Bridging and Chelation in Organoantimony(V) Chemistry

by

Martin Neil Gibbons, B.Sc.

Thesis submitted to the University of Nottingham for the degree of Doctor of Philosophy, September 1996.

To my parents

Acknowledgements

I would like to express my sincere thanks to my supervisor, Dr D.B.Sowerby, for his support, guidance and enthusiasm during the course of this work.

Many thanks also go to Dr M.J.Begley (deceased) and Dr A.J.Blake for their assistance in determination of the crystal structures presented in this thesis and to Professor M.B.Hursthouse and the EPSRC Crystallographic Service for collection of much of the crystallographic data. Thanks also go to Mr L.A.D.Hollingsworth for the mass spectral data and to Mr T.Spencer for microanalytical data.

I would also like to thank Dr M.J.Taylor (University of Auckland) for helpful discussions on the hydrolysis of $[R_3SbX]_2O$ compounds and to Dr. C.Silvestru ('Babes-Bolyai' University, Romania) for donation of a number of precursor compounds and assistance with reactions of dithiophosphinate compounds. Thanks also to Dr P.Mountford for useful discussions and the use of dry-box facilities, solvent stills, etc, etc....

Thanks also to Susan Wan, Daniel Swallow, Simon Dunn and the other people I have worked alongside with for making my stay in Nottingham an enjoyable one.

In addition, I would like to thank Arlene for her continual support and encouragement throughout the period of this work.

This project was funded by the Engineering and Physical Sciences Research Council and their assistance is gratefully acknowledged.

This research was carried out between October 1992 and September1995, during the tenure of an EPSRC Quota Award.

Abbreviations

General

^{n}Bu	*n*-butyl
^{t}Bu	*t*-butyl
Cp	cyclopentadienyl
EI	electron impact
Et	ethyl
FAB	fast atom bombardment
IR	infrared
Me	methyl
mp	melting point
Ph	phenyl
p*K*	dissociation (acidity) constant
^{i}Pr	*i*-propyl
SP	square pyramidal
TBP	trigonal bipyramidal
THF	tetrahydrofuran

Nuclear magnetic resonance spectroscopy

d	doublet
I	spin quantum number
J	coupling constant
m	multiplet
NMR	nuclear magnetic resonance
ppm	parts per million
q	quartet
s	singlet
t	triplet

Abstract

The work presented in this thesis is primarily concerned with the structural aspects of bridging and chelation in organoantimony(V) chemistry. The thesis may be essentially divided into two main parts.

The first part examines the reactions of a number of halogenated oxo-bridged organoantimony compounds (themselves subject to a study in Chapter 2) with a range of potentially bidentate groups (arsinates, phosphinates and carboxylates) to assess the capability of these groups to bridge between antimony centres. Spectroscopic and crystallographic results illustrate that arsinate groups were successfully employed in the formation of quadruply bridged compounds, whereas both arsinate and phosphinate groups enabled the preparation of several triply bridged compounds. In contrast, the shorter 'bite-length' carboxylate groups were unable to span across antimony centres in an analogous manner, although reactions between $[Ph_2SbBrO]_2$ and acetate or trimethylacetate groups led to formation of the carboxylate bridged tetra-antimony compounds, $[Ph_8Sb_4(\mu\text{-}O)_4(\mu\text{-}OR^{1,2})_2(\mu\text{-}O_2CR^3)_2]$.

The second part is concerned with antimony(V) stereochemistry. Incorporation of the chelating 2,2'-biphenylylene group led to manipulation of the coordination geometry at antimony and the preparation of compounds of the type, $PhSb(2,2'\text{-}C_{12}H_8)X_2$, with square pyramidal monomeric units. The compounds, however, possess weak intermolecular connections, giving rise to dimers in the solid state and an increase in the coordination number at antimony. In addition, the related compound, $PhSb(o\text{-}O_2C_6Cl_4)Cl_2$, also showed distinct Lewis acidity at antimony and was isolated as a diethyl ether adduct.

An additional area of work is also briefly investigated in Chapter 6. This work examines reactions between halogenated phenylantimony compounds and transition metal anions, to yield complexes incorporating the Ph_2Sb or PhSb moieties.

Contents

Appendices

CHAPTER 1

GENERAL INTRODUCTION

1.1 SCOPE OF THE THESIS

The research work documented in this thesis is primarily concerned with the topic of bridging and chelation in antimony(V) chemistry. For convenience, the thesis is divided into six chapters.

A brief introduction into the field of organoantimony chemistry is discussed in this chapter, with more specific introductions and reviews included at the beginning of each of the subsequent chapters. The uses of physical techniques employed in structural analysis are also discussed here, as well as general experimental methods.

Chapter 2 is concerned with the preparation of a number of oxo-bridged antimony(V) compounds with the formula type $[R_3SbX]_2O$. These compounds were principally prepared as precursors for the work in subsequent chapters, but an interest in the $[R_3SbX]_2O \leftrightarrow R_3Sb(OH)X$ chemical process led to a fuller study. In contrast to the other compounds prepared, which were found to exist exclusively as the $[R_3SbX]_2O$ form in the solid-state, the trimesityl derivative, $(2,4,6\text{-}Me_3C_6H_2)_3Sb(OH)Br$, was isolated as a stable compound. The chapter also details the preparation of the bis oxo-bridged compound $[Ph_2SbBrO]_2$.

Chapter 3 examines the reactions of the oxo-bridged antimony(V) compounds reported in Chapter 2 with a number of phosphinate and arsinate salts. The reactions were generally found to result in the isolation of triply or quadruply bridged diantimony products, with the antimony atoms spanned by both oxo and arsinate or phosphinate bridges. In contrast, reactions between $[Ph_2SbBrO]_2$ and dithiophosphinates led to reduction of antimony and the isolation of $Ph_2SbS_2PR_2$ compounds.

An extension of the reactions of $[R_3SbX]_2O$ compounds with carboxylates is discussed in Chapter 4. In contrast to arsinates and phosphinates, the carboxylate groups were found not to bridge across the antimony atoms, but bind in a near-unidentate manner. In addition, a number of carboxylate precursors led to the cleavage of the oxygen bridge in $[Ph_3SbBr]_2O$ and triphenylantimony dicarboxylate compounds were obtained. Bridging carboxylate groups were, however, observed in

the tetraantimony compounds, $Ph_8Sb_4O_4(OR)_2(O_2CR)_2$, obtained by reactions between $[Ph_2SbBrO]_2$ and acetate or trimethylacetate precursors.

Chapter 5 addresses the subject of the coordination geometry of five-coordinate compounds and attempts to prepare compounds with the unusual square-pyramidal geometry are described. The strategy applied in this work, involved the use of the biphenylylene and catecholato chelating groups to constrain the coordination geometry at antimony.

The final work reported herein (Chapter 6) outlines a number of reactions between halogenated phenylantimony compounds and the transition metal salts, $Na[Mo(CO)_3(\eta\text{-}C_5H_5)]$, $Na[W(CO)_3(\eta\text{-}C_5H_5)]$ and $Na[Fe(CO)_2(\eta\text{-}C_5H_5)]$. The reactions were found to be complicated and gave a number of products, but the products $[\{\mu\text{-}Ph_2Sb\}_2\{Mo(CO)_2(\eta\text{-}C_5H_5)\}_2]$ and $[PhSb\{Fe(CO)_2(\eta\text{-}C_5H_5)\}_2]$ were successfully characterised by X-ray crystallography.

The Appendices (A to R) attached at the end of this thesis detail the full results and parameters of the single crystal X-ray diffraction experiments carried out during this work.

1.2 ANTIMONY CHEMISTRY

1.2.1 History

Antimony is one of the earliest elements known to man, with the black sulfide, stibnite (Sb_2S_3), used as a cosmetic in ancient times. The name stibium was used by Pliny in *ca* 50AD and antimonium was used in writings attributed to Jabir[1] (*ca* 800AD). Between the thirteenth and the fifteenth centuries the metal became increasingly known in its elemental form and by 1707 the element was sufficiently well known for a Treatise on Antimony to be published by Lemery.

Antimony was widely used as a medicine during the fifteenth and sixteenth centuries. However, the toxicity of antimony was recognised as early as 1615 and led to a ban on the sale and use of 'tartar emetic' (hydrated potassium antimonyl tartrate; prepared by leaving wine overnight in antimony goblets). This ban was revoked in 1666 by the Paris Faculty of Medicine, which allowed 'vin emeticum' for medical use after Ludwig XIV was healed by taking it as a remedy for scarlet fever[2].

The use of antimony in medicines continues even today, where it is used in homeopathic ointments to treat chapped skin and also to treat haemorrhoids. More conventional uses of antimony rely on its toxicity and it has been used in the treatment of tropical parasitic diseases[3]. Here, the dosage has to be carefully monitored to ensure that the toxic dose for the parasite is not also a toxic dose for the host.

Alloys of antimony are used in a number of industries. Pewter, an alloy with tin, is used for drinking vessels and jewellery. Most printing 'type' alloys contain antimony as do some antifriction alloys. Battery plates are alloys with lead, whereas phosphor bronze is an alloy of copper. Addition of antimony to lead is used to greatly increase the hardness and mechanical strength.

Oxides, chlorides and sulfides of antimony are used in the manufacture of flame proofing compounds, in paints, ceramic enamels, glasses, pottery and as catalysts in the vulcanisation of rubber. These uses however, are becoming less widespread due to cheaper and less toxic alternatives becoming available.

A further use of antimony is in the electronic industry, specifically due to promoted interest in III/V type semiconductors such as InSb.

1.2.2 Reviews

Active research in organoantimony chemistry continues to this day in both the academic and industrial spheres and the subject is widely reviewed. Pre-1970 literature is summarised in a publication by Doak and Freedman[4] and there is an earlier publication by Dub[5]. Doak and Freedman have also published an annual survey on the subject of antimony chemistry since 1967[6]. The Gmelin Handbook of Inorganic Chemistry[7] also provides extensive coverage. The relevant sections of the annual R.S.C.[8] and Coordination Chemistry Reviews[9] also cover organoantimony chemistry. A recent book, edited by Patai[10], provides an extensive review of a number of topics within organoantimony chemistry.

1.2.3 Bonding and Coordination in Antimony(V) Chemistry

Organoantimony(V) compounds are known with coordination numbers four, five, six and seven, with the vast majority five or six coordinated.

Four Coordinate Structures

The pentacoordinate molecule was traditionally regarded as being unstable with respect to ionic derivatives of equivalent stoichiometry, with the ionic structure of phosphorus pentachloride often cited as an example. Such ionic examples are, in fact, rare in antimony(V) chemistry with more commonly covalent five coordinate structures found. However, a number of ionic examples have been structurally characterised and include[11,12,13], $[Me_4Sb]^+[ReO_4]^-$, $[Ph_4Sb]^+[Ph_2Sb(C_2O_4)_2]^-$ (see Figure 1.1) and $[Ph_4Sb]^+[FeI_4]^-.Ph_3SbI_2$. It should be noted that for lighter Group 15 elements, R_4E^+ cations are well known and are commonly used as stabilising (usually non-coordinating) counterions for a variety of anionic species.

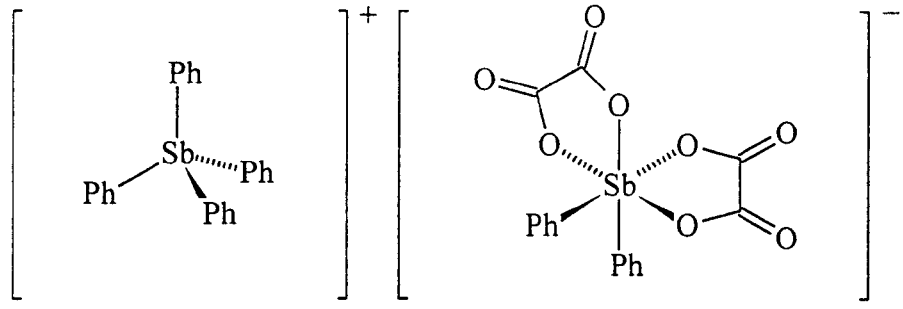

Figure 1.1 Ionic structure of triphenylantimony oxalate

Tetrahedral structures might also be expected for molecules with the stoichiometry R_3SbO. However, due to a disparity in size between antimony 5*d* and oxygen 2*p* orbitals, π bonding is very weak and stability is normally gained by formation of an additional σ bond and association into cyclic dimers or polymers[14,15]. Nevertheless, a distorted tetrahedral geometry, with a supported Sb=O bond, was found for $(2,4,6\text{-}Me_3C_6H_2)_3SbO{\cdot}HO_3SPh$[16] and surprisingly a four coordinate stibinic acid moiety is observed in $[SbO(OH)\{Co(CO)_3(PPh_3)\}_2]$[17]. The larger sulfur 3*p* orbital gives a more favourable π overlap with antimony 5*d* orbitals and indeed a stable tetrahedral monomer, with an Sb=S double bond is found for Ph_3SbS[18].

Five Coordinate Structures

Using the VSEPR theory, Gillespie[19] showed that, for minimum energy, five ligands are arranged around the central atom in either trigonal bipyramidal or square pyramidal geometry to minimise steric interactions.

The overwhelming majority of five coordinate organoantimony(V) compounds adopt a trigonal bipyramidal geometry about antimony. There are however exceptions, with one of the most notable being pentaphenylantimony, found to possess a distorted square pyramidal geometry[20,21,22]. Interestingly, crystals of the cyclohexane solvate of pentaphenylantimony[23] show the more common trigonal bipyramidal coordination, as does penta(*p*-tolyl)antimony[24].

Five coordinate organoantimony(V) structures are the subject of a greater discussion in Chapter 5.

Six Coordinate Structures

Six coordinate antimony(V) coordination is common where the Lewis acidity of the antimony(V) centre is enhanced by coordination of electronegative ligands, such as halides. For example, although triphenylantimony(V) dichloride[25] is a trigonal bipyramidal monomer, diphenylantimony(V) trichloride adopts a dimeric double chlorine bridged structure[26] with octahedral coordination about antimony. Thus, replacement of a phenyl group by a more electronegative chlorine atom increases the Lewis acidity at antimony and raises the coordination number.

Six-fold coordination may also be achieved by dative bonding in the presence of electron pair donors such as MeCN or H_2O. Hence, diphenylantimony(V) trichloride and bromide form adducts with water and acetonitrile respectively and the structures of both compounds have been reported[27]. Further, six coordination is often observed in compounds with short 'bite' ligands, with the benzamidinate compound, $Ph_2SbCl_2(PhC(NMe)_2)$[28] (see Figure 1.2), an interesting example.

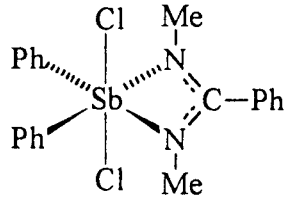

Figure 1.2 Molecular structure of $Ph_2SbCl_2(PhC(NMe)_2)$

Seven Coordinate Structures

A few seven coordinate organoantimony(V) compounds are also known. Examples include the related carboxylate compounds $[Ph_2Sb(O_2CMe)_2]_2O$[29] and $[Ph_2Sb(O_2CPh)_2]_2O$[30] in which seven coordination at each antimony is achieved by chelation of all the carboxylate groups.

Secondary Bonding

Secondary bonding has been described by Alcock and Sawyer[31] as the formation of inter or intra molecular contacts which are longer than primary bonds, but shorter

than the sum of the relevant van der Waals radii. For a bond to be described as truly secondary, the authors suggest that the interacting atoms must not be in the most favourable position for crystal packing forces and/or the interacting atom must be in a stereochemically significant position. Secondary bonding is always associated with primary bonding and the interactions are generally *trans* to each other.

Bond order can be applied to relate primary and secondary bonding. Pauling[32] related the bond order (n) to the observed bond length, $D(n)$ by the equation:

$$D(n) = D(1) - K \log n$$

where $D(1)$ is the single bond length and K is an arbitrary constant.

Thus, bond orders of less then a half are considered to be secondary bonds, while bond orders greater than a half but less than or equal to one are considered to be primary bonds.

The upper limit for secondary bonding is arbitrarily taken as the sum of the van der Waals radii of the two atoms concerned. In this work, secondary interactions have been found to occur between the antimony atom and either oxygen, sulfur, bromine or chlorine. The sum of the van der Waals radii for these atoms are listed in Table 1.1.

Table 1.1 Sum of van der Waals radii for antimony and relevant atoms

Secondary contact	Sum of van der Waals radii (Å)
Sb···O	3.6
Sb···S	4.1
Sb···Br	4.2
Sb···Cl	4.0

1.3 PHYSICAL METHODS OF STRUCTURAL ANALYSIS

X-Ray Crystallography

Single crystal X-ray diffraction provides probably the most useful tool for solid state structure elucidation, giving the spatial arrangement of atoms within a molecule. From this information relevant bond lengths and angles, as well as secondary interactions can readily be ascertained. An extensive explanation of the theoretical and practical aspects of X-ray crystallography is covered in the book by Stout and Jensen[33].

X-ray crystallography has been used extensively in this work to provide definitive structural results and to compliment conclusions drawn from spectroscopic data. For example, the work described in Chapter 4 involves investigations into the bonding modes of carboxylate groups and structural data drawn from crystallographic results were found to correlate well with trends observed from infrared spectroscopic results.

However, there are limitations to the application of X-ray crystallography; firstly the compound to be studied must be in the solid-state and provide single crystals of a suitable size and quality for a structure determination (although extensive information can be obtained from powders) and secondly (which makes, in particular, NMR spectroscopy complementary) is the poor response of X-ray diffraction to the presence of hydrogen atoms.

Infrared Spectroscopy

The vibrational spectra of molecules provide detailed information about their structure. Specifically in this work, infrared spectroscopy has provided invaluable information regarding the coordination pattern of ligands to antimony, such as phosphinates, carboxylates and thiocyanate groups. In addition, information about skeletal structures has also been obtained, with notably the Sb–O–Sb moiety providing distinctive absorptions in the commonly used frequency range.

The majority of compounds studied here were phenylantimony derivatives, which give complex infrared spectra. The most common assignment of phenyl groups is based on

work by Whiffen[34], which details the thirty fundamental vibrational modes for a monosubstituted phenyl compound, PhX, with C_{2v} symmetry.

The short time-scale (*ca.* 10^{-12} s) of infrared spectroscopy can also provide valuable information about fast chemical processes, such as isomerisation, with distinct species observable as opposed to 'time-averaged' species.

Nuclear Magnetic Resonance Spectroscopy

^{1}H and ^{13}C nuclei have been widely used to study the structures of organoantimony compounds and can provide important information, both by confirming the stoichiometry of different organic groups in the compound and by providing information about the overall structure from chemical shifts of the various nuclei. Indeed, results from this work have indicated that the chemical shifts and coupling patterns of simply a phenyl group can offer significant information regarding the oxidation state, likely coordination geometry and compound type of the antimony molecule to which they are bound.

Although not applied in this work, resonance techniques such as the nuclear Overhauser effect can also give valuable information regarding the spatial relationship between nuclei (specifically protons).

NMR study of antimony nuclei is not sufficiently developed for it to be of any great routine value in the investigation of molecular structure. The two isotopes of antimony ^{121}Sb and ^{123}Sb (natural abundancies 57.25 and 42.75% respectively) are both extremely insensitive nuclei with spins of I=5/2 and I=7/2 respectively. These factors, combined with large quadrupole moments for both isotopes lead to very broad signals in the NMR spectrum. Even for symmetrical species, line widths at half peak height can range from 300 to 9000Hz[35].

Mass Spectroscopy

Electron Impact (EI) and Fast Atom Bombardment (FAB) spectra were both used during this work and offered important structural information. For the majority of

compounds examined in this thesis, however, the parent ion was not observed; this was mainly because of the high molecular mass of the compounds and instability under mass spectroscopic conditions. Complications were also noted due to reorganisation ions and, in the case of FAB spectra, recombination with the organic matrix (in which the sample is suspended) or protons.

Important structural units, though, were observed in most cases, with the characteristic isotopic patterns extremely useful in assigning peaks (many of the atoms of interest studied in this work being polyisotopic). Piecing together of identified fragments in the spectra often led to near-complete identification of molecular composition.

The data for mass spectra included in this work have been based on lowest mass common isotopes (for example, ^{121}Sb) and are presented in monoisotopic form.

A fuller description about the physical techniques (both theoretical and practical) available for the inorganic chemist is provided in the excellent book by Ebsworth, Rankin and Cradock[36]. The book also outlines the concepts of Mössbauer spectroscopy, a further technique valuable in structural elucidation of antimony compounds.

1.4 GENERAL EXPERIMENTAL METHODS

Where necessary, manipulations were carried out under an atmosphere of dinitrogen or argon using standard Schlenk and dry-box techniques.

Solvents, triethylamine and tetramethylethylenediamine (TMEDA) were pre-dried over activated molecular sieves and refluxed over potassium (tetrahydrofuran, diglyme and hexane), sodium/potassium alloy (pentane and diethyl ether) or calcium hydride (dichloromethane, acetonitrile, triethylamine and TMEDA) under an atmosphere of dinitrogen and collected by distillation. Deuterated benzene (C_6D_6) was dried over molten potassium, while $CDCl_3$ was dried over calcium hydride or molecular sieves at room temperature. Where necessary deuterated solvents were distilled under reduced pressure and stored under dinitrogen in Young's ampoules in

a dry-box. Further, anhydrous samples were prepared in a dry-box in Teflon valve (Young's) 5mm tubes.

^{1}H and ^{13}C NMR spectra were recorded on either a Bruker WM250 or a Bruker DPX300 spectrometer at 298 K unless otherwise specified. The spectra were referenced internally to residual protio-solvent (^{1}H) or solvent (^{13}C) resonances and are reported relative to tetramethylsilane ($\delta = 0$ ppm). Chemical shifts (δ) are quoted in ppm and coupling constants in Hz.

Infrared samples were prepared either as Nujol mulls between CsI plates or as CH_2Cl_2 or tetrahydrofuran solutions in air-tight solution cells. Spectra were recorded on a Nicolet 205 FTIR spectrometer in the range 4000-400 cm^{-1}, and all data are quoted in wavenumbers.

Mass spectra were recorded by the mass spectrometry service of the Chemistry department of the University of Nottingham and were recorded on either a VG Micromass 7070E or a AEI MS902 mass spectrometer.

Elemental analysis were performed by Mr. Trevor Spencer of the Chemistry department of the University of Nottingham.

Safe Working Practices

Organoantimony compounds are highly toxic and their long-term and mutagenic properties have not been fully investigated. Standard safe working practices were therefore used in all experiments. All work was carried out in a fume cupboard and suitable protective clothing, gloves and eye protection were worn at all times. In addition, COSHH assessments were carried out before embarking on experimental work.

1.5 PREPARATON OF STARTING MATERIALS

Unless stated otherwise, chemicals were purchased from Aldrich and used as received. Dimethylarsinic acid (HO_2AsMe_2), diphenylarsinic acid (HO_2AsPh_2), diphenylphosphinic acid (HO_2PPh_2), hydrated sodium dimethyldithiophosphinate

($NaS_2PMe_2.2H_2O$) and ammonium diphenyldithiophosphinate ($NH_4S_2PPh_2$) were donated by Dr. C.Silvestru, 'Babes-Bolyai' University, Cluj-Napoca, Romania.

1.5.1 Preparation of $SbBr_3$

Antimony (powdered, 15g, 123mmol) was slowly added to a stirred solution of bromine (16.8g, 105mmol) in carbon disulfide (200ml) at 0°C and the reaction mixture was stirred for a further 2 hours at room temperature. After this time excess antimony was removed by filtration and the filtrate was evaporated to dryness. The crude obtained was purified by sublimation *in vacuo* at 70°C and the pure crystalline product was stored in a dry-box.

1.5.2 Purification of $SbCl_3$

Antimony trichloride (Aldrich) was sublimed *in vacuo* at 70°C and the resultant crystalline product was stored in a dry-box.

1.5.3 Preparation of Ph_nSbX_{3-n} compounds

Preparation of Ph_nSbX_{3-n} compounds, where X = Cl or Br and n = 1 or 2, was achieved by the method of Wesolek *et al*[37] which involved stirring or shaking together stoichiometric quantities of Ph_3Sb and the relevant SbX_3 in the solid-state. These reactions provided quantitative yields of the desired products that were used directly.

1.5.4 Preparation of $Na[C_5H_5]$

Freshly 'cracked' cyclopentadiene ($90cm^3$, 1.39mol) was added to a cooled suspension of sodium hydride (60% in mineral oil, 60g, 1.5mol) in THF (750ml) until effervescence ceased. After stirring overnight, a white suspension of solvated $Na[C_5H_5]$ had precipitated from the solution. The mixture was filtered and the remaining solid was extracted into THF and filtered away from excess NaH. The filtrate and washings were combined and the volatiles were removed under reduced pressure leaving a white solid. ^1H NMR spectroscopy (CD_3CN) showed the product to be $Na[C_5H_5].0.5THF$.

1.5 REFERENCES

1. N.N.Greenwood, A.Earnshaw, *Chemistry of the Elements*, Pergamon Press, 1984, 637.

2. W.F.Daems, *Stimmi Stibum Antimon: An Historical Examination.*, Weleda AG, 1976, Arlesheim (Switzerland).

3. A.Cushny, *A Textbook of Pharmacology and Therapeutics*, 1928, London, 676.

4. G.O.Doak, L.D.Freedman, *Organometallic Compounds of Arsenic, Antimony and Bismuth*, Wiley Interscience, London, 1970.

5. M.Dub, *Organometallic Compounds, Vol 3, Compounds of Arsenic, Antimony and Bismuth*, Wiley Interscience, London, 1970.

6. G.O.Doak, L.D.Freedman, Organometallic Chemistry Reviews, Section B, *J. Organomet. Chem.*, Annual Reviews.

7. *The Gmelin Handbook of Inorganic Chemistry*, Verlag Chemie, GMBH, Weinheim/Bergstrasse.

8. The Royal Society of Chemistry, Annual Reports, Section A, Inorganic Chemistry.

9. *Coordination Chemistry Reviews*, Chapter 5, Elsevier Science Publishers B.V., Amsterdam, Annual Reviews.

10. S.Patai, *The Chemistry of Organic Arsenic, Antimony and Bismuth Compounds*, John Wiley & Sons, London, 1994.

11. P.K.Burkert, M.Grommelt, T.T.Pietrass, J.Lachmann, G.Müller, *Z. Naturforsch.*, 1990, **B45**, 725.

12. P.L.Millington, PhD Thesis, University of Nottingham, 1982.

13. H.P.Lane, S.M.Godfrey, C.A.McAuliffe, R.G.Pritchard, *J. Chem. Soc., Dalton Trans.*, 1994, 3249.

14. J.Bordner, G.O.Doak, T.S.Everett, *J. Am. Chem. Soc.*, 1986, **108**, 4206.

15. C.J.Carmalt, J.G.Crossley, N.C.Norman, A.G.Orpen, *J. Chem. Soc., Chem. Commun.*, 1996, 1675.

16. F.Huber, T.Westhoff, H.Preut, *J. Organomet. Chem.*, 1987, **323**, 173.

17. W.Clegg, N.A.Compton, R.J.Errington, D.C.R.Hockless, N.C.Norman, M.Ramshaw, P.M.Webster, *J. Chem. Soc., Dalton Trans.*, 1990, 2375.

18. J.Pebler, F.Weller, K.Dehnicke, *Z. Anorg. Allg. Chem.*, 1982, **492**, 139.

19. R.J.Gillespie, *J. Chem. Educ.*, 1970, **47**, 18.

20. P.J.Wheatley, G.Wittig, *Proc. Chem. Soc.*, 1962, 251.

21. P.J.Wheatley, *J. Chem. Soc.*, 1964, 3718.

22. A.L.Beauchamp, M.J.Bennett, F.A.Cotton, *J. Am. Chem. Soc.*, 1968, **90**, 6675.

23. C.Brabant, B.Blanck, A.L.Beauchamp, *J. Organomet. Chem.*, 1974, **82**, 231.

24. C.Brabant, J.Hubert, A.L.Beauchamp, *Can. J. Chem.*, 1973, **51**, 2952.

25. M.J.Begley, D.B.Sowerby, *Acta Crystallogr.*, 1993, **C49**, 1044.

26. J.Bordner, G.O.Doak, J.R.Peters, *J. Am. Chem. Soc.*, 1974, **96**, 6763.

27. T.T.Bamgboye, M.J.Begley, D.B.Sowerby, *J. Organomet. Chem.*, 1989, **362**, 77.

28. F.Weller, J.Pebler, K.Dehnicke, K.Hartke, H.-M.Wolff, *Z. Anorg. Allg. Chem.*, 1982, **486**, 61.

29. D.B.Sowerby, M.J.Begley, P.L.Millington, *J. Chem. Soc., Chem. Commun.*, 1984, 896.

30. M.A.Said, K.C.Kumara Swamy, Kamlesh Babu, K.Aparna, M.Nethaji, *J. Chem. Soc., Dalton Trans.*, 1995, 2151.

31. N.W.Alcock, J.F.Sawyer, *J. Chem. Soc., Dalton Trans.*, 1977, 1090.

32. L.Pauling, *The Nature of the Chemical Bond*, 3rd Ed., Cornell Univ. Press, 1960.

33. G.H.Stout, L.H.Jensen, *X-ray Structure Determination*, 2nd Ed., Macmillan, London, 1989.

34. D.H.Whiffen, *J. Chem. Soc.*, 1956, 1350.

35. R.K.Harris, B.E.Mann, *NMR and the Periodic Table*, Academic Press, 1978, 380.

36. E.A.V.Ebsworth, D.W.H.Rankin, S.Cradock, *Structural Methods in Inorganic Chemistry*, 2nd Ed., Blackwell Scientific Publications, 1991.

37. D.M.Wesolek, M.Nunn, D.B.Sowerby, *J. Organomet. Chem.*, 1983, **251**, C45.

CHAPTER 2

OXO-BRIDGED ORGANOANTIMONY(V) HALIDES

2.1 INTRODUCTION

In contrast to the well known triorganoarsenic hydroxohalide compounds (*eg.* $Ph_3As(OH)X$, where X = Cl or Br[1]) there has been considerable confusion in the literature regarding both the analogous $R_3Sb(OH)X$ group of compounds and the corresponding dehydrated species $[R_3SbX]_2O$, where R is an organic group and X is a halide, nitrate or a carboxylate[2-8]. When R is sterically small, no $R_3Sb(OH)X$ compounds have been unambiguously isolated in the solid state, but evidence for their existence has been observed when $[R_3SbX]_2O$ is dissolved in moist solvents. For example[9], when $[Me_3SbCl]_2O$ is dissolved in water-saturated dichloromethane, infrared absorptions are observed at 3625, 3480 and 552 cm^{-1}, consistent with the expected ν(OH) and ν(Sb-OH) vibrations for $Me_3Sb(OH)Cl$. On crystallisation though, only the condensation product $[Me_3SbCl]_2O$ is recovered.

$$\underset{\text{Solid state}}{[Me_3SbCl]_2O} \underset{-H_2O}{\overset{CH_2Cl_2,\ H_2O}{\rightleftharpoons}} \underset{\text{Solution}}{2\ Me_3Sb(OH)Cl}$$

Furthermore, $[Me_3SbCl]_2O$ is also the only product isolated in a reaction between Me_3SbCl_2 and one equivalent of NaOH[9].

Infrared solution studies of $[Et_3SbBr]_2O$, $[^iPr_3SbCl]_2O$, $[Ph_3Sb(O_2CMe)]_2O$ amongst others, in non-anhydrous conditions, were also found to exhibit bands due to the corresponding $R_3Sb(OH)X$ species, but again on crystallisation only the original oxygen bridged compounds were isolated[10].

The apparent preparation of $R_3Sb(OH)X$ compounds, eg R = (*m*-MeC_6H_4), X = Cl[5], R = (*cyclo*-C_6H_{11}), X = Cl[11], has been claimed in earlier work, but without full spectroscopic and analytical data, it is likely that these compounds were in fact of the type $[R_3SbCl]_2O$. However, the genuine hydroxohalide, (*cyclo*-$C_6H_{11})_3Sb(OH)Cl$ along with its bromide, acetate and nitrate analogues has now been prepared[9], but stringent precautions must be taken to prevent the ready formation of their anhydride analogues in the solid-state.

The only 'stable' compounds possessing the hydroxohalide structural type, have been prepared by the use of bulky organo groups. The first compound reported was (2,6-$Me_2C_6H_3)_3Sb(OH)I$, formed by partial hydrolysis of (2,6-$Me_2C_6H_3)_3SbI_2$ in 10% aqueous methanol[12]. A structure determination of the compound showed it to be an ionic species, better described as [(2,6-$Me_2C_6H_3)_3Sb(OH)]^+I^-$, with near tetrahedral geometry about the antimony centre. Coordination of the iodine atom occurs via a hydrogen bond from the hydroxo hydrogen, giving a structure represented in Figure 2.1. It is interesting to note that this ionic structure is also found in related arsenic hydroxohalides, such as [*cyclo*-$(CH_2)_5$(^{t}Bu)As(OH)]Br[13] and [*cyclo*-$(CH_2)_5$(^{t}Bu)As(OH)]Cl[14].

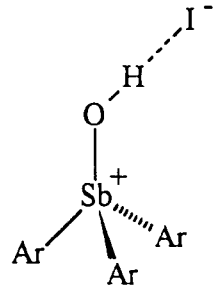

Figure 2.1 Molecular structure of [(2,6-$Me_2C_6H_3)_3Sb(OH)]^+I^-$

Mesityl groups (2,4,6-$Me_3C_6H_2$–) have also been successfully utilised to form a further series of hydroxo compounds with the general formula (2,4,6-$Me_3C_6H_2)_3Sb(OH)(O_2CR)$[15,16], where R = H, Me, $CHCl_2$, CH_2F, CF_3 and $C_{10}H_{15}$. These compounds were prepared by addition of the appropriate carboxylic acid to (2,4,6-$Me_3C_6H_2)_3Sb(OH)_2$ in acetone, *ie*.

(2,4,6-$Me_3C_6H_2)_3Sb(OH)_2$ + HO_2CR → (2,4,6-$Me_3C_6H_2)_3Sb(OH)(O_2CR)$ + H_2O

Structures of (mesityl)$_3$Sb(OH)($O_2CC_{10}H_{15}$) and (mesityl)$_3$Sb(OH)(O_2CCHCl_2) have been established by X-ray crystallography and were found to be trigonal bipyramidal covalent systems, with the hydroxo oxygen and a carboxylate oxygen occupying axial positions and the three mesityl *ipso* carbons occupying equatorial positions. It is worth noting, in passing, that antimony mesityl compounds also differ from similar

antimony compounds having smaller organo groups in the oxidation of R_3Sb compounds with anhydrous peroxides, to yield $(mesityl)_3Sb(OH)_2$ as opposed to $[R_3SbO]_2$ dimers[17].

A number of oxo-bridged $[R_3SbX]_2O$ compounds have also been structurally studied. Ferguson and co-workers[18] have reported structures of the compounds $[Me_3SbX]_2O$, where X = Cl and the pseudohalide N_3. Both compounds have crystallographically imposed $\bar{3}$ symmetry, implying that the Sb–O–Sb angle is 180°. However, substantial electron density is found in three sites about the oxygen and halides/pseudohalides, suggesting molecular disorder over three positions, giving a genuine Sb–O–Sb angle closer to 130°.

Infrared spectroscopy has proved to be a useful method of identifying the Sb–O–Sb skeleton in such compounds, with a characteristic intense band(s) normally found between 700-800 cm^{-1}. Hence, the IR spectrum of $[Me_3SbCl]_2O$, displays an absorption at 775 cm^{-1}, attributed to this ν(Sb–O–Sb) mode. Similar intense IR absorptions at *ca.* 770 cm^{-1} are also found in the phenylantimony derivatives $[Ph_3SbX]_2O$, where X = Cl, Br or N_3, all of which have been subject to a structure determination[19,20,21]. The Sb–O–Sb angles in these compounds, and other related Sb–O–Sb compounds, have been found to vary over a significant range between *ca.* 130 and 180° (139.0, 173.4(mean) and 139.8° respectively for the compounds mentioned).

This chapter primarily describes the reactions between a number of triarylantimony dihalides and one equivalent of sodium hydroxide, primarily intending to prepare $[Ar_3SbX]_2O$ compounds for use as precursors in the work described in Chapters 3 and 4. However, an interest in the $[Ar_3SbX]_2O \leftrightarrow Ar_3Sb(OH)X$ chemistry led to the full characterisation of the compounds and a study of their solution behaviour. The solution behaviour of the analogous methyl compound $[Me_3SbCl]_2O$ was also noted.

2.2 RESULTS AND DISCUSSION

2.2.1 Preparation of Compounds

Reactions of Ph_3SbBr_2 (**2.1**), (p-$MeC_6H_4)_3SbBr_2$ (**2.2**) and (o-$MeC_6H_4)_3SbBr_2$ (**2.3**) with one equivalent of NaOH led to the formation of the oxygen bridged compounds $[Ph_3SbBr]_2O$ (**2.7**), $[(p\text{-}MeC_6H_4)_3SbBr]_2O$ (**2.8**) and $[(o\text{-}MeC_6H_4)_3SbBr]_2O$ (**2.9**).

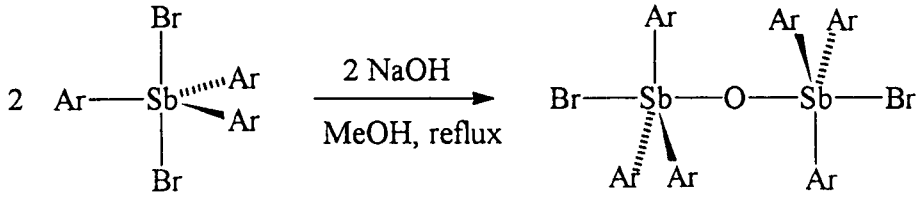

Ar = Ph (**2.7**), p-tolyl (**2.8**), o-tolyl (**2.9**)

Figure 2.2 Preparation of $[Ar_3SbBr]_2O$ compounds

All three compounds were formed in good yields and were found to be analytically pure. Compound **2.7** has been prepared previously[7] and infrared spectroscopic data reported herein were in good agreement with those previously reported.

The methyl derivative, $[Me_3SbCl]_2O$ (**2.10**) was also prepared by a reaction between stoichiometric quantities of $Me_3Sb(OH)_2$ (**2.4**) and Me_3SbCl_2 (**2.5**) and spectroscopic findings were consistent with previously reported data[6,8].

In a similar fashion to the preparations of **2.7**, **2.8** and **2.9**, (2,4,6-$Me_3C_6H_2)_3SbBr_2$ (**2.6**) was treated with one equivalent of NaOH in methanol and the resulting mixture refluxed for 20 hours. After work-up, however, the only product isolated analysed as the hydroxohalide (2,4,6-$Me_3C_6H_2)_3Sb(OH)Br$ (**2.11**), and not the corresponding oxo-bridged analogue (see Figure 2.3).

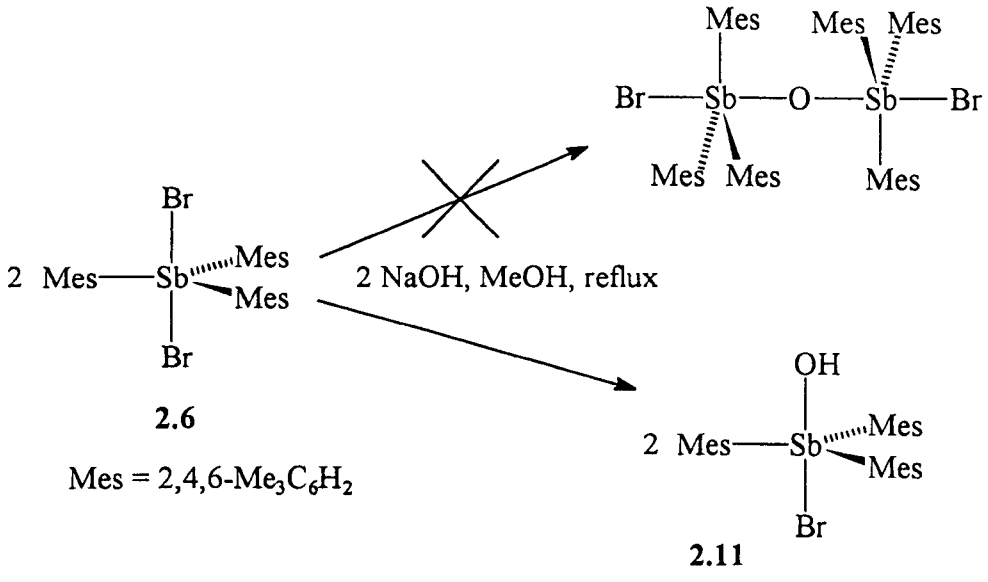

2.6

Mes = 2,4,6-$Me_3C_6H_2$

2.11

Figure 2.3 Reaction between $(2,4,6\text{-}Me_3C_6H_2)_3SbBr_2$ and NaOH

The isolated compound gave satisfactory elemental analyses and was fully characterised by NMR, IR and mass spectroscopy.

The formation of the hydroxohalide **2.11** and not the corresponding anhydride is presumably driven by the steric bulk of the mesityl groups, particularly the 2,6-methyl groups. An oxo-bridged species would clearly be very crowded with six closely positioned mesityl groups. This steric argument would also rationalise the fact that $(2,6\text{-}Me_2C_6H_3)_3Sb(OH)I$ also exists as a hydroxo halide species having similarly the 2,6- aryl positions blocked by methyl groups.

The known compound $[Ph_2SbBrO]_2$ (**2.12**) was also prepared, in good yields, by the reaction between Ph_2SbBr and ^tBuOOH (see Figure 2.4) and its spectroscopic properties are briefly discussed.

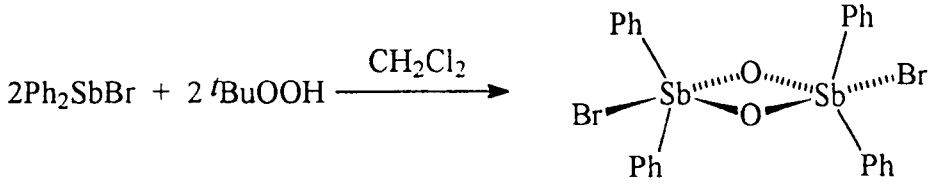

Figure 2.4 Preparation of $[Ph_2SbBrO]_2$ (2.12)

2.2.2 Infrared Spectroscopy

2.2.2.1 Oxo-bridged compounds

Spectra of M–O–M compounds, according to work carried out by Wing and Callahan[22], should show two infrared bands, *i.e.* ν_{asym} and ν_{sym}(M–O–M), whose separation is largely dependent on the M–O–M bond angle. As illustrated in Table 2.1, there is indeed a strong correlation between the magnitude of this angle and the separation of the two vibrations in the compounds listed.

Table 2.1 Comparison between M–O–M infrared modes and bond angles

Compound	ν_{asym}, cm^{-1}	ν_{sym}, cm^{-1}	M-O-M, (θ)°	Reference
$Re_2OCl_{10}^{4-}$	855	230	180	[23]
$Cr_2O(NH_3)_{10}^{4-}$	873	215	180	[23]
$Cr_2O_7^{2-}$	770	560	115	[24]
$W_2O_{11}(H_2O)_2^{2-}$	790 (750)	556	139	[23],[25]

Thus, as the angle of θ approaches 180°, the energy of ν_{sym}(M–O–M) moves out of the range of readily available spectrometers. For this reason only bands due to ν_{asym}(Sb–O–Sb) were considered in this work.

The infrared spectra of compounds **2.7**, **2.8** and **2.9** (recorded as nujol mulls) showed a great deal of structure in the region between 1500 to 400 cm^{-1}. Most of the bands can be assigned to various modes of the aryl groups following the work of Whiffen[26] and others[27]. Of particular interest though, are intense bands in the 750-780 cm^{-1} region of the spectra, assigned to ν_{asym}(Sb–O–Sb) absorptions. An intense band at 776 cm^{-1} was also observed in the infrared spectrum of $[Me_3SbCl]_2O$ (**2.10**), which also showed absorptions at 859 cm^{-1}, due to a methyl deformation mode and at 582 cm^{-1}, assigned to a ν(Sb–C) vibration. The ν_{asym}(Sb–O–Sb) bands in **2.7**, **2.8**, **2.9** and **2.10** are consistent with values obtained for related compounds and are listed in Table 2.2.

Table 2.2 Comparison of ν_{asym}(Sb–O–Sb) bands (cm^{-1})

Compound	ν_{asym}(Sb–O–Sb)	Reference
$[Ph_3SbBr]_2O$ (**2.7**)	774(772), 766(764)	This work, [7]
$[(p\text{-}MeC_6H_4)_3SbBr]_2O$ (**2.8**)	768	This work
$[(o\text{-}MeC_6H_4)_3SbBr]_2O$ (**2.9**)	760, 752	This work
$[Ph_3SbCl]_2O$	768	[8]
$[Ph_3SbN_3]_2O$	~750	[28]
$[Me_3SbCl]_2O$	777(775)	This work, [2]

Huber and co-workers[29] amongst others[30] have correlated infrared data (specifically ν_{asym}(Sb–O–Sb) modes) for a series of $[Ph_3SbX]_2O$ compounds, with their crystallographically observed Sb–O–Sb bond angles and concluded that there is sufficient agreement to enable bond angles to be predicted from IR results. Work reported later in this chapter though, casts doubt on the validity of this simple correlation. Thus, structure determinations of compounds **2.8** and **2.9**, detailed later, show that although the Sb–O–Sb bond angles are 180 and 166(mean)° respectively, there is minimal difference in the position of the ν_{asym}(Sb–O–Sb) absorptions. Moreover, this vibration in the spectrum of **2.8** is at an identical position to that reported for the compound $[Ph_3SbCl]_2O$[8], where the bond angle is only 139.0°. It is therefore apparent that other factors, such as the effect of other substituents, are also important in determining the frequency of ν_{asym}(Sb–O–Sb) absorptions.

2.2.2.2 Infrared spectrum of 2.11

The infrared spectrum of $(2,4,6\text{-}Me_3C_6H_2)_3Sb(OH)Br$ (**2.11**), showed conclusively that the species is indeed a hydroxohalide species, with absence of any notable features in the region expected for ν_{asym}(Sb–O–Sb) vibrations. In comparison with the spectrum of $(2,4,6\text{-}Me_3C_6H_2)_3SbBr_2$ (**2.6**), two distinct new bands were noted at 3501 and 542 cm^{-1}. The former broad band was assigned to the expected ν(OH) mode, with the breadth and position of the absorption implying a degree of hydrogen bonding (the corresponding ν(OH) band in $(2,4,6\text{-}Me_3C_6H_2)_3Sb(OH)_2$, found to have

no H-bonding interactions is located at 3650 cm^{-1} and is sharp). The band at 542 cm^{-1} was attributed to the ν(Sb–O) vibration, consistent with the observation of a similar band at 520 cm^{-1} in $(2,4,6\text{-}Me_3C_6H_2)_3Sb(OH)_2$ also assigned to the ν(Sb–O) vibration.

The presence of hydrogen bonding in **2.11** tends to suggest that the compound is either an ionic species, *ie.* $[(2,4,6\text{-}Me_3C_6H_2)_3Sb(OH)]^+Br^-$, with hydrogen bonding between the hydroxy hydrogen and the bromine anion, or that the hydroxy group is interacting with neighbouring molecules.

2.2.2.3 Infrared spectrum of 2.12

The infrared spectra of Sb_2O_2 compounds have been studied in some depth in previous work[17,30-34], so only a brief summary of bands in the compound $[Ph_2SbBrO]_2$ (**2.12**) will be reported here. In comparison with unoxidised diphenylantimony(III) bromide, the infrared spectrum of **2.12** displayed three very intense new bands, at 670, 648 and 495 cm^{-1}, due to Sb_2O_2 ring vibrations. Using Wing and Callahan's notation for M_2O_2 compounds[22], these bands can be assigned as the ν_1, ν_3 and ν_4 modes of the Sb_2O_2 ring respectively. According to the authors, these bands should be in similar positions for related compounds possessing similarities in ring bond angles and thus the bands in $[Ph_3SbO]_2$, with an Sb–O–Sb angle of 102.5°, should be very close to those in **2.12**, where the corresponding angle is 101.4°. Indeed, bands at 664, 649 and 477 cm^{-1} are found in the spectrum of $[Ph_3SbO]_2$[30].

2.2.3 NMR Data

2.2.3.1 Oxo-bridged compounds

The ^1H NMR spectrum of the oxo-bridged compound $[Ph_3SbBr]_2O$ (**2.7**), recorded in $CDCl_3$, without specific precautions against atmospheric moisture, showed a number of resonances in the range 7.29 to 8.26 ppm. However, on close inspection of the spectrum, the signals could be divided into two individual sets. The fact that there was no obvious correlation between the relative intensities of the two sets of signals, led to the conclusion that two individual species were present in the solution (as opposed to two chemically inequivalent types of phenyl groups being present in the molecule). The major species (**A**) displayed a triplet (7.29 ppm, *m*-Ph), triplet (7.44

ppm, *p*-Ph), doublet (7.60 ppm, *o*-Ph) phenyl coupling pattern, whereas the phenyl resonances for the minor species (**B**) were observed as two multiplets at 7.57 (*m*- and *p*-Ph) and 8.26 (*o*-Ph) ppm.

The presence of two individual species in the solution was clarified by a $^{13}C\{^{1}H\}$ spectrum that clearly showed defined signals for the two species. Species **A** gave resonances at 129.1, 130.8, 133.3 and 141.9 ppm for the *meta*, *para*, *ortho* and *ipso* phenyl carbons respectively with corresponding signals for species **B** observed at 129.5, 131.8 and 134.1 ppm for the *meta*, *para* and *ortho* carbons (the quaternary *ipso* carbon was not observed). Interestingly, on crystallisation of the NMR sample, well formed crystals of **2.7** were quantitatively recovered.

In an attempt to assess whether the presence of the two species in solution was an isomer effect or due to a partial chemical change whilst in solution, the spectrum of **2.7** was remeasured under strictly anhydrous conditions (see Section 1.4). The resultant spectrum then clearly displayed the presence of only a single species, with chemical shifts and coupling patterns identifying it to be species **A**. Not surprisingly, this was also confirmed by a $^{13}C\{^{1}H\}$ spectrum, which showed the expected four peaks in corresponding positions to those found for species **A** in the earlier mixed component spectrum.

These findings strongly suggest that the presence of a second species in the 'moist' solvent was due to a partial chemical change, that is totally reversible on crystallisation. It is proposed therefore, that the species observed in very dry conditions is the chemically unchanged parent molecule, $[Ph_3SbBr]_2O$ (**2.7**). When traces of moisture are allowed into the solution, the oxo-bridged compound is seemingly partially hydrolysed, giving rise to a second compound, which is almost certainly $Ph_3Sb(OH)Br$ (**2.13**) (see Figure 2.4). These findings are also in firm agreement with observations made by Kawasaki and co-workers[9] regarding the solution IR studies of the hydrolysis of related oxo-bridged compounds.

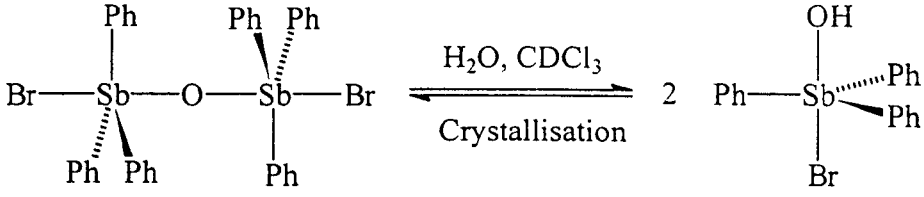

2.7 **2.13**

Figure 2.4 Hydrolysis of 2.7 in solution

The ^{1}H NMR spectrum of $[(p\text{-}MeC_6H_4)_3SbBr]_2O$ (**2.8**) illustrated a similar solution behaviour to that observed with **2.7**. Thus, when the spectrum was measured under strictly anhydrous conditions only a single species was observed, which displayed resonances at 2.40(s, Me), 7.08(d, *m*-Ar) and 7.51(d, *o*-Ar) ppm for the chemically equivalent *p*-tolyl groups. ^{13}C resonances for this species were observed at 21.4, 129.6, 133.4 and 141.0 ppm for the methyl, *meta*, *ortho* and *ipso* carbons respectively. Due to the poor solubility of the compound, a signal due to the quaternary *para* carbon was not observed.

On exposure of the sample to atmospheric conditions for a number of hours, the ^{1}H spectrum showed again the presence of a second species, expected to be the corresponding hydrolysis product $(p\text{-}MeC_6H_4)_3Sb(OH)Br$ (**2.14**) (see Figure 2.5). The spectrum of **2.14** displayed new signals at 2.42(s, Me), 7.35(d, *m*-Ar) and 8.13(d, *o*-Ar) ppm. It is of interest to note that the chemical shifts of the tolyl protons in **2.14** are very close to those observed for the related monoantimony compound $(p\text{-}MeC_6H_4)_3SbBr_2$ (**2.2**) [2.45(s, Me), 7.37(d, *m*-Ar) and 8.07(d, *o*-Ar) ppm]. This relationship adds support to the identification of the hydrolysis product as $(p\text{-}MeC_6H_4)_3Sb(OH)Br$, expected also to be a monomeric trigonal bipyramidal species, with the two most electronegative groups (*ie.* the bromine and hydroxy groups) in axial positions. **2.14** displayed ^{13}C resonances at 21.4, 130.1, 134.0 for the methyl, *meta* and *ortho* carbons respectively (no signals due to quaternary carbons were observed).

Figure 2.5 ^{1}H NMR spectrum of $[(p\text{-}MeC_6H_4)_3SbBr]_2O$ (**2.8**) and $(p\text{-}MeC_6H_4)_3Sb(OH)Br$ (**2.14**) in $CDCl_3$

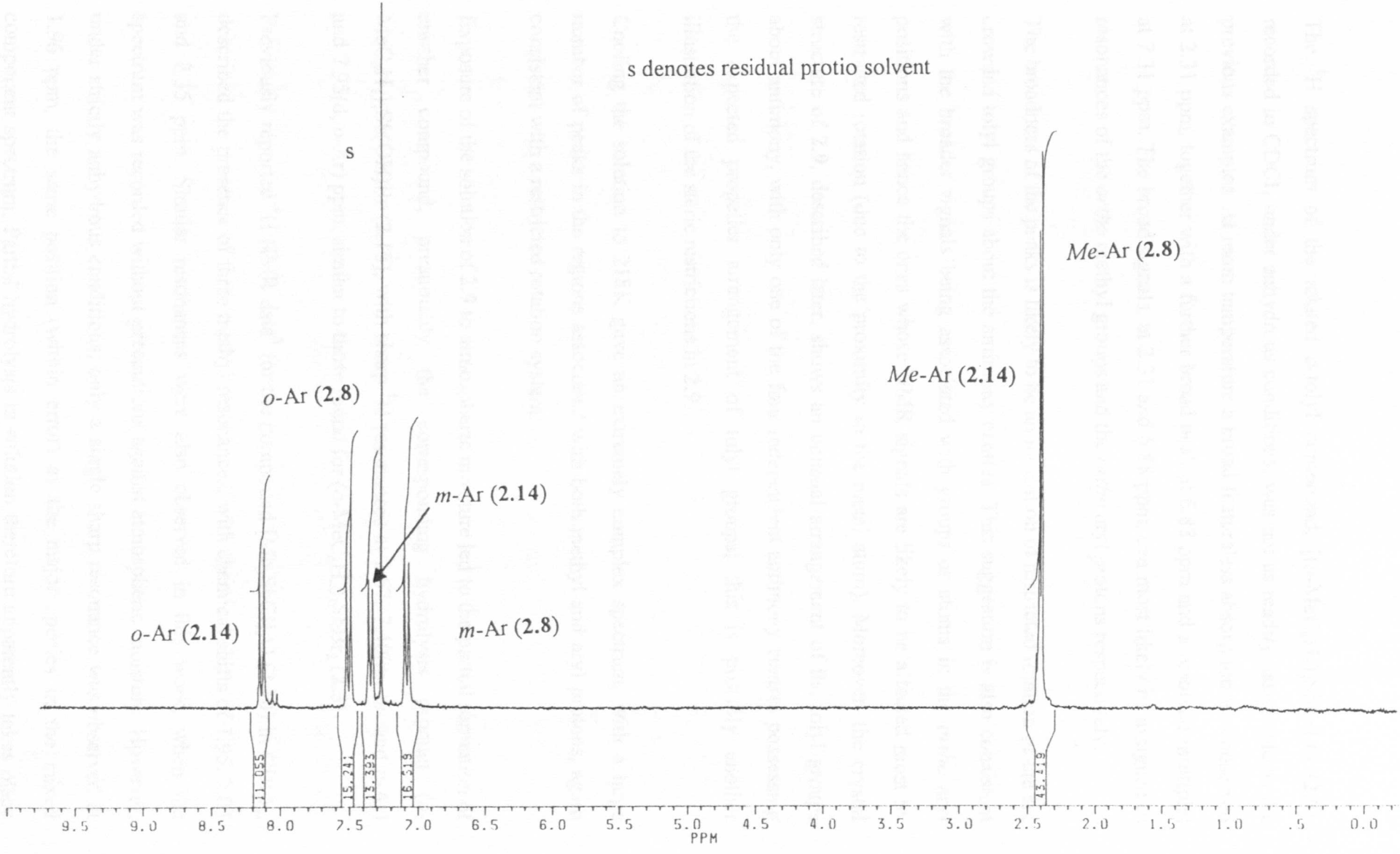

The ^{1}H spectrum of the related *o*-tolyl compound, $[(o\text{-}MeC_6H_4)_3SbBr]_2O$ (**2.9**), recorded in $CDCl_3$ under anhydrous conditions, was not as readily assignable as the previous examples. At room temperature a broad featureless absorption was observed at 2.31 ppm, together with a further broad peak at 6.88 ppm and a resolved multiplet at 7.31 ppm. The broad signals, at 2.31 and 6.88 ppm, can most likely be assigned to resonances of the *ortho* methyl groups and the *ortho* aryl protons respectively.

The broadness of the peaks is likely to be an indication of restricted rotation of the six crowded tolyl groups about the antimony centres. This suggestion is also consistent with the broader signals being associated with groups or atoms in the *ortho* aryl positions and hence the ones whose NMR signals are likely to be affected most by restricted rotation (due to the proximity to the metal atom). Moreover, the crystal structure of **2.9**, described later, shows an unusual arrangement of the tolyl groups about antimony, with only one of the four independent antimony centres possessing the expected propeller arrangement of tolyl groups; this is possibly another illustration of the steric restrictions in **2.9**.

Cooling the solution to 218K gave an extremely complex spectrum, with a large number of peaks in the regions associated with both methyl and aryl protons, again consistent with a restricted rotation system.

Exposure of the solution of **2.9** to atmospheric moisture led to the partial formation of another compound, presumably the corresponding hydrolysis product ($o\text{-}MeC_6H_4)_3Sb(OH)Br$ (**2.15**), with sharp ^{1}H resonances at 2.67, 7.40(m, *m*- and *p*-Ar) and 7.95(d, *o*-Ar) ppm, similar to those found for $(o\text{-}MeC_6H_4)_3SbBr_2$ (**2.3**).

Previously reported ^{1}H NMR data[8] for the compound $[Me_3SbCl]_2O$ (**2.10**) in $CDCl_3$, described the presence of three methyl resonances, with chemical shifts of 1.95, 2.03 and 2.35 ppm. Similar resonances were also observed in this work, when the spectrum was recorded without precautions against atmospheric moisture. However, under strictly anhydrous conditions, only a single sharp resonance was observed at 1.96 ppm, the same position (within error) as the major species in the mixed component spectrum. Partial hydrolysis in solution therefore apparently takes place

again, giving this time two different unidentified hydrolysis products. Similar to the situation with solutions of **2.7**, **2.8** and **2.9**, the starting material can be recovered quantitatively on crystallisation of the mixed component solution.

The solution NMR findings described in this section, further illustrates the ready equilibrium between $[R_3SbX]_2O$ and $R_3SbX(OH)$ compounds. In the solid state it is clear that the oxo-bridged form is preferred, except where R is large (as in **2.11**) and sterically prevents this configuration. However, in solution the parent oxo-bridged compounds readily react with traces of water to give the solution preferred configuration, $R_3SbX(OH)$.

2.2.3.2 NMR data for $(2,4,6\text{-}Me_3C_6H_2)_3Sb(OH)Br$ (2.11)

Unlike the previously mentioned compounds in this chapter, $(2,4,6\text{-}Me_3C_6H_2)_3Sb(OH)Br$ (**2.11**), is a stable hydroxohalide compound with no observed tendency to dehydrate and give an oxo bridged compound in the solid state. Moreover, in $CDCl_3$ solution the ^1H NMR spectrum of **2.11** showed the presence of only a single species, either under anhydrous conditions or without specific protection against moisture. Resonances were observed at 2.32 (*p*-Me), 2.52 (*o*-Me) and 7.01 (*m*-Ar) ppm.

The $^{13}C\{^1H\}$ spectrum showed resonances at 21.0 (*p*-Me), 24.6 (*o*-Me), 131.0 (*m*-Ar), 136.5 (*p*-Ar), 142.5 (*o*-Ar) and 142.8 (*ipso*-Ar) ppm. A comparison of chemical shifts for the compounds, $(2,4,6\text{-}Me_3C_6H_2)_3Sb$, $(2,4,6\text{-}Me_3C_6H_2)_3SbBr_2$ and $(2,4,6\text{-}Me_3C_6H_2)_3Sb(OH)Br$ is shown in Table 2.3. ^1H NMR spectra have been recorded previously[35] for $(2,4,6\text{-}Me_3C_6H_2)_3Sb$ and $(2,4,6\text{-}Me_3C_6H_2)_3SbBr_2$ with values in good agreement with those shown here.

Table 2.3 NMR shifts for mesityl compounds

Compound	^{1}H, ppm	$^{13}C\{^{1}H\}$, ppm
$(mesityl)_3Sb$	2.30, 2.32, 6.86	
$(mesityl)_3SbBr_2$ (**2.6**)	2.33, 2.71, 6.99	20.7, 26.0, 131.0, 140.7, 142.0, 145.6
$(mesityl)_3Sb(OH)Br$ (**2.11**)	2.32, 2.52, 7.01	21.0, 24.6, 131.0, 136.5, 142.5, 142.8

As expected, a pronounced downfield shift in the *ortho*-methyl resonance, due to a decrease in shielding, was observed on oxidation of the antimony(III) compound to the antimony(V) compounds and therefore increasing the Lewis acidity of the metal centre. Interestingly, the ^{1}H mesityl resonances observed in **2.11** are very similar to those reported by Huber and co-workers[15] for the $(2,4,6\text{-}Me_3C_6H_2)_3Sb(OH)(O_2CR)$ group of compounds.

From the spectroscopic data obtained, it is impossible to assess unambiguously whether **2.11** is an ionic species, similar to that of $[(2,6\text{-}Me_2C_6H_3)_3Sb(OH)]^{+}I^{-}$, or a simple covalent species like the related carboxylate derivatives $(2,4,6\text{-}Me_3C_6H_2)_3Sb(OH)(O_2CR)$. However, the presence of a degree of hydrogen bonding observed in the solid-state IR spectrum, tends to suggest an ionic structure for the solid.

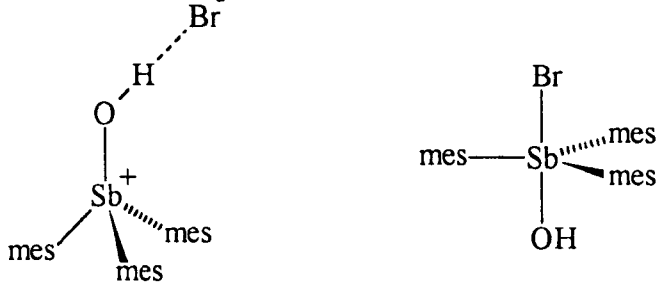

Ionic Covalent

where mes = $2,4,6\text{-}Me_3C_6H_2$

Figure 2.6 Possible molecular configurations for $(2,4,6\text{-}Me_3C_6H_2)_3Sb(OH)Br$ (2.11)

2.2.4 Mass Spectroscopy

The FAB mass spectrum of $[Ph_3SbBr]_2O$ (**2.7**) showed no sign of the parent ion but a significant ion envelope at m/z 799 can be assigned to loss of one bromine from the parent molecule. No other major diantimony species were found, but two primary monoantimony fragmentation products, $\{Ph_3SbBr\}^+$ and $\{Ph_2Sb\}^+$ were observed.

FAB spectra of both $[(p\text{-}MeC_6H_4)_3SbBr]_2O$ (**2.8**) and $[(o\text{-}MeC_6H_4)_3SbBr]_2O$ (**2.9**) were similar, with the highest mass ion, in each case, attributed to the loss of a bromine from the parent molecule. Major fragments in both spectra were monoantimony species, such as $\{tolyl_3SbBr\}^+$ and $\{tolyl_2Sb\}^+$.

Likewise, no parent ion was found in the FAB mass spectrum of $(2,4,6\text{-}Me_3C_6H_2)_3Sb(OH)Br$ (**2.11**), but several assignable ions were observed. Major fragmentation occurred by loss of bromine rather than loss of the hydroxy group from the parent molecule, as shown by the relative abundancies of the $\{(2,4,6\text{-}Me_3C_6H_2)_3Sb(OH)\}^+$ and $\{(2,4,6\text{-}Me_3C_6H_2)_3SbBr\}^+$ ions. Further fragmentation resulted from subsequent loss of complete mesityl and hydroxy groups. Important fragments are listed in Table 2.4.

Table 2.4 Important fragments in the FAB mass spectrum of 2.11

Fragment Ion	Mass m/z	Peak Height %
$\{(mesityl)_3SbBr\}^+$	557	3
$\{(mesityl)_3SbOH\}^+$	495	65
$\{(mesityl)_3Sb\}^+$	478	4
$\{(mesityl)_2SbOH\}^+$	376	3
$\{(mesityl)_2Sb\}^+$	359	8
$\{(mesityl)SbOH\}^+$	257	7
$\{(mesityl)Sb\}^+$	240	10
$\{mesityl\}^+$	119	38

2.2.5 X-Ray Crystallography

Single crystal X-ray structure determinations were carried out for both [(*p*-$MeC_6H_4)_3SbBr]_2O$ (**2.8**) and [(*o*-$MeC_6H_4)_3SbBr]_2O$ (**2.9**), obtained as a hemi-hexane solvate, on crystals obtained by slow diffusion of hexane vapour into concentrated chloroform solutions of the compounds. Crystals of (2,4,6-$Me_3C_6H_2)_3Sb(OH)Br$ (**2.11**) proved unsuitable for a structure determination.

The molecular structure of **2.8** is shown in Figure 2.7 and selected bond lengths and angles are listed in Table 2.5. Further details of the crystal structure determination are given in Appendix A.

Table 2.5 Selected bond distances and angles, with standard deviations in parentheses for [(*p*-$MeC_6H_4)_3SbBr]_2O$ (2.8)

Bond lengths, Å		Bond angles, °	
Sb(1) - Br(1)	2.7203(7)	Sb(1) - O(1) - Sb(1a)	180.0
Sb(1) - O(1)	1.9535(4)	O(1) - Sb(1) - Br(1)	180.0
Sb(1) - C(1)	2.117(3)	O(1) - Sb(1) - C(1)	90.55(7)
		C(1) - Sb(1) - C(1a)	119.99(1)
		C(1) - Sb(1) - Br(1)	89.45(8)

The structure of **2.8** is highly symmetrical with crystallographic $\bar{3}$ symmetry imposing linear Br–Sb–O and Sb–O–Sb angles. Moreover, unlike the known structures of $[Me_3SbCl]_2O$ and related compounds[18], which also have crystallographically imposed $\bar{3}$ symmetry but possess disorder problems that indicate non-linear bond angles, **2.8** illustrates genuine molecular $\bar{3}$ symmetry, with no disorder about atoms on the 3-fold axis. This level of crystallographic symmetry has not been previously noted for related compounds. For example in the structure of $[Ph_3SbBr]_2O$ (**2.7**), the angle about the bridging oxygen is close to 180° (170.2 and 176.6° for the two independent molecules) but there is no (crystallographic) molecular symmetry.

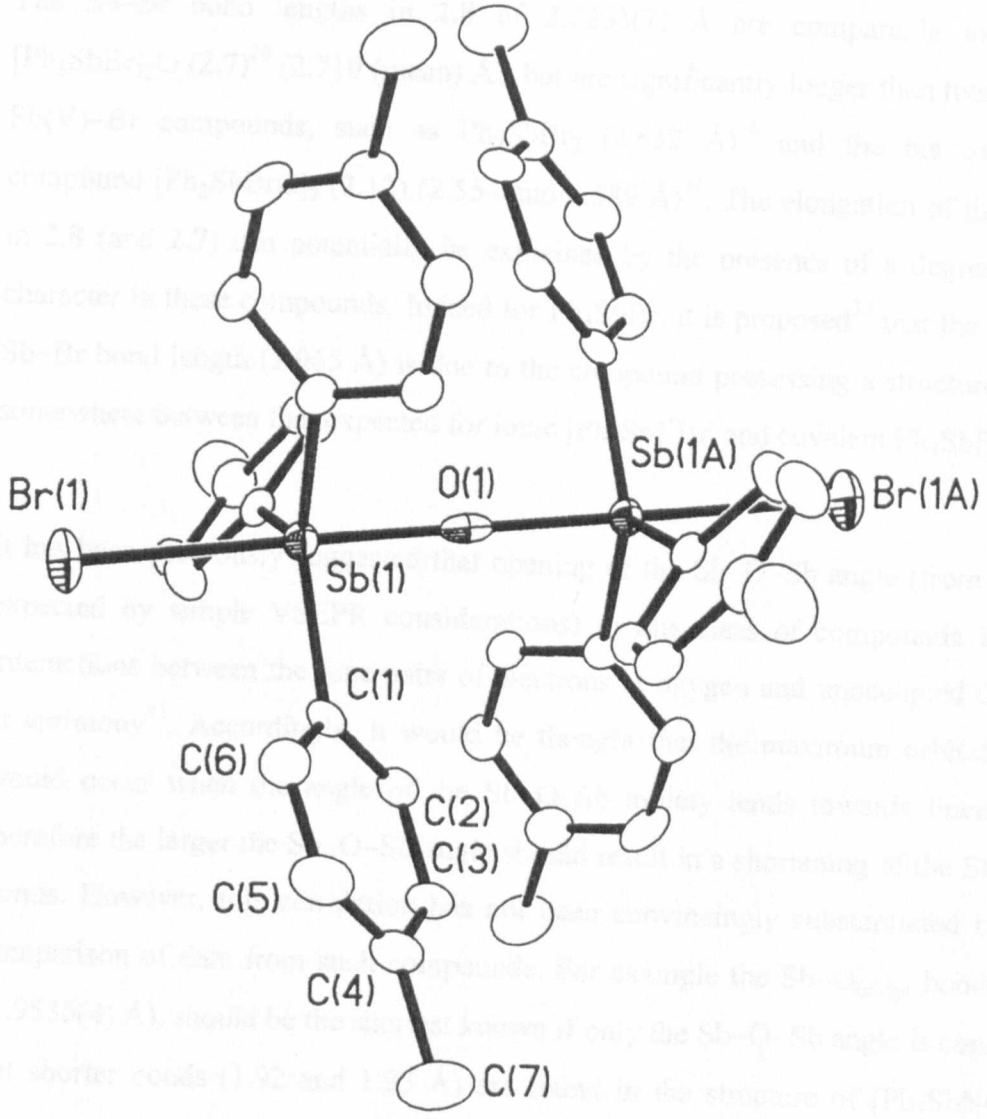

Figure 2.7 Molecular structure of $[(p\text{-}MeC_6H_4)_3SbBr]_2O$ (2.8)

Coordination about antimony in **2.8** is only very slightly distorted from true trigonal bipyramidal geometry, with each antimony bound to three *p*-tolyl *ipso* carbon atoms equatorially and with one bromine and the bridging oxygen in axial sites. The very slight distortions are due to the *ipso* carbons being bent slightly towards the bromine atoms (the C(1)–Sb(1)–Br(1) angle is 89.45(8)°).

The Sb–Br bond lengths in **2.8** of 2.7203(7) Å are comparable to those in $[Ph_3SbBr]_2O$ (**2.7**)[20] (2.710 (mean) Å), but are significantly longer than those in other Sb(V)–Br compounds, such as Ph_3SbBr_2 (2.632 Å)[36] and the bis oxo-bridged compound $[Ph_2SbBrO]_2$ (**2.12**) (2.554 and 2.589 Å)[31]. The elongation of these bonds in **2.8** (and **2.7**) can potentially be explained by the presence of a degree of ionic character in these compounds. Indeed for Ph_4SbBr, it is proposed[37] that the very long Sb–Br bond length (2.965 Å) is due to the compound possessing a structure that lies somewhere between that expected for ionic $[Ph_4Sb]^+Br^-$ and covalent Ph_4SbBr.

It has been previously suggested that opening of the Sb–O–Sb angle (from the 109° expected by simple VSEPR considerations) in this class of compounds is due to interactions between the lone pairs of electrons at oxygen and unoccupied d-orbitals at antimony[21]. Accordingly, it would be thought that the maximum orbital overlap would occur when the angle of the Sb–O–Sb moiety tends towards linearity and therefore the larger the Sb–O–Sb angle should result in a shortening of the $Sb–O_{bridge}$ bonds. However, this correlation has not been convincingly substantiated by a full comparison of data from such compounds. For example the $Sb–O_{bridge}$ bonds in **2.8** (1.9535(4) Å), should be the shortest known if only the Sb–O–Sb angle is considered, yet shorter bonds (1.92 and 1.95 Å) are found in the structure of $[Ph_3SbNO_3]_2O$[30] amongst others, which has an Sb–O–Sb angle of only 141.6°. Clearly, other factors are also significant in determining the relationship between the $Sb–O_{bridge}$ bond length and the corresponding Sb–O–Sb angle, if indeed there is a simple relationship. However, it is clear that the $Sb–O_{bridge}$ bond lengths are short in these compounds, when compared with terminal Sb–O bonds (such as those found in $(2,4,6\text{-}Me_3C_6H_2)_3Sb(OH)_2$ (2.027 Å)[17]) and this indicates that there are additional bonding

interactions, most likely to be due to a degree of delocalisation of π-electrons in the Sb–O–Sb moiety.

The molecular structure of **2.9** is shown in Figures 2.8 and 2.9 and selected bond lengths and angles are listed in Table 2.6. Further details of the crystal structure determination are given in Appendix B.

Table 2.6 Selected bond distances and angles, with standard deviations in parentheses for $[(o\text{-}MeC_6H_4)_3SbBr]_2O.\ 0.5C_6H_{14}$ (2.9)

Bond lengths, Å		Bond angles, °	
Sb(1) - Br(1)	2.750(2)	Sb(1) - O(1) - Sb(2)	161.0(2)
Sb(1) - O(1)	1.964(4)	Sb(3) - O(2) - Sb(4)	171.5(2)
Sb(1) - C(11)	2.113(5)	O(1) - Sb(1) - Br(1)	179.2(1)
Sb(1) - C(21)	2.139(4)	O(1) - Sb(1) - C(11)	95.1(2)
Sb(1) - C(31)	2.111(4)	O(1) - Sb(1) - C(21)	90.4(1)
Sb(2) - Br(2)	2.731(2)	O(1) - Sb(1) - C(31)	93.1(2)
Sb(2) - O(1)	1.962(4)	Br(1) - Sb(1) - C(11)	85.3(1)
Sb(2) - C(41)	2.112(4)	Br(1) - Sb(1) - C(21)	90.1(1)
Sb(2) - C(51)	2.125(5)	Br(1) - Sb(1) - C(31)	86.1(1)
Sb(2) - C(61)	2.133(4)	C(11) - Sb(1) - C(21)	120.9(2)
Sb(3) - Br(3)	2.739(2)	C(11) - Sb(1) - C(31)	116.9(1)
Sb(3) - O(2)	1.947(4)	C(21) - Sb(1) - C(31)	121.6(2)
Sb(3) - C(71)	2.110(4)	O(1) - Sb(2) - Br(2)	177.5(1)
Sb(3) - C(81)	2.162(3)	O(1) - Sb(2) - C(41)	90.9(2)
Sb(3) - C(91)	2.141(5)	O(1) - Sb(2) - C(51)	92.3(2)
Sb(4) - Br(4)	2.762(2)	O(1) - Sb(2) - C(61)	94.2(2)
Sb(4) - O(2)	1.964(4)	Br(2) - Sb(2) - C(41)	88.7(1)
Sb(4) - C(101)	2.109(3)	Br(2) - Sb(2) - C(51)	85.9(1)
Sb(2) - C(111)	2.121(5)	Br(2) - Sb(2) - C(61)	88.1(1)
Sb(2) - C(121)	2.149(5)	C(41) - Sb(2) - C(51)	124.8(1)
		C(41) - Sb(2) - C(61)	123.8(2)
		C(51) - Sb(2) - C(61)	110.9(2)
		O(2) - Sb(3) - Br(3)	176.6(1)
		O(2) - Sb(3) - C(71)	91.4(2)
		O(2) - Sb(3) - C(81)	88.6(2)
		O(2) - Sb(3) - C(91)	91.4(2)
		Br(3) - Sb(3) - C(71)	91.0(1)
		Br(3) - Sb(3) - C(81)	88.1(1)
		Br(3) - Sb(3) - C(91)	89.7(1)
		C(71) - Sb(3) - C(81)	117.4(2)

C(71) - Sb(3) - C(91)	117.3(2)
C(91) - Sb(3) - C(81)	125.3(2)
O(2) - Sb(4) - Br(4)	177.7(1)
O(2) - Sb(4) - C(101)	92.8(2)
O(2) - Sb(4) - C(111)	90.6(2)
O(2) - Sb(4) - C(121)	92.4(2)
Br(4) - Sb(4) - C(101)	85.9(1)
Br(4) - Sb(4) - C(111)	91.7(1)
Br(4) - Sb(4) - C(121)	86.6(1)
C(101) - Sb(4) - C(111)	120.9(2)
C(101) - Sb(4) - C(121)	116.9(1)
C(111) - Sb(4) - C(121)	124.0(2)

The dinuclear compound **2.9** consists of two (*o*-tolyl)$_3$SbBr units linked by a bridging oxygen atom. There are two independent molecules present in the asymmetric unit, [molecule A (Sb(1) and Sb(2)) and molecule B (Sb(3) and Sb(4))] possessing slight structural differences. The antimony atoms in both molecules exist in slightly distorted trigonal bipyramidal environments, with in each case the equatorial planes defined by the tolyl groups. The associated Sb–C bond lengths are in the range 2.109(3) (Sb(4)–C(101)) to 2.162(3) (Sb(3)–C(81)) and are comparable to those in related compounds.

Variations exist in the Sb–Br bond lengths, although these are moderate and all bond lengths are between 2.731(2) and 2.762(2) Å. These are slightly longer than those in both $[Ph_3SbBr]_2O$ (**2.7**)[20] and $[(p\text{-}MeC_6H_4)_3SbBr]_2O$ (**2.8**) and suggest a greater degree of ionic character in **2.9**. The moderate disparity of the Sb–Br bond distances is however not reflected in the associated Sb–O_{bridge} bonds. Furthermore, there appears to be little clear relationship between the length of the Sb–O_{bridge} bonds and the associated Sb–X bonds for $[R_3SbX]_2O$ systems in general. For example, in $[Ph_3SbO_3SCF_3)_2O$ the shorter Sb–O_{bridge} bond (1.94 Å) is *trans* to the longer Sb–X bond (Sb–O: 2.37 Å)[38], whereas in the structure of $[Ph_3SbOC(CN)=C(CN)_2]_2O$, the shorter Sb–$O_{bridge}$ bond of 1.943 Å is *trans* to the shorter Sb–X bond (Sb–O: 2.302 Å)[39].

Figure 2.8 Molecular structure of $[(o\text{-}MeC_6H_4)_3SbBr]_2O$ (2.9) - Molecule A

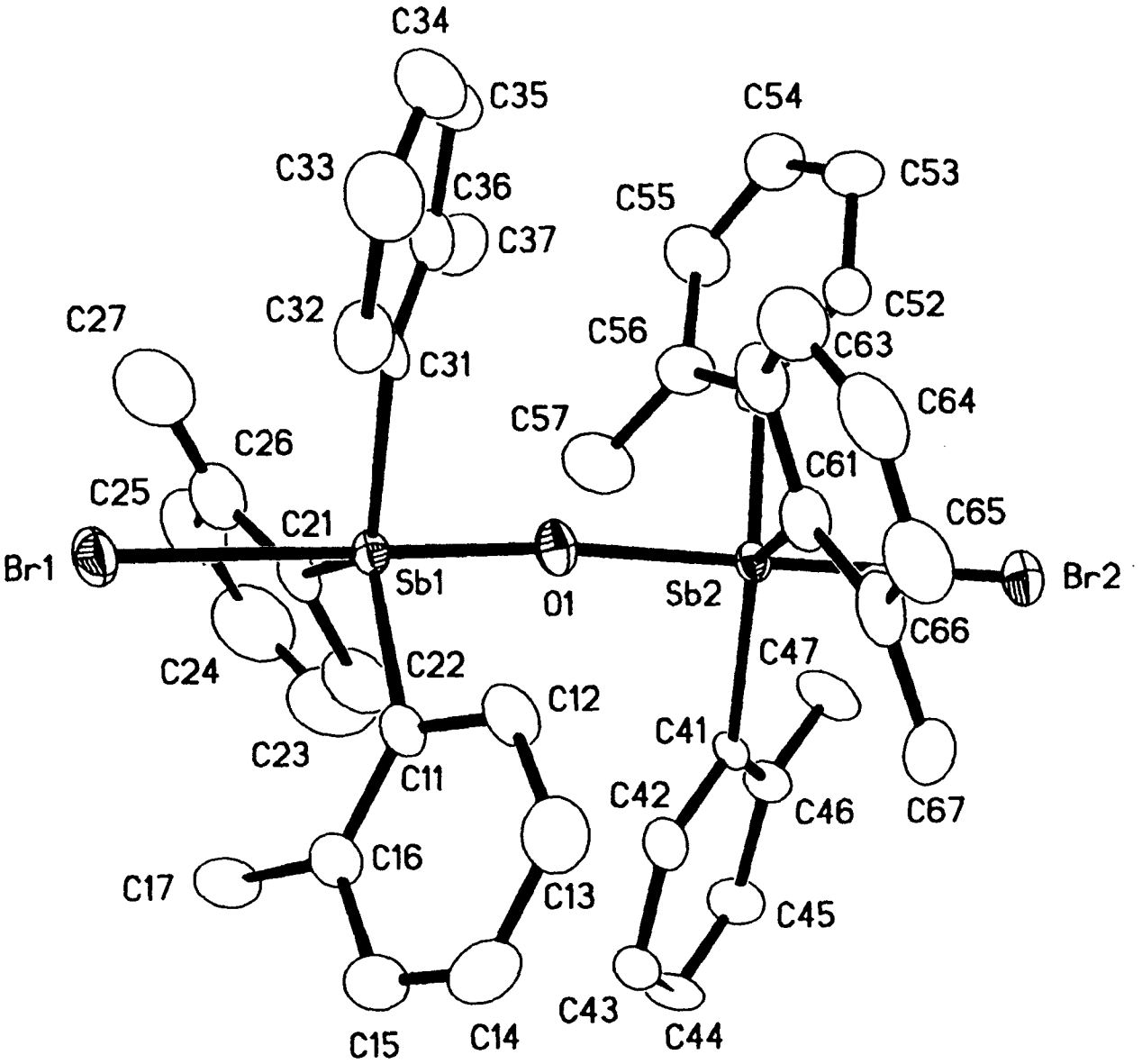

Figure 2.9 Molecular structure of $[(o\text{-}MeC_6H_4)_3SbBr]_2O$ (2.9) - Molecule B

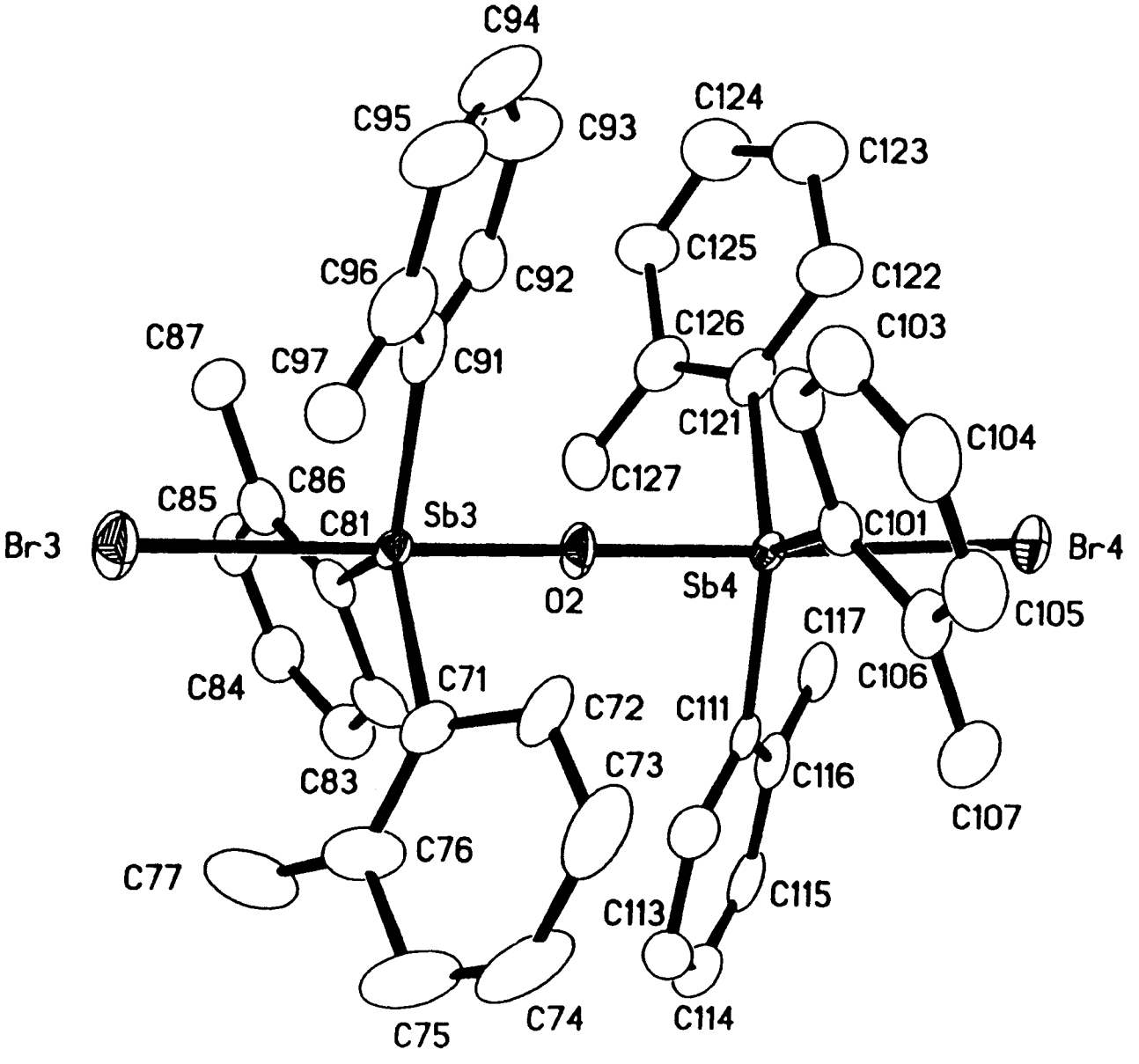

A notable difference between the two independent molecules in **2.9** is the angle about the bridging oxygens at 161.0(2)° for molecule A and 171.5(2)° for molecule B. The reason for this significant difference is not obviously clear and like previous examples is not convincingly related to differences in Sb–O_{bridge} bond lengths.

The two independent molecules also differ in the arrangement of tolyl groups about the antimony centres and this is clearly observed in the views along the Sb–Sb vectors (Figure 2.10). The groups about both Sb(1) and Sb(2) in molecule A are in a non-propeller configuration, with in each case two groups facing one direction (anticlockwise as shown in Figure 2.10) and the third facing in the opposite direction (clockwise).

In molecule B, the situation if further complicated by a non-propeller configuration of the tolyl groups about Sb(4), but a contrasting propeller configuration about Sb(3) (all groups facing in an anticlockwise direction in Figure 2.10). This unusual structural type is also illustrated by examining deviations of the tolyl methyl groups from the best-fit plane through the three *ipso* carbons about each antimony centre, listed in Table 2.7

Table 2.7 Deviations of atoms from best-fit plane of *ipso* carbons

C(11)-(31), Å		C(41)-(61), Å		C(71)-(91), Å		C(101)-(121), Å	
Sb(1)	-0.104	Sb(2)	-0.089	Sb(3)	+0.016	Sb(4)	-0.070
Br(1)	+2.642	Br(2)	+2.646	Br(3)	-2.722	Br(4)	+2.686
O(1)	-2.066	O(1)	-2.049	O(2)	+1.962	O(2)	-2.033
C(17)	+1.271	C(47)	+1.360	C(77)	-1.360	C(107)	+1.173
C(27)	+1.385	C(57)	-1.341	C(87)	-1.128	C(117)	+1.384
C(37)	-1.316	C(67)	+1.223	C(97)	-1.331	C(127)	-1.258

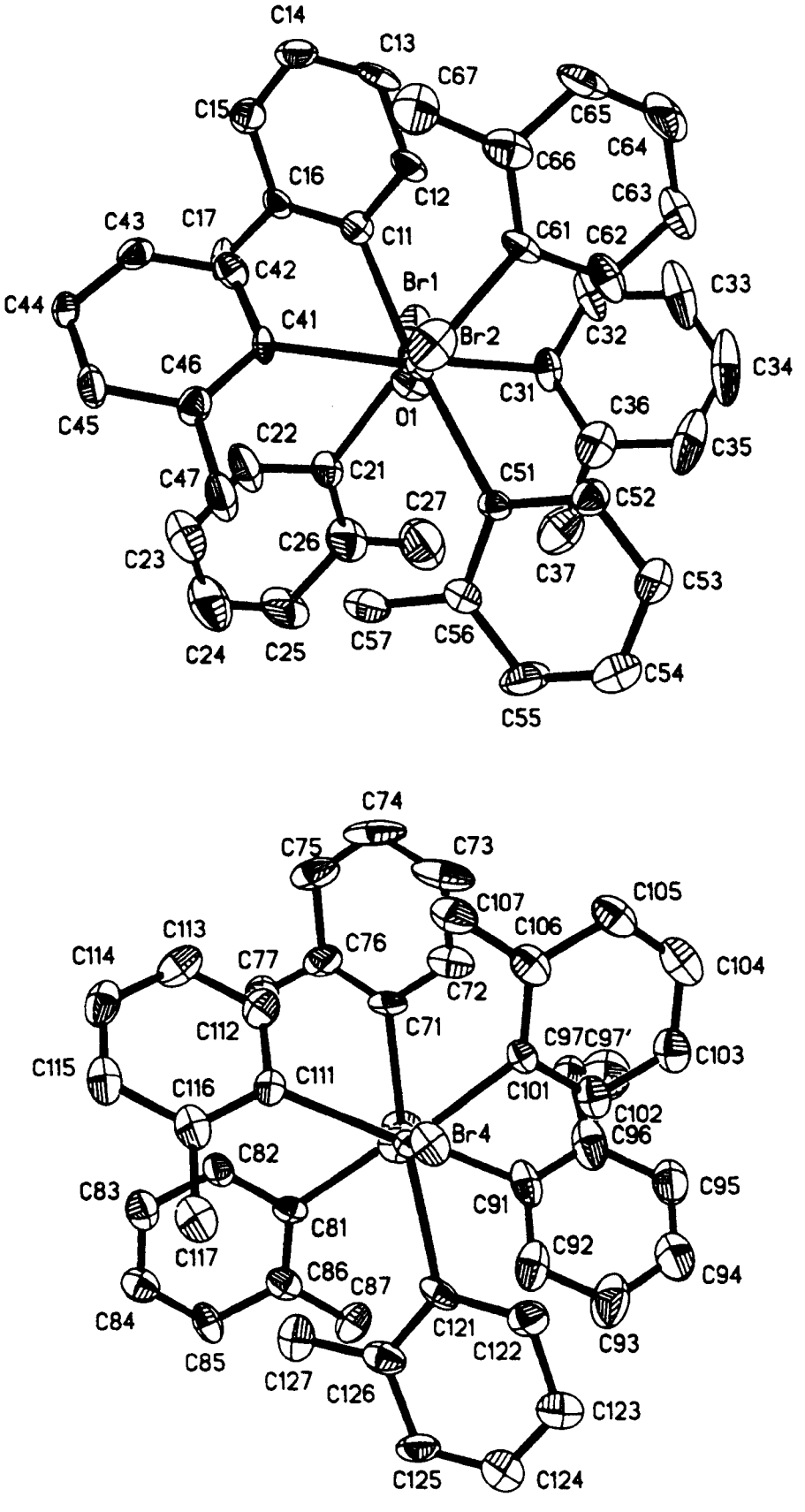

Figure 2.10 Views along Sb-Sb vectors in 2.9, Molecules A and B

Thus, only in the groups on Sb(3) do all the methyl groups lie on the same side of the best-fit plane. A further proof of the unusual configurations is demonstrated by the O_{bridge}–Sb–C_{ipso}–C_{ortho} torsion angles, with only the angles connected with Sb(3) all positive (55.0, 63.2 and 50.6° for the O(2)–Sb(3)–C(71)–C(72), O(2)–Sb(3)–C(81)–C(82) and O(2)–Sb(3)–C(91)–C(92) angles respectively).

It seems most probable that the unusual configuration of tolyl groups is a consequence of steric crowding within the molecule. Indeed, a space-filling model of molecule A is shown in Figure 2.11 and clearly demonstrates the close contacts between the six tolyl groups, especially with respect to the *ortho* methyl groups.

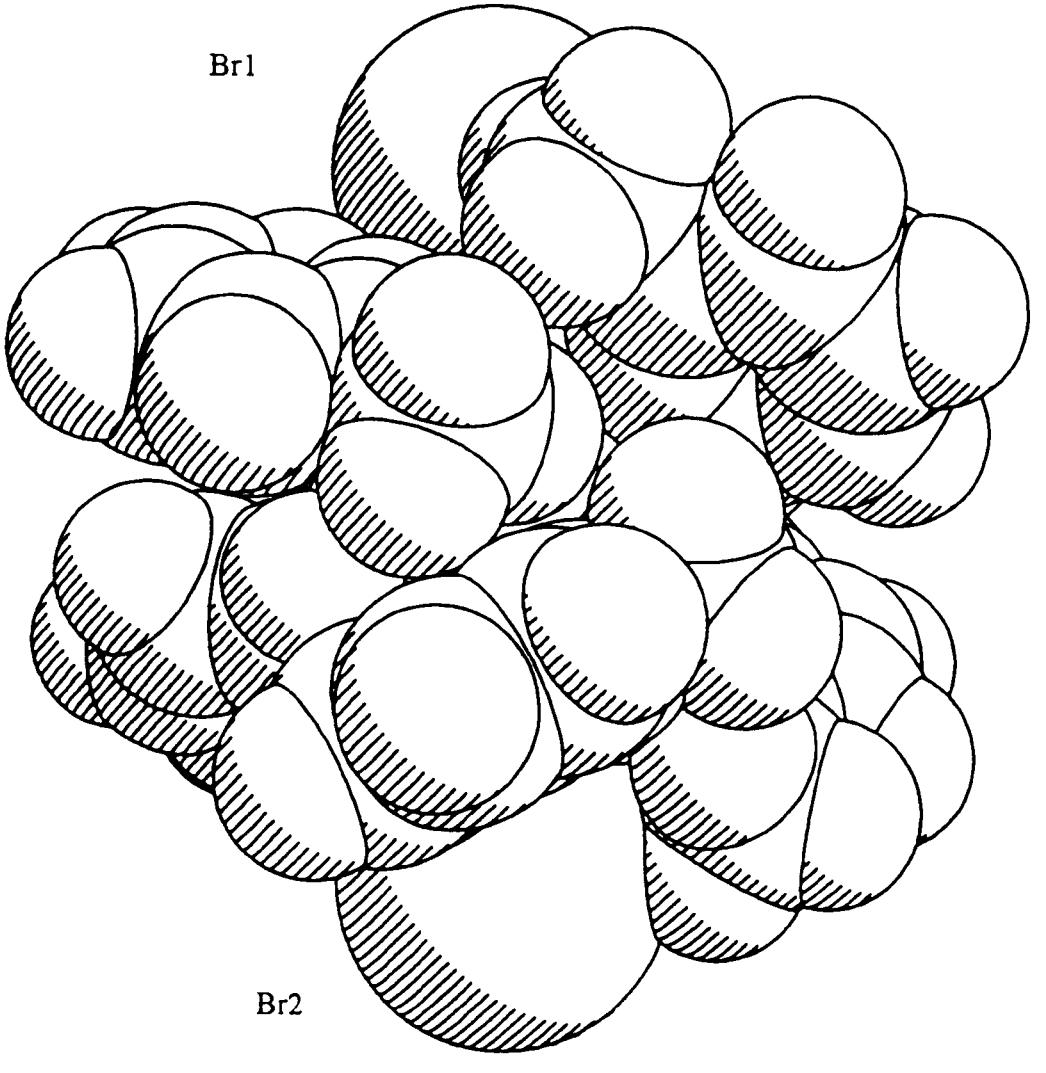

Figure 2.11 Space-filling model of 2.9 (molecule A)

SUMMARY

The oxo-bridged compounds $[Ph_3SbBr]_2O$ (**2.7**), $[(p\text{-}MeC_6H_4)_3SbBr]_2O$ (**2.8**), $[(o\text{-}MeC_6H_4)_3SbBr]_2O$ (**2.9**) were readily formed by the partial hydrolysis of the relevant triarylantimony dibromide compounds. The compounds are susceptible to hydrolysis in solution, affording monomeric hydroxohalide compounds, but quantitatively reform to the oxo-bridged parent compound on crystallisation. Solution hydrolysis was also noted with the compound $[Me_3SbCl]_2O$ (**2.10**).

In contrast, a hydrolysis reaction between $(2,4,6\text{-}Me_3C_6H_2)_3SbBr_2$ and NaOH, led to formation of a simple hydroxohalide species, $(2,4,6\text{-}Me_3C_6H_2)_3Sb(OH)Br$ (**2.11**).

The compound $[Ph_2SbBrO]_2$ (**2.12**) was also prepared for use in work described in later chapters.

2.3 EXPERIMENTAL AND CHARACTERISING DATA

2.3.1 Preparation of Triarylantimony Compounds

2.3.1.1 Preparation of $(p\text{-}MeC_6H_4)_3Sb$

A stirred suspension of lithium metal chunks (800mg, 110mmol) and diethyl ether (50ml) was cooled to 0°C under an argon atmosphere and a solution of 4-bromotoluene (8.34g, 49mmol) in diethyl ether (50ml) was added over a period of 15 minutes. The reaction mixture was then warmed to room temperature and stirred for a further 24 hours. The 4-lithiotoluene solution thus formed was then isolated from excess lithium by cannula filtration and added to a stirred solution of antimony trichloride (3.65g, 16mmol) in diethyl ether (35ml) at 0°C, also under argon. After stirring for a further 16 hours at room temperature the reaction mixture was filtered on to crushed ice. The layers were separated and the aqueous layer washed three times with diethyl ether (50ml portions). The diethyl ether fractions were combined, dried over anhydrous $MgSO_4$ and the solvent removed *in vacuo* to give a white powder. Recrystallisation from ethanol gave the title compound as colourless crystals. Yield 4.32g (68%); mp 126-130°C [Lit. 122 to 127°C[40,41]].

Found: C,63.79; H,5.49: $C_{21}H_{21}Sb$ requires C,63.83; H,5.36 %.

^{1}H NMR (250MHz, $CDCl_3$, RT) δ 2.33(s, 9H, *Me*-Ar); 7.18(d, 6H, $^3J_{HH}$ - 8Hz, *m*-Ar); 7.39(d, 6H, $^3J_{HH}$ - 8Hz, *o*-Ar).

IR (nujol mull, CsI): 1306(m), 1262(w), 1210(m), 1186(m), 1113(m), 1060(m), 1013(m), 849(w), 801(s), 572(m), 484(s).

MS (EI): $\{(p\text{-}MeC_6H_4)_3Sb\}^+$ (m/z 394, 18%); $\{(p\text{-}MeC_6H_4)_2Sb\}^+$ (m/z 303, 17%); $\{(p\text{-}MeC_6H_4)Sb\}^+$ (m/z 212, 100%); $\{(p\text{-}MeC_6H_4)_2\}^+$ (m/z 182, 83%); $\{MeC_6H_4\}^+$ (m/z 91, 96%).

2.3.1.2 Preparation of $(o\text{-}MeC_6H_4)_3Sb$

An analogous preparative method as described in 2.3.1.1 was employed, using lithium pieces (0.82g, 118mmol), 2-bromotoluene (9.24g, 54mmol) and antimony trichloride (4.10g, 18mmol). Colourless crystals of the title compound were obtained on recrystallisation from ethanol. Yield 4.55g (64%); mp 93-94°C [Lit. 96°C[42]].

Found: C,63.80; H,5.52: $C_{21}H_{21}Sb$ requires C,63.83; H,5.36 %.

^{1}H NMR (250MHz, $CDCl_3$, RT) δ 2.51(s, 9H, *Me*-Ar); 7.04(m, 6H, m_1- and *p*-Ar); 7.29(m, 6H, *o*- and m_2-Ar).

IR (nujol mull, CsI): 1266(m), 1200(m), 1157(w), 1116(m), 1033(w), 794(w), 745(vs), 539(w), 436(s), 407(m).

MS (EI): $\{(o\text{-}MeC_6H_4)_3Sb\}^+$ (m/z 394, 27%); $\{(o\text{-}MeC_6H_4)_2Sb\}^+$ (m/z 303, 16%); $\{(o\text{-}MeC_6H_4)Sb\}^+$ (m/z 212, 18%); $\{(o\text{-}MeC_6H_4)_2 - H\}^+$ (m/z 181, 62%); $\{MeC_6H_4\}^+$ (m/z 91, 100%).

2.3.1.2 $(2,4,6\text{-}Me_3C_6H_2)_3Sb$

A sample of trimesitylantimony, prepared similarly, was obtained from Dr G.E. Forster[43]; subsequent analysis showed a sufficient purity of the compound to be used for further reactions.

Found: C,65.90; H,6.12: $C_{27}H_{33}Sb$ requires C,67.66; H,6.94 %.

^{1}H NMR (250MHz, $CDCl_3$, RT) δ 2.30(s, 9H, *p*-Me); 2.32(s, 18H, *o*-Me); 6.86(s, 6H, *m*-Ar).

2.3.2 Preparation of Triarylantimony Dibromides

2.3.2.1 Preparation of Ph_3SbBr_2 (2.1)

A solution of bromine (19.54g, 0.122mol) in dichloromethane (50 ml) was added dropwise to a stirred solution of triphenylantimony (41.70g, 0.118mol) in dichloromethane (50ml) at 0°C. The resulting reaction mixture was then stirred for 3 hours at room temperature. Crude product was obtained by removal of solvent *in vacuo* and recrystallisation from chloroform, overlayered with hexane, gave the title compound as large colourless crystals. Yield 53.26g (88%); mp 216-218°C [Lit. 215-218°C[2,44]].

Found: C,42.06; H,2.90: $C_{18}H_{15}Br_2Sb$ requires C,42.15; H,2.95 %.

2.3.2.2 Preparation of $(p\text{-}MeC_6H_4)_3SbBr_2$ (2.2)

In a analogous reaction to 2.3.2.1, tri(p-tolyl)antimony (2.99g, 7.6mmol) and bromine (1.21g, 7.6mmol) were reacted in dichloromethane (30ml). Recrystallisation from chloroform/hexane gave the pure product. Yield 3.82g (91%); mp 235-239°C [Lit. 232-233°C[45,46]].

Found: C,45.42; H,3.82: $C_{21}H_{21}Br_2Sb$ requires C,45.45; H,3.81 %.

^{1}H NMR (250MHz, $CDCl_3$, RT) δ 2.45(s, 9H, *Me*-Ar); 7.37(d, 6H, $^3J_{HH}$ - 8Hz, *m*-Ar); 8.07(m, 6H, $^3J_{HH}$ - 8Hz, *o*-Ar).

IR (nujol mull, CsI): 1306(m), 1186(m), 1062(w), 1008(w), 794(vs), 582(w), 482(vs).

2.3.2.3 Preparation of $(o\text{-}MeC_6H_4)_3SbBr_2$ (2.3)

In a similar manner to 2.3.2.1, tri(o-tolyl)antimony (1.79g, 4.5mmol) and bromine (0.72g, 4.5mmol) were reacted in dichloromethane (30ml) at 0°C. Recrystallisation from chloroform/hexane gave colourless crystals of the title compound. Yield 2.15g (86%); mp 212-214°C [Lit. 209-210°C[47]].

Found: C,45.43; H,3.81: $C_{21}H_{21}Br_2Sb$ requires C,45.45; H,3.81 %.

^{1}H NMR (250MHz, $CDCl_3$, RT) δ 2.73(s, 9H, *Me*-Ar); 7.42(m, 9H, *m*- and *p*-Ar); 7.98(d, 3H, $^3J_{HH}$ - 8Hz, *o*-Ar).

IR (nujol mull, CsI): 1278(s), 1203(s), 1162(w), 1118(w), 1019(m), 866(w), 797(vs), 747(vs), 698(w), 647(w), 538(w), 487(w), 435(vs).

2.3.2.4 Preparation of $(2,4,6\text{-}Me_3C_6H_2)_3SbBr_2$ (2.6)

Bromine (270mg, 1.7mmol) was syringed into a stirred solution of trimesitylantimony (804mg, 1.7mmol) in dichloromethane (20ml) at 0 °C. The reaction mixture was then stirred for 4 hours at room temperature. Removal of volatiles afforded crude product which was recrystallised from chloroform/hexane. Yield 910mg (84%); mp 204-205°C [Lit. 202°C[35]].

Found: C,49.46; H,4.86: $C_{27}H_{33}Br_2Sb$ requires C,50.74; H,5.20 %.

^{1}H NMR (250MHz, $CDCl_3$, RT) δ 2.33(s, 9H, *p*-Me); 2.71(s, 18H, *o*-Me); 6.99(s, 6H, *m*-Ar).

$^{13}C\{^1H\}$ NMR (69 MHz, $CDCl_3$, RT) δ 20.7(*p*-Me); 26.0(*o*-Me); 131.0(*m*-Ar); 140.7(*p*-Ar); 142.0(*o*-Ar); 145.6(*ipso*-Ar).

2.3.3 Preparation of Partial Hydrolysis Products

2.3.3.1 Preparation of $[Ph_3SbBr]_2O$ (2.7)

Sodium hydroxide (0.29g, 7.25mmol) in the minimum of water was added to a stirred suspension of Ph_3SbBr_2 (**2.1**) (3.50g, 6.8mmol) and methanol (150ml) and the resulting mixture was refluxed for 18 hours. The solution was then allowed to cool to room temperature before water (100ml) was added. The precipitate formed, was collected by filtration, dried *in vacuo* and recrystallised from ethanol. Yield 2.43g (81%); mp 247-250°C [Lit. 248-250°C[48]].

Found: C,49.07; H,3.37: $C_{36}H_{30}Br_2OSb_2$ requires C,49.03; H,3.43 %.

^{1}H NMR (250MHz, $CDCl_3$, RT) δ 7.29(t, 12H, $^3J_{HH}$ - 7.5Hz, *m*-Ph-**A**); 7.44(t, 6H, $^3J_{HH}$ - 7.5Hz, *p*-Ph-**A**); 7.57(m, 9H, *m*- and *p*-Ph-**B**); 7.60(d, 12H, $^3J_{HH}$ - 7.5Hz, *o*-Ph-**A**); 8.26(m, 6H, *o*-Ph-**B**), where **A** is $[Ph_3SbBr]_2O$ and **B** is $Ph_3Sb(OH)Br$. Under strictly anhydrous conditions only signals due to **A** were observed.

$^{13}C\{^1H\}$ NMR (69 MHz, $CDCl_3$, RT) δ 129.1(*m*-Ph-**A**); 129.5(*m*-Ph-**B**); 130.8(*p*-Ph-**A**); 131.8(*p*-Ph-**B**); 133.3(*o*-Ph-**A**); 134.1(*o*-Ph-**B**); 141.9(*ipso*-Ph-**A**). Under strictly anhydrous conditions only signals due to **A** were observed.

IR (nujol mull, CsI): 1434(s), 1330(w), 1304(w), 1181(w), 1158(w), 1063(m), 1019(m), 996(m), 774(vs), 766(vs), 689(s), 457(s), 448(s).

MS (FAB): $\{[(Ph_3SbBr]_2O$ (**M**) - Br$\}^+$ (m/z 801, 3%); $\{Ph_3SbBr\}^+$ (m/z 433, 50%); $\{Ph_2Sb\}^+$ (m/z 275, 10%); $\{Ph_2\}^+$ (m/z 154, 70%); $\{Ph\}^+$ (m/z 77, 17%)

2.3.3.2 Preparation of $[(p\text{-}MeC_6H_4)_3SbBr]_2O$ (2.8)

A mixture of sodium hydroxide (0.206g, 5.2mmol), $(p\text{-}MeC_6H_4)_3SbBr_2$ (**2.2**) (2.805g, 5.1mmol) and methanol (100ml) were refluxed with stirring for 24 hours. After this time approximately half the solvent was removed *in vacuo* and crude product was precipitated by addition of water (50ml). The product was isolated by filtration and recrystallised from chloroform. Yield 1.86g (76%); mp 276-282°C.

Found: C,52.18; H,4.41: $C_{42}H_{42}Br_2OSb_2$ requires C,52.22; H,4.38 %.

^1H NMR (250MHz, $CDCl_3$, RT) δ 2.40(s, 18H, *Me*-Ar-**A**); 2.42(s, 9H, *Me*-Ar-**B**); 7.08(d, 12H, $^3J_{HH}$ - 8Hz, *m*-Ar-**A**); 7.35(d, 6H, $^3J_{HH}$ - 8Hz, *m*-Ar-**B**); 7.51(d, 12H, $^3J_{HH}$ - 8Hz, *o*-Ar-**A**); 8.13(d, 6H, $^3J_{HH}$ - 8Hz, *o*-Ar-**B**), where **A** is $[(p\text{-}MeC_6H_4)_3SbBr]_2O$ and **B** is $(p\text{-}MeC_6H_4)_3Sb(OH)Br$. Under strictly anhydrous conditions only signals due to **A** were observed.

$^{13}C\{^1H\}$ NMR (69 MHz, $CDCl_3$, RT) δ 21.4(*Me*-Ar-**A**); 21.4(*Me*-Ar-**B**); 129.6(*m*-Ar-**A**); 130.1(*m*-Ar-**B**); 133.4(*o*-Ar-**A**); 134.0(*o*-Ar-**B**); 141.0(*ipso*-Ph-**A**). Under strictly anhydrous conditions only signals due to **A** were observed.

IR (nujol mull, CsI): 1311(m), 1210(m), 1188(m), 1065(m), 1014(m), 848(w), 804(vs), 787(w), 768(s), 699(w), 484(s).

MS (FAB): $\{[(p\text{-}MeC_6H_4)_3SbBr]_2O$ (**M**) - Br$\}^+$ (m/z 885, 2%); {**M** - 2Br - $MeC_6H_4\}^+$ (m/z 715, 1%).

2.3.3.3 Preparation of $[(o\text{-}MeC_6H_4)_3SbBr]_2O$ (2.9)

An analogous experimental procedure to 2.3.3.2 was employed, using sodium hydroxide (75mg, 1.9mmol), $(o\text{-}MeC_6H_4)_3SbBr_2$ (**2.3**) (1.026g, 1.9mmol) and methanol (60ml). After recrystallisation of the crude product from chloroform/hexane, well formed crystals of the title compound were isolated. Yield 680mg (74%); mp 250-258°C.

Found: C,52.11; H,4.42: $C_{42}H_{42}Br_2OSb_2$ requires C,52.22; H,4.38 %.

^1H NMR (250MHz, $CDCl_3$, RT) δ 2.31(s, very broad, 18H, *Me*-Ar-**A**); 2.67(s, 9H, *Me*-Ar-**B**); 6.88(s, very broad, 6H, *o*-Ar-**A**); 7.31(m, 18H, *m*- and *p*-Ar-**A**); 7.40(m, 9H, *m*- and *p*-Ar-**B**); 7.95(d, 3H, $^3J_{HH}$ - 8Hz, *o*-Ar-**B**), where **A** is $[(o\text{-}MeC_6H_4)_3SbBr]_2O$ and **B** is $(o\text{-}MeC_6H_4)_3Sb(OH)Br$. Under strictly anhydrous conditions only signals due to **A** were observed.

IR (nujol mull, CsI): 1278(m), 1205(m), 1163(w), 1121(m), 908(m), 799(m), 760(vs, br), 752(vs, br), 731(s), 699(m), 485(w), 437(s).

MS (FAB): $\{[(o\text{-}MeC_6H_4)_3SbBr]_2O$ **(M)** - $Br\}^+$ (m/z 885, <1%); {**M** - 2Br - $MeC_6H_4\}^+$ (m/z 715, <1%); $\{(o\text{-}MeC_6H_4)_3SbBr\}^+$ (m/z 475, 61%); $\{(o\text{-}MeC_6H_4)_2Sb\}^+$ (m/z 303, 18%); $\{MeC_6H_4\}^+$ (m/z 91, 93%).

2.3.3.4 Preparation of $(2,4,6\text{-}Me_3C_6H_2)_3SbBr(OH)$ (2.11)

A solution of sodium hydroxide (55mg, 1.4mmol) in the minimum of water was added to a stirred suspension of $(2,4,6\text{-}Me_3C_6H_2)_3SbBr_2$ (**2.6**) (815mg, 1.3mmol) and methanol (50ml), leading to the rapid formation of a clear solution. The solution was refluxed for 20 hours, after which time the volatiles were removed *in vacuo*. The remaining solid was taken up into dichloromethane (50ml), the solution filtered and then the solvent was evaporated to yield crude product. This was then recrystallised from chloroform/hexane to give crystals of the title compound. Yield 614mg (82%); mp 188-191°C.

Found: C,55.04; H,5.67: $C_{27}H_{34}BrOSb$ requires C,56.28; H,5.95 %.

^1H NMR (250MHz, $CDCl_3$, RT) δ 2.32(s, 9H, *p*-Me); 2.52(s, 18H, *o*-Me); 7.01(s, 6H, *m*-Ar).

$^{13}C\{^1H\}$ NMR (69 MHz, $CDCl_3$, RT) δ 21.0(*p*-Me); 24.6(*o*-Me); 131.0(*m*-Ar); 136.5(*p*-Ar); 142.5(*o*-Ar); 142.8(*ipso*-Ar).

IR (nujol mull, CsI): 3501(m, br), 1596(m), 1563(m), 1403(w), 1291(m), 1264(m), 1027(m), 1008(w), 850(s), 734(s), 700(w), 570(m), 542(s).

MS (FAB): $\{(2,4,6\text{-}Me_3C_6H_2)_3SbBr\}^+$ (m/z 559, 3%); $\{(2,4,6\text{-}Me_3C_6H_2)_3SbOH\}^+$ (m/z 495, 65%); $\{(2,4,6\text{-}Me_3C_6H_2)_3Sb\}^+$ (m/z 478, 4%); $\{(2,4,6\text{-}Me_3C_6H_2)_2SbOH\}^+$ (m/z 376, 3%); $\{(2,4,6\text{-}Me_3C_6H_2)SbOH\}^+$ (m/z 257, 7%); $\{2,4,6\text{-}Me_3C_6H_2\}^+$ (m/z 119, 38%).

2.3.3.5 Preparation of $[Me_3SbCl]_2O$ (2.10)

This preparation is analogous to that reported by Long, Doak and Freedman[6] and follows a two-stage process; the first stage involving the preparation of $Me_3Sb(OH)_2$ and the second a reaction between stoichiometric quantities of $Me_3Sb(OH)_2$ and

Me_3SbCl_2. The trimethylantimony dichloride used in this reaction was provided by Dr C.Silverstru, prepared by the method of Doak *et al*[49].

2.3.3.5.1 Preparation of $Me_3Sb(OH)_2$ (2.4)

Trimethylantimony dichloride (4.80g, 20.2mmol) was dissolved in boiling water (250ml) and the resulting solution was passed through an anion exchange resin in the hydroxide form (70g, Amberlite IRA-400(OH), washed with water until the eluant was neutral). A further portion of water (300ml) was run through the resin to ensure all product was obtained in the aqueous fractions collected. These were combined and the water carefully evaporated under reduced pressure. The resulting solid obtained was dried *in vacuo*, before recrystallisation from acetone. Yield 3.98g (98%).

Found: C,16.73; H,6.16: $C_3H_{11}O_2Sb$ requires C,17.94; H,5.52: $C_3H_{11}O_2Sb.H_2O$ requires C,16.46; H,5.99 %.

^{1}H NMR (250MHz, D_2O, RT) δ 1.48(s, 9H, *Me*-Sb).

MS (EI): $\{Me_6Sb_2OH\}^+$ (m/z 351, 100%); $\{Me_4Sb_2OH\}^-$ (m/z 321, 80%); $\{Me_2Sb_2OH\}^+$ (m/z 291, 29%); $\{Me_2Sb(OH)_2\}^+$ (m/z 185, 15%); $\{Me_3SbOH\}^+$ (m/z 183, 8%); $\{Me_2SbOH\}^+$ (m/z 168, 21%); $\{Me_2Sb\}^+$ (m/z 151, 89%).

2.3.3.5.2 Preparation of $[Me_3SbCl]_2O$ (2.10)

A solution of trimethylantimony dichloride (4.64g, 19.5mmol) in water (200ml) was added to a stirred solution of $Me_3Sb(OH)_2$ (**2.4**) (3.91g, 19.5mmol) in water (100ml) and the resulting solution was stirred for 1 hour. Following this, the solvent was removed under reduced pressure and the crude product was recrystallised from ethanol, giving clear crystals. Yield 3.61g (88%).

Found: C,17.08: H,4.48: $C_6H_{18}Cl_2OSb_2$ requires C,17.13; H,4.31 %.

^{1}H NMR (250MHz, D_2O, RT) δ 1.83(s, *Me*-Sb).

^{1}H NMR (250MHz, $CDCl_3$, RT) δ 1.96(s, *Me*-Sb); 2.04(s, *Me*-Sb); 2.35(s, *Me*-Sb).

Under strictly anhydrous conditions only the signal at 1.96 ppm was observed.

IR (nujol mull, CsI): 859(m), 776(vs), 582(m).

2.3.3.6 Preparation of $[Ph_2SbBrO]_2$ (2.12)

A solution of *tert*-butylhydroperoxide (15ml, 5-6M in ^{i}octane (Fluka), *ca* 82.5mmol) was added slowly to a stirred solution of diphenylantimony bromide (26.82g, 75mmol) in dichloromethane (200ml), at 0°C. The resulting reaction mixture was then stirred at room temperature for a further 16 hours, after which the mixture was filtered and the solvent removed *in vacuo*. On recrystallising the resultant material from chloroform, well formed crystals of the desired product were isolated. Yield 23.4g (84%); mp 202-203°C [Lit. 208°C[31]].

Found: C,38.79; H,2.81: $C_{24}H_{20}Br_2O_2Sb_2$ requires C,38.76; H,2.71 %.

^{1}H NMR (250MHz, $CDCl_3$, RT) δ 7.52(m, 18H, *m*- and *p*-Ph); 8.19(m, 12H, *o*-Ph).

$^{13}C\{^{1}H\}$ NMR (69 MHz, $CDCl_3$, RT) δ 129.6(*m*-Ph); 131.6(*p*-Ph); 133.7(*o*-Ph); 141.2(*ipso*-Ph).

IR (nujol mull, CsI): 1436(s), 1330(m), 1309(w), 1188(w), 1072(w), 1057(m), 1018(w), 995(s), 742(vs), 731(vs), 690(vs), 683(vs), 670(vs), 648(vs), 537(w), 495(vs), 452(vs), 442(s).

2.4 REFERENCES

1. G.Ferguson, E.W.Macauley, *J. Chem. Soc., Chem. Commun.*, 1968, 1288.
2. G.Wittig, K.Clauss, *Ann. Chem.*, 1952, **577**, 26.
3. Y.Kawasaki, *Bull. Chem. Soc. Jpn.*, 1976, **49**, 817.
4. G.T.Morgan, F.M.G.Micklethwait, G.S.Whitby, *J. Chem. Soc.*, 1910, **97**, 34.
5. F.Challenger, F.Pritchard, J.R.A.Jinks, *J. Chem. Soc.*, 1924, **125**, 864.
6. G.G.Long, G.O.Doak, L.D.Freedman, *J. Am. Chem. Soc.*, 1964, **86**, 209.
7. G.D.Doak, G.G.Long, L.D.Freedman, *J. Organomet. Chem.*, 1965, **4**, 82.
8. R.L.McKenney, H.H.Sisler, *Inorg. Chem.*, 1967, **6**, 1178.
9. M.Shindo, R.Okawara, *J. Organomet. Chem.*, 1966, **5**, 537.
10. Y.Kawasaki, Y.Yamamoto, M.Wada, *Bull. Chem. Soc. Jpn.*, 1983, **56**, 145.
11. H.Hartmann, G.Kuhl, *Z. Anorg. Allg. Chem.*, 1961, **312**, 186.
12. G.Ferguson, G.S.Harris, A.Khan, *Acta Crystallogr.*, 1987, **C43**, 2078.
13. J.W.Pasterczyk, A.R.Barron, *J. Cryst. Spectr. Research*, 1990, **20**, 85.
14. J.W.Pasterczyk, A.M.Arif, A.R.Barron, *J. Chem. Soc., Chem. Commun.*, 1989, 829.
15. T.Westhoff, F.Huber, H.Preut, *J. Organomet. Chem.*, 1988, **348**, 185.
16. H.Preut, T.Westhoff, F.Huber, *Acta Crystallogr.*, 1989, **C45**, 49.
17. T.Westhoff, F.Huber, R.Ruther, H.Preut, *J. Organomet. Chem.*, 1988, **352**, 107.
18. G.Ferguson, F.C.March, D.R.Ridley, *Acta Crystallogr.*, 1975, **B31**, 1260.
19. E.R.T.Tiekink, *J. Organomet. Chem.*, 1987, **333**, 199.
20. A.Ouchi, S.Sato, *Bull. Chem. Soc. Jpn.*, 1988, **61**, 1806.
21. G.Ferguson, D.R.Ridley, *Acta Crystallogr.*, 1973, **B29**, 2221.
22. R.M.Wing, K.P.Callahan, *Inorg. Chem.*, 1969, **8**, 871.
23. D.J.Hewkin, W.P.Griffith, *J. Chem. Soc., A*, 1966, 472.
24. A.Bystrom, K.-A.Wilhelmi, *Acta Chem. Scand.*, 1951, **5**, 1003.
25. F.W.B.Einstein, B.R.Penfold, *Acta Crystallogr.*, 1964, **17**, 1127.
26. D.H.Whiffen, *J. Chem. Soc.*, 1956, 1350.
27. for example G.Socrates, *Infrared Characteristic Group Frequencies*, Demand, 1980.
28. R.G.Goel, D.R.Ridley, *Inorg. Nucl. Chem. Letters*, 1971, **7**, 21.

29. R.Rüther, F.Huber, H.Preut, *J. Organomet. Chem.*, 1988, **342**, 185.

30. I.G.Southerington, PhD Thesis, University of Nottingham, 1991.

31. I.G.Southerington, G.E.Forster, M.J.Begley, D.B.Sowerby *J. Chem. Soc., Dalton Trans.*, 1995, 1995.

32. J.Bordner, G.O.Doak, T.S.Everett, *J. Am. Chem. Soc.*, 1986, **108**, 4206.

33. G.N.Chremos, R.A.Zingaro, *J. Organomet. Chem.*, 1970, **22**, 637.

34. G.N.Chremos, R.A.Zingaro, *J. Organomet. Chem.*, 1970, **22**, 647.

35. M.Ates, H.J.Breunig, A.Soltami-Neshan, M.Tegeler, *Z. Naturforsch.*, 1986, **41b**, 321.

36. M.J.Begley, D.B.Sowerby, *Acta Crystallogr.*, 1993, **C49**, 1044.

37. G.Ferguson, C.Glidewell, D.Lloyd, S.Metcalfe, *J. Chem. Soc., Perkin Trans. II*, 1988, 731.

38. H.Preut, R.Ruther, F.Huber, *Acta Crystallogr.*, 1986, **C42**, 1154.

39. G.L.Breneman, *Acta Crystallogr.*, 1979, **B35**, 731.

40. F.Challenger, V.K.Wilson, *J. Chem. Soc.*, 1927, 209.

41. M.S.Malinovskii, S.P.Olifirenko, *Zh. Obshch. Khim.*, 1956, **26**, 1581.

42. M.Benmalek, H.Chermette, C.Martelet, D.Sandino, J.Tousset, *J. Organomet. Chem.*, 1974, **67**, 53.

43. G.E.Forster, PhD Thesis, University of Nottingham, 1992.

44. K.A.Jensen, *Z. Anorg. Allg. Chem.*, 1943, **250**, 257.

45. K.W.Shen, W.E.McEwen, S.J.La Placa, W.C.Hamilton, A.P.Wolf, *J. Am. Chem. Soc.*, 1968, **90**, 1718.

46. S.N.Bhattacharya, M.Singh, *Indian J. Chem.*, 1979, **18**, 515.

47. A.Michaelis, U.Genzken, *Ann. Chem.*, 1887, **242**, 164.

48. G.Ferguson, C.Glidewell, I.Gosney, D.Lloyd, S.Metcalfe, *J. Chem. Soc., Perkin Trans. II*, 1988, 1829.

49. G.O.Doak, G.G.Long, M.E.Key, *Inorg. Synth.*, 1967, **9**, 92.

CHAPTER 3

MULTIPLE BRIDGING OF DIANTIMONY COMPOUNDS

3.1 INTRODUCTION

This chapter describes the use of phosphinate and arsinate ligands to bridge between two antimony atoms using antimony precursor compounds already linked by one or two oxo bridges. The introduction includes a review of multiply bridged antimony compounds (3.1.1) and a general review of antimony phosphinate/arsinate (or their sulfur containing analogues) compounds (3.1.2).

3.1.1 Multiply Bridged Antimony Compounds

Until recently there were very few known antimony compounds, in which pairs of antimony atoms are spanned by either three or four bridging groups and even now only two compounds containing quadruple bridges have been reported. The first is the structurally characterised zwitterionic species $[(Ph_2Sb)_2(\mu\text{-}O)_2(\mu\text{-}O_2SbPh_2)_2]$[1] (see Figure 3.1), a by-product of the oxidation of triphenylantimony. It is believed that this species is identical to an earlier reported compound[2] incorrectly described as diphenylstibinic anhydride.

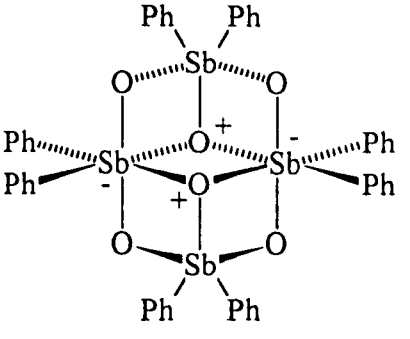

Figure 3.1 Molecular structure of $[(Ph_2Sb)_2(\mu\text{-}O)_2(\mu\text{-}O_2SbPh_2)_2]$

The second known quadruply bridged species is the ionic compound $[(Ph_2Sb)_2(\mu\text{-}O)_2(\mu\text{-}MoO_4)_2][NBu_4]_2$, in which the anion contains two oxo and two molybdate bridges spanning between Ph_2Sb fragments. This was originally prepared by Liu *et al* by a curious reaction between tetrabutylammonium molybdate and triphenylantimony diiodide[3]. It has subsequently been prepared by a more direct reaction between diphenylantimonybromide oxide dimer and the same molybdate[4].

A number of triply bridged compounds are also known. Schmidt and others have reported an extensive series of compounds with the general formula $[(Cl_3Sb)_2(\mu\text{-}O)(\mu\text{-}OR)(\mu\text{-}X)]$ with, for example: R=H, X=O_2CMe[5], O_2CCl_3[6], SO_4H[7], ClO_4[8]; R=Me, X=SO_4Me[9], SO_2Me[10], SO_3Me[10], O_2PMe_2[11], $O_2PMe(OMe)$[12] and R=Et, X=$O_2PEt(OEt)$[12], $O_2PMe(OMe)$[12]. These compounds were generally prepared by reactions between $SbCl_5$, H_2O, ROH and XH (the corresponding acid of the bridging ligands X), leading to the formation of an oxo, alkoxy (hydroxy) and ligand X bridges between two $SbCl_3$ fragments (see Figure 3.2).

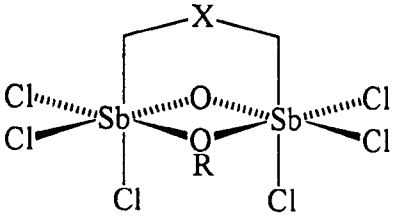

Figure 3.2 Molecular configuration of $[(Cl_3Sb)_2(\mu\text{-}O)(\mu\text{-}OR)(\mu\text{-}X)]$ compounds

The unusual tetranuclear antimony compound $[(Sb_4Ph_8O_6)(HOAc)_3]$[13] shows a similar bridging system to the above compounds, with each pair of antimony centres spanned by a hydroxo, oxo and an acetate bridge.

There are a number of compounds also reported in which pairs of antimony atoms are triply bridged by three halogens or two halogens and an oxo bridge *eg.* $[NMe_4]_3[(SbCl_3)_2(\mu\text{-}Br)_3]$[14] and $[HPy]_2[(SbCl_2)_2(\mu\text{-}O)(\mu\text{-}Br)_2]$[15]. However, this slightly different class of compounds will not be discussed further here.

Other reported triply bridged antimony species include compounds in which two antimony atoms are linked by two phosphinate and one oxo bridge, and include $[(Cl_3Sb)_2(\mu\text{-}O)(\mu\text{-}O_2PMe_2)_2]$[11] and the recently reported $[(Ph_2SbCl)_2(\mu\text{-}O)(\mu\text{-}O_2PR_2)_2]$[16], where R=cyclohexyl and cyclooctyl. Formation of the oxo bridge in these compounds was by the adventitious hydrolysis of a more highly halogenated species, *ie*:

$$2\ SbCl_5 + 2\ HO_2PMe_2 + H_2O \rightarrow [(Cl_3Sb)_2(\mu\text{-}O)(\mu\text{-}O_2PMe_2)_2] + 4\ HCl$$

$$2\ Ph_2SbCl_3 + 2\ AgO_2PR_2 + H_2O \rightarrow [(Ph_2SbCl)_2(\mu\text{-}O)(\mu\text{-}O_2PR_2)_2] + 2AgCl + 2HCl$$

X-ray crystal structures of both $[(Cl_3Sb)_2(\mu\text{-}O)(\mu\text{-}O_2PMe_2)_2]$ (see Figure 3.3) and $[(Ph_2SbCl)_2(\mu\text{-}O)(\mu\text{-}O_2P(C_6H_{11})_2)_2]$ show closely related geometries, with octahedrally coordinated antimony centres. Both compounds were also found to be in the *fac* isomeric form with the three oxygens mutually perpendicular.

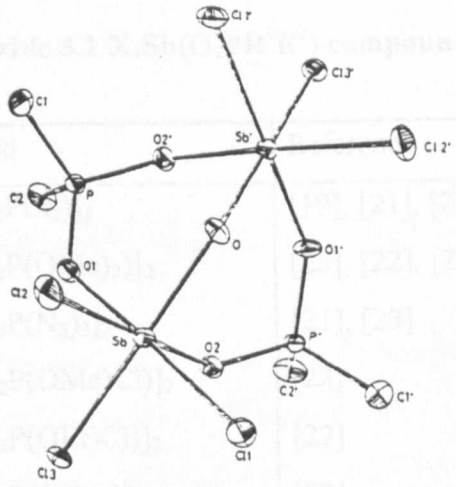

Figure 3.3 Molecular structure of $[(Cl_3Sb)_2(\mu\text{-}O)(\mu\text{-}O_2PMe_2)_2]$

It is therefore apparent that phosphinate and presumably arsinate ligands (the quadruply bridged arsenic compound $[((CF_3)_2As)_2(\mu\text{-}O)_2(\mu\text{-}O_2As(CF_3)OH)_2]$[17] having been reported) or their sulfur containing analogues are potentially valuable bridging groups. As shown in Figure 3.4, however, other forms of coordination are also possible.

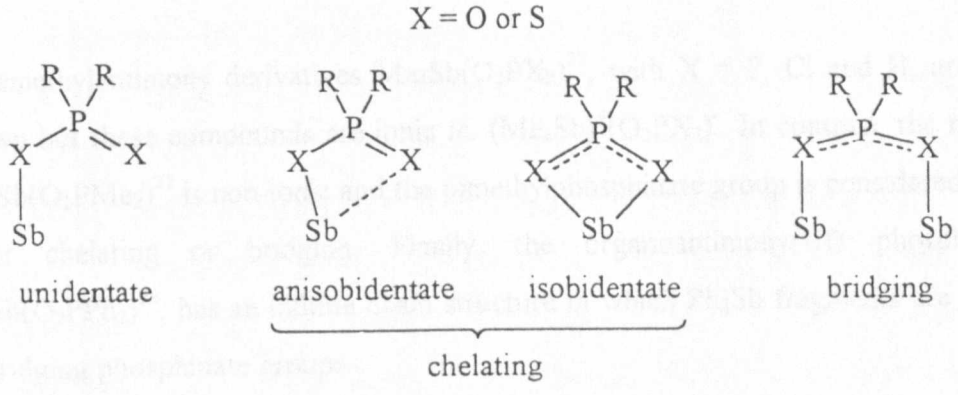

Figure 3.4 Potential coordination types of a phosphinate (or arsinate) group

3.1.2 Complexes of Antimony with Phosphinate, Arsinate and Related Ligands

3.1.2.1 Antimony phosphinates/phosphates

As well as the multiply bridged compounds described earlier, several other antimony phosphinates or phosphates are known. The majority are of the type $X_4Sb(O_2PRR')$, where X = Cl or F and R and R' are either halide, alkyl, alkoxy, azido or amino groups and are listed in Table 3.1. These compounds are all dimeric with antimony in octahedral coordination and the phosphinate groups bridging in a *cis* configuration.

Table 3.1 $X_4Sb(O_2PR^1R^2)$ compounds

Compound	Reference
$[Cl_4Sb(O_2PCl_2)]_2$	[19], [21], [23]
$[Cl_4Sb(O_2P(OMe)_2)]_2$	[20], [22], [23], [24]
$[Cl_4Sb(O_2P(N_3)_2]_2$	[21], [23]
$[Cl_4Sb(O_2P(OMe)Cl)]_2$	[22]
$[Cl_4Sb(O_2P(OEt)Cl)]_2$	[22]
$[Cl_4Sb(O_2P(OEt)_2)]_2$	[22]
$[F_4Sb(O_2PF_2)]_2$	[23]
$[Cl_4Sb(O_2PF_2)]_2$	[23]
$[Cl_4Sb(O_2P(OMe)(NMe_2)]_2$	[24]
$[Cl_4Sb(O_2PMe_2)]_2$	[25]
$[Cl_4Sb(O_2P(NMe_2)_2)]_2$	[26]
$[Cl_4Sb(O_2PMe(OMe))]_2$	[12]
$[Cl_4Sb(O_2PEt(OEt))]_2$	[12]

Tetramethylantimony derivatives $Me_4Sb(O_2PX_2)$[27], with X = F, Cl and H, are also known but these compounds are ionic *ie.* $(Me_4Sb)^+(O_2PX_2)^-$. In contrast, the related $Me_4Sb(O_2PMe_2)$[27] is non-ionic and the dimethylphosphinate group is considered to be either chelating or bridging. Finally, the organoantimony(III) phosphinate, $Ph_2Sb(O_2PPh_2)$[28], has an infinite chain structure in which Ph_2Sb fragments are linked by bridging phosphinate groups.

3.1.2.2 Antimony thiophosphinates/thiophosphates

Although antimony(III) is known to be a borderline hard-soft acid[29] and therefore should have little preference for O (**a**) over S (**b**) bonding to thiophosphinate groups (see Figure 3.5), data for known antimony thiophosphinates indicate that the ligand binds to the metal primarily by oxygen.

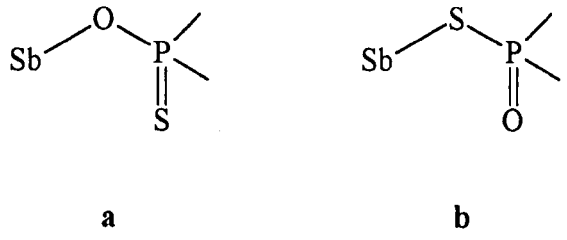

a **b**

Figure 3.5 Possible bonding modes of thiophospinate groups

Thus in both $Sb(OSPPh_2)_3$ and $Sb(OSP(C_6H_{11})_2)_3$[30], bonding is primarily to oxygen with little secondary Sb···S interaction. $Ph_2Sb(OSPPh_2)$, on the other hand, has a polymeric chain structure with again primary Sb–O bonds but the presence of secondary Sb···S bonds leads to bridging and generation of a polymeric chain structure[28]. The antimony(V) compounds, $Me_3Sb(OSPR_2)_2$[31] where R = Me, Et and Ph, have also been prepared and not surprisingly it was found that the thiophosphinate groups, which occupy axial sites in a trigonal bipyramid, are bound to the metal only through oxygen. The dimethylthiophosphinate group in $Me_4Sb(OSPMe_2)$[27,32] is also O–bonded, giving again a five-coordinate distorted trigonal bipyramidal arrangement about antimony.

3.1.2.3 Antimony dithiophosphinates/dithiophosphates

The molecular structures of several compounds of the type $Sb(S_2PR_2)_3$, where R = Ph[33,34], OMe[35], OEt[36], O^{i}Pr[35], have been investigated, showing interesting structural peculiarities. The compounds are all monomeric tris-chelates, with the majority displaying octahedral coordination. The exception to this is $Sb(S_2PPh_2)_3$, which has a pentagonal pyramidal structure. The synthesis of $Sb(S_2P(O^nBu)_2)_3$[35], $Sb(S_2P(O^iBu)_2)_3$[35], $Sb(S_2P(O^{sec}Bu)_2)_3$[35], $Sb(S_2PMe_2)_3$[35], $Sb(S_2PEt_2)_3$[35] have also been described, but structural data are lacking.

For the compound $PhSb(S_2P(O^iPr)_2)_2$[37], a structure determination shows a monomeric species, with chelating dithiophosphate groups, giving square pyramidal geometry about antimony and an apical phenyl group. The electron lone-pair on antimony in this compound is assumed to be stereochemically active and to occupy the sixth octahedral position. This type of coordination is similarly suggested for the related compounds, $PhSb(S_2P(OEt)_2)_2$[37], $PhSb(S_2P(O^nPr)_2)_2$[37], $PhSb(S_2P(OPh)_2)_2$[37] $PhSb(S_2PMe_2)_2$[38], $PhSb(S_2PEt_2)_2$[38] and $PhSb(S_2PPh_2)_2$[38]

In contrast, structure determinations of diarylantimony dithiophosphinates, show them to be dimers, with two different structural types (Type 1 and Type 2) having been observed (see Figure 3.6). In Type 1 dimers the dithiophosphinate groups are both chelating and bridging (bimetallic triconnective), whereas Type 2 dimers have solely bridging dithiophosphinate groups.

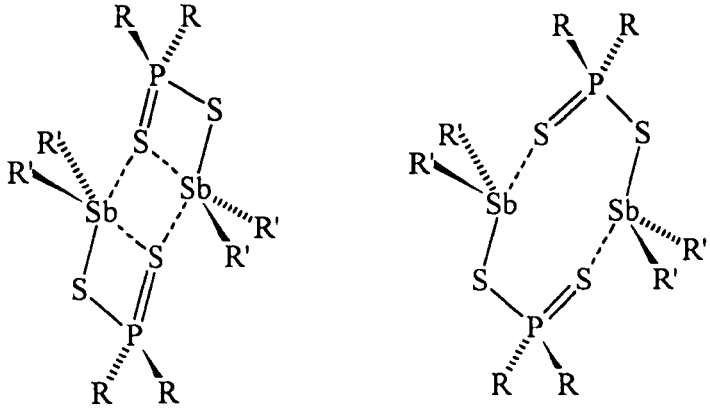

Figure 3.6 Type 1 and 2 structures of diarylantimony dithiophosphinates

The Type 1, *quasi*-tricyclic, structure can be found in $[Ph_2SbS_2PPh_2]_2$[39], which has similar secondary chelate and bridging Sb···S bond lengths of 3.440Å and 3.474Å. The Type 2 dimer is found in $[(p\text{-}MeC_6H_4)_2SbS_2PEt_2]_2$[40]. Other diarylantimony derivatives reported are $Ph_2SbS_2PMe_2$[39], $Ph_2SbS_2PEt_2$[39] and $Ph_2SbS_2PPr_2$[39], but there is a lack of data regarding their molecular structures.

The diphenylantimony dithiophosphate $[Ph_2SbS_2P(O^iPr)_2]_n$[41] is a supramolecular polymer with both secondary bridging and chelating Sb···S contacts. A similar structure is also seen in $[Me_2SbS_2PMe_2]_n$[42], which was formed by reaction between tetramethyldistibane Me_4Sb_2 and the disulfane $[Me_2P(S)S]_2$. Other reported diorganoantimony(III) dithiophosphates include $Ph_2SbS_2P(OMe)_2$[41], $Ph_2SbS_2P(OEt)_2$[41], $Ph_2SbS_2P(OPh)_2$[41], but again no structural data are available for these compounds.

The only antimony(V) analogues that have been reported are $Me_3Sb(S_2PR_2)_2$, where R = Me[38], Et[38,43] and Ph[38] and the oxo-bridged compounds $[Me_3Sb(S_2P(OR)_2)]_2O$, where R = Me, Et[44]. The molecular structure of $Me_3Sb(S_2PPh_2)_2$ has been determined, showing the presence of monomers with weakly chelating dithiophosphinate groups, leading to distortions of the trigonal bipyramidal coordination about antimony.

3.1.2.4 Antimony arsinates/dithioarsinates

Compared with the relatively large number of antimony compounds containing the $O_2P<$ or $S_2P<$ ligand grouping, analogous arsenic containing species ($O_2As<$ or $S_2As<$) are very scarce and have only recently been reported. All the known species are antimony(III) dithioarsinates and include $Sb(S_2AsMe_2)_3$[45], $PhSb(S_2AsMe_2)_2$[45], $Ph_2SbS_2AsMe_2$[39,45] and $Ph_2SbS_2AsPh_2$[39]. The compounds were prepared by reactions between the appropriate sodium dithioarsinate and the relevant phenylantimony(III) chloride (or acetate), *eg*.

$$Ph_nSbCl_{3-n} + (3-n)NaS_2AsMe_2 \rightarrow Ph_nSb(S_2AsMe_2)_{3-n} + (3-n)NaCl$$

The structures of both $Ph_2SbS_2AsMe_2$ and $Ph_2SbS_2AsPh_2$ have been elucidated, showing $Ph_2SbS_2AsMe_2$ to be a chain polymer, similar to that found for $Ph_2SbS_2P(O^iPr)_2$, and $Ph_2SbS_2AsPh_2$ to be a dimer, analogous to the Type 1 dimer in Figure 3.6.

The work reported in this chapter describes the reactions between several oxo-bridged antimony halide compounds, namely $[Ph_2SbBrO]_2$ (**2.12**), $[Ph_3SbBr]_2O$ (**2.7**), $[(p\text{-}MeC_6H_4)_3SbBr]_2O$ (**2.8**) and $[Me_3SbCl]_2O$ (**2.10**), with a range of phosphinate and arsinate salts. The aim of the work was to assess the ability of these ligands to bridge between the pairs of antimony atoms.

The work outlined in 3.2.3 also describes reactions of $[Ph_2SbBrO]_2$ (**2.12**) with dithiophosphinate salts.

3.2 RESULTS AND DISCUSSION

3.2.1 Quadruply Bridged Compounds

3.2.1.1 Preparation of Compounds

The quadruply bridged compounds $[(Ph_2Sb)_2(\mu\text{-}O)_2(\mu\text{-}O_2AsR_2)_2]$, where R=Me (**3.1**) or Ph (**3.2**) have been prepared by treatment of $[Ph_2SbBrO]_2$ with two equivalents of $Na(O_2AsMe_2)$ or $Na(O_2AsPh_2)$ in dichloromethane, the former reaction proceeding in far greater yield.

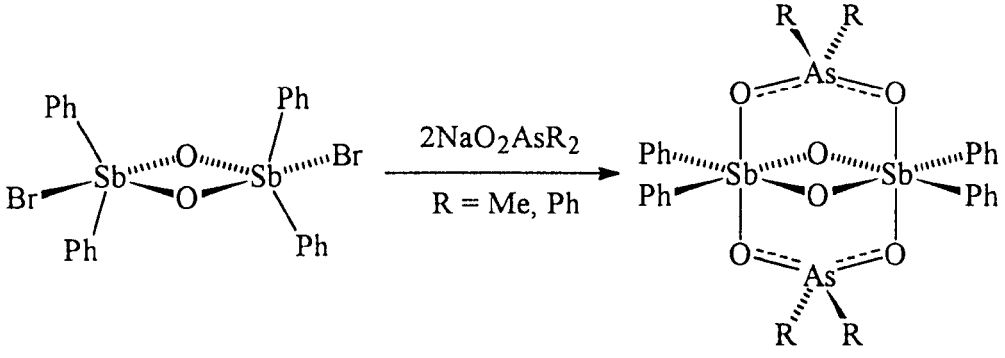

3.1 R = Me

3.2 R = Ph

Figure 3.7 Preparation of $[(Ph_2Sb)_2(\mu\text{-}O)_2(\mu\text{-}O_2AsR_2)_2]$ compounds

The compounds are high melting, air-stable compounds, although crystals obtained from chloroform readily lose solvent of crystallisation. Satisfactory microanalytical data were obtained for both compounds.

Similar reactions between $[Ph_2SbBrO]_2$ (**2.12**) and the phosphinate salts $Na(O_2PMe_2)$ and $Na(O_2PPh_2)$ failed to give quadruply bridged compounds and in the case of the dimethylphosphinate reaction a low yield of the triply bridged species, $[(Ph_3Sb)_2(\mu\text{-}O)(\mu\text{-}O_2PMe_2)_2]$ (**3.3**), was obtained. This compound has clearly undergone notable rearrangement, with the loss of an oxo bridge and the gaining of a phenyl group on each antimony when compared with the precursor compound.

Unexpectedly, a further quadruply bridged compound, $[((p\text{-}MeC_6H_4)_2Sb)_2(\mu\text{-}O)_2(\mu\text{-}O_2AsMe_2)_2]$ (**3.4**), was obtained in moderate yield by reaction between $[(p\text{-}MeC_6H_4)_3SbBr]_2O$ (**2.8**) and two equivalents of $Na(O_2AsMe_2)$ in dichloromethane. This compound has again undergone rearrangement, having gained an oxo bridge and lost a tolyl group from each antimony. As illustrated in the equation below, the rearrangement was presumably due to hydrolysis, leading to the elimination of toluene:

$$[(p\text{-}MeC_6H_4)_3SbBr]_2O\ (\mathbf{2.8}) + 2Na(O_2AsMe_2) + H_2O \rightarrow [((p\text{-}MeC_6H_4)_2Sb)_2(\mu\text{-}O)_2(\mu\text{-}O_2AsMe_2)_2]\ (\mathbf{3.4}) + 2NaBr + 2MeC_6H_5$$

It therefore seems apparent that an arsinate group has an appropriate 'bite-length' to comfortably span an Sb_2O_2 ring and facilitate the formation of quadruply bridged compounds. A possible reason for the non-formation of phosphinate (or carboxylate, see Chapter 4) derivatives is that these groups have a bite-length that is too small to comfortably bridge this gap; this would lead to strained structures where the *trans* angle θ is substantially less than 180° (see Figure 3.8).

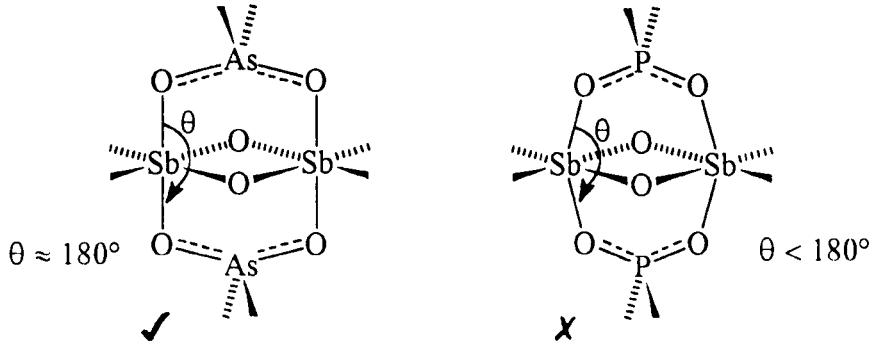

Figure 3.8 Potential quadruply bridged compounds

The results of the reactions described in this section have also illustrated the ready rearrangement of these organoantimony compounds, with aryl groups and oxo-bridges being lost or gained without the use of extreme conditions. Rearrangement and interchange of groups in antimony chemistry (notably antimony(III) chemistry) is not in itself unusual. Indeed, a ready synthetic route to arylantimony(III) halides[46] is by simple interchange of groups when triarylantimony and the relevant antimony(III) halide are mixed together, even in the absence of solvents. However, such ready reorganisations are not as prevalent in antimony(V) chemistry and accordingly it is likely that there is a strong driving force to form the multiply bridged compounds reported herein; either as quadruply bridged compounds with arsinate ligands or triply bridged species with phosphinate groups.

A reaction was also attempted between $[Ph_2SbBrO]_2$ and one equivalent of NaO_2AsMe_2 in dichloromethane, but this led to a complex reaction mixture and the small number of crystals obtained are, as yet, unidentified.

3.2.1.2 Infrared Spectroscopy

By analogy to the infrared spectra of carboxylate[47-50] and phosphinate compounds[51,52], it is expected that compounds containing arsinate ligands (local C_{2v} symmetry) should exhibit two infrared active bands, assignable to the $\nu_{asym}(AsO_2)$ and $\nu_{sym}(AsO_2)$ modes. The degree of delocalisation of the π-component would also, as is the case for phosphinates and carboxylates, be reflected in a decrease in the energy difference, $\Delta\nu(AsO_2)$, between the bands (see Figure 3.9).

However, it would be expected that the magnitude of $\Delta\nu(AsO_2)$ will be lower than that the equivalent separation in phosphinate/carboxylate compounds due to the increase in atomic weight of the central atom.

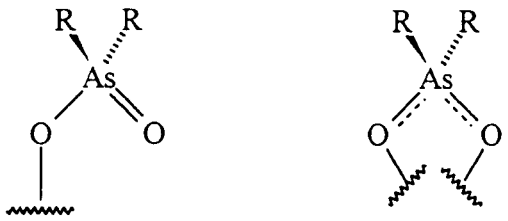

Unidentate — Chelating / Bridging

$\Delta\nu(AsO_2)$ = Larger — $\Delta\nu(AsO_2)$ = Smaller

Figure 3.9 Bonding modes of arsinate groups

The infrared spectra of the quadruply bridged compounds $[(Ph_2Sb)_2(\mu\text{-}O)_2(\mu\text{-}O_2AsR_2)_2]$ (R = Me (**3.1**) and Ph (**3.2**)) both showed an intense broad absorption centred at 796 and 812 cm^{-1} respectively. These bands are most likely due to combination of the two expected $\nu(AsO_2)$ vibrations and, as they cannot be separated into the individual $\nu_{asym}(AsO_2)$ and $\nu_{sym}(AsO_2)$ components, the arsinate groups appear to be highly delocalised. Indeed, the bridging arsinate groups in **3.1** are found by X-ray crystallography (see Section 3.2.1.5), to have nearly equivalent As–O bond lengths. A very similar infrared spectrum was displayed for $[((p\text{-}MeC_6H_4)_2Sb)_2(\mu\text{-}O)_2(\mu\text{-}O_2AsMe_2)_2]$ (**3.4**), with a broad intense peak observed at 805 cm^{-1}.

Assignment of the Sb-O vibrations in compounds **3.1**, **3.2** and **3.4**, proved to be difficult and no obvious bands due to the Sb_2O_2 ring, expected to have local D_{2h} symmetry were observed[53].

3.2.1.3 NMR Data

^1H NMR spectra of the compounds, $[(Ph_2Sb)_2(\mu\text{-}O)_2(\mu\text{-}O_2AsMe_2)_2]$ (**3.1**) and $[((p\text{-}MeC_6H_4)_2Sb)_2(\mu\text{-}O)_2(\mu\text{-}O_2AsMe_2)_2]$ (**3.4**) (see Figure 3.10), proved to be fully assignable. The spectrum of **3.1** showed a singlet at 2.00 ppm, due to the O_2AsMe_2 moiety and typical second-order phenyl multiplets at 7.33 and 7.83 ppm. The *p*-tolyl derivative displayed the equivalent O_2AsMe_2 resonance at 1.96 ppm and signals due to the tolyl groups were at 2.32(s, Me), 7.15(d, *m*-Ar) and 7.73(d, *o*-Ar) ppm (the

Figure 3.10 ^{1}H NMR spectrum of $[((p\text{-}MeC_6H_4)_2Sb)_2(\mu\text{-}O)_2(\mu\text{-}O_2AsMe_2)_2]$ (3.4) in $CDCl_3$

s denotes residual protio solvent

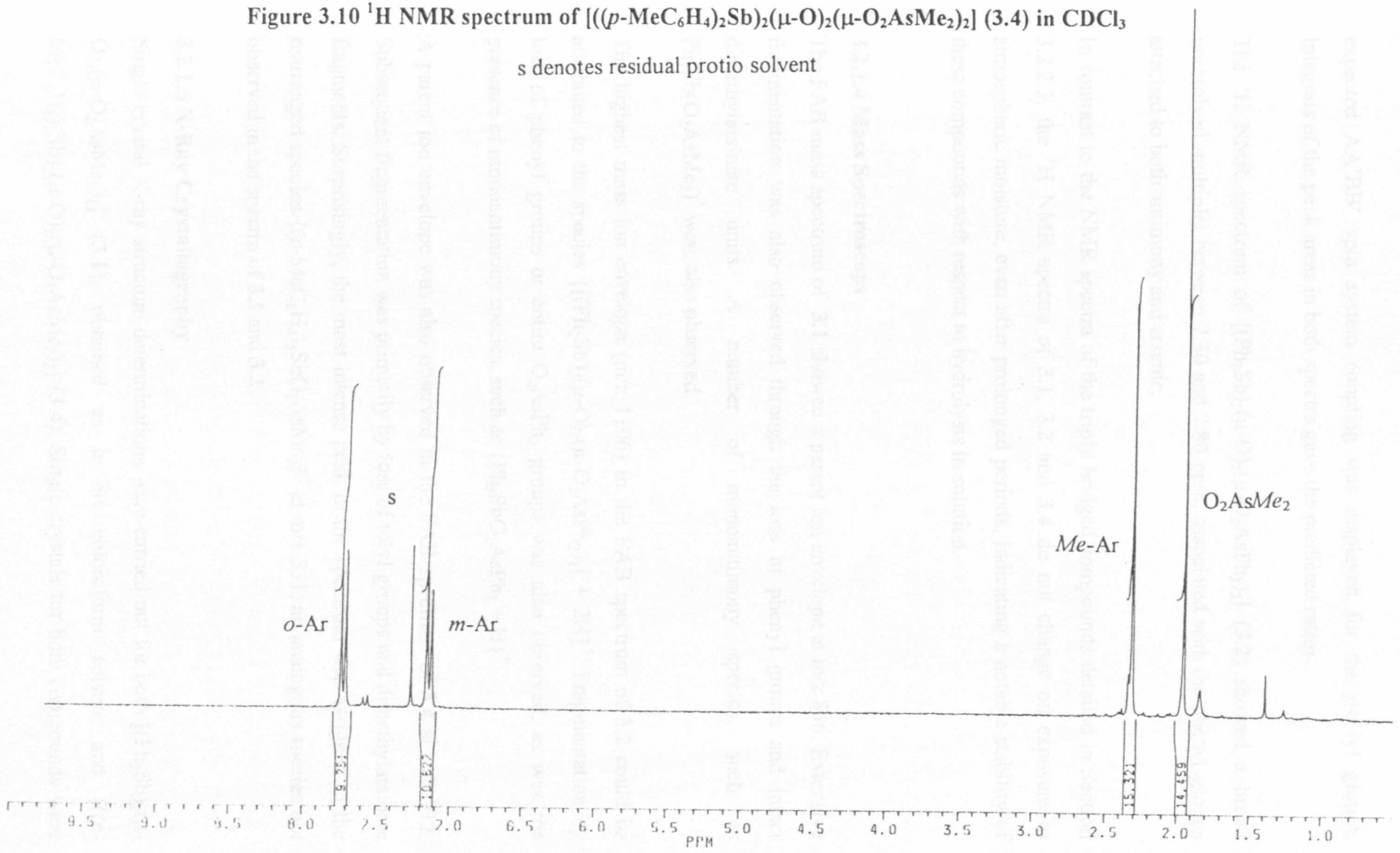

expected AA'BB' spin system coupling was displayed for the *p*-tolyl group). Integrals of the peak areas in both spectra gave the predicted ratios.

The ^{1}H NMR spectrum of $[(Ph_2Sb)_2(\mu\text{-}O)_2(\mu\text{-}O_2AsPh_2)_2]$ (**3.2**) showed a broad unresolved multiplet between 7.30 and 7.80 ppm, associated with the phenyl groups attached to both antimony and arsenic.

In contrast to the NMR spectra of the triply bridged compounds detailed in Section 3.2.2.3, the ^{1}H NMR spectra of **3.1**, **3.2** and **3.4** do not change on exposure to atmospheric moisture, even after prolonged periods, indicating a notable stability of these compounds with respect to hydrolysis in solution.

3.2.1.4 Mass Spectroscopy

The FAB mass spectrum of **3.1** showed a parent ion envelope at m/z 856. Extensive fragmentation was also observed through the loss of phenyl groups and intact dimethylarsinate units. A number of monoantimony species, such as $Ph_2Sb(O_2AsMe_2)^+$ were also observed.

The highest mass ion envelope (m/z 1106) in the FAB spectrum of **3.2** could be attributed to the species $\{[(Ph_2Sb)_2(\mu\text{-}O)_2(\mu\text{-}O_2AsPh_2)_2] + 2H\}^+$. Fragmentation by loss of phenyl groups or entire O_2AsPh_2 groups was also observed, as was the presence of monoantimony species, such as $\{Ph_2SbO_2AsPh_2 + H\}^+$.

A parent ion envelope was also observed in the FAB spectrum of **3.4** at m/z 912. Subsequent fragmentation was primarily by loss of tolyl groups and dimethylarsinate fragments. Surprisingly, the most intense peak in the spectrum was assigned to the rearranged species $\{(p\text{-}MeC_6H_4)_3SbO_2AsMe_2\}^+$ at m/z 531; an analogous species not observed in the spectra of **3.1** and **3.2**.

3.2.1.5 X-Ray Crystallography

Single crystal X-ray structure determinations were carried out for both $[(Ph_2Sb)_2(\mu\text{-}O)_2(\mu\text{-}O_2AsMe_2)_2]$ (**3.1**), obtained as a bis chloroform solvate and $[((p\text{-}MeC_6H_4)_2Sb)_2(\mu\text{-}O)_2(\mu\text{-}O_2AsMe_2)_2]$ (**3.4**). Single crystals for both compounds were

obtained by slow diffusion of hexane vapour into concentrated chloroform solutions of the compounds.

The molecular structure of **3.1** is shown in Figure 3.11 and selected bond lengths and angles are listed in Table 3.2. Further details of the crystal structure determination are given in Appendix C.

Table 3.2 Selected bond distances and angles, with standard deviations in parentheses for $[(Ph_2Sb)_2(\mu\text{-}O)_2(\mu\text{-}O_2AsMe_2)_2].2CHCl_3$ (3.1)

Bond lengths, Å		Bond angles, °	
Sb(1) - O(1)	1.995(3)	O(1) - Sb(1) - O(1')	79.5(1)
Sb(1) - O(1')	2.004(3)	O(1) - Sb(1) - O(2)	89.9(1)
Sb(1) - O(2)	2.101(3)	O(1') - Sb(1) - O(2)	85.5(1)
Sb(1) - O(3)	2.083(3)	O(1) - Sb(1) - O(3)	85.3(1)
Sb(1) - C(1)	2.157(4)	O(1') - Sb(1) - O(3)	90.7(1)
Sb(1) - C(7)	2.156(4)	O(1) - Sb(1) - C(1)	92.5(1)
As(1) - O(2)	1.709(3)	O(2) - Sb(1) - C(1)	88.6(1)
As(1) - O(3')	1.711(3)	O(3) - Sb(1) - C(1)	94.6(1)
As(1) - C(13)	1.909(4)	O(1') - Sb(1) - C(7)	91.1(1)
As(1) - C(14)	1.911(4)	O(2) - Sb(1) - C(7)	94.7(1)
		O(3) - Sb(1) - C(7)	89.6(1)
		C(1) - Sb(1) - C(7)	97.4(1)
		O(2) - Sb(1) - O(3)	174.3(1)
		O(1') - Sb(1) - C(1)	170.0(1)
		O(1) - Sb(1) - C(7)	169.3(1)
		O(2) - As(1) - O(3)	114.0(1)
		C(13) - As(1) - C(14)	110.0(2)
		Sb(1) - O(1) - Sb(1)	100.5(1)
		Sb(1) - O(2) - As(1)	119.0(1)
		Sb(1) - O(3) - As(1')	119.5(1)

As predicted by spectroscopic findings, **3.1** (obtained as a bis chloroform solvate) is a quadruply bridged species. The molecule possesses crystallographic C_i symmetry, with the inversion centre lying in the mid-point of the Sb_2O_2 ring. Coordination about the antimony centres is near-octahedral, with notable distortions being due to the constraints of the Sb_2O_2 ring, causing a constriction in the O(1)–Sb(1)–O(1') angle to 79.5(1)°.

Figure 3.11 Molecular structure of $[(Ph_2Sb)_2(\mu\text{-}O)_2(\mu\text{-}O_2AsMe_2)_2]$ (3.1)

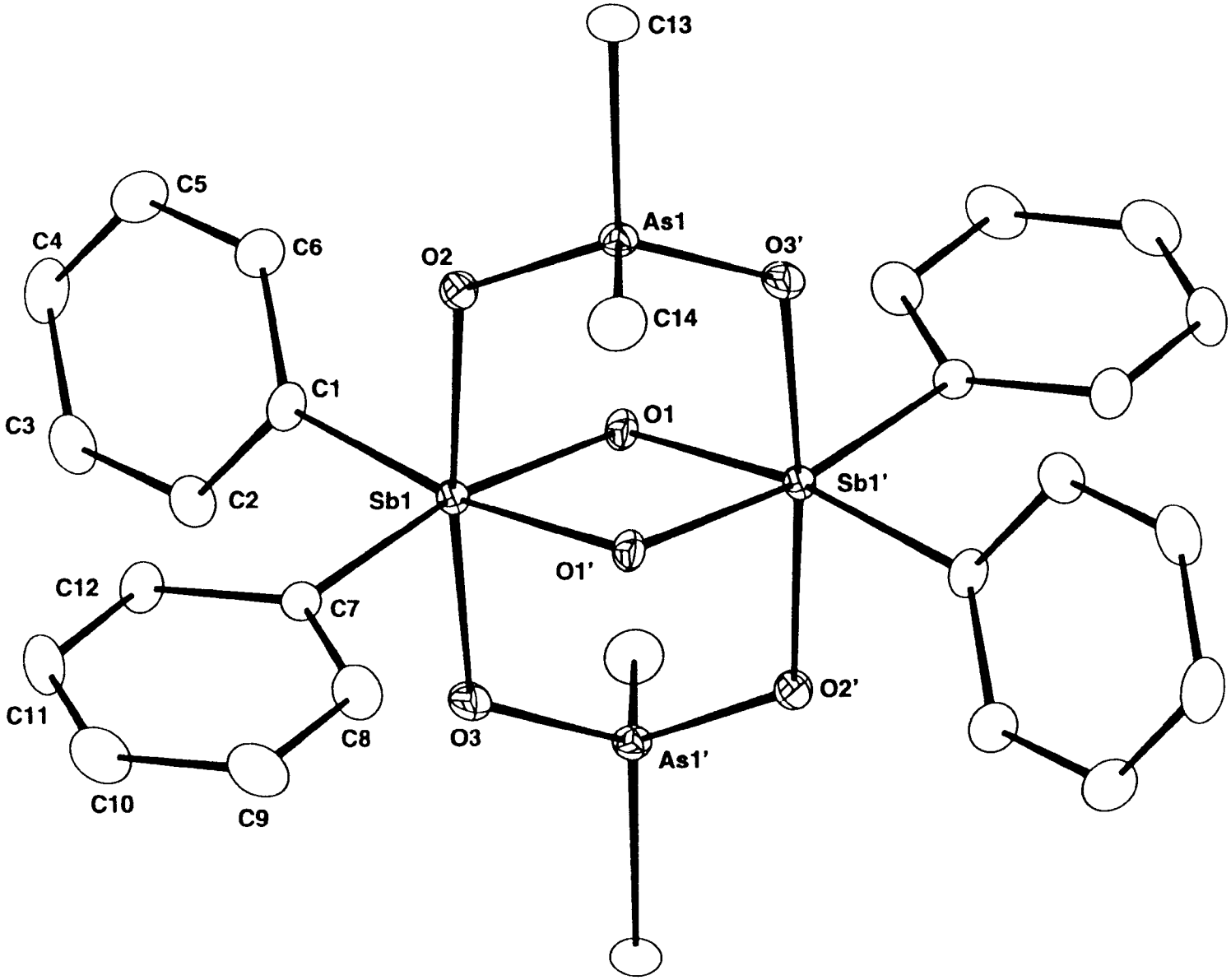

The $Sb–O_{bridge}$ bond lengths are relatively short, with the Sb(1)–O(1) bond at 1.995(3) Å and the Sb(1)–O(1') bond at 2.004(3) Å. These bond lengths are consistent with data from other known compounds containing an Sb_2O_2 ring, such as $[Ph_2SbBrO]_2$ (**2.12**) ($Sb–O_{bridge}$ = 1.936 and 2.061 Å)[54]. The bond lengths from antimony to the oxygen atoms of the *trans* dimethylarsinate ligands are slightly longer and nearly equivalent, with the Sb(1)–O(2) bond at 2.101(3) Å and the Sb(1)–O(3') bond at 2.083(3) Å. This near-equivalence is also reflected in the very similar $As–O_{ligand}$ bond lengths (As(1)–O(2) at 1.709(3) Å and As(1)–O(3') at 1.711(3) Å), illustrating the very symmetrical bonding of the groups with virtually total delocalisation of the π-component.

Coordination about the arsenic atoms is distorted tetrahedral, with the most notable distortion being the opening of the O(2)–As(1)–O(3') angle to 114.0(1)°. The As–C bond lengths are identical, within error (1.909(4) and 1.911(4) Å) and are comparable to those found in the structure of $Ph_2SbS_2AsMe_2$ (1.91 Å)[45].

The structure of $[(Ph_2Sb)_2(\mu\text{-}O)_2(\mu\text{-}O_2AsMe_2)_2]$ (**3.1**) can clearly be related to the anion in $[(Ph_2Sb)_2(\mu\text{-}O)_2(\mu\text{-}MoO_4)_2][NBu_4]_2$ reported by Liu and co-workers[3]. However, the molybdate groups in that compound have a significantly larger 'bite-length' than the arsinate groups in **3.1**, with an average $Mo–O_{ring}$ bond length of 1.83 Å. In addition, many similarities can be drawn between **3.1** and the structure of the zwitterionic $[(Ph_2Sb)_2(\mu\text{-}O)_2(\mu\text{-}O_2SbPh_2)_2]$[1], also consisting of diphenylantimony fragments quadruply bridged by two oxygen atoms and two further dioxo chelating ligands.

The molecular structure of $[((p\text{-}MeC_6H_4)_2Sb)_2(\mu\text{-}O)_2(\mu\text{-}O_2AsMe_2)_2]$ (**3.4**) is shown in Figure 3.12 and selected bond lengths and angles are listed in Table 3.3.
Further details of the crystal structure determination are given in Appendix D.

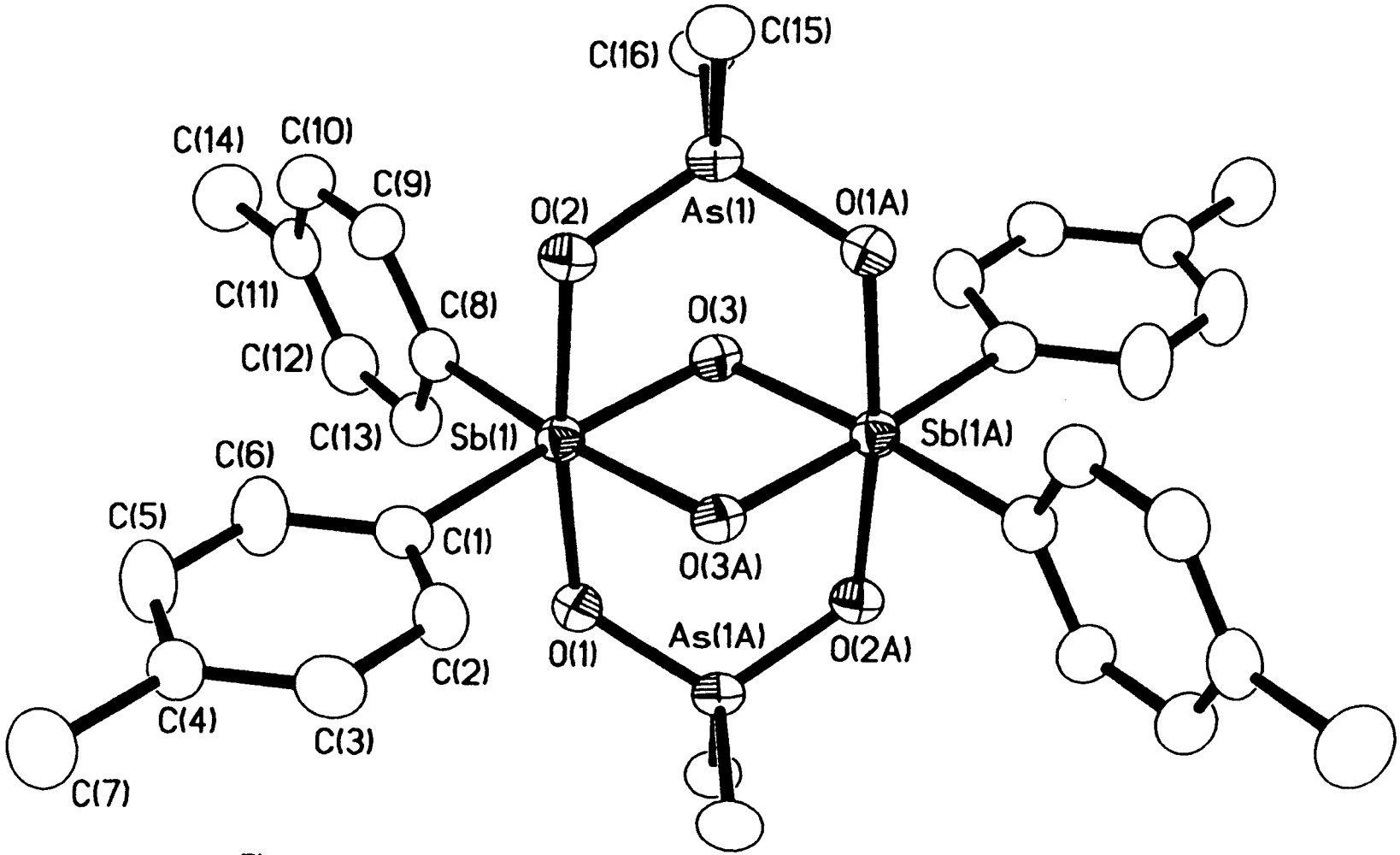

Figure 3.12 Molecular structure of $[((p\text{-}MeC_6H_4)_2Sb)_2(\mu\text{-}O)_2(\mu\text{-}O_2AsMe_2)_2]$ (3.4)

Table 3.3 Selected bond distances and angles, with standard deviations in parentheses for [((*p*-$MeC_6H_4)_2Sb)_2(\mu$-$O)_2(\mu$-$O_2AsMe_2)_2$] (3.4)

Bond lengths, Å		Bond angles, °	
Sb(1) - O(3)	2.007(3)	O(3) - Sb(1) - O(3a)	79.0(1)
Sb(1) - O(3a)	2.007(3)	O(3) - Sb(1) - O(2)	85.4(1)
Sb(1) - O(2)	2.087(3)	O(3a) - Sb(1) - O(2)	89.4(1)
Sb(1) - O(1)	2.084(3)	O(3) - Sb(1) - O(1)	89.9(1)
Sb(1) - C(1)	2.148(4)	O(3a) - Sb(1) - O(1)	84.6(1)
Sb(1) - C(8)	2.161(4)	O(3) - Sb(1) - C(8)	89.3(1)
As(1) - O(1a)	1.701(3)	O(2) - Sb(1) - C(8)	95.1(1)
As(1) - O(2)	1.703(3)	O(1) - Sb(1) - C(8)	90.1(2)
As(1) - C(15)	1.904(4)	O(3a) - Sb(1) - C(1)	92.9(1)
As(1) - C(16)	1.903(4)	O(2) - Sb(1) - C(1)	90.6(1)
		O(1) - Sb(1) - C(1)	93.2(1)
		C(1) - Sb(1) - C(8)	99.0(2)
		O(1) - Sb(1) - O(2)	173.0(1)
		O(3a) - Sb(1) - C(8)	167.2(1)
		O(3) - Sb(1) - C(1)	171.0(1)
		O(1a) - As(1) - O(2)	113.4(1)
		C(15) - As(1) - C(16)	110.4(2)
		Sb(1) - O(3) - Sb(1)	101.0(1)
		Sb(1) - O(2) - As(1)	119.0(1)
		Sb(1) - O(1) - As(1a)	119.5(1)

The structure of **3.4** is strongly reminiscent of that found for **3.1**, comprising of two (*p*-tolyl)$_2$Sb fragments quadruply bridged by two oxygen atoms and two dimethylarsinate ligands. Octahedral coordination is again noted about the antimony centres with the most significant distortion being the reduction in the O(3)–Sb(1)–O(3a) angle to 79.0(1)°, due to the constraints of the Sb_2O_2 ring.

Likewise to **3.1**, the structure has crystallographically imposed C_i symmetry and possesses a symmetrical dimethylarsinate moiety (As(1)–O(1a) and As(1)–O(2) having bond lengths of 1.701(3) and 1.703(3) Å respectively). This is also mirrored in the near identical Sb–O(1) and Sb–O(2) bond lengths (2.084(3) and 2.087(3) Å respectively).

An interesting feature of **3.4** is the relative orientation of the *p*-tolyl groups. Thus, the C(1) to C(7) tolyl group has a near coplanar configuration with respect to the Sb_2O_2

plane (4.0° twist), whereas the C(8) to C(14) group is perpendicular (94.5 ° between respective best-fit planes).

A comparison of the mean dimensions of the Sb_2O_2 rings found in **3.1** and **3.4** with some related compounds is collated in Table 3.4 below.

Table 3.4 Mean dimensions of Sb_2O_2 rings

Compound	Sb–O, Å	O–Sb–O,°	Sb–O–Sb,°	Reference
3.1	2.000	79.5*	100.5	This work
3.4	2.007	79.0*	101.0	This work
$[Ph_2Sb(MoO_4)O]_2^{2-}$	2.019	77.1*	102.9	[3]
$[Ph_2Sb(O_2SbPh_2)O]_2$	2.089	72.7*	107.3	[1]
$[Ph_3SbO]_2$	2.002	77.5*	102.5	[1]
$[Ph_2SbBrO]_2$	1.986	78.6	101.4	[54]

[Note: * indicates a centrosymmetric Sb_2O_2 ring(s)]

As shown in Table 3.4, the Sb_2O_2 ring dimensions are very similar for the selected group of compounds, with Sb–O bond lengths of *ca.* 2.00 Å and O–Sb–O angles of *ca.* 78°. The only compound that is noticeably different is $[Ph_2Sb(O_2SbPh_2)O]_2$, with relatively long Sb–O bonds (mean 2.089 Å) and small O–Sb–O angles (mean 72.7°). This, however, is probably due to the zwitterionic nature of the compound, with the bridging oxo groups involved in additional bonding to the antimony centres of the bridging diphenylstibinate moieties. In most cases, $[Ph_2SbBrO]_2$ being the only exception, the Sb_2O_2 ring possesses crystallographic C_i symmetry and all compounds show near D_{2h} local symmetry.

3.2.2 Triply Bridged Compounds

3.2.2.1 Preparation of Compounds

The triply bridged compounds $[(Ph_3Sb)_2(\mu\text{-}O)(\mu\text{-}O_2MR_2)_2]$ (M = P, R = Me (**3.3**); M = As, R = Me (**3.5**), Ph (**3.6**) were formed by reactions between the monooxo bridged species $[Ph_3SbBr]_2O$ (**2.7**) and 2 equivalents of the appropriate $Na(O_2MR_2)$ salt (see Figure 3.13). The stable products were all formed in good yield, giving crystalline products with satisfactory microanalytical data (note, **3.3** is the same as the earlier rearranged product described in Section 3.2.1).

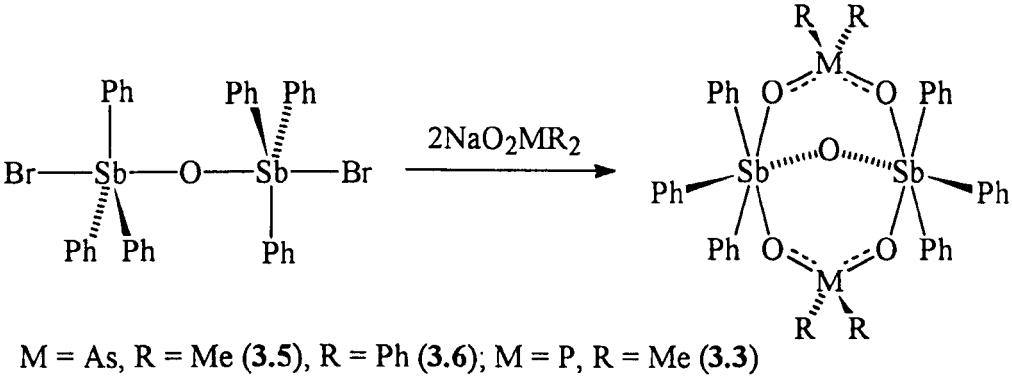

M = As, R = Me (**3.5**), R = Ph (**3.6**); M = P, R = Me (**3.3**)

Figure 3.13 Preparation of $[(Ph_3Sb)_2(\mu\text{-}O)(\mu\text{-}O_2MR_2)_2]$ compounds

A related reaction between $[Ph_3SbBr]_2O$ and two equivalents of $Na(O_2PPh_2)$ was surprisingly unsuccessful giving a mixture of unidentified products. Reaction between $[Ph_3SbBr]_2O$ and one equivalent of $Na(O_2AsMe_2)$ carried out in an attempt to form the unsymmetrical compound, $[(Ph_3Sb)_2(\mu\text{-}O)(\mu\text{-}O_2AsMe_2)Br]$, was also unsuccessful and led to the isolation of a mixture of **3.5** and unreacted starting material $[Ph_3SbBr]_2O$ (**2.7**)

A further triply bridged compound, $[((p\text{-}MeC_6H_4)_3Sb)_2(\mu\text{-}O)(\mu\text{-}O_2PMe_2)_2]$ (**3.7**), was however formed, in good yield, by a reaction between $[(p\text{-}MeC_6H_4)_3SbBr]_2O$ (**2.8**) and two equivalents of $Na(O_2PMe_2)$. In contrast, a similar reaction between $[(o\text{-}MeC_6H_4)_3SbBr]_2O$ (**2.9**) and two equivalents of $Na(O_2PMe_2)$ proved unsuccessful. This outcome was perhaps due to the steric bulk (specifically the *ortho* methyl groups) of the antimony precursor hindering reaction.

Preparation of two related compounds, $[(Me_3Sb)_2(\mu\text{-}O)(\mu\text{-}O_2PMe_2)_2]$ (**3.8**) and $[(Me_3Sb)_2(\mu\text{-}O)(\mu\text{-}O_2AsPh_2)_2]$ (**3.9**), was achieved by the reactions of $[Me_3SbCl]_2O$ (**2.10**) with two equivalents of $Na(O_2PMe_2)$ or $Na(O_2AsPh_2)$. The compounds were isolated in reasonable yields, but proved to be exceptionally sensitive to irreversible hydrolysis, with formation of a mixture of unidentified products. Handling these compounds, even with stringent Schlenk and glove-box techniques, proved extremely difficult and it was not possible to obtain reliable microanalytical results. Satisfactory ^1H and $^{13}C\{^1H\}$ NMR data, however, were obtained and, by analogy with the compounds described earlier, are also presumed to be triply bridged.

As reported earlier (Section 3.2.1.1), reaction of $[(p\text{-}MeC_6H_4)_3SbBr]_2O$ (**2.8**) with two equivalents of $Na(O_2AsMe_2)$, did not give the expected triply bridged species (*ie* $[((p\text{-}MeC_6H_4)_3Sb)_2(\mu\text{-}O)(\mu\text{-}O_2AsMe_2)_2]$), but instead a rearranged quadruply bridged compound, $[((p\text{-}MeC_6H_4)_2Sb)_2(\mu\text{-}O)_2(\mu\text{-}O_2AsMe_2)_2]$ (**3.4**), was formed. This observation is in clear contrast with the analogous reaction between $[Ph_3SbBr]_2O$ and $Na(O_2AsMe_2)$ which gave a good yield of the triply bridged compound **3.5**. However, closer investigation (by ^1H NMR) into the reaction between $[Ph_3SbBr]_2O$ and $Na(O_2AsMe_2)$ showed that rearrangement to the quadruply bridged analogue $[(Ph_2Sb)_2(\mu\text{-}O)_2(\mu\text{-}O_2AsMe_2)_2]$ (**3.1**) did occur, but only to a very minor extent, with **3.5** being formed in far greater yield.

It is not readily apparent why the reactions of the similar precursors $[Ph_3SbBr]_2O$ (**2.7**) and $[(p\text{-}MeC_6H_4)_3SbBr]_2O$ (**2.8**) with two equivalents of $Na(O_2AsMe_2)$ give very different products, but it again demonstrates the ease at which rearrangement occurs in these systems.

The mechanism of formation of the successful triply bridged compounds is a matter of interest. As few precautions were taken to avoid atmospheric moisture [except for reactions involving $[Me_3SbCl]_2O$ (**2.10**)], it is likely that the oxo-bridged precursors will have hydrolysed to some extent whilst in solution (see Chapter 2). Thus, it is possible that the compounds **3.5**, **3.6** and **3.7** were initially formed as hydroxo species in solution and subsequently condense on crystallisation to give the triply bridged compounds isolated, as illustrated in Figure 3.14.

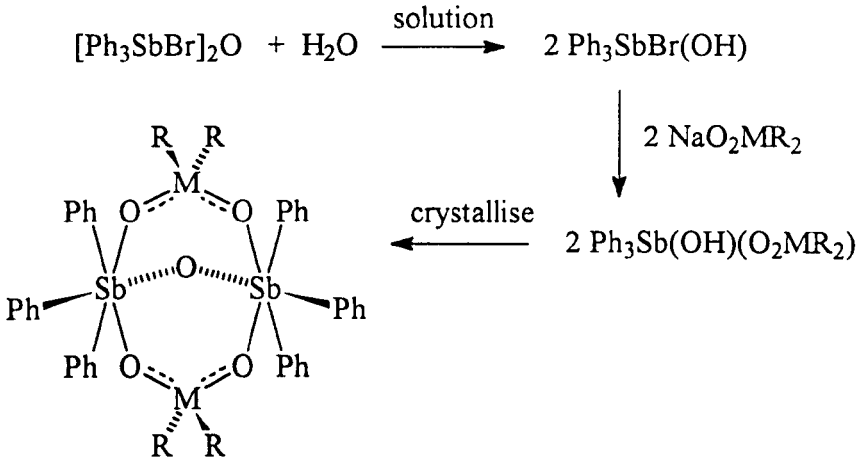

Figure 3.14 Potential mechanism for formation of triply bridged compounds

Furthermore, NMR data for compounds **3.5**, **3.6** and **3.7** illustrates that solution hydrolysis readily occurs, giving the hydroxo species that are proposed as being intermediates in their formation.

As all manipulations carried out to prepare and handle $[(Me_3Sb)_2(\mu\text{-}O)(\mu\text{-}O_2PMe_2)_2]$ (**3.8**) and $[(Me_3Sb)_2(\mu\text{-}O)(\mu\text{-}O_2AsPh_2)_2]$ (**3.9**) were performed under strictly anhydrous conditions it is highly unlikely that the formation of any hydroxo species could have occurred. Therefore, drawing similarities between the solid state structures of these compounds and those of **3.5**, **3.6** and **3.7** is potentially unreliable.

3.2.2.2 Infrared Spectroscopy

In addition to bands due to many phenyl modes, the infrared spectrum (see Figure 3.15) of the triply bridged compound, $[(Ph_3Sb)_2(\mu\text{-}O)(\mu\text{-}O_2PMe_2)_2]$ (**3.3**) exhibited a strong, broad band at 1112 cm^{-1} assigned to the $\nu_{asym}(PO_2)$ mode. A doublet at 1046 and 1032 cm^{-1} was also observed, due to the in- and out-of-phase components of the $\nu_{sym}(PO_2)$ mode. Shihada and co-workers[51,52] have reported that in related tin dimethylphosphinate compounds, if the $\nu(PO_2)$ bands are found between 1200 and 1000 cm^{-1}, the dimethylphosphinate ligand is likely to be bound in a bidentate fashion, either as a chelate or a bridge, which is in agreement with the triply bridged structure of **3.3** illustrated by a crystal structure determination detailed later (Section 3.2.2.5).

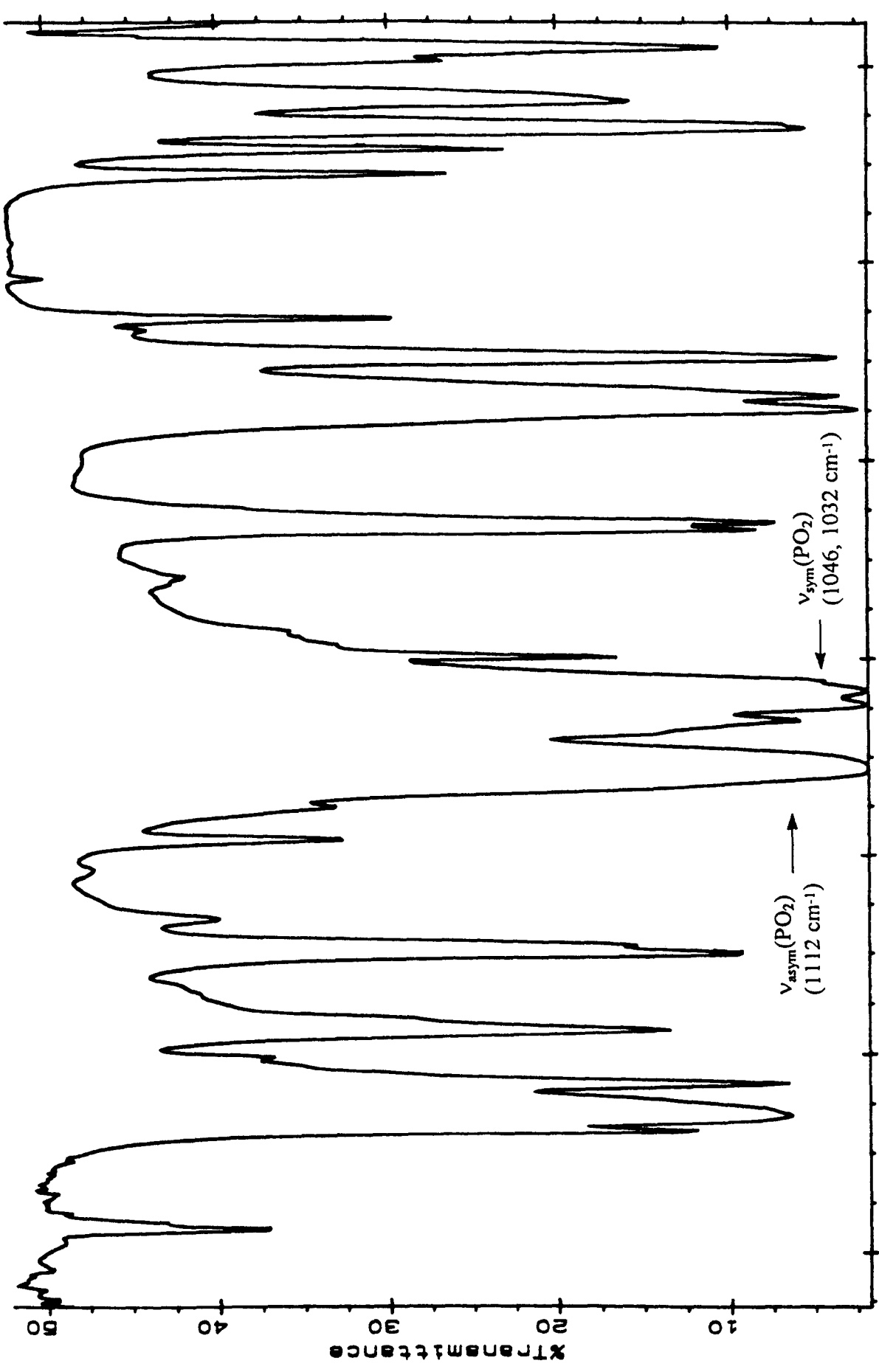

Figure 3.15 Infrared spectrum (nujol mull) of $[(Ph_3Sb)_2(\mu\text{-}O)(\mu\text{-}O_2PMe_2)_2]$ (3.3) from 1650 to 350 cm^{-1}

Analogous $\nu(PO_2)$ bands in the related compound $[((p\text{-}MeC_6H_4)_3Sb)_2(\mu\text{-}O)(\mu\text{-}O_2PMe_2)_2]$ (**3.7**) showed a similar structure to that observed for **3.3**. However, splitting of the $\nu_{asym}(PO_2)$ band was also noted here, giving rise to peaks at 1120 and 1111 cm^{-1}. The $\nu_{sym}(PO_2)$ absorptions were found at 1048 and 1033 cm^{-1}.

The infrared spectra of the compounds, $[(Ph_3Sb)_2(\mu\text{-}O)(\mu\text{-}O_2AsMe_2)_2]$ (**3.5**) and $[(Ph_3Sb)_2(\mu\text{-}O)(\mu\text{-}O_2AsPh_2)_2]$ (**3.6**), exhibited (in addition to many other, primarily phenyl, bands) intense broad absorptions at *ca.* 850 cm^{-1}, assigned to the $\nu(AsO_2)$ absorptions of the bridging arsinate groups. The band was centred at 852 cm^{-1} in **3.5** and at 831 cm^{-1} in **3.6** (likely to be of lower energy than that in **3.5** due to the electron-withdrawing effects of the phenyl groups). It is notable that the $\nu(AsO_2)$ absorptions in **3.5** and **3.6** are at significantly higher energy than those found for the quadruply bridged compounds **3.1**, **3.2** and **3.4** (*ca.* 800 cm^{-1}) described in Section 3.2.1.2. This observation tends to suggest that the arsinate groups possess stronger (and therefore shorter) As–O bonds in the triply bridged compounds. This conclusion is indeed illustrated by comparisons of their molecular structures, reported herein.

Due to partial decomposition in the nujol mull, even when prepared in a glove-box, infrared spectra for the compounds, $[(Me_3Sb)_2(\mu\text{-}O)(\mu\text{-}O_2PMe_2)_2]$ (**3.8**) and $[(Me_3Sb)_2(\mu\text{-}O)(\mu\text{-}O_2AsPh_2)_2]$ (**3.9**), were not particularly informative or reliable, although tentative assignments have been made. The spectrum of **3.8** displayed a broad band centred at 1172 cm^{-1} assigned to the stretching mode $\nu_{asym}(PO_2)$ and another broad band at 1020 cm^{-1} is likely to be due to the $\nu_{sym}(PO_2)$ absorption. These bands lie within the range quoted by Shihada and co-workers[51] for bidentate coordination of a dimethylphosphinate group. Compound **3.9** displayed a broad intense band, centred at 795 cm^{-1}, likely to be due to the $\nu(AsO_2)$ of the (probably bridging) diphenylarsinate moiety.

3.2.2.3 NMR Data

A ^1H NMR spectrum of $[(Ph_3Sb)_2(\mu\text{-}O)(\mu\text{-}O_2PMe_2)_2]$ (**3.3**) illustrated an unusual behaviour of this compound in solution. If the spectrum was obtained using $CDCl_3$ without precaution against atmospheric moisture, only a single species was observed,

which showed the expected ratio of three phenyl groups to each dimethylphosphinate group. Following the observations made in Chapter 2, this species seems likely to be a hydrolysis product and probably the monometallic hydroxo species, $Ph_3Sb(O_2PMe_2)OH$ (**3.10**). Crystallisation of the NMR sample leads to the quantitative recovery of the triply bridged parent compound **3.3**.

$$[(Ph_3Sb)_2(\mu\text{-}O)(\mu\text{-}O_2PMe_2)_2] \underset{-H_2O}{\overset{H_2O}{\rightleftharpoons}} 2Ph_3Sb(O_2PMe_2)OH$$

Solid state Solution

However, when the spectrum was recorded under strictly anhydrous conditions, a very different spectrum was obtained, showing resonances from two different species (or isomers), neither of which corresponded to the resonances of the hydrolysed species mentioned above. Under these conditions, it seems highly unlikely that hydrolysis could have occurred and the oxo bridge is therefore presumed to be intact in these species. The methyl groups of the dimethylphosphinate fragment in the first species (**A**) were observed as a doublet at 0.72 ppm ($^2J_{HP}$ = 14Hz) with the phenyl region defined into a triplet, triplet and doublet (7.16, 7.45 and 7.56 ppm respectively). In the second species (**B**) the O_2PMe_2 signal was collapsed and only a broad featureless absorption was seen. The phenyl resonances were observed as two second-order multiplets, centred at 7.38 and 7.68 ppm. The ratio of the two compounds (**A**) and (**B**) was approximately 2:3.

Further work would be needed to fully identify these two solution species, although a feasible explanation would be the presence of species that differ in the coordination mode of the dimethylphosphinate group (even though the solid state structure of the compound shows exclusively a triply bridged species). As well as bridging, it is possible that in solution the dimethylphosphinate group could be either chelating, unidentate or even ionized. Chelating is perhaps the more reasonable possibility, due to antimony coordinative unsaturation and with the known chemistry of R_2PO_2 groups[25,27,28] indicating a distinct preference for bidentate coordination (see Figure 3.16).

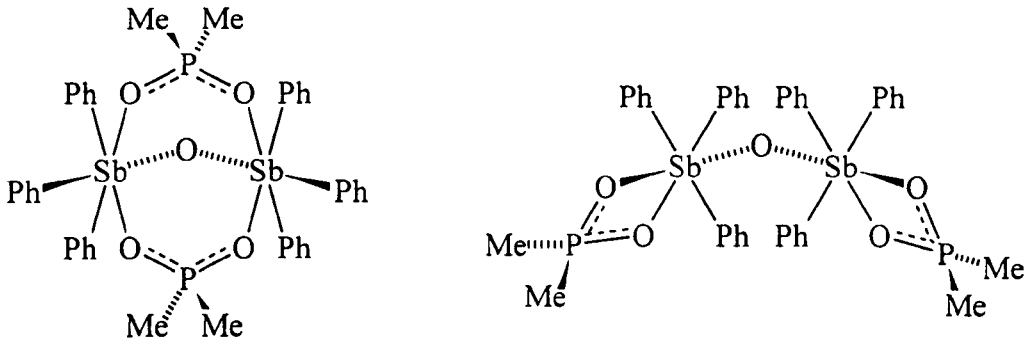

Figure 3.16 Possible solution species of 3.3 under anhydrous conditions

The ^{1}H NMR spectrum of the *p*-tolyl derivative **3.7** displayed a very similar solution behaviour to that observed for **3.3**. Thus, in non-anhydrous $CDCl_3$, a single species was observed, assumed to be the hydrolysed monometallic compound, (*p*-$MeC_6H_4)_3Sb(O_2PMe_2)OH$, while under anhydrous conditions, two species were again seen (**A** and **B**), with chemical shifts of the corresponding resonances closely related to those of the phenyl analogue (**3.3**). Species **A** in the anhydrous spectrum of **3.7** was the dominant isomer, with an **A**:**B** ratio of *ca.* 5:1.

Unusual solution effects were also present in the ^{1}H NMR spectrum of [$(Ph_3Sb)_2(\mu$-$O)(\mu$-$O_2AsMe_2)_2$] (**3.5**). Here, in anhydrous $CDCl_3$, resonances due to two different species (**A** and **B**) were again observed. Signals due to the dimethylarsinate group (0.71 and 1.89 ppm), in both species, were very broad and featureless, giving unreliable integrals and making detailed assignments difficult. The phenyl region however, was clearly defined with two distinct environments observed. The first (**A**) displayed a triplet, triplet, doublet coupling pattern at chemical shifts of 7.17, 7.27 (masked by a multiplet from second species) and 7.61 ppm for the *meta*, *para* and *ortho* protons respectively. The phenyl resonances of the second species (**B**) were observed as two multiplets at 7.27 and 7.71 ppm. The relative intensities of **A**:**B** was *ca.* 2:1. The identity of the solution species **A** and **B** is again unknown, although it is presumed that the oxo-bridge has remained intact due to the absence of moisture.

In contrast to the triarylantimony triply bridged compounds, the ^{1}H NMR spectra of $[(Me_3Sb)_2(\mu\text{-}O)(\mu\text{-}O_2PMe_2)_2]$ (**3.8**) and $[(Me_3Sb)_2(\mu\text{-}O)(\mu\text{-}O_2AsPh_2)_2]$ (**3.9**) were readily assignable with only one solution species observed in each case. Chemical shifts of the Me_3Sb signals were found in relatively high field positions (1.66 ppm for both compounds) in comparison with related compounds, *ie.* 1.96 ppm in $[Me_3SbCl]_2O$ (**2.10**) and 2.07 ppm in $[Me_3Sb(S_2P(OMe)_2)]_2O$[44]. A doublet at 1.13 ppm, assigned to the O_2PMe_2 fragment, was also observed in the spectrum of **3.8**, whereas second-order phenyl multiplets at 7.41 and 7.70 ppm were observed in the spectrum of **3.9**, along with a resonance associated with solvating dichloromethane (1:1 solvate).

The ^{13}C shifts of the methyl groups on antimony are also closely related at 16.3 ppm for **3.8** and 16.8 ppm for **3.9**, notably higher field than the equivalent resonance in $[Me_3Sb(S_2P(OMe)_2)]_2O$ (18.6 ppm). A further signal in the $^{13}C\{^1H\}$ spectrum of **3.8** at 18.8 ppm (doublet, $^1J_{CP}$ = 104Hz) was assigned to the methyl carbons of the dimethylphosphinate group. In addition to the *Me*–Sb resonance (at 16.8 ppm) in the $^{13}C\{^1H\}$ spectrum of **3.9**, signals were observed at 128.7 (*m*-Ph), 130.4 (*p*-Ph), 131.2 (*o*-Ph) and 138.2 (*ipso*-Ph) ppm.

From these NMR data (as well as the poor infrared data), it is impossible to define convincingly compounds **3.8** and **3.9** as being triply bridged species. Analogy with the molecular structures of the triarylantimony compounds, reported in Section 3.2.2.5, would suggest they would be, although the presence of the electron-donating methyl groups will lead to a marked decrease in Lewis acidity at the metal centres and therefore the possibility of less secondary bonding from the phosphinate (or arsinate) ligands. It is also dubious whether conclusions about the solid state structures of these compounds can be drawn from the different behaviour displayed in the anhydrous NMR studies reported here, *ie.* only one species observed in solution for **3.8** and **3.9** and at least two for the triarylantimony compounds.

3.2.2.4 Mass Spectroscopy

In contrast to the previously reported quadruply bridged compounds (Section 3.2.1.4), the FAB mass spectrum of $[(Ph_3Sb)_2(\mu\text{-}O)(\mu\text{-}O_2PMe_2)_2]$ (**3.3**) did not

display a peak assignable to the parent ion. However, fragments were observed in which the parent had lost either a phenyl group or an intact dimethylphosphinate group, with the intensities of the peaks indicating preferential loss of the dimethylphosphinate group. The most intense peak in the spectrum was assigned to the monoantimony cation $\{Ph_3Sb(O_2PMe_2)\}^+$ at m/z 445.

Similarly, FAB mass spectra of the related compounds, $[(Ph_3Sb)_2(\mu\text{-}O)(\mu\text{-}O_2AsMe_2)_2]$ (**3.5**) and $[((p\text{-}MeC_6H_4)_3Sb)_2(\mu\text{-}O)(\mu\text{-}O_2PMe_2)_2]$ (**3.7**), did not exhibit their respective parent ions. However, both spectra showed significant ion envelopes assignable to the respective $\{(Ar_3Sb)_2(\mu\text{-}O)(\mu\text{-}O_2MMe_2)\}^+$ (*ie* loss of one ligand group) and $\{Ar_3Sb(O_2MMe_2)\}^+$ ions [where M = As (**3.5**) or P (**3.7**)].

3.2.2.5 X-Ray Crystallography

Single crystal X-ray structure determinations were carried out for $[(Ph_3Sb)_2(\mu\text{-}O)(\mu\text{-}O_2PMe_2)_2]$ (**3.3**), obtained as a hemi-hexane solvate; $[(Ph_3Sb)_2(\mu\text{-}O)(\mu\text{-}O_2AsMe_2)_2].0.5C_6H_{14}$ (**3.5**), isomorphous with **3.3**; $[(Ph_3Sb)_2(\mu\text{-}O)(\mu\text{-}O_2AsPh_2)_2].CHCl_3$ (**3.6**) and $[((p\text{-}MeC_6H_4)_3Sb)_2(\mu\text{-}O)(\mu\text{-}O_2PMe_2)_2].0.5C_6H_{14}$ (**3.7**). Crystallographic quality crystals for all compounds were obtained by slow diffusion of hexane vapour into concentrated chloroform solutions of the relevant compound.

Structure of $[(Ph_3Sb)_2(\mu\text{-}O)(\mu\text{-}O_2PMe_2)_2].0.5C_6H_{14}$ (3.3)

The molecular structure of **3.3** is shown in Figure 3.18 and selected bond lengths and angles are listed in Table 3.5. Further details of the crystal structure determination are given in Appendix E.

Figure 3.18 Molecular structure of $[(Ph_3Sb)_2(\mu\text{-}O)(\mu\text{-}O_2PMe_2)_2]$ (3.3)

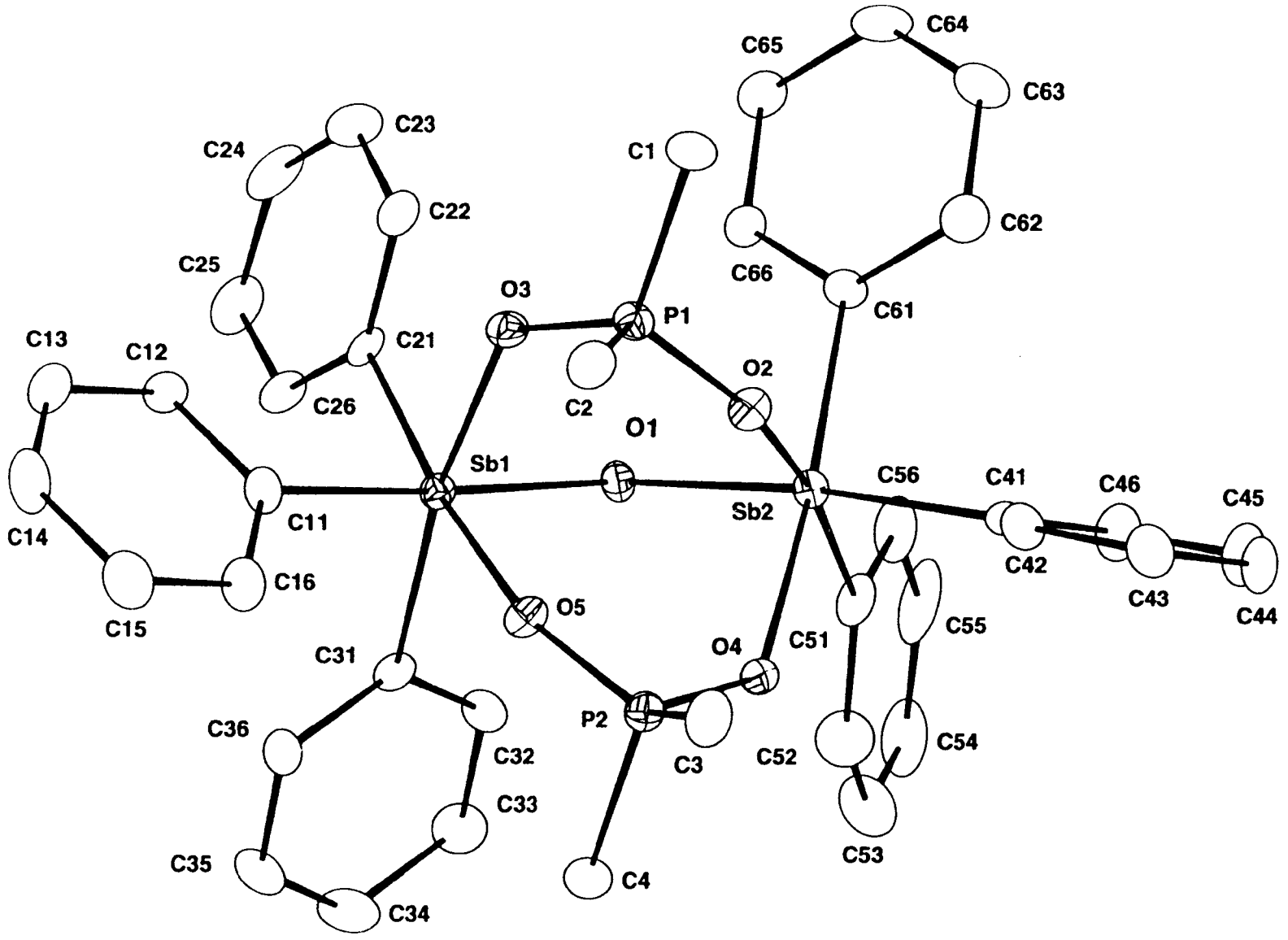

Table 3.5 Selected bond distances and angles, with standard deviations in parentheses for $[(Ph_3Sb)_2(\mu\text{-}O)(\mu\text{-}O_2PMe_2)_2].0.5C_6H_{14}$ (3.3)

Bond lengths, Å		Bond angles, °	
Sb(1) - O(1)	1.958(3)	O(1) - Sb(1) - O(3)	83.8(1)
Sb(1) - O(3)	2.153(3)	O(1) - Sb(1) - O(5)	85.8(1)
Sb(1) - O(5)	2.171(3)	O(3) - Sb(1) - O(5)	83.7(1)
Sb(1) - C(11)	2.164(5)	O(3) - Sb(1) - C(11)	83.7(2)
Sb(1) - C(21)	2.152(5)	O(5) - Sb(1) - C(11)	83.7(2)
Sb(1) - C(31)	2.155(5)	O(1) - Sb(1) - C(21)	91.5(2)
Sb(2) - O(1)	1.952(3)	O(3) - Sb(1) - C(21)	88.9(2)
Sb(2) - O(2)	2.194(3)	C(11) - Sb(1) - C(21)	97.4(2)
Sb(2) - O(4)	2.154(3)	O(1) - Sb(1) - C(31)	91.5(2)
Sb(2) - C(41)	2.153(5)	O(5) - Sb(1) - C(31)	88.5(2)
Sb(2) - C(51)	2.163(5)	C(11) - Sb(1) - C(31)	99.6(2)
Sb(2) - C(61)	2.151(5)	C(21) - Sb(1) - C(31)	98.7(2)
P(1) - O(2)	1.519(4)	O(1) - Sb(1) - C(11)	164.5(2)
P(1) - O(3)	1.528(4)	O(5) - Sb(1) - C(21)	172.4(2)
P(1) - C(1)	1.798(5)	O(3) - Sb(1) - C(31)	171.2(2)
P(1) - C(2)	1.789(6)	O(1) - Sb(2) - O(2)	84.9(1)
P(2) - O(4)	1.514(4)	O(1) - Sb(2) - O(4)	84.3(1)
P(2) - O(5)	1.525(4)	O(2) - Sb(2) - O(4)	82.0(1)
P(2) - C(3)	1.787(6)	O(2) - Sb(2) - C(41)	84.1(2)
P(2) - C(4)	1.795(6)	O(4) - Sb(2) - C(41)	84.0(2)
		O(1) - Sb(2) - C(51)	91.8(2)
		O(4) - Sb(2) - C(51)	88.4(2)
		C(41) - Sb(2) - C(51)	97.3(2)
		O(1) - Sb(2) - C(61)	91.8(2)
		O(2) - Sb(2) - C(61)	89.7(2)
		C(41) - Sb(2) - C(61)	98.4(2)
		C(51) - Sb(2) - C(61)	99.7(2)
		O(1) - Sb(2) - C(41)	165.0(2)
		O(2) - Sb(2) - C(51)	170.2(2)
		O(4) - Sb(2) - C(61)	171.2(2)
		O(2) - P(1) - O(3)	115.5(2)
		C(1) - P(1) - C(2)	107.7(3)
		O(4) - P(2) - O(5)	115.0(2)
		C(3) - P(2) - C(4)	106.7(3)
		Sb(1) - O(1) - Sb(2)	144.2(2)
		Sb(2) - O(2) - P(1)	133.6(2)
		Sb(1) - O(3) - P(1)	128.4(2)
		Sb(2) - O(4) - P(2)	130.6(2)
		Sb(1) - O(5) - P(2)	133.5(2)

The structure of $[(Ph_3Sb)_2(\mu\text{-}O)(\mu\text{-}O_2PMe_2)_2]$ (**3.3**), obtained as a hemi-hexane solvate, consists of two triphenylantimony fragments, bridged by an oxygen atom and two *cis* dimethylphosphinate groups. Coordination about both antimony atoms is distorted octahedral with *cis* angles ranging between 82.0(1)° (O(2)–Sb(2)–O(4)) and 99.7(2)° (C(51)–Sb(2)–C(61)). The three oxygen atoms (and phenyl *ipso* carbons) are configured about each antimony centre in a *fac* geometry.

The Sb–C bond lengths lie within the range 2.151(5) (Sb(2)–C(61)) to 2.164(5) (Sb(1) - C(11)) Å and are comparable with related structures[16]. As could be expected, distinct differences are found between the $Sb–O_{bridge}$ and $Sb–O_{phosphinate}$ bond lengths, with significantly shorter distances found for the $Sb–O_{bridge}$ bonds (1.955 Å mean) than for the $Sb–O_{phosphinate}$ bonds (2.168 Å mean). Moreover, the $Sb–O_{bridge}$ bonds are comparable with the short distances observed for single oxygen bridged compounds such as $[Ph_3SbBr]_2O$ (1.944 Å mean)[55]. The angle about the bridging oxygen in **3.3** is 144.2(2)°, similar to that found for $[(Ph_2SbCl)_2(\mu\text{-}O)(\mu\text{-}O_2P(C_6H_{11})_2)_2]$[16] at 144.7°.

The π-components of the phosphinate ligands are substantially delocalised over the P–O bonds, with bond lengths ranging between 1.514(4) [P(2)–O(4)] and 1.528(4) [P(1)–O(3)] Å. Surprisingly, there is no obvious correlation between shorter P–O bonds and longer Sb–O bond lengths at a specific oxygen atom, for example the short P(2)–O(4) bond of 1.514(4) Å is also associated with a relatively short Sb(2)–O(4) bond of 2.154(3) Å.

The triply bridged structure of **3.3** can be closely compared to those of $[(Cl_3Sb)_2(\mu\text{-}O)(\mu\text{-}O_2PMe_2)_2]$[11] and $[(Ph_2SbCl)_2(\mu\text{-}O)(\mu\text{-}O_2P(C_6H_{11})_2)_2]$[16] with all compounds possessing similar geometries and a *fac* configuration about the antimony centres. The compounds also possess a similar skewing of the octahedral coordination spheres about the antimony atoms relative to the adjacent antimony, presumably to ease the incorporation of the bridging phosphinate ligands.

Structure of $[(Ph_3Sb)_2(\mu\text{-}O)(\mu\text{-}O_2AsMe_2)_2].0.5C_6H_{14}$ (3.5)

The molecular structure of **3.5** is shown in Figure 3.19 and selected bond lengths and angles are listed in Table 3.6. Further details of the crystal structure determination are given in Appendix F.

Table 3.6 Selected bond distances and angles, with standard deviations in parentheses for $[(Ph_3Sb)_2(\mu\text{-}O)(\mu\text{-}O_2AsMe_2)_2].0.5C_6H_{14}$ (3.5)

Bond lengths, Å		Bond angles, °	
Sb(1) - O(1)	1.968(4)	O(1) - Sb(1) - O(3)	85.3(2)
Sb(1) - O(3)	2.124(4)	O(1) - Sb(1) - O(5)	87.9(2)
Sb(1) - O(5)	2.141(4)	O(3) - Sb(1) - O(5)	82.7(2)
Sb(1) - C(11)	2.183(6)	O(3) - Sb(1) - C(11)	85.4(2)
Sb(1) - C(21)	2.156(6)	O(5) - Sb(1) - C(11)	83.3(2)
Sb(1) - C(31)	2.171(6)	O(1) - Sb(1) - C(21)	90.7(2)
Sb(2) - O(1)	1.964(4)	O(3) - Sb(1) - C(21)	88.4(2)
Sb(2) - O(2)	2.156(4)	C(11) - Sb(1) - C(21)	96.7(2)
Sb(2) - O(4)	2.102(4)	O(1) - Sb(1) - C(31)	91.2(2)
Sb(2) - C(41)	2.176(6)	O(5) - Sb(1) - C(31)	91.0(2)
Sb(2) - C(51)	2.173(6)	C(11) - Sb(1) - C(31)	97.2(2)
Sb(2) - C(61)	2.162(6)	C(21) - Sb(1) - C(31)	97.9(2)
As(1) - O(2)	1.675(4)	O(1) - Sb(1) - C(11)	167.9(2)
As(1) - O(3)	1.687(4)	O(5) - Sb(1) - C(21)	171.1(2)
As(1) - C(1)	1.907(7)	O(3) - Sb(1) - C(31)	172.8(2)
As(1) - C(2)	1.911(6)	O(1) - Sb(2) - O(2)	85.9(2)
As(2) - O(4)	1.687(4)	O(1) - Sb(2) - O(4)	86.0(2)
As(2) - O(5)	1.690(4)	O(2) - Sb(2) - O(4)	83.1(2)
As(2) - C(3)	1.903(6)	O(2) - Sb(2) - C(41)	84.9(2)
As(2) - C(4)	1.897(7)	O(4) - Sb(2) - C(41)	84.9(2)
		O(1) - Sb(2) - C(51)	92.4(2)
		O(4) - Sb(2) - C(51)	88.1(2)
		C(41) - Sb(2) - C(51)	95.9(2)
		O(1) - Sb(2) - C(61)	90.8(2)
		O(2) - Sb(2) - C(61)	90.2(2)
		C(41) - Sb(2) - C(61)	97.1(2)
		C(51) - Sb(2) - C(61)	98.5(2)
		O(1) - Sb(2) - C(41)	167.5(2)
		O(2) - Sb(2) - C(51)	171.2(2)
		O(4) - Sb(2) - C(61)	172.8(2)
		O(2) - As(1) - O(3)	115.9(2)
		C(1) - As(1) - C(2)	109.8(3)
		O(4) - As(2) - O(5)	113.8(2)
		C(3) - As(2) - C(4)	108.3(3)
		Sb(1) - O(1) - Sb(2)	145.1(2)
		Sb(2) - O(2) - As(1)	129.8(2)
		Sb(1) - O(3) - As(1)	123.8(2)
		Sb(2) - O(4) - As(2)	126.0(2)
		Sb(1) - O(5) - As(2)	129.2(2)

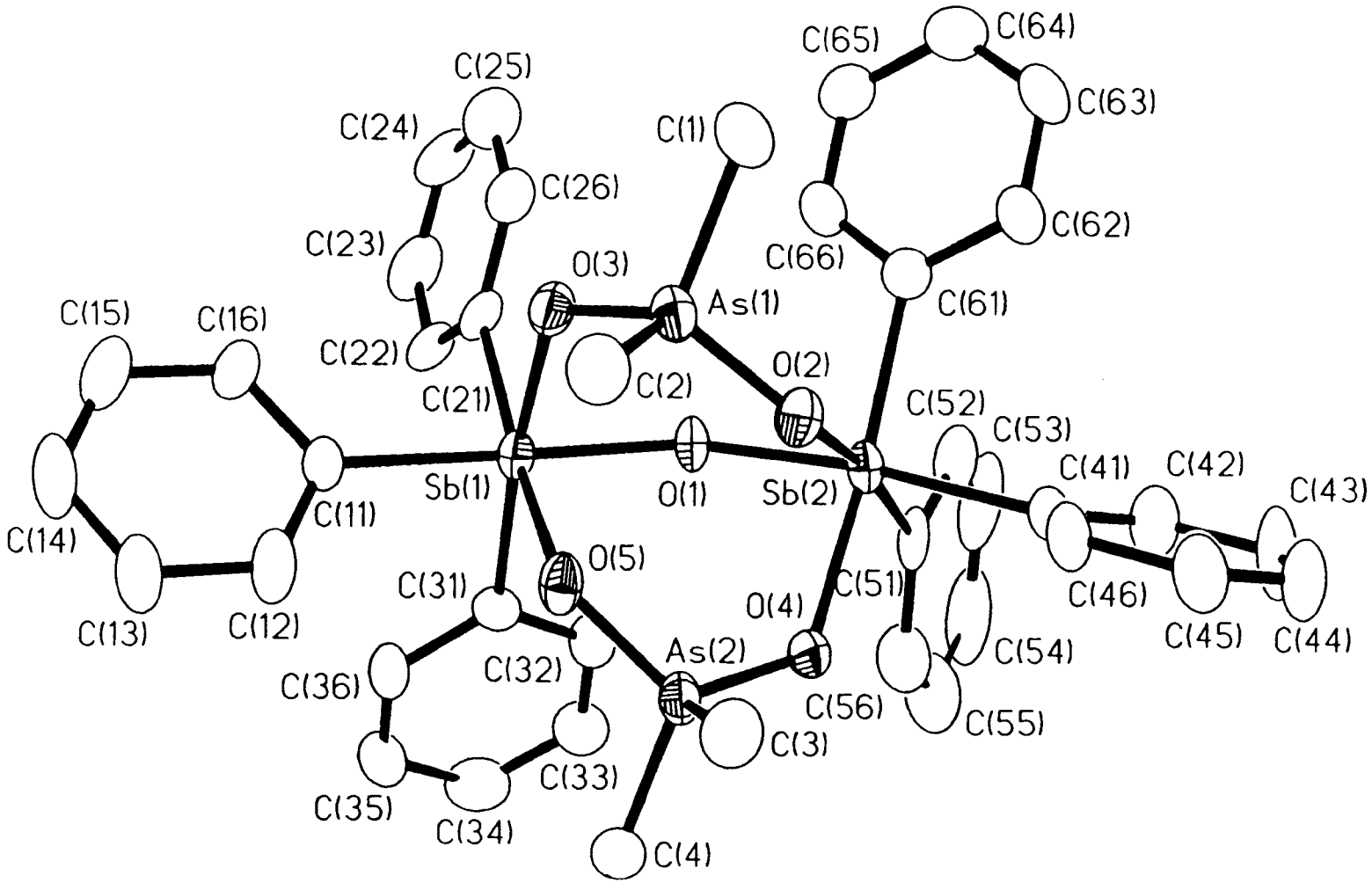

Figure 3.19 Molecular structure of $[(Ph_3Sb)_2(\mu\text{-}O)(\mu\text{-}O_2AsMe_2)_2]$ (3.5)

The structure of **3.5** is isomorphous with that of **3.3**. As in **3.3**, the antimony atoms are each bound to three phenyl groups and are bridged by an oxygen atom. The antimony atoms in **3.5** are further bridged by two dimethylarsinate groups. As expected, coordination about the antimony atoms is octahedral, with the groups arranged in a *fac* configuration.

A notable feature of the structure is the short As–O bond lengths (mean, 1.685 Å) in the dimethylarsinate groups, when compared to those reported earlier (Section 3.2.1.5) for the quadruply bridged compounds **3.1** (mean, 1.710 Å) and **3.4** (mean, 1.702 Å). This could perhaps have been expected from the infrared spectroscopic data, as the ν(As–O) vibrations in **3.5** were found to be at higher wavenumber than those found for the quadruply bridged compounds. Differences between As–O bond lengths show no convincing correlation with the corresponding Sb–O bond lengths at a specific oxygen.

A further feature of interest is the slight elongation of the Sb(1)–C(11) and Sb(2)–C(41) bonds (2.183(6) and 2.176(6) Å), when compared to the remaining Sb–C bonds. This observation is likely to be an effect of the *trans* influence exerted by the tightly bound $Sb–O_{bridge}$ bonds.

Structure of $[(Ph_3Sb)_2(\mu\text{-}O)(\mu\text{-}O_2AsPh_2)_2].CHCl_3$ (3.6)

The molecular structure of **3.6** is shown in Figure 3.20 and selected bond lengths and angles are listed in Table 3.7. Further details of the crystal structure determination are given in Appendix G.

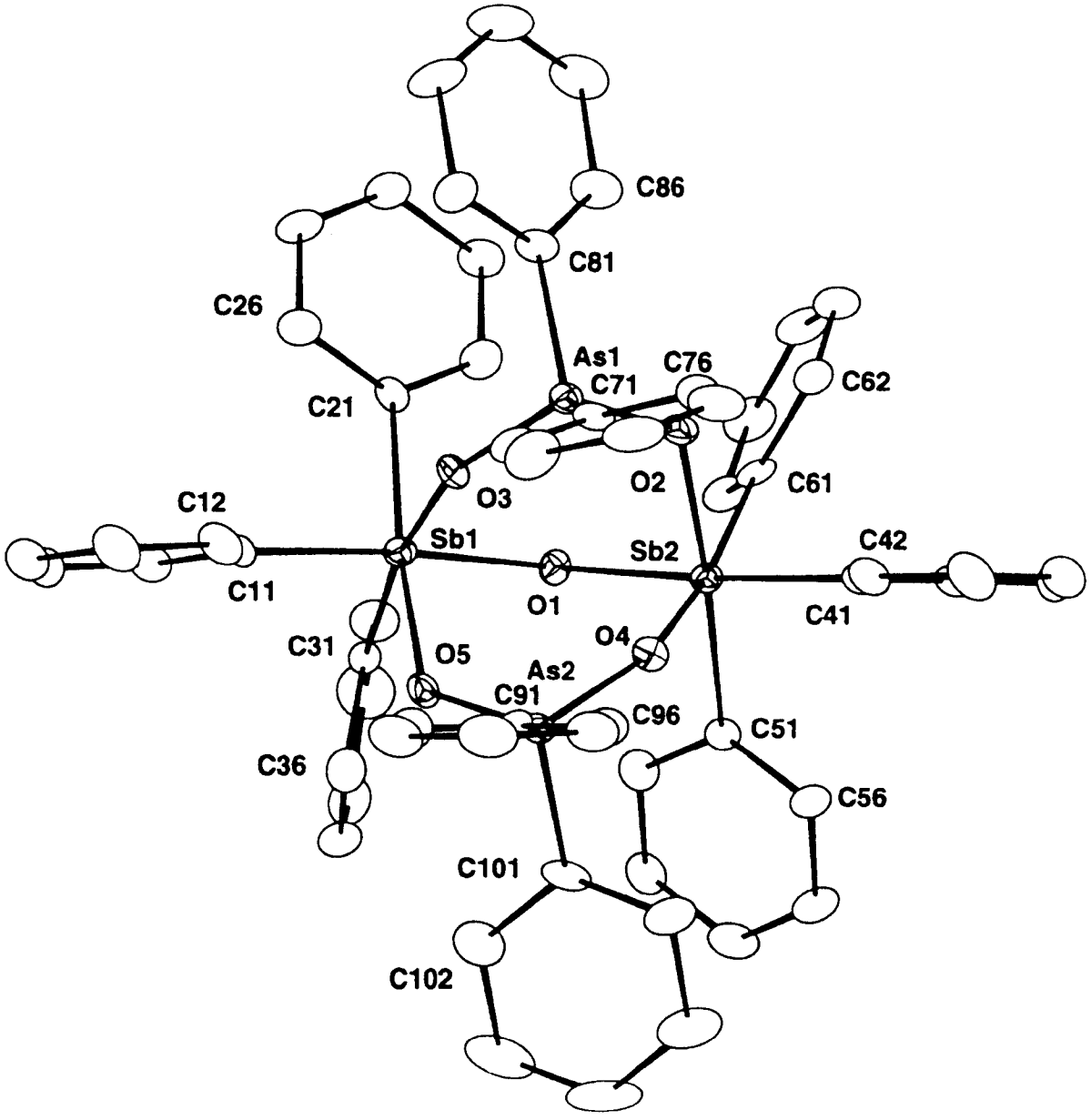

Figure 3.20 Molecular structure of $[(Ph_3Sb)_2(\mu\text{-}O)(\mu\text{-}O_2AsPh_2)_2]$ (3.6)

Table 3.7 Selected bond distances and angles, with standard deviations in parentheses for $[(Ph_3Sb)_2(\mu\text{-}O)(\mu\text{-}O_2AsPh_2)_2].CHCl_3$ (3.6)

Bond lengths, Å		Bond angles, °	
Sb(1) - O(1)	1.967(5)	O(1) - Sb(1) - O(3)	86.6(2)
Sb(1) - O(3)	2.148(5)	O(1) - Sb(1) - O(5)	86.4(2)
Sb(1) - O(5)	2.152(5)	O(3) - Sb(1) - O(5)	80.2(2)
Sb(1) - C(11)	2.135(7)	O(3) - Sb(1) - C(11)	86.3(2)
Sb(1) - C(21)	2.156(7)	O(5) - Sb(1) - C(11)	83.4(2)
Sb(1) - C(31)	2.158(7)	O(1) - Sb(1) - C(21)	90.9(2)
Sb(2) - O(1)	1.947(4)	O(3) - Sb(1) - C(21)	89.5(2)
Sb(2) - O(2)	2.169(4)	C(11) - Sb(1) - C(21)	98.1(3)
Sb(2) - O(4)	2.141(5)	O(1) - Sb(1) - C(31)	87.7(2)
Sb(2) - C(41)	2.167(7)	O(5) - Sb(1) - C(31)	89.7(2)
Sb(2) - C(51)	2.166(7)	C(11) - Sb(1) - C(31)	97.7(3)
Sb(2) - C(61)	2.148(7)	C(21) - Sb(1) - C(31)	100.4(3)
As(1) - O(2)	1.699(5)	O(1) - Sb(1) - C(11)	168.4(2)
As(1) - O(3)	1.680(4)	O(5) - Sb(1) - C(21)	169.4(2)
As(1) - C(71)	1.926(7)	O(3) - Sb(1) - C(31)	168.7(2)
As(1) - C(81)	1.921(7)	O(1) - Sb(2) - O(2)	86.3(2)
As(2) - O(4)	1.686(5)	O(1) - Sb(2) - O(4)	85.9(2)
As(2) - O(5)	1.677(5)	O(2) - Sb(2) - O(4)	82.8(2)
As(2) - C(91)	1.919(7)	O(2) - Sb(2) - C(41)	83.3(2)
As(2) - C(101)	1.923(7)	O(4) - Sb(2) - C(41)	83.9(2)
		O(1) - Sb(2) - C(51)	91.9(2)
		O(4) - Sb(2) - C(51)	90.4(2)
		C(41) - Sb(2) - C(51)	97.4(3)
		O(1) - Sb(2) - C(61)	92.6(2)
		O(2) - Sb(2) - C(61)	86.7(2)
		C(41) - Sb(2) - C(61)	95.7(3)
		C(51) - Sb(2) - C(61)	100.1(3)
		O(1) - Sb(2) - C(41)	166.2(3)
		O(2) - Sb(2) - C(51)	173.1(2)
		O(4) - Sb(2) - C(61)	169.4(2)
		O(2) - As(1) - O(3)	118.8(2)
		C(71) - As(1) - C(81)	109.3(3)
		O(4) - As(2) - O(5)	118.6(2)
		C(91) - As(2) - C(101)	106.8(3)
		Sb(1) - O(1) - Sb(2)	151.7(3)
		Sb(2) - O(2) - As(1)	125.9(2)
		Sb(1) - O(3) - As(1)	129.1(3)
		Sb(2) - O(4) - As(2)	128.6(2)
		Sb(1) - O(5) - As(2)	127.4(2)

In similarity to **3.5**, the structure of **3.6** consists of two triphenylantimony moieties triply bridged by an oxo group and two arsinate groups (diphenylarsinate groups in the case of **3.6**).

Distortions are evident about the *fac* octahedral antimony centres, with the most significant distortions being due to the expansion of the C–Sb–C angles (up to 100.4(3)° for the C(21)–Sb(1)–C(31) angle) and a corresponding contraction of the O–Sb–O angles as far as 80.2(2)° for the O(3)–Sb(1)–O(5) angle.

As was also observed in the structure of **3.5**, there appears to be no simple correlation between As–O bond lengths within the diphenylarsinate groups and Sb–O bond lengths to the same oxygen.

Coordination about the arsenic atoms is distorted tetrahedral with As–O bond lengths lying between 1.677(5) and 1.699(5) Å, comparable to those in **3.5**. However, As–C bond lengths are slightly longer than those in **3.5** and fall within the range 1.919(7) to 1.926(7) Å (which are shorter than those found for the diphenyldithioarsinate groups in the structure of $Ph_2SbS_2AsPh_2$; mean As–C, 1.942 Å[39]).

Structure of $[((p\text{-}MeC_6H_4)_3Sb)_2(\mu\text{-}O)(\mu\text{-}O_2PMe_2)_2].0.5C_6H_{14}$ (3.7)

The molecular structure of **3.7** is shown in Figure 3.21 and selected bond lengths and angles are listed in Table 3.8. Further details of the crystal structure determination are given in Appendix H.

Figure 3.21 Molecular structure of $[((p\text{-}MeC_6H_4)_3Sb)_2(\mu\text{-}O)(\mu\text{-}O_2PMe_2)_2]$ (3.7)

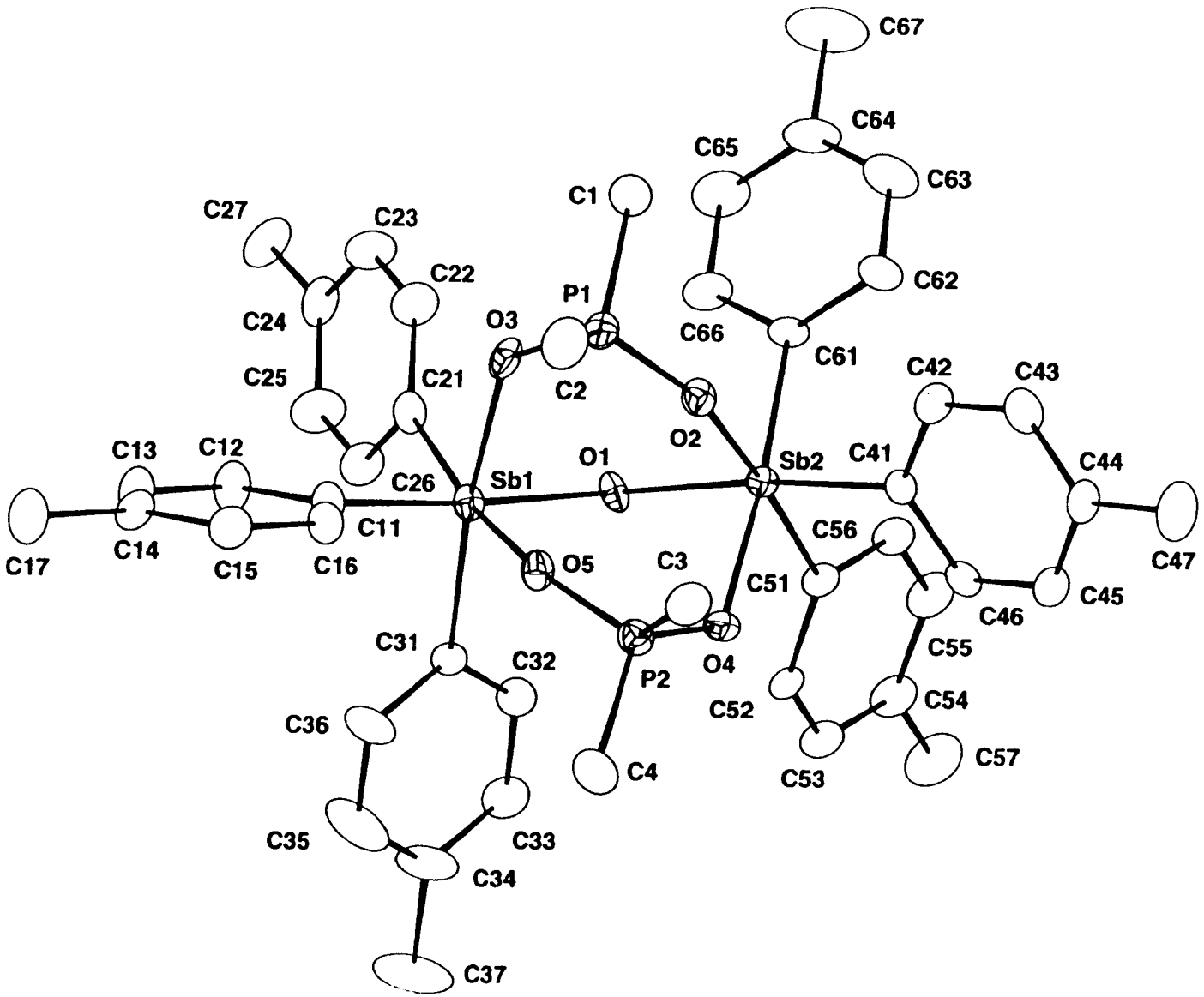

Table 3.8 Selected bond distances and angles, with standard deviations in parentheses for $[((p\text{-}MeC_6H_4)_3Sb)_2(\mu\text{-}O)(\mu\text{-}O_2PMe_2)_2].0.5C_6H_{14}$ (3.7)

Bond lengths, Å		Bond angles, °	
Sb(1) - O(1)	1.972(5)	O(1) - Sb(1) - O(3)	84.3(2)
Sb(1) - O(3)	2.139(5)	O(1) - Sb(1) - O(5)	85.8(2)
Sb(1) - O(5)	2.170(5)	O(3) - Sb(1) - O(5)	82.4(2)
Sb(1) - C(11)	2.158(7)	O(3) - Sb(1) - C(11)	85.5(2)
Sb(1) - C(21)	2.163(8)	O(5) - Sb(1) - C(11)	83.5(2)
Sb(1) - C(31)	2.159(7)	O(1) - Sb(1) - C(21)	91.9(2)
Sb(2) - O(1)	1.954(5)	O(3) - Sb(1) - C(21)	88.4(3)
Sb(2) - O(2)	2.215(5)	C(11) - Sb(1) - C(21)	97.2(3)
Sb(2) - O(4)	2.213(5)	O(1) - Sb(1) - C(31)	92.4(2)
Sb(2) - C(41)	2.144(7)	O(5) - Sb(1) - C(31)	89.3(2)
Sb(2) - C(51)	2.144(7)	C(11) - Sb(1) - C(31)	96.3(3)
Sb(2) - C(61)	2.156(7)	C(21) - Sb(1) - C(31)	99.8(3)
P(1) - O(2)	1.521(5)	O(1) - Sb(1) - C(11)	166.1(2)
P(1) - O(3)	1.533(5)	O(5) - Sb(1) - C(21)	170.8(2)
P(1) - C(1)	1.783(8)	O(3) - Sb(1) - C(31)	171.3(2)
P(1) - C(2)	1.800(8)	O(1) - Sb(2) - O(2)	84.6(2)
P(2) - O(4)	1.524(5)	O(1) - Sb(2) - O(4)	82.2(2)
P(2) - O(5)	1.526(5)	O(2) - Sb(2) - O(4)	85.8(2)
P(2) - C(3)	1.788(8)	O(2) - Sb(2) - C(41)	81.6(2)
P(2) - C(4)	1.792(8)	O(4) - Sb(2) - C(41)	82.4(2)
		O(1) - Sb(2) - C(51)	94.8(3)
		O(4) - Sb(2) - C(51)	87.4(2)
		C(41) - Sb(2) - C(51)	97.2(3)
		O(1) - Sb(2) - C(61)	94.1(3)
		O(2) - Sb(2) - C(61)	89.0(2)
		C(41) - Sb(2) - C(61)	100.0(3)
		C(51) - Sb(2) - C(61)	97.8(3)
		O(1) - Sb(2) - C(41)	160.0(2)
		O(2) - Sb(2) - C(51)	173.2(2)
		O(4) - Sb(2) - C(61)	174.0(2)
		O(2) - P(1) - O(3)	115.1(3)
		C(1) - P(1) - C(2)	107.1(4)
		O(4) - P(2) - O(5)	114.8(3)
		C(3) - P(2) - C(4)	106.4(4)
		Sb(1) - O(1) - Sb(2)	143.6(3)
		Sb(2) - O(2) - P(1)	134.1(3)
		Sb(1) - O(3) - P(1)	129.2(3)
		Sb(2) - O(4) - P(2)	125.8(3)
		Sb(1) - O(5) - P(2)	133.1(3)

Distinct similarities can be drawn between the structure of **3.7** and that of $[(Ph_3Sb)_2(\mu\text{-}O)(\mu\text{-}O_2PMe_2)_2]$ (**3.3**), with both compounds possessing identical bridging groups between antimony centres. As would be therefore expected, coordination about the antimony atoms in **3.7** is distorted octahedral with again a *fac* configuration of the ligands. Both Sb–O and Sb–C bond lengths are similar to those found for **3.3**.

Coordination about the bridging dimethylphosphinate groups is distorted tetrahedral, with bond lengths and angles very similar to those found for **3.3**. The groups also show near complete delocalisation of the π-component having P–O bonds identical within error.

Further discussion

The intersecting six-ring $Sb–O_{ligand}–E–O_{ligand}–Sb–O_{bridge}$ metallacycles, where E = P or As, found in all the triply bridged structures reported herein (**3.3**, **3.5**, **3.6** and **3.7**) have a boat conformation, with the bridging oxo and the phosphorus or arsenic atoms in the 'prow' positions. The similar conformation in $[(Ph_2SbCl)_2(\mu\text{-}O)(\mu\text{-}O_2P(C_6H_{11})_2)_2]$ was justified by a calculated reduction in steric interactions between substituents on the two phosphinate ligands, when compared with a chair conformation[16].

Listings of mean Sb–O bond lengths and Sb–O–Sb angles for the compounds reported here along with related structures have been listed in Table 3.9. On comparison of the data, there is no convincing correlation between shorter $Sb–O_{bridge}$ bond lengths and greater Sb–O–Sb angles, as would be expected using Ferguson and Ridley's suggestions regarding interactions between lone pairs of electrons at the bridging oxygen and unoccupied *d*-orbitals at antimony[56]. Clearly though, the $Sb–O_{bridge}$ bond lengths are short, and tend to suggest that a degree of additional π bonding is present.

Table 3.9 Comparison of Sb–O–Sb dimensions for triply bridged compounds

Compound	Sb–O, Å	Sb–O–Sb, °	Reference
3.3	1.955	144.2	This work
3.5	1.963	145.5	This work
3.6	1.957	151.7	This work
3.7	1.963	143.6	This work
$[SbCl_3(O_2PMe_2)]_2O$	1.942	136.0	[11]
$[Ph_2SbCl(O_2P(C_6H_{11})_2)]_2O$	1.937	144.7	[16]
$[SbF_3(O_2CCF_3)]_2O$	1.893	131.1	[57]

3.2.3 Reduction Compounds

3.2.3.1 Preparation of Compounds

This work was carried out in collaboration with Dr. C.Silvestru, a visiting chemist from 'Babes-Bolyai' University, Cluj-Napoca, Romania.

Reaction of $[Ph_2SbBrO]_2$ (**2.12**) with either two equivalents of $Na(S_2PMe_2).2H_2O$ or $NH_4(S_2PPh_2)$ were found to give non-simple reactions and on fractional crystallisation of the reaction products, the previously reported[39] reduced species $Ph_2SbS_2PMe_2$ (**3.11**) and $Ph_2SbS_2PPh_2$ (**3.12**) were isolated.

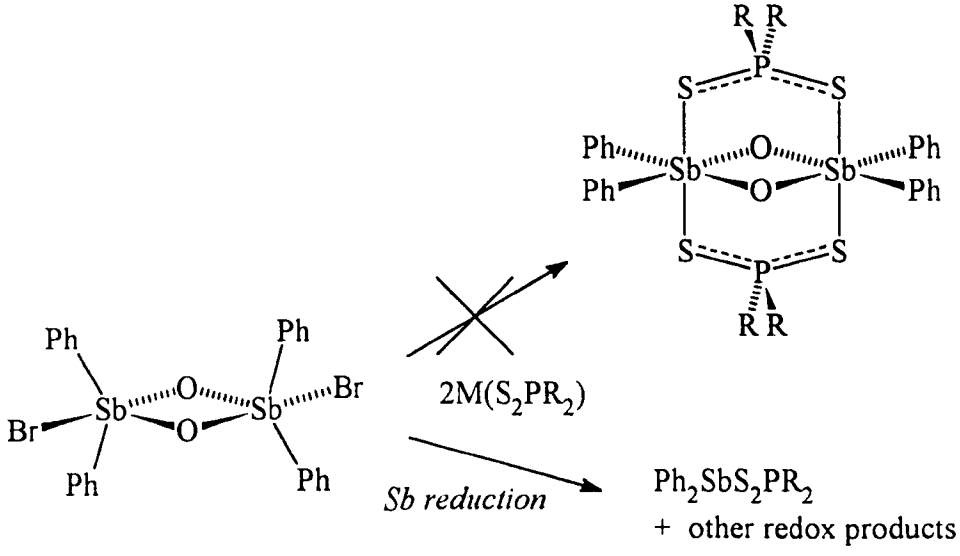

Figure 3.22 Reaction between $[Ph_2SbBrO]_2$ and dithiophosphinate anions

Further analysis into the nature of the redox products was carried out by Dr. Silvestru by repeating reactions in NMR tubes and observing the new products formed. Furthermore, it was also noted that elemental sulfur was precipitated in the reaction between $[Ph_2SbBrO]_2$ and $Na(S_2PMe_2).2H_2O$. From the observations made, a likely equation for this reaction was deemed to be:

$$[Ph_2SbBrO]_2 + 2\,Na(S_2PMe_2).2H_2O \rightarrow Ph_2SbS_2PMe_2\,(\mathbf{3.11}) + Ph_2SbO_2PMe_2 + 2NaBr + 2S + 4H_2O$$

The reaction between $[Ph_2SbBrO]_2$ and $NH_4(S_2PPh_2)$ was also followed by NMR (specifically ^{31}P) and it was found that, in addition to resonances due to **3.12**, signals were also observed that could be assigned to the disulfane $(Ph_2PS_2)_2$ and therefore the reaction seemed to follow a different route from that of the previous reaction.

The reducing nature of dithiophosphinate ligands towards antimony(V) has been previously noted[38] and the only known examples of organoantimony(V) dithiophosphinates are stabilised by the presence of electron donating methyl groups on antimony, *eg.* $Me_3Sb(S_2PPh_2)_2$[38]. Due to the relatively poor (especially NMR) data originally reported, **3.11** and **3.12** have been fully characterised and the crystal structure of **3.11** determined.

3.2.3.2 Infrared Spectroscopy

In addition to many bands due to phenyl modes, the infrared spectrum of $Ph_2SbS_2PPh_2$ (**3.12**) displayed absorptions at 643 and 613 cm^{-1}, assigned to the split $\nu_{asym}(PS_2)$ mode and bands at 532 and 491 cm^{-1} due to $\nu_{sym}(PS_2)$ modes. The separation of the main bands ($\Delta\nu$) of 111 cm^{-1} suggests, according to work reported by Haiduc and co-workers[58], that the ligand is behaving in a unidentate fashion. Indeed, the known solid-state structure of **3.12** shows primarily unidentate behaviour with distinctly different P–S and P=S bond lengths[39]. However, the presence of weak chelating and bridging secondary interactions move the bonding towards a bidentate model. Splitting of the $\nu_{asym}(PS_2)$ and $\nu_{sym}(PS_2)$ bands is considered to be due to the in-phase and out-of-phase components, consistent with the dimeric structure.

Previously reported infrared data for $Ph_2SbS_2PMe_2$ (**3.11**) gives a $\Delta\nu(PS_2)$ value of 121 cm^{-1}, again indicative of unidentate bonding. The structure determination of the compound reported in Section 3.2.3.5, confirms that the ligand is primarily unidentate, although weak secondary interactions are also present from the P=S sulfur.

3.2.3.3 NMR Data

The ^1H NMR spectrum of the compound $Ph_2SbS_2PMe_2$ (**3.11**) was readily assignable and displayed a doublet at 2.08 ppm ($^2J_{HP}$ = 13Hz) due to the S_2PMe_2 moiety and typical second-order phenyl multiplets at 7.39 and 7.69 ppm. The $^{13}C\{^1H\}$ spectrum showed resonances at 29.6(d, $^1J_{CP}$ = 56Hz, P-*Me*), 129.0(*m*-Ph), 129.4(*p*-Ph), 135.9(*o*-Ph) and 140.7(*ipso*-Ph).

Assignment of both the ^1H and $^{13}C\{^1H\}$ spectra of $Ph_2SbS_2PPh_2$ (**3.12**) was greatly aided by a two dimensional $^{13}C/^1H$ correlation spectrum (see Figure 3.23) and the resonances are listed in Table 3.10, along with those for **3.11**. It is of interest to note the very similar chemical shifts of the common Ph_2Sb fragments, indicating a closely related solution behaviour of these two compounds.

Table 3.10 ^1H and ^{13}C resonances for 3.11 and 3.12

		$Ph_2SbS_2PMe_2$ (**3.11**)	$Ph_2SbS_2PPh_2$ (**3.12**)
^1H	S_2PR_2	2.08(d, $^2J_{HP}$ - 13Hz)	7.44(m), 7.96(m)
	Ph_2Sb	7.39(m), 7.69(m)	7.35(m), 7.63(m)
$^{13}C\{^1H\}$	S_2PR_2	29.6(d, $^1J_{CP}$ - 56Hz)	128.1, 128.4, 131.1(d, $^2J_{CP}$ - 12Hz), 137.1(d, $^1J_{CP}$ - 82Hz)
	Ph_2Sb	129.0, 129.4, 135.9, 140.7	128.9, 129.3, 136.0, 140.7

The ^{31}P (non ^1H decoupled) spectrum of **3.11** displayed a binomial septet at 56.5 ppm, whereas the $^{31}P\{^1H\}$ spectrum showed a resonance at 61.4 ppm.

Figure 3.23 $^{13}C/^{1}H$ correlation NMR spectrum of $Ph_2SbS_2PPh_2$ (3.12) in $CDCl_3$

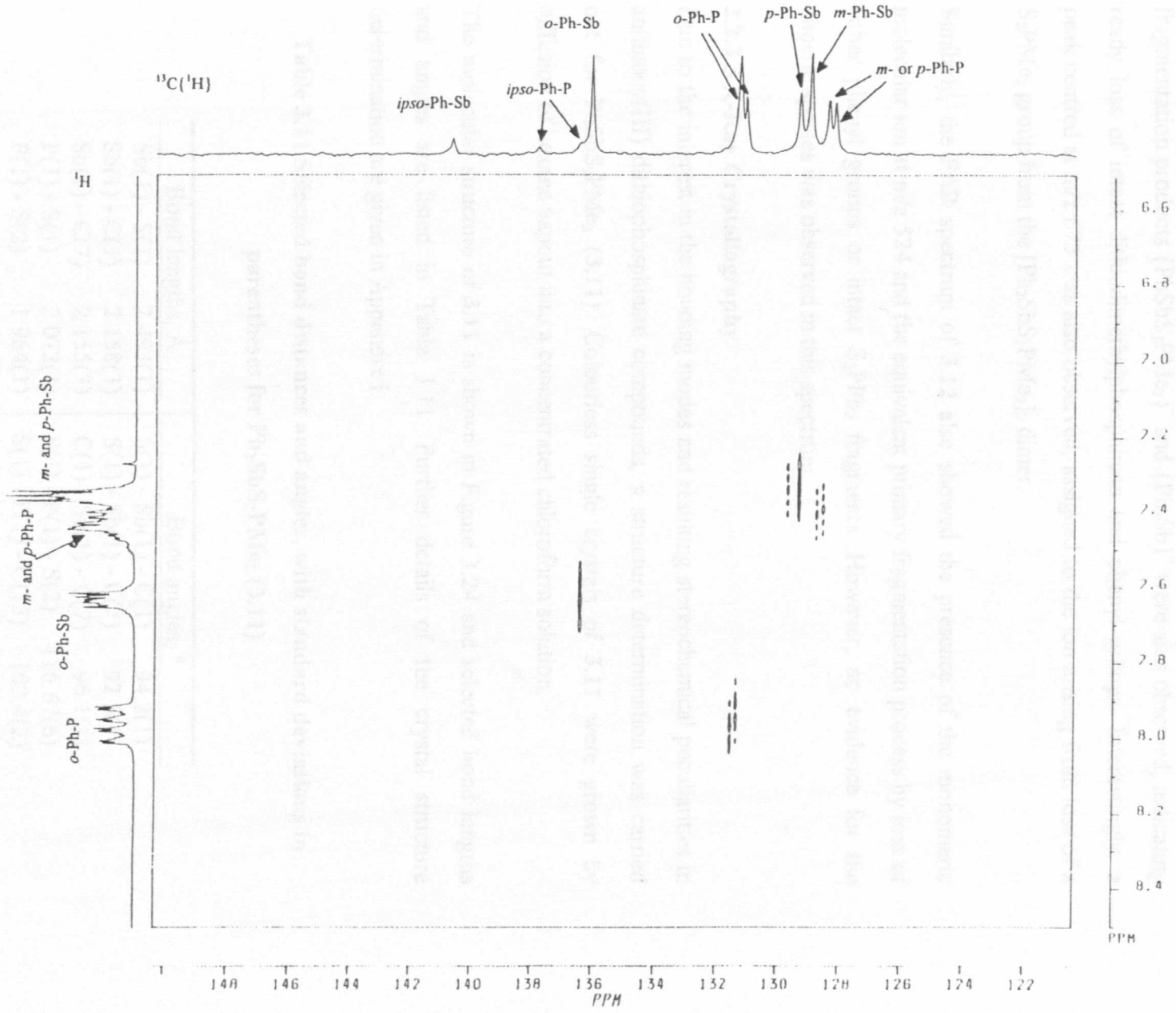

3.2.3.4 Mass Spectroscopy

The FAB mass spectrum of $Ph_2SbS_2PMe_2$ contained an intense ion envelope attributable to the parent ion centred at m/z 400 and peaks due to the two primary fragmentation products $\{PhSbS_2PMe_2\}^+$ and $\{Ph_2Sb\}^+$ were also observed, indicating ready loss of intact dithiodimethylphosphinate and phenyl groups. Interestingly, a peak centred at m/z 675 was also observed, assigned to the ion arising from loss of a S_2PMe_2 group from the $[Ph_2SbS_2PMe_2]_2$ dimer.

Similarly, the FAB spectrum of **3.12** also showed the presence of the monomeric molecular ion at m/z 524 and the equivalent primary fragmentation process by loss of either phenyl groups or intact S_2PPh_2 fragments. However, no evidence for the dimeric species was observed in this spectrum.

3.2.3.5 X-Ray Crystallography

Due to the interest in the bonding modes and resulting stereochemical peculiarities in antimony(III) dithiophosphinate compounds, a structure determination was carried out for $PhSbS_2PMe_2$ (**3.11**). Colourless single crystals of **3.11** were grown by diffusion of hexane vapour into a concentrated chloroform solution.

The molecular structure of **3.11** is shown in Figure 3.24 and selected bond lengths and angles are listed in Table 3.11. Further details of the crystal structure determination are given in Appendix I.

Table 3.11 Selected bond distances and angles, with standard deviations in parentheses for $Ph_2SbS_2PMe_2$ (3.11)

Bond lengths, Å		Bond angles, °	
Sb(1) - S(1)	2.493(1)	S(1) - Sb(1) - C(1)	94.2(1)
Sb(1) - C(1)	2.158(3)	S(1) - Sb(1) - C(7)	92.5(1)
Sb(1) - C(7)	2.155(3)	C(1) - Sb(1) - C(7)	96.1(1)
P(1) - S(1)	2.072(1)	S(1) - P(1) - S(2)	116.67(6)
P(1) - S(2)	1.964(1)	S(1) - P(1) - C(13)	102.4(2)
P(1) - C(13)	1.794(5)	S(2) - P(1) - C(13)	112.9(2)
P(1) - C(14)	1.800(4)	S(1) - P(1) - C(14)	108.3(2)
Sb(1) - S(2')	3.450(1)	S(2) - P(1) - C(14)	110.7(2)
Sb(1) - S(2)	3.779(1)	C(13) - P(1) - C(14)	105.0(3)
		S(1) - Sb(1) - S(2')	173.83(3)
		S(1) - Sb(1) - S(2)	62.52(3)

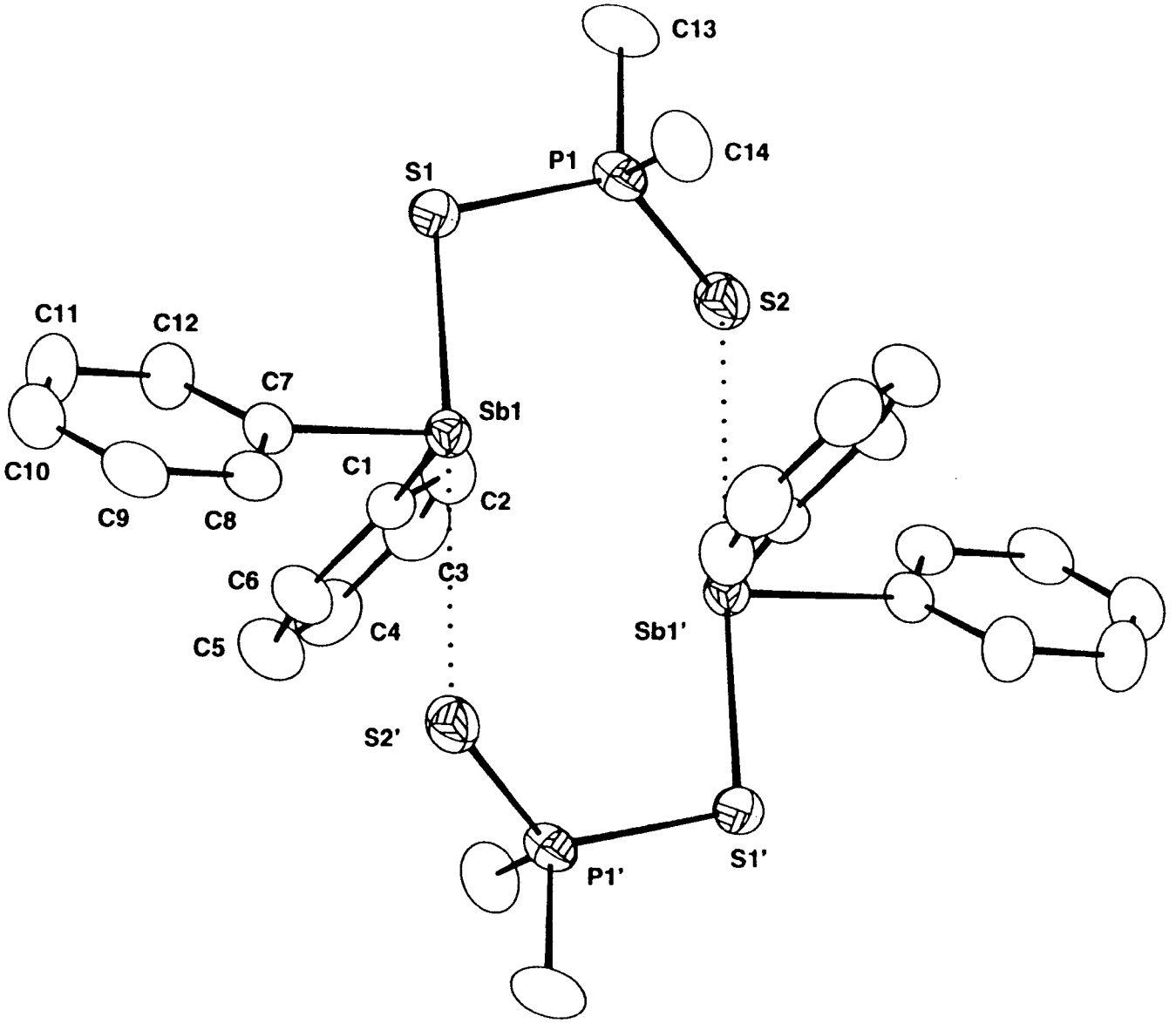

Figure 3.24 Molecular structure of dimeric $Ph_2SbS_2PMe_2$ (3.11)

The crystal structure determination of **3.11** confirms the stoichiometry of the compound, showing it to crystallise as a loose centrosymmetric dimer.

The Sb–S distances [Sb(1)–S(1) 2.493(1), Sb(1)···S(2') 3.450(1) (bridge) and Sb(1)···S(2) 3.779(1) Å (chelate)] indicate effectively unidentate bonding of the dithiophosphinate group. This is reinforced by the P–S bond lengths of 1.964(1) and 2.072(1) Å for the bonds to S(2) and S(1) respectively, close to the values, *ca.* 1.95 and 2.00 Å expected for P=S and P–S bonds[18] (*cf.* values found for the acid Ph_2PS_2H[59], P=S, 1.954; P–S, 2.076 Å). If this view is taken, coordination at antimony in the monomeric unit is trigonal pyramidal with angles at antimony ranging between 92.5(1) [S(1)–Sb(1)–C(7)] and 96.1(1)° [C(1)–Sb(1)–C(7)]. Geometry at phosphorus is distorted tetrahedral, with angles falling between 102.4(2) [S(1)–P(1)–C(13)] and 116.67(6) [S(1)–P(1)–S(2)].

If, however, the secondary Sb···S are considered and in particular the shorter bridging Sb(1)···S(2') interaction (3.450(1) Å), which leads to dimerisation and the formation of an eight membered $Sb_2S_4P_2$ ring, the coordination number about antimony increases. Therefore, if the inter-molecular bridging interaction is considered and a stereochemically active lone pair is assumed to be present, the geometry about antimony is best classed as ψ-trigonal bipyramidal, with the lone pair occupying a coplanar (equatorial) position with respect to the phenyl *ipso*-carbons.

Comparisons with the structures of the related compounds $Ph_2SbS_2PPh_2$ (**3.12**)[39] and $(p\text{-}MeC_6H_4)_2SbS_2PEt_2$[40], show how the structures of these compounds are intimately dependent on 'remote' changes to either the peripheral substituents on either phosphorus or antimony (see Table 3.12). Hence for $(p\text{-}MeC_6H_4)_2SbS_2PEt_2$ the dithiophosphinate ligands are solely bridging, whereas the S_2PPh_2 groups in **3.12** were found to be mainly chelating but also bridged to a lesser extent. Clearly, the structure of **3.11** represents an intermediate position, where the bridging ability of the ligand is more highly developed but the weaker chelating interactions (Sb(1)···S(2), 3.779(1) Å) cannot be ignored.

Table 3.12 Comparison of Sb–S distances (Å) in $R_2SbS_2PR'_2$ dimers

Compound	Sb–S (primary)	Sb···S (chelate)	Sb···S (bridge)
$Ph_2SbS_2PPh_2$[39]	2.490	3.440	3.474
$Ph_2SbS_2PMe_2$	2.493	3.779	3.450
$(p\text{-}MeC_6H_4)_2SbS_2PEt_2$[40]	2.497	3.977	3.437

Discussion

It is notable that the bridging Sb(1)···S(2') interaction in **3.11**, occurs in a position *trans* to the primary bonded sulfur (S(1)–Sb(1)···S(2'), 173.83(3)°). This observation suggests that the primary Lewis acidity displayed at antimony occurs through occupation of the Sb(1)–S(1) σ^* orbital (by one of the S(2') lone pairs).

Coordination chemistry of antimony(III) halides and organoantimony(III) halides have been extensively studied by Norman[60] amongst others and it is generally noted that the secondary interactions at antimony occur in positions *trans* to the more electronegative group(s) (X) on antimony. Furthermore, it is also observed that as the Lewis base···Sb interaction becomes stronger (and hence the distance becomes shorter) the Sb–X bond becomes lengthened due to increasing population of the Sb–X σ^* orbital.

Similarly, in the formation of halogenoantimony(III) anions from neutral SbX_3 and X^- anions, the X^- ion always appears to be attached in a position *trans* to one of the existing Sb–X bonds. Thus, it is possible to generate SbX_4^-, SbX_5^{2-} and SbX_6^{3-} species with successive occupation of Sb–X σ^* orbitals[61,62,63].

An analogous bonding argument can seemingly be extended to compounds of the type $R_2SbX_2PR'_2$ with X = O or S, using structural data from the compounds $Ph_2SbO_2PPh_2$[28], $Ph_2SbOSPPh_2$[28], $Ph_2SbS_2PPh_2$[39], $(p\text{-}MeC_6H_4)_2SbS_2PEt_2$[40], $Me_2SbS_2PMe_2$[42] and $Ph_2SbS_2P(O^iPr)_2$[41] as well as from **3.11**. In all cases bridging (in addition to weaker chelation in some cases) is observed between antimony and the X atom of the ligand that is not formally bonded to antimony and this bridge is always

found in a *trans* position with respect to the primary bonded X atom, giving near linear X–Sb–X configurations. Moreover, it is also found that the primary Sb–X bond is elongated when the secondary bridging interaction becomes shorter, for example in $Ph_2SbS_2PPh_2$ the primary Sb–S bond is 2.490 Å and the secondary bridging Sb···S bond is 3.474 Å, whereas in $Ph_2SbS_2P(O^iPr)_2$ the primary Sb–S bonds are 2.543 (mean) Å and the secondary bridging Sb···S bonds are an average of 3.219 Å. Accordingly, secondary bonding as a result of interactions with the Sb–X σ^* orbitals seems plausible and is consistent with the structural findings.

SUMMARY

The bis-oxo bridged compound $[Ph_2SbBrO]_2$ (**2.12**) reacts with two equivalents of NaO_2AsMe_2 or NaO_2AsPh_2, to give the relevant quadruply bridged compounds $[(Ph_2Sb)_2(\mu\text{-}O)_2(\mu\text{-}O_2AsR_2)_2]$ (R = Me, **3.1**; R = Ph, **3.2**). A related quadruply bridged compound $[((p\text{-}MeC_6H_4)_2Sb)_2(\mu\text{-}O)_2(\mu\text{-}O_2AsMe_2)_2]$ (**3.4**) has also been unexpectedly prepared by a reaction between $[(p\text{-}MeC_6H_4)_3SbBr]_2O$ and NaO_2AsMe_2.

The reaction of $[Ph_2SbBrO]_2$ with two equivalents of NaO_2PMe_2, however, did not give a quadruply bridged product, but instead the rearranged triply bridged species $[(Ph_3Sb)_2(\mu\text{-}O)(\mu\text{-}O_2PMe_2)_2]$ (**3.3**). A better synthesis of the same compound was afforded by reaction of $[Ph_3SbBr]_2O$ (**2.7**) with two equivalents of the same phosphinate salt. Reactions of $[Ph_3SbBr]_2O$ with two equivalents of NaO_2AsMe_2 or NaO_2AsPh_2, led to the formation of further triply bridged species, $[(Ph_3Sb)_2(\mu\text{-}O)(\mu\text{-}O_2AsMe_2)_2]$ (**3.5**) and $[(Ph_3Sb)_2(\mu\text{-}O)(\mu\text{-}O_2AsPh_2)_2]$ (**3.6**). Synthesis of $[((p\text{-}MeC_6H_4)_3Sb)_2(\mu\text{-}O)(\mu\text{-}O_2PMe_2)_2]$ (**3.7**) was also achieved, by a reaction between $[(p\text{-}MeC_6H_4)_3SbBr]_2O$ and two equivalents of NaO_2PMe_2.

The compounds $[Me_3Sb(O_2PMe_2)]_2O$ (**3.8**) and $[Me_3Sb(O_2AsPh_2)]_2O$ (**3.9**) were formed by reaction between $[Me_3SbCl]_2O$ and the relevant sodium phosphinate or sodium arsinate. Lack of structural data or convincing infrared results, however, leads to uncertainties in the identification of the coordination style of the ligands.

Problems of reduction were encountered in the reaction between $[Ph_2SbBrO]_2$ and dithiophosphinate reagents, yielding the antimony(III) compounds $Ph_2SbS_2PMe_2$ (**3.11**) and $Ph_2SbS_2PPh_2$ (**3.12**). A structure determination of the former compound, shows a dimeric species, with weak secondary Sb···S bonds.

3.3 EXPERIMENTAL AND CHARACTERISING DATA

The sodium salts NaO_2AsMe_2, NaO_2AsPh_2, NaO_2PMe_2, NaO_2PPh_2, $NaS_2PMe_2.2H_2O$ were prepared by reaction of a stoichiometric amount of the relevant acid with sodium ethoxide (prepared *in situ* by adding lumps of sodium to ethanol) in ethanol. $NH_4S_2PPh_2$ was donated by Dr. C.Silvestru and used as received.

3.3.1 Preparation of dimethylphosphinic acid

This preparation was adapted from the method of Reinhardt, Bianchi and Molle[64]

3.3.1.1 Preparation of $[Me_2(S)P]_2$

Methyl iodide (31ml, 70.97g, 0.50mol) was added dropwise to a stirred suspension of magnesium (11.8g, 0.48mol) in diethyl ether (200ml) under argon. The addition was such as to maintain the diethyl ether at a gentle reflux. After complete addition of the methyl iodide a grey solution resulted, which was then cooled to -30°C and thiophosphoryl chloride (16.5ml, 25.41g, 0.15mol) in diethyl ether (30ml), also under argon, was then slowly added with stirring. The reaction mixture was allowed to warm to room temperature and stirred for a further 16 hours. After this time, dilute sulfuric acid (100ml, 2M) was then carefully added to ensure complete hydrolysis of the mixture. The resultant precipitate was isolated by filtration, dried and recrystallised from toluene/ethanol (3:1 v/v) yielding clear crystals. Yield 9.2g (66%); mp 223-225°C [lit 227-228°C[64]].

Found: C,25.77; H,6.73: $C_4H_{12}P_2S_2$ requires C,25.80; H,6.50 %.

^{1}H NMR (250MHz, $CDCl_3$, RT) δ 1.97(q, 12H, $^{2,3}J_{HP}$ - 6Hz, *Me*-P).

MS (E.I.): $\{(SPMe_2)_2\ (\mathbf{M})\}^+$ (m/z 186, 53%); $\{\mathbf{M}$ - Me$\}^+$ (m/z 171, 63%); $\{\mathbf{M}$ - Me - S$\}^+$ (m/z 139, 8%); $\{\mathbf{M}$ - 2Me - S$\}^+$ (m/z 125, 5%); $\{SPMe_2\}^+$ (m/z 93, 100%).

3.3.1.2 Preparation of Me_2PO_2H

A solution of hydrogen peroxide (110ml, 30% v/v in H_2O, 110mmol) was added dropwise to a stirring and refluxing suspension of bis(dimethylthiophosphine) (6.58g, 35.3mmol) and carbon tetrachloride (30ml) and the mixture was refluxed for a further 2 hours. The mixture was then cooled and filtered to remove elemental sulfur. Removal of volatiles *in vacuo* gave crude product that was recrystallised from benzene to give clear crystals. Yield 5.11g (77%); mp 86-88°C [lit 89-91°C[64]].

Found: C,24.63; H,7.70: $C_2H_7O_2P$ requires C,25.54; H,7.50 %.

^{1}H NMR (250MHz, $CDCl_3$, RT) δ 1.51(d, 6H, $^2J_{HP}$ - 14Hz, *Me*-P); 8.85(s, 1H, PO_2H).

3.3.2 Preparation of $[(Ph_2Sb)_2(\mu\text{-}O)_2(\mu\text{-}O_2AsMe_2)_2]$ (3.1)

A solution of $[Ph_2SbBrO]_2$ (**2.12**) (4.00g, 5.4mmol) in dichloromethane (50ml) was added to a stirred suspension of sodium dimethylarsinate (1.90g, 11.9mmol) and dichloromethane (10ml) and the resultant reaction mixture was refluxed for 24 hours. After this time the mixture was filtered and the solvent removed *in vacuo* affording crude product. Recrystallisation from chloroform overlayered with twice the volume of hexane afforded the compound as clear crystals. Yield 3.98g (86%); mp 324-327°C.

Found: C,39.38; H,3.83: $C_{28}H_{32}As_2O_6Sb_2$ requires C,39.20; H,3.76 % (non-crystalline sample).

^{1}H NMR (250MHz, $CDCl_3$, RT) δ 2.00(s, 12H, *Me*-As); 7.33(m, 12H, *m*- and *p*-Ph); 7.83(m, 8H, *o*-Ph).

IR (nujol mull, CsI): 1430(s), 1072(m), 817(vs, sh), 796(vs), 738(s), 696(s), 652(m), 608(m), 518(s), 487(s), 466(m).

MS (FAB): $\{[Ph_2Sb(O_2AsMe_2)O]_2(\mathbf{M})\}^+$ (m/z 858, 100%); $\{\mathbf{M} - (O_2AsMe_2)\}^+$ (m/z 721, 30%); $\{\mathbf{M} - 2Ph\}^+$ (m/z 704, 28%); $\{\mathbf{M} - 2Ph - (O_2AsMe_2)\}^+$ (m/z 567, 43%);$\{[SbO]_2(O_2AsMe_2)\}^+$ (m/z 413, 26%).

3.3.3 Preparation of $[(Ph_2Sb)_2(\mu\text{-}O)_2(\mu\text{-}O_2AsPh_2)_2]$ (3.2)

A solution of $[Ph_2SbBrO]_2$ (**2.12**) (3.20g, 4.3mmol) in dichloromethane (80ml) was added to a stirred suspension of sodium diphenylarsinate (2.60g, 9.2mmol) and dichloromethane (10ml) and the resultant reaction mixture was refluxed for 40 hours. After this time the mixture was filtered and the solvent removed from the filtrate *in vacuo*, giving a white precipitate. Purification of the product proved difficult, but repeated recrystallisations from chloroform/hexane gave a very low yield of crystalline material. Yield 143mg (3%); mp 260-266°C.

Found: C,51.22; H,3.41: $C_{48}H_{40}As_2O_6Sb_2$ requires C,52.12; H,3.64 %.

^{1}H NMR (250MHz, $CDCl_3$, RT) δ 7.30-7.80(m, very broad, 40H, *Ph*-As and *Ph*-Sb)

IR (nujol mull, CsI): 1087(w), 823(vs, sh), 812(vs), 735(s), 691(s), 490(m), 457(m).

MS (FAB): $\{[Ph_2Sb(O_2AsPh_2)O]_2$ **(M)** + 2H$\}^+$ (m/z 1108, 73%); {**M** - 2Ph + H$\}^+$ (m/z 953, 16%); {**M** - $(O_2AsPh_2)\}^+$ (m/z 845, 38%); $\{[Ph_2SbO]_2(O_2As)\}^+$ (m/z 691, 100%); $\{Ph_2SbO_2AsPh_2\}^+$ (m/z 537, 75%); $\{PhSbO_2AsPh_2\}^+$ (m/z 459, 36%).

3.3.4 Preparation of $[((p\text{-}MeC_6H_4)_2Sb)_2(\mu\text{-}O)_2(\mu\text{-}O_2AsMe_2)_2]$ (3.4)

A mixture of $[(p\text{-}MeC_6H_4)_3SbBr]_2O$ (**2.8**) (423mg, 0.438mmol), sodium dimethylarsinate (170mg, 1.063mmol) and dichloromethane (20ml) was stirred together under reflux for 16 hours. The precipitated white solid was filtered off and the clear filtrate was then evaporated *in vacuo*. Recrystallisation from chloroform/hexane gave a small amount of crystalline product. Yield 104mg (26%); mp 313-320°C.

Found: C,41.67; H,4.45: $C_{32}H_{40}As_2O_6Sb_2$ requires C,42.05; H,4.41 %

($C_{46}H_{54}As_2O_5Sb_2$ requires C,51.14; H,5.04 %).

^{1}H NMR (250MHz, $CDCl_3$, RT) δ 1.96(s, 12H, *Me*-As); 2.32(s, 12H, *Me*-Ar); 7.15(d, 8H, $^3J_{HH}$ - 8Hz, *m*-Ar); 7.73(d, 8H, $^3J_{HH}$ - 8Hz, *o*-Ar).

IR (nujol mull, CsI): 1492(m), 1307(w), 1270(w), 1183(m), 1070(m), 1018(w), 901(m), 869(m), 824(vs, sh), 805(vs), 793(s, sh), 722(w), 652(m), 609(m), 578(m), 516(s), 488(s), 430(w).

MS (FAB): $\{[(p\text{-}MeC_6H_4)_2Sb(O_2AsMe_2)O]_2$ **(M)** + H$\}^+$ (m/z 915, 24%); $\{[(p\text{-}MeC_6H_4)_2Sb(O_2AsMe_2)\}^+$ (m/z 577, 13%); $\{[(p\text{-}MeC_6H_4)_3Sb(O_2AsMe_2)\}^+$ (m/z 531, 100%); $\{[(p\text{-}MeC_6H_4)Sb(O_2AsMe_2)\}^+$ (m/z 349, 12%).

3.3.5(a) Preparation of $[(Ph_3Sb)_2(\mu\text{-}O)(\mu\text{-}O_2PMe_2)_2]$ (3.3) - Method A

A solution of $[Ph_3SbBr]_2O$ (**2.7**) (532mg, 0.60mmol) in dichloromethane (20ml), was added to a stirred suspension of sodium dimethylphosphinate (156mg, 1.34mmol) and dichloromethane (10ml) and the resultant reaction mixture was refluxed for 24 hours. After this time the mixture was filtered and the solvent removed from the filtrate *in vacuo*, giving a white precipitate. Pure crystalline product was obtained by overlayering a chloroform solution with twice the volume of hexane. Yield 480mg (88%); mp 188-192°C.

Found: C,53.08; H,5.07: $C_{40}H_{42}O_5P_2Sb_2$ requires C,52.90; H,4.66 % (non-crystalline sample).

^{1}H NMR (250MHz, $CDCl_3$, RT) Damp solvent: δ 1.00(d, 6H, $^2J_{HP}$ - 14Hz, *Me*-P); 7.57(m, 9H, *m*- and *p*-Ph); 8.21(m, 6H, *o*-Ph), species thought to be $Ph_3Sb(O_2PMe_2)OH$ (**3.10**).

Anhydrous conditions: δ 0.72(d, 12H, $^2J_{HP}$ - 14Hz, *Me*-P-**A**); 1.03(broad hump, 12H, *Me*-P-**B**); 7.16(t, 12H, $^3J_{HH}$ - 7Hz, *m*-Ph-**A**); 7.38(m, 18H, *m*- and *p*-Ph-**B**); 7.45(t, 6H, $^3J_{HH}$ - 7Hz, *p*-Ph-**A**); 7.56(d, 12H, $^3J_{HH}$ - 7Hz, *o*-Ph-**A**); 7.68(m, 12H, *o*-Ph-**B**), where **A** and **B** are distinct, unidentified solution species.

IR (nujol mull, CsI): 1430(m), 1301(m), 1112(vs), 1062(m), 1046(vs), 1032(vs), 998(w), 871(m), 863(m), 749(s), 735(s), 693(s), 659(w), 512(w), 487(w), 464(m), 437(w).

MS (FAB): $\{[Ph_3Sb(O_2PMe_2)]_2O$ (**M**) - Ph$\}^+$ (m/z 831, 4.4%); {**M** - $(O_2PMe_2)\}^+$ (m/z 815, 9.4%); $\{[Ph_2Sb]_2O(O_2PMe_2)\}^+$ (m/z 661, 5.1%); $\{Ph_3Sb(O_2PMe_2)\}^+$ (m/z 445, 100%).

3.3.5(b) Preparation of $[(Ph_3Sb)_2(\mu\text{-}O)(\mu\text{-}O_2PMe_2)_2]$ (3.3) - Method B

A mixture of $[Ph_2SbBrO]_2$ (**2.12**) (527mg, 0.71mmol), sodium dimethylphosphinate (173mg, 1.49mmol) and toluene (30ml) were stirred together at reflux for 24 hours. After this time the mixture was filtered and the solvent removed from the filtrate *in vacuo*, giving crude product. After recrystallising from chloroform/hexane, a crop of crystals of **3.3** was isolated from the remaining oily residue. Yield 77mg (12%).

3.3.6 Preparation of $[(Ph_3Sb)_2(\mu\text{-}O)(\mu\text{-}O_2AsMe_2)_2]$ (3.5)

A mixture of $[Ph_3SbBr]_2O$ (**2.7**) (744mg, 0.84mmol), sodium dimethylarsinate (361mg, 2.3mmol) and dichloromethane (35ml) was stirred at reflux for 20 hours. The resulting mixture was filtered and the solvent was removed *in vacuo*, giving crude product. Analytically and spectroscopically pure crystals were obtained by diffusion of hexane vapour into a concentrated chloroform solution. Yield 620mg (74%); mp 241-245°C.

Found: C,47.85; H,4.28: $C_{40}H_{42}As_2O_5Sb_2$ requires C,48.23; H,4.25 % (non-crystalline sample).

^{1}H NMR (250MHz, $CDCl_3$, RT) Anhydrous conditions: δ 0.71(s, broad, *Me*-As); 1.89(s, broad, *Me*-As); 7.17(t, 12H, $^3J_{HH}$ - 7Hz, *m*-Ph-**A**); 7.27(masked t, 6H, *p*-Ph-**A**); 7.27(m, 18H, *m*- and *p*-Ph-**B**); 7.61(d, 12H, $^3J_{HH}$ - 7Hz, *o*-Ph-**A**); 7.71(m, 12H, *o*-Ph-**B**), where **A** and **B** are distinct, unidentified solution species.

IR (nujol mull, CsI): 1429(s), 1265(m), 1185(m), 1069(s), 1023(w), 852(vs, br), 738(vs), 698(vs), 657(m), 641(m), 465(s), 421(m).

MS (FAB): $\{[Ph_3Sb(O_2AsMe_2)]_2O$ **(M)**$\}^+$ (m/z 996, 0.4%); $\{$**M** - $(O_2AsMe_2)\}^+$ (m/z 859, 5.5%); $\{Ph_3Sb(O_2AsMe_2)\}^+$ (m/z 489, 60.8%); $\{PhSb(O_2AsMe_2)\}^+$ (m/z 335, 27.7%); $\{Ph_2Sb\}^+$ (m/z 275, 38.9%).

3.3.7 Preparation of $[(Ph_3Sb)_2(\mu\text{-}O)(\mu\text{-}O_2AsPh_2)_2]$ (3.6)

A mixture of $[Ph_3SbBr]_2O$ (**2.7**) (598mg, 0.68mmol), sodium diphenylarsinate (489mg, 1.7mmol) and dichloromethane (35ml) was stirred at reflux for 24 hours. The resulting mixture was filtered and the solvent was removed *in vacuo*, giving crude product. Analytically and spectroscopically pure crystals were obtained by diffusion of hexane vapour into a concentrated chloroform solution. Yield 626mg (74%); mp 244-247°C.

Found: C,53.06; H,3.68: $C_{60}H_{50}As_2O_5Sb_2$ requires C,57.91; H,4.05: $C_{60}H_{50}As_2O_5Sb_2.CHCl_3$ requires C,53.72; H,3.77 % (crystalline sample).

^{1}H NMR (250MHz, $CDCl_3$, RT) Anhydrous conditions: δ 6.97(m); 7.08(m); 7.33(m); 7.43(m); 7.58(d, $^3J_{HH}$ - 7Hz); 8.04(m) assignment of the resonances was not achieved.

IR (nujol mull, CsI): 1440(s), 1430(s), 1306(m), 1183(m), 1090(s), 1069(s), 1023(m), 999(m), 831(vs, br), 735(vs), 692(vs), 658(m), 609(w), 536(m), 464(s), 410(m).

3.3.8 Preparation of $[((p\text{-}MeC_6H_4)_3Sb)_2(\mu\text{-}O)(\mu\text{-}O_2PMe_2)_2]$ (3.7)

A solution of $[(p\text{-}MeC_6H_4)_3SbBr]_2O$ (**2.8**) (591mg, 0.61mmol) in dichloromethane (20ml) was added to a stirring suspension of sodium dimethylphosphinate (152mg, 1.31mmol) and dichloromethane (10ml) and the resultant reaction mixture was stirred at room temperature for 18 hours. After this time the mixture was filtered and the solvent removed *in vacuo*, giving a white precipitate. Pure crystalline product was obtained by overlayering a chloroform solution with three times the volume of hexane. Yield 352mg (58%).

Found: C,55.17; H,5.42: $C_{46}H_{54}O_5P_2Sb_2$ requires C,55.67; H,5.48 % (non-crystalline sample).

^{1}H NMR (250MHz, $CDCl_3$, RT) Damp solvent: δ 0.97(d, 6H, $^2J_{HP}$ - 14Hz, *Me*-P); 2.40(s, 9H, *Me*-Ar); 7.51(d, 6H, $^3J_{HH}$ - 8Hz, *m*-Ar); 8.12(d, 6H, $^3J_{HH}$ - 8Hz, *o*-Ph), species thought to be $(p\text{-}MeC_6H_4)_3Sb(O_2PMe_2)OH$.

Anhydrous conditions: δ 0.70(d, 12H, $^2J_{HP}$ - 14Hz, *Me*-P-**A**); 1.05(broad hump, 12H, *Me*-P-**B**); 2.38(s, 18H, *Me*-Ar-**A**); 2.39(s, 18H, Me-Ar-**B**); 7.10(d, 12H, $^3J_{HH}$ - 8Hz, *m*-Ar-**A**); 7.25(d, 12H, $^3J_{HH}$ - 8Hz, *m*-Ph-**B**); 7.55(d, 12H, $^3J_{HH}$ - 8Hz, *o*-Ph-**A**); 7.61(d, 12H, $^3J_{HH}$ - 8Hz, *o*-Ph-**B**), where **A** and **B** are distinct, unidentified solution species.

IR (nujol mull, CsI): 1298(m), 1187(m), 1111(vs), 1048(vs), 1033(vs), 863(s), 801(s), 732(s), 705(w), 576(w), 487(s).

MS (FAB): $\{[(p\text{-}MeC_6H_4)_3Sb(O_2PMe_2)]_2O$ (**M**) - 2Me$\}^+$ (m/z 962, 4%); {**M** - $(O_2PMe_2)\}^+$ (m/z 899, 0.4%); $\{(p\text{-}MeC_6H_4)_3Sb(O_2PMe_2)\}^+$ (m/z 487, 100%).

3.3.9 Reaction of $[(o\text{-}MeC_6H_4)_3SbBr]_2O$ with NaO_2PMe_2

A solution of $[(o\text{-}MeC_6H_4)_3SbBr]_2O$ (**2.9**) (294mg, 0.30mmol) in dichloromethane (20ml) was added to a stirring suspension of sodium dimethylphosphinate (76mg, 0.65mmol) and dichloromethane (5ml) and the resulting mixture was refluxed for 24

hours. After filtration and removal of volatiles *in vacuo* crude unidentified product was isolated. ^{1}H NMR showed the material contained no dimethylphosphinate groups.

3.3.10 Reaction of $(Ph_3SbBr)_2O$ with one equivalent of NaO_2AsMe_2

A mixture of $[Ph_3SbBr]_2O$ (**2.7**) (645mg, 0.73mmol), sodium dimethylarsinate (122mg, 0.76mmol) and dichloromethane (25ml) was stirred together at reflux for 6 hours. The resulting mixture was filtered and the solvent was removed *in vacuo*, giving crude product. Analysis of this material, showed the presence of a mixture of $[Ph_3SbBr]_2O$ and $[(Ph_3Sb)_2(\mu\text{-}O)(\mu\text{-}O_2AsMe_2)_2]$ (**3.5**).

3.3.11 Reaction of $[Ph_2SbBrO]_2$ with one equivalent of NaO_2AsMe_2

Sodium dimethylarsinate (395mg, 2.47mmol) was added to a solution of $[Ph_2SbBrO]_2$ (**2.12**) (1.829g, 2.46mmol) in dichloromethane (50ml). The mixture was then stirred at reflux for 6 hours, after which time the insolubles were removed by filtration and the solvent was removed *in vacuo*. Recrystallisation from chloroform gave a small amount of crystalline product, in addition to a thick oil. The crystals were isolated, but are as yet identified. Yield 230mg.

Crystal cell data: Orthorhombic; a = 7.855(2), b = 19.729(5), c = 24.322(7); Space group $P2_12_12_1$. The crystal was not of sufficient quality for complete data collection.

3.3.12 Reaction of $[Ph_3SbBr]_2O$ with NaO_2PPh_2

Sodium diphenylphosphinate (746mg, 3.11mmol) was added to a stirred solution of $[Ph_3SbBr]_2O$ (**2.7**) (1.29g, 1.46mmol) in dichloromethane (30ml) and the resulting mixture was refluxed for 5 hours. The mixture was then filtered and the volatiles removed from the filtrate *in vacuo*. Analysis of the residue showed a mixture of unidentified products.

3.3.13 Preparation of $[(Me_3Sb)_2(\mu\text{-}O)(\mu\text{-}O_2AsPh_2)_2]$ (3.9)

A solution of $[Me_3SbCl]_2O$ (**2.10**) (392mg, 0.93mmol) in dichloromethane (20ml), was added to a stirred suspension of sodium diphenylarsinate (556mg, 1.96mmol) and dichloromethane (15ml) at 0°C under argon. The resultant reaction mixture was then stirred at room temperature for 6 hours after which time it was filtered. The clear filtrate was then concentrated (*ca.* 5ml) and overlayered with hexane (15ml). After 3 days clumps of crystals appeared that were isolated by decanting off the mother liquor and were dried *in vacuo*. Yield 601mg (74%).

Due to the extremely air sensitive nature of this compound satisfactory micro-analytical results could not be obtained.

^{1}H NMR (250MHz, $CDCl_3$, RT) Anhydrous conditions: δ 1.66(s, 18H, *Me*-Sb); 5.27(s, 2H, CH_2Cl_2); 7.41(m, 12H, *m*- and *p*-Ph); 7.70(m, 8H, *o*-Ph).

^{13}C{^{1}H} NMR (69 MHz, $CDCl_3$, RT) δ 16.8(*Me*-Sb); 128.7(*m*-Ph); 130.4(*p*-Ph); 131.2(*o*-Ph); 138.2(*ipso*-Ph).

IR (nujol mull, CsI, very poor spectrum, apparent decomposition in mull): 1307(m), 1216(w), 1180(w), 1157(w), 1088(s), 1066(m), 1025(m), 998(m), 896(s), 795(vs, br), 740(vs, br), 720(vs, br), 692(vs, br), 574(s), 526(w), 481(s), 462(s).

3.3.14 Preparation of $[(Me_3Sb)_2(\mu\text{-}O)(\mu\text{-}O_2PMe_2)_2]$ (3.8)

An analogous procedure to that employed in Experiment 3.3.13 was carried out, using $[Me_3SbCl]_2O$ (**2.10**) (844mg, 2.01mmol), sodium dimethylphosphinate (510mg, 4.40mmol) and dichloromethane (35ml). After filtration to remove NaCl and evaporation of volatiles, spectroscopically pure product was isolated. Yield 901mg (84%).

Due to the extremely air sensitive nature of this compound satisfactory micro-analytical results could not be obtained.

^{1}H NMR (250MHz, $CDCl_3$, RT) Anhydrous conditions: δ 1.13(d, 12H, $^2J_{HP}$ - 14Hz, *Me*-P); 1.66(s, 18H, *Me*-Sb).

^{13}C{^{1}H} NMR (69 MHz, $CDCl_3$, RT) δ 16.3(*Me*-Sb); 18.8(d, $^1J_{CP}$ - 104Hz, *Me*-P).

IR (nujol mull, CsI, very poor spectrum, apparent decomposition in mull): 1421(s), 1286(s), 1262(w), 1221(s), 1172(vs, br), 1002(vs, br), 851(vs, br), 753(vs, br), 692(s), 578(s), 531(m), 512(w), 482(vs), 420(vs).

3.3.15 Reaction of $[Me_3SbCl]_2O$ with NaO_2PPh_2

An analogous procedure to that in experiment 3.3.13 was carried out, using $[Me_3SbCl]_2O$ (**2.10**) (461mg, 1.10mmol), sodium diphenylphosphinate (568mg, 2.36mmol) and dichloromethane (20ml). After filtration, and removal of volatiles from the filtrate, only the starting material $[Me_3SbCl]_2O$ was isolated.

3.3.16 Preparation of $Ph_2SbS_2PMe_2$ (3.11)

Hydrated sodium dimethyldithiophosphinate (0.46g, 2.5mmol) was added to a solution of $[Ph_2SbBrO]_2$ (**2.12**) (0.93g, 1.25mmol) in benzene (25ml) and the mixture was stirred under reflux for 2 hours. The resulting yellowish reaction mixture was filtered to remove insolubles and then the clear filtrate was evaporated to dryness. On standing white and yellow crystals were deposited from the oily residue. Subsequent treatment with acetone allowed the separation of the yellow product, which proved to be elemental sulfur (Found: C,0.52; H,0.00 %). The acetone solution containing the soluble white product was evaporated *in vacuo* and the residue crystallised from chloroform. Yield 130mg (13% with respect to $[Ph_2SbBrO]_2$); mp 114°C [lit 104-105°C[39]].

Found: C,40.98; H,3.94: $C_{14}H_{16}PS_2Sb$ requires C,41.92; H,4.02 %.

^1H NMR (250MHz, $CDCl_3$, RT) δ 2.08(d, 6H, $^2J_{HP}$ - 13Hz, *Me*-P); 7.39(m, 6H, *m*- and *p*-Ph); 7.69(m, 4H, *o*-Ph).

$^{13}C\{^1H\}$ NMR (69 MHz, $CDCl_3$, RT) δ 29.6(d, $^1J_{CP}$ - 56Hz, P-*C*); 129.0(*m*-Ph); 129.4(*p*-Ph); 135.9(*o*-Ph); 140.7(*ipso*-Ph).

^{31}P NMR (121 MHz, $CDCl_3$, RT) δ 56.5(sept, $^2J_{PH}$ - 13Hz).

MS (FAB): $\{[Ph_2Sb(S_2PMe_2)]_2$ (**M_2**) - $(S_2PMe_2)\}^+$ (m/z 677, 56%); $\{Ph_2SbS_2PMe_2$ (**M**)$\}^+$ (m/z 400, 71%); {**M** - Ph}$^+$ (m/z 323, 100%); $\{Ph_2Sb\}^+$ (m/z 275, 72%).

3.3.17 Preparation of $Ph_2SbS_2PPh_2$ (3.12)

A similar reaction to 3.3.16 was carried out between $[Ph_2SbBrO]_2$ (**2.12**) (0.497g, 0.66mmol) and ammonium dithiodiphenylphosphinate $[NH_4S_2PPh_2]$ (0.356g, 1.33mmol) in benzene. The crude product was recrystallised from acetonitrile. Yield 130mg (18%); mp 142-144°C [lit 140-142°C[39]].

Found: C,54.40; H,3.88: $C_{24}H_{20}PS_2Sb$ requires C,54.88; H,3.84 %.

^1H NMR (250MHz, $CDCl_3$, RT) δ 7.35(m, 6H, *m*- and *p*-Ph-Sb); 7.44(m, 6H, *m*- and *p*-Ph-P); 7.63(m, 4H, *o*-Ph-Sb); 7.96(m, 4H, *o*-Ph-P) .

$^{13}C\{^1H\}$ NMR (69 MHz, $CDCl_3$, RT) δ 128.1(*m*- or *p*-Ph-P); 128.4(*m*- or *p*-Ph-P); 128.9(*m*-Ph-Sb); 129.3(*p*-Ph-Sb); 131.1(d, $^2J_{CP}$ - 12Hz, *o*-Ph-P); 136.0(*o*-Ph-Sb); 137.1(d, $^1J_{CP}$ - 82Hz, *ipso*-Ph-P); 140.7(*ipso*-Ph-Sb).

$^{31}P\{^1H\}$ NMR (121 MHz, $CDCl_3$, RT) δ 61.4

IR (nujol mull, CsI): 1437(s), 1430(s), 1095(s), 1066(m), 1061(m), 997(m), 750(s), 736(s), 728(vs), 711(s), 693(vs), 643(vs), 613(m), 532(vs), 491(s), 442(m).

MS (FAB): $\{Ph_2SbS_2PPh_2$ (**M**)$\}^+$ (m/z 524, 22%); {**M** - Ph}$^+$ (m/z 447, 80%); $\{Ph_2Sb\}^+$ (m/z 275, 33%).

3.4 REFERENCES

1. J.Bordner, G.O.Doak, T.S.Everett, *J. Am. Chem. Soc.*, 1986, **108**, 4206.

2. W.E.McEwan, G.H.Briles, D.N.Schulz, *Phosphorus and Sulfur*, 1972, **2**, 147.

3. B.-Y.Liu,Y.-T.Ku, M.Wang, B.-Y.Wang, P.-J.Zheng, *J. Chem. Soc., Chem. Commun.*, 1989, 651.

4. I.G.Southerington, M.J.Begley, D.B.Sowerby, *J. Chem. Soc., Chem. Commun.*, 1991, 1555.

5. F.J.Koller, W.Schwarz, A.Schmidt, *Z. Naturforsch.*, 1979, **34b**, 563.

6. S.Blösl, W.Schwarz, A.Schmidt, *Z. Anorg. Allg. Chem.*, 1981, **474**, 51.

7. S.Blösl, W.Schwarz, A.Schmidt, *Z. Anorg. Allg. Chem.*, 1982, **495**, 165.

8. C.H.Belin, M.Chaabouni, J.L.Pascal, J.Potier, *Inorg. Chem.*, 1982, **21**, 3557.

9. S.Blösl, W.Schwarz, A.Schmidt, *Z. Anorg. Allg. Chem.*, 1982, **495**, 177.

10. S.Blösl, A.Schmidt, *Z. Anorg. Allg. Chem.*, 1985, **523**, 99.

11. S.Blösl, W.Schwarz, A.Schmidt, *Z. Naturforsch.*, 1983, **38b**, 143.

12. A.Sauvigny, J.E.Faerber, A.Rihm, H.Thurn, A.Schmidt, *Z. Anorg. Allg. Chem.*, 1995, **621**, 640.

13. D.B.Sowerby, M.J.Begley, P.L.Millington, *J. Chem. Soc., Chem. Commun.*, 1984, 896.

14. M.Hall, M.Nunn, M.J.Begley, D.B.Sowerby, *J. Chem. Soc., Dalton Trans.*, 1986, 1231.

15. M.J.Begley, M.Hall, M.Nunn, D.B.Sowerby, *J. Chem. Soc., Dalton Trans.*, 1986, 1735.

16. M.A.Said, K.C.K.Swamy, K.Babu, K.Aparna, M.Nethaji, *J. Chem. Soc., Dalton Trans.*, 1995, 2151.

17. R.Bohra, H.W.Roesky, M.Noltemeyer, G.M.Sheldrick, *J. Chem. Soc., Dalton Trans.*, 1984, 2011.

18. I.Haiduc, D.B.Sowerby, S.-F.Lu, *Polyhedron*, 1995, **14**, 3389.

19. K.Dehnicke, R.Schmitt, *Z. Anorg. Allg. Chem.*, 1968, **358**, 1.

20. R.Schmitt, K.Dehnicke, E.Fluck, *Z. Anorg. Allg. Chem.*, 1969, **366**, 310.

21. P.Volgnandt, R.A. Laber, A.Schmidt, *Z. Anorg. Allg. Chem.*, 1976, **427**, 17.

22. R.A.Laber, A.Schmidt, *Z. Anorg. Allg. Chem.*, 1977, **428**, 209

23. N.Kruger, K.Dehnicke, A.-F.Shihada, *Z. Anorg. Allg. Chem.*, 1978, **438**, 169.

24. M.Brauninger, W.Schwarz, A.Schmidt, *Z. Naturforsch.*, 1979, **34b**, 1703.

25. A.-F.Shihada, F.Weller, *Z. Anorg. Allg. Chem.*, 1981, **472**, 102.

26. F.Knodler, W.Schwarz, A.Schmidt, *Z. Naturforsch.*, 1987, **42b**, 1282.

27. B.Eberwein, J.Weidlein, *Z. Anorg. Allg. Chem.*, 1976, **420**, 229.

28. M.J.Begley, D.B.Sowerby, D.M.Wesolek, C.Silvestru, I.Haiduc, *J. Organomet. Chem.*, 1986, **316**, 281.

29. R.Mattes, D.Ruhl, *Inorg. Chim. Acta.*, 1984, **84**, 125.

30. R.Mattes, D.Ruhl, *Z. Anorg. Allg. Chem.*, 1984, **508**, 19.

31. C.Silvestru, I.Haiduc, K.H.Ebert, H.J.Breunig, D.B.Sowerby, *J. Organomet. Chem.*, 1994, **468**, 113.

32. W.Schwarz, H.D.Hausen, *Z. Anorg. Allg. Chem.*, 1978, **441**, 175.

33. M.J.Begley, D.B.Sowerby, I.Haiduc, *J. Chem. Soc., Dalton Trans.*, 1987, 145.

34. M.J.Begley, D.B.Sowerby, I.Haiduc, *J. Chem. Soc., Chem. Commun.*, 1980, 64.

35. D.B.Sowerby, I.Haiduc, A.Barbul-Rusu, M.Salajan, *Inorg. Chim. Acta*, 1983, **68**, 87.

36. R.O.Day, M.M.Chauvin, W.E.McEwan, *Phosphorus and Sulfur*, 1980, **8**, 121.

37. R.K.Gupta, A.K.Rai, R.C.Mehrotra, V.K.Jain, B.F.Hoskins, E.R.T.Tiekink, *Inorg. Chem.*, 1985, **24**, 3280.

38. C.Silvestru, D.B.Sowerby, I.Haiduc, K.H.Ebert, H.J.Breunig, *Main Group Met. Chem.*, 1994, **17**, 505.

39. C.Silvestru, L.Silaghi-Dumitrescu, I.Haiduc, M.J.Begley, M.Nunn, D.B.Sowerby, *J. Chem. Soc., Dalton Trans.*, 1986, 1031.

40. C.Silvestru, I.Haiduc, R.Kaller, K.H.Ebert, H.J.Breunig, *Polyhedron*, 1993, **12**, 2611.

41. C.Silvestru, M.Curtui, I.Haiduc, M.J.Begley, D.B.Sowerby, *J. Organomet. Chem.*, 1992, **426**, 49.

42. K.H.Ebert, H.J.Breunig, C.Silvestru, I.Haiduc, *Polyhedron*, 1994, **13**, 2531.

43. J.G.Stevens, J.M.Trooster, *J. Chem. Soc., Dalton Trans.*, 1979, 740.

44. S.Kraft, M.Wieber, *Z. Anorg. Allg. Chem.*, 1992, **607**, 153.

45. D.B.Sowerby, M.J.Begley, L.Silaghi-Dumitrescu, I.Silaghi-Dumitrescu, I.Haiduc, *J. Organomet. Chem.*, 1994, **469**, 45.

46. D.M.Wesolek, M.Nunn, D.B.Sowerby, *J. Organomet. Chem.*, 1983, **251**, C45.

47. K.Nakomoto, *Infrared and Raman Spectra of Inorganic and Co-ordination Compounds*, 3rd Edn., Wiley, 1978.

48. M.Tsutsui (Editor), *Characterisation of Organometallic Compounds*, Interscience, 1969.

49. N.W.Alcock, V.M.Tracy, T.C.Waddington, *J. Chem. Soc., Dalton Trans.*, 1976, 2243.

50. G.B.Deacon, F.Huber, R.J.Phillips, *Inorg. Chim. Acta.*, 1985, **104**, 41.

51. A.-F.Shihada, *Z. Naturforsch.*, 1994, **49b**, 1319.

52. A.-F.Shihada, H.R.Yousif, *Z. Naturforsch.*, 1991, **46b**, 1568.

53. R.M.Wing, K.P.Callahan, *Inorg. Chem.*, 1969, **8**, 871.

54. I.G.Southerington, G.E.Forster, M.J.Begley, D.B.Sowerby *J. Chem. Soc., Dalton Trans.*, 1995, 1995.

55. A.Ouchi, S.Sato, *Bull. Chem. Soc. Jpn.*, 1988, **61**, 1806.

56. G.Ferguson, D.R.Ridley, *Acta Crystallogr., Sect.B*, 1973, **29**, 2221.

57. D.P.Bullivant, M.F.A.Dove, M.J.Haley, *J. Chem. Soc., Dalton Trans.*, 1980, 109.

58. I.Haiduc, I.Silaghi-Dumitrescu, R.Grecu, R.Constantinescu, L.Silaghi-Dumitrescu, *J. Mol. Struct.*, 1984, **114**, 467.

59. B.Krebs, G.Henkel, *Z. Anorg. Allg. Chem.*, 1981, **475**, 143.

60. see for example N.C.Norman, *Phosphorus, Sulfur and Silicon*, 1994, **87**, 167 and references therein.

61. S.K.Porter, R.A.Jacobson, *J. Chem. Soc., A*, 1970, 1359.

62. M.Webster, S.Keats, *J. Chem. Soc., A*, 1971, 298.

63. G.Birke, H.P.Latscha, H.Pritzkow, *Z. Naturforsch.*, 1976, **B31**, 1285.

64. H.Reinhardt, D.Bianchi, D.Molle, *Chem. Ber.*, 1957, **90**, 1656.

65. M.A.Said, K.C.K.Swamy, D.M.Poojary, A.Clearfield, M.Veith, V.Huch, *Inorg. Chem.*, 1996, **35**, 3235.

POST SCRIPTUM

Following the preparation of this chapter, Swamy[65] and co-workers reported the preparation of the quadruply bridged compounds, $[(Ph_2Sb)_2(\mu\text{-}O)_2(\mu\text{-}O_2P(C_6H_{11})_2)_2]$ and $[(Ph_2Sb)_2(\mu\text{-}O)_2(\mu\text{-}O_2P(C_8H_{15})_2)_2]$, by the reaction routes shown below:

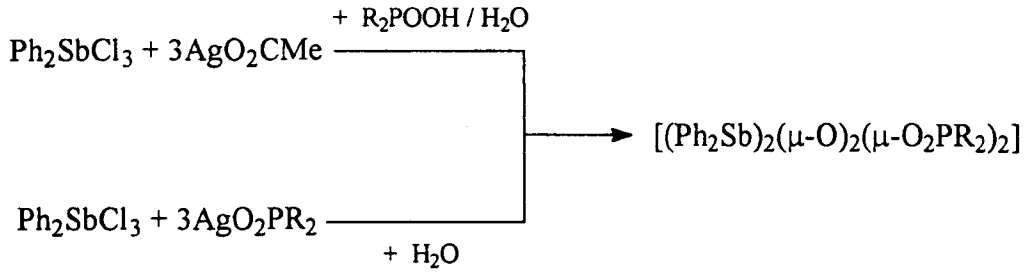

The compounds are clearly related to the arsinate bridged compounds **3.1**, **3.2** and **3.4** reported in this chapter. Further, formation of the compounds is in contrast to the findings discussed in this chapter, where attempts at forming a quadruply bridged compound with dimethylphosphinate groups, led instead to rearrangement and isolation of a triply bridged compound (**3.3**). The conclusion that rearrangement occurred because the phosphinate groups had too small a 'bite-length' to form quadruply bridged compounds is now distinctly dubious, although the P–O bond lengths found in **3.3** (mean, 1.522 Å) are shorter than those found for both $[(Ph_2Sb)_2(\mu\text{-}O)_2(\mu\text{-}O_2P(C_6H_{11})_2)_2]$ (mean, 1.534 Å) and $[(Ph_2Sb)_2(\mu\text{-}O)_2(\mu\text{-}O_2P(C_8H_{15})_2)_2]$ (mean, 1.544 Å).

The same publication also details the preparation of further triply bridged compounds, based on Sb_4O_6 structures, with phosphinate groups spanning each pair of antimony atoms. The structures are strongly reminiscent of the acetate bridged 'cage' compound reported by Sowerby, Begley and Millington[13] (see also Section 4.2.4).

CHAPTER 4

OXO-BRIDGED ORGANOANTIMONY(V) CARBOXYLATES

4.1 INTRODUCTION

This chapter describes the reaction of carboxylate ligands with oxo-bridged antimony compounds, in an attempt to assess the capability of such groups to bridge between antimony centres and thus compare with the behaviour of phosphinate and arsinates, as described in Chapter 3. The introduction includes a brief review of antimony compounds containing carboxylate bridges (4.1.1) and of other antimony carboxylate compounds (4.1.2).

Carboxylate coordination in organometallic compounds has received considerable attention[1], with a number of groups attempting to correlate the mode of carboxylate coordination obtained from crystallographic studies with infrared data[2,3].

Carboxylate coordination to a metallic centre may be divided into four general types, as shown in Figure 4.1. The extent to which infrared data and specifically the $\nu_{asym}(CO_2)$ and $\nu_{sym}(CO_2)$ vibration modes, can be used to identify the coordination type is a subject of contention[4,5]. However, these bands can generally be used with some degree of certainty to distinguish between unidentate and bidentate (or ionic) coordination types.

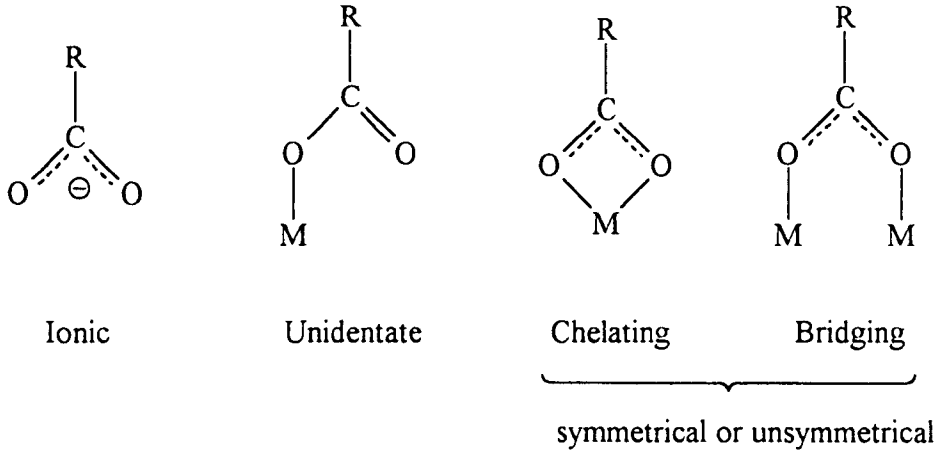

Figure 4.1 Carboxylate coordination

4.1.1 Bridging Carboxylate Compounds

There are only a few compounds reported that contain carboxylate group(s) spanning two antimony centres. As outlined in Section 3.1.1, Schmidt and co-workers have

prepared compounds of the type $[(Cl_3Sb)_2(\mu\text{-}O)(\mu\text{-}OR^1)(\mu\text{-}O_2CR^2)]$, where R^1 = H, R^2 = Me[6], CCl_3, ^iPr[7] and R^1 = Me, R^2 = CF_3, Et[8] amongst others. Structural investigations indicate the presence of symmetrically bridging carboxylate groups in all these compounds.

Another species containing bridging acetate groups is the unusual 'cage' compound[9], $[Ph_8Sb_4(\mu\text{-}O)_4(\mu\text{-}OH)_2(\mu\text{-}O_2CMe)_2].HO_2CMe$, formed by the adventitious hydrolysis of $Ph_2Sb(OAc)_3$. This compound also contains symmetrically bridging acetate groups and possesses the same skeletal fragment as Schmidt's compounds, illustrated in Figure 4.2.

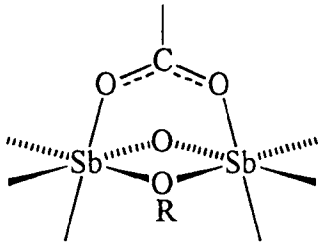

Figure 4.2 Structural skeleton of $[(Cl_3Sb)_2(\mu\text{-}O)(\mu\text{-}OR^1)(\mu\text{-}O_2CR^2)]$ compounds

A further compound containing bridging carboxylates is $[(F_3Sb)_2(\mu\text{-}O)(\mu\text{-}O_2CCF_3)_2]$, reported by Dove and co-workers[10]. This compound is structurally closely related to the triply bridged compounds discussed in Chapter 3 and a schematic view of the structure is shown in Figure 4.3.

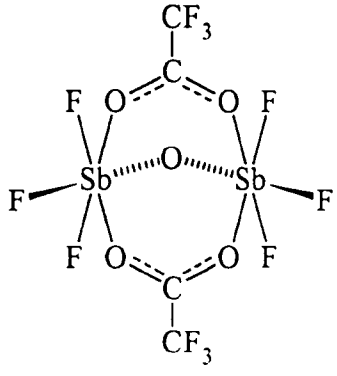

Figure 4.3 Structure of $[(F_3Sb)_2(\mu\text{-}O)(\mu\text{-}O_2CCF_3)_2]$

The same publication also reports the structure of a second trifluoroacetate bridged compound $[(F_4Sb)_2(\mu\text{-}F)(\mu\text{-}O_2CCF_3)]$, in which the two antimony centres are spanned by a fluorine atom and a single trifluoroacetate group.

Structural investigations have shown the presence of bridging interactions, in addition to chelation in the antimony(III) tris-(thio)carboxylates, $Sb(O_2CMe)_3$, $Sb(OSCMe)_3$ and $Sb(O_2CCF_3)_3$ giving seven coordinate compounds[11,12]. However, secondary chelate and bridging interactions were found to be notably less pronounced for $Sb(O_2CCF_3)_3$. Interestingly, bonding in the thioacetate derivative $Sb(OSCMe)_3$ is primarily to sulfur, in contrast to the related thiophosphinate compounds, such as $Sb(OSPPh_2)_3$, which are primarily O-bonded[13].

Another antimony(III) compound that possesses bridging acetates is the well known compound $Ph_2Sb(O_2CMe)$[14]. X-ray crystallography reveals a polymeric structure with acetate groups bridging between adjacent antimony atoms. The secondary bridging occurs in a position *trans* to the primary bonded oxygen, suggesting interaction with the Sb–O σ^* orbital.

A further range of diarylantimony(III) carboxylates, presumably with similar carboxylate coordination, have been prepared by the reactions shown below, where Ar = Ph or *p*-MeC_6H_4, R = CF_3, CH_2Cl and CH_2I amongst others and M = Na or Ag[15].

$$Ar_2SbCl + RCO_2H + Et_3N \rightarrow Ar_2SbO_2CR + Et_3NHCl$$

$$Ar_2SbCl + RCO_2M \rightarrow Ar_2SbO_2CR + MCl$$

4.1.2 Other Antimony Carboxylate Compounds

Coordination of carboxylate ligands to monomeric antimony(V) compounds is generally found to be either unidentate or chelating.

Wieber and co-workers have reported the synthesis and crystal structure of $PhSb(O_2CMe)_4$, synthesised by a metathesis reaction between $Ag(O_2CMe)$ and $PhSbCl_4$ (prepared *in situ* by the reaction between $PhSbCl_2$ and SO_2Cl_2). The

molecular structure displayed the presence of three unidentate acetate groups and one isobidentate chelating group, giving a distorted octahedral geometry about the antimony centre[16].

From infrared and Raman spectroscopic data, the structures of a range of dialkylantimony(V) tricarboxylates have also been proposed to be octahedral, with two unidentate and one bidentate acetate groups[17,18] (see Figure 4.4). The presence of only one set of ^{1}H NMR acetate resonances for the compound $Me_2Sb(O_2CMe)_3$ is considered to be a consequence of stereochemical non-rigidity on the NMR timescale.

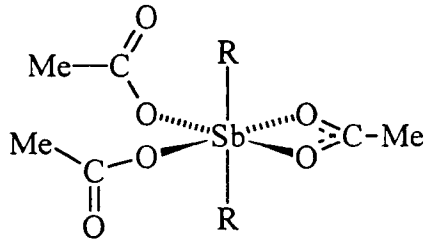

Figure 4.4 Proposed structure of dialkylantimony(V) tricarboxylates

A similar structure has been suggested[19,20] for the compound $Ph_2Sb(O_2CMe)_3$, with again two different acetate coordination types identified from infrared vibrational data. All diorganoantimony tricarboxylates are reported to be very sensitive to hydrolysis and indeed attempted recrystallisations of $Ph_2Sb(O_2CMe)_3$ led to the formation of the 'cage' compound $[Ph_8Sb_4(\mu\text{-}O)_4(\mu\text{-}OH)_2(\mu\text{-}O_2CMe)_2].HO_2CMe$ and also the oxo-bridged species, $[Ph_2Sb(O_2CMe)_2]_2O$, discussed later.

A large number of triorganoantimony dicarboxylate compounds having the general formula $R^1{}_3Sb(O_2CR^2)_2$, are also known[21,22]. Most are prepared by reaction of the corresponding $R^1{}_3SbX_2$ compound with the relevant carboxylic acid or salt, although a recent publication describes the preparation of a number of $Ar_3Sb(O_2CR)_2$ by a direct oxidative reaction between triarylantimony(III) compounds and two equivalents of the relevant acid[23], *ie.*

$$Ar_3Sb + 2RCO_2H \rightarrow Ar_3Sb(O_2CR)_2 + H_2$$

Structures have been determined for a number of these compounds and a common feature is the presence of distorted trigonal bipyramidal geometry at antimony with the three organo groups occupying equatorial positions and the carboxylate groups taking axial positions. Most compounds also have additional chelate interactions from the second carboxylate oxygen, as shown in Figure 4.5.

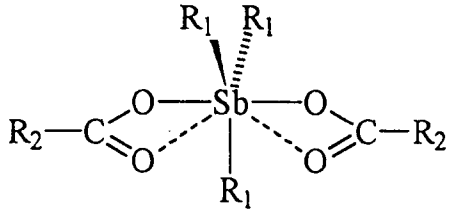

Figure 4.5 Molecular configuration of triorganoantimony dicarboxylates

The trimethylantimony compounds, $Me_3Sb(O_2C\text{-}2\text{-}C_4H_3S)_2$[24] and $Me_3Sb(O_2C\text{-}2\text{-}C_5H_4N)_2$[25], indeed possess this structural type, but there are only weak chelating interactions from the second carboxylate oxygen (Sb···O greater than 3 Å) which slightly distorts the geometry about antimony from true trigonal bipyramidal.

Secondary chelating interactions in the related triphenylantimony(V) dicarboxylates, $Ph_3Sb(O_2CMe)_2$[26], $Ph_3Sb(O_2CPh)_2$[27] and $Ph_3Sb(O_2CCF_3)_2$[28], show a clear correlation to the p*K* values of the corresponding free acids (HO_2CR). Thus the first two compounds possess similar coordination geometries (as does the compound $Ph_3Sb(O_2C\text{-}2\text{-}C_4H_3S)_2$[29]), with significant chelate interactions (Sb···O *ca.* 2.8 Å) and correspondingly both acetic and benzoic acids possess similar p*K* values (4.75 and 4.19 respectively). The much lower p*K* value of trifluoroacetic acid (0.2) is reflected in weaker secondary interactions (Sb···O *ca.* 3.2 Å) observed in the structure of $Ph_3Sb(O_2CCF_3)_2$.

In contrast, a related compound, $Ph_3Sb(O_2C\text{-}2\text{-}C_5H_4N)_2$, displays a very different coordination geometry, with one of the 2-pyridinecarboxylate groups acting as a chelate through the two oxygen atoms while the other carboxylate chelates through one oxygen and the nitrogen of its pyridyl ring[25].

A series of unusual hydroxo tris(mesityl)antimony carboxylate compounds has also been prepared[30] by the reaction shown below.

$$(mesityl)_3Sb(OH)_2 + HO_2CR \rightarrow (mesityl)_3Sb(OH)(O_2CR) + H_2O$$

Structure determinations for $(mesityl)_3Sb(OH)(O_2CC_{10}H_{15})$[30] and $(mesityl)_3Sb(OH)(O_2CCHCl_2)$[31] show negligible secondary interactions from the second carboxylate oxygen. Antimony in both cases is trigonal bipyramidally coordinated, with the mesityl groups in equatorial sites and the hydroxo and a carboxylate oxygen in the axial positions.

The crystal structure of tetraphenylantimony formate, $Ph_4Sb(O_2CH)$, has also been reported[32]. Coordination about the antimony centre was found to be basically trigonal bipyramidal, with only very weak secondary Sb···O chelating interactions of 3.291 Å. The corresponding acetate analogue, $Ph_4Sb(O_2CMe)$ has also been the subject of a structure determination[33], showing the presence of stronger chelate interactions than the formate with secondary Sb···O bonds of 2.585 Å.

Antimony carboxylates containing oxo-bridges between two antimony centres compounds are also known. One of the first to be reported resulted from hydrolysis of $Ph_2Sb(O_2CMe)_3$, leading to the formation of $[Ph_2Sb(O_2CMe)_2]_2O$. The antimony centres in this compound are seven coordinate with all acetate groups chelating[19]. A recent publication[34] details the preparation of a series of related compounds having the general formula $[Ph_2Sb(O_2CAr)_2]_2O$. The molecular structure of one of the compounds, $[Ph_2Sb(O_2CPh)_2]_2O$ was found to be similar to that of the previously described acetate compound, again with seven coordinate antimony centres. In addition, Pandey and Srivastava have also outlined the preparations of a series of compounds of the type $[Ph_3Sb(O_2CR)]_2O$[35].

The work reported in this chapter describes reactions of the oxo-bridged precursors $[Ph_3SbBr]_2O$ (**2.7**) and $[Ph_2SbBrO]_2$ (**2.12**) with a range of carboxylate acids or salts. The aim of the work was to assess the capability of the carboxylate groups to bridge between the antimony centres already spanned by the oxygen atom(s) and hence draw

similarities and contrasts between the behaviour of the carboxylates with that of phosphinate and arsinate ligands, as described in Chapter 3.

4.2 RESULTS AND DISCUSSION

4.2.1 Phenyl Substituted Oxo-Bridged Compounds

4.2.1.1 Preparation of Compounds

The compounds $[Ph_3Sb(O_2CCF_3)]_2O$ (**4.1**), $[Ph_3Sb(O_2CCCl_3)]_2O$ (**4.2**) and $[Ph_3Sb(O_2CCHCl_2)]_2O$ (**4.3**) have been prepared (using a synthetic strategy related to that of Pandey and Srivastava[35]) by reactions of the precursor $[Ph_3SbBr]_2O$ (**2.7**) with the appropriate carboxylic acid in the presence of triethylamine.

$$[Ph_3SbBr]_2O + 2\,HO_2CR + 2\,Et_3N \rightarrow [Ph_3Sb(O_2CR)]_2O + 2\,Et_3NHBr$$

R = CF_3 (**4.1**), CCl_3 (**4.2**) and $CHCl_2$ (**4.3**)

The crystalline products were isolated in reasonable yields, with satisfactory elemental analyses and were characterised by spectroscopic methods. In addition, a structure determination was carried out for the compound $[Ph_3Sb(O_2CCF_3)]_2O$ (**4.1**).

4.2.1.2 Infrared Spectroscopy

Attempts have been made[4,20] to definitively assign the coordination type of a carboxylate group by the position (and separation, $\Delta\nu$) of the $\nu_{asym}(CO_2)$ and $\nu_{sym}(CO_2)$ absorptions in the infrared spectrum. More recent publications though[5], cast doubt on the validity of these simple correlations. Deacon and co-workers[3,5] performed an exhaustive search on all acetate and trifluoroacetate organometallic compounds with both reliable infrared and crystallographic data and conclude that the use of $\nu(CO_2)$ frequencies in structural diagnosis is limited to:

1. Recognition of complexes with unidentate carboxylate coordination, in which $\Delta\nu_{unidentate} > \Delta\nu_{ionic}$.
2. Identification of some complexes with bridging and/or chelating bidentate carboxylate groups ($\Delta\nu_{bridging\ and/or\ chelating}$ often $< \Delta\nu_{ionic}$).

Commonly accepted values for ionic modes are taken from the spectra of NaO_2CMe ($\nu_{asym}(CO_2)$, 1578; $\nu_{sym}(CO_2)$, 1414; $\Delta\nu(CO_2)$, 164 cm^{-1}) and NaO_2CCF_3 ($\nu_{asym}(CO_2)$, 1680; $\nu_{sym}(CO_2)$, 1457; $\Delta\nu(CO_2)$, 223 cm^{-1}).

The infrared criterion for differentiation between unidentate and bidentate bonding is clearly observed for the acetate containing compounds, $Ph_2Sb(O_2CMe)_3$ and $[(Cl_3Sb)_2(\mu\text{-}O)(\mu\text{-}OH)(\mu\text{-}O_2CMe)]$[7]. The proposed unidentate coordination of two of the acetate groups in $Ph_2Sb(O_2CMe)_3$ is reflected in the infrared spectrum[20], which displayed $\nu_{asym}(CO_2)$ and $\nu_{sym}(CO_2)$ absorptions at 1714 and 1377cm^{-1} assigned to the unidentate acetates, giving a relatively large $\Delta\nu(CO_2)$ value of 337 cm^{-1} (equivalent bands for the chelating acetate group were found at 1553 and 1410 cm^{-1}, giving a $\Delta\nu(CO_2)$ value of 143 cm^{-1}). In contrast, the $\nu_{asym}(CO_2)$ and $\nu_{sym}(CO_2)$ bands for $[(Cl_3Sb)_2(\mu\text{-}O)(\mu\text{-}OH)(\mu\text{-}O_2CMe)]$, having a crystallographically observed symmetrically bridging acetate group, were observed at 1490 and 1435 cm^{-1} respectively, giving a $\Delta\nu(CO_2)$ value of only 55 cm^{-1}.

The infrared spectrum of $[Ph_3Sb(O_2CCF_3)]_2O$ (**4.1**), recorded as a nujol mull, displayed a sharp, intense band at 1714 cm^{-1}, assigned to the $\nu_{asym}(CO_2)$ band of the trifluoroacetate group. A further sharp band at 1437 cm^{-1} was assigned to the $\nu_{sym}(CO_2)$ absorption, giving a $\Delta\nu(CO_2)$ value of 277 cm^{-1}, closer to the value for $Sb(O_2CCF_3)_3$ (293 cm^{-1}) known to have near-unidentate trifluoroacetate groups[12], than for $[(Cl_3Sb)_2(\mu\text{-}O)(\mu\text{-}OH)(\mu\text{-}O_2CCF_3)]$[7] (153 cm^{-1}) presumed, by analogy with related compounds, to have symmetrically bridging trifluoroacetate groups. Other significant bands were observed at 1185 cm^{-1}, due to a ν(C–F) mode and at 742 cm^{-1}, due to the ν_{asym}(Sb–O–Sb) mode. The position of the latter band is comparable with those found for the $[Ar_3SbBr]_2O$ compounds reported in Section 2.2.2.1.

The $\nu(CO_2)$ modes for $[Ph_3Sb(O_2CCCl_3)]_2O$ (**4.2**) were observed at 1701 and 1289 cm^{-1} (*cf.* 1710 and 1290 cm^{-1} reported previously[35]) giving a relatively large $\Delta\nu(CO_2)$ value of 412 cm^{-1}. A sharp absorption assigned to the ν_{asym}(Sb–O–Sb) mode was also observed at 737 cm^{-1}, similar to that found for **4.1**.

The $\nu_{asym}(CO_2)$ absorption in $[Ph_3Sb(O_2CCHCl_2)]_2O$ (**4.3**) was split into two bands at 1694 and 1669 cm^{-1}, with the corresponding $\nu_{sym}(CO_2)$ vibration at 1325 cm^{-1} (mean $\Delta\nu(CO_2)$ = 357 cm^{-1}). Further, the spectrum displayed an intense absorption, at 740 cm^{-1}, assignable to the ν_{asym}(Sb–O–Sb) mode.

The values of $\Delta\nu(CO_2)$ for the spectra of **4.1**, **4.2** and **4.3** point to a general conclusion that all three compounds contain carboxylate groups bound to antimony in a near unidentate fashion in the solid state. Notably, the value of $\Delta\nu(CO_2)$, 277 cm^{-1}, for the trifluoroacetate derivative **4.1** is greater than the accepted ionic value and therefore according to Deacon's observations should be unidentate. Accordingly, this suggests that **4.1** is very different from the empirically similar $[F_3Sb(O_2CCF_3)]_2O$[10], which is known to contain symmetrically bridging trifluoroacetate groups. Indeed, a structure determination of **4.1** described later, illustrates the presence of near-unidentate coordination of the carboxylate groups.

The reason for the very different behaviour of the carboxylate groups in $[F_3Sb(O_2CCF_3)]_2O$ must therefore lie in the presence of the fluorine atoms attached to antimony. Simplistically, it could be thought that the increase in electron-withdrawing effect on moving from phenyl groups in **4.1** to fluorine atoms in $[F_3Sb(O_2CCF_3)]_2O$ would enhance the Lewis acidity at antimony and therefore increase its susceptibility to secondary bonding and hence promote the bridging of the trifluoroacetate groups.

A noted trend in the spectra of **4.1**, **4.2** and **4.3** is the steady decrease in frequency of the $\nu_{asym}(CO_2)$ carboxylate band with a corresponding increase in the p*K* value of the corresponding parent carboxylic acids. Thus, trifluoroacetic acid has the lowest p*K* value of *ca.* 0.2 and the $\nu_{asym}(CO_2)$ band for **4.1** is observed at the highest wavenumber (1714 cm^{-1}), whereas the p*K* value for the weakest acid, dichloroacetic acid, is 1.48 and the $\nu_{asym}(CO_2)$ bands for **4.3** are found at the lowest frequencies *ie.* 1694 and 1669 cm^{-1}.

A further point of interest is the similarity of ν_{asym}(Sb–O–Sb) vibrations in **4.1**, **4.2** and **4.3** (*ca.* 740 cm^{-1}) perhaps suggesting close similarities in the Sb–O–Sb structural skeleton.

Table 4.1 Comparison of the infrared absorptions (cm^{-1}) for 4.1, 4.2 and 4.3

Compound	$\nu_{asym}(CO_2)$	$\nu_{sym}(CO_2)$	$\Delta\nu(CO_2)$	$\nu_{asym}(Sb-O-Sb)$
4.1	1714	1437	277	742
4.2	1701	1289	412	737
4.3	1682 (mean)	1325	357	740

4.2.1.3 NMR Data

In a similar manner to the precursor compounds, such as $[Ph_3SbBr]_2O$ (**2.7**) (see Section 2.2.3.1), the oxo-bridged antimony carboxylate compound $[Ph_3Sb(O_2CCF_3)]_2O$ (**4.1**), showed a marked tendency to hydrolyse in solution, presumably (in keeping with the observations noted in Section 2.2.3.1) forming the hydroxo species $Ph_3Sb(OH)(O_2CCF_3)$. Thus, the ^1H NMR spectrum of **4.1** recorded without significant precautions against atmospheric moisture, clearly exhibited the presence of two individual species (**A** and **B**). The species presumed to be the non-hydrolysed parent compound **4.1** (**A**), displayed aromatic resonances at 7.31 (triplet), 7.45 (triplet) and 7.52 (doublet) ppm for the phenyl *meta*, *para* and *ortho* protons respectively, whereas the hydrolysed species (**B**) showed second order phenyl multiplets at 7.53 and 8.06 ppm. The similarity of chemical shifts and coupling structure of the resonances in the hydrolysed species $Ph_3Sb(OH)(O_2CCF_3)$ (**B**), with those of compounds such as Ph_3SbBr_2 and $Ph_3Sb(O_2CMe)_2$, suggests that the species has a related monomeric trigonal bipyramidal structure with phenyl groups in equatorial positions and the trifluoroacetate and hydroxo groups in axial sites.

The ^1H NMR spectrum of $[Ph_3Sb(O_2CCCl_3)]_2O$ (**4.2**) was very similar to that of **4.1** with two species (**A** and **B**) observed in non-anhydrous solution. The parent oxo-bridged species (**A**) displayed a triplet, triplet, doublet phenyl coupling pattern for the phenyl *meta*, *para* and *ortho* protons respectively, at chemical shifts of 7.35, 7.48 and 7.53 ppm. Phenyl resonances assigned to the hydrolysed hydroxo species, $Ph_3Sb(OH)(O_2CCCl_3)$ (**B**), were observed at 7.53 and 8.12 ppm.

Under strictly anhydrous conditions, the ^{1}H NMR spectrum of $[Ph_3Sb(O_2CCHCl_2)]_2O$ (**4.3**) displayed resonances for the chemically unchanged parent compound only. The phenyl protons displayed a triplet (7.30 ppm, *meta*), triplet (7.45 ppm, *para*) and doublet (7.60 ppm, *ortho*) coupling structure, with a singlet observed at 5.55 ppm for the dichloroacetate protons (see Figure 4.6). On exposure to the atmosphere for 24 hours, further signals appeared which can be assigned to the corresponding hydrolysis product $Ph_3Sb(OH)(O_2CCHCl_2)$, with resonances at 5.75 (singlet, $CHCl_2$), 7.53 (multiplet, *meta*- and *para*-Ph) and 8.11 (multiplet, *ortho*-Ph) ppm.

A single species was also clearly evident in the $^{13}C\{^1H\}$ spectrum of **4.3**, when recorded under anhydrous conditions. The resonances for non-hydrolysed $[Ph_3Sb(O_2CCHCl_2)]_2O$ were at 67.8 (Cl_2CH), 129.3 (*m*-Ph), 131.1 (*p*-Ph), 133.7(*o*-Ph) and 138.1(*ipso*-Ph) (the quaternary carboxylate carbon was not observed).

Crystallisation of the non-anhydrous NMR samples of **4.1** and **4.2**, which contained varying amounts of the hydrolysis products, $Ph_3Sb(OH)(O_2CR)$, gave quantitative recovery of the parent oxo-bridged compound. This was consistent with the findings in Section 2.2.3.1, showing the clear instability of the hydroxo compounds in the solid state.

As was noted for the bromo compounds described in Chapter 2, the presence of sterically demanding groups, such as mesityl groups, are required to stabilise these hydroxo species in the solid state, with a range of stable $(mesityl)_3Sb(OH)(O_2CR)$ compounds having been successfully prepared[24,25].

Figure 4.6 ^{1}H NMR spectrum of $[Ph_3Sb(O_2CCHCl_2)]_2O$ (4.3) in $CDCl_3$

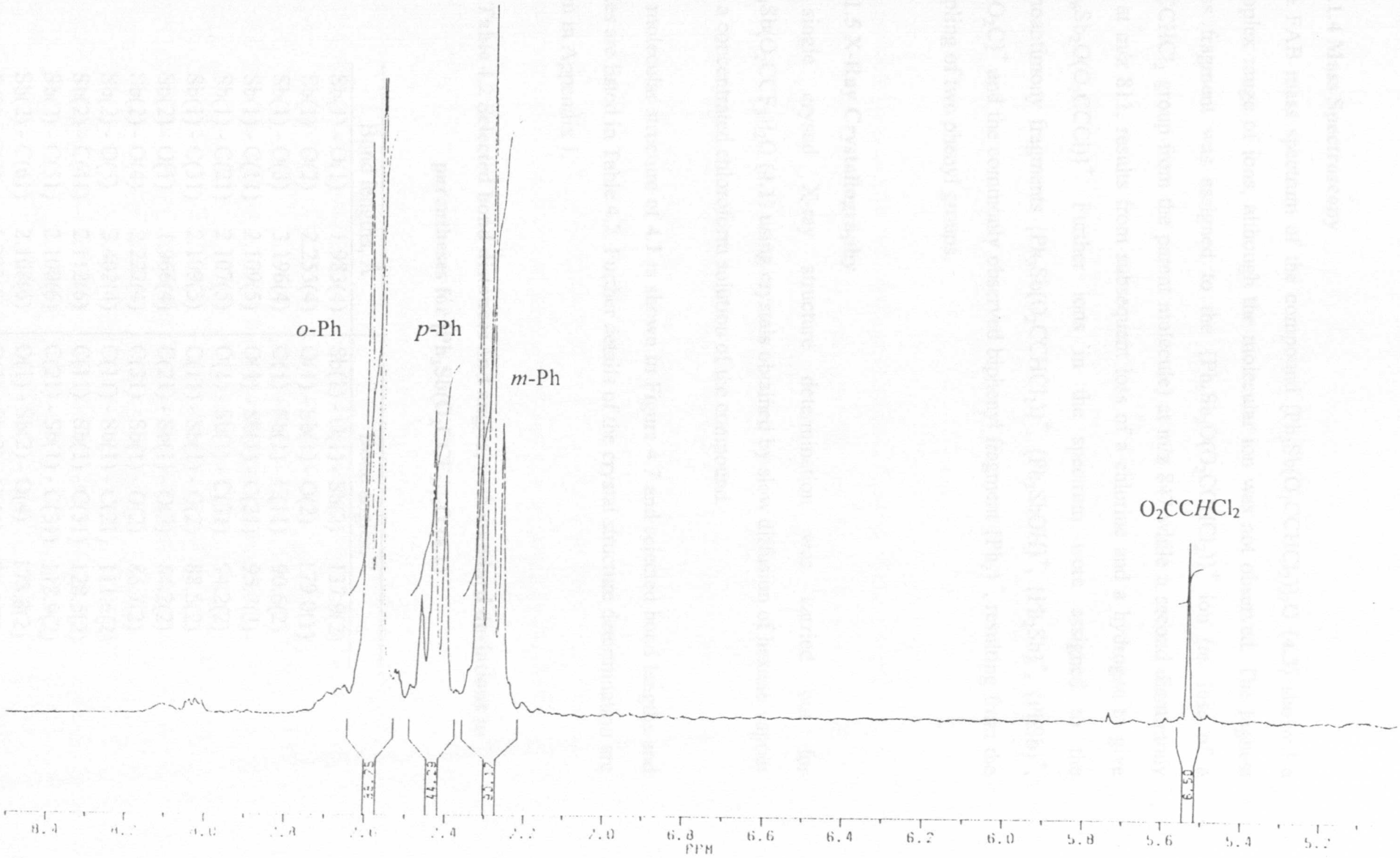

4.2.1.4 Mass Spectroscopy

The FAB mass spectrum of the compound $[Ph_3Sb(O_2CCHCl_2)]_2O$ (**4.3**) showed a complex range of ions, although the molecular ion was not observed. The highest mass fragment was assigned to the $\{Ph_6Sb_2O(O_2CCHCl_2)\}^+$ ion (*ie.* loss of a O_2CCHCl_2 group from the parent molecule) at m/z 847 while a second diantimony ion at m/z 811, results from subsequent loss of a chlorine and a hydrogen to give $\{Ph_6Sb_2O(O_2CCCl)\}^+$. Further ions in the spectrum were assigned to the monoantimony fragments $\{Ph_3Sb(O_2CCHCl_2)\}^+$, $\{Ph_3SbOH\}^+$, $\{Ph_2Sb\}^+$, $\{PhSb\}^+$, $\{SbO_2C\}^+$ and the commonly observed biphenyl fragment $\{Ph_2\}^+$, resulting from the coupling of two phenyl groups.

4.2.1.5 X-Ray Crystallography

A single crystal X-ray structure determination was carried out for $[Ph_3Sb(O_2CCF_3)]_2O$ (**4.1**) using crystals obtained by slow diffusion of hexane vapour into a concentrated chloroform solution of the compound.

The molecular structure of **4.1** is shown in Figure 4.7 and selected bond lengths and angles are listed in Table 4.2. Further details of the crystal structure determination are given in Appendix J.

Table 4.2 Selected bond distances and angles, with standard deviations in parentheses for $[Ph_3Sb(O_2CCF_3)]_2O$ (4.1)

Bond lengths, Å		Bond angles, °	
Sb(1) - O(1)	1.983(4)	Sb(1) - O(1) - Sb(2)	137.9(2)
Sb(1) - O(2)	2.255(4)	O(1) - Sb(1) - O(2)	179.0(1)
Sb(1) - O(3)	3.196(4)	O(1) - Sb(1) - C(11)	90.6(2)
Sb(1) - C(11)	2.109(5)	O(1) - Sb(1) - C(21)	95.7(2)
Sb(1) - C(21)	2.107(5)	O(1) - Sb(1) - C(31)	94.2(2)
Sb(1) - C(31)	2.109(5)	C(11) - Sb(1) - O(2)	88.5(2)
Sb(2) - O(1)	1.966(4)	C(21) - Sb(1) - O(2)	84.2(2)
Sb(2) - O(4)	2.222(4)	C(31) - Sb(1) - O(2)	86.7(2)
Sb(2) - O(5)	3.402(4)	C(11) - Sb(1) - C(21)	111.6(2)
Sb(2) - C(41)	2.112(6)	C(11) - Sb(1) - C(31)	128.5(2)
Sb(2) - C(51)	2.100(6)	C(21) - Sb(1) - C(31)	118.9(2)
Sb(2) - C(61)	2.108(6)	O(1) - Sb(2) - O(4)	178.8(2)
O(3) - C(1)	1.235(5)	O(1) - Sb(2) - C(41)	91.0(2)

O(2) - C(1)	1.258(5)	O(1) - Sb(2) - C(51)	100.3(2)
C(1) - C(2)	1.509(6)	O(1) - Sb(2) - C(61)	92.5(2)
		C(41) - Sb(2) - O(4)	88.1(2)
		C(51) - Sb(2) - O(4)	79.5(2)
		C(61) - Sb(2) - O(4)	88.7(2)
		C(41) - Sb(2) - C(51)	119.2(2)
		C(41) - Sb(2) - C(61)	123.9(2)
		C(51) - Sb(2) - C(61)	115.1(2)
		O(3) - C(1) - O(2)	128.6(4)

(Note: parameters for the C(3) trifluoroacetate group have been omitted as there are problems of disorder, giving unreliable information)

The molecular structure of **4.1** confirms unidentate bonding of the trifluoroacetate groups as indicated by earlier reported spectroscopic data. Secondary bonding interactions through the formally non-bonded oxygens are very weak, with the Sb(1)···O(3) distance of 3.196(4) Å and Sb(2)···O(5) of 3.402(4) Å. Both distances though are comfortably within the sum of the antimony and oxygen van de Waals radii (3.6 Å). The near-unidentate coordination of the trifluoroacetate groups is also reflected in the C–O bond lengths; the C(1)=O(3) bond, as expected, shorter (1.235(5) Å) than the C(1)–O(2) bond (1.258(5) Å). However, the difference between these bond lengths is less pronounced than was found for $Ph_3Sb(O_2CCF_3)_2$[28] (mean Sb=O, 1.193 Å; mean Sb–O, 1.295 Å), also showing unidentate coordination of the trifluoroacetate groups.

Coordination about the antimony atoms is trigonal bipyramidal, with three phenyl *ipso* carbons (having Sb–C bond lengths comparable to those in related structures and within the range between 2.100(6) [Sb(2)–C(51)] and 2.112(6) [Sb(2)–C(41)] Å) in equatorial positions and the bridging oxygen and a trifluoroacetate oxygen in axial positions. Significant deviations are observed in the equatorial plane about each antimony due to an opening of an angle between two phenyl groups at both antimony atoms [C(11)–Sb(1)–C(31) at 128.5(2)° and C(41)–Sb(2)–C(61) at 123.9(2)°]. The opening of the angles seems likely to be a consequence of the weak chelating interaction from the second carboxylate oxygens O(3) and O(5), that occur in positions at antimony between those phenyl groups.

Figure 4.7 Molecular structure of $[Ph_3Sb(O_2CCF_3)]_2O$ (4.3)

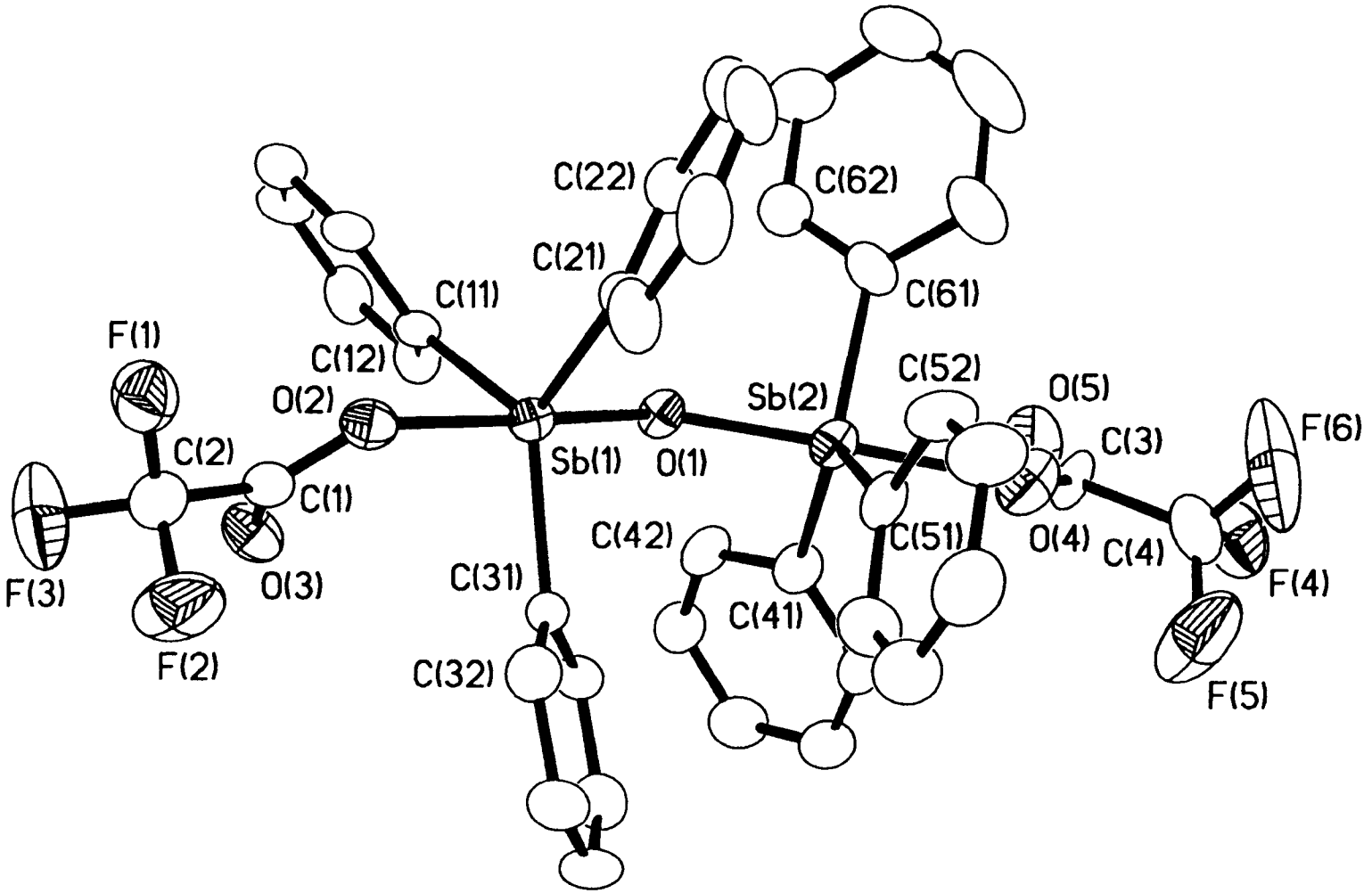

The angle about the bridging oxygen [Sb(1)–O(1)–Sb(2)] is 137.9(2)°, with corresponding Sb–O_{bridge} distances of 1.983(4) and 1.966(4) Å to Sb(1) and Sb(2) respectively. The angle about O(1) is fairly low in comparison to other structurally characterised Sb–O–Sb compounds and similar to those found for $[Ph_3SbCl]_2O$ (139.0°)[36] and $[Ph_3Sb(NO_3)]_2O$ (141.6°)[20].

Marked differences are observed in the Sb–O bond lengths, with the Sb–$O_{carboxylate}$ bonds significantly longer (Sb(1)–O(2), 2.255(4) Å and Sb(2)–O(4), 2.222(4) Å) than the Sb–O_{bridge} bonds. Moreover, the Sb–$O_{carboxylate}$ bond lengths are longer than normally found in compounds containing formal Sb–O single bonds, for example those found for $Ph_3Sb(OMe)_2$ are *ca.* 2.03 Å[37]. The possible explanation for the elongation found for **4.1** could either be a result of a lower degree of back-bonding from the oxygen to antimony or due to a partial ionic character of the compound, in which the observed structure lies along the coordinate between $[Ph_3Sb(O_2CCF_3)]_2O$ and $[Ph_3Sb]_2O^{2+}(O_2CCF_3)_2^-$ (see Figure 4.8). This explanation is consistent with the observed bending of the phenyl *ipso* carbons away from the bridging oxygen, with an angle as high as 100.3(2)° for the C(51)–Sb(2)–O(1) angle, and hence a distortion towards tetrahedral coordination about antimony.

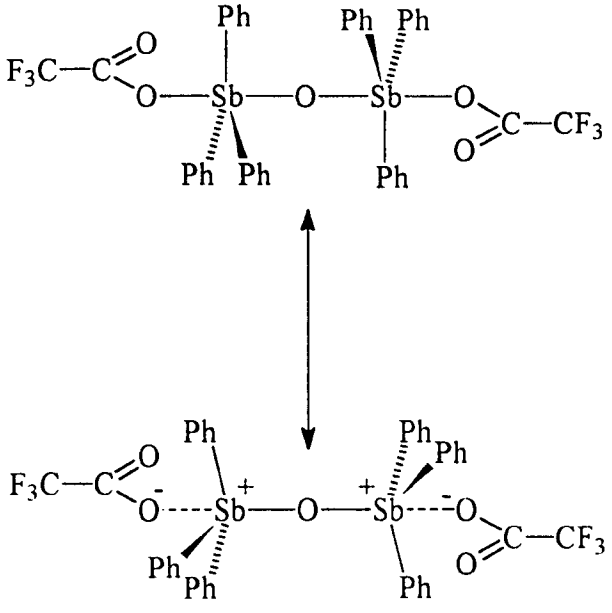

Figure 4.8 Structural coordinate between $[Ph_3Sb(O_2CCF_3)]_2O$ and $[Ph_3Sb]_2O^{2+}(O_2CCF_3)_2^-$

It is of interest to note that elongation of Sb–Br bonds was observed in the structures of the related compounds $[(p\text{-}MeC_6H_4)_3SbBr]_2O$ (**2.8**) and $[(o\text{-}MeC_6H_4)_3SbBr]_2O$ (**2.9**) (see Section 2.2.5), suggesting a similar partially ionic character of these compounds.

A further possible explanation for the elongation of the $Sb–O_{carboxylate}$ bond length could be due to a marked *trans* influence exerted by the strong $Sb–O_{bridge}$ bonds.

The structure determination of **4.1** confirms that there is a marked structural difference between this compound and $[F_3Sb(O_2CCF_3)]_2O$, in spite of the formal similarity in stoichiometry; the latter containing symmetrically bridging trifluoroacetate groups giving a triply bridged species with octahedral geometry at antimony[10]. The Sb–O bond lengths to all four carboxylate oxygens in $[F_3Sb(O_2CCF_3)]_2O$ fall between 2.028 and 2.107 Å, and are shorter than any of the equivalent bonds in **4.1**. Clearly replacement of fluorine atoms with phenyl groups as in **4.1**, significantly reduces Lewis acidity at antimony and consequently secondary interactions from the carboxylate groups are dramatically reduced.

4.2.2 Oxo-Bridge Cleavage Reactions

4.2.2.1 Preparation of Compounds

Although the reactions described in Section 4.2.1.1, maintained the oxo-bridge, analogous reactions between $[Ph_3SbBr]_2O$ (**2.7**) and chloroacetic acid (HO_2CCH_2Cl) or benzoic acid (HO_2CPh) in the presence of triethylamine, led to cleavage of the oxo-bridge between the antimony atoms, giving $Ph_3Sb(O_2CCH_2Cl)_2$ (**4.4**) and $Ph_3Sb(O_2CPh)_2$ (**4.5**) as the only products isolated after work-up. A similar cleavage of the oxo-bridge was observed in a reaction between $[Ph_3SbBr]_2O$ and two equivalents of $Ag(O_2CMe)$, yielding the well known compound $Ph_3Sb(O_2CMe)_2$ (**4.6**). In contrast, there was no reaction between $[Ph_3SbBr]_2O$ and either $Na(O_2CMe)$ or $(MeCO)_2O$ and even after prolonged reaction times only unreacted starting materials were recovered.

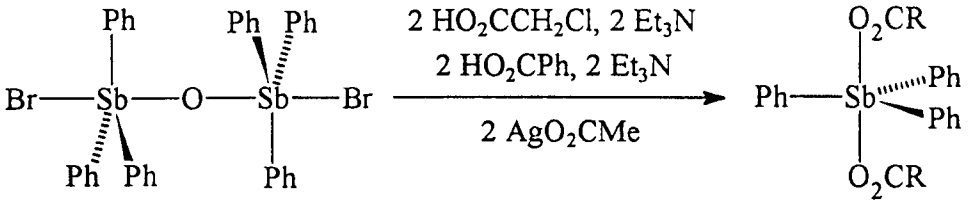

R = CH_2Cl (**4.4**), Ph (**4.5**), Me (**4.6**

Figure 4.9 Oxo-bridge cleavage reactions

4.2.2.2 Infrared Spectroscopy

In addition to many phenyl modes, the infrared spectrum of $Ph_3Sb(O_2CCH_2Cl)_2$ (**4.4**) displayed a split $\nu_{asym}(CO_2)$ mode at 1672 and 1654, likely to be due to the in-phase and out-of-phase components. Splitting of the $\nu_{sym}(CO_2)$ mode was also noted, with bands found at 1346 and 1332 cm^{-1}. The band separation (mean $\Delta\nu(CO_2)$, 324 cm^{-1}) is indicative of unidentate coordination. It should be noted that the infrared results reported here are in agreement with those previously reported for the same compound[38].

The equivalent $\nu(CO_2)$ bands in the dibenzoate derivative, **4.5**, were observed at 1645 [$\nu_{asym}(CO_2)$] and 1324 cm^{-1} [$\nu_{sym}(CO_2)$], giving a relatively large $\Delta\nu(CO_2)$ value of 321 cm^{-1} again implying unidentate coordination. Indeed, the known molecular structure[27] of **4.5** shows primarily unidentate benzoate groups, although secondary chelate interactions are present, with Sb···O distances of 2.70 and 2.81 Å, well within the sum of the van der Waals radii of the atoms (*ca.* 3.6 Å).

The asymmetric and symmetric acetate stretches were located at 1630 and 1318 cm^{-1} in the infrared spectrum of $Ph_3Sb(O_2CMe)_2$ (**4.6**) (in good agreement with previously reported values[38] of 1633 and 1320 cm^{-1}). Following Deacon and co-workers observations[5], the structurally observed[26] near-unidentate coordination of the acetate groups correlates well with the large $\Delta\nu(CO_2)$ value of 312 cm^{-1}, which is considerably greater than that for an ionic acetate (164 cm^{-1}).

4.2.2.3 NMR Data

The compounds $Ph_3Sb(O_2CCH_2Cl)_2$ (**4.4**), $Ph_3Sb(O_2CPh)_2$ (**4.5**) and $Ph_3Sb(O_2CMe)_2$ (**4.6**) have been fully characterised by ^1H NMR spectroscopy and in the case of **4.4** and **4.6** also by $^{13}C\{^1H\}$ spectroscopy. All the compounds show complex second order phenyl multiplets, typical of a monomeric trigonal bipyramidal Ph_3SbX_2 compound, and the results are tabulated in Table 4.3.

Table 4.3 NMR data for 4.4, 4.5 and 4.6

	$Ph_3Sb(O_2CCH_2Cl)_2$ (**4.4**)	$Ph_3Sb(O_2CPh)_2$ (**4.5**)	$Ph_3Sb(O_2CMe)_2$ (**4.6**)
^1H (Ph), ppm	7.55, 8.03	7.51, 8.14	7.49, 8.01
^1H (carboxy), ppm	3.86	7.36, 7.47, 7.96	1.84
^{13}C (Ph), ppm	129.6, 131.7, 133.9, 135.8		129.1, 130.9, 133.8, 139.0
^{13}C (carboxy), ppm	42.5, 169.9		22.1, 175.7

4.2.2.4 Mass Spectroscopy

The E.I. mass spectrum of $Ph_3Sb(O_2CCH_2Cl)_2$ (**4.4**) showed no evidence of the molecular ion, although a series of fragmentation products was observed. From the peak intensities (see Table 4.4), the major fragmentation route occurs through loss of the carboxylate groups giving major species such as $\{Ph_3Sb(O_2CCH_2Cl)\}^+$ and $\{Ph_2Sb\}^+$. Loss of phenyl groups, as perhaps expected, is less probable although there is reasonable intensity for the species $\{Sb(O_2CCH_2Cl)\}^+$. Rearrangement to give the species $\{Ph_3SbCl\}^+$ was also noted.

Primary fragmentation for $Ph_3Sb(O_2CMe)_2$ (**4.6**) was similar in that loss of the carboxylate groups from the parent (the parent ion not being seen) was more probable than loss of phenyl groups. Major fragments in the spectrum of **4.6** are summarised in Table 4.4, together with data from the spectrum of **4.4**.

Table 4.4 Major fragments in the EI mass spectra of 4.4 and 4.6

Fragment Ion	$Ph_3Sb(O_2CCH_2Cl)_2$ (**4.4**), m/z (% height)	$Ph_3Sb(O_2CMe)_2$ (**4.6**), m/z (% height)
$\{Ph_3Sb(O_2CR)\}^+$	445 (74)	411 (61)
$\{Ph_2Sb(O_2CR)_2\}^+$	461 (6)	393 (20)
$\{Ph_3SbCl\}^+$	387 (17)	
$\{Ph_3SbOH\}^+$		369 (11)
$\{Ph_3Sb\}^+$		352 (7)
$\{Ph_2Sb(O_2CR)\}^+$		334 (8)
$\{Ph_2Sb\}^+$	275 (14)	275 (18)
$\{PhSb(O_2CR)\}^+$		257 (27)
$\{Sb(O_2CR)\}^+$	214 (33)	180 (35)
$\{PhSb\}^+$	198 (47)	198 (100)
$\{Ph_2\}^+$	154 (100)	154 (91)
$\{Ph\}^+$	77 (38)	77 (41)

4.2.3 Methyl Substituted Oxo-Bridged Compounds

4.2.3.1 Preparation of Compounds

Both $[Me_3Sb(O_2CMe)]_2O$ (**4.7**) and $[Me_3Sb(O_2C^tBu)]_2O$ (**4.8**) were prepared in good yield by reaction of the precursor $[Me_3SbCl]_2O$ (**2.10**) with two equivalents of either $Ag(O_2CMe)$ or $Na(O_2C^tBu)$ under anhydrous conditions. Although, the compounds were sensitive to moisture, the hydrolysis was far less extreme and rapid as for the phosphinate and arsinate derivatives, described in Section 3.2.2.

The crystalline products gave satisfactory elemental analysis and were characterised by spectroscopic means. In addition, a structure determination was carried out for the compound **4.7**.

Clearly, the reaction of $[Me_3SbCl]_2O$ with $Ag(O_2CMe)$ follows a different course than the analogous reaction between $[Ph_3SbBr]_2O$ and the same acetate salt, which yielded the oxo-bridged cleaved product $Ph_3Sb(O_2CMe)_2$ (**4.6**).

Interest in the compounds **4.7** and **4.8** again lies in the coordination mode of the carboxylate groups, which as shown in Figure 4.10 could be either unidentate, chelating or bridging.

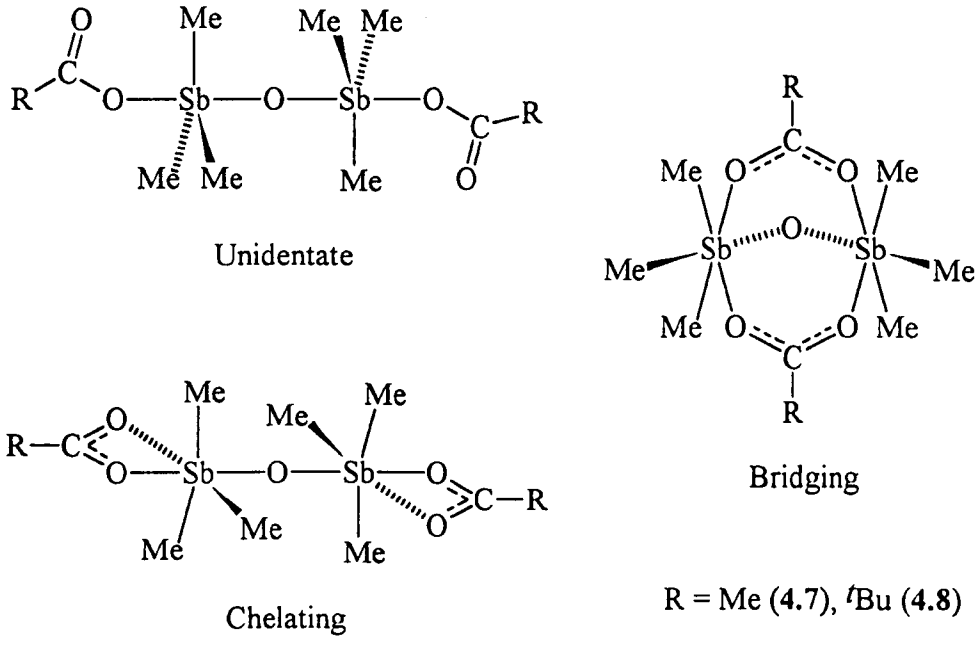

Figure 4.10 Potential molecular configurations for 4.7 and 4.8

A reaction between $[Me_3SbCl]_2O$ (**2.10**) and two equivalents of HO_2CCF_3 in the presence of triethylamine did not yield the expected substitution product, but instead ^1H NMR spectroscopy showed the presence of a number of unidentified products.

4.2.3.2 Infrared Spectroscopy

The solid-state infrared spectra of **4.7**, displayed an intense band at 1623 cm^{-1}, assigned to the $\nu_{asym}(CO_2)$ stretching vibration, whilst a second intense band at 1374 cm^{-1}, due to the corresponding $\nu_{sym}(CO_2)$ stretch, leads to a $\Delta\nu(CO_2)$ value of 249 cm^{-1}. The magnitude of $\Delta\nu(CO_2)$ is greater than that for $Na(O_2CMe)$ and so the coordination of the acetate group is likely to be unidentate. A further intense band at

710 cm^{-1} was tentatively assigned to the ν_{asym}(Sb–O–Sb) vibration, although this is of notably lower frequency than the equivalent bands for the phenyl compounds **4.1**, **4.2** and **4.3** (*ca.* 740 cm^{-1}), reported in Section 4.2.1.1, and also significantly lower than that found for $[Me_3SbCl]_2O$ (777 cm^{-1}).

The corresponding carboxylate bands in the spectrum of $[Me_3Sb(O_2C^tBu)]_2O$ (**4.8**) were at 1620 and 1326 cm^{-1}, with the band separation ($\Delta\nu(CO_2)$ = 294 cm^{-1}) implying unidentate coordination of the trimethylacetate groups. In addition, a broad intense band at 750 cm^{-1}, was assigned to the ν_{asym}(Sb–O–Sb) mode. Interestingly, the ν_{asym}(Sb–O–Sb) bands observed for **4.7** and **4.8**, are similar to those found for the related group of compounds $[Me_3Sb(S_2CR)]_2O$[39], where S_2CR = dithiocarbamate or xanthate, which fell in the range between 710 and 744 cm^{-1}.

4.2.3.3 NMR Data

The ^1H NMR spectrum of $[Me_3Sb(O_2CMe)]_2O$ (**4.7**), recorded under anhydrous conditions in $CDCl_3$, was straightforward and displayed two singlets at 1.62 and 1.83 ppm, assigned to the *Me*-Sb and *Me*-CO_2 resonances respectively. On exposure to atmospheric moisture however, new peaks appeared at 1.82 and 1.90 ppm (see Figure 4.11) suggesting that hydrolysis had occurred (possibly to produce $Me_3Sb(OH)O_2CMe$), but in contrast to the situation observed with solutions of **4.1** and **4.2**, the parent compound could not be recovered on crystallisation of the sample. It is therefore concluded that the compound was subject to an irreversible hydrolysis process whilst in the solution.

As expected, three resonances were observed in the anhydrous $^{13}C\{^1H\}$ NMR spectrum of **4.7**, at 14.5 (*Me*-Sb), 23.3 (*Me*-CO_2) and 176.4 (Me*C*O_2) ppm. Differences in the acetate carbon shifts when compared with $Ph_3Sb(O_2CMe)_2$ (22.1 and 175.7 ppm) may be associated with the reduced secondary interactions observed in the structure of **4.7** (see Section 4.2.3.5).

Figure 4.11 ^{1}H NMR spectrum of $[Me_3Sb(O_2CMe)]_2O$ (4.7) in $CDCl_3$

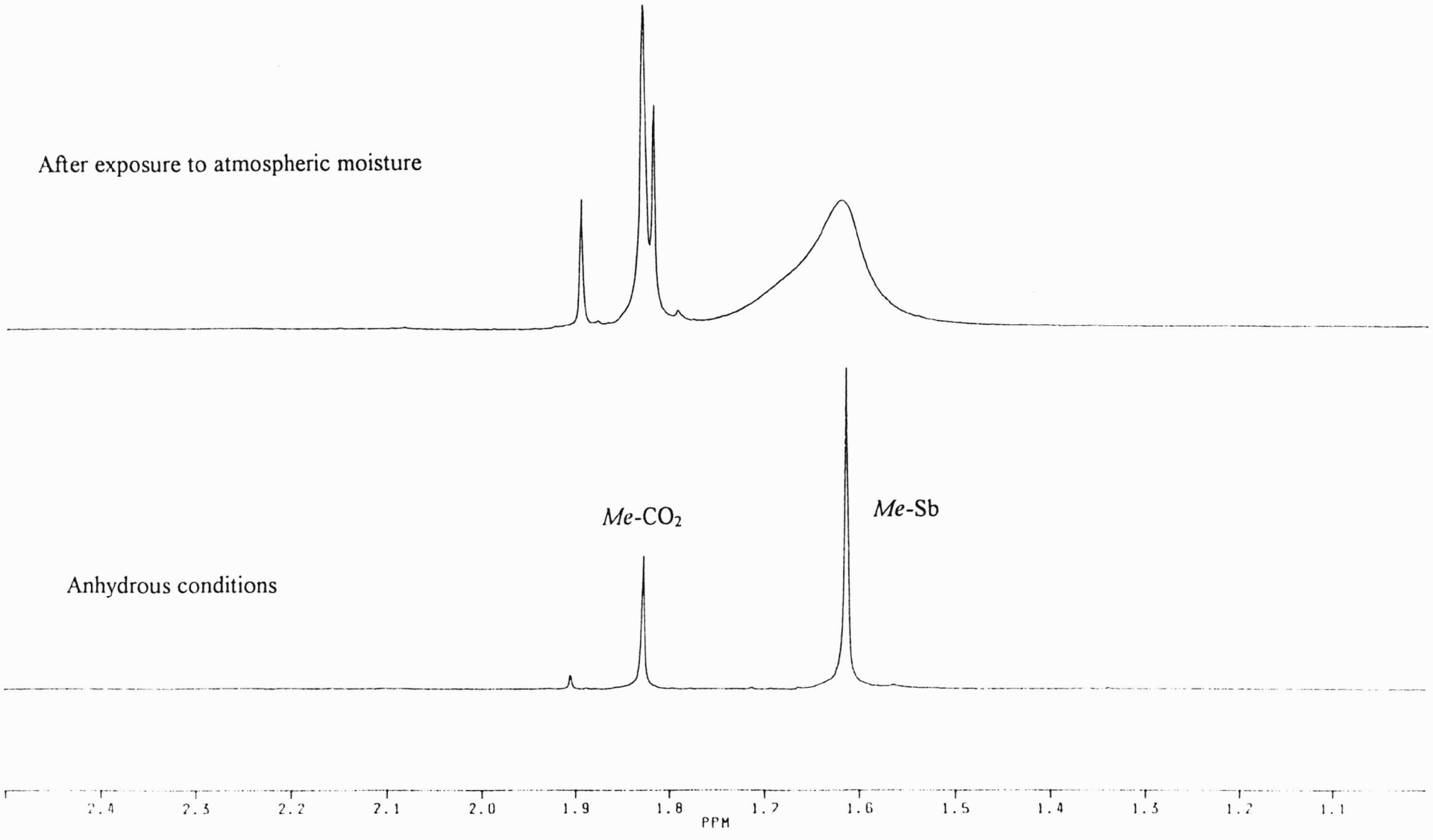

Figure 4.12 $^{13}C\{^{1}H\}$ NMR spectrum of $[Me_3Sb(O_2C^tBu)]_2O$ (4.8) in $CDCl_3$

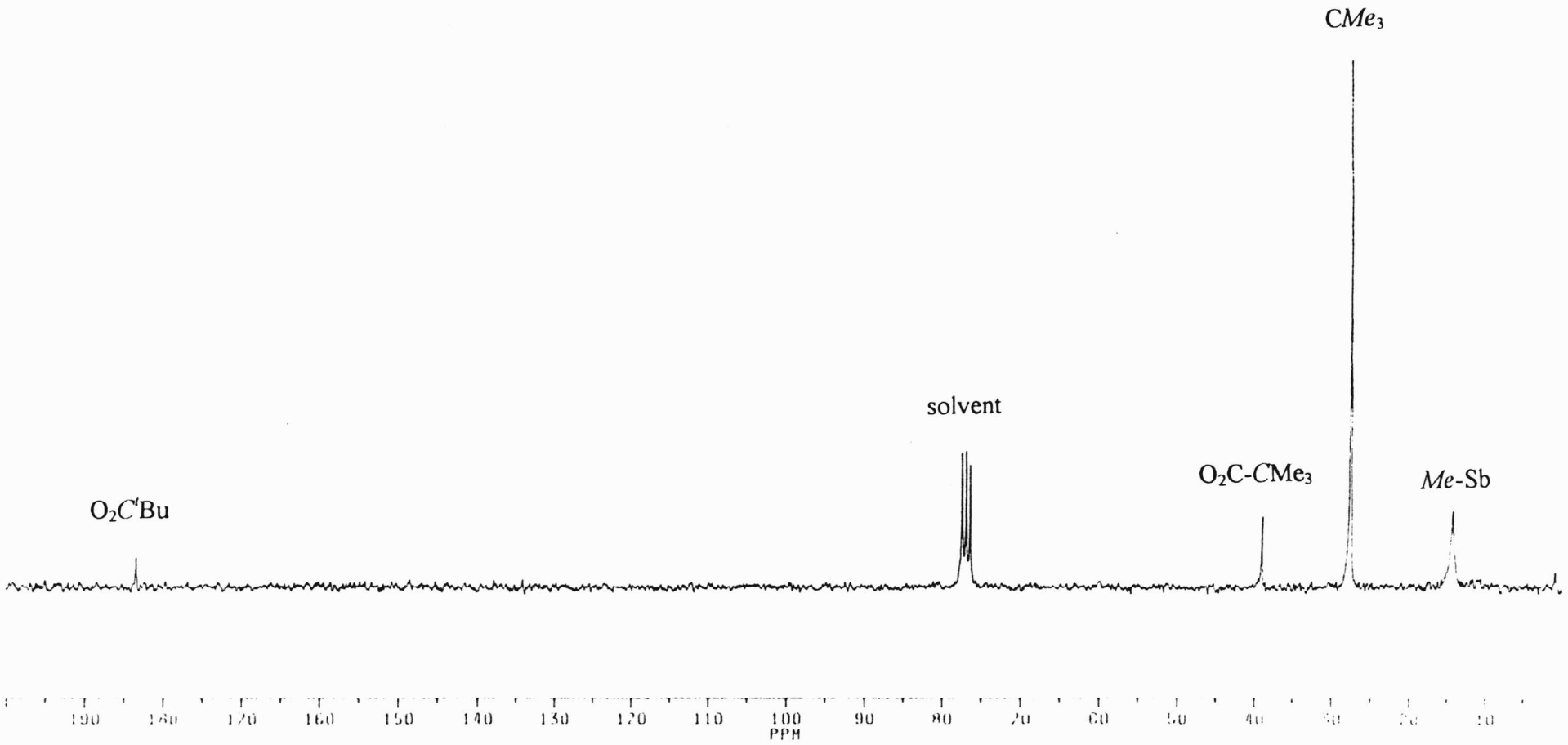

The chemical shift of the *Me*-Sb resonance in the anhydrous ^{1}H spectrum of $[Me_3Sb(O_2C^tBu)]_2O$ (**4.8**) was observed at 1.59 ppm, with a singlet for the ^tBu protons at 1.03 ppm. In the $^{13}C\{^1H\}$ NMR of the same solution, resonances were observed at 14.3(*Me*-Sb), 27.7(CMe_3), 39.1(O_2C-CMe_3) and 183.5(O_2C^tBu) (see Figure 4.12). The similarity of the *Me*-Sb signals with those found for **4.7** point to a closely related solution-state configuration.

4.2.3.4 Mass Spectroscopy

Although the molecular ion was not observed, several diantimony fragments were evident in the EI mass spectrum of $[Me_3Sb(O_2CMe)]_2O$ (**4.7**). The highest mass ion envelope was assigned to the $\{Me_6Sb_2O(O_2CMe)\}^+$ species (*ie.* loss of one acetate group from the parent) at m/z 407. In addition, two other diantimony fragments were observed, $\{Me_6Sb_2O\}^+$ and $\{Me_4Sb_2O\}^+$. Other notable peaks were assigned to $\{Me_3Sb(O_2CMe)\}^+$, $\{Me_3SbOH\}^+$, $\{MeSbOH\}^+$ and $\{Me_2Sb\}^+$.

In contrast to the spectrum of **4.7**, the EI spectra of $[Me_3Sb(O_2C^tBu)]_2O$ (**4.8**) showed an extremely complex fragmentation pattern, but with few assignable peaks. The only ions clearly observed were $\{Me_3Sb_2O\}^+$ at m/z 303, $\{Me_2Sb\}^+$ and $\{Sb\}^+$.

4.2.3.5 X-Ray Crystallography

A single crystal X-ray structure determination was carried out for $[Me_3Sb(O_2CMe)]_2O$ (**4.7**). Good quality single crystals were obtained by overlayering a concentrated dichloromethane solution of **4.7** with about twice the volume of pentane.

The molecular structure of **4.7** is shown in Figure 4.13 and selected bond lengths and angles are listed in Table 4.5. Further details of the crystal structure determination are given in Appendix K.

Figure 4.13 Molecular structure of $[Me_3Sb(O_2CMe)]_2O$ (4.7)

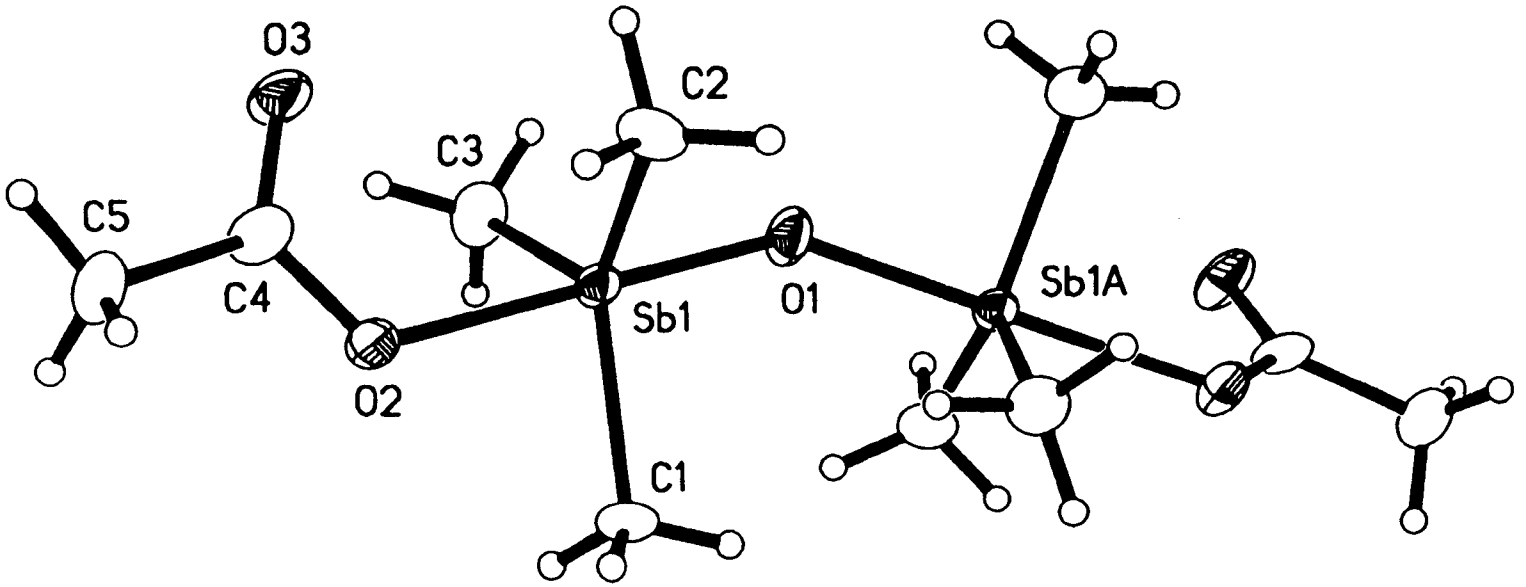

Table 4.5 Selected bond distances and angles, with standard deviations in parentheses for $[Me_3Sb(O_2CMe)]_2O$ (4.7)

Bond lengths, Å		Bond angles, °	
Sb(1) - O(1)	1.978(2)	Sb(1) - O(1) - Sb(1A)	140.1(4)
Sb(1) - O(2)	2.197(4)	O(1) - Sb(1) - O(2)	179.8(2)
Sb(1) - O(3)	3.207(4)	O(1) - Sb(1) - C(1)	97.4(2)
Sb(1) - C(1)	2.104(6)	O(1) - Sb(1) - C(2)	92.4(2)
Sb(1) - C(2)	2.098(8)	O(1) - Sb(1) - C(3)	90.7(3)
Sb(1) - C(3)	2.102(7)	C(1) - Sb(1) - O(2)	82.4(2)
O(2) - C(4)	1.304(9)	C(2) - Sb(1) - O(2)	87.6(2)
O(3) - C(4)	1.218(8)	C(3) - Sb(1) - O(2)	89.5(3)
C(4) - C(5)	1.506(11)	C(1) - Sb(1) - C(2)	123.2(3)
		C(1) - Sb(1) - C(3)	113.2(3)
		C(2) - Sb(1) - C(3)	122.5(3)
		O(3) - C(4) - O(2)	124.0(7)

The structure of **4.7** consists of two trimethylantimony acetate fragments bridged by an oxygen atom. The bridging oxygen lies on a crystallographic two-fold axis and thus provides crystallographic equivalence of the antimony centres. The geometry about antimony is trigonal bipyramidal, with three methyl groups occupying equatorial positions and an acetate oxygen and the bridging oxygen taking the axial positions.

As expected from the spectroscopic findings, the coordination of the acetate groups is near-unidentate, with only weak secondary chelate interactions (Sb(1)···O(3), 3.207(4) Å). The unidentate coordination is also mirrored in the C–O bond lengths, with a longer C(4)–O(2) bond length of 1.304(9) Å and a correspondingly shorter C(4)=O(3) double bond of 1.218(8) Å. The equivalent bond lengths found for $Ph_3Sb(O_2CMe)_2$ are 1.298 and 1.214 Å[26].

The most notable distortions from local D_{3h} symmetry about antimony are due to deviations in angles between methyl groups in the equatorial plane. However, in contrast to the situation found for $[Ph_3Sb(O_2CCF_3)]_2O$ (**4.1**), the deviations in **4.7** cannot be simply attributed to the weak chelate interactions from the formally non-bonded acetate oxygen pushing apart the two organo groups. Thus the chelate interaction [Sb(1)···O(3)] occurs in a position between C(2) and C(3) with a

corresponding C(2)–Sb(1)–C(3) angle of 122.5(3)°, but a larger angle of 123.2(3)° is observed for the C(1)–Sb(1)–C(2) angle with no apparent reason.

As found for **4.1**, the $Sb–O_{acetate}$ bond length is significantly longer than normally found for Sb–O single bonds. However, the elongation is less pronounced for **4.7** with the Sb(1)–O(2) bond lengths of 2.197(4) Å (*cf* mean 2.239 Å for **4.1**), which are comparable with the $Sb–O_{acetate}$ bond lengths in $Ph_3Sb(O_2CMe)_2$[26] of 2.130 Å.

The angle about the bridging oxygen is 140.1(4)°, with $Sb–O_{bridge}$ bond lengths of 1.978(2) Å, parameters similar to those found in **4.1** and for $[Ph_3SbCl]_2O$[36] amongst others. As has been observed in other structures reported in this work, little correlation can seemingly be drawn from comparisons between Sb–O–Sb angles and the corresponding $Sb–O_{bridge}$ bond lengths.

4.2.4 Tetrametallic 'Cage' Compounds

4.2.4.1 Preparation of Compounds

The reactions of $[Ph_2SbBrO]_2$ (**2.12**) with $Na(O_2AsR_2)$ to give quadruply bridged compounds has been discussed in Chapter 3. In the hope of preparing analogous compounds with bridging carboxylate groups in place of arsinates, related reactions were carried out between $[Ph_2SbBrO]_2$ and carboxylate salts. However, in these cases the reaction takes a different course and instead of there being simple substitution of both the bromine atoms, further reaction clearly takes place and the products isolated are based on tetraantimony 'cages' (see Figure 4.14).

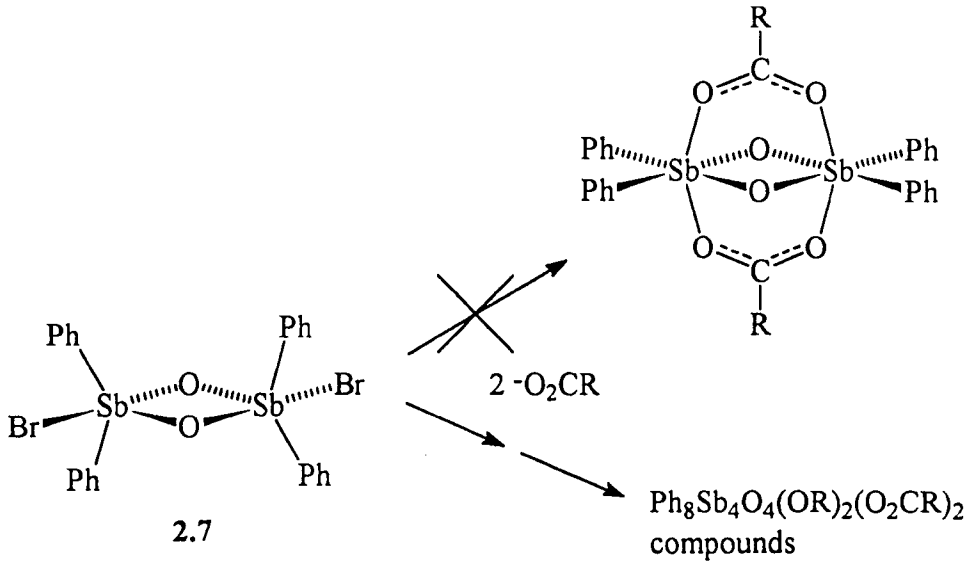

Figure 4.14 Reaction between $[Ph_2SbBrO]_2$ and carboxylate anions

One compound of this type, $[Ph_8Sb_4(\mu\text{-}O)_4(\mu\text{-}OH)_2(\mu\text{-}O_2CMe)_2].HO_2CMe$ has already been identified and is considered to arise from the hydrolysis of $Ph_2Sb(O_2CMe)_3$. The work described in this section, details the isolation of the same compound (**4.9**) (albeit from a different reaction course) in addition to two further compounds of this type, $[Ph_8Sb_4(\mu\text{-}O)_4(\mu\text{-}OH)(\mu\text{-}OEt)(\mu\text{-}O_2CMe)_2]$ (**4.10**) and $[Ph_8Sb_4(\mu\text{-}O)_4(\mu\text{-}OH)_2(\mu\text{-}O_2C^tBu)_2].HO_2C^tBu$ (**4.11**). Clearly compound **4.11** is closely related to that of **4.9**, with the only change being replacement of the acetate groups by trimethylacetate groups (pivalate groups) and incorporation of a trimethylacetic acid molecule, instead of an acetic acid molecule. The composition of compound **4.10**, is also related to that of **4.9**, although one of the bridging hydroxy groups is replaced by an ethoxy group and there is an absence of the acetic acid adduct.

The mechanism of formation of the tetrametallic compounds is clearly important in understanding the driving force behind their formation. The most probable route for the formation of compounds **4.9** and **4.10** (with an analogous scheme proposed for **4.11**) is shown in Figure 4.15.

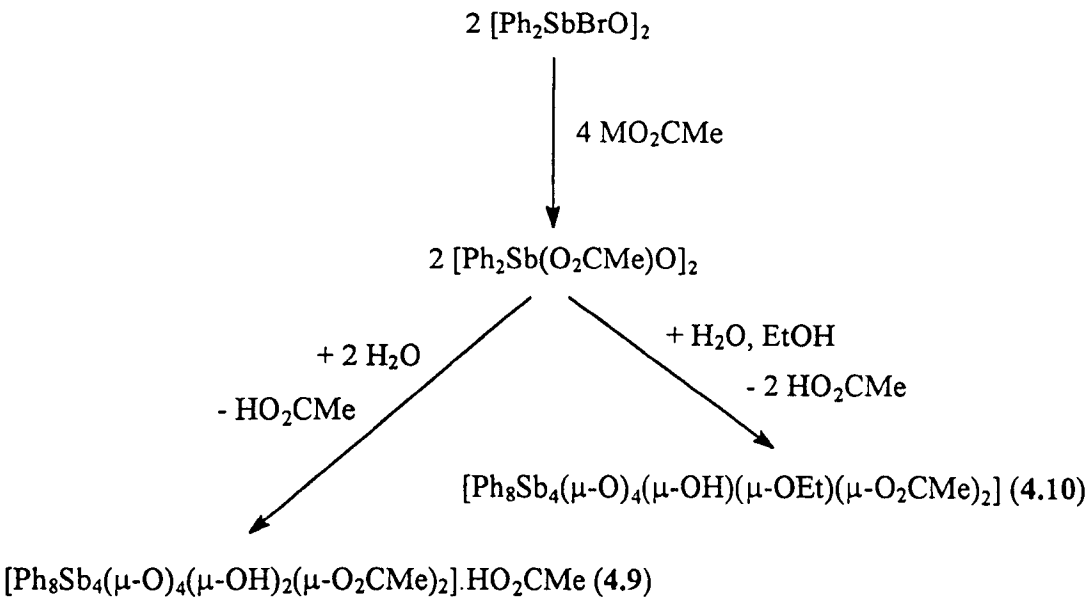

Figure 4.15 Mechanistic route to 'cage' compounds

As illustrated in the reaction scheme the formation of the 'cage' compounds must surely occur as a result of hydrolysis or alcoholysis. Thus, the reaction carried out to produce **4.9** is likely to have initially produced the intermediate species $[Ph_2Sb(O_2CMe)O]_2$ and then a subsequent reaction with traces of water (probably in the solvent) gives the isolated compound.

The reaction to produce **4.10** and subsequent handling of the compound was carried out under anhydrous conditions. Consequently, it seems that there must exist a strong driving force to promote the formation of the tetrametallic compounds to the extent that water and ethanol is 'scavenged' during the course of the reaction. Indeed, the source of the ethanol required in the formation of **4.10** is not known, but it is perhaps most likely that it was introduced as a contaminant from the ethanol/potassium hydroxide wash bath used for glassware cleaning. However, the glassware was subsequently rinsed in an aqueous acidic bath, washed with water and thoroughly oven-dried, thus the drive to form the tetrametallic compounds seems particularly powerful.

Another possible explanation (although not very probable) for the presence of ethanol, is contamination from the solvents used throughout the reaction and 'work-

up' stages. However, all solvents used were distilled over drying agents, under an inert atmosphere and stored in teflon-valve sealed vessels (see Chapter 1).

The structure of **4.9** has been previously elucidated by X-ray crystallography[19], the results of which showed the presence of the $[Ph_8Sb_4(\mu\text{-}O)_4(\mu\text{-}OH)_2(\mu\text{-}O_2CMe)_2]$ structural core, reminiscent of the tin 'crown' compounds[40]. A schematic view of the compound is shown below.

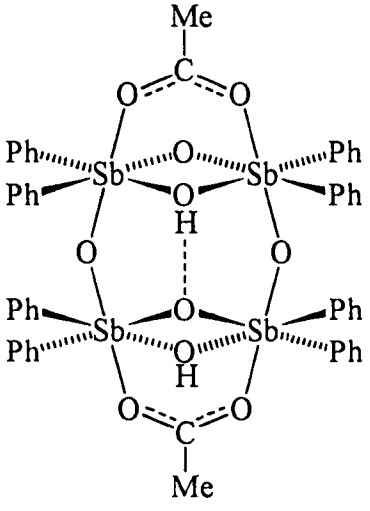

Figure 4.16 Molecular structure of $[Ph_8Sb_4(\mu\text{-}O)_4(\mu\text{-}OH)_2(\mu\text{-}O_2CMe)_2]$ (4.9)

The structure of **4.9** also showed the presence of a molecule of acetic acid, hydrogen bound from the second (bottom) bridging hydroxo group to the acid carbonyl oxygen and also from the acid hydroxy hydrogen to the top bridging oxygen atom.

4.2.4.2 Infrared Spectroscopy

The acetate groups in **4.9** are known from a structure determination[19] to be symmetrically bridging and as the compound also contains a molecule of hydrogen-bonded acetic acid there should be two different sets of acetate absorptions in the infrared spectrum. These can be clearly identified in the spectrum of **4.9**, obtained as a nujol mull, with bands at 1550 and 1433 cm^{-1} assigned to the $\nu_{asym}(CO_2)$ and $\nu_{sym}(CO_2)$ modes respectively of the bridging acetate groups and bands at 1691 and

1318 cm^{-1} assigned to the corresponding modes in the hydrogen-bonded acetic acid molecule.

The frequencies of the carboxylate bands for the bridging acetate groups, reflect their symmetrical coordination, with the $\Delta\nu(CO_2)$ value of only 117 cm^{-1} considerably lower than that found in the compounds $Ph_3Sb(O_2CMe)_2$ (**4.6**) and $[Me_3Sb(O_2CMe)]_2O$ (**4.7**), both having near unidentate acetate groups. Indeed, the band positions are similar to those found for $[(Cl_3Sb)_2(\mu\text{-}O)(\mu\text{-}OH)(\mu\text{-}O_2CMe)]$, also known to contain symmetrically bridging acetate groups (*ie.* $\nu_{asym}(CO_2)$ = 1490, $\nu_{sym}(CO_2)$ = 1435 and $\Delta\nu(CO_2)$ = 55 cm^{-1}).

Another significant absorption in the spectrum of **4.9** was observed at 791 cm^{-1}, likely to be due to a Sb–O–Sb stretch. Other expected Sb–O bands were not clearly assignable.

The infrared spectrum of **4.10** displayed only one acetate environment with a band at 1543 cm^{-1} assigned to the $\nu_{asym}(CO_2)$ mode of the bridging acetate groups, with the corresponding $\nu_{sym}(CO_2)$ band observed at 1434 cm^{-1}. The similarity of these band positions to those observed for **4.9** suggests a very similar structural skeleton and this is indeed shown in the crystal structure reported in Section 4.2.4.5. Further, an intense broad band was observed at 786 cm^{-1}, assigned to a ν(Sb–O–Sb) mode, again bearing close comparison to that found in the spectrum of **4.9**.

Two distinct sets of carboxylate absorptions were clearly observed in the solid-state infrared spectrum of $[Ph_8Sb_4(\mu\text{-}O)_4(\mu\text{-}OH)_2(\mu\text{-}O_2C^tBu)_2].HO_2C^tBu$ (**4.11**), with bands characteristic of a symmetrically coordinated carboxylate group noted at 1535 and 1433 cm^{-1} ($\Delta\nu(CO_2)$ = 102 cm^{-1}). The bands assigned to the trimethylacetic acid adduct were observed at 1678 and 1367 cm^{-1}. As would be expected, the band separation [$\Delta\nu(CO_2)$] of 311 cm^{-1} suggests non-delocalisation of the π-component within the acid molecule. A ν(Sb–O–Sb) band of similar frequency and appearance to both **4.9** and **4.10** was also seen in the spectrum of **4.11** at 793 cm^{-1}.

Table 4.6 Comparison of carboxylate bands (cm^{-1}) with coordination type

Compound	$\nu_{asym}(CO_2)$	$\nu_{sym}(CO_2)$	$\Delta\nu(CO_2)$	Coordination type
4.9	1550	1433	117	bridging
4.10	1543	1434	109	bridging
$[(Cl_3Sb)_2(\mu\text{-}O)(\mu\text{-}OH)(\mu\text{-}O_2CMe)]$	1490	1435	55	bridging[7]
$[Ph_2Sb(O_2CMe)_2]_2O$	1550	1405	145	chelating[41]
$Ph_3Sb(O_2CMe)_2$ (**4.6**)	1630	1318	312	near-unidentate[26]
4.11	1535	1433	102	bridging
$[Me_3Sb(O_2C^tBu)]_2O$ (**4.8**)	1620	1326	294	near-unidentate ?
$[(Cl_3Sb)_2(\mu\text{-}O)(\mu\text{-}OH)(\mu\text{-}O_2CCF_3)]$	1608	1455	153	bridging[7]
$[Ph_3Sb(O_2CCF_3)]_2O$ (**4.1**)	1714	1437	277	near-unidentate

4.2.4.3 NMR Data

Phenyl resonances in the ^1H NMR spectra of the compounds **4.9**, **4.10** and **4.11** proved to be closely related and provide a useful diagnostic 'handle' for identification of this compound type. At 250 MHz in $CDCl_3$ solution, all three compounds displayed two overlapping triplets, centred at *ca.* 7.16 and 7.21 ppm, assigned respectively to the *meta* and *para* protons of the chemically equivalent phenyl groups. Doublets at *ca.* 7.64 ppm were assigned to the *ortho* phenyl protons in each case. The $^3J_{HH}$ couplings for each compound were *ca.* 7.0 Hz and showed no significant second order coupling (in contrast to the anhydrous spectra of the oxo-bridged diantimony compounds such as $[Ph_3SbBr]_2O$, which tended to show a degree of $^4J_{HH}$ coupling and hence additional satellite peaks).

Full ^1H NMR data for $[Ph_8Sb_4(\mu\text{-}O)_4(\mu\text{-}OH)_2(\mu\text{-}O_2CMe)_2].HO_2CMe$ (**4.9**), $[Ph_8Sb_4(\mu\text{-}O)_4(\mu\text{-}OH)(\mu\text{-}OEt)(\mu\text{-}O_2CMe)_2]$ (**4.10**) and $[Ph_8Sb_4(\mu\text{-}O)_4(\mu\text{-}OH)_2(\mu\text{-}O_2C^tBu)_2].HO_2C^tBu$ (**4.11**) are tabulated in Table 4.7.

Table 4.7 ^{1}H NMR spectra of 4.9, 4.10 and 4.11

	^{1}H (Ph), ppm	^{1}H (other), ppm
4.9	7.16, 7.21, 7.63	1.88(s, HO_2CMe), 2.00(s, O_2CMe), 5.30(s, CH_2Cl_2), 5.72(s, br, OH)
4.10	7.17, 7.21, 7.65	1.03(t, OCH_2CH_3), 2.00(s, O_2CMe), 3.51(q, OCH_2CH_3), 5.30(s, CH_2Cl_2), 6.27(s, br, OH)
4.11	7.15, 7.21, 7.64	1.00(s, O_2C^tBu), 1.08(s, HO_2C^tBu), 6.02(s, br, OH)

As shown in Table 4.7, the chemical shift of the bridging acetate methyl group in both **4.9** and **4.10** occurred at 2.00 ppm, notably lower field than the corresponding signal for the compounds $Ph_3Sb(O_2CMe)_2$ (**4.6**) and $[Me_3Sb(O_2CMe)]_2O$ (**4.7**) (1.84 and 1.83 ppm respectively), in which the acetate groups are coordinated in a near-unidentate manner. Potentially, this observation could be used as a further characterising 'handle' for identification of bridging acetate groups and reflects the increased deshielding of the acetate protons, possibly due to the additional secondary interactions of the acetate oxygens.

Reliable $^{13}C\{^1H\}$ NMR data were only obtained for **4.11** due to the low solubility of the other compounds in common deuterated solvents. Resonances for **4.11** were observed at 27.1(CMe_3), 40.8(CMe_3), 127.7(*m*-Ph), 128.9(*p*-Ph), 133.4(*o*-Ph) and 148.4(*ipso*-Ph). The quaternary bridging O_2C resonances and signals due to the trimethylacetic acid adduct were not observed.

4.2.4.4 Mass Spectroscopy

Although no parent ion peaks, nor any ions associated with species containing all four antimony atoms, were observed peaks associated with triantimony ions were found in the FAB spectra of **4.10** and **4.11**. A signal common to both spectra was found at m/z 735, assigned to the $\{Sb_3Ph_4O_4\}^+$ fragment, showing the expected isotopic pattern for a triantimony species. In addition, the spectrum of **4.11** showed peaks assignable to

the further triantimony ions $\{Sb_3Ph_6O_4\}^+$,$\{Sb_3Ph_2O_4\}^+$ and $\{Sb_3O_4\}^+$ indicating that loss of the trimethylacetate groups was a primary fragmentation route.

A further common peak in both the spectra of **4.10** and **4.11** was observed at m/z 505 assigned to the diantimony species $\{Sb_2Ph_3O_2\}^+$, whilst the richer spectrum of **4.11** also showed peaks assigned to $\{Sb_2Ph_4O_2(O_2C^tBu)\}^+$ and $\{Sb_2Ph_4O_3\}^+$. Both spectra also showed a number of peaks assignable to simple monoantimony ions such as $\{Ph_2Sb\}^+$ and $\{PhSb\}^+$.

4.2.4.5 X-Ray Crystallography

A single crystal X-ray structure determination was carried out for $[Ph_8Sb_4(\mu\text{-}O)_4(\mu\text{-}OH)(\mu\text{-}OEt)(\mu\text{-}O_2CMe)_2].CHCl_2$ (**4.10**). Single crystals were obtained by slow diffusion of hexane vapour into a concentrated dichloromethane solution of the compound.

The molecular structure of **4.10** is shown in Figure 4.17 and selected bond lengths and angles are listed in Table 4.8. Further details of the crystal structure determination are given in Appendix L.

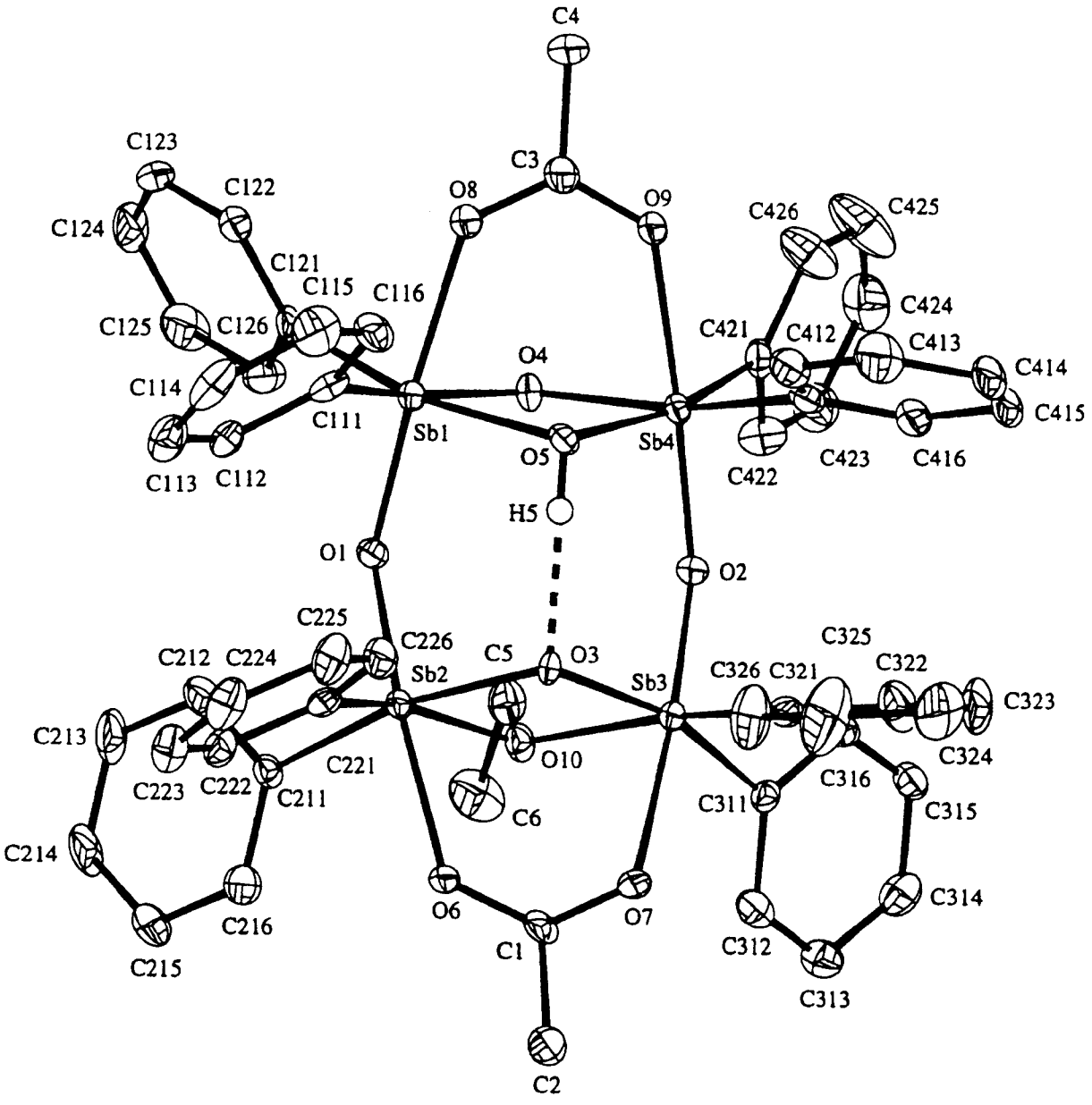

Figure 4.17 Molecular structure of $[Ph_8Sb_4(\mu\text{-}O)_4(\mu\text{-}OH)(\mu\text{-}OEt)(\mu\text{-}O_2CMe)_2]$ (4.10)

Table 4.8 Selected bond distances (Å) and angles (°), with standard deviations in parentheses for $[Ph_8Sb_4(\mu\text{-}O)_4(\mu\text{-}OH)(\mu\text{-}OEt)(\mu\text{-}O_2CMe)_2].CHCl_2$ (4.10)

Sb(1) - O(1)	1.957(3)	Sb(3) - O(2)	1.939(3)
Sb(1) - O(4)	1.966(3)	Sb(3) - O(3)	1.984(3)
Sb(1) - O(5)	2.143(3)	Sb(3) - O(7)	2.170(3)
Sb(1) - O(8)	2.190(3)	Sb(3) - O(10)	2.157(3)
Sb(1) - C(111)	2.133(2)	Sb(3) - C(311)	2.154(2)
Sb(1) - C(121)	2.135(2)	Sb(3) - C(321)	2.133(2)
Sb(2) - O(1)	1.937(3)	Sb(4) - O(2)	1.950(3)
Sb(2) - O(3)	1.973(3)	Sb(4) - O(4)	1.961(3)
Sb(2) - O(6)	2.213(3)	Sb(4) - O(5)	2.151(3)
Sb(2) - O(10)	2.155(3)	Sb(4) - O(9)	2.203(3)
Sb(2) - C(211)	2.164(2)	Sb(4) - C(411)	2.122(2)
Sb(2) - C(221)	2.141(2)	Sb(4) - C(421)	2.144(2)
C(1) - O(6)	1.265(5)	C(3) - C(4)	1.485(7)
C(1) - O(7)	1.272(5)	O(10) - C(5)	1.457(6)
C(1) - C(2)	1.488(7)	C(5) - C(6)	1.505(7)
C(3) - O(8)	1.266(6)	O(3) - O(5)	2.719(5)
C(3) - O(9)	1.273(6)	O(3) - H(5)	1.88(5)
Sb(1) - O(1) - Sb(2)	141.4(2)	Sb(1) - O(4) - Sb(4)	109.7(2)
Sb(3) - O(2) - Sb(4)	141.2(2)	Sb(1) - O(5) - Sb(4)	96.8(1)
Sb(2) - O(3) - Sb(3)	111.5(2)	Sb(2) - O(10) - Sb(3)	98.7(1)
O(1) - Sb(1) - O(8)	176.4(1)	O(2) - Sb(3) - O(7)	171.9(1)
O(4) - Sb(1) - C(111)	162.6(1)	O(3) - Sb(3) - C(311)	163.5(1)
O(5) - Sb(1) - C(121)	166.6(1)	O(10) - Sb(3) - C(321)	161.4(1)
O(1) - Sb(1) - O(4)	93.9(1)	O(2) - Sb(3) - O(3)	95.3(1)
O(1) - Sb(1) - O(5)	94.0(1)	O(2) - Sb(3) - O(10)	91.3(1)
O(1) - Sb(1) - C(111)	95.2(1)	O(2) - Sb(3) - C(311)	91.1(1)
O(1) - Sb(1) - C(121)	95.4(1)	O(2) - Sb(3) - C(321)	102.1(1)
O(4) - Sb(1) - O(5)	76.4(1)	O(3) - Sb(3) - O(10)	74.3(1)
O(4) - Sb(1) - O(8)	84.9(1)	O(3) - Sb(3) - O(7)	85.0(1)
O(4) - Sb(1) - C(121)	93.5(1)	O(3) - Sb(3) - C(321)	91.4(1)
O(5) - Sb(1) - O(8)	82.4(1)	O(10) - Sb(3) - O(7)	81.0(1)
O(5) - Sb(1) - C(111)	88.2(1)	O(10) - Sb(3) - C(311)	90.4(1)
O(8) - Sb(1) - C(111)	85.1(1)	O(7) - Sb(3) - C(311)	86.6(1)
O(8) - Sb(1) - C(121)	88.1(1)	O(7) - Sb(3) - C(321)	86.0(1)
C(111) - Sb(1) - C(121)	100.4(1)	C(311) - Sb(3) - C(321)	102.1(1)
O(1) - Sb(2) - O(6)	172.3(1)	O(2) - Sb(4) - O(9)	176.2(1)
O(3) - Sb(2) - C(211)	164.5(1)	O(4) - Sb(4) - C(411)	161.3(1)
O(10) - Sb(2) - C(221)	159.5(1)	O(5) - Sb(4) - C(421)	167.8(1)
O(1) - Sb(2) - O(3)	94.0(1)	O(2) - Sb(4) - O(4)	95.3(1)
O(1) - Sb(2) - O(10)	93.3(1)	O(2) - Sb(4) - O(5)	92.7(1)
O(1) - Sb(2) - C(211)	91.6(1)	O(2) - Sb(4) - C(411)	97.1(1)

O(1) - Sb(2) - C(221)	103.1(1)	O(2) - Sb(4) - C(421)	93.2(1)
O(3) - Sb(2) - O(10)	74.6(1)	O(4) - Sb(4) - O(5)	76.3(1)
O(3) - Sb(2) - O(6)	84.8(1)	O(4) - Sb(4) - O(9)	83.3(1)
O(3) - Sb(2) - C(221)	91.8(1)	O(4) - Sb(4) - C(421)	92.5(1)
O(10) - Sb(2) - O(6)	79.1(1)	O(5) - Sb(4) - O(9)	83.5(1)
O(10) - Sb(2) - C(211)	90.7(1)	O(5) - Sb(4) - C(411)	89.2(1)
O(6) - Sb(2) - C(211)	87.6(1)	O(9) - Sb(4) - C(411)	83.2(1)
O(6) - Sb(2) - C(221)	84.6(1)	O(9) - Sb(4) - C(421)	90.5(1)
C(211) - Sb(2) - C(221)	101.0(1)	C(411) - Sb(4) - C(421)	100.7(1)
O(6) - C(1) - O(7)	124.7(4)	O(8) - C(3) - O(9)	125.0(5)

The molecular structure of **4.10** confirms the formula of the compound to be $[Ph_8Sb_4(\mu\text{-}O)_4(\mu\text{-}OH)(\mu\text{-}OEt)(\mu\text{-}O_2CMe)_2]$ with a structural skeleton closely related to that found for $[Ph_8Sb_4(\mu\text{-}O)_4(\mu\text{-}OH)_2(\mu\text{-}O_2CMe)_2].HO_2CMe$ (**4.9**)[19]. Each antimony is bound to two phenyl groups, with pairs of antimony atoms bridged by an acetate group, an oxo bridge and a hydroxy or ethoxy bridge. The oxygen atoms O(1) and O(2) further interlink the two antimony pairs. The two Sb_2O_2 ring systems are further connected by a hydrogen bond from the O(5) hydroxy group to the O(3) oxygen which leads to a 'tilting' of the Sb_2O_2 planes with respect to each other.

The basic structural unit is an Sb_4O_6 'cage' (with two of the oxygens being those from the hydroxy and ethoxy group) that represents a structural variant of the usual M_4X_6 arrangement which is based on the 'adamantane' type of skeleton. The Sb_4O_6 unit found for **4.10** is however similar to that found in one form of the phosphorus(III) compound $P_4(N^iPr)_6$[42] and clearly very closely related to that found for **4.9**, comprising of two interlinked 4-membered rings.

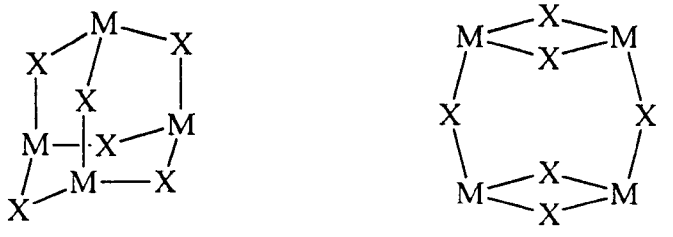

6-membered rings
'Adamantane-like'

4-membered rings

Figure 4.18 Alternate configurations for M_4X_6 systems

Coordination at antimony is basically octahedral, although significant distortions are evident, with *trans* angles as low as 159.5(1)° for the O(10)–Sb(2)–C(221) angle and *cis* angles distorted due to the constraints of the Sb_2O_2 rings. Internal ring angles are reduced to as little as 74.3(1)° (O(3)–Sb(3)–O(10)), with a corresponding opening of the angles between phenyl groups, for example the C(311)–Sb(3)–C(321) bond angle is 102.1(1)°.

Bond lengths from antimony to the single oxo bridges O(1) and O(2) are short, with a mean Sb–O bond length of 1.946 Å and corresponding Sb–O–Sb bond angles of 141.4(2)° and 141.2(2)° for the Sb(1)–O(1)–Sb(2) and Sb(3)–O(2)–Sb(4) angles respectively.

An interesting and unusual feature in the structure of **4.10** is the incorporation of the ethoxy bridge between Sb(2) and Sb(3) as opposed to the two hydroxo bridges found for **4.9**. The corresponding $Sb–O_{ethoxy}$ bond lengths are notably longer (mean 2.156 Å) than the Sb–O(3) bond lengths (mean 1.979 Å) completing that Sb_2O_2 ring. Bridging alkoxy groups are, however, not unknown in antimony chemistry and specifically ethoxy bridges are found in $[(Cl_3Sb)_2(\mu\text{-}O)(\mu\text{-}OEt)(\mu\text{-}O_2P(OEt)Et)]$[43] and the antimony(III) dimer $\{[(Me_2NH)Cl_2Sb]_2[\mu\text{-}OEt]_2\}$[44] amongst others.

The two independent acetate groups symmetrically bridge between antimony atoms with near-equivalent $Sb–O_{acetate}$ bond lengths in the range between 2.170(3) and 2.213(3) Å and corresponding C–O bond lengths within the range 1.265(5) to 1.273(6) Å, indicating almost complete delocalisation of the π component. Thus a good correlation is noted between the low $\Delta\nu(CO_2)$ value observed in the infrared spectrum and the symmetrical coordination of the acetate group.

The structure of **4.10** provides an indication to why the 'cage' compounds are formed in preference to the intended quadruply bridged products $[Ph_2Sb(O_2CR)O]_2$. A quadruply bridged compound with two acetate bridges, analogous to the compounds reported in Chapter 3 (such as $[(Ph_2Sb)_2(\mu\text{-}O)_2(\mu\text{-}O_2AsMe_2)_2]$ (**3.1**)), would seemingly be considerably strained as the 'bite-length' of the carboxylate groups is too short to bridge comfortably in this manner. However, the presence of only one

bridge in these tetra-antimony compounds would partially alleviate this strain, as the oxo bridges *trans* to the acetate groups are free to 'open' the structure and hence give *trans* angles closer to linearity (see Figure 4.19).

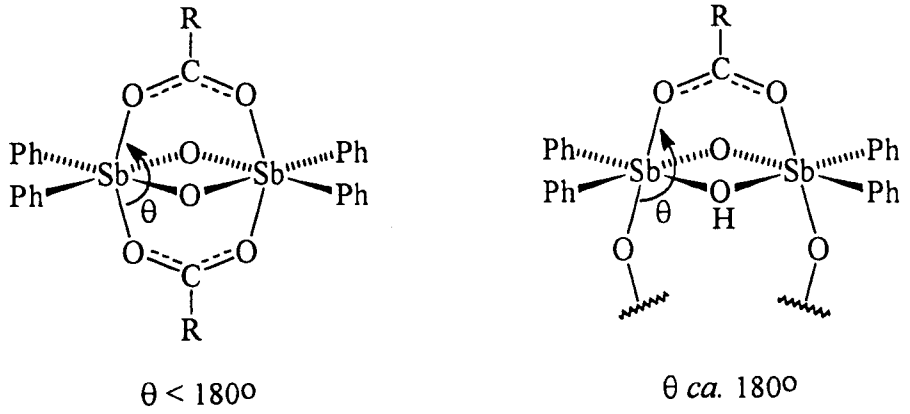

Figure 4.19 Comparison of *trans* angles between the expected quadruply bridged species and the 'cage' compound isolated

SUMMARY

The oxo-bridged carboxylate compounds, $[Ph_3Sb(O_2CCF_3)]_2O$ (**4.1**), $[Ph_3Sb(O_2CCCl_3)]_2O$ (**4.2**) and $[Ph_3Sb(O_2CCHCl_2)]_2O$ (**4.3**), were isolated in reactions between $[Ph_3SbBr]_2O$ (**2.7**) and the appropriate carboxylic acid in the presence of triethylamine. Spectroscopic results suggested that the carboxylate groups were coordinated in a unidentate fashion and this was confirmed by a structure determination of $[Ph_3Sb(O_2CCF_3)]_2O$.

A related reaction between $[Ph_3SbBr]_2O$ and two equivalents of HO_2CCH_2Cl and Et_3N however, led to cleavage of the oxo-bridge and $Ph_3Sb(O_2CCH_2Cl)_2$ (**4.4**) was isolated after work-up. Similarly, cleavage of the oxo-bridge was noted in reactions between $[Ph_3SbBr]_2O$ and HO_2CPh or $Ag(O_2CMe)$ giving the relevant triphenylantimony dicarboxylate compounds (**4.5** and **4.6** respectively).

In contrast, the oxo-bridge remained intact in reactions between $[Me_3SbCl]_2O$ (**2.10**) and both $Ag(O_2CMe)$ and $Na(O_2C^tBu)$ giving the compounds $[Me_3Sb(O_2CMe)]_2O$

(**4.7**) and $[Me_3Sb(O_2C^tBu)]_2O$ (**4.8**), both proposed to have near-unidentate coordinated carboxylate groups. Indeed, a structure determination of $[Me_3Sb(O_2CMe)]_2O$ showed that secondary interactions from the carboxylate carbonyl oxygen were very weak, with Sb···O chelate interactions of 3.207(4) Å.

Reactions between $[Ph_2SbBrO]_2$ (**2.12**) and two equivalents of carboxylate anions were found to be more complex and the products isolated after work-up were based on tetraantimony units with bridging carboxylate groups *ie.* $[Ph_8Sb_4(\mu\text{-}O)_4(\mu\text{-}OH)_2(\mu\text{-}O_2CMe)_2].HO_2CMe$ (**4.9**), $[Ph_8Sb_4(\mu\text{-}O)_4(\mu\text{-}OH)(\mu\text{-}OEt)(\mu\text{-}O_2CMe)_2]$ (**4.10**) and $[Ph_8Sb_4(\mu\text{-}O)_4(\mu\text{-}OH)_2(\mu\text{-}O_2C^tBu)_2].HO_2C^tBu$ (**4.11**). Compound **4.9** was previously isolated in a reaction between Ph_2SbCl_3 and three equivalents of $Ag(O_2CMe)$. The unusual compounds are based on a Sb_4O_6 skeleton consisting of interlinked Sb_2O_2 four-membered rings. Structural data for **4.10** was consistent with spectroscopic results which indicated the presence of symmetrically coordinated carboxylate groups.

4.3 EXPERIMENTAL AND CHARACTERISING DATA

4.3.1 Preparation of $[Ph_3Sb(O_2CCF_3)]_2O$ (4.1)

Trifluoroacetic acid (240mg, 2.08mmol) was added slowly to a stirred suspension of $[Ph_3SbBr]_2O$ (**2.7**) (920mg, 1.04mmol) and toluene (25ml), leading to dissolution. Triethylamine (210mg, 2.08mmol) was then added and the reaction mixture was stirred at room temperature for a further 16 hours. Removal of precipitated triethylammonium bromide by filtration and evaporation of solvent *in vacuo* yielded crude product, which was recrystallised from chloroform/hexane. Yield 610mg (62%); mp 228-230°C.

Found: C,50.45; H,3.38: $C_{40}H_{30}F_6O_5Sb_2$ requires C,50.67; H,3.19 %

^1H NMR (250MHz, $CDCl_3$, RT) Damp solvent: δ 7.31(t, 12H, $^3J_{HH}$ - 7Hz, *m*-Ph-**B**); 7.45(t, 6H, $^3J_{HH}$ - 7Hz, *p*-Ph-**B**); 7.52(d, 12H, $^3J_{HH}$ - 7Hz, *o*-Ph-**B**); 7.53(m, 18H, *m*- and *p*-Ph-**A**); 8.06(m, 12H, *o*-Ph-**A**), where **A** is $Ph_3Sb(OH)(O_2CCF_3)$ and **B** is $[Ph_3Sb(O_2CCF_3)]_2O$.

IR (nujol mull, CsI): 1714(vs), 1437(s), 1393(m), 1185(vs), 1144(s), 998(w), 841(w), 794(w), 742(vs), 721(m), 691(m), 456(m).

4.3.2 Preparation of $[Ph_3Sb(O_2CCCl_3)]_2O$ (4.2)

In a similar method to that outlined in 4.3.1, $[Ph_3SbBr]_2O$ (**2.7**) (1.00g, 1.13mmol) was treated with trichloroacetic acid (370mg, 2.27mmol) and triethylamine (230mg, 2.28mmol) in toluene (30ml). Precipitated triethylammonium bromide was removed by filtration, the volatiles removed *in vacuo* and the residue recrystallised from chloroform. Yield 380mg (32%); mp 170-174°C [lit 177°C[35]].

Found: C,46.79; H,3.81: $C_{40}H_{30}Cl_6O_5Sb_2$ requires C,45.89; H,2.89 %.

^{1}H NMR (250MHz, $CDCl_3$, RT) Damp solvent: δ 7.35(t, 12H, $^3J_{HH}$ - 7Hz, *m*-Ph-**B**); 7.48(t, 6H, $^3J_{HH}$ - 7Hz, *p*-Ph-**B**); 7.53(d, 12H, $^3J_{HH}$ - 7Hz, *o*-Ph-**B**); 7.53(m, 18H, *m*- and *p*-Ph-**A**); 8.12(m, 12H, *o*-Ph-**A**), where **A** is $Ph_3Sb(OH)(O_2CCCl_3)$ and **B** is $[Ph_3Sb(O_2CCCl_3)]_2O$.

IR (nujol mull, CsI): 1701(vs), 1435(s), 1289(vs), 1074(w), 997(w), 834(s), 738(vs), 691(vs), 454(m).

4.3.3 Preparation of $[Ph_3Sb(O_2CCHCl_2)]_2O$ (4.3)

In a similar method to 4.3.1, a reaction was carried out between dichloroacetic acid (360mg, 2.81mmol), $[Ph_3SbBr]_2O$ (**2.7**) (1.00g, 1.13mmol) and triethylamine (285mg, 2.81mmol) in toluene (20ml). Recrystallisation of the crude product from chloroform afforded a crystalline sample of the title compound. Yield 510mg (46%); mp 211-214°C.

Found: C,48.30; H,3.30: $C_{40}H_{32}Cl_4O_5Sb_2$ requires C,49.12; H,3.30 %.

^{1}H NMR (250MHz, $CDCl_3$, RT) Damp solvent: δ 5.55(s, 2H, $CHCl_2$-**B**); 5.75(s, 2H, $CHCl_2$-**A**); 7.30(t, 12H, $^3J_{HH}$ - 7Hz, *m*-Ph-**B**); 7.45(t, 6H, $^3J_{HH}$ - 7Hz, *p*-Ph-**B**); 7.60(d, 12H, $^3J_{HH}$ - 7Hz, *o*-Ph-**B**); 7.53(m, 18H, *m*- and *p*-Ph-**A**); 8.11(m, 12H, *o*-Ph-**A**), where **A** is $Ph_3Sb(OH)(O_2CCHCl_2)$ and **B** is $[Ph_3Sb(O_2CCHCl_2)]_2O$. Under strictly anhydrous conditions signals due to **B** only were observed.

$^{13}C\{^1H\}$ NMR (69 MHz, $CDCl_3$, RT, anhydrous (only **B**)) δ 67.8(Cl_2CH); 129.3(*m*-Ph); 131.1(*p*-Ph); 133.7(*o*-Ph); 138.1(*ipso*-Ph), quaternary carboxylate carbon not observed.

IR (nujol mull, CsI): 1694(s), 1669(s), 1435(s), 1325(vs), 1193(m), 740(vs), 692(s), 459(s).

MS (FAB): $\{Ph_6Sb_2O(O_2CCHCl_2)\}^+$(m/z 847, 49%); $\{Ph_6Sb_2O(O_2CCCl)\}^+$(m/z 811, 18%); $\{Ph_3Sb(O_2CCHCl_2)\}^+$(m/z 479, 23%); $\{Ph_3SbOH\}^+$(m/z 369, 5%); $\{Ph_2Sb\}^+$(m/z 275, 23%); $\{PhSb\}^+$ (m/z 198, 23%); $\{Ph_2\}^+$ (m/z 154, 100%); $\{Ph\}^+$ (m/z 77, 43%).

4.3.4 Reaction of $[Ph_3SbBr]_2O$ with two equivalents of HO_2CCH_2Cl

A stirred suspension of $[Ph_3SbBr]_2O$ (**2.7**) (990mg, 1.12mmol) and toluene (20ml) was treated with chloroacetic acid (223mg, 2.36mmol) giving a clear solution. Addition of triethylamine (239mg, 2.36mmol) led to the immediate formation of a white precipitate. The mixture was stirred at ambient temperature for 24 hours and then filtered to remove insolubles. Removal of solvent *in vacuo* gave a crude product that was recrystallised from chloroform/hexane to give crystals of a material identified as $Ph_3Sb(O_2CCH_2Cl)_2$ (**4.4**). Yield 557mg (46% with respect to $[Ph_3SbBr]_2O$); mp 132-135°C [lit 132-133°C[38]].

Found: C,48.78; H,3.54: $C_{22}H_{19}Cl_2O_4Sb$ requires C,48.93; H,3.55 %

^1H NMR (250MHz, $CDCl_3$, RT) δ 3.86(s, 4H, CH_2Cl); 7.55(m, 9H, *m*- and *p*-Ph); 8.03(m, 6H, *o*-Ph).

$^{13}C\{^1H\}$ NMR (69 MHz, $CDCl_3$, RT) δ 42.5($ClCH_2$); 129.6(*m*-Ph); 131.7(*p*-Ph); 133.9(*o*-Ph); 135.8(*ipso*-Ph); 169.9(O_2C).

IR (nujol mull, CsI): 1673(w,sh), 1646(vs), 1481(m), 1435(s), 1366(m), 1332(vs), 1259(m), 1228(w), 1073(m), 1021(m), 998(m), 773(vs), 737(s), 692(s), 461(s), 452(s).

MS (EI): $\{Ph_2Sb(O_2CCH_2Cl)_2\}^+$ (m/z 461, 6%); $\{Ph_3Sb(O_2CCH_2Cl)\}^+$ (m/z 445, 74%); $\{Ph_3SbCl\}^+$ (m/z 387, 17%); $\{Ph_2Sb\}^+$ (m/z 275, 14%); $\{Sb(O_2CCH_2Cl)\}^+$ (m/z 214, 33%); $\{PhSb\}^+$ (m/z 198, 47%); $\{Ph_2\}^+$ (m/z 154, 100%); $\{Ph\}^+$ (m/z 77, 38%).

4.3.5 Reaction of $[Ph_3SbBr]_2O$ with two equivalents of HO_2CPh

Following an analogous procedure to 4.3.4, $[Ph_3SbBr]_2O$ (**2.7**) (1.02g, 1.15mmol), benzoic acid (300mg, 2.42mmol) and triethylamine (245mg, 2.42mmol) were stirred together in toluene (25ml). After filtration to remove precipitated triethylammonium

bromide the solvent was evaporated yielding an oily residue. Recrystallisation from chloroform/hexane gave a white crystalline product, analysing as $Ph_3Sb(O_2CPh)_2$ (**4.5**). Yield 220mg (16% with respect to $[Ph_3SbBr]_2O$); mp 172-175°C [lit 176-177°C[45]].

Found: C,64.01; H,4.11: $C_{32}H_{25}O_4Sb$ requires C,64.56; H,4.23 %

^1H NMR (250MHz, $CDCl_3$, RT) δ 7.36(t, 4H, $^3J_{HH}$ - 7.5Hz, *m*-Ph-benzoate); 7.47(t, 2H, $^3J_{HH}$ - 7.5Hz, *p*-Ph-benzoate); 7.51(m, 9H, *m*- and *p*-Ph-Sb); 7.96(d, 4H, $^3J_{HH}$ - 7.5Hz, *o*-Ph-benzoate); 8.14(m, 6H, *o*-Ph-Sb).

IR (nujol mull, CsI): 1645(s), 1577(w), 1536(w), 1435(s), 1324(vs), 1300(s), 1125(w), 1068(w), 1024(w), 998(w), 764(vs), 734(vs), 718(s), 691(s), 449(s).

4.3.6 Reaction of $[Ph_3SbBr]_2O$ with two equivalents of AgO_2CMe

Silver acetate (329mg, 1.97mmol) was added to a stirred solution of $[Ph_3SbBr]_2O$ (**2.7**) (697mg, 0.79mmol) in dichloromethane (30ml) and the resultant reaction mixture was stirred in the dark under reflux for 16 hours. After filtration to remove insolubles, the solvent was evaporated to give an off-white product. Recrystallisation from chloroform/hexane gave well-formed crystals of a compound analysing as $Ph_3Sb(O_2CMe)_2$ (**4.6**). Yield 340mg (46% with respect to $[Ph_3SbBr]_2O$); mp 209-212°C [lit 213-215°C[45]].

Found: C,56.08; H,4.59: $C_{22}H_{21}O_4Sb$ requires C,56.08; H,4.49 %

^1H NMR (250MHz, $CDCl_3$, RT) δ 1.84(s, 6H, O_2CMe); 7.49(m, 9H, *m*- and *p*-Ph); 8.01(m, 6H, *o*-Ph).

$^{13}C\{^1H\}$ NMR (69 MHz, $CDCl_3$, RT) δ 22.1(CH_3); 129.1(*m*-Ph); 130.9(*p*-Ph); 133.8(*o*-Ph); 139.0(*ipso*-Ph); 175.7(O_2C).

IR (nujol mull, CsI): 1630(s), 1318(s), 1008(w), 932(m), 915(w), 688(m), 672(w), 609(w), 486(m).

MS (EI): $\{Ph_3Sb(O_2CMe)\}^+$ (m/z 411, 61%); $\{Ph_2Sb(O_2CMe)_2\}^+$ (m/z 393, 20%); $\{Ph_3SbOH\}^+$ (m/z 369, 11%); $\{Ph_3Sb\}^+$ (m/z 352, 7%); $\{Ph_2Sb(O_2CMe)\}^+$ (m/z 334, 8%); $\{Ph_2Sb\}^+$ (m/z 275, 18%); $\{PhSb(O_2CMe)\}^+$ (m/z 257, 27%); $\{PhSbOH\}^+$ (m/z 215, 22%); $\{PhSb\}^+$ (m/z 198, 100%); $\{Sb(O_2CMe)\}^+$ (m/z 180, 35%); $\{Ph_2\}^+$ (m/z 154, 91%); $\{Ph\}^+$ (m/z 77, 41%); $\{HO_2CMe\}^+$ (m/z 60, 10%).

4.3.7 Attempted reaction of $[Ph_3SbBr]_2O$ with two equivalents of NaO_2CMe

Sodium acetate (153mg, 1.87mmol) was added to a stirred solution of $[Ph_3SbBr]_2O$ (**2.7**) (719mg, 0.82mmol) in dichloromethane (35ml) and the resultant mixture was stirred at reflux for 19 hours. After filtration, the solvent was removed *in vacuo* to yield crude product. Recrystallisation afforded a crystalline product that proved to be unreacted $[Ph_3SbBr]_2O$.

4.3.8 Attempted reaction of $[Ph_3SbBr]_2O$ with two equivalents of $(MeCO)_2O$

Acetic anhydride (97mg, 0.95mmol) was syringed into a solution of $[Ph_3SbBr]_2O$ (**2.7**) (370mg, 0.42mmol) in dichloromethane (20ml) and the resulting solution was stirred for 4 hours. After this time volatiles were removed *in vacuo* giving an off-white material. Recrystallisation gave crystals of the unreacted starting material $[Ph_3SbBr]_2O$.

4.3.9 Preparation of $[Me_3Sb(O_2CMe)]_2O$ (4.7)

A solution of $[Me_3SbCl]_2O$ (**2.10**) (668mg, 1.59mmol) in dichloromethane (20ml) was added to a suspension of silver acetate (581mg, 3.5mmol) and dichloromethane (10ml) under an argon atmosphere, in darkness. The resulting mixture was then stirred for *ca.* 24 hours at room temperature, after which time precipitated silver salts were removed by cannula filtration. The pale purple solution was then evaporated, affording a grey-white powder. The crude product was purified by recrystallisation from dichloromethane/pentane, giving good quality crystals of the title compound (**4.7**). Yield 600mg (81%); mp 174-176°C.

Found: C,25.61; H,5.24: $C_{10}H_{24}O_5Sb_2$ requires C,25.68; H,5.17 %

^1H NMR (250MHz, $CDCl_3$, RT) δ 1.62(s, 18H, *Me*-Sb); 1.83(s, 6H, O_2C*Me*); decomposition was noted after exposure to atmospheric moisture.

$^{13}C\{^1H\}$ NMR (69 MHz, $CDCl_3$, RT) δ 14.5(*Me*-Sb); 23.3(O_2C*Me*); 176.4(O_2CMe).

IR (nujol mull, CsI): 1623(s), 1374(s), 1311(s), 1097(w,br), 1015(m), 925(m), 851(s), 710(s), 658(s), 577(m), 527(w), 493(m).

MS (EI): $\{Me_6Sb_2O(O_2CMe)\}^+$ (m/z 409, 3%); $\{Me_6Sb_2O\}^+$ (m/z 351, 30%); $\{Me_4Sb_2O\}^+$ (m/z 321, 18%); $\{Me_3Sb(O_2CMe)\}^+$ (m/z 225, 100%); $\{Me_3SbOH\}^+$ (m/z 183, 49%); $\{MeSbOH\}^+$ (m/z 153, 28%); $\{Me_2Sb\}^+$ (m/z 151, 23%).

4.3.10 Preparation of $[Me_3Sb(O_2C^tBu)]_2O$ (4.8)

A solution of $[Me_3SbCl]_2O$ (**2.10**) (370mg, 0.88mmol) in dichloromethane (20ml) was added under argon to a suspension of sodium trimethylacetate (224mg, 1.80mmol) and dichloromethane (10ml). After stirring at room temperature for 16 hours, the mixture was filtered to give a clear solution. Evaporation of volatiles *in vacuo* gave a crude product that was recrystallised from toluene/hexane yielding crystals of $[Me_3Sb(O_2C^tBu)]_2O$ (**4.8**). Yield 320mg (66%).

Found: C,34.13; H,6.59: $C_{16}H_{36}O_5Sb_2$ requires C,34.82; H,6.57 %

^1H NMR (250MHz, $CDCl_3$, RT) δ 1.03(s, 18H, O_2C^tBu); 1.59(s, 18H, *Me*-Sb).

Traces of the compound $Me_3Sb(O_2C^tBu)_2$ were also detected prior to recrystallisation {δ 1.08(s, 18H, O_2C^tBu); 1.77(s, 9H, *Me*-Sb)}.

$^{13}C\{^1H\}$ NMR (69 MHz, $CDCl_3$, RT) δ 14.3(*Me*-Sb); 27.7(CMe_3); 39.1(CMe_3); 183.5(O_2C^tBu).

IR (nujol mull, CsI): 1620(s), 1326(s), 1211(s), 849(w, br), 750(s), 603(m), 550(w).

MS (EI): $\{Me_3Sb_2O\}^+$ (m/z 303, 7%); $\{Me_2Sb\}^+$ (m/z 151, 80%); $\{Sb\}^+$ (m/z 121, 61%).

4.3.11 Reaction of $[Me_3SbCl]_2O$ with two equivalents of HO_2CCF_3

Trifluoroacetic acid (222mg, 1.95mmol) was added slowly to a stirred solution of $[Me_3SbCl]_2O$ (**2.10**) (404mg, 0.96mmol) and toluene (30ml) under argon. Triethylamine (182mg, 1.79mmol) was then added and the reaction mixture stirred at room temperature for a further 24 hours. Removal of precipitated material by filtration and evaporation of solvent *in vacuo* yielded crude product. ^1H NMR spectroscopy showed the material to be a mixture of several compounds which were not identified.

4.3.12 Preparation of $[Ph_8Sb_4(\mu\text{-}O)_4(\mu\text{-}OH)_2(\mu\text{-}O_2CMe)_2].HO_2CMe$ (4.9)

Silver acetate (541mg, 3.24mmol) was added to a solution of $[Ph_2SbBrO]_2$ (**2.12**) (1.146g, 1.54mmol) in dichloromethane (30ml) in the dark and the resulting mixture was stirred for 24 hours at room temperature, with no specific attempts to exclude atmospheric moisture. The mixture was then filtered to remove insoluble materials and crude product obtained by evaporation of the solvent. The title compound (**4.9**) as a dichloromethane solvate was separated from traces of $Ph_3Sb(O_2CMe)_2$ (observed by ^1H NMR spectroscopy) by recrystallisation from dichloromethane/pentane. Yield 810mg (76%). Gradual melting with decomposition above 170°C.

Found: C,45.28; H,3.61: $C_{52}H_{48}O_{10}Sb_4.HO_2CCH_3.CH_2Cl_2$ requires C,45.09; H,3.72 %

^1H NMR (250MHz, $CDCl_3$, RT) δ 1.88(s, 3H, $HO_2C\mathit{Me}$); 2.00(s, 6H, $O_2C\mathit{Me}$); 5.30(s, 2H, $C\mathit{H}_2Cl_2$); 5.72(position varies with concentration, s, br, O*H*); 7.16(t, 16H, $^3J_{HH}$ - 7Hz, *m*-Ph); 7.21(t, 8H, $^3J_{HH}$ - 7Hz, *p*-Ph); 7.63(d, 16H, $^3J_{HH}$ - 7Hz, *o*-Ph).

IR (nujol mull, CsI): 1691(m), 1550(vs), 1433(vs), 1318(w), 1074(w), 1023(w), 999(w), 791(s), 735(m), 693(s), 664(m), 628(w), 483(w), 459(m).

4.2.13 Preparation of $[Ph_8Sb_4(\mu\text{-}O)_4(\mu\text{-}OH)(\mu\text{-}OEt)(\mu\text{-}O_2CMe)_2]$ (4.10)

A solution of $[Ph_2SbBrO]_2$ (**2.12**) (2.010g, 2.70mmol) in dichloromethane (50ml) was added, under an argon atmosphere, to a slurry of sodium acetate (508mg, 6.19mmol) and dichloromethane (10ml). The reaction mixture was then stirred at room temperature for 4 days to ensure complete reaction, after which time insolubles were removed by cannula filtration. Evaporation of the solvent *in vacuo* gave a white powder, that was recrystallised from dichloromethane/hexane. After a few days a quantity of well-formed crystals was isolated. Yield 1.05g (58%). Gradual melting with decomposition above 185°C.

Found: C,46.01; H,3.81: $C_{54}H_{52}O_{10}Sb_4.CH_2Cl_2$ requires C,46.10; H,3.80 %

^1H NMR (250MHz, $CDCl_3$, RT) δ 1.03(t, 3H, $^3J_{HH}$ - 7Hz, $OCH_2C\mathit{H}_3$); 2.00(s, 6H, $O_2C\mathit{Me}$); 3.51(q, 2H, $OC\mathit{H}_2CH_3$); 5.30(s, 2H, $C\mathit{H}_2Cl_2$); 6.27(position varies with concentration, s, br, O*H*); 7.17(t, 16H, $^3J_{HH}$ - 7Hz, *m*-Ph); 7.21(t, 8H, $^3J_{HH}$ - 7Hz, *p*-Ph); 7.65(d, 16H, $^3J_{HH}$ - 7Hz, *o*-Ph).

IR (nujol mull, CsI): 1543(vs), 1434(vs), 1351(m), 1073(m), 1023(w), 786(vs), 736(m), 729(m), 692(s), 670(s), 458(s).

MS (FAB): $\{Sb_3Ph_4O_4\}^+$ (m/z 735, 9%); $\{Sb_2Ph_3O_2\}^+$ (m/z 505, 8%); $\{Ph_2Sb\}^+$ (m/z 275, 21%); $\{PhSb\}^+$ (m/z 198, 12%).

4.2.14 Preparation of $[Ph_8Sb_4(\mu\text{-}O)_4(\mu\text{-}OH)_2(\mu\text{-}O_2C^tBu)_2].HO_2C^tBu$ (4.11)

A solution of $[Ph_2SbBrO]_2$ (**2.12**) (1.600g, 2.15mmol) in dichloromethane (35ml) was added to a stirred slurry of sodium trimethylacetate (576mg, 4.64mmol) in dichloromethane (15ml) and the mixture was stirred at room temperature for 48 hours. Precipitated sodium salts were then removed by filtration and crude product was obtained by evaporation of volatiles *in vacuo*. Crystalline product was obtained on recrystallising from chloroform/hexane. Yield 910mg (56%). Gradual melting with decomposition above 130°C.

Found: C,49.03; H,4.65: $C_{58}H_{60}O_{10}Sb_4.HO_2CC(CH_3)_3$ requires C,50.24; H,4.68 %.

^1H NMR (250MHz, $CDCl_3$, RT) δ 1.00(s, 18H, O_2C^tBu); 1.08(s, 9H, HO_2C^tBu); 6.02(position varies with concentration, s, br, O*H*); 7.15(t, 16H, $^3J_{HH}$ - 7Hz, *m*-Ph); 7.21(t, 8H, $^3J_{HH}$ - 7Hz, *p*-Ph); 7.64(d, 16H, $^3J_{HH}$ - 7Hz, *o*-Ph).

$^{13}C\{^1H\}$ NMR (69 MHz, $CDCl_3$, RT) δ 27.1(CMe_3); 40.8(CMe_3); 127.7(*m*-Ph); 128.9(*p*-Ph); 133.4(*o*-Ph); 148.4(*ipso*-Ph), quaternary O_2C resonance and signals due to acid adduct not observed.

IR (nujol mull, CsI): 3145(w, br), 1678(s), 1535(vs), 1484(m), 1433(s), 1423(m), 1367(m), 1227(m), 1192(w), 1069(m), 793(vs), 730(s), 693(s), 660(m), 624(m), 615(m), 482(m), 463(m).

MS (FAB): $\{Sb_3Ph_6O_4\}^+$ (m/z 889, 36%); $\{Sb_3Ph_4O_4\}^+$ (m/z 735, 82%); $\{Sb_2Ph_4O_2(O_2C^tBu)\}^+$ (m/z 683, 16%); $\{Sb_2Ph_4O_3\}^+$ (m/z 598, 14%); $\{Sb_3Ph_2O_4\}^+$ (m/z 581, 100%); $\{Sb_2Ph_3O_2\}^+$ (m/z 505, 84%); $\{Sb_3O_4\}^+$ (m/z 427, 31%); $\{Ph_2Sb\}^+$ (m/z 275, 28%); $\{PhSb\}^+$ (m/z 198, 16%); $\{Ph_2\}^+$ (m/z 154, 26%).

4.4 REFERENCES

1. See for example N.W.Alcock, V.M.Tracy, T.C.Waddington, *J. Chem. Soc., Dalton Trans.*, 1976, 2243.

2. S.P.Bone, PhD Thesis, University of Nottingham, 1979.

3. G.B.Deacon, R.J.Phillips, *Coord. Chem. Rev.*, 1980, **33**, 227 and references cited therein.

4. B.S.Manhas, A.K.Trikha, *J. Indian Chem. Soc.*, 1982, **59**, 315.

5. G.B.Deacon, F.Huber, R.J.Phillips, *Inorg. Chim. Acta*, 1985, **104**, 41.

6. F.J.Koller, W.Schwarz, A.Schmidt, *Z. Naturforsch.*, 1979, **34b**, 563.

7. S.Blösl, W.Schwarz, A.Schmidt, *Z. Anorg. Allg. Chem.*, 1981, **474**, 51.

8. S.Blösl, W.Rozdzinski, A.Schmidt, *Z. Anorg. Allg. Chem.*, 1986, **538**, 61.

9. D.B.Sowerby, M.J.Begley, P.L.Millington, *J. Chem. Soc., Chem. Commun.*, 1984, 896.

10. D.P.Bullivant, M.F.A.Dove, M.J.Haley, *J. Chem. Soc., Dalton Trans.*, 1980, 109.

11. M.Hall, D.B.Sowerby, *J. Chem. Soc., Dalton Trans.*, 1980, 1292.

12. D.P.Bullivant, M.F.A.Dove, M.J.Haley, *J. Chem. Soc., Dalton Trans.*, 1980, 105.

13. R.Mattes, D.Ruhl, *Z. Anorg. Allg. Chem.*, 1984, **508**, 19.

14. S.Bone, D.B.Sowerby, *J. Organomet. Chem.*, 1980, **184**, 181.

15. P.Raj, A.K.Aggarwal, *Synth. React. Inorg. Met.-Org. Chem.*, 1992, **22**, 509.

16. M.Wieber, I.Fetzer-Kremling, H.Reith, C.Burschka, *Z. Naturforsch.*, 1987, **42b**, 815.

17. H.A.Meinema, J.G.Noltes, *J. Organomet. Chem.*, 1972, **36**, 313.

18. J.G.Stevens, J.M.Trooster, H.A.Meinema, *Inorg. Chim. Acta.*, 1980, **40**, 263.

19. D.B.Sowerby, M.J.Begley, P.L.Millington, *J. Chem. Soc., Chem. Commun.*, 1984, 896.

20. I.G.Southerington, PhD Thesis, University of Nottingham, 1991.

21. See for example R.G.Goel, D.R.Ridley, *J. Organomet. Chem.*, 1972, **38**, 83; and

22. G.O.Doak, G.G.Long, L.D.Freedman, *J. Organomet. Chem.*, 1965, **4**, 82 and references therein.

23. A.K.S. Chauhan, R.Sharma, R.C.Srivastava, *Indian J. Chem.*, 1992, **31A**, 475.

24. H.Preut, M.Domagala, F.Huber, *Acta Crystallogr.*, 1987, **C43**, 416.

25. M.Domagala, F.Huber, H.Preut, *Z. Anorg. Allg. Chem.*, 1990, **582**, 37.

26. D.B.Sowerby, *J. Chem. Res.*, 1979, **S80**, M1001.

27. V.A.Lebedev, R.I.Bochkova, L.F.Kuzubova, E.A.Kuz'min, V.V.Sharutin, N.V.Belov, *Dokl. Akad. Nauk. SSSR*, 1982, **265**, 332.

28. G.Ferguson, B.Kaitner, C.Glidewell, S.Smith, *J. Organomet. Chem.*, 1991, **419**, 283.

29. M.Domagala, F.Huber, H.Preut, *Z. Anorg. Allg. Chem.*, 1989, **574**, 130.

30. T.Westhoff, F.Huber, H.Preut, *J. Organomet. Chem.*, 1988, **348**, 185.

31. H.Preut, T.Westhoff, F.Huber, *Acta Crystallogr.*, 1989, **C45**, 49.

32. S.P.Bone, D.B. Sowerby, *J. Chem. Res.*, 1979, **S82**, M1029.

33. S.P.Bone, D.B. Sowerby, *Phosphorus, Sulphur and Silicon*, 1989, **45**, 23.

34. M.A.Said, K.C.K.Swamy, K.Babu, K.Aparna, M.Nethaji, *J. Chem. Soc., Dalton Trans*, 1995, 2151.

35. K.Pandey, R.C.Srivastava, *Synth. React. Inorg. Met.-Org. Chem.*, 1985, **15**, 327.

36. E.R.T.Tiekink, *J. Organomet. Chem.*, 1988, **333**, 199.

37. K.Shen, W.E.McEwen, S.J.Laplaca, W.C.Hamilton, A.P.Wolf, *J. Am. Chem. Soc.*, 1968, **90**, 1718.

38. R.G.Goel, D.R.Ridley, *J. Organomet. Chem.*, 1972, **38**, 83.

39. S.Kraft, M.Wieber, *Z. Anorg. Allg. Chem.*, 1992, **607**, 153.

40. see for example K.C.Kumara Swamy, C.G.Schmid, R.O.Day, R.R.Holmes, *J. Am. Chem. Soc.*, 1988, **110**, 1067.

41. P.L.Millington, PhD Thesis, University of Nottingham, 1982.

42. O.J.Scherer, K.Andres, C.Kruger, Y.-H.Tsay, G.Wolmershauser, *Angew. Chem., Int. Ed. Engl.*, 1980, **19**, 571.

43. A.Sauvigny, J.E.Faerber, A.Rihm, H.Thurn, A.Schmidt, *Z. Anorg. Allg. Chem.*, 1995, **621**, 640.

44. A.J.Edwards, N.E.Leadbeater, M.A.Paver, P.R.Raithby, C.A.Russell, D.S.Wright, *J. Chem. Soc., Dalton Trans.*, 1994, 1479.

45. J.Havranek, J.Mleziva, A.Lycka, *J. Organomet. Chem.*, 1978, **157**, 163.

CHAPTER 5

FIVE COORDINATION IN ANTIMONY(V) CHEMISTRY

5.1 INTRODUCTION

This chapter addresses a different problem in antimony chemistry and is concerned with the possibility of isolating antimony(V) compounds in which the ligands are arranged at the corners of a square pyramid.

The vast majority of five-coordinate Group 15 compounds have been shown to have trigonal bipyramidal (TBP) structures, although it has been calculated that the conformational energy difference between this arrangement and the alternative square pyramidal (SP) structure is small[1]. The two alternative arrangements are linked by the Berry pseudorotation coordinate[2], as illustrated in Figure 5.1, which describes the interconversion of the two forms by slight bond bending. Five coordinate structures are therefore considered to be stereochemically non-rigid.

Figure 5.1 Berry Pseudorotation

As shown in Figure 5.1, the bond angles in the original trigonal bipyramid, $\theta_{15} = 180°$ and $\theta_{24} = 120°$, are distorted to give equal values (θ_{15} and $\theta_{24} \approx 150°$) in the square pyramidal structure. Further, Berry pseudorotation is also proposed to be the mechanism by which axial/equatorial ligands exchange in isolable TBP compounds, via SP intermediates (*ie.* the final trigonal bipyramidal structure will have reversed bond angles of $\theta_{15} = 120°$ and $\theta_{24} = 180°$)[3,4].

Structures of phosphorus(V) compounds have been the most widely investigated of the Group 15 elements, with a range of structures noted along the Berry coordinate, including a number of SP structures. In all the SP examples, phosphorus is contained within four or/and five membered rings[5-9]. Indeed, SP geometry seems to be favoured

in compounds containing multiple unsaturated five-membered rings. Geometric considerations for phosphorus(V) compounds having five-membered phosphorus heterocycles suggest that lower ring strain is encountered if rings are located in *cis* basal positions of a square pyramid[1]. An example of this is noted in the compound $Ph(C_6H_4O_2\text{-}o)P(o\text{-}O_2Cl_4C_6)$ having near perfect SP geometry[5] (see Figure 5.2).

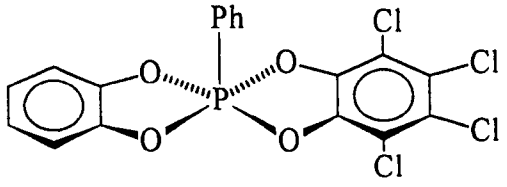

Figure 5.2 Molecular configuration of $Ph(C_6H_4O_2\text{-}o)P(o\text{-}O_2Cl_4C_6)$

Arsenic(V) compounds have been less widely investigated, but square pyramidal species are also known. Similar to the situation with phosphorus, SP geometries are promoted by the use of unsaturated dioxo chelating groups which tend to be located in *cis* basal positions[10,11]. This is indeed found for the bis-catecholate compound $(C_6H_4O_2\text{-}o)_2AsPh$, which has an undistorted SP geometry[11].

In contrast to the analogous phosphorus and arsenic derivatives, pentaphenylantimony unexpectedly has a square pyramidal structure[12,13] and for a considerable period of time this was unique for a Group 15 compound having solely monodentate substituents. However, crystal structures of the cyclohexane solvate of pentaphenylantimony[14], $Ph_5Sb.0.5C_6H_{12}$ and the *p*-tolyl derivative, $(p\text{-}MeC_6H_4)_5Sb$[15] were later reported, showing TBP geometries at antimony. These findings suggested that the SP geometry found for Ph_5Sb was due to lattice stabilisation effects and indeed this assumption was supported by molecular calculations[16].

Two cyclic antimony compounds are also known to have SP geometry. Hall and Sowerby[17] reported the structure of the hemi-hydrate species, $[Ph_3Sb(o\text{-}O_2C_6H_4)]_2.H_2O$, found to have both SP five-coordinated (non-hydrated) and octahedral six-coordinated (hydrated) antimony atoms within the crystal. A similar SP five-coordinate structure was also found for $PhSb(o\text{-}O_2C_6Cl_4)(2,2'\text{-}C_{12}H_8)$, with the

basal sites occupied by the tetrachlorocatecholate and a biphenylylene group[18], as illustrated in Figure 5.3.

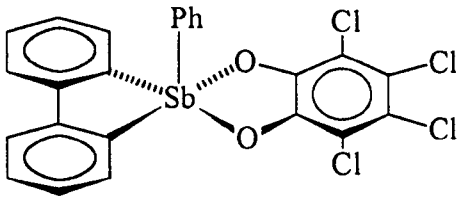

Figure 5.3 Molecular configuration of PhSb(o-$O_2C_6Cl_4$)(2,2'-$C_{12}H_8$)

Square pyramidal geometry is also found for pentaphenylbismuth, Ph_5Bi[19], where the conformation is essentially identical to that in Ph_5Sb. More recently, Seppelt and co-workers have investigated a wide range of pentaarylbismuth (Ar_5Bi) compounds to show that in the majority of cases SP geometry is favoured[20,21,22]. Furthermore, the compound $Ph_3Bi(2,2'\text{-}C_{12}H_8)$[22] was also found to possess a distorted SP configuration, in contrast to the trigonal bipyramidal structure for the corresponding antimony derivative[23]. Interesting and unexpected properties of the SP Ar_5Bi compounds are their strong colours and marked dichroic effects. Seppelt[22] has investigated correlations between the optical properties of the compounds and the bonding characteristics and concluded that the SP geometry found for the Ar_5Bi compounds is a result of overwhelming *p*-character in the bonding, with the 6*s* electrons playing only a very small part (*cf.* 'Inert Pair Effect'). This bonding leads to a short apical bond and four longer basal Sb–C bonds that are claimed to be electron-deficient and polarised according to $Bi(\delta^+)$–$C(\delta^-)$. The electron excitation leading to the optical effects displayed, is therefore thought to be charge transfer from the basal ligands to the central bismuth atom.

In order to quantify the configuration of five coordinate structures a definition must be applied to measure SP and TBP character; this is especially important for intermediate cases. Pioneering work on the definition of five coordinate configurations was reported by Muetterties and Guggenberger[24], who described a

quantitative measure of shape, obtained from the dihedral angles formed by the normals to adjacent polytopal faces.

A later publication by Holmes and Deiters[3] described how closely varyingly distorted cyclic phosphoranes structures follow the Berry coordinate (which follows a local C_{2v} constraint), by the use of the dihedral angle method to characterise structural types. The same publication also showed how five-coordinate structures could be expressed as percentage values along the Berry coordinate.

The general aim of the work described in this chapter was to prepare a range of square pyramidal antimony compounds. In a contrasting manner to previously reported SP antimony compounds, a simple strategy was applied in an attempt to engineer the formation of SP geometry at antimony. As illustrated in Figure 5.4, the methodology applied involved the use of a chelating group and two strongly electronegative (and therefore mutually repulsive) halogen (pseudohalogen) groups to constrain SP geometry. The fifth coordination site was occupied by a phenyl group acting simply as a 'spectator' group and playing no part in control of stereochemistry. To apply a chelate angle of *ca.* 90° the most sensible choice of metallacycle would be a five-membered ring (with top-row elements occupying other ring positions), *eg.* the chelate angles at antimony in the spirocyclic compound $(p\text{-}MeC_6H_4)Sb(O_2C_2Me_4)_2$[25] are 84.2°.

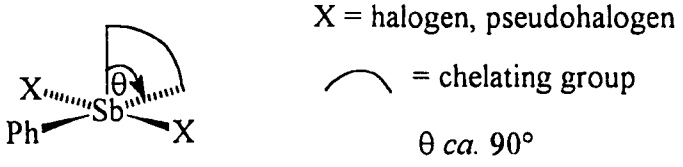

Figure 5.4 Proposed coordination of compounds prepared in this chapter

It was considered that if the (pseudo)halogens assumed positions *trans* to each other, SP coordination would be favoured (as opposed to a highly distorted TBP geometry, with the chelating group in equatorial positions). However, it should be noted that a related compound, $(\text{-}(CH_2)_4\text{-})MeSbCl_2$, has been previously prepared and shown to have distorted trigonal bipyramidal geometry[26].

The chelating ligand chosen for the majority of this work was the 2,2'-biphenylylene group which gives stibafluorene heterocycles, as shown in Figure 5.5.

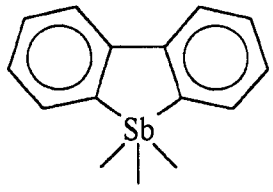

Figure 5.5 Coordination of the 2,2'-biphenylylene group

Biphenylylene complexes of antimony were the subject of considerable attention by Hellwinkel *et al* who prepared a number of compounds with chelating and in some cases bridging biphenylylene groups[27]. Synthetic strategies towards the incorporation of the biphenylylene group to antimony(III) compounds, involved the use of a biphenylylene cadmium intermediate (see Figure 5.6).

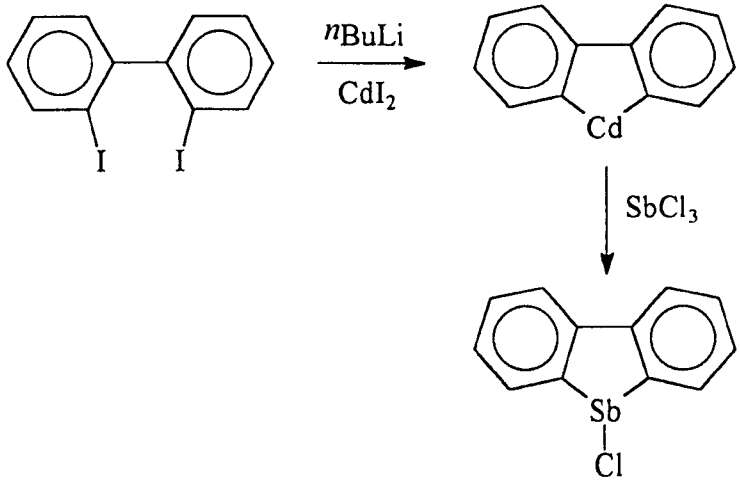

Figure 5.6 Preparation of antimony biphenylylene compounds using cadmium intermediates

To simplify the preparative approach, the biphenylylene precursor compound for this work, PhSb(2,2'-$C_{12}H_8$), was synthesised by a direct reaction between $PhSbCl_2$ and 2,2'-dilithiobiphenyl.2TMEDA[28]. The antimony(V) compounds of interest were then

prepared by either oxidative addition reactions or by metathesis reactions with the products so formed.

Recently, an alternative approach has been used in the synthesis of these stibole-like compounds. This method involves the use of zirconacyclopentadiene compounds as 'metallacycle transfer' reagents and several antimony heterocycles have been prepared in high yields using this technique[29]. An example is 1-phenyl-2,3,4,5-tetramethylstibole[29] formed by the reaction scheme shown in Figure 5.7.

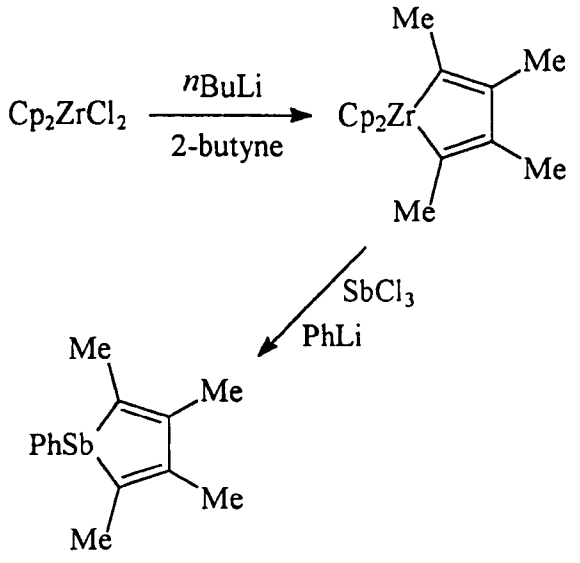

Figure 5.7 Preparation of antimony heterocycles using zirconacycle intermediates

A second area of work reported in this chapter describes the use of a number of dioxo chelating groups, again in attempts to constrain SP geometry at antimony. The chelate groups in successfully prepared antimony(V) compounds were introduced by oxidative addition reactions between $PhSbCl_2$ and substituted *ortho*-quinones. Incorporation of a catecholate group via oxidative addition reactions between antimony(III) compounds and *ortho*-quinones has been reported previously by the groups of Holmes[18] and Tuck[30]. An example of this reaction type is shown in the reaction between Ph_3Sb and *o*-$O_2C_6Cl_4$ giving $Ph_3Sb(O_2C_6Cl_4)$[18] (see Figure 5.8).

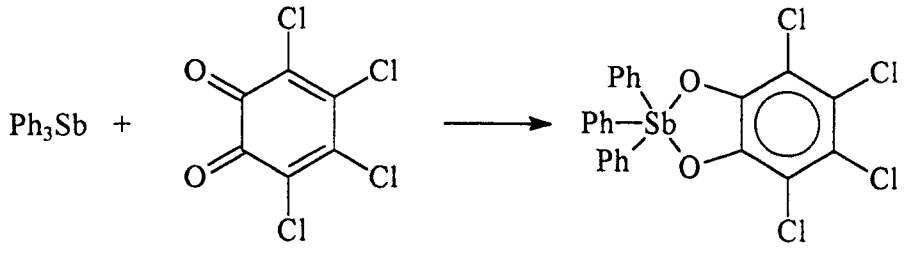

Figure 5.8 Preparation of $Ph_3Sb(O_2C_6Cl_4)$

5.2 RESULTS AND DISCUSSION

5.2.1 Biphenylylene Compounds

5.2.1.1 Preparation of Compounds

The compound $PhSb(2,2'\text{-}C_{12}H_8)$ (**5.1**) was prepared in moderate yield by reaction between stoichiometric quantities of $PhSbCl_2$ and $(2,2'\text{-}Li_2C_{12}H_8).2TMEDA$ in diethyl ether solution. Spectroscopic and physical properties were found to be in agreement with previously reported data for the compound[27].

Compound **5.1** was than converted on treatment with elemental bromine to the corresponding dibromide, $PhSb(2,2'\text{-}C_{12}H_8)Br_2$ (**5.2**). The analogous dichloride, $PhSb(2,2'\text{-}C_{12}H_8)Cl_2$ (**5.3**), was prepared by a similar reaction of **5.1** with sulfuryl chloride:

$$PhSb(2,2'\text{-}C_{12}H_8) + SO_2Cl_2 \rightarrow PhSb(2,2'\text{-}C_{12}H_8)Cl_2 + SO_2$$

Both compounds, **5.2** and **5.3**, gave satisfactory elemental analyses and were fully characterised by spectroscopic means. To assess the coordination geometry at antimony, both compounds were subjected to X-ray structure determinations.

Metathesis reactions between the dichloride (**5.3**) and two equivalents of either KF or KSCN led to two further biphenylylene compounds, $PhSb(2,2'\text{-}C_{12}H_8)F_2$ (**5.4**) and the dithiocyanate derivative, $PhSb(2,2'\text{-}C_{12}H_8)(NCS)_2$ (**5.5**) respectively. The coordination geometry of **5.5** was determined by X-ray crystallography.

5.2.1.2 Infrared Spectroscopy

Infrared spectra for the compounds **5.1** to **5.5** were all clearly dominated by aryl modes, assignment of which was not attempted in this work. However, assignment of the infrared spectrum of the related biphenylylene compound, $Ph_3Sb(2,2'\text{-}C_{12}H_8)$, has been carried out by Millington[31] and can be used for reference.

The most intense absorptions in the solid-state spectrum of $PhSb(2,2'\text{-}C_{12}H_8)(NCS)_2$ (**5.5**) could be assigned to modes of the thiocyanate groups. In the region normally associated with ν(CN) absorptions, two bands were observed at 2077 and 1994 cm^{-1}. The sharp, intense band at 2077 cm^{-1} is in the region often associated with either 1,3-bridging or terminal S-bonded thiocyanate groups[32]. According to hard/soft acid/base rules the latter assignment is unlikely, with Sb(V) centres showing a distinct preference for N-bonding, for example $Ph_3Sb(NCS)_2$ has only N-bonded thiocyanate groups[33]. The second broad band at 1994 cm^{-1} was consistent with a terminal N-bonded thiocyanate group. The position and breadth of this band was similar to the ν(CN) band in $Ph_3Sb(NCS)_2$ (2009 cm^{-1}), the crystal structure of which indeed showed the presence of terminal N-bonded thiocyanate groups.

A further band at 743 cm^{-1}, was assigned to the ν(CS) thiocyanate stretch, comparable with the analogous mode in related compounds. Assignment of the weak δ(NCS) mode proved to be complicated due to the abundance of aryl modes in the relevant region. A listing of ν(CN) and ν(CS) bands for **5.5** and other triorganodithiocyanate compounds is given in Table 5.1.

Table 5.1 Thiocyanate group stretches (cm^{-1}) for $R_3Sb(NCS)_2$ compounds

R	ν(CN)	ν(CS)	Reference
Ph(2,2'-$C_{12}H_8$) (**5.5**)	2077, 1994	743	This work
phenyl	2009	876	[33]
p-tolyl	2040		[33]
o-tolyl	2027		[33]
2,6-$Me_2C_6H_4$	2049	767	[33]
mesityl	2052, 2030	750	[33]
p-fluorophenyl	2004	720	[33]
p-chlorophenyl	2010	830	[34]
methyl	2016	848	[35]
methyl	2045, 2015	843	[36]

The two ν(CN) bands in **5.5** show distinct similarities in position and appearance to the two bands found for the compound $Ph_2SbBr(NCS)_2$ (2092 and 1993 cm^{-1}), reported by Forster, Begley and Sowerby[33]. The authors argue that the ν(CN) bands in that compound were consistent with a dimeric species with one thiocyanate group coordinating as a 1,3-bridging group and the second NCS group N-bonded and terminal. One of the possible isomers suggested is illustrated in Figure 5.9.

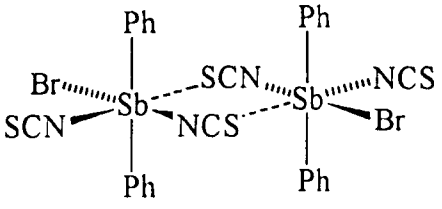

Figure 5.9 Possible molecular configuration of $Ph_2SbBr(NCS)_2$

The solid-state structure of PhSb(2,2'-$C_{12}H_8$)$(NCS)_2$ (**5.5**) is therefore likely to have a related arrangement of the thiocyanate groups. If, as expected, the formally bonded (N-bonded) thiocyanate groups assume mutually *trans* positions then the most probable structure, shown in Figure 5.10, will be a *pseudo*-octahedral species with the

bridging thiocyanate groups forming a dimeric (or alternatively polymeric) system. Indeed, a X-ray structure determination of **5.5** detailed in Section 5.2.1.4, confirms this dimeric coordination style.

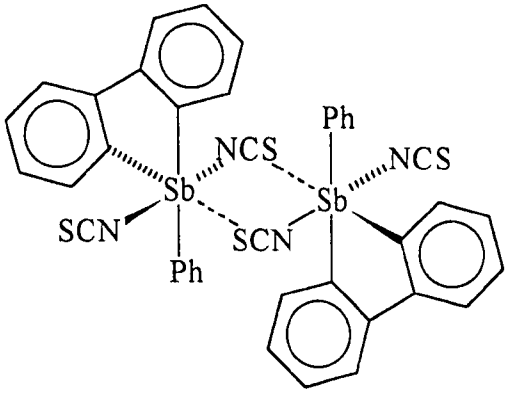

Figure 5.10 Proposed structure of 5.5 from infrared data

5.2.1.3 NMR Data

The ^{1}H NMR spectrum of the compound PhSb(2,2'-$C_{12}H_8$)Br_2 (**5.2**), recorded in $CDCl_3$ solution, showed two multiplets centred at 7.56 and 8.06 ppm (see Figure 5.12). Integration of the two resonance areas indicated that they were seven and six proton multiplets respectively. The higher field multiplet (7.56 ppm) was assigned to the *meta* and *para* phenyl protons and to the H_2 and H_3-biphenylylene protons (using the numbering scheme shown in Figure 5.11). Correspondingly, the 8.06 ppm signal was assigned to the *ortho* phenyl protons and the H_1 and H_4-biphenylylene protons. Indeed, two doublets due to the H_1 and H_4-biphenylylene protons can be resolved within the multiplet.

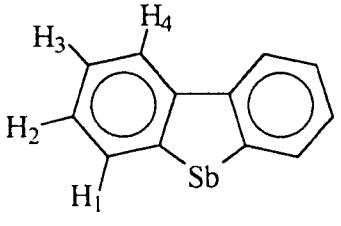

Figure 5.11 Numbering scheme for biphenylylene protons

Figure 5.12 ^{1}H NMR spectrum of PhSb(2,2'-$C_{12}H_8$)Br_2 (5.2) in $CDCl_3$

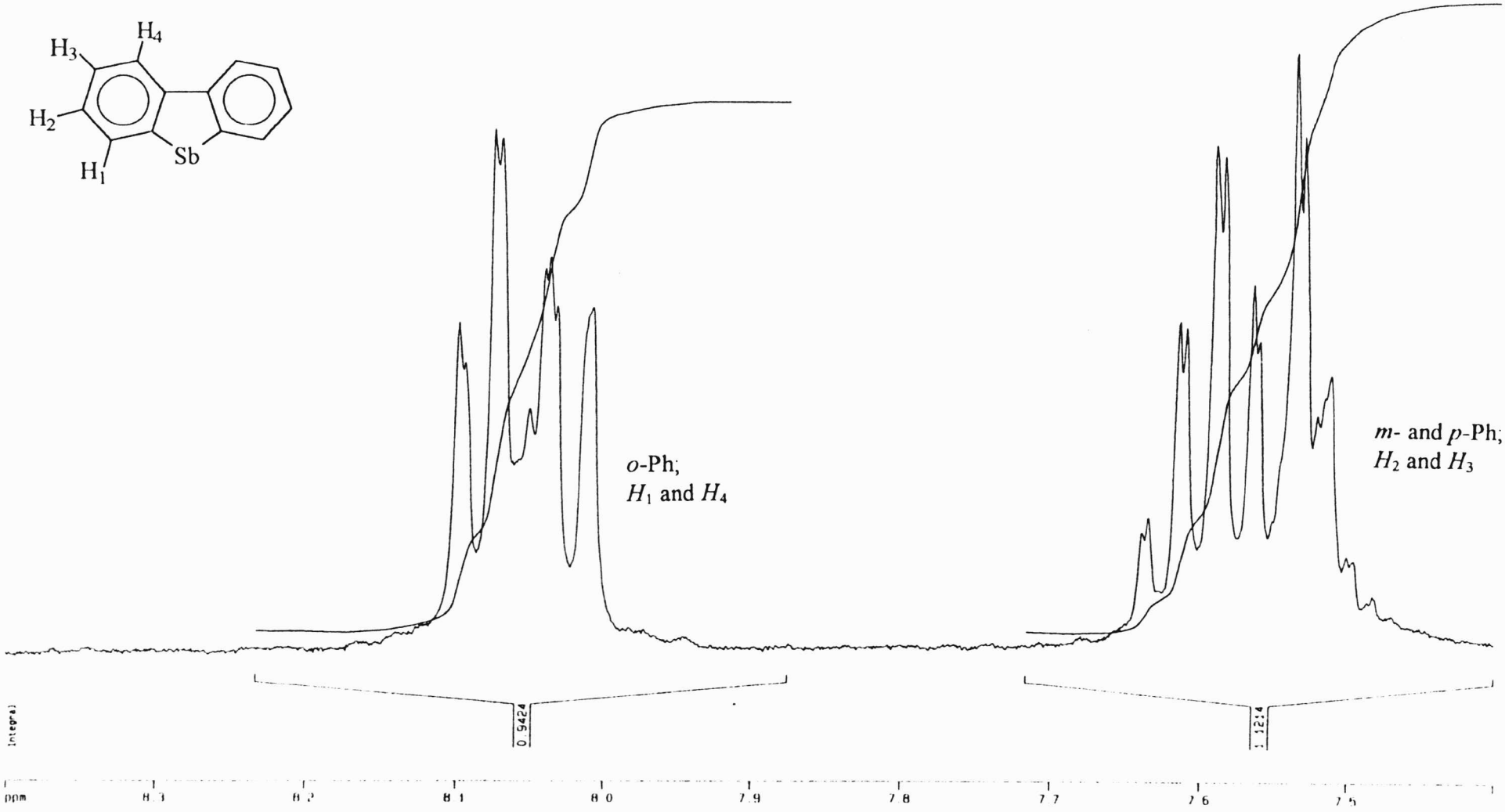

The ^{1}H spectrum of PhSb(2,2'-$C_{12}H_8$)Cl_2 (**5.3**) showed distinct differences from **5.2**, with greater resolution of the signals assigned to the biphenylylene group. A resonance at 7.60 ppm, could be separated into two triplets ($^3J_{HH}$ = 7.5Hz) of doublets ($^4J_{HH}$ = 1.4Hz) at 7.55 and 7.63 ppm which were assigned to the H_2 and H_3-biphenylylene protons, with an overlapping multiplet due to the phenyl *meta* and *para* protons (centred at 7.60 ppm). The H_4 and H_1-biphenylylene protons were observed as doublets (with a degree of second order coupling) at 8.02 and 8.08 ppm. The resonance due to the phenyl *ortho* protons was found at 8.27 ppm (multiplet), notably lower field than the corresponding signal for **5.2**.

The resonances for the biphenylylene group in the ^{1}H NMR spectrum of PhSb(2,2'-$C_{12}H_8$)$(NCS)_2$ (**5.5**), displayed doublet, triplet, triplet, doublet coupling patterns for the H_1 to H_4 protons respectively. The protons associated with the phenyl group were observed as broad unresolved multiplets at 7.70 ppm (*meta* and *para*) and 8.23 ppm (*ortho*).

It is of significance to note the presence of only four resonances for the protons of the biphenylylene groups in each of the spectra of **5.2**, **5.3** and **5.5**. This observation suggests that either an element of symmetry is present in their solution-state structures, making both benzenoid rings chemically equivalent, or alternatively that a pseudorotation mechanism is operating, exchanging ligand positions at a rate faster than the NMR timescale. If the molecules exist with the proposed SP geometry (see Figure 5.13), the former proposition is unlikely as the biphenylylene group would be spanning between the chemically distinct apical and basal sites.

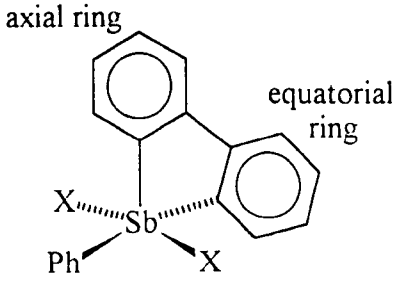

Figure 5.13 Chemical non-equivalence of the benzenoid rings for SP geometry

5.2.1.4 Mass Spectroscopy

The monoisotopically scaled EI mass spectral data for $PhSb(2,2'\text{-}C_{12}H_8)Br_2$ (**5.2**) are listed in Table 5.2 and Tables 5.3, 5.4 and 5.5 list similar data for $PhSb(2,2'\text{-}C_{12}H_8)Cl_2$ (**5.3**), $PhSb(2,2'\text{-}C_{12}H_8)F_2$ (**5.4**) and $PhSb(2,2'\text{-}C_{12}H_8)(NCS)_2$ (**5.5**). Additional data obtained from a FAB mass spectrum of **5.5** are also reported in Table 5.5.

Table 5.2 Important fragments in the EI mass spectrum of 5.2

Fragment Ion	Mass (m/z)	Peak Height, %
$\{PhSb(2,2'\text{-}C_{12}H_8)Br\}^+$	429	5
$\{PhSb(2,2'\text{-}C_{12}H_8)\}^+$	350	99
$\{Sb(2,2'\text{-}C_{12}H_8)\}^+$	273	58
$\{PhC_{12}H_8\}^+$	229	100
$\{Ph\}^+$	77	15

Table 5.3 Important fragments in the EI mass spectrum of 5.3

Fragment Ion	Mass (m/z)	Peak Height, %
$\{PhSb(2,2'\text{-}C_{12}H_8)Cl\}^+$	385	3
$\{PhSb(2,2'\text{-}C_{12}H_8)\}^+$	350	76
$\{Sb(2,2'\text{-}C_{12}H_8)Cl\}^+$	308	6
$\{Sb(2,2'\text{-}C_{12}H_8)\}^+$	273	60
$\{PhC_{12}H_8\}^+$	229	100
$\{C_{12}H_8\}^+$	152	98
$\{Ph\}^+$	77	15

Table 5.4 Important fragments in the EI mass spectrum of 5.4

Fragment Ion	Mass (m/z)	Peak Height, %
$\{PhSb(2,2'\text{-}C_{12}H_8)F\}^+$	369	59
$\{PhSb(2,2'\text{-}C_{12}H_8)\}^+$	350	13
$\{Sb(2,2'\text{-}C_{12}H_8)\}^+$	273	19
$\{PhC_{12}H_8\}^+$	229	49
$\{C_{12}H_8\}^+$	152	61
$\{Ph\}^+$	77	30

Table 5.5 Important fragments in the FAB and EI mass spectra of 5.5

Fragment Ion	Mass (m/z)	FAB (%)	EI (%)
$\{PhSb(2,2'\text{-}C_{12}H_8)(NCS)\}^+$	408	7	-
$\{PhSb(2,2'\text{-}C_{12}H_8)NH_3\}^+$	367	16	-
$\{PhSb(2,2'\text{-}C_{12}H_8)\}^+$	350	16	87
$\{Sb(2,2'\text{-}C_{12}H_8)\}^+$	273	44	70
$\{PhC_{12}H_8\}^+$	229	48	90
$\{C_{12}H_8\}^+$	152	100	100
$\{Ph\}^+$	77	43	15

The appropriate parent ion was not observed in any of the EI spectra nor even in the FAB spectrum of **5.5**, involving comparatively more gentle conditions. With the exception of the EI spectrum of **5.5**, all the spectra showed a fragment which could be assigned to the respective $\{PhSb(2,2'\text{-}C_{12}H_8)X\}^+$ ions. Accordingly, the first step in the fragmentation process appeared to be the loss of a halide (pseudohalide) group. Loss of the second halide (pseudohalide) also appeared to be more favourable than the loss of the organo groups, with the ion $\{Sb(2,2'\text{-}C_{12}H_8)Cl\}^+$ seen in the spectra of **5.3**, being the only observed example of a halide remaining after loss of an organic group.

Further, loss of the phenyl groups appears to be more favourable than elimination of the biphenylylene groups, likely to be due to the necessary two-bond cleavage that would be required for the latter. This leads to the presence of the $\{PhSb(2,2'\text{-}C_{12}H_8)\}^+$ and $\{Sb(2,2'\text{-}C_{12}H_8)\}^+$ ions in all spectra, whereas the $\{PhSb\}^+$ ion was not observed. Indeed, both the former species were found to be of notable intensity in all spectra.

A further interesting feature of all the spectra (also noted in the EI spectrum of the precursor $PhSb(2,2'\text{-}C_{12}H_8)$ **[5.1]**) was a high intensity peak assigned to the $\{PhC_{12}H_8\}^+$ ion (m/z 229), *ie* a product formed by the fusing of a phenyl and biphenylylene group. However, the fusing of organo-fragments in mass spectra of organoantimony compounds is not unusual, with the $\{Ph_2\}^+$ ion seen in most phenylantimony compounds reported in this work.

From the information obtained from the spectra reported here, the primary fragmentation pathway shown in Figure 5.14 has been devised, with the major routes indicated by the bold arrows:

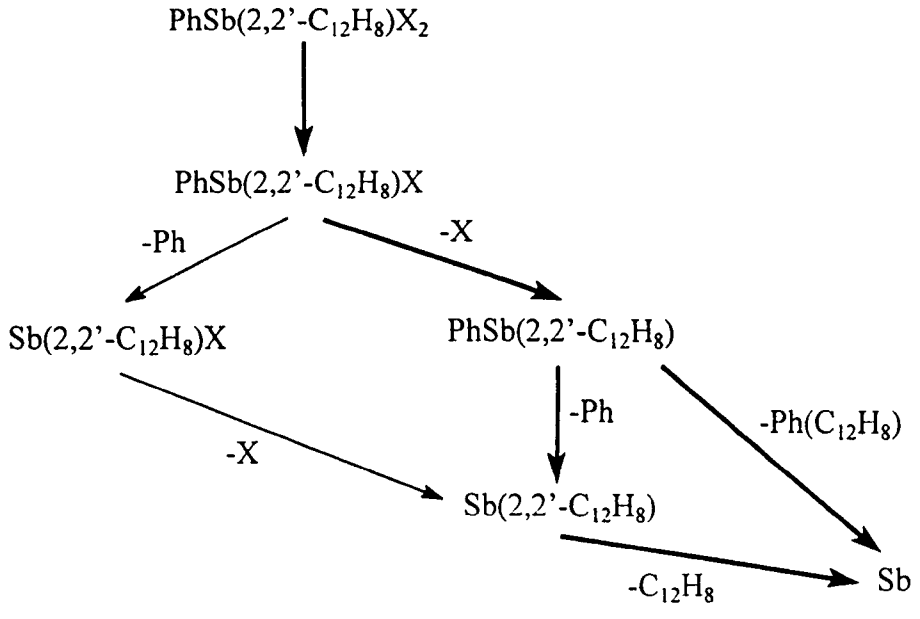

Figure 5.14 Fragmentation pathway for $PhSb(2,2'\text{-}C_{12}H_8)X_2$ compounds

5.2.1.5 X-Ray Crystallography

Single crystal X-ray structure determinations were carried out for the compounds $PhSb(2,2'\text{-}C_{12}H_8)Br_2$ (**5.2**), $PhSb(2,2'\text{-}C_{12}H_8)Cl_2$ (**5.3**) and $PhSb(2,2'\text{-}C_{12}H_8)(NCS)_2$ (**5.5**) to assess the coordination geometry at antimony in each case. Single crystals of the compounds in each case were obtained by diffusion of hexane vapour into concentrated chloroform solutions of the compounds.

The molecular structure of **5.2** is shown in Figure 5.15 and selected bond lengths and angles are listed in Table 5.6. Further details of the crystal structure determination are given in Appendix M.

Table 5.6 Selected bond distances and angles, with standard deviations in parentheses for $PhSb(2,2'\text{-}C_{12}H_8)Br_2$ (5.2)

Bond lengths, Å		Bond angles, °	
Sb(1) - Br(2)	2.5924(8)	Br(2) - Sb(1) - Br(1)	170.72(3)
Sb(1) - Br(1)	2.7080(8)	Br(2) - Sb(1) - C(1)	89.9(2)
Sb(1) - Br(1')	3.346(1)	Br(1) - Sb(1) - C(1)	89.7(2)
Sb(1) - C(1)	2.124(6)	Br(2) - Sb(1) - C(7)	97.9(2)
Sb(1) - C(7)	2.106(6)	Br(1) - Sb(1) - C(7)	90.9(2)
Sb(1) - C(14)	2.119(6)	C(1) - Sb(1) - C(7)	110.7(3)
		Br(2) - Sb(1) - C(14)	89.0(2)
		Br(1) - Sb(1) - C(14)	88.9(2)
		C(1) - Sb(1) - C(14)	165.0(2)
		C(7) - Sb(1) - C(14)	84.3(2)
		Br(1) - Sb(1) - Br(1')	81.39(2)
		Br(2) - Sb(1) - Br(1')	89.42(2)
		C(7) - Sb(1) - Br(1')	167.2(2)
		C(14) - Sb(1) - Br(1')	85.3(2)
		C(1) - Sb(1) - Br(1')	79.7(2)

The asymmetric unit in the structure of **5.2** comprises an antimony bound to a chelating biphenylylene group attached in the 2,2'- positions, two bromine atoms and a phenyl group. The geometry about antimony is square pyramidal (SP) with the biphenylylene group spanning between the apical position and a basal site. The remaining groups occupy the further basal positions with the bromine atoms in mutually *trans* positions.

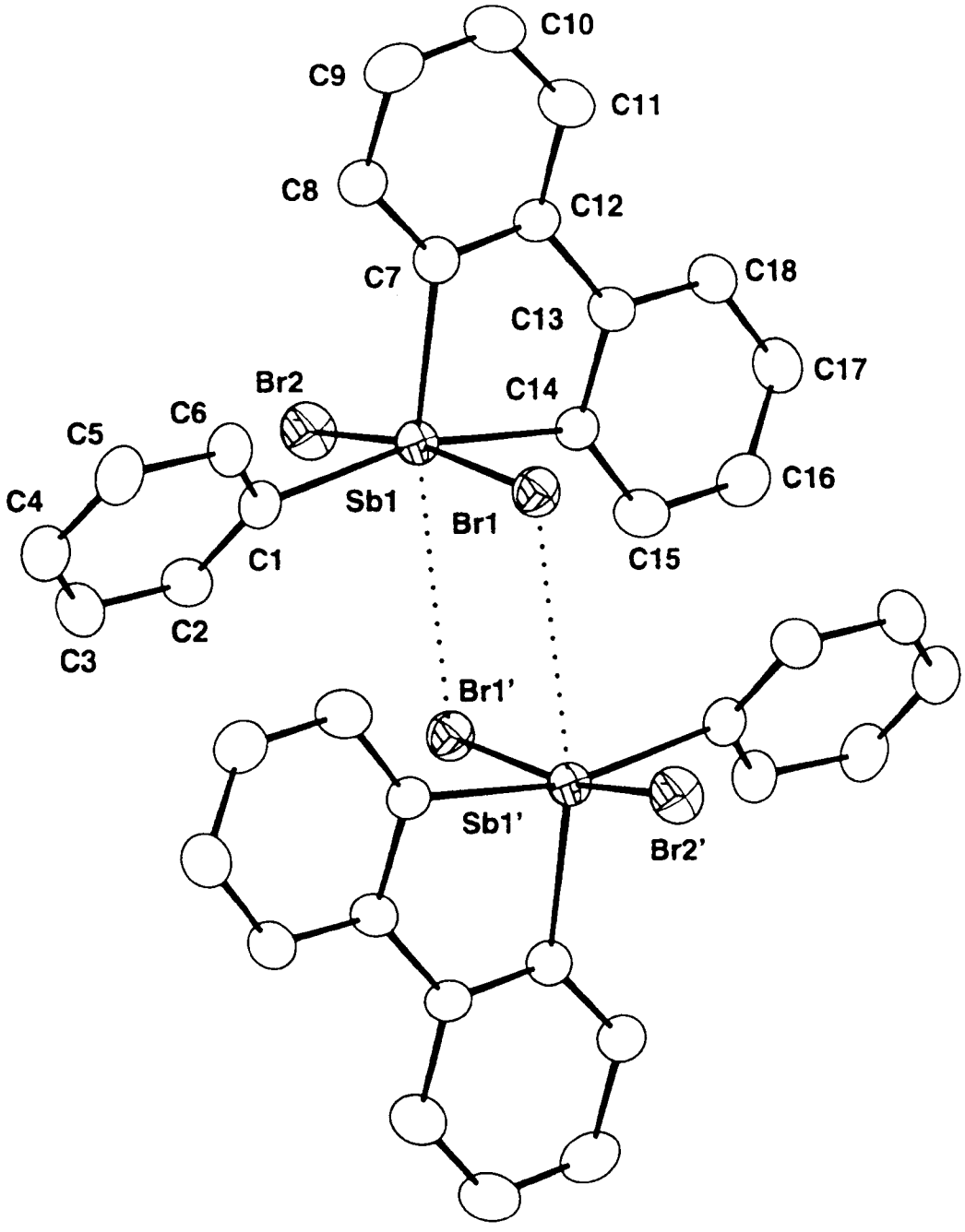

Figure 5.15 Molecular structure of dimeric $PhSb(2,2'\text{-}C_{12}H_8)Br_2$ (5.2)

Clear differences are noted for the Sb–C bond lengths, with the two Sb–C_{basal} bonds longer at 2.124(6) and 2.119(6) Å (Sb(1)–C(1) and Sb(1)–C(14) respectively) and the apical bond, Sb(1)–C(7) shorter at 2.106(6) Å. Shorter apical bond lengths are a typical feature of SP main-group compounds, for example the Sb–C_{apical} bond in the five coordinate SP molecule in $[Ph_3Sb(o\text{-}O_2C_6H_4)]_2.H_2O$[17] is the shortest of the Sb–C bonds in the compound at 2.099 Å.

Significant differences are also observed in the Sb–Br bond lengths with the Sb(1)–Br(1) bond length of 2.7080(8) Å considerably longer than the Sb(1)–Br(2) bond of 2.5924(8) Å (which is comparable to those in related compounds, such as Ph_3SbBr_2 (2.632 Å)[37]). The lengthening of the former bond is undoubtedly associated with secondary bonding of the Br(1) atom to a symmetry related antimony [Sb(1')]. The weak interactions (Sb(1')···Br(1), 3.346(1) Å) lead to association of the molecules into loose dimers (related by an inversion centre) and an increase in the coordination number about antimony to six, giving a coordination geometry best described as octahedral. The Sb···Br interaction occurs *trans* to the C(7) carbon of the biphenylylene group and gives a distorted C(7)–Sb(1)–Br(1') angle of 167.2(2)°. Further discussions will ignore these weak intermolecular connections and consider the geometry of **5.2** to be square pyramidal.

The *trans* angles about antimony to the basal atoms are found to be greater than expected for a simple SP molecule (*ca.* 150°), with a Br(2)–Sb(1)–Br(1) angle of 170.72(3)° and a C(1)–Sb(1)–C(14) angle of 165.0(2)°. This feature is again likely to be associated with the intermolecular interaction, pushing the structure towards octahedral geometry. Deviations from the best-fit basal plane are slight, with the Br(1) and Br(2) atoms lying slightly above the plane (0.031 and 0.032 Å respectively) and the two carbon atoms, C(1) and C(14) slightly lower (-0.031 and -0.032 Å respectively). The antimony is 0.245 Å above the basal plane and is enclosed within a stibole-like ring by the chelating biphenylylene group. The chelate angle [C(7)–Sb(1)–C(14)] is 84.3(2)° and therefore imposes constraints on the SP geometry; this angle should be compared with an axial-basal angle of *ca.* 100° expected for undistorted SP

geometry. Co-planarity of the two benzenoid rings of the biphenylylene group is illustrated by a twist angle of only 3.5° between the respective best-fit planes.

To assess the degree of SP character in the structure of the monomeric unit, Muetterties and Guggenberger's criterion[24] has been used. To apply this method, a base TBP conformation must be assigned, from which (Berry) deviations occur to give the observed SP geometry. The most likely model shown in Figure 5.16, will have the biphenylylene group spanning between axial and equatorial sites, with the bromine atoms in the remaining equatorial positions. Indeed, a similar TBP structure was found for the compound $Ph_3Sb(2,2'\text{-}C_{12}H_8)$ with the two bromine atoms replaced by further phenyl groups[31]. Figure 5.16 also illustrates the possible TBP↔SP interconversion by Berry pseudorotation.

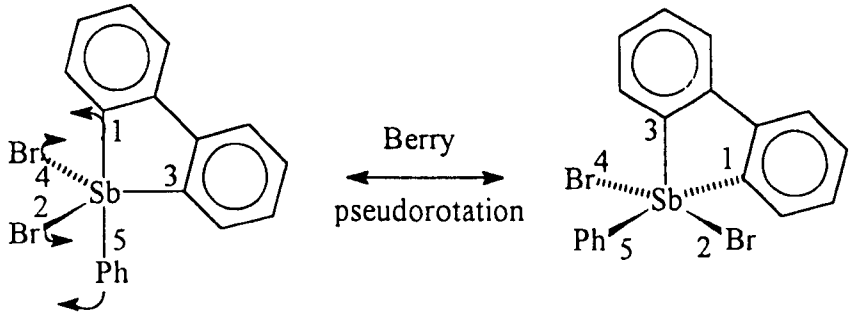

Figure 5.16 Berry pseudorotation for $PhSb(2,2'\text{-}C_{12}H_8)Br_2$ (5.2)

The basic principle of Muetterties and Guggenberger's method is the measurement of the dihedral angles relating to a number of 'shape determining' edges of the polyhedron defined by the molecule. For a ML_5 system the determining angles are taken as the δe_1, δe_2 and δe_3 angles (*ie* the angle between the planes meeting at edges e_1, e_2 and e_3 as shown in Figure 5.17), with values of 53.1, 53.1 and 53.1° respectively for a regular TBP geometry or 75.7, 75.7 and 0° for an undistorted SP molecule. The transposition of **5.2** into the relevant ML_5 polyhedron systems is shown in Figure 5.17 along with the labelling of the angles between the faces.

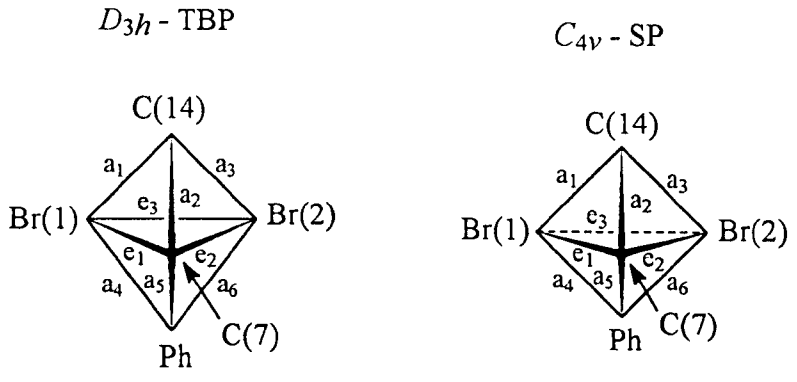

Figure 5.17 Polyhedral alternatives for 5.2

The structure of **5.2** will necessarily possess distortions using the dihedral method because of the constraints of the chelating biphenylylene group and substantial differences in bond lengths (the bond length ratio in this model taken as being unity). However, the determining values obtained, $\delta e_3 = 3.5°$, $\delta e_1 = 83.1°$ and $\delta e_2 = 79.2°$, are close to the ideal SP angles (0, 75.7 and 75.7° respectively).

The molecular structure of **5.3** is shown in Figure 5.18 and selected bond lengths and angles are listed in Table 5.7. Further details of the crystal structure determination are given in Appendix N.

Table 5.7 Selected bond distances and angles, with standard deviations in parentheses for PhSb(2,2'-$C_{12}H_8$)Cl_2 (5.3)

Bond lengths, Å		Bond angles, °	
Sb(1) - Cl(2)	2.444(4)	Cl(2) - Sb(1) - Cl(1)	170.2(1)
Sb(1) - Cl(1)	2.544(4)	Cl(2) - Sb(1) - C(1)	89.3(5)
Sb(1) - Cl(1')	3.191(4)	Cl(1) - Sb(1) - C(1)	90.0(5)
Sb(1) - C(1)	2.13(1)	Cl(2) - Sb(1) - C(7)	98.9(4)
Sb(1) - C(7)	2.12(1)	Cl(1) - Sb(1) - C(7)	90.6(4)
Sb(1) - C(14)	2.10(1)	C(1) - Sb(1) - C(7)	109.6(5)
		Cl(2) - Sb(1) - C(14)	89.0(4)
		Cl(1) - Sb(1) - C(14)	89.2(4)
		C(1) - Sb(1) - C(14)	165.4(5)
		C(7) - Sb(1) - C(14)	85.0(5)
		Cl(1) - Sb(1) - Cl(1')	79.0(1)
		Cl(2) - Sb(1) - Cl(1')	91.3(1)
		C(7) - Sb(1) - Cl(1')	165.8(5)
		C(14) - Sb(1) - Cl(1')	85.2(5)
		C(1) - Sb(1) - Cl(1')	80.5(5)

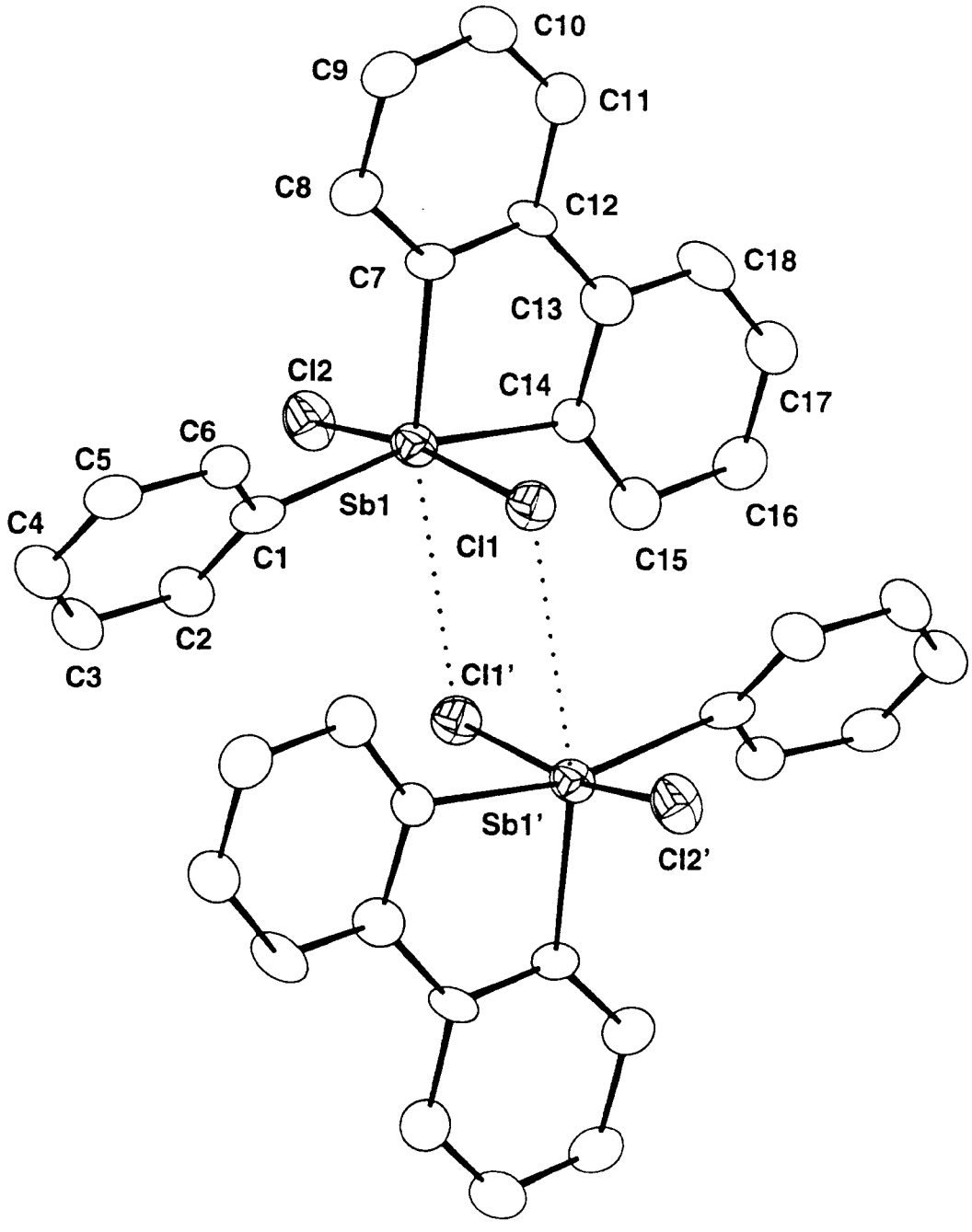

Figure 5.18 Molecular structure of dimeric $PhSb(2,2'\text{-}C_{12}H_8)Cl_2$ (5.3)

The structure of **5.3** is isomorphous with **5.2** and a very closely related structure is therefore observed. Geometry at the monomeric units is similarly square pyramidal, with shape determining dihedral angles close to those for an ideal square pyramid, with values of $\delta e_3 = 3.0°$, $\delta e_1 = 82.2°$ and $\delta e_2 = 77.3°$.

The biphenylylene group spans across the axial and a basal position with a chelate angle, C(7)–Sb(1)–C(14), of 85.0(5)°. Deviations from the best-fit basal plane are again small with, as was noted for **5.2**, the halogens sitting just above the plane (Cl(1) +0.027 and Cl(2) +0.028 Å) and the relevant carbon atoms just below (C(1) -0.027 and C(14) -0.028 Å). The antimony atom lies 0.241 Å above the plane. Coplanarity of the biphenylylene moiety is again shown by a twist angle of only 2.6° between the two benzenoid rings.

Probably due to the poorer quality data, the expected shortening of the axial Sb(1)–C(7) bond is not apparent for **5.3**, with the Sb–C bonds found to be effectively equal within the resolution obtained. Differences in Sb–Cl bond lengths, however, are clearly resolved with the terminal Sb(1)–Cl(2) bond (2.444(4) Å) shorter than the Sb(1)–Cl(1) bond (2.544(4) Å). The elongation of the latter bond is undoubtedly related to the participation of the chlorine in secondary bonding to the symmetry related antimony [Sb(1')].

The intermolecular bridging interaction Sb(1)···Cl(1') is weak, with separations of 3.191(4) Å (*cf* the van der Waals separation of 4.0 Å); the analogous bridging interaction in the Ph_2SbCl_3 dimer[38] is significantly shorter at 2.839 Å. The C(7)–Sb(1)···Cl(1') *trans* angle is distorted from linearity, at 165.8(5)°.

The molecular structure of **5.5** is shown in Figure 5.19 and selected bond lengths and angles are listed in Table 5.8. Further details of the crystal structure determination are given in Appendix O.

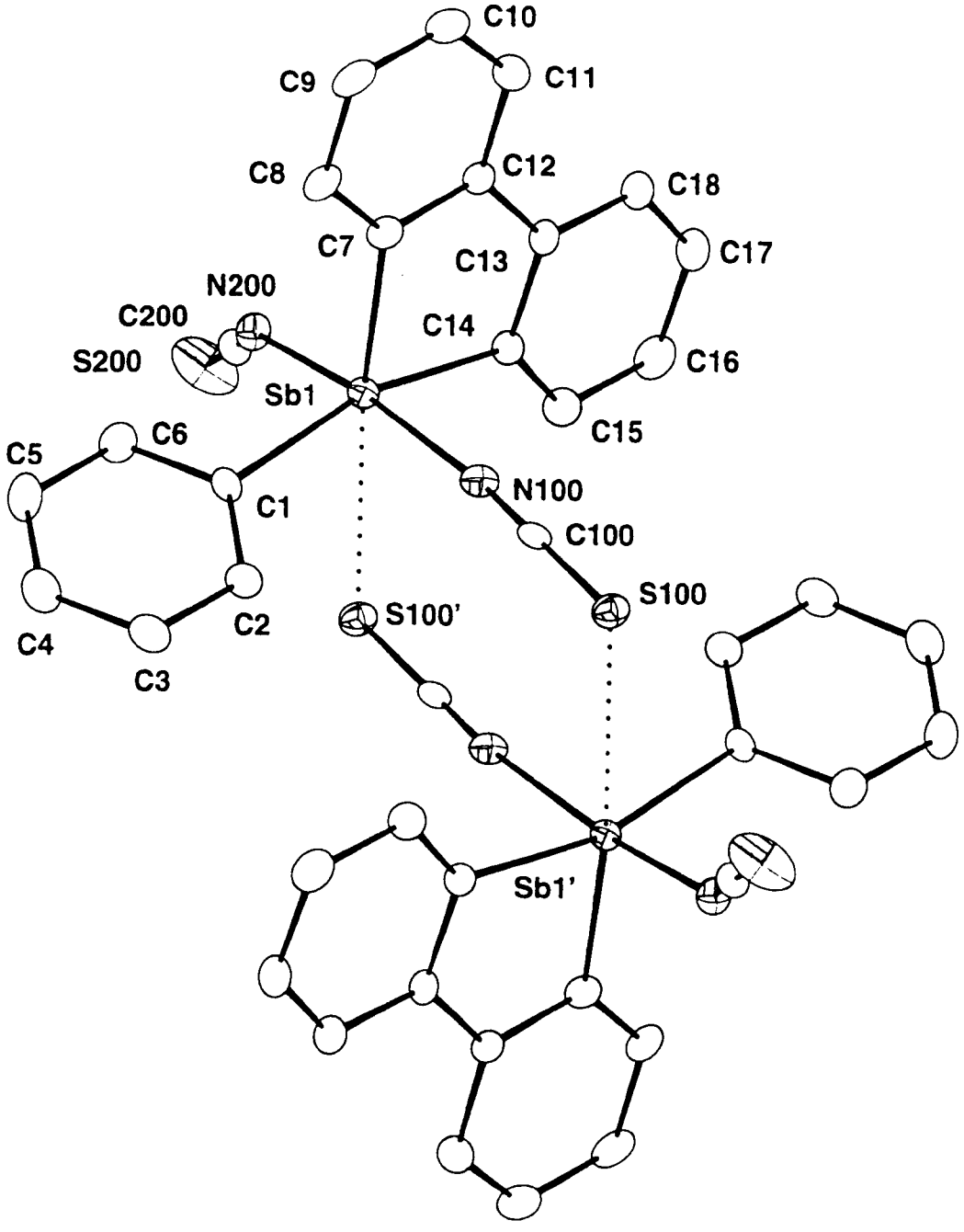

Figure 5.19 Molecular structure of dimeric $PhSb(2,2'\text{-}C_{12}H_8)(NCS)_2$ (5.5)

Table 5.8 Selected bond distances and angles, with standard deviations in parentheses for $PhSb(2,2'\text{-}C_{12}H_8)(NCS)_2$ (5.5)

Bond lengths, Å		Bond angles, °	
Sb(1) - N(100)	2.216(4)	N(100)- Sb(1) - N(200)	171.1(1)
Sb(1) - N(200)	2.146(4)	N(100)- Sb(1) - C(1)	88.5(2)
Sb(1) - S(100')	3.191(4)	N(200)- Sb(1) - C(1)	91.1(2)
Sb(1) - C(1)	2.137(4)	N(100)- Sb(1) - C(7)	93.0(2)
Sb(1) - C(7)	2.090(4)	N(200)- Sb(1) - C(7)	95.5(2)
Sb(1) - C(14)	2.135(4)	C(1) - Sb(1) - C(7)	110.7(2)
N(100) - C(100)	1.165(6)	N(100)- Sb(1) - C(14)	87.2(2)
N(200) - C(200)	1.169(6)	N(200)- Sb(1) - C(14)	90.8(2)
S(100) - C(100)	1.639(5)	C(1) - Sb(1) - C(14)	164.0(2)
S(200) - C(200)	1.601(6)	C(7) - Sb(1) - C(14)	84.9(2)
		N(100) - Sb(1) - S(100')	88.8(1)
		N(200) - Sb(1) - S(100')	82.4(1)
		C(7) - Sb(1) - S(100')	170.6(1)
		C(14) - Sb(1) - S(100')	85.9(1)
		C(1) - Sb(1) - S(100')	78.6(1)
		Sb(1) - N(100)- C(100)	173.5(4)
		Sb(1) - N(200)- C(200)	139.6(4)
		S(100)- C(100)- N(100)	179.3(4)
		S(200)- C(200)- N(200)	178.0(5)

The structure of **5.5** shows many similarities to the previous two structures with basically SP monomeric units connected by intermolecular Sb···N interactions to give dimers (with near-octahedral geometry). The coordination about antimony is analogous to that found for **5.2** and **5.3** with the biphenylylene group spanning between the apical site and a basal position and the remaining three basal positions occupied by the phenyl *ipso* carbon and the thiocyanate nitrogens.

Moreover, the structure is consistent with the assumptions derived from the infrared data, having two differing thiocyanate environments, one N-bonded and terminal and the other, though primarily N-bonded, participating in 1,3-bridging.

Although the intermolecular thiocyanate bridging is through the sulfur atom, distinct differences are found for the Sb–N bond lengths, with the terminal Sb(1)–N(200) bond length at 2.146(4) Å and the Sb(1)–N(100) bond longer at 2.216(4) Å. The former bond length is comparable with the terminal thiocyanate groups in

$Ph_3Sb(NCS)_2$ (mean Sb–N = 2.142 Å)[33]. The C(100)–S(100) bond length [1.639(5) Å] associated with the bridging thiocyanate group is also longer than the equivalent for the terminal group [C(200)–S(200), 1.601(6) Å]. Both thiocyanate groups, as would be expected, are effectively linear with angles at C(100) and C(200) of 179.3(4) and 178.0(5)° respectively. The C–N bond lengths are both short and virtually equivalent (N(100)–C(100) 1.165(6) and N(200)–C(200) 1.169(6) Å) and are effectively triple bonds (*cf* C≡N, 1.16 Å and C=N, 1.30 Å)[39].

One of the most striking features of the structure is the pronounced difference in the angles at the thiocyanate nitrogens. For the terminal N(200) group, the angle at nitrogen is noticeably bent at 139.6(4)° and significantly lower than any of the corresponding angles in $Ph_3Sb(NCS)_2$, which contains three crystallographically independent molecules. In contrast, the C(100)–N(100)–Sb(1) angle is near-linear at 173.5(4)°. The near-linearity of the C(100)–N(100)–Sb(1) angle is clearly associated with the 1,3-bridging interaction of the group and potentially alleviates steric interactions.

Deviations from the best-fit basal plane about antimony are slightly greater than those in **5.2** and **5.3** (C(1) -0.061, C(14) -0.062, N(100) +0.062 and N(200) +0.061 Å) with the antimony 0.231 Å above. Near co-planarity of the biphenylylene group is confirmed by a twist angle of only 1.8° between the benzenoid rings.

The geometry about antimony, considering just the monomeric unit, has been assessed by the dihedral angle method and again shows good agreement with the ideal values for SP geometry. The three determining angles have been evaluated as δe_3 = 6.7°, δe_1 = 75.9° and δe_2 = 76.9° (*cf.* ideal angles δe_3 = 0°, δe_1 = δe_2 = 75.7°).

Values of the structure determining dihedral angles of the compounds **5.2**, **5.3** and **5.5** are listed in Table 5.9.

Table 5.9 Structure determining dihedral angles for 5.2, 5.3 and 5.5 in comparison to Ph_5Sb and ideal TBP and SP geometries

Compound	δe_3 (°)	δe_1, δe_2 (°)
Ideal TBP	53.1	53.1, 53.1
Ph_5Sb	14.4	68.5, 69.2
$PhSb(2,2'\text{-}C_{12}H_8)Br_2$ (**5.2**)	3.5	83.1, 79.2
$PhSb(2,2'\text{-}C_{12}H_8)Cl_2$ (**5.3**)	3.0	82.2, 77.3
$PhSb(2,2'\text{-}C_{12}H_8)(NCS)_2$ (**5.5**)	6.7	75.9, 76.9
Ideal SP	0	75.7, 75.7

An interesting feature of the structures of **5.2**, **5.3** and **5.5** is not only their unusual SP geometry at antimony, but also their inherent Lewis acidity leading to the observed intermolecular interactions and formation of dimers. In comparison with Ph_3SbX_2 compounds, which exhibit very low Lewis acidity in their solid-state structures[37,33], this finding is perhaps surprising. Whether this behaviour is simply a consequence of the steric restrictions of the biphenylylene group is uncertain, but with the stabilisation of SP geometry there is an accessible coordination site *trans* to the apical carbon atom.

The stereochemical non-rigidity of five coordinate structures is clearly apparent from these compounds, with small changes in individual parameters, such as exchanging two phenyl groups for a biphenylylene group, leading to considerable structural changes.

5.2.2 Dioxo-Chelate Compounds

5.2.2.1 Preparation of Compounds

In an attempt to determine how a variation in the type of chelating group present would affect the geometry at antimony centres, attempts were made to prepare a range of compounds with the general formula $PhSbX_2$(dioxo-chelate). Two different approaches were used. The first strategy was related to that adopted in the biphenylylene work and involved the oxidative addition of elemental halogens to

PhSb(chelate) compounds. The chelate groups utilised were the well-known pinacolate ($O_2C_2Me_4$) and catecholate (o-$O_2C_6H_4$) groups. However, reactions with halogens led an unidentified mixture of products, probably resulting from concurrent oxidation of the chelate groups.

A second, more successful strategy, involved the oxidation of $PhSbCl_2$ with the *ortho* benzoquinones, o-$O_2C_6Cl_4$ and o-$O_2C_6H_2$-3,5-^{t}Bu$_2$ to give the antimony(V) products PhSb(cat)Cl_2, where cat = 3,4,5,6-tetrachlorocatecholate dianion or 3,5-di-*tert*-butylcatecholate dianion.

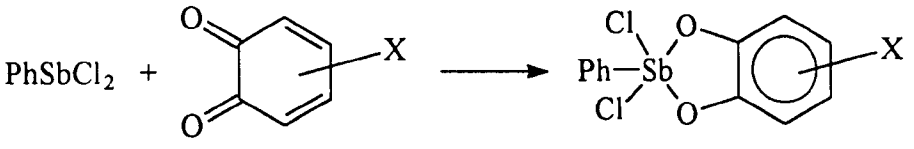

Figure 5.20 Preparation of PhSb(cat)Cl_2 compounds

Unfortunately, the only crystalline product obtained in this work resulted from a reaction between $PhSbCl_2$ and o-$O_2C_6Cl_4$ in diethyl ether and the product was shown by spectroscopic and crystallographic means to be the adduct, PhSb(o-$O_2C_6Cl_4$)Cl_2.OEt_2 (**5.6**). ^{1}H NMR spectroscopy showed that **5.6** remained unchanged as an ether adduct on recrystallisation from hot dichloromethane pointing to substantial Lewis acidity at the antimony centre. Dissolution of **5.6** in tetrahydrofuran, followed by evaporation of volatiles, led to isolation of the corresponding thf adduct PhSb(o-$O_2C_6Cl_4$)Cl_2.OC_4H_8 (**5.7**).

Attempted preparations of an authentic, solvent-free, five-coordinate compound using 3,4,5,6-tetrachloro-*ortho*-benzoquinone as the oxidising chelate were unsuccessful, but a reaction between $PhSbCl_2$ and 3,5-di-*tert*-*ortho*-benzoquinone (o-$O_2C_6H_2$-3,5-^{t}Bu$_2$) in dichloromethane did give uncomplexed PhSb(o-$O_2C_6H_2$-3,5-^{t}Bu$_2$)Cl_2 (**5.8**).

An X-ray structure determination was carried out on compound **5.6** to assess whether the compound would be structurally related to the biphenylylene compounds reported earlier, as shown in Figure 5.21, or whether the dioxo chelate group would promote

an alternative configuration. Unfortunately, it was not possible to grow single crystals of the uncomplexed compound **5.8**, which could have provided more definitive information.

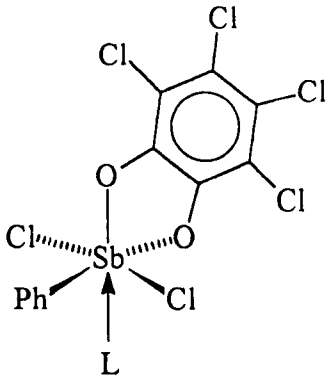

Figure 5.21 Expected configuration of 5.6 by analogy with biphenylylene compounds

5.2.2.2 Infrared Spectroscopy

The infrared spectrum of **5.6**, recorded as a nujol mull, showed the presence of the catecholato group, with strong bands at 1249 and 1242 cm^{-1} tentatively assigned to ν(C–O) vibrations. These bands are substantially lower than the ν(C=O) in the original *ortho*-quinone and no evidence of any residual ν(C=O) bands was observed. Many other bands were observed between 1500 and 400 cm^{-1}, due to phenyl, catecholato and ether modes but full assignment of these bands is beyond the scope of this work.

Similarly, the spectrum of PhSb(*o*-$O_2C_6H_2$-3,5-$^tBu_2$)Cl_2 (**5.8**) showed complete absence of any ν(C=O) bands, indicating a successful oxidative addition reaction between the $PhSbCl_2$ and the *ortho*-quinone had occurred. As for **5.6** above, a number of bands between 1236 and 1314 cm^{-1} could be assigned to ν(C–O) bands.

5.2.2.3 NMR Data

The ^1H NMR spectrum of PhSb(*o*-$O_2C_6Cl_4$)Cl_2.OEt_2 (**5.6**), clearly showed the presence of both the phenyl group and the diethyl ether molecule. Resonances

assignable to the latter were observed at 1.03 (triplet) and 3.73 (quartet) ppm, notably shifted from those expected for free Et_2O (1.20, 3.48 ppm). The phenyl group protons were observed as broad, unresolved multiplets at 7.64 (*meta* and *para*) and 8.17 (*ortho*) ppm. Integration of the peak areas gave the expected 1:1 ratio of phenyl groups to ether molecules.

Due to the low solubility of the compound in commonly available deuterated solvents a $^{13}C\{^1H\}$ DEPT-135 spectrum of **5.6** gave a very poor signal/noise ratio but the expected non-quaternary carbons were located. Hence, the diethyl ether signals were observed at 13.8 ($O(CH_2\mathit{C}H_3)_2$) and 65.6 ($O(\mathit{C}H_2CH_3)_2$) ppm and resonances due to the phenyl carbons were observed at 130.2(*m*-Ph), 132.0(*p*-Ph) and 133.0(*o*-Ph) ppm.

The ^1H spectrum of the tetrahydrofuran adduct, $PhSb(o\text{-}O_2C_6Cl_4)Cl_2.OC_4H_8$ (**5.7**), showed signals at 1.80 and 3.82 for the thf molecule, in addition to broad unresolved multiplets at 7.63 (*meta* and *para*) and 8.17 (*ortho*) ppm for the phenyl protons. Peak area integrals give the expected ratios, *ie*. a 1:1 phenyl to tetrahydrofuran ratio.

Signals in the ^1H NMR spectrum ($CDCl_3$ solution) of $PhSb(o\text{-}O_2C_6H_2\text{-}3,5\text{-}^tBu_2)Cl_2$ (**5.8**) proved to be broad and gave low resolution. However, full assignment of the spectrum was achieved, with integration of peak areas giving the expected ratios. In the high field area of the spectrum resonances due to the two *tert*-butyl groups were observed at 1.31 and 1.51 ppm (tentatively assigned to the 3- and 5- substituted groups respectively). The two aromatic protons showed resonances at 6.83 and 7.07 ppm, noticeably shifted from the corresponding signals in the (non-aromatic) quinone precursor (6.21 and 6.93 ppm). Resonances due to the phenyl protons were assigned to unresolved multiplets at 7.59 (*meta* and *para*) and 8.23 (*ortho*) ppm.

5.2.2.4 X-Ray Crystallography

A single crystal X-ray structure determination was carried out for the compound $PhSb(o\text{-}O_2C_6Cl_4)Cl_2.OEt_2$ (**5.6**) to assess the coordination geometry at antimony. Yellow crystals were obtained by overlayering a concentrated dichloromethane solution of the compound with twice the volume of pentane.

The molecular structure of **5.6** is shown in Figure 5.22 and selected bond lengths and angles are listed in Table 5.10. Further details of the structure determination are given in Appendix P.

Table 5.10 Selected bond distances and angles, with standard deviations in parentheses for $PhSb(o\text{-}O_2C_6Cl_4)Cl_2.OEt_2$ (5.6)

Bond lengths, Å		Bond angles, °	
Sb - Cl(1)	2.342(2)	Cl(1) - Sb - Cl(2)	94.76(7)
Sb - Cl(2)	2.346(2)	O(22) - Sb - O(21)	82.2(1)
Sb - O(21)	2.026(3)	O(22) - Sb - C(11)	168.9(1)
Sb - O(22)	1.991(3)	O(21) - Sb - C(11)	93.9(1)
Sb - C(11)	2.117(4)	O(22) - Sb - O(1)	81.7(1)
Sb - O(1)	2.302(3)	O(21) - Sb - O(1)	82.6(1)
O(21) - C(21)	1.343(5)	C(11) - Sb - O(1)	87.5(1)
O(22) - C(22)	1.354(5)	O(22) - Sb - Cl(1)	92.7(1)
		O(21) - Sb - Cl(1)	92.6(1)
		C(11) - Sb - Cl(1)	97.9(1)
		O(1) - Sb - Cl(1)	172.98(9)
		O(22) - Sb - Cl(2)	84.69(9)
		O(21) - Sb - Cl(2)	165.20(9)
		C(11) - Sb - Cl(2)	97.8(1)
		O(1) - Sb - Cl(2)	88.9(1)

Coordination geometry at antimony in **5.6** is, as expected, octahedral with the antimony bound to the chelating tetrachlorocatecholato group, two chlorine atoms, a phenyl group and with the diethyl ether molecule occupying the sixth octahedral site. The three oxygens occupy a common triangular face of the octahedron, giving the *fac* isomeric form. As a result, this conformation is not as proposed earlier (see Figure 5.21), using a simple geometric analogy to the biphenylylene structures reported earlier in this chapter; here the oxygen atoms would occupy *mer* sites. If the formal covalent bonds only are considered, the molecule could be classed as SP but in stark contrast to the biphenylylene compounds the tetrachlorocatecholato chelate group occupies two basal positions, with the halogens assuming mutually *cis* positions (one basal and the other apical).

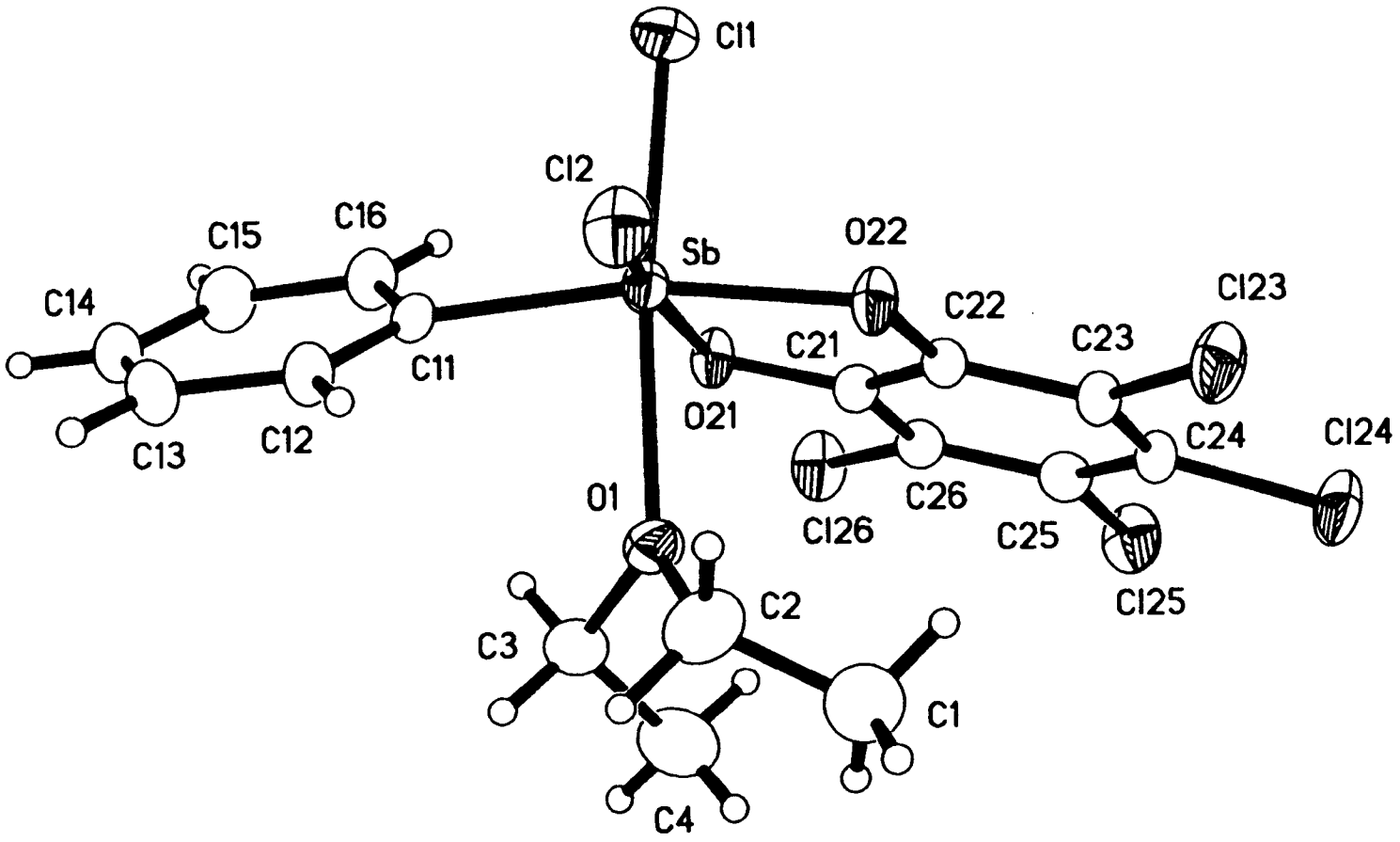

Figure 5.22 Molecular structure of $PhSb(o\text{-}O_2C_6Cl_4)Cl_2.OEt_2$ (5.6)

The chelate angle at antimony (O(21)–Sb–O(22)) of 82.2(1)° is however very similar to that found in the biphenylylene compounds (mean 84.7°) so simple geometric arguments for the differing behaviour are clearly invalid. The electronic properties of the catecholato group are therefore important in stereochemical control, with the consequence that the halogens assume *cis* positions.

The structure of **5.6** is related to that of the six-coordinate hydrated molecule in $[Ph_3Sb(o\text{-}O_2C_6H_4)]_2.H_2O$[17], in which the water molecule occupies a position *cis* to both catecholato oxygen atoms giving a similar *fac* isomeric geometry. Bond lengths in **5.6** are effectively as expected, although the $Sb–O_{catecholato}$ bonds are short. Notably, the Sb–O(22) bond length of 1.991(3) Å is particularly short and substantially less than the equivalent bonds in both $Ph_3Sb(o\text{-}O_2C_6Cl_4)$[18] (average $Sb–O_{catecholato}$ = 2.063 Å) and $PhSb(2,2'\text{-}C_{12}H_8)(o\text{-}O_2C_6Cl_4)$[18] (average $Sb–O_{catecholato}$ = 2.045 Å). The *trans* influence exerted by Cl(2) is the probable reason for slight elongation of the Sb–O(21) bond to 2.026(3) Å.

The distance between Sb and O(1), the oxygen atom of the ether group (2.302(3) Å) implies a relatively weak interaction between oxygen and antimony. This distance is comparable with the corresponding Sb←O interaction found for the mono-hydrate of diphenylantimony trichloride (2.311 Å)[40]. The equivalent distances for other known compounds containing the Sb←O linkage have been found to be spread over a significant range, for example in $SbCl_5.OPMe_3$ the Sb←O distance is 1.94 Å[41], whereas the equivalent distance is increased to 2.512 Å in $Ph_3Sb(o\text{-}O_2C_6H_4).H_2O$[17].

If the diethyl ether molecule is ignored, the residue clearly shows SP character with the *trans* 'basal' angles O(22)–Sb–C(11) (168.9(1)°) and O(21)–Sb–Cl(2) (165.20(9)°) significantly distorted from linearity. The four atoms C(11) (-0.017 Å) Cl(2) (0.018 Å) O(22) (-0.023 Å) and O(21) (0.022 Å) deviate only slightly from the best-fit basal plane, with the antimony atom lying 0.171 Å above.

As observed with the biphenylylene compounds described earlier, **5.6** clearly displays substantial Lewis acidity at the antimony centre, illustrated by the formation of the diethyl ether adduct. It would be of considerable interest to be able to determine the

structure of a compound with the PhSb(catecholato)X_2 to assess whether it would possess genuine SP geometry related to that found here in **5.6**, but without a donor molecule. However, there is a strong possibility that such a structure would include intermolecular interactions, perhaps to form dimers, as was observed with the biphenylylene compounds reported herein, or even that a TBP structure would result.

SUMMARY

Oxidative addition reactions between PhSb(2,2'-$C_{12}H_8$) and Br_2 or SO_2Cl_2 afforded the compounds PhSb(2,2'-$C_{12}H_8$)Br_2 (**5.2**) and PhSb(2,2'-$C_{12}H_8$)Cl_2 (**5.3**) respectively. Further metathesis reactions between **5.3** and KF or KSCN led to the isolation of the fluoride derivative, PhSb(2,2'-$C_{12}H_8$)F_2 (**5.4**) and the thiocyanate derivative, PhSb(2,2'-$C_{12}H_8$)$(NCS)_2$ (**5.5**). The structures of **5.2** and **5.3** are isomorphous, with square planar (SP) coordinated antimony as the monomeric unit, and the biphenylylene group spanning between the apical site and a basal position. However, long-range Sb···X interactions, giving dimers, were noted at positions *trans* to the apical (carbon) atom. This unexpected formation of dimers in the solid state implies some degree of Lewis acidity which is not present in related TBP analogous, such as the Ph_3SbX_2 group of compounds.

In a similar fashion to **5.2** and **5.3**, the monomeric unit of PhSb(2,2'-$C_{12}H_8$)$(NCS)_2$ (**5.5**) is a SP coordinated antimony structure which again is associated into dimers as a result of 1,3-bridging by one of the thiocyanate groups. The Sb···S interaction is again *trans* to the apical carbon.

The geometry at antimony in the monomeric units of **5.2**, **5.3** and **5.5** was evaluated by Muetterties and Guggenberger's method of dihedral angles and, if intermolecular interactions are ignored, near ideal SP geometry was confirmed.

Formation of catecholato analogues of the biphenylylene compound **5.3** was achieved by oxidative addition reactions between $PhSbCl_2$ and the *ortho*-benzoquinones, *o*-$O_2C_6Cl_4$ and *o*-$O_2C_6H_2$-3,5-^{t}Bu_2. However, the former reaction carried out in diethyl

ether led to formation of the six-coordinate diethyl ether adduct, PhSb(*o*-$O_2C_6Cl_4$)Cl_2.OEt_2 (**5.6**). If the diethyl ether molecule is ignored, the arrangement of the five atoms coordinated to antimony in this compound is very different from that found for the biphenylylene analogue, with the chelate group occupying two 'basal' positions and the chlorine atoms mutually *cis*. A non-solvated compound, PhSb(*o*-$O_2C_6H_2$-3,5-^{t}Bu$_2$)Cl_2 (**5.8**), was also prepared but did not give suitable crystals for a structure determination.

5.3 EXPERIMENTAL AND CHARACTERISING DATA

5.3.1 Preparation of (2,2'-$Li_2C_{12}H_8$).2TMEDA

Biphenyl (1.980g, 12.8mmol) was added to a stirred solution of ^{n}BuLi (20mls, 1.6M in hexanes, 32mmol) and tetramethylethylenediamine [TMEDA] (380mg, 33mol) under an argon atmosphere at 0°C. The resulting yellow solution was stirred for 72 hours at room temperature and then cooled to -30°C for a further 48 hours to allow crystallisation. Yellow crystals of (2,2'-$Li_2C_{12}H_8$).2TMEDA were isolated by decanting the supernatant liquid. A typical yield was 2.96g (58%).

5.3.2 Preparation of PhSb(2, 2'-$C_{12}H_8$) (5.1)

A solution of freshly prepared (2,2'-$Li_2C_{12}H_8$).2TMEDA (2.50g, 6.27mmol) in diethyl ether (20ml) was slowly added under argon to a stirred solution of $PhSbCl_2$ (1.69g, 6.27mmol) in diethyl ether (20ml) at -75°C. The resultant yellow solution was then slowly warmed to room temperature and stirred for 15 hours, after which time the mixture was filtered and added to water (50ml). The layers were separated and the aqueous layer washed three times with diethyl ether (25ml portions). The diethyl ether fractions were then combined, dried over anhydrous $MgSO_4$, filtered and the solvent removed *in vacuo* to give crude product. Recrystallisation from ethanol/ether gave PhSb(2,2'-$C_{12}H_8$) as a white powder. Yield 700mg (32%); mp 95-101°C [lit 98-100°C[27]].

Found: C,61.52; H,3.82: $C_{18}H_{13}Sb$ requires C,61.59; H,3.73 %.

^{1}H NMR (300MHz, $CDCl_3$, RT) δ 7.20(m, 7H), 7.40(m, 6H).

IR (nujol mull, CsI): 1433(m), 1298(w), 1158(w), 1108(w), 1065(w), 1057(w), 1020(w), 745(vs), 731(m), 715(w), 693(m), 480(w), 471(w), 448(w), 408(w).

MS (EI): $\{PhSb(C_{12}H_8)\}^+$ (m/z 350, 25%); $\{Sb(C_{12}H_8)\}^+$ (m/z 273, 89%); $\{PhC_{12}H_8\}^+$ (m/z 229, 40%); $\{PhSb\}^+$ (m/z 198, 21%); $\{C_{12}H_8\}^+$ (m/z 152, 100%); $\{Ph\}^+$ (m/z 77, 21%).

5.3.3 Preparation of $PhSb(2,2'\text{-}C_{12}H_8)Br_2$ (5.2)

Bromine (2.8ml, 0.485M solution in chloroform, 1.37mmol) was slowly added to a stirred solution of $PhSb(2,2'\text{-}C_{12}H_8)$ (480mg, 1.37mmol) in chloroform (30ml) at 0°C. The resulting solution was then warmed to room temperature and stirred for a further 12 hours after which time the volatiles were removed *in vacuo*. The crude product was then recrystallised from chloroform/hexane giving pure $PhSb(2,2'\text{-}C_{12}H_8)Br_2$. Yield 504mg (72%); m.p.211-215°C.

Found: C,43.05; H,2.67: $C_{18}H_{13}Br_2Sb$ requires C,42.32; H,2.57 %.

^{1}H NMR (300MHz, $CDCl_3$, RT) δ 7.56(m, 7H, biphenylyl-H_3,H_2, *m*- and *p*-Ph); 8.06(m, 6H, biphenylyl-H_3,H_2, *o*-Ph). The labelling scheme for the biphenylylene group is illustrated below:

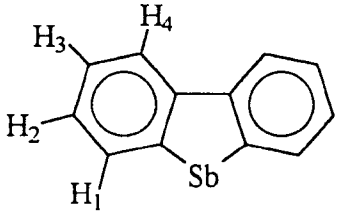

IR (nujol mull, CsI): 1431(s), 747(m), 724(s), 685(m).

MS (EI): $\{PhSb(C_{12}H_8)Br\}^+$ (m/z 429, 5%); $\{PhSb(C_{12}H_8)\}^+$ (m/z 350, 99%); $\{Sb(C_{12}H_8)\}^+$ (m/z 273, 58%); $\{PhC_{12}H_8\}^+$ (m/z 229, 100%); $\{Ph\}^+$ (m/z 77, 15%).

5.3.4 Preparation of $PhSb(2,2'\text{-}C_{12}H_8)Cl_2$ (5.3)

A solution of sulfuryl chloride (210mg, 1.55mmol) in dichloromethane (5ml) was slowly added to a stirred solution of $PhSb(2,2'\text{-}C_{12}H_8)$ (500mg, 1.45mmol) in dichloromethane (30ml) at 0°C. On warming to room temperature and stirring for 16 hours, a white precipitate was noted. Removal of volatiles from the reaction mixture

gave a white powder that was recrystallised from chloroform to give a crystalline sample of the title compound. Yield 410mg (67%); mp 216-218°C [lit: 220-223[27]].
Found: C,50.41; H,3.03: $C_{18}H_{13}Cl_2Sb$ requires C,51.25; H,3.08 %.
^{1}H NMR (300MHz, $CDCl_3$, RT) δ 7.55(td, 2H, $^3J_{HH}$ - 7.4Hz, $^4J_{HH}$ - 1.4Hz, biphenylyl-H_3); 7.61(m, 3H, *m*- and *p*-Ph); 7.63(td, 2H, $^3J_{HH}$ - 7.6Hz, $^4J_{HH}$ - 1.4Hz, biphenylyl-H_2); 8.02(dd, 2H, $^3J_{HH}$ - 7.4Hz, $^4J_{HH}$ - 1.4Hz, biphenylyl-H_4); 8.08(dd, 2H, $^3J_{HH}$ - 7.6Hz, $^4J_{HH}$ - 1.4Hz, biphenylyl-H_1); 8.27(m, 2H, *o*-Ph).
IR (nujol mull, CsI): 1437(s), 1321(w), 1305(w), 1286(w), 1261(w), 1091(w, br), 1064(w), 1044(w, br), 1014(w), 992(m), 746(s), 727(s), 682(m), 475(w), 455(w), 420(w).
MS (EI): $\{PhSb(C_{12}H_8)Cl\}^+$ (m/z 385, 3%); $\{PhSb(C_{12}H_8)\}^+$ (m/z 350, 76%); $\{Sb(2,2'\text{-}C_{12}H_8)Cl\}^+$ (m/z 308, 6%); $\{Sb(C_{12}H_8)\}^+$ (m/z 273, 60%); $\{PhC_{12}H_8\}^+$ (m/z 229, 100%); $\{C_{12}H_8\}^+$ (m/z 152, 98%); $\{Ph\}^+$ (m/z 77, 12%).

5.3.5 Preparation of $PhSb(2,2'\text{-}C_{12}H_8)F_2$ (5.4)

Potassium fluoride (140mg, 2.41mmol) was added to a stirred solution of $PhSb(2,2'\text{-}C_{12}H_8)Cl_2$ (**5.3**) (500mg, 1.18mmol) in acetone (30ml). The resulting reaction mixture was then refluxed for 16 hours, after which time volatiles were removed *in vacuo*. Crude $PhSb(2,2'\text{-}C_{12}H_8)F_2$ was extracted into hot chloroform and insoluble potassium chloride was removed by filtration. On removal of the solvent a white powder was isolated that was recrystallised from chloroform/hexane. Yield 240mg (52%).
Found: C,54.62; H,3.08: $C_{18}H_{13}F_2Sb$ requires C,55.57; H,3.37 %.
MS (EI): $\{PhSb(C_{12}H_8)F\}^+$ (m/z 369, 59%); $\{PhSb(C_{12}H_8)\}^+$ (m/z 350, 13%); $\{Sb(C_{12}H_8)\}^+$ (m/z 273, 19%); $\{PhC_{12}H_8\}^+$ (m/z 229, 49%); $\{C_{12}H_8\}^+$ (m/z 152, 61%); $\{Ph\}^+$ (m/z 77, 30%).

5.3.6 Preparation of $PhSb(2,2'\text{-}C_{12}H_8)(NCS)_2$ (5.5)

A solution of potassium thiocyanate (230mg, 2.37mmol) in acetonitrile (15ml) was added under argon to a stirred suspension of $PhSb(2,2'\text{-}C_{12}H_8)Cl_2$ (**5.3**) (500mg, 1.18mmol) and acetonitrile (20ml) and the resultant mixture was stirred at room temperature for 24 hours. After filtration, the solvent was removed *in vacuo* giving a

red oily product that was taken up into toluene, filtered again and the solvent evaporated. Recrystallisation of the oily material from chloroform/hexane afforded a small quantity of crystals of the title compound. Yield 286mg (34%); compound decomposes above *ca.* 180°C.

Found: C,51.02; H,2.68; N,5.73: $C_{20}H_{13}N_2S_2Sb$ requires C,51.42; H,2.80; N,6.00 %.

^{1}H NMR (300MHz, $CDCl_3$, RT) δ 7.56(t, 2H, $^3J_{HH}$ - 7.3Hz, biphenylyl-H_3); 7.70(t, 2H, $^3J_{HH}$ - 7.8Hz, biphenylyl-H_2); 7.70(m, masked, 3H, *m*- and *p*-Ph); 7.84(d, 2H, $^3J_{HH}$ - 7.3Hz, biphenylyl-H_4); 8.17(d, 2H, $^3J_{HH}$ - 7.8Hz, biphenylyl-H_1); 8.23(m, 2H, *o*-Ph).

IR (nujol mull, CsI): 2077(vs), 1994(vs, br), 743(s), 450(m).

MS (EI): $\{PhSb(C_{12}H_8)\}^+$ (m/z 350, 87%); $\{Sb(C_{12}H_8)\}^+$ (m/z 273, 70%); $\{PhC_{12}H_8\}^+$ (m/z 229, 90%); $\{C_{12}H_8\}^+$ (m/z 152, 100%); $\{Ph\}^+$ (m/z 77, 15%).

MS (FAB): $\{PhSb(C_{12}H_8)NCS\}^+$ (m/z 408, 7%); $\{PhSb(C_{12}H_8)NH_3\}^+$ (m/z 367, 16%); $\{PhSb(C_{12}H_8)\}^+$ (m/z 350, 16%); $\{Sb(C_{12}H_8)\}^+$ (m/z 273, 44%); $\{PhC_{12}H_8\}^+$ (m/z 229, 48%); $\{C_{12}H_8\}^+$ (m/z 152, 100%); $\{Ph\}^+$ (m/z 77, 43%).

5.3.7 Preparation of PhSb(*o*-$O_2C_6Cl_4$)Cl_2.OEt_2 (5.6)

A solution of tetrachloro-1,2-benzoquinone (3.697g, 15.0mmol) in diethyl ether (40ml) was slowly added at 0°C (leading to immediate dissipation of the deep red colour) to a stirred solution of $PhSbCl_2$ (4.052g, 15.0mmol) in diethyl ether (20ml), under an argon atmosphere. After stirring for a further 6 hours a yellow precipitate was evident and the precipitate was isolated by filtration. Recrystallisation from dichloromethane overlayered with pentane afforded yellow crystals of PhSb(*o*-$O_2C_6Cl_4$)Cl_2.OEt_2. Yield 7.785g (88%); the compound decomposes above *ca.* 140°C.

Found: C,32.35; H,2.44: $C_{12}H_5Cl_6O_2Sb.C_4H_{10}O$ requires C,32.59; H,2.56 %.

^{1}H NMR (250MHz, $CDCl_3$, RT) δ 1.03(t, 6H, $^3J_{HH}$ - 7Hz, $O(CH_2CH_3)_2$); 3.73(q, 4H, $^3J_{HH}$ - 7Hz, $O(CH_2CH_3)_2$); 7.64(m, br, 3H, *m*- and *p*-Ph); 8.17(m, br, 2H, *o*-Ph).

$^{13}C\{^1H\}$ DEPT -135 NMR (69 MHz, $CDCl_3$, RT) δ 13.8($O(CH_2CH_3)_2$); 65.6($O(CH_2CH_3)_2$); 130.2(*m*-Ph); 132.0(*p*-Ph); 133.0(*o*-Ph).

IR (nujol mull, CsI): 1429(vs), 1386(s), 1353(w), 1332(w), 1286(w), 1249(s), 1242(s), 1086(w), 1017(m), 993(m), 980(s), 890(w), 818(s), 801(m), 750(m), 739(m), 684(w), 609(w), 494(m), 452(m).

MS (EI): No antimony containing fragments observed.

5.3.8 Preparation of PhSb(*o*-$O_2C_6Cl_4$)Cl_2.OC_4H_8 (5.7)

Dissolution of PhSb(*o*-$O_2C_6Cl_4$)Cl_2.OEt_2 (**5.6**) (500mg, 0.90mmol) in tetrahydrofuran (25ml) under argon, followed by evaporation of volatiles *in vacuo* gave a quantitative conversion to the thf adduct, PhSb(*o*-$O_2C_6Cl_4$)Cl_2.OC_4H_8.

^{1}H NMR (250MHz, $CDCl_3$, RT) δ 1.80(m, 4H, -OCH_2CH_2-); 3.82(m, 4H, -OCH_2CH_2-); 7.63(m, br, 3H, *m*- and *p*-Ph); 8.17(m, br, 2H, *o*-Ph).

5.3.9 Preparation of PhSb(*o*-$O_2C_6H_2$-3,5-^{t}Bu_2)Cl_2 (5.8)

A solution of 3,5-di-*tert*-butyl-1,2-benzoquinone [dbbq] (1.961g, 8.90mmol) in dichloromethane (20ml) was added to a stirred solution of $PhSbCl_2$ (2.396g, 8.88mmol) in dichloromethane (25ml) under an argon atmosphere. The resultant green solution was then stirred at room temperature for 48 hours to ensure complete reaction. Removal of volatiles *in vacuo* yielded a fluffy yellow/green product. Yield 3.0g (69%).

Found: C,48.64; H,4.89: $C_{20}H_{25}Cl_2O_2Sb$ requires C,49.02; H,5.14 %.

^{1}H NMR (250MHz, $CDCl_3$, RT) δ 1.31(s, br, 9H, ^{t}Bu); 1.51(s, br, 9H, ^{t}Bu); 6.83(s, br, 1H, dbbq-*H*); 7.07(s, br, 1H, dbbq-*H*); 7.59(m, br, 3H, *m*- and *p*-Ph); 8.23(m, br, 2H, *o*-Ph).

IR (nujol mull, CsI): 1450(vs,br), 1414(vs), 1363(s), 1313(s), 1282(s), 1261(s), 1236(vs), 1202(m), 1091(m), 1062(m), 1027(m), 996(w), 975(s), 862(m), 827(s), 808(s), 751(m), 734(vs), 687(s), 581(m), 452(s).

5.3.10 Preparation of PhSb($O_2C_2Me_4$)

A solution of pinacol (2.570g, 21.7mmol) in toluene (10ml) was added to a stirred solution of $PhSbCl_2$ (5.859g, 21.7mmol) in toluene (40ml) at room temperature. Addition of triethylamine (4.396g, 43.4mmol) caused immediate precipitation of a white precipitate. After stirring for 24 hours the precipitate was collected by filtration, washed with further toluene (20ml) and shaken with methanol (50ml) to dissolve

Et_3NHCl. The product was isolated by filtration and washed with methanol. Yield 2.430g (36%).

Found: C,45.21; H,5.92: $C_{12}H_{17}O_2Sb$ requires C,45.75; H,5.44 %.

5.3.11 Preparation of PhSb(*o*-$O_2C_6H_4$)

A solution of $PhSbCl_2$ (5.211g, 19.3mmol) in toluene (50ml) was added to a stirred suspension of catechol (2.129g, 19.3mmol) and toluene (20ml) at room temperature. After stirring for *ca.* 30 minutes, triethylamine (3.910g, 38.6mmol) was added leading to immediate formation of a thick white suspension. After stirring for a further 3 hours the precipitate was collected by filtration and dried under vacuum. Stirring of the dried material with methanol (60ml) at room temperature, led to dissolution of Et_3NHCl and the insoluble PhSb(*o*-$O_2C_6H_4$) was collected by filtration. The crude product was washed with further methanol (20ml) and dried *in vacuo*. Yield 3.820g (64%).

Found: C,47.32; H,3.62: $C_{12}H_9O_2Sb$ requires C,46.96; H,2.96 %.

5.3.12 Attempted preparation of PhSb($O_2C_2Me_4$)Br_2

A solution of bromine (930mg, 5.82mmol) in dichloromethane (10ml) was added slowly to a stirred suspension of PhSb($O_2C_2Me_4$) (1.816g, 5.76mmol) in dichloromethane (50ml) at 0°C. The resultant orange reaction mixture was stirred for a further 12 hours, after which time all volatiles were removed *in vacuo*. ^1H NMR analysis of the material recovered showed the presence of a number of unidentified products.

5.3.13 Attempted preparation of PhSb(*o*-$O_2C_6H_4$)Br_2

A solution of bromine (560mg, 3.50mmol) in dichloromethane (5ml) was added to a stirred suspension of PhSb(*o*-$O_2C_6H_4$) (1.075g, 3.50mmol) in dichloromethane (50ml) at 0°C and the reaction mixture was stirred for 16 hours at reflux. The blue solution formed was evaporated to dryness, giving a green oil. ^1H NMR analysis showed the material to be a complex mixture of unidentified products.

5.4 REFERENCES

1. R.R.Holmes, *J. Am. Chem. Soc.*, 1985, **97**, 5379.

2. R.S.Berry, *J. Chem. Phys.*, 1960, **32**, 933.

3. R.R.Holmes, J.A.Dieters, *J. Am. Chem. Soc.*, 1977, **99**, 3318.

4. L.W.Dennis, V.J.Bartuska, G.E.Maciel, *J. Am. Chem. Soc.*, 1982, **104**, 230.

5. for example T.E.Clark, R.O.Day, R.R.Holmes, *Inorg. Chem.*, 1979, **18**, 1668.

6. J.A.Howard, D.R.Russel, S.J.Trippett, *J. Chem. Soc., Chem Commun.*, 1973, 856.

7. W.Althoff, R.O.Day, R.Brown, R.R.Holmes, *J. Am. Chem. Soc.*, 1977, **99**, 3332.

8. T.E.Clark, R.O.Day, R.R.Holmes, *Inorg. Chem.*, 1979, **18**, 1660.

9. R.O.Day, R.R.Holmes, *Inorg. Chem.*, 1983, **22**, 1771.

10. H.Wunderlich, *Acta Crystallogr.*, 1978, **B34**, 1000.

11. R.O.Day, J.M.Holmes, A.C.Sau, J.R.Devillers, R.R.Holmes, J.A.Dieters, *J. Am. Chem. Soc.*, 1982, **104**, 2127.

12. P.J.Wheatley, *J. Chem. Soc.*, 1964, 3718.

13. A.L.Beauchamp, M.J.Bennett, F.A.Cotton, *J. Am. Chem. Soc.*, 1968, **90**, 6675.

14. C.Brabant, B.Blanck, A.L.Beauchamp, *J. Organomet. Chem.*, 1974, **82**, 231.

15. C.Brabant, H.Hubert, A.L.Beauchamp, *Can. J. Chem.*, 1973, **51**, 2952.

16. C.P.Brock, *Acta Crystallogr.*, 1977, **A33**, 193.

17. M.Hall, D.B.Sowerby, *J. Am. Chem. Soc.*, 1980, **102**, 628.

18. R.R.Holmes, R.O.Day, V.Chandrasekhar, J.M.Holmes, *Inorg. Chem.*, 1987, **26**, 157.

19. A.Schmuck, J.Buschmann, J.Fuchs, K.Seppelt, *Angew. Chem., Int. Ed. Engl.*, 1987, **26**, 1180.

20. A.Schmuck, D.Leopold, K.Seppelt, *Chem. Ber.*, 1989, **122**, 803.

21. A.Schmuck, P.Pyykkö, K.Seppelt, *Angew. Chem., Int. Ed. Engl.*, 1990, **29**, 213.

22. K.Seppelt, *Heteroatom Chemistry*, Ed. E.Block, VCH, Ch. 19.

23. P.L.Millington, D.B.Sowerby, *J. Chem. Soc., Dalton Trans.*, 1981, 2011.

24. E.L.Muetterties, L.J.Guggenberger, *J. Am. Chem. Soc.*, 1974, **96**, 1748..

25. R.R.Holmes, R.O.Day, V.Chandrasekhar, J.M.Holmes, *Inorg. Chem.*, 1987, **26**, 163.

26. H.A.Meinema, J.G.Noltes, A.L.Spek, A.J.M.Duisenberg, *Recl. Trav. Chim.*, 1988, **107**, 226.

27. see for example D.Hellwinkel, M.Bach, *J. Organomet. Chem.*, 1969, **17**, 389.

28. W.Neugebauer, A.J.Kos, P.v.R.Schleyer, *J. Organomet. Chem.*, 1982, **228**, 107.

29. P.J.Fagan, W.A.Nugent, J.C.Calabrese, *J. Am. Chem. Soc.*, 1994, **116**, 1880 and references therein.

30. Z.Tian, D.G.Tuck, *J. Chem. Soc., Dalton Trans.*, 1993, 1381.

31. P.L.Millington, PhD Thesis, University of Nottingham, 1982.

32. A.M.Golub, H.Kohler, V.V.Skopenko, *Chemistry of the Pseudohalides*, Amsterdam, 1986.

33. G.E.Forster, M.J.Begley, D.B.Sowerby, *J. Organomet. Chem.*, 1996, **507**, 263.

34. P.Raj, R.Rastogi, R.Firojee, *Indian J. Chem.*, 1987, **A26**, 682.

35. R.G.Goel, E.Maslovsky Jr., C.V.Senoff, *Inorg. Chem.*, 1971, **10**, 2573.

36. T.Wizemann, H.Muller, D.Seybold, K.Dehnicke, *J. Organomet. Chem.*, 1969, **20**, 211.

37. M.J.Begley, D.B.Sowerby, *Acta Crystallogr.*, 1993, **C49**, 1044.

38. J.Bordner, G.O.Doak, J.R.Peters Jr., *J. Am. Chem. Soc.*, 1974, **96**, 6763.

39. J.Emsley, *The Elements*, 2nd edn., Clarendon Press, Oxford, 1991.

40. T.T.Bamgboye, M.J.Begley, D.B.Sowerby, *J. Organomet. Chem.*, 1989, **362**, 77.

41. C.I.Branden, I.Lindqvist, *Acta Chem. Scand.*, 1963, **17**, 253.

CHAPTER 6

TRANSITION METAL COMPLEXES INCORPORATING ANTIMONY

6.1 INTRODUCTION

The preparation of transition metal complexes incorporating antimony atoms or fragments has been a subject of significant interest over recent years. In addition to offering structural and reactivity interest, these compounds have potential interest regarding the synthesis of 'new materials'[1].

This chapter describes the preparation of a number of complexes containing phenylantimony or diphenylantimony fragments and the introduction provides a brief review of transition metal complexes incorporating antimony.

Stibine (R_3Sb) compounds

Perhaps the simplest type of compounds containing antimony–transition metal bonds are stibine complexes, in which R_3Sb (where R = alkyl, aryl, etc.) species acts as electron-pair σ-donors to unsaturated transition metal fragments. These complexes, analogous to the well known phosphine complexes, are typified by the compound $[Fe(CO)_4(SbPh_3)]$[2]. Distibines, $R_2Sb–SbR_2$, can also complex and, as in $(CO)_5Cr(Ph_4Sb_2)Cr(CO)_5$ they generally bridge between two metal centres[3]. In $Ni_2(CO)_4(\mu_2\text{-}Ph_2SbOSbPh_2)_2$ the oxobis-diphenylstibine groups also bridge between two nickel dicarbonyl fragments giving an eight-membered cyclo-$(NiSbOSb)_2$ system[4], as shown in Figure 6.1.

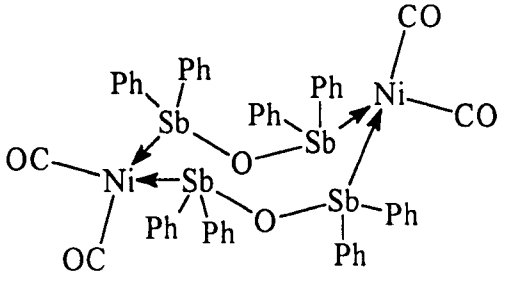

Figure 6.1 Molecular configuration of $Ni_2(CO)_4(\mu_2\text{-}Ph_2SbOSbPh_2)_2$

Interesting structural features of stibine and distibine complexes include the opening of the C–Sb–C angles and a shortening of the Sb–C bond lengths in comparison with the relevant uncomplexed stibine. These changes are considered[4,5] to reflect increased

Sb 5*s* orbital character in the Sb–C bonds. In turn, this argument suggests that the hybridised lone-pair Sb orbital used in forming antimony-transition metal bonds has less 5*s* (and more 5*p*) character (and hence moves towards that expected for sp^3 hybridisation) than that of the corresponding orbital in the 'free' stibine.

Stibane[6] (R_2Sb) compounds

A number of stibane (R_2Sb) complexes have been reported. Simple $R_2Sb–ML_n$ examples, where ML_n is a 17-electron fragment, are most appropriately described as having covalent Sb–M bonds, with retention of the lone pair on antimony. The compounds $[SbBr_2\{Fe(CO)_2(\eta\text{-}C_5H_5)\}]$[7] and $[Me_2Sb\{Fe(CO)_2(\eta\text{-}C_5H_5)\}]$[7] are examples of this complex type. Dative interactions between such compounds, using the antimony lone pair, and 16-electron transition metal fragments, has led to isolation of bis-transition metal complexes with bridging stibane groups. An interesting recent example of this type of complex is $[Fe(CO)_4]\{(\eta\text{-}C_5H_5)(CO)_nM\}Sb(N^tBu)_2SiMe_2$, where M = Mo, W or Fe, formed in a reaction between $(\eta\text{-}C_5H_5)(CO)_nMSb(N^tBu)_2SiMe_2$ and $Fe_2(CO)_9$[8] (see Figure 6.2).

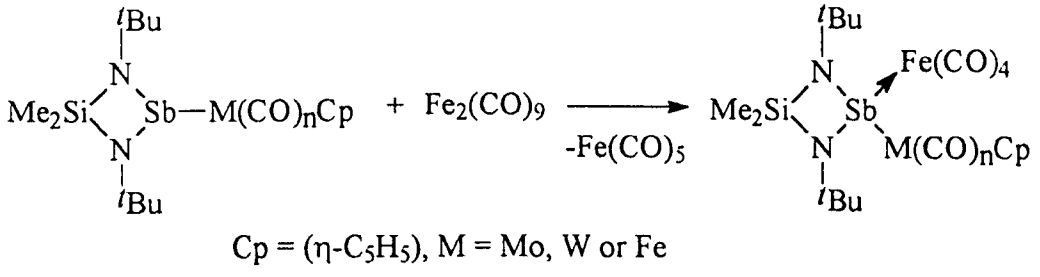

Cp = $(\eta\text{-}C_5H_5)$, M = Mo, W or Fe

Figure 6.2 Preparation of $[Fe(CO)_4]\{(\eta\text{-}C_5H_5)(CO)_nM\}Sb(N^tBu)_2SiMe_2$

Other examples of stibane groups acting as bridging, three electron donors are observed in the compounds $Cu_2(PMe_3)_4[\mu\text{-}(mesityl)_2Sb]_2$[9] and $(\mu\text{-}H)Os_3(CO)_{10}(\mu\text{-}SbPh_2)$[10].

Stibinidene (RSb) compounds

A variety of complexes containing the stibinidene (RSb) fragment is also known, which show a range of different coordination modes. These include compounds with the general formula $L_nM–Sb(R)–ML_n$, where ML_n is a 17-electron fragment, such as the chlorostibinidene compounds $[SbCl\{M(CO)_n(\eta\text{-}C_5H_5)\}_2]$ (M = Mo, W or Fe, n = 2 or 3), reported by Norman and co-workers[11]. Preparation of these compounds was achieved by reactions between $SbCl_3$ and two equivalents of the relevant $Na[M(CO)_n(\eta\text{-}C_5H_5)]$ species. An alternative route to the preparation of $[SbCl\{Mo(CO)_3(\eta\text{-}C_5H_5)\}_2]$ is by the exchange reaction shown below[11]:

$$2[Sb\{Mo(CO)_3(\eta\text{-}C_5H_5)\}_3] + SbCl_3 \rightarrow 3[SbCl\{Mo(CO)_3(\eta\text{-}C_5H_5)\}_2]$$

Organostibinidene complexes have also been prepared; for example, a bridging methylstibinidene group is proposed for the compound $[MeSb\{Fe(CO)_2(\eta\text{-}C_5H_5)\}_2]$[12]. Dative interactions between such stibinidene compounds and further 16-electron fragments can lead to tri-metallic compounds, such as $[Mn(CO)_2(\eta\text{-}C_5H_5)][SbBr\{Fe(CO)_2(\eta\text{-}C_5H_5)\}_2]$[7].

A further important class of stibinidene compounds includes di-metal complexes containing trigonal planar antimony bound to two 16-electron transition metal fragments, such as $[SbBr\{Mn(CO)_2(\eta\text{-}C_5H_4Me)\}_2]$[13], which are considered to possess a degree of $Sb–ML_n$ multiple bonding. A general preparative route to these compounds is typified by the reaction between $RSbCl_2$ (R = ^{t}Bu, Cl) and $Na_2Cr_2(CO)_{10}$, which affords the compound $[RSb\{Cr(CO)_5\}_2]$[13], as shown in Figure 6.3.

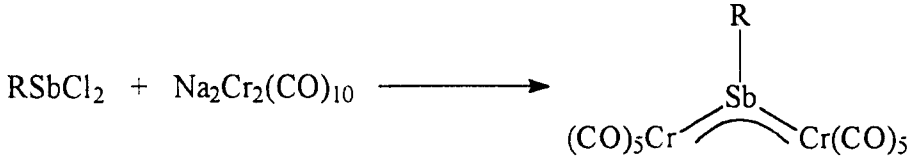

Figure 6.3 Preparation of $(CO)_5Cr–Sb(R)–Cr(CO)_5$ compounds

An alternative route to this class of complex is by reduction of a stibine complex where, for example, treatment of $[(\eta\text{-}C_5H_5)(CO)_2Mn\text{–}SbPhI_2]$ with metallic potassium, in the presence of [18]-crown-6, gives $[PhSb\{Mn(CO)_2(\eta\text{-}C_5H_5)\}_2]$[14]. Huttner[15] has described complexes of this type as being Sb(I) compounds, in which two SbR lone pairs are σ-donated to the electron deficient 16-electron transition metal fragments. This bonding is further accompanied by π-interactions from two transition metal occupied *d* orbitals to the empty 5*p*-Sb orbital (sp^2 hybridised). The π bonding is hence classed as a 3-centre-4π system[15]. The trigonal planar coordination about antimony and the short Sb–transition metal bonds are consistent with this proposal.

Interestingly, these stibinidene complexes have been found to react with both Lewis bases (B:) and Lewis acids. Thus, reaction of $RSb[W(CO)_5]_2$ (where R= ^{t}Bu, Cl) with Lewis bases gives the adducts $B\rightarrow Sb(R)[W(CO)_5]_2$, whilst reaction of the same stibinidene complex with the Lewis acid $W(CO)_5$, gives the tri-metallic species $RSb[W(CO)_5]_3$[16]. These findings are consistent with the presence of two valence tautomers, as illustrated in Figure 6.4. The first has the previously described 'open' 3-centre-4π system, while the second 'closed' structure contains a direct $L_nM\text{–}ML_n$ bond and an available lone pair on antimony. Indeed, both compound types have been isolated and characterised[16,17].

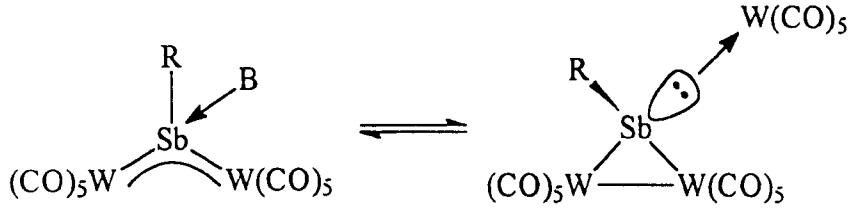

'open' structure - Lewis acid 'closed' structure - Lewis base

Figure 6.4 Valence tautomers for stibinidene complexes

In contrast to the 'open' structure generally observed for dimetallastibinidenes (where the antimony is not further acting as a Lewis base), the compound $[(Me_3Si)_2CHSb\{Fe(CO)_4\}_2]$[18] was found to possess a 'closed' structure. Clearly, the equilibrium between the two tautomeric forms is delicately controlled by steric and electronic factors[15].

Interestingly, several publications[16,18,19] have reported the formation of products characterised as containing π-coordinated RSb=SbR ligands, during preparations of stibinidene complexes, although no R–Sb=Sb–R compound has yet been isolated in the 'free' state. An example of this is the reaction between ^{t}BuSbCl$_2$ and $Na_2Cr_2(CO)_{10}$ which yields not only the 'open' stibinidene compound ^{t}BuSb[Cr(CO)$_5$]$_2$ but also [^{t}BuSb=Sb^{t}Bu][Cr(CO)$_5$]$_3$[16], illustrated as the π-complex shown in Figure 6.5.

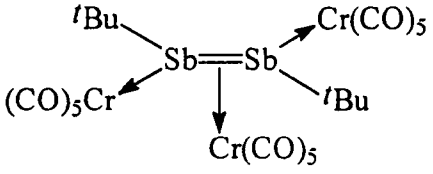

Figure 6.5 Molecular representation of the complex [^{t}BuSb=Sb^{t}Bu][Cr(CO)$_5$]$_3$

A further class of stibinidene compounds are those in which the RSb fragment is incorporated into a transition metal carbonyl cluster. Most examples of this type are anionic, such as $[Ni_{10}(SbPh)_2(CO)_{18}]^{2-}$ where the PhSb fragments 'cap' the $Ni_{10}Sb_2$ icosahedron[4]. A second example is the dianion, $[Fe_3(ClSb)(CO)_{12}]^{2-}$, in which the antimony is four-coordinate, bound to three $Fe(CO)_4$ groups in addition to the chlorine atom[20].

Stibido ('naked' Sb) compounds

Coordination complexes incorporating 'naked' antimony (stibido complexes) are also known. Norman and co-workers have prepared a range of such compounds in which the antimony is bound to three 17-electron fragments, as in $[Sb\{M(CO)_n(\eta\text{-}C_5R_5)\}_3]$, where M = Mo, W, Fe (R = H)[11] or Ni (R = Me)[21] and $[Sb\{Re(CO)_5\}_3]$[22]. All these

compounds were prepared by metathesis reactions between $SbCl_3$ and three equivalents of either the sodium or potassium salts of the ML_n anion. Interestingly, the unusual stibido product $[(\mu\text{-}Sb)_2Mo_5(CO)_{14}(\eta\text{-}C_5H_5)_4]$ was isolated in a reaction between $SbCl_3$ and one equivalent of $Na[Mo(CO)_3(\eta\text{-}C_5H_5)]$[23].

When $SbCl_3$ was treated with three mols of $Na[Co(CO)_3L]$, where L = carbonyl or phosphine, the initial products were the expected $[Sb\{Co(CO)_3L\}_3]$ species, but their ready decomposition led to aggregation and isolation of more complex species, such as $[Sb_2Co_4(CO)_{11}]^{n-}$ (n = 1 or 2)[24,25] and $[Sb_2Co_2(CO)_4(PPh_3)_2]$[26].

Incorporation of 'naked' antimony into metal carbonyl clusters, is also known. Examples of this type include[27-30], $[Sb_2Fe_6(CO)_{20}]^{2-}$, $[Sb_2Fe_6(CO)_{22}]$, $[SbFe_3Cr(CO)_{17}]^-$ and $[SbRh_{12}(CO)_{27}]^{3-}$. A reaction between $Fe_5C(CO)_{15}$ and $SbCl_5$ has also led to the preparation of the antimony carbyne cluster $[SbFe_3(CO)_9CH]$[31].

Sb_2 coordination

The heavier dinitrogen homologue Sb_2, clearly unstable in the 'free' state, can be stabilised by coordination to transition metal fragments. Harper and Rheingold have described the preparation of the supported Sb_2 compound, $[Mo(CO)_2(\eta\text{-}C_5H_5)]_2(\mu,\eta^2\text{-}Sb_2)$, by a reaction between the dimer $[Mo(CO)_3(\eta\text{-}C_5H_5)]_2$ and elemental antimony[32]. The side-on, μ,η^2 coordination of the diantimony moiety gives a tetrahedral framework, simplistically illustrated in Figure 6.6.

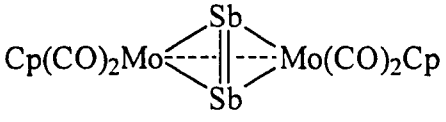

Figure 6.6 Molecular representation for $[Mo(CO)_2(\eta\text{-}C_5H_5)]_2(\mu,\eta^2\text{-}Sb_2)$

A supported Sb_2 fragment, having the shortest Sb–Sb bond (2.663 Å) reported, is also present in the triangular pinwheel compound $\{[W(CO)_5]_3(\mu_3,\eta^2\text{-}Sb_2)\}$[19]. Huttner has rationalised the coordination of the Sb_2 fragment by a donation of the 4π-electrons and also the σ-bonding electron pair[15]. This bonding model hence fulfils the

18-electron requirements of the three 16-electron $W(CO)_5$ fragments with the Sb_2 group donating a total of six electrons.

Antimony–transition metal multiple bonding

Unlike the lighter congeners RP (phosphinidene) and RN (imido), terminal $L_nM{=}SbR$ complexes are not known. However, doubly bonded cations with the general formula $[L_nM{=}Sb{=}ML_n]^+$ have been successfully prepared[33]. For example, treatment of $[SbCl\{Cr(CO)_2(\eta\text{-}C_6Me_6)\}_2]$ with $GaCl_3$ afforded the compound $[(\eta\text{-}C_6Me_6)(CO)_2Cr{=}Sb{=}Cr(CO)_2(\eta\text{-}C_6Me_6)]^+[GaCl_4]^-$ (see Figure 6.7)

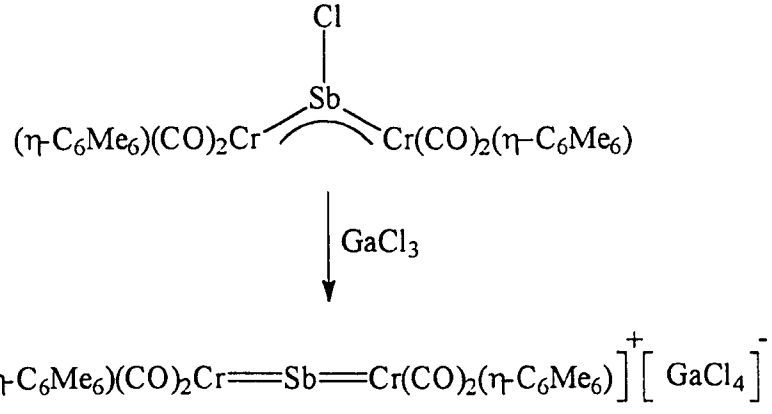

Figure 6.7 Preparation of antimony-chromium doubly bonded cations

Not perhaps surprisingly, compounds containing terminal Sb≡transition metal triple bonds have not been isolated, although recent work by Rheingold and co-workers, has shown evidence of $[(CO)_nM{\equiv}Sb]^-$ compounds in the gas phase. These complexes were produced by interaction of Sb_2^- (formed by laser ablation of elemental antimony) and binary metal carbonyls (Cr, Mo, W and Fe)[34].

Sb(V) containing complexes

There are a few examples in the literature in which Sb(V) fragments are bound to transition metal species. Malisch and co-workers have reported the preparation and crystal structure of the chiral complex, $[Me_2SbCl_2\{Fe(CO)(PMe_3)(\eta\text{-}C_5H_5)\}]$[35] and a further example is $[Rf_2Sb\{Fe(CO)_2(\eta\text{-}C_5H_5)\}]$, where Rf = *o*-$C_6H_4C(CF_3)_2O$-,

prepared by a reaction between $[Rf_2Sb][NEt_4]$ and $Fe(CO)_2(\eta\text{-}C_5H_5)I$[36]. In addition, aerobic oxidation of solutions containing $[Sb_2Co_2(CO)_4(PAr_3)_2]$, where Ar = Ph or *p*-tolyl, leads to the isolation of the corresponding dimetallastibinic acids $[SbO(OH)\{Co(CO)_3(PAr_3)\}_2]$[37]. Interestingly, these stibinic acids are the only structurally characterised compounds containing an unsupported Sb=O double bond.

The work described in this chapter involves an investigation into diphenylstibane and phenylstibinidene complexes, to develop further their relatively unexplored chemistry. The majority of the reactions reported involve Sb(III) substrates although reactions involving Sb(V) precursors were also attempted.

6.2 RESULTS AND DISCUSSION

6.2.1 Preparation of Compounds

It is possible to envisage a simple metathesis reaction taking place when the bis oxo-bridged compound $[Ph_2SbBrO]_2$ (**2.12**) is treated with two equivalents of $Na[Mo(CO)_3(\eta\text{-}C_5H_5)]$ in tetrahydrofuran, to give $[Ph_2Sb\{Mo(CO)_3(\eta\text{-}C_5H_5)\}O]_2$. This, however, was not observed and instead an unusual antimony reduction compound, $[\{\mu\text{-}Ph_2Sb\}_2\{Mo(CO)_2(\eta\text{-}C_5H_5)\}_2]$ (**6.1**) was isolated. Purification of the compound by column chromatography (alumina) and subsequent recrystallisation yielded purple crystals of the compound, suitable for X-ray diffraction.

Although the preparation and subsequent manipulations of the complex were carried out using Schlenk and glove-box techniques, **6.1** appeared to be stable under atmospheric conditions for prolonged periods of time.

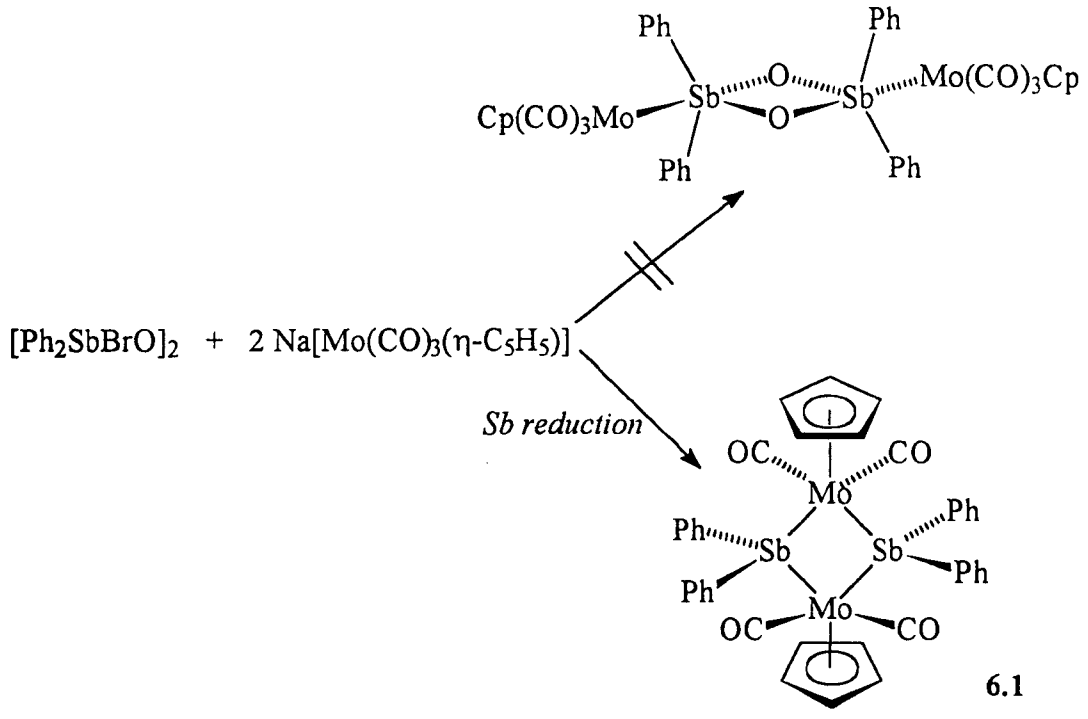

Figure 6.8 Preparation of [{μ-Ph_2Sb}$_2${$Mo(CO)_2(\eta\text{-}C_5H_5)$}$_2$] (6.1)

The mechanism by which **6.1** was formed is a matter of discussion, although it seems highly probable that it is formed by 'dimerisation' (with corresponding carbonyl loss) of an intermediate [Ph_2Sb{$Mo(CO)_3(\eta\text{-}C_5H_5)$}] (**6.2**) (see Figure 6.9). Indeed Malisch *et al* have previously reported that the dimethylarsane analogue [Me_2As{$Mo(CO)_3(\eta\text{-}C_5H_5)$}] is known to 'dimerise' with CO loss on thermal or photochemical treatment, to give [{μ-Me_2As}$_2${$Mo(CO)_2(\eta\text{-}C_5H_5)$}$_2$][38,39]. Similarly, loss of the phosphine group from [Me_2As{$Mo(CO)_2(PR_3)(\eta\text{-}C_5H_5)$}$_2$] is reported to give the same compound[40].

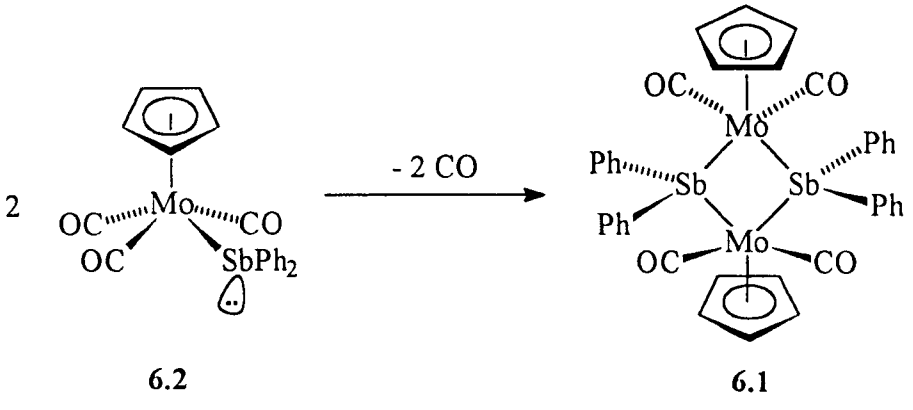

Figure 6.9 Proposed mechanism of formation for 6.1

In an attempt to prepare the proposed and previously unreported intermediate **6.2**, a reaction was carried out between Ph_2SbCl and $Na[Mo(CO)_3(\eta\text{-}C_5H_5)]$ in THF. Although the material obtained after work-up proved to be a mixture of products that could not be readily separated, ^1H NMR spectroscopy showed that the main component was consistent with the composition $[Ph_2Sb\{Mo(CO)_3(\eta\text{-}C_5H_5)\}]$ (**6.2**). Surprisingly, heating of the material in solution gave no indication (by ^1H NMR spectroscopy) of aggregation to give **6.1**. Furthermore, exposure of the sample to daylight and ambient temperatures for prolonged periods still showed no conversion of the ^1H NMR signals associated with **6.2** into those for **6.1**.

It is therefore not possible to confirm the proposed mechanism for formation of **6.1** via **6.2** as an intermediate. In addition, further uncertainties lie in the fact that pure **6.2** could not be isolated and unambiguously characterised.

An analogous reaction between Ph_2SbCl and $Na[W(CO)_3(\eta\text{-}C_5H_5)]$ (see Figure 6.10) also gave a mixture of products, although again the ^1H NMR spectrum was consistent with the major component being the expected product, $[Ph_2Sb\{W(CO)_3(\eta\text{-}C_5H_5)\}]$ (**6.3**). As was found for **6.2**, the mixture could not be readily separated and thus unambiguous characterisation was not possible. However, a FAB mass spectrum of the mixture showed signals due to the expected molecular ion and expected fragments.

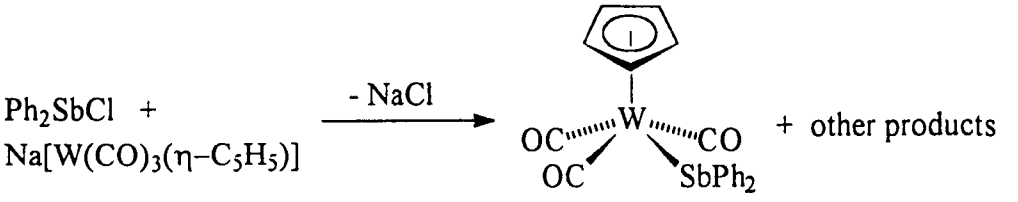

6.3

Figure 6.10 Reaction between Ph_2SbCl and $Na[W(CO)_3(\eta\text{-}C_5H_5)]$

In an attempt to form an iron analogue of **6.1**, a solution of $[Ph_2SbBrO]_2$ (**2.12**) in THF was treated with two equivalents of $Na[Fe(CO)_2(\eta\text{-}C_5H_5)]$ (formed by the sodium amalgam reduction of $[Fe(CO)_2(\eta\text{-}C_5H_5)]_2$). However, the reaction gave a mixture of unidentified products and is clearly complex. In contrast, identifiable products were obtained from a reaction between the antimony(III) precursor, Ph_2SbCl and $Na[Fe(CO)_2(\eta\text{-}C_5H_5)]$, which afforded a mixture of two products identified as $[PhSb\{Fe(CO)_2(\eta\text{-}C_5H_5)\}_2]$ (**6.4**) and $[Ph_2Sb\{Fe(CO)_2(\eta\text{-}C_5H_5)\}]$ (**6.5**). Repeated recrystallisations of the material led to the continued isolation of crystalline mixtures and the compounds **6.4** and **6.5** were therefore characterised as a mixture. A crystal selected from the mixture was subjected to a structure determination and was found to be the phenylstibinidene bridged compound $[PhSb\{Fe(CO)_2(\eta\text{-}C_5H_5)\}_2]$ (**6.4**).

In contrast to the reactions between antimony(III) halides and two or three equivalents of $Na[ML_n]$ (ML_n = 17-electron transition metal fragment) which give good yields of the metathesis products, $Sb\{ML_n\}_3$ or $XSb\{ML_n\}_2$, respectively[7,11], it is surprising that related reactions between Ph_2SbCl and $Na[ML_n]$, reported here, give complex mixtures of products. However, it is clear that a number of competitive reactions take place, in addition to the expected 'salt-elimination' metathesis reactions to give Ph_2SbML_n complexes. Interestingly, a non-straightforward reaction was also noted in the reaction between $^tBuSbCl_2$ and one equivalent of $Na[M(CO)_3(\eta\text{-}C_5H_5)]$ (where M = Mo or W) which, after prolonged periods in solution, yielded $[ClSb\{M(CO)_3(\eta\text{-}C_5H_5)\}_2]$[41].

The differing behaviour between phenyl and methyl substituents on antimony is also apparent as Malisch and Panster have reported the ready synthesis of Me_2SbML_n compounds via similar reactions between Me_2SbBr and $Na[ML_n]$[7]. It is likely that the increased lability of the phenyl groups plays a significant role in the differing chemistry and indeed reaction between Ph_2SbCl and $[Ni_6(CO)_{12}]^{2-}$ has been shown[4] to give a phenyl elimination product, $[Ni_{10}(SbPh)_2(CO)_{18}]^{2-}$, rather than one containing the intact Ph_2Sb unit. It also appears that the presence of methyl substituents reduces the susceptibility of antimony(V) to reduction, with the complex,

$[Me_2SbCl_2\{Fe(CO)(PMe_3)(\eta\text{-}C_5H_5)\}]$[35] previously prepared, whilst the use of an antimony(V) precursor, $[Ph_2SbBrO]_2$ (**2.12**), in this work, led to reduction and the isolation (in the case of **6.1**) of antimony(III) products.

6.2.2 Infrared Spectroscopy

The solid state infrared spectrum of $[\{\mu\text{-}Ph_2Sb\}_2\{Mo(CO)_2(\eta\text{-}C_5H_5)\}_2]$ (**6.1**), displayed, in addition to a number of bands assignable to phenyl and cyclopentadienyl modes, intense ν(CO) absorptions at 1924, 1870, 1857 and 1846 cm^{-1}, consistent with the presence of terminal carbonyl groups. The splitting of the lower frequency bands (1870 to 1846 cm^{-1}) is considered to be a solid-state effect.

In CH_2Cl_2 solution, the spectrum was simplified and showed major ν(CO) bands at 1929(vs) and 1866(s) cm^{-1}, together with an unresolved shoulder at 1946 cm^{-1}. If this shoulder is ignored, the spectrum is comparable with the two band spectra of the related compounds $[Mo(CO)_2(\eta\text{-}C_5H_5)]_2(\mu,\eta^2\text{-}Sb_2)$ (1936 and 1885 cm^{-1}, CH_2Cl_2 solution[32]) and $[Mo(CO)_2(\eta\text{-}C_5H_5)]_2(\mu,\eta^2\text{-}Bi_2)$ (1917 and 1866 cm^{-1}, THF solution[42]), both of which contain the same two $Mo(CO)_2(\eta\text{-}C_5H_5)$ fragments. However, the non-trivial shoulder in the CH_2Cl_2 spectrum of **6.1**, together with the possibility that further splitting is masked within the broad 1866 cm^{-1} band, indicates the possible existence of isomerisation occurring in the polar CH_2Cl_2 solution. Indeed, a ^1H NMR spectrum of **6.1** in $CDCl_3$ solution (Section 6.2.3) showed the clear presence of two differing cyclopentadienyl environments (one significantly more dominant than the other).

The most likely form of isomerism in the CH_2Cl_2 solution spectrum of **6.1** (and in the ^1H NMR spectrum in similarly polar $CDCl_3$) is a *cis* ↔ *trans* isomerisation of the molybdenum fragments. It should be noted that the solid-state structure of **6.1**, detailed in Section 6.2.5, shows a basically *trans* configuration of the two molybdenum centres. Moreover, a ^1H NMR spectrum of **6.1** recorded in C_6D_6 solution, showed only a single isomer (presumably the *trans* form).

The reason why only a single isomer was observed in the infrared spectrum of $[Mo(CO)_2(\eta\text{-}C_5H_5)]_2(\mu,\eta^2\text{-}Sb_2)$, when recorded in CH_2Cl_2 solution, is not known, although it is possible that the multiply bonded Sb_2 moiety prevents a related isomerisation occurring.

As other reactions yielded unseparated mixtures, limited information can be obtained from their infrared spectra. A solution spectrum (CH_2Cl_2) of the mixture containing $[Ph_2Sb\{W(CO)_3(\eta\text{-}C_5H_5)\}]$ (**6.3**) showed bands at 2027, 1995, 1933 and 1889 cm^{-1}, consistent with the presence of solely terminal carbonyl groups. Likewise, a solution spectrum (THF) of the mixture of **6.4** and **6.5** showed ν(CO) bands expected for terminal carbonyl groups attached to a neutral iron centre, with absorptions at 1995, 1977 and 1946 cm^{-1}.

6.2.3 NMR Data

The ^1H NMR spectrum of **6.1**, measured in C_6D_6 solution (see Figure 6.11), displayed fully assignable resonances, with a singlet at 4.90 ppm due to the cyclopentadienyl protons and multiplets at 7.23 (*meta* and *para*) and 7.76 (*ortho*) ppm assigned to the phenyl proton resonances. However, when the spectrum was recorded in $CDCl_3$ solution, two distinctly different cyclopentadienyl singlets (δ 5.16 and 5.32 ppm) were observed. The resonance at 5.16 ppm was considerably more intense and integration of the two peak areas gave a ratio of *ca* 4:1. The phenyl protons signals were observed as a complex multiplet between 7.20 and 7.60 ppm, *ie.* the distinct separation of the *ortho* and *meta/para* resonances observed in the C_6D_6 spectrum, had collapsed in the $CDCl_3$ spectrum. As crystallisation of the $CDCl_3$ solution afforded quantitative recovery of **6.1**, it seems apparent that the presence of two sets of resonances in the polar $CDCl_3$, is due to a form of isomerisation as opposed to degradation whilst in solution. As discussed in Section 6.2.2, the isomerisation is likely to be a *cis* ↔ *trans* process.

Figure 6.11 ^{1}H NMR spectrum of $[\{\mu\text{-}Ph_2Sb\}_2\{Mo(CO)_2(\eta\text{-}C_5H_5)\}_2]$ (6.1) in C_6D_6

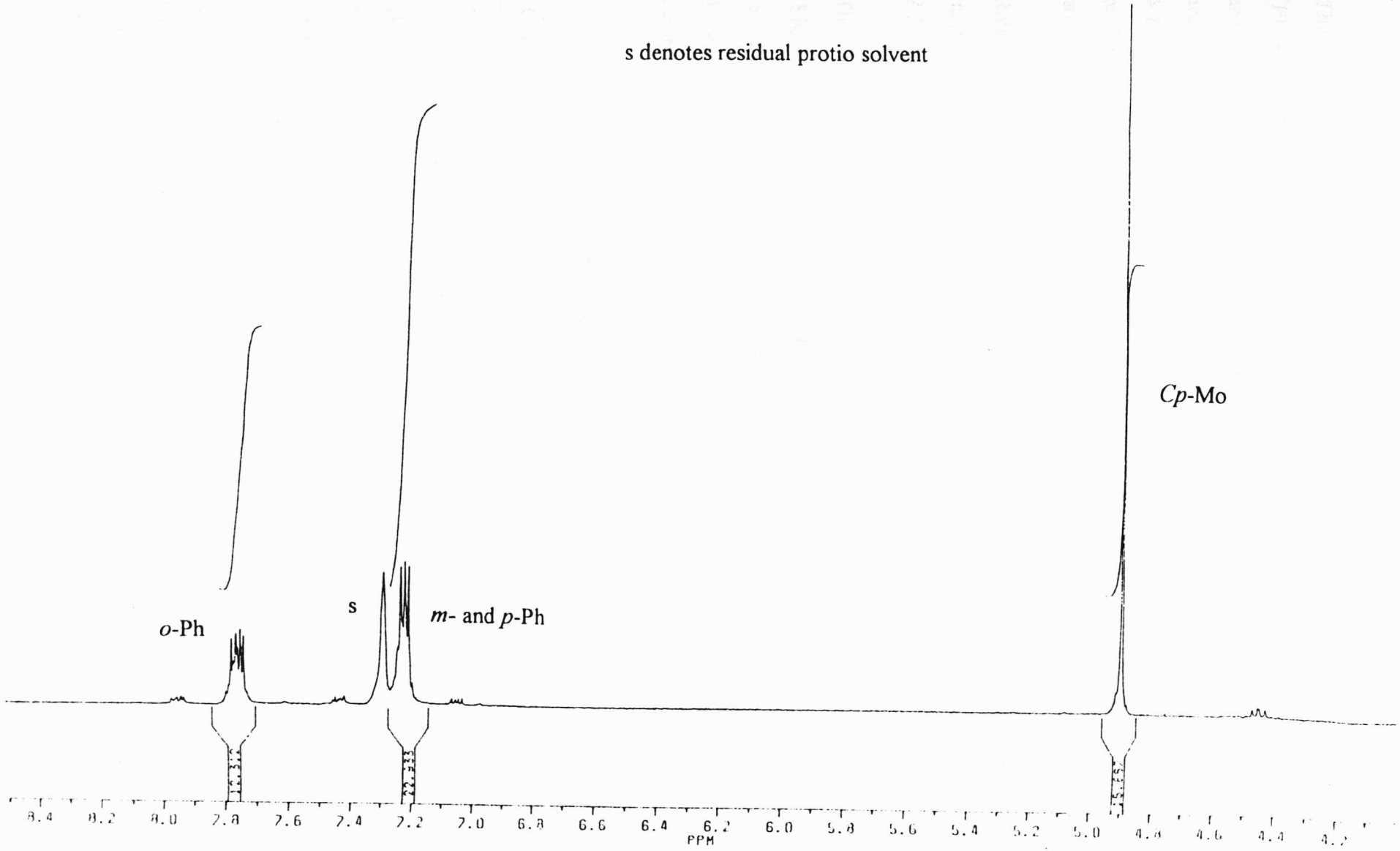

The ^{1}H NMR spectrum (C_6D_6 solution) of the mixture considered to contain $[Ph_2Sb\{Mo(CO)_3(\eta\text{-}C_5H_5)\}]$ (**6.2**), showed resonances at 4.78(s, C_5H_5), 7.21(m, *m*- and *p*-Ph) and 7.80(d, *o*-Ph) ppm attributed to that species, with integrals of peak areas giving the expected ratios. As reported earlier (Section 6.2.1), no signals due to **6.1** were evident in the spectrum, even after heating the C_6D_6 solution or exposure to prolonged periods of daylight. Moreover, if anhydrous conditions were maintained, no notable changes to the initial signals were observed.

Related resonances were observed in the ^{1}H NMR spectrum (C_6D_6 solution) of the mixture containing $[Ph_2Sb\{W(CO)_3(\eta\text{-}C_5H_5)\}]$ (**6.3**), with signals at 4.66(s, C_5H_5), 7.27(m, *m*- and *p*-Ph) and 7.84(d, *o*-Ph) ppm attributed to **6.3**.

The ^{1}H NMR spectrum of the mixture of $[PhSb\{Fe(CO)_2(\eta\text{-}C_5H_5)\}_2]$ (**6.4**) and $[Ph_2Sb\{Fe(CO)_2(\eta\text{-}C_5H_5)\}]$ (**6.5**) in C_6D_6 solution, clearly showed the presence of the two individual complexes. Resonances at 4.35(s, C_5H_5), 7.27(m, *m*- and *p*-Ph) and 8.19(d, *o*-Ph) ppm could be assigned to the compound **6.4**, whereas **6.5** showed signals at 4.12(s, C_5H_5), 7.27(m, *m*- and *p*-Ph) and 7.92(d, *o*-Ph) ppm.

Table 6.1 ^{1}H chemical shifts (ppm) for compounds 6.1 to 6.5

Compound	Cp resonance	Ph resonances
$[\{\mu\text{-}Ph_2Sb\}_2\{Mo(CO)_2(\eta\text{-}C_5H_5)\}_2]$ (**6.1**)	4.90	7.23, 7.76
$[Ph_2Sb\{Mo(CO)_3(\eta\text{-}C_5H_5)\}]$ (**6.2**)	4.78	7.21, 7.80
$[Ph_2Sb\{W(CO)_3(\eta\text{-}C_5H_5)\}]$ (**6.3**)	4.66	7.27, 7.84
$[PhSb\{Fe(CO)_2(\eta\text{-}C_5H_5)\}_2]$ (**6.4**)	4.35	7.27, 8.19
$[Ph_2Sb\{Fe(CO)_2(\eta\text{-}C_5H_5)\}]$ (**6.5**)	4.12	7.27, 7.92

6.2.4 Mass Spectroscopy

The FAB mass spectrum of $[\{\mu\text{-}Ph_2Sb\}_2\{Mo(CO)_2(\eta\text{-}C_5H_5)\}_2]$ (**6.1**) proved to be particularly informative. A parent ion peak, showing the appropriate isotopic peaks, was observed at m/z 988, while a peak at m/z 932 can be assigned to the parent minus two carbonyl groups. Several monoantimony fragments were also observed, including $\{Ph_2SbMo_2Cp_2(CO)_3\}^+$ (m/z 685), $\{Ph_2SbMoCp(CO)_3\}^+$ (m/z 522) and

$\{Ph_2SbMoCp\}^+$ (m/z 438). Interestingly, the $\{Ph_2SbMoCp(CO)_3\}^+$ fragment peak was of significant intensity, which seems to imply rearrangement of **6.1** to **6.2** under the mass spectroscopy conditions.

The FAB mass spectrum of the mixture containing $[Ph_2Sb\{W(CO)_3(\eta\text{-}C_5H_5)\}]$ (**6.3**) displayed a low intensity peak assigned to the molecular ion, $\{Ph_2SbWCp(CO)_3\}^+$, at m/z 608. Primary fragmentation through loss of carbonyls was also evident, with peaks at m/z 580 and 524 assigned to the ions $\{Ph_2SbWCp(CO)_2\}^+$ and $\{Ph_2SbWCp\}^+$ respectively. Furthermore, significant peaks were also observed due to the monophenyl fragments, $\{PhSbWCp(CO)_2\}^+$ (m/z 503) and $\{PhSbWCp\}^+$ (m/z 447).

An EI mass spectrum of the mixture of $[PhSb\{Fe(CO)_2(\eta\text{-}C_5H_5)\}_2]$ (**6.4**) and $[Ph_2Sb\{Fe(CO)_2(\eta\text{-}C_5H_5)\}]$ (**6.5**) showed peaks attributable to both compounds and results are listed in Table 6.2

Table 6.2 Major fragments in the EI mass spectrum of a mixture of 6.4 and 6.5

Fragment Ion	**6.4**, m/z (% height)	**6.5**, m/z (% height)
$\{PhSbFe_2Cp_2(CO)_4\}^+$	552 (3)	
$\{PhSbFe_2Cp_2(CO)_3\}^+$	524 (0.5)	
$\{PhSbFe_2Cp_2(CO)_2\}^+$	496 (1)	
$\{PhSbFe_2Cp_2(CO)\}^+$	468 (1)	
$\{Ph_2SbFeCp(CO)_2\}^+$		452 (3)
$\{PhSbFe_2Cp_2\}^+$	440 (3)	
$\{Ph_2SbFeCp\}^+$		396 (18)
$\{Ph_2Sb\}^+$		275 (11)
$\{PhSb\}^+$	198 (22)	198 (22)
$\{CpFe(CO)_2\}^+$	177 (22)	177 (22)
$\{CpFe(CO)\}^+$	149 (21)	149 (21)
$\{CpFe\}^+$	121 (100)	121 (100)
$\{Ph\}^+$	77 (9)	77 (9)
$\{C_2O_2\}^+$	56 (41)	56 (41)

6.2.5 X-Ray Crystallography

Single crystal X-ray structure determinations were carried out for the compounds $[\{\mu\text{-}Ph_2Sb\}_2\{Mo(CO)_2(\eta\text{-}C_5H_5)\}_2].CHCl_3$ (**6.1**) and $[PhSb\{Fe(CO)_2(\eta\text{-}C_5H_5)\}_2]$ (**6.4**). Single crystals were obtained for **6.1** by diffusion of hexane vapour into a concentrated chloroform solution, whereas crystals of **6.4** were obtained by overlayering a tetrahydrofuran solution with hexane. The molecular structure of **6.1** is shown in Figure 6.12 and selected bond lengths and angles are listed in Table 6.3. Further details of the crystal structure determination are given in Appendix Q.

Table 6.3 Selected bond distances and angles, with standard deviations in parentheses for $[\{\mu\text{-}Ph_2Sb\}_2\{Mo(CO)_2(\eta\text{-}C_5H_5)\}_2].CHCl_3$ (6.1)

Bond lengths, Å		Bond angles, °	
Sb(1) - Sb(2)	3.0996(8)	Mo(1) - Sb(1) - Mo(2)	104.46(3)
Sb(1) - Mo(1)	2.796(1)	Mo(1) - Sb(1) - C(11)	114.6(3)
Sb(1) - Mo(2)	2.777(1)	Mo(2) - Sb(1) - C(11)	113.9(3)
Sb(1) - C(11)	2.141(9)	Mo(1) - Sb(1) - C(21)	114.4(3)
Sb(1) - C(21)	2.16(1)	Mo(2) - Sb(1) - C(21)	117.5(3)
Sb(2) - Mo(1)	2.774(1)	C(11) - Sb(1) - C(21)	92.3(4)
Sb(2) - Mo(2)	2.760(1)	Mo(1) - Sb(2) - Mo(2)	105.51(3)
Sb(2) - C(31)	2.152(9)	Mo(1) - Sb(2) - C(31)	116.8(3)
Sb(2) - C(41)	2.151(9)	Mo(2) - Sb(2) - C(31)	114.5(3)
Mo(1) - C(1)	1.94(1)	Mo(1) - Sb(2) - C(41)	109.9(3)
Mo(1) - C(2)	1.94(1)	Mo(2) - Sb(2) - C(41)	115.9(3)
Mo(1) - C(51)	2.34(1)	C(31) - Sb(2) - C(41)	94.3(3)
Mo(1) - C(52)	2.29(1)	Sb(1) - Mo(1) - Sb(2)	67.63(2)
Mo(1) - C(53)	2.26(1)	Sb(1) - Mo(1) - C(1)	116.6(3)
Mo(1) - C(54)	2.27(1)	Sb(2) - Mo(1) - C(1)	76.9(3)
Mo(1) - C(55)	2.30(1)	Sb(1) - Mo(1) - C(2)	75.4(3)
Mo(1) - Cp_{cent}	2.00	Sb(2) - Mo(1) - C(2)	114.8(3)
Mo(2) - C(3)	1.96(1)	C(1) - Mo(1) - C(2)	74.4(4)
Mo(2) - C(4)	1.94(1)	Sb(1) - Mo(2) - Sb(2)	68.09(3)
Mo(2) - C(61)	2.29(1)	Sb(1) - Mo(2) - C(3)	79.2(4)
Mo(2) - C(62)	2.31(1)	Sb(2) - Mo(2) - C(3)	121.9(3)
Mo(2) - C(63)	2.36(1)	Sb(1) - Mo(2) - C(4)	122.7(4)
Mo(2) - C(64)	2.36(1)	Sb(2) - Mo(2) - C(4)	79.2(3)
Mo(2) - C(65)	2.32(1)	C(3) - Mo(2) - C(4)	80.2(5)
Mo(2) - Cp_{cent}	2.00	Mo(1) - C(1) - O(1)	176.0(9)
O(1) - C(1)	1.17(1)	Mo(1) - C(2) - O(2)	175.0(10)
O(2) - C(2)	1.15(1)	Mo(2) - C(3) - O(3)	176.6(11)
O(3) - C(3)	1.15(1)	Mo(2) - C(4) - O(4)	178.2(11)
O(4) - C(4)	1.17(1)		

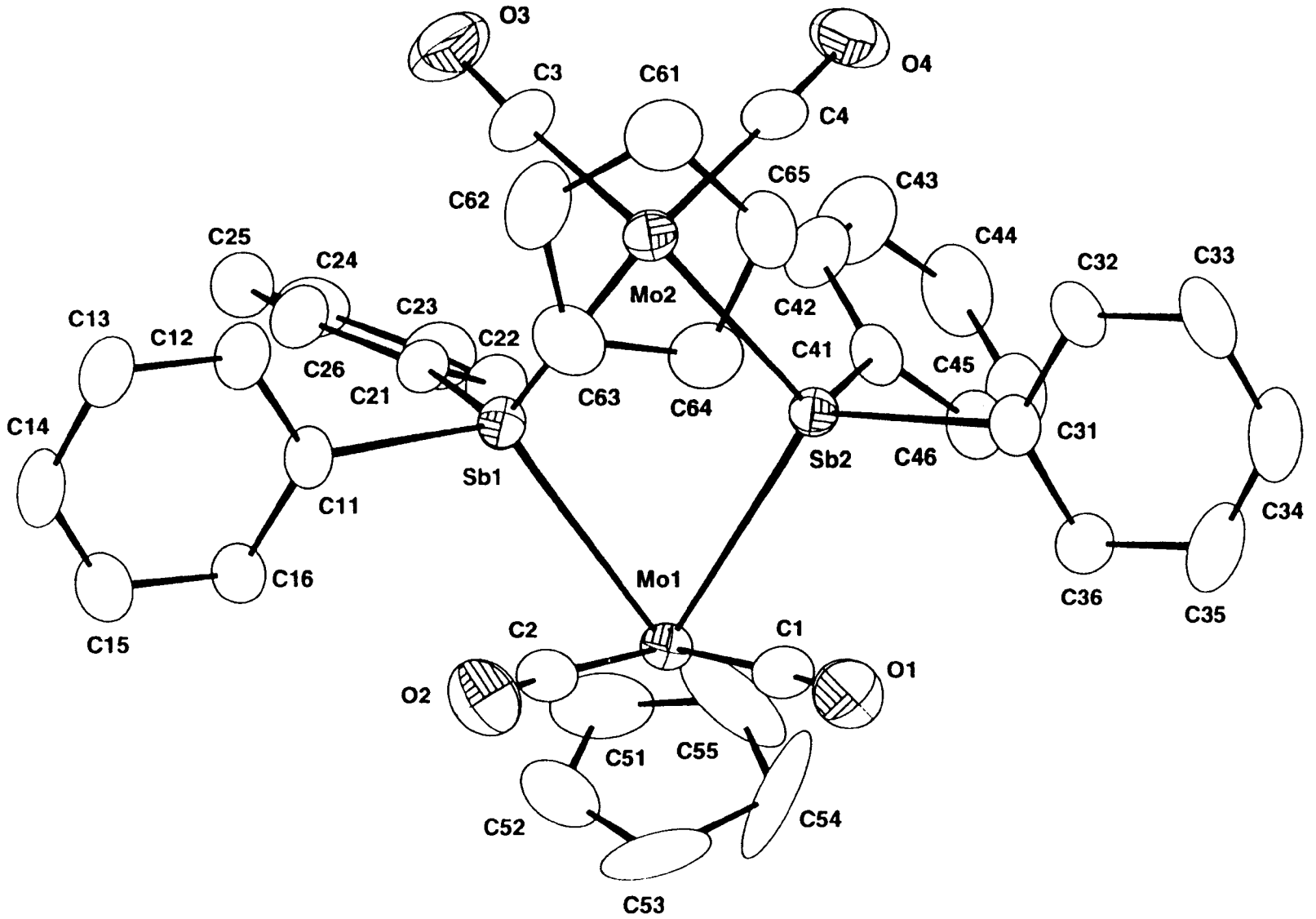

Figure 6.12 Molecular structure of $[\{\mu\text{-}Ph_2Sb\}_2\{Mo(CO)_2(\eta\text{-}C_5H_5)\}_2]$

The crystal structure of the chloroform solvate of **6.1**, consists of two 15-electron $Mo(CO)_2(\eta\text{-}C_5H_5)$ fragments, bridged by two diphenylstibane groups. Coordination about the two antimony atoms is best described as distorted tetrahedral, with angles between 104.46(3) [Mo(1)–Sb(1)–Mo(2)] and 117.5(3)° [Mo(2)–Sb(1)–C(21)].

Bond lengths to the phenyl *ipso* carbons [2.141(9) to 2.16(1) Å] are comparable to those in related structures, but the Sb–Mo bonds are short. The Sb(2)–Mo(2) bond is the shortest at 2.760(1) Å and indeed is one of the shortest Sb–Mo bonds reported for this class of compound. The Sb–Mo bonds in the stibine complex $[Mo(CO)_3\{Ph_2(PhS)Sb\}_3]$ (mean, 2.746 Å)[43], however, are slightly shorter and the shortest Sb–Mo bond separations in the compounds $[Mo(CO)_2(\eta\text{-}C_5H_5)]_2(\mu,\eta^2\text{-}Sb_2)$[32] and $[(\mu\text{-}Sb)_2Mo_5(CO)_{14}(\eta\text{-}C_5H_5)_4]$[23] are very similar (2.762 and 2.764 Å respectively) to the Sb(2)–Mo(2) bond reported here. The shortness of the Sb–Mo bonds is a likely consequence of some degree of multiple bonding, with the diphenylstibido groups each acting as three-electron donors to the two neighbouring molybdenum atoms.

In addition to the two bonds to antimony, each molybdenum atom is further ligated by an η^5-cyclopentadienyl group and two carbonyl ligands, giving an overall '4-legged piano-stool' geometry. Bond lengths to the carbonyl carbons (1.94(1) to 1.96(1) Å) and the cyclopentadienyl centroids (2.00 Å) are unexceptional and are comparable with those in related compounds; for example, the $Mo\text{–}Cp_{centroid}$ bond in $[Mo(CO)_2(\eta\text{-}C_5H_5)]_2(\mu,\eta^2\text{-}Sb_2)$ is 2.03 Å.

The Sb_2Mo_2 skeleton is best described as a 'butterfly' type structure. This is clearly illustrated in the view along the Sb(1)–Sb(2) vector (Figure 6.13), which also shows the *trans* arrangement of the two cyclopentadienyl groups.

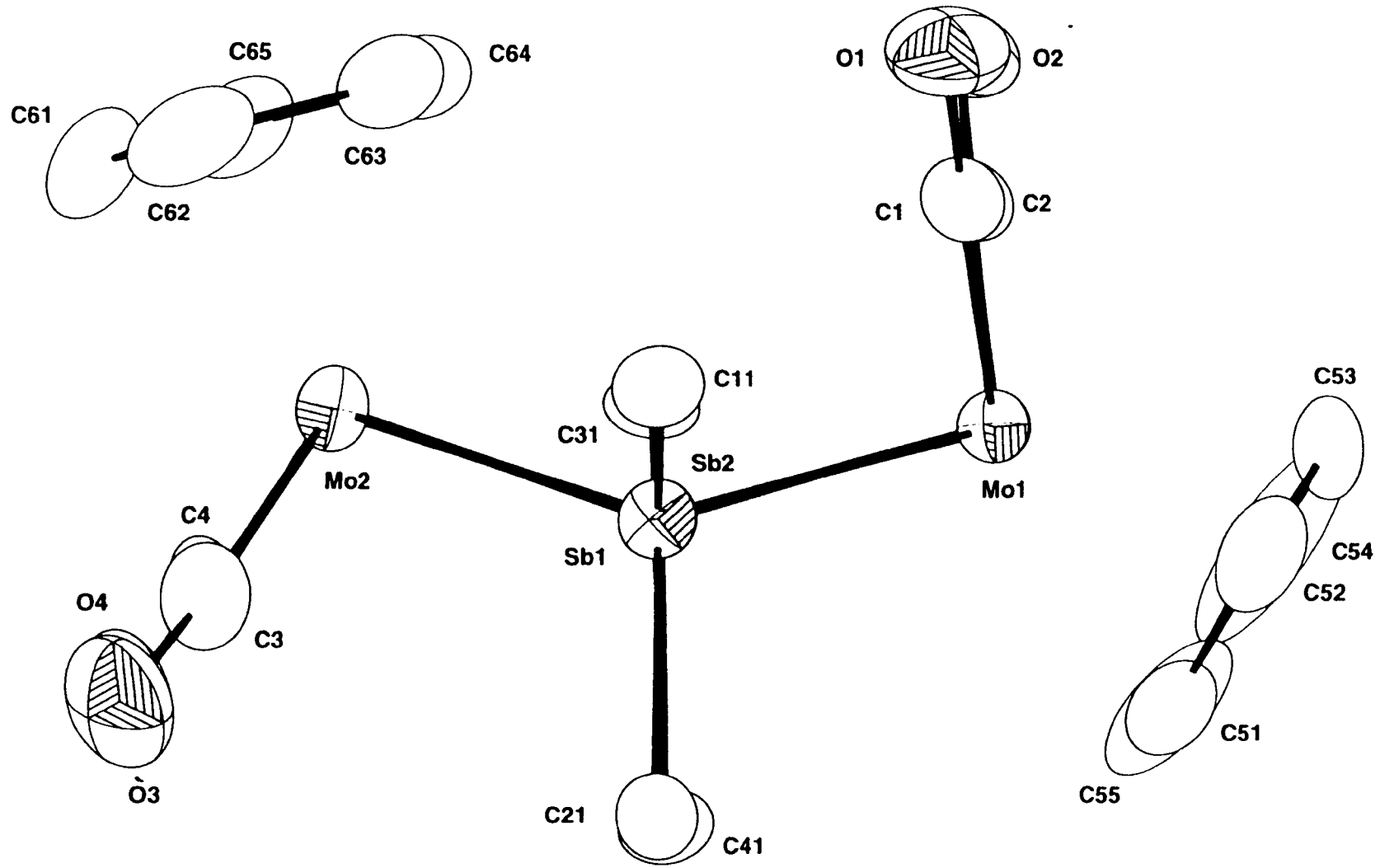

Figure 6.13 Molecular structure of $[\{\mu\text{-}Ph_2Sb\}_2\{Mo(CO)_2(\eta\text{-}C_5H_5)\}_2]$ viewed along the Sb–Sb vector

The Mo(1)–Mo(2) separation of 4.405(1) Å precludes any type of bonding interaction between these atoms, but there is a short separation (3.0996(8) Å) between the antimony atoms. This 'interaction' is almost in the realms of being classed as a formal bond, with typical Sb–Sb single bonds falling in the region of 2.85 Å (eg. 2.837 Å in *cyclo*$(PhSb)_6$[44] and 2.867 Å in $[(Me_3Si)_2Sb]_2$[45]). For comparison, the van de Waals separation is 4.4 Å. Whether this short separation is simply due to the constraints imposed by the Sb_2Mo_2 ring, or a 'real' interaction is a matter of discussion; it is however, comparable with the Sb···Sb separation found for $[(\mu\text{-}Sb)_2Mo_5(CO)_{14}(\eta\text{-}C_5H_5)_4]$[23] (3.050 Å).

In many respects, the structure of **6.1** is similar to that found for $Cu_2(PMe)_4[\mu\text{-}(mesityl)_2Sb]_2$[9], with both compounds containing diarylstibane groups bridging between 15-electron transition metal fragments. The near tetrahedral coordination geometry about antimony in both compounds is also similar, but the ML_n–Sb–ML_n angle in **6.1** (mean, 104.99°) is considerably more 'open' in comparison with that found in $Cu_2(PMe_3)_4[\mu\text{-}(mesityl)_2Sb]_2$, (mean, 95.11°). The smaller angle for $Cu_2(PMe_3)_4[\mu\text{-}(mesityl)_2Sb]_2$ is probably associated with the steric requirements of the mesityl groups.

The molecular structure of **6.4** is shown in Figure 6.14 and selected bond lengths and angles are listed in Table 6.4. Further details of the crystal structure determination are given in Appendix R.

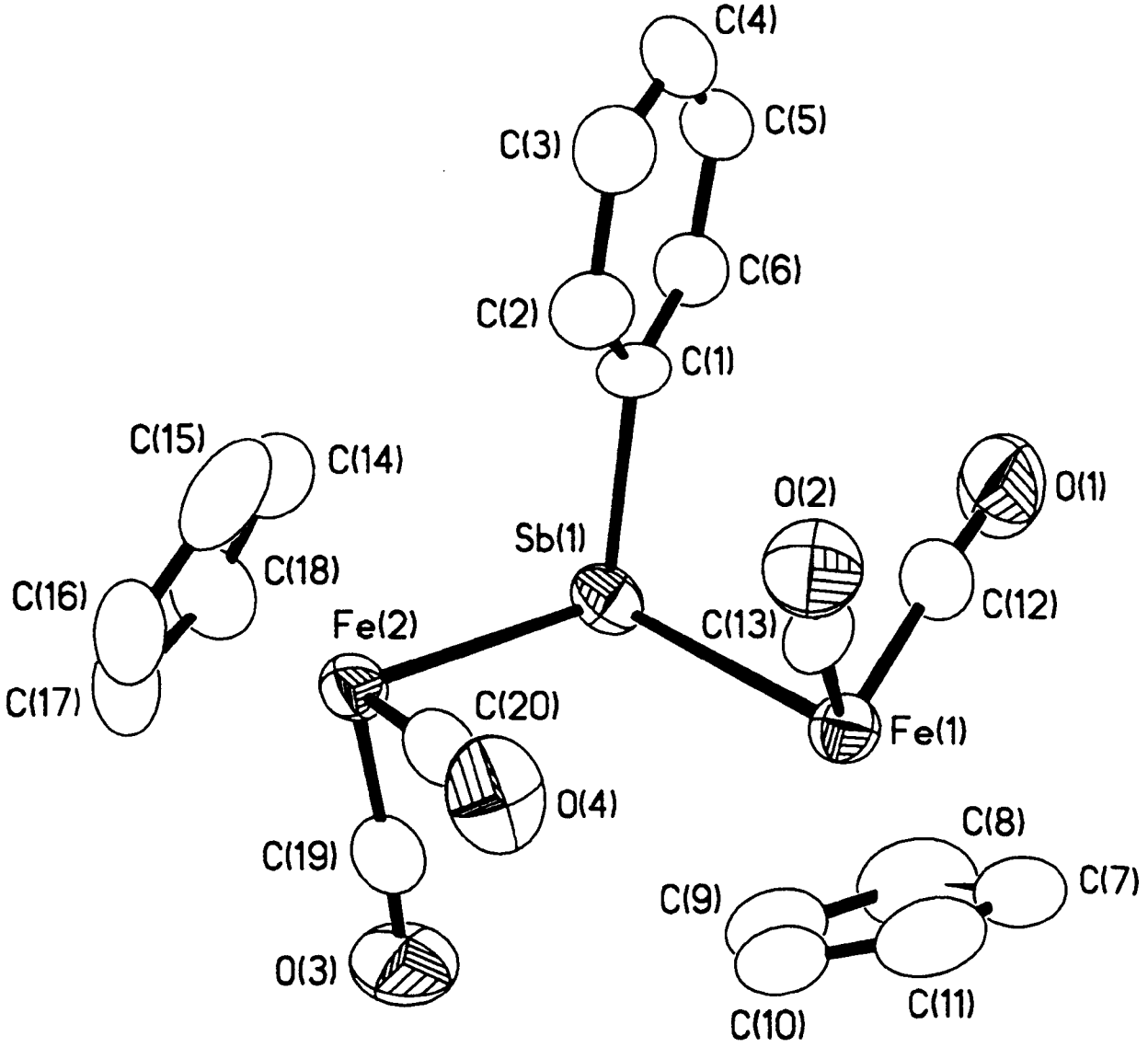

Figure 6.14 Molecular structure of $[PhSb\{Fe(CO)_2(\eta\text{-}C_5H_5)\}_2]$ (6.4)

Table 6.4 Selected bond distances and angles, with standard deviations in parentheses for $[PhSb\{Fe(CO)_2(\eta\text{-}C_5H_5)\}_2]$ (6.4)

Bond lengths, Å		Bond angles, °	
Sb(1) - Fe(1)	2.639(2)	Fe(1) - Sb(1) - Fe(2)	111.96(5)
Sb(1) - Fe(2)	2.634(1)	C(1) - Sb(1) - Fe(1)	98.7(2)
Sb(1) - C(1)	2.177(9)	C(1) - Sb(1) - Fe(2)	102.2(3)
Fe(1) - C(12)	1.74(1)	C(12) - Fe(1) - C(13)	95.1(5)
Fe(1) - C(13)	1.737(8)	C(12) - Fe(1) - Sb(1)	84.8(3)
Fe(1) - C(7)	2.10(1)	C(13) - Fe(1) - Sb(1)	89.9(3)
Fe(1) - C(8)	2.07(1)	C(19) - Fe(2) - C(20)	94.7(4)
Fe(1) - C(9)	2.12(1)	C(19) - Fe(2) - Sb(1)	86.3(3)
Fe(1) - C(10)	2.11(1)	C(20) - Fe(2) - Sb(1)	91.9(3)
Fe(1) - C(11)	2.09(1)	O(1) - C(12) - Fe(1)	176.0(11)
Fe(1) - Cp_{cent}	1.73	O(2) - C(13) - Fe(1)	174.3(8)
Fe(2) - C(19)	1.75(1)	O(3) - C(19) - Fe(2)	177.0(9)
Fe(2) - C(20)	1.75(1)	O(4) - C(20) - Fe(2)	177.0(8)
Fe(2) - C(14)	2.12(1)		
Fe(2) - C(15)	2.10(1)		
Fe(2) - C(16)	2.09(1)		
Fe(2) - C(17)	2.097(9)		
Fe(2) - C(18)	2.08(1)		
Fe(2) - Cp_{cent}	1.73		
O(1) - C(12)	1.15(1)		
O(2) - C(13)	1.140(9)		
O(3) - C(19)	1.16(1)		
O(4) - C(20)	1.14(1)		

The molecular structure of **6.4** consists of a phenylstibinidene fragment bridging between two iron atoms, which in turn are each ligated by a cyclopentadienyl group and two carbonyl groups.

Coordination about antimony is pyramidal, with angles ranging between 98.7(2) [C(1)–Sb(1)–Fe(1)] and 111.96(5)° [Fe(1)–Sb(1)–Fe(2)]. The sum of the angles about antimony is 312.86° and the pyramid is therefore slightly more contracted than that in $[Sb\{Fe(CO)_2(\eta\text{-}C_5H_5)\}_3]$[11], where the sum is 330.9°. The Sb–Fe bond lengths are effectively identical (mean Sb–Fe, 2.637 Å) and are comparable with those in related compounds, such as $[Sb\{Fe(CO)_2(\eta\text{-}C_5H_5)\}_3]$ (mean Sb–Fe, 2.652 Å) and $[SbCl\{Fe(CO)_2(\eta\text{-}C_5H_5)\}_3]_2[FeCl_4]$ (mean Sb–Fe, 2.539 Å)[46], containing covalent Sb–Fe bonds.

The overall geometry about the iron atoms is the familiar $CpML_3$ 'three-legged piano-stool' type. Bond lengths from iron to the carbonyl carbons are identical within experimental error, lying in the range 1.737(8) [Fe(1)–C(13)] to 1.75(1) Å [Fe(2)–C(19) and Fe(2)–C(20)], as are the distances from iron to the η^5-cyclopentadienyl centroids (1.73 Å). The two cyclopentadienyl rings are arranged in a *trans*-like configuration, both facing away from the antimony atom in an arrangement similar to that for the related compound $[SbCl\{Mo(CO)_3(\eta\text{-}C_5H_5)\}_2]$[11].

The plane of the phenyl group is almost orthogonal to the Sb(1)–Fe(1) bond, with a C(2)–C(1)–Sb(1)–Fe(1) torsion angle of -81.0(8)°. The corresponding C(2)–C(1)–Sb(1)–Fe(2) torsion angle is 33.9(9)°.

SUMMARY

Reaction between $[Ph_2SbBrO]_2$ (**2.12**) and two equivalents of $Na[Mo(CO)_3(\eta\text{-}C_5H_5)]$ does not give the expected simple metathesis product $[Ph_2Sb\{Mo(CO)_3(\eta\text{-}C_5H_5)\}O]_2$, but instead an unusual antimony reduction compound, $[\{\mu\text{-}Ph_2Sb\}_2\{Mo(CO)_2(\eta\text{-}C_5H_5)\}_2]$ (**6.1**) has been isolated. A structure determination of **6.1** showed it to possess a 'butterfly'-like configuration, when viewed along the short Sb···Sb vector. Solution infrared and NMR spectroscopy pointed to the presence of two isomeric forms in the polar solvents, CH_2Cl_2 and $CDCl_3$; this was in contrast to the observation of only a single isomer in C_6D_6 solution.

In an attempt to employ a more direct approach to the preparation of antimony(III) complexes, further reactions were carried out between the antimony(III) substrate, Ph_2SbCl and the transition metal salts, $Na[Mo(CO)_3(\eta\text{-}C_5H_5)]$, $Na[W(CO)_3(\eta\text{-}C_5H_5)]$ and $Na[Fe(CO)_2(\eta\text{-}C_5H_5)]$. These reactions were non-straightforward and in each case afforded a mixture of products, albeit that spectroscopic results were consistent with the presence of the expected products $[Ph_2Sb\{Mo(CO)_3(\eta\text{-}C_5H_5)\}]$ (**6.2**), $[Ph_2Sb\{W(CO)_3(\eta\text{-}C_5H_5)\}]$ (**6.3**) and $[Ph_2Sb\{Fe(CO)_2(\eta\text{-}C_5H_5)\}]$ (**6.5**) as major components in the mixtures. In addition to **6.5** a further compound, identified as the phenylstibinidene bridged species $[PhSb\{Fe(CO)_2(\eta\text{-}C_5H_5)\}_2]$ (**6.4**) was

isolated from the reaction between Ph_2SbCl and $Na[Fe(CO)_2(\eta\text{-}C_5H_5)]$. A structure determination of **6.4** showed the presence of monomers with pyramidal coordination about antimony.

6.3 EXPERIMENTAL AND CHARACTERISING DATA

All experiments in this chapter were performed using stringent Schlenk techniques under an argon atmosphere. Further handling of compounds was performed in a dry oxygen-free glovebox.

6.3.1 Preparation of $[\{\mu\text{-}Ph_2Sb\}_2\{Mo(CO)_2(\eta\text{-}C_5H_5)\}_2]$ (6.1)

A solution of sodium cyclopentadienylide (NaCp.0.5THF) (528mg, 4.25mmol) in tetrahydrofuran (THF) (40ml) was added to a solution of molybdenum hexacarbonyl (1.142g, 4.33mmol) in THF (40ml) and the resultant solution was refluxed with stirring for 18 hours (CARE: reaction releases CO and should be vented). After cooling to room temperature, the pale yellow/green solution was added to a stirred slurry of $[Ph_2SbBrO]_2$ (**2.12**) (1.580g, 2.12mmol) in THF (50ml) at -80°C. The reaction mixture was then slowly warmed to room temperature and stirred for a further 24 hours. The mixture was then filtered and the solvent was removed *in vacuo*. The resulting purple solid was then extracted into dichloromethane (50ml), filtered and evaporated to dryness. A low yield of pure, purple crystals of **6.1** was obtained by column chromatography (CH_2Cl_2/hexane 2:5 v/v, Al_2O_3). Yield 250mg (12% with respect to $[Ph_2SbBrO]_2$); mp 259-262(dec.)°C.

Found: C,46.01; H,3.24: $C_{38}H_{30}O_4Mo_2Sb_2$ requires C,46.29; H,3.07 %.

^{1}H NMR (250MHz, C_6D_6, RT) δ 4.90(s, 10H, *Cp*-Mo); 7.23(m, 12H, *m*- and *p*-Ph); 7.76(m, 8H, *o*-Ph).

^{1}H NMR (250MHz, $CDCl_3$, RT) δ 5.16(s, 10H, *Cp*-Mo major isomer); 5.32(s, 10H, *Cp*-Mo minor isomer); 7.32(m, 20H, *Ph*-Sb both isomers).

IR (CH_2Cl_2 solution): 1946(m,sh), 1929(vs), 1866(m,br).

IR (nujol mull, CsI): 1924(vs), 1870(m), 1857(s), 1846(s), 1431(m), 1062(w), 1019(w), 819(w), 736(w), 728(w), 696(w), 556(w), 549(w), 449(w).

MS (FAB): $\{Ph_4Sb_2Mo_2Cp_2(CO)_4\}^+$ (m/z 988, 6%); $\{Ph_4Sb_2Mo_2Cp_2(CO)_2\}^+$ (m/z 932, 7%); $\{Ph_4Sb_2Mo_2Cp_2\}^+$ (m/z 876, 2%); $\{Ph_2SbMo_2Cp_2(CO)_3\}^+$ (m/z 685, 6%); $\{Ph_2SbMoCp(CO)_3\}^+$ (m/z 522, 18%); $\{Ph_2SbMoCp\}^+$ (m/z 438, 14%).

6.3.2 Reaction between Ph_2SbCl and $Na[Mo(CO)_3(\eta\text{-}C_5H_5)]$

A solution of $Na[Mo(CO)_3(\eta\text{-}C_5H_5)]$ prepared *in situ* (as in 6.3.1) from NaCp.0.5THF (914mg, 7.36mmol) and molybdenum hexacarbonyl (1.923g, 7.28mmol) in THF (35ml) was added to a stirred solution of Ph_2SbCl (2.187g, 7.02mmol) in THF (25ml) at -45°C causing an immediate purple colouration. After stirring for a further 24 hours at room temperature, the reaction mixture was filtered through Celite and the solvent was removed *in vacuo* to give a red oily product. The crude material was recrystallised from toluene to give a red powder which was a mixture of compounds, that could not be separated by further recrystallisations. ^1H NMR analysis of the unseparated mixture suggested that the major compound was $[Ph_2Sb\{Mo(CO)_3(\eta\text{-}C_5H_5)\}]$ (**6.2**): (C_6D_6, 250MHz, RT) δ 4.78(s, 5H, *Cp*-Mo); 7.21(m, 6H, *m*- and *p*-Ph); 7.80(m, 4H, *o*-Ph).

6.3.3 Reaction between Ph_2SbCl and $Na[W(CO)_3(\eta\text{-}C_5H_5)]$

A solution of NaCp.0.5THF (897mg, 7.23mmol) in diglyme (40ml) was added to a solution of tungsten hexacarbonyl (2.544g, 7.23mmol) in diglyme (40ml) and the resultant mixture was stirred at reflux for 18 hours. The $Na[W(CO)_3(\eta\text{-}C_5H_5)]$ thus formed was added to a stirred solution of Ph_2SbCl (2.227g, 7.15mmol) in THF (20ml) at -65°C and the mixture slowly warmed to room temperature and stirred for a further 16 hours. After this time insolubles were removed by filtration through Celite and the solvent was removed *in vacuo*. ^1H NMR spectroscopy showed that the remaining material was a mixture of products that could not be purified by subsequent recrystallisations. The major species in the mixture was consistent with the composition $[Ph_2Sb\{W(CO)_3(\eta\text{-}C_5H_5)\}]$ (**6.3**): (C_6D_6, 250MHz, RT) δ 4.66(s, 5H, *Cp*-W); 7.27(m, 6H, *m*- and *p*-Ph); 7.84(d, 4H, $^3J_{HH}$ - 7.5Hz, *o*-Ph).

IR (CH_2Cl_2 solution): 2027(m), 1995(s), 1933(vs,br), 1889(s).

MS (FAB): $\{Ph_2SbWCp(CO)_3\}^+$ (m/z 608, 2%); $\{Ph_2SbWCp(CO)_2\}^+$ (m/z 580, 8%); $\{Ph_2SbWCp\}^+$ (m/z 524, 11%); $\{PhSbWCp(CO)_2\}^+$ (m/z 503, 32%); $\{PhSbWCp\}^+$ (m/z 447, 37%); $\{Ph_2Sb\}^+$ (m/z 275, 53%); $\{PhSb\}^+$ (m/z 198, 18%).

6.3.4 Reaction between Ph_2SbCl and $Na[Fe(CO)_2(\eta\text{-}C_5H_5)]$

A slurry of $[Fe(CO)_2(\eta\text{-}C_5H_5)]_2$ (1.393g, 3.94mmol) and THF (30ml) was added to sodium amalgam (37g, 0.593% w/w, 8.7mmol Na) and the resulting mixture was stirred for 48 hours. After this time the $Na[Fe(CO)_2(\eta\text{-}C_5H_5)]$ thus formed was filtered into a solution of Ph_2SbCl (2.392g, 7.68mmol) in THF (50ml) at -80°C and the mixture stirred at room temperature for 24 hours. Following filtration through Celite, the solvent volume was reduced to *ca.* 10ml and hexane (30ml) was overlayered. After 3 days at -30°C, a quantity of crystalline product was isolated, that was shown spectroscopically to be a mixture of $[PhSb\{Fe(CO)_2(\eta\text{-}C_5H_5)\}_2]$ (**6.4**) and $[Ph_2Sb\{Fe(CO)_2(\eta\text{-}C_5H_5)\}]$ (**6.5**). Attempted separation of the mixture by recrystallisation proved to be unsuccessful and the compounds were characterised as a mixture. Yield 2.03g.

IR (THF solution, **6.4** and **6.5** mixture): 1995(vs), 1977(m), 1946(vs).

$[PhSb\{Fe(CO)_2(\eta\text{-}C_5H_5)\}_2]$ (**6.4**):

^1H NMR (250MHz, C_6D_6, RT) δ 4.35(s, 10H, *Cp*-Fe); 7.27(m, 3H, *m*- and *p*-Ph); 8.19(d, 2H, $^3J_{HH}$ - 6.5Hz, *o*-Ph).

MS (EI): $\{PhSbFe_2Cp_2(CO)_4\}^+$ (m/z 552, 3%); $\{PhSbFe_2Cp_2(CO)_3\}^+$ (m/z 524, 0.5%); $\{PhSbFe_2Cp_2(CO)_2\}^+$ (m/z 496, 1%); $\{PhSbFe_2Cp_2(CO)_3\}^+$ (m/z 468, 1%); $\{PhSbFe_2Cp_2\}^+$ (m/z 440, 3%); $\{PhSb\}^+$ (m/z 198, 22%); $\{CpFe(CO)_2\}^+$ (m/z 177, 22%); $\{CpFe(CO)\}^+$ (m/z 149, 21%); $\{CpFe\}^+$ (m/z 121, 100%); $\{Ph\}^+$ (m/z 77, 9%); $\{C_2O_2\}^+$ (m/z 56, 41%).

$[Ph_2Sb\{Fe(CO)_2(\eta\text{-}C_5H_5)\}]$ (**6.5**):

^1H NMR (250MHz, C_6D_6, RT) δ 4.12(s, 5H, *Cp*-Fe); 7.27(m, 6H, *m*- and *p*-Ph); 7.92(d, 4H, $^3J_{HH}$ - 6.2Hz, *o*-Ph).

MS (EI): $\{Ph_2SbFeCp(CO)_2\}^+$ (m/z 452, 3%); $\{Ph_2SbFeCp\}^+$ (m/z 396, 18%); $\{Ph_2Sb\}^+$ (m/z 275, 11%) and other fragments in common with **6.4**.

6.3.5 Reaction between $[Ph_2SbBrO]_2$ and $Na[Fe(CO)_2(\eta\text{-}C_5H_5)]$

A slurry of $[Fe(CO)_2(\eta\text{-}C_5H_5)]_2$ (466mg, 1.32mmol) and THF (25ml) was added to sodium amalgam (14g, 0.593% w/w, 3.3mmol Na) and the resulting mixture was stirred for 20 hours at room temperature. After this time the resultant $Na[Fe(CO)_2(\eta\text{-}C_5H_5)]$ was filtered into a slurry of $[Ph_2SbBrO]_2$ (**2.12**) (984mg, 1.32mmol) in THF (20ml) at -80°C and the mixture stirred at room temperature for 20 hours. The reaction mixture was then filtered and the solution evaporated to dryness to give a complex mixture of unidentified products.

6.4 REFERENCES

1. K.H.Whitmire, *J. Coord. Chem.*, 1988, **17**, 95.

2. R.F.Bryan, W.C.Schmidt Jr., *J. Chem. Soc., Dalton Trans.*, 1974, 2337.

3. J.v.Seyerl, G. Huttner, *Cryst. Struct. Comm.*, 1980, **9**, 1099.

4. R.E.DesEnfants II, J.A.Gavney Jr., R.K.Hayashi, A.D.Rae, L.F.Dahl, A.Bjarnason, *J. Organomet. Chem.*, 1990, **383**, 543.

5. A.J.Carty, N.J.Taylor, A.W.Coleman, M.F.Lappert, *J. Chem. Soc., Chem. Commun.*, 1979, 639.

6. The naming of R_2Sb–transition metal compounds as 'stibane' complexes is somewhat arbitrary, but has been taken from the naming scheme used in publications from Malisch's group. Perhaps a more suitable name would be diorganostibide (stibido), although this could lead to confusion with Sb^{3-} compounds (stibide or stibido).

7. P.Panster, W.Malisch, *Chem. Ber.*, 1976, **109**, 692.

8. A.-M.Caminade, M.Veith, V.Huch, W.Malisch, *Organometallics*, 1990, **9**, 1798.

9. A.H.Cowley, R.A.Jones, C.M.Nunn, D.L.Westmoreland, *Angew. Chem., Int. Ed. Engl.*, 1989, **28**, 1018.

10. B.F.G.Johnson, J.Lewis, A.J.Whitton, S.G.Bott, *J. Organomet. Chem.*, 1990, **389**, 129.

11. A.M.Barr, M.D.Kerlogue, N.C.Norman, P.M.Webster, L.J.Farrugia, *Polyhedron*, 1989, **8**, 2495.

12. W.Malisch, P.Panster, *Chem. Ber.*, 1975, **108**, 700.

13. U.Weber, L.Zsolnai, G.Huttner, *J. Organomet. Chem.*, 1984, **260**, 281.

14. J.v.Seyerl, G.Huttner, *Angew. Chem., Int. Ed. Engl.*, 1978, **17**, 843.

15. G.Huttner, *Pure & Appl. Chem.*, 1986, **58**, 585.

16. U.Weber, G.Huttner, O.Scheidsteger, L.Zsolnai, *J. Organomet. Chem.* 1985, **289**, 357.

17. B.Sigwarth, U.Weber, L.Zsolnai, G.Huttner, *Chem. Ber.*, 1985, **118**, 3114.

18. A.H.Cowley, N.C.Norman, M.Palulski, D.L.Bricker, D.H.Russell, *J. Am. Chem. Soc.*, 1985, **107**, 8211.

19. G.Huttner, U.Weber, B.Sigwarth, O.Scheidsteger, *Angew. Chem., Int. Ed. Engl.*, 1982, **21**, 215.

20. S.Luo, K.H.Whitmire, *Inorg. Chem.*, 1989, **28**, 1424.

21. N.C.Norman, N.L.Pickett, W.D.Storr, N.M.Boag, A.J.Goodby, *Polyhedron*, 1994, **13**, 2525.

22. N.A.Compton, R.J.Errington, G.A.Fisher, N.C.Norman, P.M.Webster, P.S.Jarrett, S.J.Nichols, A.G.Orpen, S.E.Stratford, *J. Chem. Soc., Dalton Trans.*, 1991, 669.

23. M.Gorzellik, B.Nuber, M.L.Ziegler, *J. Organomet. Chem.*, 1992, **431**, 171.

24. J.S.Leigh, K.H.Whitmire, K.A.Yee, T.A.Albright, *J. Am. Chem. Soc.*, 1989, **111**, 2726.

25. T.A.Albright, K.A.Yee, J.-Y.Saillard, S.Kahlal, J.-F.Halet, J.S.Leigh, K.H.Whitmire, *Inorg. Chem.*, 1991, **30**, 1179.

26. W.Clegg, N.A.Compton, R.J.Errington, D.C.R.Hockless, N.C.Norman, M.Ramshaw, P.M.Webster, *J. Chem. Soc., Dalton Trans.*, 1990, 2375.

27. S.Luo, K.H.Whitmire, *J. Organomet. Chem.*, 1989, **376**, 297.

28. A.L.Rheingold, S.J.Geib, M.Shieh, K.H.Whitmire, *Inorg. Chem.*, 1987, **26**, 463,

29. K.H.Whitmire, M.Shieh, J.Cassidy, *Inorg. Chem.*, 1989, **28**, 3164.

30. J.L.Vidal, J.M.Troup, *J. Organomet. Chem.*, 1981, **213**, 351.

31. C.Caballero, B.Nuber, M.L.Ziegler, *J. Organomet. Chem.*, 1990, **386**, 209.

32. J.R.Harper, A.L.Rheingold, *J. Organomet. Chem.*, 1990, **390**, C36.

33. F.Bringewski, G.Huttner, W.Imhof, *J. Organomet. Chem.*, 1993, **448**, C3.

34. F.P.Arnold Jr., D.P.Ridge, A,L.Rheingold, *J. Am. Chem. Soc.*, 1995, **117**, 4427.

35. W.Malisch, H.-A.Kaul, E.Gross, U.Thewalt, *Angew. Chem., Int. Ed. Engl.*, 1982, **21**, 549.

36. Y.Yamamoto, M.Okazaki, Y.Makisaka, K.-Y.Akiba, *Organometallics*, 1995, **14**, 3364.

37. W.Clegg, N.A.Compton, R.J.Errington, D.C.R.Hockless, N.C.Norman, M.Ramshaw, P.M.Webster, *J. Chem. Soc., Dalton Trans.*, 1990, 2375.

38. W.Malisch, M.Kuhn, W.Albert, H.Rossner, *Chem. Ber.*, 1980, **113**, 3318.

39. P.Panster, W.Malisch, *Chem. Ber.*, 1976, **109**, 3842.

40. W.Malisch, H.Rossner, K.Keller, R.Janta, *J. Organomet. Chem.*, 1977, **133**, C21.

41. R.Schemm, W.Malisch, *J. Organomet. Chem.*, 1985, **288**, C9.

42. W.Clegg, N.A.Compton, R.J.Errington, N.C.Norman, *Polyhedron*, 1988, 7, 2239.

43. M.Wieber, H.Hohl, C.Burschka, *Z. Anorg. Allg. Chem.*, 1990, **583**, 113.

44. H.J.Breunig, K.Häberle, M.Dräger, T.Severengiz, *Angew. Chem., Int. Ed. Engl.*, 1985, **24**, 72.

45. G.Becker, H.Freudenblu, C.Witthauer, *Z. Anorg. Allg. Chem.*, 1982, **492**, 37.

46. Trinh-toan, L.F.Dahl, *J. Am. Chem. Soc.*, 1971, **93**, 2654.

APPENDIX A

Table A.1 Data collection and processing parameters for $[(p\text{-}MeC_6H_4)_3SbBr]_2O$ (2.8)

Chemical formula	$C_{42}H_{42}Br_2OSb_2$
Formula weight	966.08
Crystal size/mm	0.36 x 0.32 x 0.28
Crystal system	Trigonal - hexagonal axis
Space group	$R\bar{3}$
a / Å	13.1564(14)
c / Å	19.506(3)
α / °	90
β / °	90
γ / °	120
Volume / Å^3	2923.9(6)
Z	3
D_c/gcm^{-3}	1.646
Radiation (λ / Å)	Mo-K_α (0.71069)
μ / cm^{-1}	34.66
F(000)	1422
2θ limits / °	4.14 to 49.92
Index ranges	-14<=h<=12, -11<=k<=14, -21<=l<= 22
Temperature / K	150
Total data collected	3461
Unique data	1033 [(R(int) = 0.0936]
Absorption correction	None
Structure solution	Patterson (SHELXS-86)[1]
Refinement procedure	Full matrix-LS on F^2
Number of data / variables	1022 / 74
Goodness-of-fit on F^2	1.073
Max/min peaks in final diff. map / e Å^3	+1.348, -0.724
R observed data [$I > 2\sigma(I)$], (all data)	0.0308, (0.0343)
R_w observed data, (all data)	0.0668, (0.0747)

Table A.2 Atomic coordinates (x 10^4) and equivalent isotropic displacement parameters ($Å^2$ x 10^3) with estimated standard deviations in parentheses for $[(p\text{-}MeC_6H_4)_3SbBr]_2O$ (2.8)

Atom	x	y	z	U(eq)
Br(1)	6667	3333	5937(1)	39(1)
Sb(1)	6667	3333	7332(1)	18(1)
O(1)	6667	3333	8333	22(1)
C(1)	6175(3)	4639(3)	7321(1)	20(1)
C(2)	5324(3)	4536(3)	7785(2)	22(1)
C(3)	5095(3)	5450(3)	7859(2)	26(1)
C(4)	5726(3)	6491(3)	7495(2)	31(1)
C(5)	6571(3)	6570(3)	7033(2)	36(1)
C(6)	6784(3)	5654(3)	6937(2)	30(1)
C(7)	5483(4)	7491(4)	7589(2)	53(1)

Table A.3 Calculated hydrogen coordinates (x 10^4) and isotropic displacement parameters ($Å^2$ x 10^3) with estimated standard deviations in parentheses for $[(p\text{-}MeC_6H_4)_3SbBr]_2O$ (2.8)

Atom	x	y	z	U(iso)
H(2)	4901(3)	3841(3)	8049(2)	27
H(3)	4496(3)	5364(3)	8166(2)	32
H(5)	7012(3)	7273(3)	6777(2)	44
H(6)	7346(3)	5719(3)	6608(2)	36
H(7A)	5016(22)	7508(15)	7202(8)	79
H(7B)	6227(4)	8235(5)	7610(15)	79
H(7C)	5047(23)	7378(14)	8016(8)	79

Table A.4 Anisotropic thermal parameters ($Å^2$ x 10^3) with estimated standard deviations in parentheses for $[(p\text{-}MeC_6H_4)_3SbBr]_2O$ (2.8)

Atom	U11	U22	U33	U23	U13	U12
Br(1)	51(1)	51(1)	15(1)	0	0	26(1)
Sb(1)	19(1)	19(1)	16(1)	0	0	10(1)
O(1)	12(2)	12(2)	44(3)	0	0	6(1)
C(1)	19(2)	21(2)	20(1)	2(1)	-5(1)	10(1)
C(2)	22(2)	23(2)	22(2)	3(1)	-1(1)	11(1)
C(3)	23(2)	34(2)	30(2)	2(2)	-1(1)	19(2)
C(4)	36(2)	28(2)	35(2)	4(2)	-4(2)	20(2)
C(5)	40(2)	28(2)	42(2)	18(2)	10(2)	17(2)
C(6)	33(2)	29(2)	28(2)	9(1)	8(2)	16(2)
C(7)	67(3)	38(2)	69(3)	14(2)	12(2)	38(2)

Table A.5 Bond lengths (Å) with estimated standard deviations in parentheses for [(*p*-$MeC_6H_4)_3SbBr]_2O$ (2.8)

Br(1)-Sb(1)	2.7203(7)
Sb(1)-O(1)	1.9535(4)
Sb(1)-C(1)#1	2.117(3)
Sb(1)-C(1)#2	2.117(3)
Sb(1)-C(1)	2.117(3)
O(1)-Sb(1)#3	1.9534(4)
C(1)-C(6)	1.385(4)
C(1)-C(2)	1.392(4)
C(2)-C(3)	1.386(4)
C(3)-C(4)	1.390(5)
C(4)-C(5)	1.395(5)
C(4)-C(7)	1.513(5)
C(5)-C(6)	1.379(5)

Table A.6 Bond angles (°) with estimated standard deviations in parentheses for [(*p*-$MeC_6H_4)_3SbBr]_2O$ (2.8)

O(1)-Sb(1)-C(1)#1	90.55(8)
O(1)-Sb(1)-C(1)#2	90.55(7)
C(1)#1-Sb(1)-C(1)#2	119.994(3)
O(1)-Sb(1)-C(1)	90.55(8)
C(1)#1-Sb(1)-C(1)	119.990(2)
C(1)#2-Sb(1)-C(1)	119.988(3)
O(1)-Sb(1)-Br(1)	180.0
C(1)#1-Sb(1)-Br(1)	89.45(7)
C(1)#2-Sb(1)-Br(1)	89.45(8)
C(1)-Sb(1)-Br(1)	89.44(8)
Sb(1)-O(1)-Sb(1)#3	180.0
C(6)-C(1)-C(2)	119.7(3)
C(6)-C(1)-Sb(1)	121.6(2)
C(2)-C(1)-Sb(1)	118.2(2)
C(3)-C(2)-C(1)	119.8(3)
C(2)-C(3)-C(4)	121.3(3)
C(3)-C(4)-C(5)	117.7(3)
C(3)-C(4)-C(7)	120.9(3)
C(5)-C(4)-C(7)	121.4(3)
C(6)-C(5)-C(4)	121.6(3)
C(5)-C(6)-C(1)	119.8(3)

Symmetry transformations used to generate equivalent atoms:

#1 -x+y+1,-x+1,z #2 -y+1,x-y,z #3 -x+4/3,-y+2/3,-z+5/3

Experimental Details

Slightly more than one hemisphere of data were collected on a Delft Instruments FAST TV area detector, equipped with a rotating anode FR591 generator. The data were corrected for Lorentz and polarisation effects, merged and systematically absent reflections were rejected. The Sb atom position was located from a Patterson synthesis and subsequent Fourier difference syntheses revealed the positions of all the other non-hydrogen atoms. Refinement was carried out against all F_o^2 data by full matrix procedures (SHELXL-93)[2]. Hydrogen atoms were placed in estimated positions [C–H = 0.95 (aromatic ring hydrogens), 0.98 (methyl group) Å], with fixed isotropic parameters (1.2 x equivalent isotropic temperature factors of the carbon atom to which they were bonded for aryl protons and 1.5 x for methyl protons) and refined 'riding' their respective carbon atoms. A standard weighting scheme was applied and the data were corrected for isotropic extinction. All crystallographic calculations were performed using the SHELXS-86[1] and SHELXL-93[2] programs and neutral atom scattering factors were taken from the usual sources[3].

APPENDIX B

Table B.1 Data collection and processing parameters for [(*o*-$MeC_6H_4)_3SbBr]_2O.0.5C_6H_{14}$ ($2.9.0.5C_6H_{14}$)

Chemical formula	$C_{45}H_{49}Br_2OSb_2$
Formula weight	1009.16
Crystal size/mm	0.31 x 0.27 x 0.21
Crystal system	Triclinic
Space group	$P\bar{1}$
a / Å	12.100(8)
b / Å	19.622(12)
c / Å	19.623(9)
α / °	112.17(4)
β / °	94.68(5)
γ / °	107.44(5)
Volume / Å^3	4015(4)
Z	4
D_c/gcm^{-3}	1.669
Radiation (λ / Å)	Mo-K_α (0.71069)
μ / cm^{-1}	33.69
F(000)	1996
2θ limits / °	5.00 to 45.00
Index ranges	-13<=h<=12, -21<=k<=19, 0<=l<= 21
Temperature / K	150
Total unique data collected	10452
Absorption correction	Numerical (min = 0.666, max = 0.721)
Structure solution	Direct (SHELXS-86)[1]
Refinement procedure	Full matrix-LS on F^2
Number of data / variables	10409 / 910
Goodness-of-fit on F^2	1.016
Max/min peaks in final diff. map / e Å^{-3}	+1.32, -1.24
R observed data [$I > 2\sigma(I)$], (all data)	0.0602, (0.1114)
R_w observed data, (all data)	0.1277, (0.1565)

Table B.2 Atomic coordinates (x 10^4) and equivalent isotropic displacement parameters ($Å^2$ x 10^3) with estimated standard deviations in parentheses for $[(o\text{-}MeC_6H_4)_3SbBr]_2O.0.5C_6H_{14}$ ($2.9.0.5C_6H_{14}$)

Atom	x	y	z	U(eq)
Sb(1)	-268(1)	-2708(1)	6516(1)	27(1)
Br(1)	1445(1)	-3042(1)	5750(1)	52(1)
O(1)	-1477(3)	-2467(2)	7077(2)	38(1)
Sb(2)	-2313(1)	-1872(1)	7738(1)	25(1)
Br(2)	-3556(1)	-1104(1)	8642(1)	56(1)
O(2)	5870(3)	2350(2)	7964(2)	41(1)
Sb(3)	4483(1)	2121(1)	7223(1)	25(1)
Br(3)	2472(1)	1835(1)	6249(1)	55(1)
Sb(4)	7352(1)	2494(1)	8584(1)	24(1)
Br(4)	9409(1)	2632(1)	9434(1)	42(1)
C(11)	156(2)	-1703(2)	6283(2)	38(2)
C(12)	570(2)	-986(2)	6922(3)	42(2)
C(13)	811(3)	-287(3)	6856(3)	52(2)
C(14)	638(5)	-304(3)	6149(3)	57(2)
C(15)	229(5)	-1002(3)	5512(3)	50(2)
C(16)	-20(4)	-1720(3)	5565(3)	36(2)
C(17)	-453(5)	-2448(4)	4850(3)	60(3)
C(21)	-1562(3)	-3810(2)	5728(1)	44(2)
C(22)	-2568(3)	-3718(3)	5404(1)	73(2)
C(23)	-3520(4)	-4354(3)	4923(2)	112(3)
C(24)	-3446(6)	-5075(3)	4772(4)	116(3)
C(25)	-2524(6)	-5223(3)	5045(3)	85(3)
C(26)	-1537(5)	-4558(3)	5564(3)	70(3)
C(27)	-559(6)	-4683(5)	5872(4)	105(5)
C(31)	827(2)	-2618(2)	7464(2)	43(2)
C(32)	1978(3)	-2061(2)	7691(2)	64(2)
C(33)	2732(4)	-1913(3)	8344(3)	109(3)
C(34)	2286(6)	-2335(4)	8746(3)	119(3)
C(35)	1179(6)	-2882(3)	8545(3)	96(3)
C(36)	407(5)	-3038(3)	7882(3)	62(2)
C(37)	-758(6)	-3630(4)	7713(5)	79(3)
C(41)	-3355(3)	-1902(1)	6802(2)	27(2)
C(42)	-2691(3)	-1584(1)	6372(2)	37(2)
C(43)	-3242(4)	-1607(2)	5723(3)	40(2)
C(44)	-4454(4)	-1944(3)	5496(3)	44(2)
C(45)	-5126(4)	-2265(3)	5907(3)	48(2)
C(46)	-4597(4)	-2245(3)	6579(3)	40(2)
C(47)	-5378(5)	-2615(3)	6990(3)	56(3)
C(51)	-2818(2)	-2702(2)	8209(2)	33(2)
C(52)	-2414(2)	-2366(2)	8999(2)	41(2)
C(53)	-2586(3)	-2823(3)	9387(3)	56(2)
C(54)	-3178(5)	-3630(3)	8979(3)	63(2)
C(55)	-3576(6)	-3962(3)	8220(3)	71(3)
C(56)	-3396(5)	-3506(3)	7810(3)	51(2)
C(57)	-3828(6)	-3895(4)	6982(4)	70(3)
C(61)	-727(3)	-911(3)	8427(1)	42(2)
C(62)	51(3)	-1138(3)	8809(1)	54(2)
C(63)	1088(4)	-583(3)	9286(2)	70(2)
C(64)	1336(5)	188(3)	9380(3)	81(3)
C(65)	617(5)	426(3)	9020(3)	69(3)

C(66)	-455(5)	-141(3)	8529(3)	58(2)
C(67)	-1216(6)	129(4)	8155(3)	64(3)
C(71)	5564(3)	2596(3)	6602(2)	42(2)
C(72)	6423(3)	2237(3)	6397(2)	57(2)
C(73)	7275(4)	2548(3)	6069(2)	85(2)
C(74)	7273(5)	3193(3)	5948(3)	96(2)
C(75)	6469(5)	3552(3)	6145(3)	91(2)
C(76)	5576(5)	3236(3)	6478(3)	66(2)
C(77)	4758(6)	3640(4)	6651(4)	83(3)
C(81)	3932(3)	2919(2)	8108(2)	39(2)
C(82)	4759(3)	3705(2)	8412(2)	49(2)
C(83)	4509(4)	4283(2)	8962(2)	57(2)
C(84)	3471(5)	4079(3)	9191(3)	58(2)
C(85)	2656(5)	3329(3)	8912(3)	53(2)
C(86)	2891(4)	2732(3)	8343(3)	50(2)
C(87)	2066(6)	1938(3)	8058(4)	62(3)
C(91)	3986(2)	882(3)	6907(3)	61(2)
C(92)	3975(2)	733(3)	7585(3)	68(2)
C(93)	3804(3)	-12(3)	7485(3)	99(3)
C(94)	3639(5)	-574(3)	6758(3)	89(3)
C(95)	3644(5)	-474(3)	6118(4)	90(3)
C(96)	3845(5)	324(3)	6216(3)	80(2)
C(97)	3880(7)	587(6)	5639(5)	49(4)
C(97')	3807(7)	243(10)	5478(6)	121(8)
C(101)	7830(3)	1757(2)	7652(2)	34(2)
C(102)	7015(3)	980(2)	7320(2)	49(2)
C(103)	7204(4)	426(2)	6707(2)	57(2)
C(104)	8198(5)	648(3)	6431(3)	67(2)
C(105)	9014(5)	1392(3)	6740(3)	62(2)
C(106)	8833(4)	1970(3)	7369(3)	52(2)
C(107)	9677(6)	2766(4)	7682(4)	62(3)
C(111)	7944(2)	3728(2)	8911(3)	35(2)
C(112)	7944(2)	3926(2)	8297(3)	50(2)
C(113)	8262(3)	4692(3)	8406(3)	60(2)
C(114)	8591(5)	5262(3)	9149(3)	61(2)
C(115)	8605(4)	5097(3)	9756(3)	53(2)
C(116)	8275(4)	4303(3)	9651(3)	46(2)
C(117)	8257(5)	4129(4)	10307(3)	51(3)
C(121)	6414(3)	1920(3)	9217(2)	41(2)
C(122)	6605(3)	1217(3)	9147(2)	55(2)
C(123)	5925(4)	749(3)	9437(2)	80(2)
C(124)	5072(5)	983(3)	9780(3)	77(2)
C(125)	4872(5)	1652(3)	9872(3)	57(2)
C(126)	5553(5)	2139(3)	9579(3)	52(2)
C(127)	5321(6)	2839(3)	9673(4)	56(3)
C(1S)	7514(12)	5742(8)	2994(8)	53(4)
C(2S)	8191(18)	5268(11)	3276(12)	99(7)
C(3S)	7633(7)	4245(4)	2725(5)	66(3)
C(4S)	6619(16)	4327(10)	2037(10)	82(6)
C(1S')	7392(14)	5464(9)	2384(9)	66(5)
C(2S')	7749(11)	4903(7)	3475(7)	37(3)
C(4S')	6722(21)	4046(14)	2084(14)	122(9)
C(5S)	9269(7)	5238(5)	2538(5)	82(3)
C(6S)	9613(11)	5667(6)	3191(6)	115(5)

Table B.3 Calculated hydrogen coordinates (x 10^4) and isotropic displacement parameters ($Å^2$ x 10^3) with estimated standard deviations in parentheses for $[(o\text{-}MeC_6H_4)_3SbBr]_2O.0.5C_6H_{14}$ ($2.9.0.5C_6H_{14}$)

Atom	x	y	z	U(iso)
H(12A)	687(2)	-981(2)	7409(3)	51
H(13A)	1093(3)	201(3)	7292(3)	62
H(14A)	806(5)	177(3)	6099(3)	68
H(15A)	113(5)	-996(3)	5030(3)	61
H(17A)	-125(35)	-2332(8)	4449(7)	90
H(17B)	-1322(6)	-2640(17)	4711(15)	90
H(17C)	-198(37)	-2852(10)	4917(9)	90
H(22A)	-2577(3)	-3203(3)	5525(1)	88
H(23A)	-4200(4)	-4299(3)	4704(2)	134
H(24A)	-4114(6)	-5520(3)	4440(4)	139
H(25A)	-2534(6)	-5746(3)	4897(3)	103
H(27A)	-552(40)	-5200(20)	5542(23)	157
H(27B)	-626(36)	-4664(46)	6373(19)	157
H(27C)	179(7)	-4271(27)	5916(41)	157
H(32A)	2247(3)	-1782(2)	7397(2)	77
H(33A)	3519(4)	-1537(3)	8506(3)	131
H(34A)	2791(6)	-2236(4)	9196(3)	142
H(35A)	926(6)	-3156(3)	8847(3)	116
H(37A)	-1091(23)	-3514(20)	8165(10)	118
H(37B)	-692(9)	-4151(6)	7552(33)	118
H(37C)	-1281(16)	-3626(24)	7307(24)	118
H(42A)	-1851(3)	-1349(1)	6533(2)	45
H(43A)	-2788(4)	-1392(2)	5431(3)	48
H(44A)	-4838(4)	-1956(3)	5047(3)	53
H(45A)	-5964(4)	-2504(3)	5732(3)	57
H(47A)	-5455(34)	-2202(3)	7439(15)	84
H(47B)	-5028(22)	-2940(23)	7143(24)	84
H(47C)	-6164(14)	-2946(22)	6658(9)	84
H(52A)	-2016(2)	-1812(2)	9265(2)	49
H(53A)	-2310(3)	-2598(3)	9919(3)	67
H(54A)	-3307(5)	-3959(3)	9239(3)	75
H(55A)	-3985(6)	-4516(3)	7961(3)	85
H(57A)	-3514(40)	-4318(22)	6766(5)	106
H(57B)	-3558(41)	-3508(8)	6773(5)	106
H(57C)	-4698(6)	-4119(28)	6857(4)	106
H(62A)	-152(3)	-1672(3)	8731(1)	65
H(63A)	1622(4)	-719(3)	9545(2)	84
H(64A)	2054(5)	577(3)	9717(3)	97
H(65A)	837(5)	963(3)	9101(3)	82
H(67A)	-878(25)	704(5)	8350(21)	96
H(67B)	-2012(14)	-29(26)	8257(24)	96
H(67C)	-1269(37)	-109(24)	7610(5)	96
H(72A)	6405(3)	1791(3)	6486(2)	68
H(73A)	7860(4)	2321(3)	5928(2)	102
H(74A)	7863(5)	3399(3)	5715(3)	115
H(75A)	6507(5)	4004(3)	6061(3)	109
H(77A)	3944(7)	3255(4)	6474(32)	125
H(77B)	4851(39)	3994(28)	6399(29)	125
H(77C)	4918(37)	3948(30)	7198(5)	125
H(82A)	5471(3)	3827(2)	8239(2)	58
H(83A)	5046(4)	4814(2)	9179(2)	69

H(84A)	3304(5)	4486(3)	9569(3)	70
H(85A)	1954(5)	3217(3)	9099(3)	63
H(87A)	1352(19)	1936(4)	8261(23)	92
H(87B)	2432(17)	1621(8)	8211(24)	92
H(87C)	1848(35)	1715(11)	7506(4)	92
H(92A)	4082(2)	1140(3)	8069(3)	81
H(93A)	3797(3)	-149(3)	7900(3)	118
H(94A)	3505(5)	-1095(3)	6707(3)	107
H(95A)	3525(5)	-894(3)	5640(4)	109
H(97A)	3841(80)	1116(22)	5833(15)	74
H(97B)	3202(44)	225(29)	5216(21)	74
H(97C)	4621(36)	602(50)	5467(35)	74
H(97D)	3378(128)	-310(20)	5128(6)	182
H(97E)	4619(8)	409(93)	5402(27)	182
H(97F)	3400(131)	572(76)	5384(29)	182
H(10A)	6334(3)	838(2)	7518(2)	59
H(10B)	6657(4)	-102(2)	6477(2)	68
H(10C)	8318(5)	262(3)	6004(3)	80
H(10D)	9693(5)	1521(3)	6538(3)	75
H(10E)	9396(23)	3072(9)	7461(21)	93
H(10F)	10448(13)	2760(4)	7567(25)	93
H(10G)	9760(34)	3007(10)	8230(5)	93
H(11A)	7720(2)	3522(2)	7798(3)	60
H(11B)	8259(3)	4833(3)	7993(3)	72
H(11C)	8820(5)	5799(3)	9232(3)	73
H(11D)	8835(4)	5511(3)	10250(3)	64
H(11E)	7686(29)	4314(24)	10579(14)	77
H(11F)	9050(11)	4396(22)	10640(13)	77
H(11G)	8024(39)	3558(4)	10144(4)	77
H(12B)	7199(3)	1076(3)	8900(2)	66
H(12C)	6037(4)	279(3)	9404(2)	96
H(12D)	4584(5)	648(3)	9967(3)	92
H(12E)	4283(5)	1786(3)	10129(3)	68
H(12F)	5818(31)	3109(15)	9414(23)	84
H(12G)	5504(41)	3190(13)	10211(4)	84
H(12H)	4482(11)	2699(4)	9457(24)	84

Table B.4 Anisotropic thermal parameters ($Å^2$ x 10^3) with estimated standard deviations in parentheses for $[(o\text{-}MeC_6H_4)_3SbBr]_2O.0.5C_6H_{14}$ (2.9.0.5C_6H_{14})

Atom	U11	U22	U33	U23	U13	U12
Sb(1)	21(1)	32(1)	23(1)	6(1)	4(1)	9(1)
Br(1)	43(1)	84(1)	40(1)	25(1)	21(1)	35(1)
O(1)	33(2)	34(2)	37(2)	8(2)	14(2)	7(2)
Sb(2)	23(1)	25(1)	21(1)	5(1)	4(1)	7(1)
Br(2)	77(1)	60(1)	44(1)	21(1)	32(1)	42(1)
O(2)	26(2)	58(2)	36(2)	20(2)	-6(2)	12(2)
Sb(3)	21(1)	27(1)	21(1)	9(1)	2(1)	4(1)
Br(3)	39(1)	78(1)	43(1)	26(1)	-4(1)	16(1)
Sb(4)	20(1)	25(1)	22(1)	6(1)	2(1)	6(1)
Br(4)	30(1)	52(1)	37(1)	11(1)	-2(1)	16(1)
C(11)	40(3)	43(2)	32(2)	14(2)	14(3)	14(3)
C(12)	30(3)	41(2)	36(3)	10(2)	6(3)	-7(3)
C(13)	26(3)	34(2)	67(3)	11(2)	7(3)	-14(3)
C(14)	42(4)	40(2)	87(3)	34(2)	10(4)	6(3)
C(15)	40(4)	58(2)	59(3)	34(2)	12(3)	12(3)
C(16)	21(3)	39(2)	37(2)	14(2)	2(3)	0(2)
C(17)	65(4)	80(4)	34(4)	25(3)	-6(3)	31(3)
C(21)	56(3)	42(2)	19(3)	2(2)	6(2)	14(2)
C(22)	41(3)	101(3)	49(4)	24(3)	-9(3)	2(3)
C(23)	82(4)	118(3)	92(6)	40(4)	-28(4)	-4(3)
C(24)	119(4)	101(3)	61(6)	2(5)	-25(4)	2(4)
C(25)	105(5)	49(3)	49(5)	-9(4)	9(4)	-3(3)
C(26)	85(4)	61(3)	44(4)	4(3)	12(3)	21(3)
C(27)	84(7)	123(7)	87(6)	40(5)	12(5)	16(6)
C(31)	43(3)	62(3)	21(2)	8(2)	13(2)	27(2)
C(32)	48(3)	73(4)	40(3)	-7(3)	-12(3)	25(3)
C(33)	77(4)	153(5)	55(4)	0(3)	-21(3)	51(4)
C(34)	139(4)	187(5)	32(3)	17(3)	-3(4)	105(4)
C(35)	167(5)	125(4)	42(3)	38(3)	29(3)	106(3)
C(36)	94(4)	59(3)	43(3)	13(2)	26(3)	50(3)
C(37)	92(5)	89(4)	90(5)	54(4)	37(4)	53(4)
C(41)	31(2)	36(3)	11(2)	4(2)	0(2)	15(2)
C(42)	29(3)	42(3)	34(3)	10(2)	8(2)	10(2)
C(43)	56(3)	33(3)	32(2)	15(2)	13(2)	15(2)
C(44)	57(3)	39(3)	23(2)	14(2)	-12(2)	3(3)
C(45)	32(3)	63(3)	42(3)	23(2)	-7(2)	11(3)
C(46)	37(3)	52(3)	38(2)	26(2)	12(2)	17(2)
C(47)	29(4)	92(5)	37(3)	32(3)	-1(3)	2(3)
C(51)	18(3)	31(2)	48(2)	19(2)	2(3)	7(2)
C(52)	47(3)	38(2)	39(3)	16(2)	11(3)	16(3)
C(53)	60(4)	62(3)	54(3)	33(2)	5(3)	24(3)
C(54)	70(5)	58(3)	74(3)	40(2)	26(4)	23(3)
C(55)	98(6)	40(3)	69(3)	32(2)	25(4)	7(4)
C(56)	47(4)	40(3)	51(3)	18(2)	-1(3)	1(3)
C(57)	69(5)	50(4)	67(5)	27(3)	3(4)	-11(4)
C(61)	32(3)	30(2)	39(3)	2(2)	6(2)	-3(2)
C(62)	28(3)	72(3)	39(4)	3(3)	3(3)	13(2)
C(63)	55(4)	73(3)	48(4)	1(3)	-14(3)	16(3)
C(64)	101(4)	57(3)	36(4)	-10(3)	0(3)	7(3)
C(65)	77(4)	34(3)	54(4)	1(3)	12(3)	-13(3)
C(66)	67(4)	42(2)	48(4)	5(3)	26(3)	13(3)
C(67)	81(4)	62(4)	54(4)	15(3)	19(4)	43(3)

C(71)	39(3)	56(2)	11(2)	12(2)	-1(2)	-4(2)
C(72)	27(3)	85(3)	34(3)	19(2)	-5(2)	-3(2)
C(73)	43(3)	160(3)	27(3)	37(3)	4(2)	9(3)
C(74)	72(3)	128(3)	32(3)	33(3)	7(3)	-37(3)
C(75)	115(4)	75(3)	32(3)	19(3)	9(3)	-28(3)
C(76)	96(4)	53(3)	27(3)	18(2)	11(3)	-1(3)
C(77)	153(7)	57(4)	54(4)	31(3)	43(5)	42(4)
C(81)	46(3)	58(3)	32(3)	31(2)	12(2)	28(2)
C(82)	79(3)	51(3)	29(3)	21(2)	15(2)	36(2)
C(83)	66(3)	52(3)	48(4)	14(3)	9(3)	24(3)
C(84)	56(3)	70(3)	46(4)	23(3)	12(3)	22(3)
C(85)	55(3)	56(3)	32(3)	1(3)	-4(3)	26(2)
C(86)	53(3)	66(3)	42(3)	27(2)	11(2)	30(2)
C(87)	48(4)	51(4)	74(5)	26(3)	-3(4)	5(3)
C(91)	27(3)	58(3)	79(3)	3(2)	7(3)	24(3)
C(92)	38(4)	52(2)	108(3)	26(3)	4(4)	22(3)
C(93)	89(6)	50(3)	127(3)	21(3)	15(6)	9(4)
C(94)	52(4)	55(3)	121(3)	9(2)	36(4)	0(4)
C(95)	65(5)	54(3)	140(3)	25(3)	52(5)	17(4)
C(96)	50(4)	58(3)	98(3)	1(3)	6(4)	15(4)
C(101)	37(3)	41(3)	23(3)	9(2)	1(2)	18(2)
C(102)	54(3)	49(3)	37(3)	9(2)	-2(2)	23(2)
C(103)	66(3)	54(3)	38(4)	8(3)	-3(3)	22(3)
C(104)	64(3)	85(4)	49(4)	15(3)	10(3)	42(3)
C(105)	67(3)	85(4)	41(3)	23(3)	17(3)	39(3)
C(106)	42(3)	67(3)	49(4)	21(3)	8(2)	27(2)
C(107)	46(4)	79(5)	58(4)	27(4)	21(3)	19(3)
C(111)	14(3)	35(2)	51(3)	13(2)	2(3)	9(2)
C(112)	40(4)	46(2)	50(3)	16(2)	-1(3)	6(3)
C(113)	46(4)	62(2)	73(3)	43(2)	-3(3)	8(3)
C(114)	35(4)	40(3)	99(3)	21(2)	15(4)	11(3)
C(115)	19(3)	43(2)	74(3)	2(2)	2(3)	12(3)
C(116)	22(3)	50(2)	48(3)	6(2)	-4(3)	14(3)
C(117)	29(3)	62(4)	51(4)	13(3)	-1(3)	17(3)
C(121)	34(3)	55(2)	17(3)	2(2)	3(2)	9(2)
C(122)	65(3)	52(3)	30(3)	14(2)	3(3)	4(2)
C(123)	93(4)	81(3)	76(4)	42(3)	45(3)	28(3)
C(124)	92(4)	72(3)	72(4)	30(3)	36(3)	33(3)
C(125)	70(4)	66(3)	38(3)	34(2)	17(3)	14(2)
C(126)	46(3)	63(3)	32(3)	15(2)	8(3)	8(2)
C(127)	55(4)	50(4)	48(4)	12(3)	-14(3)	16(3)
C(3S)	68(4)	34(3)	95(5)	19(3)	35(4)	22(3)
C(5S)	90(5)	102(5)	99(5)	70(4)	65(4)	47(4)
C(6S)	133(9)	83(6)	86(7)	9(6)	-13(7)	24(6)

Table B.5 Bond lengths (Å) with estimated standard deviations in parentheses for [(*o*-$MeC_6H_4)_3SbBr]_2O.0.5C_6H_{14}$ (2.9.0.5C_6H_{14})

Sb(1)-O(1)	1.964(4)	C(61)-C(66)	1.376(7)
Sb(1)-Br(1)	2.750(2)	C(61)-C(62)	1.427(7)
Sb(1)-C(11)	2.113(5)	C(62)-C(63)	1.362(5)
Sb(1)-C(21)	2.139(4)	C(63)-C(64)	1.385(8)
Sb(1)-C(31)	2.111(4)	C(64)-C(65)	1.366(9)
Sb(2)-O(1)	1.962(4)	C(65)-C(66)	1.404(7)

Sb(2)-Br(2)	2.731(2)	C(66)-C(67)	1.463(9)
Sb(2)-C(41)	2.112(4)	C(71)-C(76)	1.361(8)
Sb(2)-C(51)	2.125(5)	C(71)-C(72)	1.425(7)
Sb(2)-C(61)	2.133(4)	C(72)-C(73)	1.370(7)
Sb(3)-O(2)	1.947(4)	C(73)-C(74)	1.372(9)
Sb(3)-Br(3)	2.739(2)	C(74)-C(75)	1.365(9)
Sb(3)-C(71)	2.110(4)	C(75)-C(76)	1.413(8)
Sb(3)-C(91)	2.141(5)	C(76)-C(77)	1.430(10)
Sb(3)-C(81)	2.162(3)	C(81)-C(86)	1.371(6)
Sb(4)-O(2)	1.964(4)	C(81)-C(82)	1.420(4)
Sb(4)-Br(4)	2.762(2)	C(82)-C(83)	1.370(5)
Sb(4)-C(101)	2.109(3)	C(83)-C(84)	1.366(7)
Sb(4)-C(111)	2.121(5)	C(84)-C(85)	1.369(7)
Sb(4)-C(121)	2.149(5)	C(85)-C(86)	1.403(7)
C(11)-C(12)	1.395(5)	C(86)-C(87)	1.433(7)
C(11)-C(16)	1.395(7)	C(91)-C(96)	1.341(7)
C(12)-C(13)	1.373(7)	C(91)-C(92)	1.467(9)
C(13)-C(14)	1.372(8)	C(92)-C(93)	1.347(8)
C(14)-C(15)	1.371(6)	C(93)-C(94)	1.386(7)
C(15)-C(16)	1.396(8)	C(94)-C(95)	1.343(9)
C(16)-C(17)	1.484(7)	C(95)-C(96)	1.445(8)
C(21)-C(26)	1.389(7)	C(96)-C(97')	1.390(13)
C(21)-C(22)	1.418(6)	C(96)-C(97)	1.408(12)
C(22)-C(23)	1.359(5)	C(101)-C(106)	1.392(6)
C(23)-C(24)	1.365(9)	C(101)-C(102)	1.401(4)
C(24)-C(25)	1.354(10)	C(102)-C(103)	1.374(5)
C(25)-C(26)	1.426(7)	C(103)-C(104)	1.379(7)
C(26)-C(27)	1.413(10)	C(104)-C(105)	1.358(7)
C(31)-C(32)	1.397(4)	C(105)-C(106)	1.411(7)
C(31)-C(36)	1.391(7)	C(106)-C(107)	1.442(7)
C(32)-C(33)	1.388(7)	C(111)-C(116)	1.394(6)
C(33)-C(34)	1.377(9)	C(111)-C(112)	1.399(8)
C(34)-C(35)	1.354(8)	C(112)-C(113)	1.360(7)
C(35)-C(36)	1.410(8)	C(113)-C(114)	1.393(7)
C(36)-C(37)	1.449(8)	C(114)-C(115)	1.347(9)
C(41)-C(42)	1.398(6)	C(115)-C(116)	1.414(7)
C(41)-C(46)	1.402(6)	C(116)-C(117)	1.451(9)
C(42)-C(43)	1.367(7)	C(121)-C(126)	1.390(7)
C(43)-C(44)	1.371(6)	C(121)-C(122)	1.424(8)
C(44)-C(45)	1.374(8)	C(122)-C(123)	1.366(7)
C(45)-C(46)	1.400(7)	C(123)-C(124)	1.375(8)
C(46)-C(47)	1.492(8)	C(124)-C(125)	1.355(8)
C(51)-C(56)	1.382(6)	C(125)-C(126)	1.393(8)
C(51)-C(52)	1.410(6)	C(126)-C(127)	1.433(9)
C(52)-C(53)	1.363(8)	C(1S)-C(2S)	1.62(3)
C(53)-C(54)	1.390(6)	C(2S)-C(6S)	1.71(2)
C(54)-C(55)	1.356(7)	C(2S)-C(3S)	1.76(2)
C(55)-C(56)	1.395(8)	C(3S)-C(4S')	1.45(3)
C(56)-C(57)	1.478(8)	C(3S)-C(2S')	1.509(13)
		C(5S)-C(6S)	1.189(12)

Table B.6 Bond angles (°) with estimated standard deviations in parentheses for [(*o*-$MeC_6H_4)_3SbBr]_2O.0.5C_6H_{14}$ (2.9.0.5C_6H_{14})

Sb(1)-O(1)-Sb(2)	161.0(2)	C(55)-C(56)-C(57)	119.3(5)
Sb(3)-O(2)-Sb(4)	171.5(2)	C(66)-C(61)-C(62)	121.4(3)
O(1)-Sb(1)-Br(1)	179.16(13)	C(66)-C(61)-Sb(2)	125.8(3)
O(1)-Sb(1)-C(11)	95.1(2)	C(62)-C(61)-Sb(2)	112.8(3)
O(1)-Sb(1)-C(21)	90.40(14)	C(63)-C(62)-C(61)	119.6(5)
O(1)-Sb(1)-C(31)	93.1(2)	C(62)-C(63)-C(64)	117.7(5)
Br(1)-Sb(1)-C(11)	85.27(10)	C(65)-C(64)-C(63)	124.4(5)
Br(1)-Sb(1)-C(21)	90.06(11)	C(64)-C(65)-C(66)	118.3(5)
Br(1)-Sb(1)-C(31)	86.10(11)	C(61)-C(66)-C(65)	118.6(5)
C(11)-Sb(1)-C(21)	120.9(2)	C(61)-C(66)-C(67)	124.0(4)
C(11)-Sb(1)-C(31)	116.85(13)	C(65)-C(66)-C(67)	117.4(5)
C(21)-Sb(1)-C(31)	121.6(2)	C(76)-C(71)-C(72)	121.5(4)
O(1)-Sb(2)-Br(2)	177.49(11)	C(76)-C(71)-Sb(3)	125.7(4)
O(1)-Sb(2)-C(41)	90.9(2)	C(72)-C(71)-Sb(3)	112.3(4)
O(1)-Sb(2)-C(51)	92.3(2)	C(73)-C(72)-C(71)	118.7(5)
O(1)-Sb(2)-C(61)	94.2(2)	C(72)-C(73)-C(74)	119.0(6)
Br(2)-Sb(2)-C(41)	88.69(11)	C(75)-C(74)-C(73)	123.4(6)
Br(2)-Sb(2)-C(51)	85.90(10)	C(74)-C(75)-C(76)	118.3(6)
Br(2)-Sb(2)-C(61)	88.06(11)	C(71)-C(76)-C(75)	119.0(5)
C(41)-Sb(2)-C(51)	124.81(12)	C(71)-C(76)-C(77)	126.6(6)
C(41)-Sb(2)-C(61)	123.8(2)	C(75)-C(76)-C(77)	114.5(6)
C(51)-Sb(2)-C(61)	110.9(2)	C(86)-C(81)-C(82)	121.6(3)
O(2)-Sb(3)-Br(3)	176.59(13)	C(86)-C(81)-Sb(3)	126.3(3)
O(2)-Sb(3)-C(71)	91.4(2)	C(82)-C(81)-Sb(3)	112.0(3)
O(2)-Sb(3)-C(81)	88.6(2)	C(83)-C(82)-C(81)	118.7(4)
O(2)-Sb(3)-C(91)	91.4(2)	C(84)-C(83)-C(82)	118.4(4)
Br(3)-Sb(3)-C(71)	91.01(12)	C(83)-C(84)-C(85)	124.5(5)
Br(3)-Sb(3)-C(81)	88.12(10)	C(84)-C(85)-C(86)	117.8(5)
Br(3)-Sb(3)-C(91)	89.67(12)	C(81)-C(86)-C(85)	118.9(4)
C(71)-Sb(3)-C(81)	117.4(2)	C(81)-C(86)-C(87)	122.3(5)
C(71)-Sb(3)-C(91)	117.3(2)	C(85)-C(86)-C(87)	118.7(5)
C(91)-Sb(3)-C(81)	125.3(2)	C(96)-C(91)-C(92)	123.5(5)
O(2)-Sb(4)-Br(4)	177.71(12)	C(96)-C(91)-Sb(3)	126.5(5)
O(2)-Sb(4)-C(101)	92.8(2)	C(92)-C(91)-Sb(3)	109.5(3)
O(2)-Sb(4)-C(111)	90.6(2)	C(93)-C(92)-C(91)	116.5(5)
O(2)-Sb(4)-C(121)	92.4(2)	C(92)-C(93)-C(94)	118.1(7)
Br(4)-Sb(4)-C(101)	85.85(10)	C(95)-C(94)-C(93)	128.2(6)
Br(4)-Sb(4)-C(111)	91.69(11)	C(94)-C(95)-C(96)	114.5(5)
Br(4)-Sb(4)-C(121)	86.55(11)	C(91)-C(96)-C(97')	139.6(10)
C(101)-Sb(4)-C(111)	120.5(2)	C(91)-C(96)-C(97)	114.7(6)
C(101)-Sb(4)-C(121)	115.1(2)	C(91)-C(96)-C(95)	119.2(6)
C(111)-Sb(4)-C(121)	124.0(2)	C(97')-C(96)-C(95)	101.2(9)
C(12)-C(11)-C(16)	120.2(5)	C(97)-C(96)-C(95)	126.0(6)
C(12)-C(11)-Sb(1)	114.5(4)	C(106)-C(101)-C(102)	120.5(3)
C(16)-C(11)-Sb(1)	125.1(3)	C(106)-C(101)-Sb(4)	126.8(2)
C(13)-C(12)-C(11)	120.8(5)	C(102)-C(101)-Sb(4)	112.6(2)
C(14)-C(13)-C(12)	118.8(4)	C(103)-C(102)-C(101)	119.7(4)
C(15)-C(14)-C(13)	121.5(5)	C(102)-C(103)-C(104)	119.0(4)
C(14)-C(15)-C(16)	120.7(5)	C(105)-C(104)-C(103)	123.0(5)
C(15)-C(16)-C(11)	117.9(4)	C(104)-C(105)-C(106)	118.7(5)
C(15)-C(16)-C(17)	117.4(5)	C(101)-C(106)-C(105)	118.9(4)
C(11)-C(16)-C(17)	124.7(5)	C(101)-C(106)-C(107)	122.3(5)
C(26)-C(21)-C(22)	120.4(3)	C(105)-C(106)-C(107)	118.8(5)
C(26)-C(21)-Sb(1)	127.3(3)	C(116)-C(111)-C(112)	121.4(4)

C(22)-C(21)-Sb(1)	112.2(3)	C(116)-C(111)-Sb(4)	125.4(4)
C(23)-C(22)-C(21)	121.1(5)	C(112)-C(111)-Sb(4)	113.1(3)
C(22)-C(23)-C(24)	116.3(6)	C(113)-C(112)-C(111)	120.8(4)
C(25)-C(24)-C(23)	127.0(5)	C(112)-C(113)-C(114)	117.1(6)
C(24)-C(25)-C(26)	116.7(6)	C(115)-C(114)-C(113)	124.1(5)
C(21)-C(26)-C(27)	122.7(5)	C(114)-C(115)-C(116)	119.4(4)
C(21)-C(26)-C(25)	118.4(5)	C(111)-C(116)-C(115)	117.2(5)
C(27)-C(26)-C(25)	118.9(6)	C(111)-C(116)-C(117)	123.7(5)
C(32)-C(31)-C(36)	121.2(4)	C(115)-C(116)-C(117)	119.1(5)
C(32)-C(31)-Sb(1)	116.2(3)	C(126)-C(121)-C(122)	121.2(4)
C(36)-C(31)-Sb(1)	122.4(3)	C(126)-C(121)-Sb(4)	123.5(4)
C(33)-C(32)-C(31)	120.5(5)	C(122)-C(121)-Sb(4)	114.6(3)
C(34)-C(33)-C(32)	116.8(4)	C(123)-C(122)-C(121)	119.2(4)
C(35)-C(34)-C(33)	124.7(6)	C(122)-C(123)-C(124)	117.5(6)
C(34)-C(35)-C(36)	118.9(6)	C(125)-C(124)-C(123)	125.3(6)
C(31)-C(36)-C(35)	117.9(4)	C(124)-C(125)-C(126)	118.2(6)
C(31)-C(36)-C(37)	127.0(6)	C(121)-C(126)-C(125)	118.5(5)
C(35)-C(36)-C(37)	115.1(6)	C(121)-C(126)-C(127)	123.9(6)
C(42)-C(41)-C(46)	120.7(4)	C(125)-C(126)-C(127)	117.5(6)
C(42)-C(41)-Sb(2)	113.9(3)	C(1S)-C(2S)-C(6S)	102.3(14)
C(46)-C(41)-Sb(2)	125.3(3)	C(1S)-C(2S)-C(3S)	114.1(12)
C(43)-C(42)-C(41)	120.5(3)	C(6S)-C(2S)-C(3S)	109.8(13)
C(42)-C(43)-C(44)	119.4(5)	C(1S)-C(2S)-C(5S)	94.2(13)
C(43)-C(44)-C(45)	121.2(5)	C(6S)-C(2S)-C(5S)	35.9(6)
C(44)-C(45)-C(46)	121.1(5)	C(3S)-C(2S)-C(5S)	82.0(9)
C(41)-C(46)-C(45)	117.0(5)	C(4S')-C(3S)-C(2S')	120.0(13)
C(41)-C(46)-C(47)	124.6(5)	C(4S')-C(3S)-C(4S)	17.9(11)
C(45)-C(46)-C(47)	118.3(4)	C(2S')-C(3S)-C(4S)	105.8(9)
C(56)-C(51)-C(52)	120.5(5)	C(2S)-C(3S)-C(4S)	92.2(10)
C(56)-C(51)-Sb(2)	126.1(4)	C(4S')-C(4S)-C(3S)	44(2)
C(52)-C(51)-Sb(2)	113.3(3)	C(4S')-C(4S)-C(1S')	138(3)
C(53)-C(52)-C(51)	121.0(3)	C(3S)-C(4S)-C(1S')	95.3(9)
C(52)-C(53)-C(54)	117.8(5)	C(4S)-C(4S')-C(3S)	118(3)
C(55)-C(54)-C(53)	121.9(6)	C(6S)-C(5S)-C(2S)	57.7(8)
C(54)-C(55)-C(56)	121.2(5)	C(5S)-C(6S)-C(2S)	86.4(10)
C(51)-C(56)-C(55)	117.6(4)		
C(51)-C(56)-C(57)	123.1(6)		

Experimental Details

A set of unique data were collected on a Stoe Stadi-4 four-circle diffractometer and the data were corrected for absorption (numerical), Lorentz and polarisation effects. The structure was solved by direct methods (SHELXS-86)[1] and subsequent Fourier difference syntheses revealed the positions of all the other non-hydrogen atoms. Refinement was carried out against all F_o^2 data by full matrix procedures (SHELXL-93)[2] with tolyl groups restrained to be flat and have local two-fold symmetry. Bonds to methyl groups were restrained to be similar in all twelve groups. One methyl group, C97/C97', is disordered over two sites. The disordered solvate region was modelled using three fully-occupied and three partly-occupied carbon atoms. Hydrogen atoms were placed in estimated positions (except methyl hydrogens that were located from a difference synthesis) [C–H = 0.95 (aromatic ring hydrogens), 0.98 (methyl group) Å], with fixed isotropic parameters (1.2 x equivalent isotropic temperature factors of the carbon atom to which they were bonded for aryl protons and 1.5 x for methyl protons) and refined 'riding' their respective carbon atoms. A standard weighting scheme was applied but no extinction correction was found to be necessary.

All crystallographic calculations were performed using the SHELXS-86[1] and SHELXL-93[2] programs and neutral atom scattering factors were taken from the usual sources[3].

APPENDIX C

Table C.1 Data collection and processing parameters for $[(Ph_2Sb)_2(\mu\text{-}O)_2(\mu\text{-}O_2AsMe_2)_2].2CHCl_3$ (3.1.2CHCl$_3$)

Chemical formula	$C_{30}H_{34}As_2Cl_6O_6Sb_2$
Formula weight	1096.61
Crystal size/mm	0.30 x 0.25 x 0.15
Crystal system	Monoclinic
Space group	$P2_1/a$
a / Å	13.830(3)
b / Å	10.2590(3)
c / Å	14.5744(12)
β / °	113.13(2)
Volume / Å^3	1901.57
Z	2
D_c/gcm^{-3}	1.915
Radiation (λ / Å)	Mo-K_α (0.71069)
μ / cm^{-1}	36.09
F(000)	1064
2θ limits / °	5-50
Index ranges (for unique data)	-16<=h<=14, 0<=k<=12, 0<=l<=17
Temperature / K	150
Total data collected	8051
Unique data	2932 [(R(int) = 0.0766]
Observed data [$I > 3\sigma(I)$]	2172
Absorption correction	DIFABS (min, 0.961, max, 1.044)[4]
Structure solution	Direct (SIR-92)[5]
Refinement procedure	Full matrix-LS on F
Number of data / variables	2172 / 209
S	1.039
Max/min peaks in final diff. map / e Å^{-3}	+1.18, -0.70
R	0.0276
R_w	0.0306

Table C.2 Fractional atomic coordinates and equivalent isotropic displacement parameters ($Å^2$) with estimated standard deviations in parentheses for $[(Ph_2Sb)_2(\mu\text{-}O)_2(\mu\text{-}O_2AsMe_2)_2].2CHCl_3$ (3.1.2CHCl$_3$)

Atom	x/a	y/b	z/c	U(eq)
Sb(1)	0.49402(2)	0.44061(2)	0.90108(2)	0.0095
As(1)	0.27577(3)	0.55271(4)	0.91152(3)	0.0106
O(1)	0.5420(2)	0.6026(3)	0.9820(2)	0.0116
O(2)	0.3410(2)	0.5169(3)	0.8364(2)	0.0128
O(3)	0.6474(2)	0.3751(3)	0.9780(2)	0.0141
C(1)	0.5246(3)	0.5211(4)	0.7783(3)	0.0122
C(2)	0.6077(3)	0.4744(4)	0.7567(3)	0.0175
C(3)	0.6222(4)	0.5179(4)	0.6718(3)	0.0201
C(4)	0.5526(4)	0.6089(4)	0.6087(3)	0.0202
C(5)	0.4724(3)	0.6579(4)	0.6312(3)	0.0215
C(6)	0.4568(3)	0.6137(4)	0.7153(3)	0.0175
C(7)	0.4492(3)	0.2478(4)	0.8402(3)	0.0132
C(8)	0.4314(3)	0.1499(4)	0.8990(3)	0.0208
C(9)	0.4107(4)	0.0224(4)	0.8630(4)	0.0231
C(10)	0.4055(4)	-0.0074(5)	0.7681(4)	0.0233
C(11)	0.4218(4)	0.0886(4)	0.7098(3)	0.0213
C(12)	0.4433(3)	0.2160(4)	0.7447(3)	0.0180
C(13)	0.1723(3)	0.6797(4)	0.8412(3)	0.0187
C(14)	0.2090(3)	0.3989(4)	0.9322(3)	0.0191
C(100)	0.7817(4)	0.5622(4)	0.3883(3)	0.0202
Cl(1)	0.74148(9)	0.6064(1)	0.48497(8)	0.0289
Cl(2)	0.8526(1)	0.4160(1)	0.4167(1)	0.0395
Cl(3)	0.8558(1)	0.6883(1)	0.3659(1)	0.0354

Table C.3 Calculated hydrogen coordinates and isotropic displacement parameters ($Å^2$) with estimated standard deviations in parentheses for $[(Ph_2Sb)_2(\mu\text{-}O)_2(\mu\text{-}O_2AsMe_2)_2].2CHCl_3$ (3.1.2CHCl$_3$)

Atom	x/a	y/b	z/c	U(iso)
H(21)	0.6576(3)	0.4101(4)	0.8027(3)	0.0350
H(31)	0.6826(4)	0.4845(4)	0.6572(3)	0.0350
H(41)	0.5609(4)	0.6376(4)	0.5466(3)	0.0350
H(51)	0.4242(3)	0.7257(4)	0.5875(3)	0.0350
H(61)	0.3969(3)	0.6476(4)	0.7305(3)	0.0350
H(81)	0.4332(3)	0.1721(4)	0.9664(3)	0.0350
H(91)	0.3996(4)	-0.0476(4)	0.9056(4)	0.0350
H(101)	0.3893(4)	-0.0985(5)	0.7419(4)	0.0350
H(111)	0.4192(4)	0.0661(4)	0.6421(3)	0.0350
H(121)	0.4535(3)	0.2852(4)	0.7010(3)	0.0350
H(131)	0.1314(3)	0.7048(4)	0.8819(3)	0.0350
H(132)	0.2077(3)	0.7587(4)	0.8285(3)	0.0350
H(133)	0.1236(3)	0.6421(4)	0.7762(3)	0.0350
H(141)	0.1710(3)	0.4201(4)	0.9762(3)	0.0350
H(142)	0.2633(3)	0.3307(4)	0.9647(3)	0.0350
H(143)	0.1576(3)	0.3657(4)	0.8666(3)	0.0350
H(1001)	0.7167(4)	0.5473(4)	0.3269(3)	0.0350

Table C.4 Anisotropic thermal parameters ($Å^2$) with estimated standard deviations in parentheses for $[(Ph_2Sb)_2(\mu\text{-}O)_2(\mu\text{-}O_2AsMe_2)_2].2CHCl_3$ (3.1.2CHCl$_3$)

Atom	U(11)	U(22)	U(33)	U(23)	U(13)	U(12)
Sb(1)	0.0097(2)	0.0098(2)	0.0091(2)	-0.0010(1)	0.0036(1)	0.0006(1)
As(1)	0.0090(2)	0.0115(2)	0.0112(2)	0.0005(2)	0.0037(2)	0.0009(2)
O(1)	0.014(1)	0.012(1)	0.009(1)	-0.002(1)	0.004(1)	-0.001(1)
O(2)	0.012(1)	0.019(1)	0.012(1)	0.001(1)	0.006(1)	0.004(1)
O(3)	0.011(1)	0.017(1)	0.015(1)	-0.001(1)	0.003(1)	0.004(1)
C(1)	0.014(2)	0.014(2)	0.011(2)	-0.004(2)	0.002(2)	-0.006(2)
C(2)	0.017(2)	0.020(2)	0.019(2)	-0.002(2)	0.010(2)	-0.000(2)
C(3)	0.025(2)	0.023(2)	0.024(2)	-0.004(2)	0.017(2)	-0.003(2)
C(4)	0.032(3)	0.021(2)	0.017(2)	-0.004(2)	0.013(2)	-0.010(2)
C(5)	0.022(2)	0.021(2)	0.020(2)	0.003(2)	0.006(2)	-0.002(2)
C(6)	0.017(2)	0.019(2)	0.017(2)	0.001(2)	0.007(2)	-0.002(2)
C(7)	0.011(2)	0.016(2)	0.012(2)	-0.002(2)	0.002(2)	0.002(2)
C(8)	0.023(2)	0.019(2)	0.023(2)	-0.002(2)	0.012(2)	-0.002(2)
C(9)	0.029(3)	0.014(2)	0.033(3)	-0.002(2)	0.013(2)	-0.001(2)
C(10)	0.022(2)	0.018(2)	0.033(3)	-0.008(2)	0.007(2)	-0.003(2)
C(11)	0.027(2)	0.024(2)	0.019(2)	-0.009(2)	0.009(2)	-0.001(2)
C(12)	0.019(2)	0.020(2)	0.015(2)	-0.002(2)	0.006(2)	-0.001(2)
C(13)	0.017(2)	0.022(2)	0.019(2)	0.002(2)	0.004(2)	0.009(2)
C(14)	0.018(2)	0.019(2)	0.025(2)	0.001(2)	0.009(2)	-0.006(2)
C(100)	0.025(2)	0.019(2)	0.017(2)	0.001(2)	0.008(2)	0.001(2)
Cl(1)	0.0294(6)	0.0447(7)	0.0228(6)	-0.0027(5)	0.0145(5)	-0.0004(5)
Cl(2)	0.063(1)	0.0349(7)	0.0346(8)	0.0045(6)	0.0168(7)	0.0218(7)
Cl(3)	0.0436(8)	0.0429(8)	0.0383(7)	0.0002(6)	0.0232(6)	-0.0168(6)

Table C.5 Bond lengths (Å) with estimated standard deviations in parentheses for $[(Ph_2Sb)_2(\mu\text{-}O)_2(\mu\text{-}O_2AsMe_2)_2].2CHCl_3$ (3.1.2CHCl$_3$)

Sb(1) - Sb(1')	3.0743(5)
Sb(1) - O(1)	1.995(3)
Sb(1) - O(1')	2.004(3)
Sb(1) - O(2)	2.101(3)
Sb(1) - O(3)	2.083(3)
Sb(1) - C(1)	2.157(4)
Sb(1) - C(7)	2.156(4)
As(1) - O(2)	1.709(3)
As(1) - O(3')	1.711(3)
As(1) - C(13)	1.909(4)
As(1) - C(14)	1.911(4)
C(1) - C(2)	1.391(6)
C(1) - C(6)	1.396(6)
C(2) - C(3)	1.401(6)
C(3) - C(4)	1.396(7)
C(4) - C(5)	1.371(6)
C(5) - C(6)	1.400(6)
C(7) - C(8)	1.404(6)
C(7) - C(12)	1.400(6)
C(8) - C(9)	1.396(6)

C(9) - C(10)	1.390(7)
C(10) - C(11)	1.376(7)
C(11) - C(12)	1.392(6)
C(100)- Cl(1)	1.766(5)
C(100)- Cl(2)	1.750(4)
C(100)- Cl(3)	1.758(5)

Table C.6 Bond angles (°) with estimated standard deviations in parentheses for $[(Ph_2Sb)_2(\mu\text{-}O)_2(\mu\text{-}O_2AsMe_2)_2].2CHCl_3$ ($3.1.2CHCl_3$)

O(1) - Sb(1) - O(1')	79.5(1)
O(1) - Sb(1) - O(2)	89.9(1)
O(1') - Sb(1) - O(2)	85.5(1)
O(1) - Sb(1) - O(3)	85.3(1)
O(1') - Sb(1) - O(3)	90.7(1)
O(2) - Sb(1) - O(3)	174.3(1)
O(1) - Sb(1) - C(1)	92.5(1)
O(1') - Sb(1) - C(1)	170.0(1)
O(2) - Sb(1) - C(1)	88.6(1)
O(3) - Sb(1) - C(1)	94.6(1)
O(1) - Sb(1) - C(7)	169.3(1)
O(1') - Sb(1) - C(7)	91.1(1)
O(2) - Sb(1) - C(7)	94.7(1)
O(3) - Sb(1) - C(7)	89.6(1)
C(1) - Sb(1) - C(7)	97.4(1)
O(2) - As(1) - O(3')	114.0(1)
O(2) - As(1) - C(13)	106.0(2)
O(3') - As(1) - C(13)	105.5(2)
O(2) - As(1) - C(14)	109.4(2)
O(3') - As(1) - C(14)	111.7(2)
C(13) - As(1) - C(14)	110.0(2)
Sb(1) - O(1) - Sb(1')	100.5(1)
Sb(1) - O(2) - As(1)	119.0(1)
Sb(1) - O(3) - As(1')	119.5(1)
Sb(1) - C(1) - C(2)	120.3(3)
Sb(1) - C(1) - C(6)	120.5(3)
C(2) - C(1) - C(6)	119.0(4)
C(1) - C(2) - C(3)	120.6(4)
C(2) - C(3) - C(4)	119.6(4)
C(3) - C(4) - C(5)	120.0(4)
C(4) - C(5) - C(6)	120.5(4)
C(1) - C(6) - C(5)	120.2(4)
Sb(1) - C(7) - C(8)	119.8(3)
Sb(1) - C(7) - C(12)	121.2(3)
C(8) - C(7) - C(12)	118.9(4)
C(7) - C(8) - C(9)	120.0(4)
C(8) - C(9) - C(10)	120.2(4)
C(9) - C(10) - C(11)	119.9(4)
C(10) - C(11) - C(12)	120.7(4)
C(7) - C(12) - C(11)	120.2(4)
Cl(1) - C(100)- Cl(2)	110.7(2)
Cl(1) - C(100)- Cl(3)	110.4(2)
Cl(2) - C(100)- Cl(3)	111.2(3)

Symmetry operation: (') = 1-x, 1-y, 2-z

Experimental Details

Slightly more than one hemisphere of data were collected on a Delft Instruments FAST TV area detector, equipped with a rotating anode FR591 generator. The data were corrected for Lorentz and polarisation effects, merged and systematically absent reflections were rejected. The structure was solved by direct methods (SIR-92)[5] and subsequent Fourier difference syntheses revealed the positions of all the other non-hydrogen atoms. Refinement was carried out against 'observed' F_o data by full matrix procedures. Hydrogen atoms were placed in estimated positions (C–H = 1.00 Å), assigned a common fixed thermal parameter and refined 'riding' their respective carbon atoms. Data were corrected by a Chebyshev weighting scheme[6] (4 coefficient) and also for the effects of absorption[4], anomalous dispersion and isotropic extinction[7]. All crystallographic calculations were performed using the CRYSTALS suite of programs[8] and neutral atom scattering factors were taken from the usual sources[3].

APPENDIX D

Table D.1 Data collection and processing parameters for [((*p*-$MeC_6H_4)_2Sb)_2(\mu$-$O)_2(\mu$-$O_2AsMe_2)_2$] (3.4)

Chemical formula	$C_{32}H_{40}As_2O_6Sb_2$
Formula weight	913.98
Crystal size/mm	0.35 x 0.24 x 0.06
Crystal system	Monoclinic
Space group	$P2_1/c$
a / Å	13.3821(13)
b / Å	11.4790(10)
c / Å	11.2265(10)
β / °	99.411(5)
Volume / Å^3	1701.3(3)
Z	2
D_c/gcm^{-3}	1.784
Radiation (λ / Å)	Mo-K_α (0.71069)
μ / cm^{-1}	35.58
F(000)	896
2θ limits / °	4.70 to 51.78
Index ranges	-10<=h<=16, -12<=k<=13, -11<=l<=13
Temperature / K	150
Total data collected	7176
Unique data	2960 [R(int) = 0.0502]
Absorption correction	Gaussian (min, 0.394, max, 0.810)
Structure solution	Direct (SHELXS-86)[1]
Refinement procedure	Full matrix-LS on F^2
Number of data / variables	2933 / 195
Goodness-of-fit on F^2	1.065
Max/min peaks in final diff. map / e Å^{-3}	+0.640, -1.120
R observed data [$I > 2\sigma(I)$], (all data)	0.0315, (0.0355)
R_w observed data, (all data)	0.0794, (0.0873)

Table D.2 Atomic coordinates (x 10^4) and equivalent isotropic displacement parameters ($Å^2$ x 10^3) with estimated standard deviations in parentheses for [((*p*-$MeC_6H_4)_2Sb)_2(\mu$-$O)_2(\mu$-$O_2AsMe_2)_2$] (3.4)

Atom	x	y	z	U(eq)
Sb(1)	1165(1)	5114(1)	335(1)	23(1)
As(1)	-238(1)	7180(1)	1185(1)	24(1)
O(1)	1233(2)	3390(3)	-227(3)	29(1)
O(2)	908(2)	6833(3)	810(3)	28(1)
O(3)	-54(2)	4731(3)	1092(2)	26(1)
C(1)	2309(3)	5678(4)	-675(4)	28(1)
C(2)	2039(3)	5988(4)	-1884(4)	34(1)
C(3)	2764(4)	6341(4)	-2550(4)	37(1)
C(4)	3784(3)	6394(4)	-2029(4)	36(1)
C(5)	4037(4)	6098(6)	-831(5)	51(1)
C(6)	3312(4)	5731(5)	-158(5)	45(1)
C(7)	4577(4)	6812(6)	-2754(5)	57(2)
C(8)	2125(3)	4690(4)	2020(4)	28(1)
C(9)	2421(3)	5557(4)	2877(4)	32(1)
C(10)	2984(4)	5274(5)	3993(4)	38(1)
C(11)	3246(3)	4124(5)	4285(4)	36(1)
C(12)	2957(3)	3269(4)	3425(4)	37(1)
C(13)	2411(3)	3553(4)	2301(4)	30(1)
C(14)	3851(4)	3812(6)	5506(5)	53(1)
C(15)	-380(3)	8818(4)	953(4)	30(1)
C(16)	-257(4)	6789(4)	2829(4)	31(1)

Table D.3 Anisotropic thermal parameters ($Å^2$ x 10^3) with estimated standard deviations in parentheses for [((*p*-$MeC_6H_4)_2Sb)_2(\mu$-$O)_2(\mu$-$O_2AsMe_2)_2$] (3.4)

Atom	U11	U22	U33	U23	U13	U12
Sb(1)	24(1)	23(1)	22(1)	0(1)	5(1)	0(1)
As(1)	29(1)	22(1)	22(1)	-1(1)	5(1)	1(1)
O(1)	27(2)	30(2)	28(2)	-3(1)	5(1)	2(1)
O(2)	31(2)	25(2)	27(2)	-2(1)	6(1)	2(1)
O(3)	28(2)	25(2)	24(2)	-2(1)	4(1)	0(1)
C(1)	32(2)	26(2)	28(2)	0(2)	9(2)	-1(2)
C(2)	27(2)	45(3)	32(2)	4(2)	6(2)	-1(2)
C(3)	39(3)	45(3)	27(2)	3(2)	9(2)	3(2)
C(4)	31(2)	45(3)	33(2)	-5(2)	13(2)	-10(2)
C(5)	29(3)	83(4)	40(3)	6(3)	4(2)	-9(3)
C(6)	31(2)	66(4)	37(3)	10(3)	4(2)	-7(2)
C(7)	45(3)	88(5)	42(3)	-4(3)	17(2)	-20(3)
C(8)	26(2)	33(2)	24(2)	3(2)	6(2)	0(2)
C(9)	32(2)	33(2)	30(2)	0(2)	4(2)	-3(2)
C(10)	35(3)	42(3)	36(3)	-4(2)	2(2)	0(2)
C(11)	26(2)	52(3)	30(2)	7(2)	4(2)	3(2)
C(12)	34(2)	39(3)	37(3)	7(2)	5(2)	3(2)
C(13)	31(2)	32(2)	28(2)	4(2)	4(2)	0(2)
C(14)	56(3)	66(4)	35(3)	8(3)	-2(2)	4(3)
C(15)	36(2)	25(2)	29(2)	-1(2)	7(2)	0(2)
C(16)	41(2)	26(2)	28(2)	0(2)	10(2)	4(2)

Table D.4 Bond lengths (Å) with estimated standard deviations in parentheses for [((*p*-$MeC_6H_4)_2Sb)_2(\mu\text{-}O)_2(\mu\text{-}O_2AsMe_2)_2$] (3.4)

Sb(1)-O(3)#1	2.007(3)
Sb(1)-O(3)	2.007(3)
Sb(1)-O(1)	2.084(3)
Sb(1)-O(2)	2.087(3)
Sb(1)-C(1)	2.148(4)
Sb(1)-C(8)	2.161(4)
Sb(1)-Sb(1)#1	3.0975(6)
As(1)-O(1)#1	1.701(3)
As(1)-O(2)	1.703(3)
As(1)-C(16)	1.903(4)
As(1)-C(15)	1.904(4)
O(1)-As(1)#1	1.701(3)
O(3)-Sb(1)#1	2.007(3)
C(1)-C(6)	1.374(6)
C(1)-C(2)	1.392(6)
C(2)-C(3)	1.379(6)
C(3)-C(4)	1.396(6)
C(4)-C(5)	1.374(7)
C(4)-C(7)	1.517(6)
C(5)-C(6)	1.389(7)
C(8)-C(13)	1.382(6)
C(8)-C(9)	1.395(6)
C(9)-C(10)	1.391(7)
C(10)-C(11)	1.392(7)
C(11)-C(12)	1.386(7)
C(11)-C(14)	1.517(7)
C(12)-C(13)	1.390(6)

Table D.5 Bond angles (°) with estimated standard deviations in parentheses for [((*p*-$MeC_6H_4)_2Sb)_2(\mu\text{-}O)_2(\mu\text{-}O_2AsMe_2)_2$] (3.4)

O(3)#1-Sb(1)-O(3)	79.02(12)
O(3)#1-Sb(1)-O(1)	84.60(12)
O(3)-Sb(1)-O(1)	89.92(12)
O(3)#1-Sb(1)-O(2)	89.36(11)
O(3)-Sb(1)-O(2)	85.41(11)
O(1)-Sb(1)-O(2)	172.98(11)
O(3)#1-Sb(1)-C(1)	92.92(14)
O(3)-Sb(1)-C(1)	171.04(14)
O(1)-Sb(1)-C(1)	93.23(14)
O(2)-Sb(1)-C(1)	90.64(14)
O(3)#1-Sb(1)-C(8)	167.18(14)
O(3)-Sb(1)-C(8)	89.33(14)
O(1)-Sb(1)-C(8)	90.1(2)
O(2)-Sb(1)-C(8)	95.08(14)
C(1)-Sb(1)-C(8)	99.0(2)
O(3)#1-Sb(1)-Sb(1)#1	39.51(8)
O(3)-Sb(1)-Sb(1)#1	39.51(8)
O(1)-Sb(1)-Sb(1)#1	86.46(8)
O(2)-Sb(1)-Sb(1)#1	86.61(8)
C(1)-Sb(1)-Sb(1)#1	132.31(12)
C(8)-Sb(1)-Sb(1)#1	128.63(11)
O(1)#1-As(1)-O(2)	113.43(14)
O(1)#1-As(1)-C(16)	112.9(2)
O(2)-As(1)-C(16)	109.9(2)
O(1)#1-As(1)-C(15)	104.0(2)
O(2)-As(1)-C(15)	105.7(2)
C(16)-As(1)-C(15)	110.4(2)
As(1)#1-O(1)-Sb(1)	119.2(2)
As(1)-O(2)-Sb(1)	118.5(2)
Sb(1)#1-O(3)-Sb(1)	100.98(12)
C(6)-C(1)-C(2)	118.7(4)
C(6)-C(1)-Sb(1)	121.5(3)
C(2)-C(1)-Sb(1)	119.9(3)
C(3)-C(2)-C(1)	120.7(4)
C(2)-C(3)-C(4)	120.7(4)
C(5)-C(4)-C(3)	117.8(4)
C(5)-C(4)-C(7)	121.5(5)
C(3)-C(4)-C(7)	120.7(4)
C(4)-C(5)-C(6)	121.7(5)
C(1)-C(6)-C(5)	120.3(5)
C(13)-C(8)-C(9)	118.6(4)
C(13)-C(8)-Sb(1)	121.0(3)
C(9)-C(8)-Sb(1)	120.3(3)
C(10)-C(9)-C(8)	120.4(4)
C(9)-C(10)-C(11)	120.8(5)
C(12)-C(11)-C(10)	118.5(4)
C(12)-C(11)-C(14)	120.6(5)
C(10)-C(11)-C(14)	120.9(5)
C(11)-C(12)-C(13)	120.8(4)
C(8)-C(13)-C(12)	120.9(4)

Symmetry transformations used to generate equivalent atoms: #1 -x,-y+1,-z

Experimental Details

A hemisphere of data were collected on a Siemens SMART area detector. The data were corrected for Lorentz, polarisation and absorption effects (Gaussian), merged and systematically absent reflections rejected. The structure was solved by direct methods (SHELXS-86)[1] and subsequent Fourier difference syntheses revealed the positions of all the other non-hydrogen atoms. Refinement was carried out against all F_o^2 data by full matrix procedures (SHELXL-93)[2]. Hydrogen atoms were placed in estimated positions [C–H = 0.95 (aromatic ring hydrogens), 0.98 (methyl group) Å], with fixed isotropic parameters (1.2 x equivalent isotropic temperature factors of the carbon atom to which they were bonded for aryl protons and 1.5 x for methyl protons) and refined 'riding' their respective carbon atoms. A standard weighting scheme was applied and the data were corrected for isotropic extinction. All crystallographic calculations were performed using the SHELXS-86[1] and SHELXL-93[2] programs and neutral atom scattering factors were taken from the usual sources[3].

APPENDIX E

Table E.1 Data collection and processing parameters for $[(Ph_3Sb)_2(\mu\text{-}O)(\mu\text{-}O_2PMe_2)_2].0.5C_6H_{14}$ ($3.3.0.5C_6H_{14}$)

Chemical formula	$C_{43}H_{49}O_5P_2Sb_2$
Formula weight	951.30
Crystal size/mm	0.20 x 0.18 x 0.14
Crystal system	Monoclinic
Space group	*C*2/*c*
a / Å	26.704(3)
b / Å	16.879(3)
c / Å	22.1874(12)
β / °	125.35(1)
Volume / Å^3	8157.06
Z	8
D_c/gcm^{-3}	1.5493
Radiation (λ / Å)	Mo-K_α (0.71069)
μ / cm^{-1}	14.518
F(000)	3832
2θ limits / °	5-50
Index ranges (for unique data set)	-29<=h<=23, 0<=k<=18, 0<=l<=25
Temperature / K	120
Total data collected	17558
Unique data	6171 [(R(int) = 0.0481]
Observed data [$I > 2\sigma(I)$]	4315
Absorption correction	DIFABS (min, 0.855, max, 1.160)[4]
Structure solution	Direct (SIR-92)[5]
Refinement procedure	Full matrix-LS on F^2
Number of data / variables	4315 / 455
S	1.080
Max/min peaks in final diff. map / e Å^{-3}	+1.10, -0.728
R	0.0344
R_w	0.0698

Table E.2 Fractional atomic coordinates and equivalent isotropic displacement parameters ($Å^2$) with estimated standard deviations in parentheses for $[(Ph_3Sb)_2(\mu\text{-}O)(\mu\text{-}O_2PMe_2)_2].0.5C_6H_{14}$ ($3.3.0.5C_6H_{14}$)

Atom	x/a	y/b	z/c	U(eq)
Sb(1)	0.66345(1)	0.19840(2)	0.62521(2)	0.0152
Sb(2)	0.71994(1)	0.16343(2)	0.82053(2)	0.0150
P(1)	0.58436(6)	0.09249(8)	0.66989(7)	0.0182
P(2)	0.75026(6)	0.03997(8)	0.72769(7)	0.0187
O(1)	0.6984(2)	0.2153(2)	0.7298(2)	0.0175
O(2)	0.6438(2)	0.0830(2)	0.7463(2)	0.0190
O(3)	0.5856(2)	0.1544(2)	0.6205(2)	0.0198
O(4)	0.7697(2)	0.0824(2)	0.7982(2)	0.0187
O(5)	0.6964(2)	0.0776(2)	0.6569(2)	0.0175
C(1)	0.5243(2)	0.1184(4)	0.6800(3)	0.0263
C(2)	0.5650(3)	-0.0011(3)	0.6236(3)	0.0261
C(3)	0.7310(3)	-0.0604(3)	0.7315(3)	0.0256
C(4)	0.8161(3)	0.0368(4)	0.7249(3)	0.0288
C(11)	0.6146(2)	0.1517(3)	0.5141(3)	0.0180
C(12)	0.5664(2)	0.1966(4)	0.4574(3)	0.0233
C(13)	0.5339(3)	0.1698(4)	0.3846(3)	0.0284
C(14)	0.5489(3)	0.0988(4)	0.3670(3)	0.0275
C(15)	0.5975(3)	0.0548(4)	0.4237(3)	0.0294
C(16)	0.6296(3)	0.0802(3)	0.4960(3)	0.0250
C(21)	0.6221(2)	0.3141(3)	0.5968(3)	0.0166
C(22)	0.5720(2)	0.3333(3)	0.5978(3)	0.0245
C(23)	0.5495(3)	0.4110(4)	0.5835(3)	0.0320
C(24)	0.5766(3)	0.4687(4)	0.5675(3)	0.0308
C(25)	0.6251(3)	0.4500(4)	0.5636(3)	0.0339
C(26)	0.6482(2)	0.3727(3)	0.5787(3)	0.0239
C(31)	0.7493(2)	0.2285(3)	0.6425(3)	0.0154
C(32)	0.7960(2)	0.2623(3)	0.7103(3)	0.0224
C(33)	0.8523(3)	0.2808(3)	0.7235(3)	0.0289
C(34)	0.8636(3)	0.2640(4)	0.6712(3)	0.0306
C(35)	0.8182(3)	0.2312(3)	0.6050(3)	0.0259
C(36)	0.7609(3)	0.2132(3)	0.5905(3)	0.0208
C(41)	0.7403(2)	0.0786(3)	0.9043(3)	0.0171
C(42)	0.7206(2)	0.0006(3)	0.8901(3)	0.0215
C(43)	0.7379(3)	-0.0513(3)	0.9480(3)	0.0250
C(44)	0.7741(3)	-0.0241(3)	1.0202(3)	0.0269
C(45)	0.7929(3)	0.0532(4)	1.0348(3)	0.0313
C(46)	0.7765(3)	0.1046(3)	0.9774(3)	0.0252
C(51)	0.8030(2)	0.2328(3)	0.8866(3)	0.0200
C(52)	0.8584(3)	0.2101(4)	0.8981(3)	0.0355
C(53)	0.9101(3)	0.2576(5)	0.9380(4)	0.0405
C(54)	0.9088(3)	0.3265(4)	0.9682(3)	0.0340
C(55)	0.8558(3)	0.3504(4)	0.9600(3)	0.0301
C(56)	0.8020(3)	0.3036(3)	0.9191(3)	0.0273
C(61)	0.6578(2)	0.2375(3)	0.8273(3)	0.0206
C(62)	0.6406(3)	0.2193(3)	0.8743(3)	0.0251
C(63)	0.5991(3)	0.2677(4)	0.8766(3)	0.0290
C(64)	0.5744(2)	0.3329(4)	0.8321(3)	0.0279
C(65)	0.5916(3)	0.3527(3)	0.7851(3)	0.0284
C(66)	0.6327(2)	0.3049(3)	0.7825(3)	0.0203
C(101)	0.5142(5)	0.3899(7)	0.1425(7)	0.100(3)
C(102)	0.4597(7)	0.410(1)	0.1461(9)	0.154(6)
C(103)	0.474(1)	0.413(1)	0.225(1)	0.21(1)

Table E.3 Calculated hydrogen coordinates and isotropic displacement parameters ($Å^2$) with estimated standard deviations in parentheses for $[(Ph_3Sb)_2(\mu\text{-}O)(\mu\text{-}O_2PMe_2)_2].0.5C_6H_{14}$ ($3.3.0.5C_6H_{14}$)

Atom	x/a	y/b	z/c	U(iso)
H(1)	0.5338(2)	0.1706(4)	0.7059(3)	0.0350
H(2)	0.5212(2)	0.0766(4)	0.7096(3)	0.0350
H(3)	0.4844(2)	0.1222(4)	0.6301(3)	0.0350
H(4)	0.5975(3)	-0.0173(3)	0.6170(3)	0.0350
H(5)	0.5615(3)	-0.0418(3)	0.6537(3)	0.0350
H(6)	0.5248(3)	0.0038(3)	0.5742(3)	0.0350
H(7)	0.6946(3)	-0.0610(3)	0.7335(3)	0.0350
H(8)	0.7665(3)	-0.0865(3)	0.7767(3)	0.0350
H(9)	0.7210(3)	-0.0897(3)	0.6866(3)	0.0350
H(10)	0.8283(3)	0.0921(4)	0.7225(3)	0.0350
H(11)	0.8509(3)	0.0099(4)	0.7701(3)	0.0350
H(12)	0.8054(3)	0.0068(4)	0.6800(3)	0.0350
H(121)	0.5550(2)	0.2478(4)	0.4692(3)	0.0350
H(131)	0.4989(3)	0.2022(4)	0.3445(3)	0.0350
H(141)	0.5253(3)	0.0803(4)	0.3146(3)	0.0350
H(151)	0.6093(3)	0.0044(4)	0.4114(3)	0.0350
H(161)	0.6637(3)	0.0471(3)	0.5364(3)	0.0350
H(221)	0.5518(2)	0.2912(3)	0.6085(3)	0.0350
H(231)	0.5137(3)	0.4245(4)	0.5849(3)	0.0350
H(241)	0.5612(3)	0.5244(4)	0.5592(3)	0.0350
H(251)	0.6436(3)	0.4915(4)	0.5498(3)	0.0350
H(261)	0.6840(2)	0.3593(3)	0.5775(3)	0.0350
H(321)	0.7887(2)	0.2729(3)	0.7491(3)	0.0350
H(331)	0.8845(3)	0.3070(3)	0.7712(3)	0.0350
H(341)	0.9048(3)	0.2756(4)	0.6822(3)	0.0350
H(351)	0.8257(3)	0.2202(3)	0.5665(3)	0.0350
H(361)	0.7280(3)	0.1888(3)	0.5422(3)	0.0350
H(421)	0.6945(2)	-0.0188(3)	0.8380(3)	0.0350
H(431)	0.7237(3)	-0.1076(3)	0.9374(3)	0.0350
H(441)	0.7867(3)	-0.0613(3)	1.0618(3)	0.0350
H(451)	0.8189(3)	0.0726(4)	1.0870(3)	0.0350
H(461)	0.7902(3)	0.1611(3)	0.9883(3)	0.0350
H(521)	0.8606(3)	0.1582(4)	0.8780(3)	0.0350
H(531)	0.9485(3)	0.2408(5)	0.9436(4)	0.0350
H(541)	0.9465(3)	0.3602(4)	0.9967(3)	0.0350
H(551)	0.8556(3)	0.4011(4)	0.9831(3)	0.0350
H(561)	0.7637(3)	0.3205(3)	0.9137(3)	0.0350
H(621)	0.6583(3)	0.1715(3)	0.9068(3)	0.0350
H(631)	0.5876(3)	0.2544(4)	0.9110(3)	0.0350
H(641)	0.5443(2)	0.3670(4)	0.8331(3)	0.0350
H(651)	0.5739(3)	0.4007(3)	0.7528(3)	0.0350
H(661)	0.6448(2)	0.3190(3)	0.7489(3)	0.0350
H(1011)	0.5034(5)	0.3923(7)	0.0912(7)	0.1200
H(1012)	0.5492(5)	0.4266(7)	0.1751(7)	0.1200
H(1013)	0.5264(5)	0.3345(7)	0.1617(7)	0.1200
H(1021)	0.4472(7)	0.466(1)	0.1275(9)	0.1200
H(1022)	0.4244(7)	0.374(1)	0.1141(9)	0.1200

Table E.4 Anisotropic thermal parameters ($Å^2$) with estimated standard deviations in parentheses for $[(Ph_3Sb)_2(\mu\text{-}O)(\mu\text{-}O_2PMe_2)_2].0.5C_6H_{14}$ ($3.3.0.5C_6H_{14}$)

Atom	U(11)	U(22)	U(33)	U(23)	U(13)	U(12)
Sb(1)	0.0150(2)	0.0148(2)	0.0156(2)	0.0009(1)	0.0086(1)	-0.0001(1)
Sb(2)	0.0170(2)	0.0130(2)	0.0157(2)	-0.0009(1)	0.0096(1)	-0.0014(1)
P(1)	0.0171(7)	0.0196(7)	0.0204(7)	-0.0011(5)	0.0116(6)	-0.0036(5)
P(2)	0.0219(7)	0.0157(7)	0.0191(7)	0.0004(5)	0.0117(6)	0.0025(5)
O(1)	0.022(2)	0.018(2)	0.015(2)	0.001(1)	0.012(2)	0.001(1)
O(2)	0.020(2)	0.015(2)	0.022(2)	-0.000(1)	0.011(2)	-0.004(1)
O(3)	0.016(2)	0.023(2)	0.021(2)	0.001(1)	0.010(2)	-0.000(1)
O(4)	0.018(2)	0.021(2)	0.017(2)	0.001(1)	0.010(2)	0.003(1)
O(5)	0.021(2)	0.011(2)	0.021(2)	-0.002(1)	0.009(2)	0.001(1)
C(1)	0.019(3)	0.037(4)	0.029(3)	-0.001(2)	0.015(3)	0.000(2)
C(2)	0.023(3)	0.026(3)	0.027(3)	-0.003(2)	0.011(3)	-0.006(2)
C(3)	0.041(3)	0.014(3)	0.027(3)	0.000(2)	0.017(3)	0.001(2)
C(4)	0.031(3)	0.036(4)	0.032(3)	0.004(3)	0.021(3)	0.013(3)
C(11)	0.018(3)	0.025(3)	0.017(3)	0.000(2)	0.010(2)	-0.009(2)
C(12)	0.016(3)	0.032(3)	0.022(3)	0.001(2)	0.010(2)	-0.002(2)
C(13)	0.018(3)	0.052(4)	0.018(3)	0.004(3)	0.005(2)	-0.004(3)
C(14)	0.031(3)	0.045(4)	0.019(3)	-0.007(3)	0.012(3)	-0.021(3)
C(15)	0.038(4)	0.027(3)	0.031(3)	-0.008(3)	0.021(3)	-0.012(3)
C(16)	0.034(3)	0.020(3)	0.025(3)	0.001(2)	0.017(3)	-0.004(2)
C(21)	0.014(3)	0.018(3)	0.013(2)	0.003(2)	0.003(2)	0.003(2)
C(22)	0.026(3)	0.025(3)	0.022(3)	0.007(2)	0.012(2)	0.006(2)
C(23)	0.029(3)	0.037(4)	0.034(3)	0.001(3)	0.016(3)	0.012(3)
C(24)	0.031(4)	0.025(3)	0.030(3)	0.006(2)	0.006(3)	0.009(3)
C(25)	0.036(4)	0.028(4)	0.031(3)	0.006(3)	0.012(3)	0.000(3)
C(26)	0.018(3)	0.026(3)	0.026(3)	0.008(2)	0.009(2)	0.003(2)
C(31)	0.015(3)	0.011(3)	0.022(3)	0.003(2)	0.008(2)	-0.002(2)
C(32)	0.024(3)	0.022(3)	0.026(3)	-0.003(2)	0.017(3)	-0.003(2)
C(33)	0.024(3)	0.030(3)	0.035(3)	-0.004(2)	0.015(3)	-0.009(2)
C(34)	0.028(3)	0.034(4)	0.052(4)	0.004(3)	0.029(3)	-0.001(3)
C(35)	0.037(3)	0.025(3)	0.041(3)	0.005(3)	0.032(3)	0.003(3)
C(36)	0.030(3)	0.017(3)	0.022(3)	0.004(2)	0.017(2)	0.003(2)
C(41)	0.016(3)	0.018(3)	0.021(3)	0.004(2)	0.012(2)	0.003(2)
C(42)	0.028(3)	0.017(3)	0.024(3)	-0.002(2)	0.017(3)	-0.003(2)
C(43)	0.037(3)	0.017(3)	0.033(3)	0.000(2)	0.024(3)	-0.004(2)
C(44)	0.034(3)	0.032(3)	0.021(3)	0.008(2)	0.016(3)	-0.001(3)
C(45)	0.036(4)	0.034(4)	0.021(3)	-0.001(2)	0.012(3)	-0.007(3)
C(46)	0.034(3)	0.018(3)	0.025(3)	-0.001(2)	0.014(3)	-0.007(2)
C(51)	0.023(3)	0.019(3)	0.016(3)	0.000(2)	0.005(2)	-0.008(2)
C(52)	0.027(3)	0.049(4)	0.033(3)	-0.011(3)	0.013(3)	-0.013(3)
C(53)	0.027(4)	0.093(6)	0.033(4)	-0.011(4)	0.018(3)	-0.022(4)
C(54)	0.038(4)	0.062(5)	0.023(3)	-0.001(3)	0.009(3)	-0.031(3)
C(55)	0.064(5)	0.022(4)	0.018(3)	0.001(2)	0.008(3)	-0.016(3)
C(56)	0.042(4)	0.023(3)	0.019(3)	-0.003(2)	0.013(3)	-0.009(3)
C(61)	0.018(3)	0.025(3)	0.020(3)	-0.006(2)	0.011(2)	-0.002(2)
C(62)	0.026(3)	0.020(3)	0.028(3)	-0.002(2)	0.014(3)	-0.004(2)
C(63)	0.028(3)	0.035(4)	0.038(3)	-0.006(3)	0.024(3)	-0.004(3)
C(64)	0.019(3)	0.035(4)	0.038(3)	-0.008(3)	0.015(3)	0.001(2)
C(65)	0.031(3)	0.027(3)	0.029(3)	0.004(2)	0.017(3)	0.009(2)
C(66)	0.020(3)	0.021(3)	0.018(3)	-0.003(2)	0.009(2)	-0.001(2)

Table E.5 Bond lengths (Å) with estimated standard deviations in parentheses for $[(Ph_3Sb)_2(\mu\text{-}O)(\mu\text{-}O_2PMe_2)_2].0.5C_6H_{14}$ ($3.3.0.5C_6H_{14}$)

Sb(1) - O(1)	1.958(3)	C(23) - C(24)	1.376(9)
Sb(1) - O(3)	2.153(3)	C(24) - C(25)	1.385(9)
Sb(1) - O(5)	2.171(3)	C(25) - C(26)	1.398(8)
Sb(1) - C(11)	2.164(5)	C(31) - C(32)	1.406(7)
Sb(1) - C(21)	2.152(5)	C(31) - C(36)	1.383(7)
Sb(1) - C(31)	2.155(5)	C(32) - C(33)	1.390(8)
Sb(2) - O(1)	1.952(3)	C(33) - C(34)	1.388(8)
Sb(2) - O(2)	2.194(3)	C(34) - C(35)	1.367(8)
Sb(2) - O(4)	2.154(3)	C(35) - C(36)	1.402(8)
Sb(2) - C(41)	2.153(5)	C(41) - C(42)	1.384(7)
Sb(2) - C(51)	2.163(5)	C(41) - C(46)	1.393(7)
Sb(2) - C(61)	2.151(5)	C(42) - C(43)	1.394(7)
P(1) - O(2)	1.519(4)	C(43) - C(44)	1.385(8)
P(1) - O(3)	1.528(4)	C(44) - C(45)	1.369(8)
P(1) - C(1)	1.798(5)	C(45) - C(46)	1.385(8)
P(1) - C(2)	1.789(6)	C(51) - C(52)	1.402(9)
P(2) - O(4)	1.514(4)	C(51) - C(56)	1.405(8)
P(2) - O(5)	1.525(4)	C(52) - C(53)	1.384(9)
P(2) - C(3)	1.787(6)	C(53) - C(54)	1.35(1)
P(2) - C(4)	1.795(6)	C(54) - C(55)	1.38(1)
C(11) - C(12)	1.393(7)	C(55) - C(56)	1.415(9)
C(11) - C(16)	1.400(8)	C(61) - C(62)	1.397(8)
C(12) - C(13)	1.393(8)	C(61) - C(66)	1.400(8)
C(13) - C(14)	1.391(9)	C(62) - C(63)	1.399(8)
C(14) - C(15)	1.388(9)	C(63) - C(64)	1.367(8)
C(15) - C(16)	1.378(8)	C(64) - C(65)	1.401(8)
C(21) - C(22)	1.388(7)	C(65) - C(66)	1.389(8)
C(21) - C(26)	1.395(7)	C(101)- C(102)	1.54(2)
C(22) - C(23)	1.400(8)	C(102)- C(103)	1.56(3)
		C(103)- C(103')	1.18(4)

Table E.6 Bond angles (°) with estimated standard deviations in parentheses for $[(Ph_3Sb)_2(\mu\text{-}O)(\mu\text{-}O_2PMe_2)_2].0.5C_6H_{14}$ ($3.3.0.5C_6H_{14}$)

O(1) - Sb(1) - O(3)	83.8(1)	C(12) - C(11) - C(16)	118.6(5)
O(1) - Sb(1) - O(5)	85.8(1)	C(11) - C(12) - C(13)	120.0(6)
O(3) - Sb(1) - O(5)	83.7(1)	C(12) - C(13) - C(14)	121.1(5)
O(1) - Sb(1) - C(11)	164.5(2)	C(13) - C(14) - C(15)	118.4(5)
O(3) - Sb(1) - C(11)	83.7(2)	C(14) - C(15) - C(16)	121.0(6)
O(5) - Sb(1) - C(11)	83.7(2)	C(11) - C(16) - C(15)	120.8(5)
O(1) - Sb(1) - C(21)	91.5(2)	Sb(1) - C(21) - C(22)	122.9(4)
O(3) - Sb(1) - C(21)	88.9(2)	Sb(1) - C(21) - C(26)	118.1(4)
O(5) - Sb(1) - C(21)	172.4(2)	C(22) - C(21) - C(26)	119.0(5)
C(11) - Sb(1) - C(21)	97.4(2)	C(21) - C(22) - C(23)	120.4(5)
O(1) - Sb(1) - C(31)	91.5(2)	C(22) - C(23) - C(24)	120.0(6)
O(3) - Sb(1) - C(31)	171.2(2)	C(23) - C(24) - C(25)	120.4(6)
O(5) - Sb(1) - C(31)	88.5(2)	C(24) - C(25) - C(26)	119.7(6)
C(11) - Sb(1) - C(31)	99.6(2)	C(21) - C(26) - C(25)	120.5(5)
C(21) - Sb(1) - C(31)	98.7(2)	Sb(1) - C(31) - C(32)	118.7(4)

O(1) - Sb(2) - O(2)	84.9(1)	Sb(1) - C(31) - C(36)	122.5(4)
O(1) - Sb(2) - O(4)	84.3(1)	C(32) - C(31) - C(36)	118.8(5)
O(2) - Sb(2) - O(4)	82.0(1)	C(31) - C(32) - C(33)	119.9(5)
O(1) - Sb(2) - C(41)	165.0(2)	C(32) - C(33) - C(34)	120.6(5)
O(2) - Sb(2) - C(41)	84.1(2)	C(33) - C(34) - C(35)	119.7(5)
O(4) - Sb(2) - C(41)	84.0(2)	C(34) - C(35) - C(36)	120.4(5)
O(1) - Sb(2) - C(51)	91.8(2)	C(31) - C(36) - C(35)	120.7(5)
O(2) - Sb(2) - C(51)	170.2(2)	Sb(2) - C(41) - C(42)	124.3(4)
O(4) - Sb(2) - C(51)	88.4(2)	Sb(2) - C(41) - C(46)	116.9(4)
C(41) - Sb(2) - C(51)	97.3(2)	C(42) - C(41) - C(46)	118.8(5)
O(1) - Sb(2) - C(61)	91.8(2)	C(41) - C(42) - C(43)	120.5(5)
O(2) - Sb(2) - C(61)	89.7(2)	C(42) - C(43) - C(44)	119.6(5)
O(4) - Sb(2) - C(61)	171.2(2)	C(43) - C(44) - C(45)	120.3(5)
C(41) - Sb(2) - C(61)	98.4(2)	C(44) - C(45) - C(46)	120.1(5)
C(51) - Sb(2) - C(61)	99.7(2)	C(41) - C(46) - C(45)	120.6(5)
O(2) - P(1) - O(3)	115.5(2)	Sb(2) - C(51) - C(52)	122.5(4)
O(2) - P(1) - C(1)	108.6(2)	Sb(2) - C(51) - C(56)	119.5(4)
O(3) - P(1) - C(1)	108.3(2)	C(52) - C(51) - C(56)	118.1(5)
O(2) - P(1) - C(2)	108.4(2)	C(51) - C(52) - C(53)	121.0(7)
O(3) - P(1) - C(2)	108.1(2)	C(52) - C(53) - C(54)	120.9(7)
C(1) - P(1) - C(2)	107.7(3)	C(53) - C(54) - C(55)	120.2(6)
O(4) - P(2) - O(5)	115.0(2)	C(54) - C(55) - C(56)	120.4(6)
O(4) - P(2) - C(3)	109.6(2)	C(51) - C(56) - C(55)	119.4(6)
O(5) - P(2) - C(3)	108.5(2)	Sb(2) - C(61) - C(62)	121.7(4)
O(4) - P(2) - C(4)	107.1(2)	Sb(2) - C(61) - C(66)	119.7(4)
O(5) - P(2) - C(4)	109.6(2)	C(62) - C(61) - C(66)	118.6(5)
C(3) - P(2) - C(4)	106.7(3)	C(61) - C(62) - C(63)	120.5(5)
Sb(1) - O(1) - Sb(2)	144.2(2)	C(62) - C(63) - C(64)	120.4(5)
Sb(2) - O(2) - P(1)	133.6(2)	C(63) - C(64) - C(65)	120.1(5)
Sb(1) - O(3) - P(1)	128.4(2)	C(64) - C(65) - C(66)	119.8(5)
Sb(2) - O(4) - P(2)	130.6(2)	C(61) - C(66) - C(65)	120.6(5)
Sb(1) - O(5) - P(2)	133.5(2)	C(101)- C(102)- C(103)	116.0(15)
Sb(1) - C(11) - C(12)	117.6(4)	C(102)- C(103)- C(103')	116.7(35)
Sb(1) - C(11) - C(16)	123.8(4)		

Symmetry operation: (') = 1-x, y, 0.5-z

Experimental Details

Slightly more than one hemisphere of data were collected on a Delft Instruments FAST TV area detector, equipped with a rotating anode FR591 generator. The data were corrected for Lorentz and polarisation effects, merged and systematically absent reflections were rejected. The structure was solved by direct methods (SIR-92)[5] and subsequent Fourier difference syntheses revealed the positions of all the other non-hydrogen atoms. Refinement was carried out against 'observed' F_o^2 data by full matrix procedures, using an anisotropic model for all non-hydrogen atoms except for the carbon atoms of the disordered solvent molecule that were refined isotropically. Hydrogen atoms were placed in estimated positions (C–H = 1.00 Å) (except for those associated with the poorly defined C(103) that were ignored), assigned a common fixed thermal parameter and refined 'riding' their respective carbon atoms. Data were corrected by a Chebyshev weighting scheme[6] (4 coefficient) and also for the effects of absorption[4], anomalous dispersion and isotropic extinction[7]. All crystallographic calculations were performed using the CRYSTALS suite of programs[8] and neutral atom scattering factors were taken from the usual sources[3].

APPENDIX F

Table F.1 Data collection and processing parameters for $[(Ph_3Sb)_2(\mu\text{-}O)(\mu\text{-}O_2AsMe_2)_2].0.5C_6H_{14}$ ($3.5.0.5C_6H_{14}$)

Chemical formula	$C_{43}H_{49}As_2O_5Sb_2$
Formula weight	1039.16
Crystal size/mm	0.32 x 0.20 x 0.16
Crystal system	Monoclinic
Space group	*C*2/*c*
a / Å	27.176(3)
b / Å	16.826(2)
c / Å	22.637(3)
β / °	126.887(8)
Volume / Å^3	8279(2)
Z	8
D_c/gcm^{-3}	1.667
Radiation (λ / Å)	Mo-K_α (0.71069)
μ / cm^{-1}	29.34
F(000)	4120
2θ limits / °	3.74 to 50.28
Index ranges	-29<=h<=30, -16<=k<=18, -26<=l<=21
Temperature / K	150
Total data collected	17594
Unique data	6432 [R(int) = 0.0913]
Absorption correction	None
Structure solution	Direct (SHELXS-86)[1]
Refinement procedure	Full matrix-LS on F^2
Number of data / variables	6406 / 467
Goodness-of-fit on F^2	0.935
Max/min peaks in final diff. map / e Å^{-3}	+1.736, -0.643
R observed data [$I > 2\sigma(I)$], (all data)	0.0422, (0.0633)
R_w observed data, (all data)	0.0940, (0.1247)

Table F.2 Atomic coordinates (x 10^4) and equivalent isotropic displacement parameters ($Å^2$ x 10^3) with estimated standard deviations in parentheses for $[(Ph_3Sb)_2(\mu\text{-}O)(\mu\text{-}O_2AsMe_2)_2].0.5C_6H_{14}$ ($3.5.0.5C_6H_{14}$)

Atom	x	y	z	U(eq)
Sb(1)	2134(1)	5620(1)	1236(1)	24(1)
Sb(2)	3496(1)	5961(1)	3203(1)	24(1)
As(1)	3353(1)	6702(1)	1673(1)	28(1)
As(2)	2300(1)	7244(1)	2284(1)	28(1)
O(1)	2827(2)	5447(2)	2280(2)	26(1)
O(2)	3512(2)	6819(2)	2506(2)	29(1)
O(3)	2814(2)	6017(2)	1120(2)	31(1)
O(4)	2814(2)	6717(2)	3053(2)	28(1)
O(5)	2140(2)	6843(2)	1502(2)	29(1)
C(1)	4088(3)	6387(4)	1806(4)	40(2)
C(2)	3079(3)	7703(4)	1175(4)	41(2)
C(3)	2591(3)	8295(3)	2360(4)	40(2)
C(4)	1575(3)	7305(4)	2225(4)	42(2)
C(11)	1472(3)	6037(3)	104(3)	27(2)
C(12)	1131(3)	6731(4)	-76(4)	42(2)
C(13)	698(3)	6953(4)	-797(4)	41(2)
C(14)	593(3)	6490(5)	-1353(4)	47(2)
C(15)	932(4)	5800(4)	-1198(4)	45(2)
C(16)	1362(3)	5576(4)	-474(4)	37(2)
C(21)	2244(3)	4439(3)	961(3)	27(2)
C(22)	1818(3)	3858(4)	790(3)	33(2)
C(23)	1892(4)	3080(4)	648(4)	47(2)
C(24)	2386(4)	2877(4)	665(4)	48(2)
C(25)	2810(4)	3457(5)	819(4)	53(2)
C(26)	2738(3)	4229(4)	960(4)	38(2)
C(31)	1477(3)	5335(3)	1453(3)	24(2)
C(32)	1685(3)	5065(3)	2144(4)	32(2)
C(33)	1278(3)	4873(4)	2295(4)	42(2)
C(34)	655(4)	4939(4)	1752(4)	44(2)
C(35)	437(3)	5207(4)	1065(4)	40(2)
C(36)	843(3)	5404(3)	911(4)	31(2)
C(41)	4139(3)	6768(3)	4094(3)	27(2)
C(42)	4484(3)	6485(4)	4807(4)	40(2)
C(43)	4893(3)	6960(4)	5394(4)	50(2)
C(44)	4963(3)	7741(4)	5280(4)	45(2)
C(45)	4627(3)	8044(4)	4575(4)	43(2)
C(46)	4220(3)	7548(3)	3982(4)	33(2)
C(51)	3359(3)	5198(4)	3866(3)	31(2)
C(52)	3702(3)	4482(4)	4158(4)	42(2)
C(53)	3613(5)	3978(4)	4573(4)	65(3)
C(54)	3192(5)	4181(6)	4707(5)	70(3)
C(55)	2871(4)	4872(6)	4437(5)	70(3)
C(56)	2952(4)	5384(5)	4016(4)	50(2)
C(61)	4172(3)	5248(3)	3231(3)	28(2)
C(62)	4802(3)	5414(4)	3717(4)	33(2)
C(63)	5227(3)	4934(4)	3747(4)	41(2)
C(64)	5031(4)	4290(4)	3290(4)	45(2)
C(65)	4411(3)	4113(4)	2802(4)	41(2)
C(66)	3984(3)	4577(4)	2777(4)	34(2)
C(100)	-301(19)	6522(22)	2161(24)	201(16)
C(101)	-754(14)	7442(18)	1479(17)	147(11)

C(102)	103(19)	6888(19)	2184(23)	160(13)
C(103)	-912(12)	6606(14)	1361(13)	103(7)
C(104)	-410(10)	6123(11)	1412(12)	83(6)
C(105)	-1334(6)	6303(8)	1450(8)	37(3)

Table F.3 Calculated hydrogen coordinates (x 10^4) and isotropic displacement parameters ($Å^2$ x 10^3) with estimated standard deviations in parentheses for $[(Ph_3Sb)_2(\mu\text{-}O)(\mu\text{-}O_2AsMe_2)_2].0.5C_6H_{14}$ ($3.5.0.5C_6H_{14}$)

Atom	x	y	z	U(eq)
H(1A)	4003(3)	6316(4)	1323(4)	60
H(1B)	4236(3)	5885(4)	2080(4)	60
H(1C)	4403(3)	6798(4)	2085(4)	60
H(2A)	2983(3)	7651(4)	685(4)	61
H(2B)	3404(3)	8100(4)	1462(4)	61
H(2C)	2710(3)	7871(4)	1123(4)	61
H(3A)	2287(3)	8591(3)	1909(4)	60
H(3B)	2981(3)	8273(3)	2424(4)	60
H(3C)	2655(3)	8561(3)	2786(4)	60
H(4B)	1260(3)	7607(4)	1785(4)	63
H(4C)	1667(3)	7571(4)	2666(4)	63
H(4A)	1421(3)	6767(4)	2194(4)	63
H(12A)	1200(3)	7059(4)	309(4)	51
H(13A)	472(3)	7431(4)	-907(4)	50
H(14A)	287(3)	6639(5)	-1852(4)	57
H(15A)	867(4)	5485(4)	-1588(4)	54
H(16A)	1588(3)	5098(4)	-368(4)	44
H(22A)	1468(3)	3992(4)	769(3)	39
H(23A)	1596(4)	2688(4)	537(4)	56
H(24A)	2439(4)	2345(4)	574(4)	57
H(25A)	3153(4)	3322(5)	828(4)	64
H(26A)	3029(3)	4622(4)	1058(4)	46
H(32A)	2115(3)	5010(3)	2520(4)	39
H(33A)	1427(3)	4695(4)	2774(4)	51
H(34A)	376(4)	4798(4)	1855(4)	53
H(35A)	7(3)	5257(4)	694(4)	49
H(36A)	689(3)	5588(3)	432(4)	37
H(42A)	4438(3)	5947(4)	4893(4)	48
H(43A)	5128(3)	6751(4)	5882(4)	60
H(44A)	5245(3)	8072(4)	5689(4)	53
H(45A)	4671(3)	8584(4)	4494(4)	51
H(46A)	3995(3)	7750(3)	3493(4)	39
H(52A)	3993(3)	4348(4)	4071(4)	51
H(53A)	3838(5)	3496(4)	4764(4)	78
H(54A)	3130(5)	3836(6)	4988(5)	84
H(55A)	2587(4)	5008(6)	4536(5)	84
H(56A)	2723(4)	5864(5)	3831(4)	61
H(62A)	4939(3)	5865(4)	4032(4)	40
H(63A)	5654(3)	5050(4)	4084(4)	49
H(64A)	5324(4)	3961(4)	3307(4)	54
H(65A)	4280(3)	3667(4)	2482(4)	49
H(66A)	3560(3)	4443(4)	2451(4)	41

Table F.4 Anisotropic thermal parameters ($Å^2 \times 10^3$) with estimated standard deviations in parentheses for $[(Ph_3Sb)_2(\mu\text{-}O)(\mu\text{-}O_2AsMe_2)_2].0.5C_6H_{14}$ ($3.5.0.5C_6H_{14}$)

Atom	U11	U22	U33	U23	U13	U12
Sb(1)	22(1)	26(1)	18(1)	-2(1)	8(1)	-2(1)
Sb(2)	21(1)	25(1)	18(1)	1(1)	7(1)	-1(1)
As(1)	23(1)	32(1)	23(1)	3(1)	11(1)	-2(1)
As(2)	24(1)	28(1)	21(1)	-2(1)	8(1)	3(1)
O(1)	22(2)	28(2)	16(2)	1(2)	5(2)	-4(2)
O(2)	31(3)	28(2)	23(2)	1(2)	14(2)	-4(2)
O(3)	27(3)	43(3)	23(3)	-6(2)	15(2)	-9(2)
O(4)	25(3)	32(2)	21(2)	2(2)	10(2)	6(2)
O(5)	32(3)	22(2)	21(2)	3(2)	9(2)	0(2)
C(1)	29(4)	47(4)	36(4)	7(3)	16(4)	3(3)
C(2)	45(5)	41(4)	35(4)	14(3)	23(4)	7(3)
C(3)	47(5)	22(4)	39(5)	-1(3)	19(4)	2(3)
C(4)	34(4)	48(4)	38(4)	-8(3)	18(4)	6(3)
C(11)	21(4)	37(4)	20(4)	0(3)	10(3)	-5(3)
C(12)	39(5)	44(4)	22(4)	-1(3)	6(4)	-1(3)
C(13)	38(5)	45(4)	25(4)	13(3)	10(4)	2(3)
C(14)	33(5)	68(5)	23(4)	16(4)	7(4)	-9(4)
C(15)	50(5)	56(5)	24(4)	-5(3)	19(4)	-14(4)
C(16)	38(4)	45(4)	23(4)	-6(3)	16(4)	-5(3)
C(21)	41(4)	22(3)	19(3)	-1(3)	17(3)	1(3)
C(22)	45(5)	31(4)	26(4)	-5(3)	24(4)	-3(3)
C(23)	66(6)	39(5)	36(5)	-3(3)	31(5)	-13(4)
C(24)	78(7)	34(4)	42(5)	-1(3)	41(5)	6(4)
C(25)	56(6)	56(5)	43(5)	-3(4)	28(5)	10(4)
C(26)	39(5)	41(4)	30(4)	-7(3)	18(4)	-3(3)
C(31)	25(4)	16(3)	33(4)	-2(3)	18(3)	-3(2)
C(32)	32(4)	31(4)	30(4)	3(3)	16(4)	0(3)
C(33)	40(5)	51(5)	42(5)	6(3)	28(4)	0(3)
C(34)	47(5)	44(4)	60(6)	-2(4)	42(5)	-9(3)
C(35)	24(4)	47(4)	39(5)	-8(4)	12(4)	-6(3)
C(36)	26(4)	32(4)	23(4)	-2(3)	8(3)	-4(3)
C(41)	23(4)	26(4)	23(4)	0(3)	9(3)	-2(3)
C(42)	41(5)	33(4)	29(4)	3(3)	12(4)	-6(3)
C(43)	43(5)	45(5)	21(4)	8(3)	-3(4)	-13(3)
C(44)	37(5)	45(5)	29(4)	-8(3)	8(4)	-13(3)
C(45)	35(5)	30(4)	41(5)	-2(3)	12(4)	-4(3)
C(46)	27(4)	27(4)	24(4)	2(3)	5(3)	-2(3)
C(51)	29(4)	38(4)	13(3)	1(3)	5(3)	-12(3)
C(52)	45(5)	33(4)	28(4)	-3(3)	11(4)	-12(3)
C(53)	92(8)	30(4)	25(4)	5(3)	9(5)	-28(4)
C(54)	69(7)	86(7)	27(5)	3(5)	15(5)	-46(6)
C(55)	47(6)	120(8)	40(5)	8(5)	25(5)	-18(5)
C(56)	42(5)	78(6)	32(5)	10(4)	23(4)	-5(4)
C(61)	31(4)	28(4)	26(4)	8(3)	18(3)	1(3)
C(62)	25(4)	35(4)	31(4)	1(3)	13(4)	-4(3)
C(63)	23(4)	54(5)	35(4)	7(4)	12(4)	5(3)
C(64)	46(5)	49(5)	44(5)	7(4)	29(4)	15(4)
C(65)	46(5)	38(4)	40(5)	-4(3)	26(4)	1(3)
C(66)	26(4)	42(4)	28(4)	7(3)	13(3)	2(3)

Table F.5 Bond lengths (Å) with estimated standard deviations in parentheses for $[(Ph_3Sb)_2(\mu\text{-}O)(\mu\text{-}O_2AsMe_2)_2].0.5C_6H_{14}$ ($3.5.0.5C_6H_{14}$)

Sb(1)-O(1)	1.968(4)	C(31)-C(36)	1.396(8)
Sb(1)-O(3)	2.124(4)	C(32)-C(33)	1.378(9)
Sb(1)-O(5)	2.141(4)	C(33)-C(34)	1.375(10)
Sb(1)-C(21)	2.156(6)	C(34)-C(35)	1.364(10)
Sb(1)-C(31)	2.171(6)	C(35)-C(36)	1.382(9)
Sb(1)-C(11)	2.183(6)	C(41)-C(42)	1.376(9)
Sb(2)-O(1)	1.964(4)	C(41)-C(46)	1.379(8)
Sb(2)-O(4)	2.102(4)	C(42)-C(43)	1.366(9)
Sb(2)-O(2)	2.156(4)	C(43)-C(44)	1.374(9)
Sb(2)-C(61)	2.162(6)	C(44)-C(45)	1.374(9)
Sb(2)-C(51)	2.173(6)	C(45)-C(46)	1.392(9)
Sb(2)-C(41)	2.176(6)	C(51)-C(56)	1.373(10)
As(1)-O(2)	1.675(4)	C(51)-C(52)	1.421(9)
As(1)-O(3)	1.687(4)	C(52)-C(53)	1.390(11)
As(1)-C(1)	1.907(7)	C(53)-C(54)	1.390(13)
As(1)-C(2)	1.911(6)	C(54)-C(55)	1.358(13)
As(2)-O(4)	1.687(4)	C(55)-C(56)	1.398(11)
As(2)-O(5)	1.690(4)	C(61)-C(66)	1.401(9)
As(2)-C(4)	1.897(7)	C(61)-C(62)	1.399(9)
As(2)-C(3)	1.903(6)	C(62)-C(63)	1.377(9)
C(11)-C(12)	1.391(9)	C(63)-C(64)	1.367(10)
C(11)-C(16)	1.392(9)	C(64)-C(65)	1.385(10)
C(12)-C(13)	1.373(9)	C(65)-C(66)	1.370(9)
C(13)-C(14)	1.357(10)	C(100)-C(102)	1.23(5)
C(14)-C(15)	1.390(11)	C(100)-C(100)#1	1.42(8)
C(15)-C(16)	1.376(9)	C(100)-C(102)#1	1.38(4)
C(21)-C(22)	1.381(9)	C(100)-C(103)	1.56(4)
C(21)-C(26)	1.389(9)	C(100)-C(104)	1.68(5)
C(22)-C(23)	1.391(9)	C(101)-C(103)	1.45(3)
C(23)-C(24)	1.361(11)	C(102)-C(100)#1	1.38(4)
C(24)-C(25)	1.385(11)	C(102)-C(102)#1	1.82(7)
C(25)-C(26)	1.379(9)	C(102)-C(104)	1.93(4)
C(31)-C(32)	1.383(9)	C(103)-C(105)	1.38(3)
		C(103)-C(104)	1.53(3)

Table F.6 Bond angles (°) with estimated standard deviations in parentheses for $[(Ph_3Sb)_2(\mu\text{-}O)(\mu\text{-}O_2AsMe_2)_2].0.5C_6H_{14}$ ($3.5.0.5C_6H_{14}$)

O(1)-Sb(1)-O(3)	85.3(2)	C(23)-C(24)-C(25)	119.1(7)
O(1)-Sb(1)-O(5)	87.9(2)	C(26)-C(25)-C(24)	120.7(8)
O(3)-Sb(1)-O(5)	82.7(2)	C(25)-C(26)-C(21)	120.7(7)
O(1)-Sb(1)-C(21)	90.7(2)	C(32)-C(31)-C(36)	118.2(6)
O(3)-Sb(1)-C(21)	88.4(2)	C(32)-C(31)-Sb(1)	119.6(5)
O(5)-Sb(1)-C(21)	171.1(2)	C(36)-C(31)-Sb(1)	122.2(5)
O(1)-Sb(1)-C(31)	91.2(2)	C(33)-C(32)-C(31)	120.8(6)
O(3)-Sb(1)-C(31)	172.8(2)	C(34)-C(33)-C(32)	120.0(7)
O(5)-Sb(1)-C(31)	91.0(2)	C(35)-C(34)-C(33)	120.4(7)
C(21)-Sb(1)-C(31)	97.9(2)	C(34)-C(35)-C(36)	120.0(7)
O(1)-Sb(1)-C(11)	167.9(2)	C(35)-C(36)-C(31)	120.6(6)
O(3)-Sb(1)-C(11)	85.4(2)	C(42)-C(41)-C(46)	118.3(6)

O(5)-Sb(1)-C(11)	83.3(2)	C(42)-C(41)-Sb(2)	118.3(4)
C(21)-Sb(1)-C(11)	96.7(2)	C(46)-C(41)-Sb(2)	123.4(4)
C(31)-Sb(1)-C(11)	97.2(2)	C(43)-C(42)-C(41)	121.5(6)
O(1)-Sb(2)-O(4)	86.0(2)	C(42)-C(43)-C(44)	119.9(7)
O(1)-Sb(2)-O(2)	85.9(2)	C(45)-C(44)-C(43)	120.2(6)
O(4)-Sb(2)-O(2)	83.1(2)	C(44)-C(45)-C(46)	119.2(6)
O(1)-Sb(2)-C(61)	90.8(2)	C(41)-C(46)-C(45)	120.9(6)
O(4)-Sb(2)-C(61)	172.8(2)	C(56)-C(51)-C(52)	118.6(6)
O(2)-Sb(2)-C(61)	90.2(2)	C(56)-C(51)-Sb(2)	122.3(5)
O(1)-Sb(2)-C(51)	92.4(2)	C(52)-C(51)-Sb(2)	119.0(5)
O(4)-Sb(2)-C(51)	88.1(2)	C(53)-C(52)-C(51)	119.9(8)
O(2)-Sb(2)-C(51)	171.2(2)	C(54)-C(53)-C(52)	119.8(8)
C(61)-Sb(2)-C(51)	98.5(2)	C(55)-C(54)-C(53)	120.3(8)
O(1)-Sb(2)-C(41)	167.5(2)	C(54)-C(55)-C(56)	120.7(9)
O(4)-Sb(2)-C(41)	84.9(2)	C(51)-C(56)-C(55)	120.6(8)
O(2)-Sb(2)-C(41)	84.5(2)	C(66)-C(61)-C(62)	118.3(6)
C(61)-Sb(2)-C(41)	97.1(2)	C(66)-C(61)-Sb(2)	119.7(5)
C(51)-Sb(2)-C(41)	95.9(2)	C(62)-C(61)-Sb(2)	121.9(5)
O(2)-As(1)-O(3)	115.9(2)	C(63)-C(62)-C(61)	121.0(6)
O(2)-As(1)-C(1)	108.5(3)	C(64)-C(63)-C(62)	119.6(7)
O(3)-As(1)-C(1)	106.8(3)	C(63)-C(64)-C(65)	120.6(7)
O(2)-As(1)-C(2)	107.9(3)	C(66)-C(65)-C(64)	120.4(7)
O(3)-As(1)-C(2)	107.9(3)	C(65)-C(66)-C(61)	120.1(6)
C(1)-As(1)-C(2)	109.8(3)	C(102)-C(100)-C(100)#1	62(3)
O(4)-As(2)-O(5)	113.8(2)	C(102)-C(100)-C(102)#1	88(4)
O(4)-As(2)-C(4)	106.4(3)	C(100)#1-C(100)-C(102)#1	52(3)
O(5)-As(2)-C(4)	110.2(3)	C(102)-C(100)-C(103)	108(4)
O(4)-As(2)-C(3)	110.7(3)	C(100)#1-C(100)-C(103)	170(6)
O(5)-As(2)-C(3)	107.3(3)	C(102)#1-C(100)-C(103)	131(4)
C(4)-As(2)-C(3)	108.3(3)	C(102)-C(100)-C(104)	82(4)
Sb(2)-O(1)-Sb(1)	145.1(2)	C(100)#1-C(100)-C(104)	119(5)
As(1)-O(2)-Sb(2)	129.8(2)	C(102)#1-C(100)-C(104)	169(4)
As(1)-O(3)-Sb(1)	123.8(2)	C(103)-C(100)-C(104)	56(2)
As(2)-O(4)-Sb(2)	126.0(2)	C(100)-C(102)-C(100)#1	66(4)
As(2)-O(5)-Sb(1)	129.2(2)	C(100)-C(102)-C(102)#1	49(3)
C(12)-C(11)-C(16)	117.7(6)	C(100)#1-C(102)-C(102)#1	43(2)
C(12)-C(11)-Sb(1)	123.3(5)	C(100)-C(102)-C(104)	59(3)
C(16)-C(11)-Sb(1)	119.0(5)	C(100)#1-C(102)-C(104)	106(3)
C(13)-C(12)-C(11)	121.4(7)	C(102)#1-C(102)-C(104)	108(3)
C(14)-C(13)-C(12)	120.0(7)	C(105)-C(103)-C(101)	121(2)
C(13)-C(14)-C(15)	120.5(7)	C(105)-C(103)-C(104)	125(2)
C(16)-C(15)-C(14)	119.4(7)	C(101)-C(103)-C(104)	111(2)
C(15)-C(16)-C(11)	121.1(7)	C(105)-C(103)-C(100)	101(3)
C(22)-C(21)-C(26)	118.0(6)	C(101)-C(103)-C(100)	83(2)
C(22)-C(21)-Sb(1)	119.7(5)	C(104)-C(103)-C(100)	66(2)
C(26)-C(21)-Sb(1)	122.4(5)	C(103)-C(104)-C(100)	58(2)
C(21)-C(22)-C(23)	121.1(7)	C(103)-C(104)-C(102)	81(2)
C(24)-C(23)-C(22)	120.4(7)	C(100)-C(104)-C(102)	39(2)

Symmetry transformation used to generate equivalent atoms:

#1 -x,y,-z+1/2

Experimental Details

Slightly more than one hemisphere of data were collected on a Delft Instruments FAST TV area detector, equipped with a rotating anode FR591 generator. The data were corrected for Lorentz and polarisation effects, merged and systematically absent reflections were rejected. The structure was solved by direct methods (SHELXS-86)[1] and subsequent Fourier difference syntheses revealed the positions of all the other non-hydrogen atoms. Refinement was carried out against all F_o^2 data by full matrix procedures (SHELXL-93)[2] with the disordered solvate region modelled using six half-occupied carbon atoms (all with isotropic temperature factors and with the associated hydrogen atoms ignored). Hydrogen atoms were placed in estimated positions [C–H = 0.95 (phenyl hydrogens), 0.98 (methyl hydrogens) Å], with fixed isotropic parameters (1.2 x equivalent isotropic temperature factors of the carbon atom to which they were bonded for phenyl protons and 1.5 x for methyl protons) and refined 'riding' their respective carbon atoms. A standard weighting scheme was applied but no extinction correction was found to be necessary. All crystallographic calculations were performed using the SHELXS-86[1] and SHELXL-93[2] programs and neutral atom scattering factors were taken from the usual sources[3].

APPENDIX G

Table G.1 Data collection and processing parameters for $[(Ph_3Sb)_2(\mu\text{-}O)(\mu\text{-}O_2AsPh_2)_2].CHCl_3$ (3.6.$CHCl_3$)

Chemical formula	$C_{61}H_{51}Cl_3O_5As_2Sb_2$
Formula weight	1363.77
Crystal size/mm	0.15 x 0.10 x 0.10
Crystal system	Monoclinic
Space group	$P2_1/a$
a / Å	11.804(12)
b / Å	40.910(4)
c / Å	12.738(7)
β / °	115.71(4)
Volume / Å^3	5542.26
Z	4
D_c/gcm^{-3}	1.6345
Radiation (λ / Å)	Mo-K_α (0.71069)
μ / cm^{-1}	23.569
F(000)	2704
2θ limits / °	5-50
Index ranges (for unique data set)	-13<=h<=11, 0<=k<=45, 0<=l<=14
Temperature / K	120
Total data collected	21169
Unique data	7933 [(R(int) = 0.1616]
Observed data [$I > 3\sigma(I)$]	6128
Absorption correction	DIFABS (min, 0.773, max, 1.115)[4]
Structure solution	Direct (SIR-92)[5]
Refinement procedure	Full matrix-LS on F^2
Number of data / variables	6128 / 658
S	1.073
Max/min peaks in final diff. map / e Å^{-3}	+2.09, -2.04
R	0.0702
R_w	0.0942

Table G.2 Fractional atomic coordinates and equivalent isotropic displacement parameters ($Å^2$) with estimated standard deviations in parentheses for $[(Ph_3Sb)_2(\mu\text{-}O)(\mu\text{-}O_2AsPh_2)_2].CHCl_3$ ($3.6.CHCl_3$)

Atom	x/a	y/b	z/c	U(eq)
Sb(1)	0.39508(5)	0.08166(1)	-0.13741(4)	0.0150
Sb(2)	0.48955(4)	0.14599(1)	-0.29903(4)	0.0146
As(1)	0.20656(7)	0.10481(2)	-0.42203(6)	0.0157
As(2)	0.32829(7)	0.16340(2)	-0.13521(6)	0.0159
Cl(1)	0.0652(3)	0.11301(9)	0.1699(3)	0.0619
Cl(2)	0.2319(4)	0.16806(7)	0.2270(3)	0.0717
Cl(3)	0.3161(2)	0.10430(7)	0.1943(2)	0.0479
O(1)	0.4843(4)	0.1096(1)	-0.2029(4)	0.0155
O(2)	0.3260(5)	0.1240(1)	-0.4378(4)	0.0177
O(3)	0.2259(5)	0.0947(1)	-0.2874(4)	0.0181
O(4)	0.3507(4)	0.1682(1)	-0.2564(4)	0.0166
O(5)	0.3480(5)	0.1261(1)	-0.0751(4)	0.0179
C(1)	0.2184(9)	0.1262(2)	0.2429(8)	0.0400
C(11)	0.2750(7)	0.0599(2)	-0.0711(6)	0.0185
C(12)	0.1476(7)	0.0687(2)	-0.1068(6)	0.0253
C(13)	0.0773(8)	0.0543(2)	-0.0566(7)	0.0336
C(14)	0.1282(9)	0.0311(2)	0.0305(7)	0.0326
C(15)	0.2543(8)	0.0220(2)	0.0670(6)	0.0271
C(16)	0.3245(7)	0.0365(2)	0.0169(6)	0.0215
C(21)	0.4160(7)	0.0399(2)	-0.2307(6)	0.0176
C(22)	0.4910(8)	0.0425(2)	-0.2896(6)	0.0247
C(23)	0.5066(8)	0.0166(2)	-0.3524(6)	0.0261
C(24)	0.4470(8)	-0.0133(2)	-0.3544(7)	0.0292
C(25)	0.3730(9)	-0.0159(2)	-0.2954(7)	0.0291
C(26)	0.3552(8)	0.0102(2)	-0.2334(6)	0.0281
C(31)	0.5683(7)	0.0788(2)	0.0200(5)	0.0158
C(32)	0.6677(8)	0.0603(2)	0.0226(7)	0.0301
C(33)	0.7855(8)	0.0612(2)	0.1179(7)	0.0333
C(34)	0.8063(8)	0.0814(2)	0.2111(7)	0.0304
C(35)	0.7089(8)	0.1003(2)	0.2104(7)	0.0285
C(36)	0.5899(7)	0.0990(2)	0.1170(6)	0.0246
C(41)	0.4469(7)	0.1862(2)	-0.4210(6)	0.0207
C(42)	0.3301(8)	0.2015(2)	-0.4693(6)	0.0245
C(43)	0.3074(9)	0.2275(2)	-0.5484(7)	0.0326
C(44)	0.400(1)	0.2373(2)	-0.5794(7)	0.0331
C(45)	0.5191(9)	0.2224(2)	-0.5282(7)	0.0289
C(46)	0.5410(9)	0.1967(2)	-0.4510(6)	0.0249
C(51)	0.6377(7)	0.1698(2)	-0.1514(6)	0.0180
C(52)	0.6996(7)	0.1523(2)	-0.0474(6)	0.0246
C(53)	0.7916(7)	0.1682(2)	0.0508(6)	0.0257
C(54)	0.8191(8)	0.2004(2)	0.0449(6)	0.0280
C(55)	0.7594(7)	0.2177(2)	-0.0568(7)	0.0260
C(56)	0.6661(7)	0.2025(2)	-0.1570(6)	0.0207
C(61)	0.6001(7)	0.1189(2)	-0.3658(6)	0.0155
C(62)	0.5575(8)	0.1141(2)	-0.4851(6)	0.0237
C(63)	0.6237(8)	0.0939(2)	-0.5279(7)	0.0267
C(64)	0.7314(7)	0.0785(2)	-0.4507(7)	0.0260
C(65)	0.7791(8)	0.0834(2)	-0.3343(7)	0.0289
C(66)	0.7120(8)	0.1034(2)	-0.2905(7)	0.0258
C(71)	0.0612(7)	0.1329(2)	-0.4796(6)	0.0153
C(72)	-0.0212(7)	0.1314(2)	-0.4329(7)	0.0244

C(73)	-0.1298(7)	0.1508(2)	-0.4774(7)	0.0279
C(74)	-0.1506(8)	0.1713(2)	-0.5695(7)	0.0269
C(75)	-0.0665(8)	0.1728(2)	-0.6184(7)	0.0286
C(76)	0.0419(8)	0.1534(2)	-0.5749(6)	0.0257
C(81)	0.1699(7)	0.0662(2)	-0.5170(6)	0.0167
C(82)	0.0618(8)	0.0482(2)	-0.5348(7)	0.0280
C(83)	0.0332(9)	0.0204(2)	-0.6088(7)	0.0323
C(84)	0.107(1)	0.0128(2)	-0.6643(7)	0.0345
C(85)	0.2128(9)	0.0308(2)	-0.6452(7)	0.0369
C(86)	0.2448(8)	0.0573(2)	-0.5708(7)	0.0287
C(91)	0.1588(7)	0.1776(2)	-0.1791(6)	0.0177
C(92)	0.0865(8)	0.1635(2)	-0.1303(7)	0.0301
C(93)	-0.0352(8)	0.1766(2)	-0.1585(7)	0.0320
C(94)	-0.0760(8)	0.2023(2)	-0.2364(7)	0.0312
C(95)	-0.0034(8)	0.2161(2)	-0.2869(7)	0.0290
C(96)	0.1145(8)	0.2040(2)	-0.2581(6)	0.0247
C(101)	0.4359(7)	0.1930(2)	-0.0166(6)	0.0202
C(102)	0.4621(8)	0.1861(2)	0.0990(7)	0.0336
C(103)	0.5327(9)	0.2093(3)	0.1845(7)	0.0392
C(104)	0.5761(8)	0.2370(2)	0.1537(8)	0.0318
C(105)	0.5498(8)	0.2433(2)	0.0393(8)	0.0340
C(106)	0.4775(7)	0.2211(2)	-0.0471(7)	0.0217

Table G.3 Calculated hydrogen coordinates and isotropic displacement parameters ($Å^2$) with estimated standard deviations in parentheses for $[(Ph_3Sb)_2(\mu\text{-}O)(\mu\text{-}O_2AsPh_2)_2].CHCl_3$ ($3.6.CHCl_3$)

Atom	x/a	y/b	z/c	U(iso)
H(1)	0.2400	0.1214	0.3275	0.0500
H(121)	0.1079(7)	0.0852(2)	-0.1702(6)	0.0350
H(131)	-0.0122(8)	0.0613(2)	-0.0838(7)	0.0350
H(141)	0.0755(9)	0.0209(2)	0.0656(7)	0.0350
H(151)	0.2935(8)	0.0054(2)	0.1300(6)	0.0350
H(161)	0.4144(7)	0.0298(2)	0.0447(6)	0.0350
H(221)	0.5335(8)	0.0638(2)	-0.2872(6)	0.0350
H(231)	0.5606(8)	0.0191(2)	-0.3945(6)	0.0350
H(241)	0.4582(8)	-0.0325(2)	-0.3976(7)	0.0350
H(251)	0.3295(9)	-0.0371(2)	-0.2983(7)	0.0350
H(261)	0.3013(8)	0.0078(2)	-0.1913(6)	0.0350
H(321)	0.6540(8)	0.0457(2)	-0.0450(7)	0.0350
H(331)	0.8554(8)	0.0474(2)	0.1174(7)	0.0350
H(341)	0.8910(8)	0.0821(2)	0.2792(7)	0.0350
H(351)	0.7247(8)	0.1152(2)	0.2777(7)	0.0350
H(361)	0.5205(7)	0.1126(2)	0.1191(6)	0.0350
H(421)	0.2625(8)	0.1939(2)	-0.4475(6)	0.0350
H(431)	0.2235(9)	0.2385(2)	-0.5830(7)	0.0350
H(441)	0.384(1)	0.2552(2)	-0.6376(7)	0.0350
H(451)	0.5882(9)	0.2302(2)	-0.5474(7)	0.0350
H(461)	0.6244(9)	0.1855(2)	-0.4168(6)	0.0350
H(521)	0.6786(7)	0.1288(2)	-0.0433(6)	0.0350
H(531)	0.8364(7)	0.1559(2)	0.1254(6)	0.0350
H(541)	0.8850(8)	0.2114(2)	0.1148(6)	0.0350

H(551)	0.7811(7)	0.2412(2)	-0.0597(7)	0.0350
H(561)	0.6208(7)	0.2152(2)	-0.2306(6)	0.0350
H(621)	0.4791(8)	0.1253(2)	-0.5407(6)	0.0350
H(631)	0.5936(8)	0.0905(2)	-0.6136(7)	0.0350
H(641)	0.7754(7)	0.0631(2)	-0.4817(7)	0.0350
H(651)	0.8613(8)	0.0733(2)	-0.2812(7)	0.0350
H(661)	0.7442(8)	0.1064(2)	-0.2044(7)	0.0350
H(721)	-0.0053(7)	0.1163(2)	-0.3661(7)	0.0350
H(731)	-0.1919(7)	0.1496(2)	-0.4436(7)	0.0350
H(741)	-0.2269(8)	0.1856(2)	-0.6004(7)	0.0350
H(751)	-0.0840(8)	0.1879(2)	-0.6854(7)	0.0350
H(761)	0.1032(8)	0.1541(2)	-0.6098(6)	0.0350
H(821)	0.0065(8)	0.0552(2)	-0.4977(7)	0.0350
H(831)	-0.0404(9)	0.0064(2)	-0.6190(7)	0.0350
H(841)	0.083(1)	-0.0065(2)	-0.7181(7)	0.0350
H(851)	0.2646(9)	0.0248(2)	-0.6871(7)	0.0350
H(861)	0.3229(8)	0.0700(2)	-0.5552(7)	0.0350
H(921)	0.1190(8)	0.1443(2)	-0.0771(7)	0.0350
H(931)	-0.0898(8)	0.1680(2)	-0.1229(7)	0.0350
H(941)	-0.1621(8)	0.2114(2)	-0.2587(7)	0.0350
H(951)	-0.0370(8)	0.2347(2)	-0.3430(7)	0.0350
H(961)	0.1685(8)	0.2134(2)	-0.2932(6)	0.0350
H(1021)	0.4324(8)	0.1654(2)	0.1207(7)	0.0350
H(1031)	0.5506(9)	0.2057(3)	0.2679(7)	0.0350
H(1041)	0.6273(8)	0.2530(2)	0.2154(8)	0.0350
H(1051)	0.5832(8)	0.2635(2)	0.0183(8)	0.0350
H(1061)	0.4564(7)	0.2255(2)	-0.1308(7)	0.0350

Table G.4 Anisotropic thermal parameters ($Å^2$) with estimated standard deviations in parentheses for $[(Ph_3Sb)_2(\mu\text{-}O)(\mu\text{-}O_2AsPh_2)_2].CHCl_3$ (3.6.$CHCl_3$)

Atom	U(11)	U(22)	U(33)	U(23)	U(13)	U(12)
Sb(1)	0.0192(3)	0.0127(2)	0.0116(2)	0.0005(2)	0.0028(2)	0.0001(2)
Sb(2)	0.0163(3)	0.0134(2)	0.0123(2)	-0.0002(2)	0.0032(2)	-0.0003(2)
As(1)	0.0165(4)	0.0165(4)	0.0121(3)	0.0006(3)	0.0025(3)	0.0001(3)
As(2)	0.0201(4)	0.0146(4)	0.0128(4)	0.0000(3)	0.0052(3)	0.0023(3)
Cl(1)	0.036(2)	0.098(2)	0.069(2)	-0.032(2)	0.010(1)	0.005(1)
Cl(2)	0.156(4)	0.039(2)	0.102(2)	-0.015(2)	0.088(3)	-0.013(2)
Cl(3)	0.044(2)	0.064(2)	0.047(1)	-0.016(1)	0.022(1)	-0.001(1)
O(1)	0.018(3)	0.015(2)	0.014(2)	0.005(2)	0.002(2)	0.001(2)
O(2)	0.017(3)	0.024(3)	0.014(2)	-0.004(2)	0.005(2)	-0.005(2)
O(3)	0.025(3)	0.022(3)	0.010(2)	0.002(2)	0.005(2)	-0.003(2)
O(4)	0.015(3)	0.018(2)	0.016(2)	0.001(2)	0.006(2)	0.004(2)
O(5)	0.031(3)	0.015(3)	0.019(3)	0.001(2)	0.016(2)	0.004(2)
C(1)	0.047(6)	0.037(5)	0.037(5)	-0.006(4)	0.016(4)	-0.006(4)
C(11)	0.036(5)	0.017(4)	0.012(3)	0.001(3)	0.010(3)	-0.004(3)
C(12)	0.023(5)	0.039(5)	0.016(4)	0.001(3)	0.005(3)	0.000(4)
C(13)	0.033(5)	0.050(5)	0.021(4)	0.000(4)	0.008(4)	-0.005(4)
C(14)	0.044(6)	0.037(5)	0.023(4)	-0.003(4)	0.014(4)	-0.010(4)
C(15)	0.047(6)	0.022(4)	0.019(4)	0.003(3)	0.012(4)	-0.004(4)
C(16)	0.026(5)	0.019(4)	0.018(4)	0.001(3)	0.006(3)	0.005(3)
C(21)	0.022(4)	0.019(4)	0.015(3)	0.001(3)	0.009(3)	0.003(3)

C(22)	0.032(5)	0.017(4)	0.024(4)	0.003(3)	0.007(3)	0.003(3)
C(23)	0.038(5)	0.020(4)	0.026(4)	-0.001(3)	0.013(4)	0.007(3)
C(24)	0.049(6)	0.018(4)	0.030(4)	-0.004(3)	0.017(4)	-0.002(4)
C(25)	0.064(7)	0.015(4)	0.031(5)	-0.009(3)	0.020(4)	-0.007(4)
C(26)	0.044(6)	0.021(4)	0.024(4)	-0.003(3)	0.012(4)	-0.001(4)
C(31)	0.025(4)	0.012(3)	0.012(3)	0.003(3)	0.003(3)	0.000(3)
C(32)	0.030(5)	0.031(5)	0.024(4)	0.001(3)	0.003(4)	0.002(4)
C(33)	0.025(5)	0.044(5)	0.034(5)	0.008(4)	-0.001(4)	0.012(4)
C(34)	0.031(5)	0.041(5)	0.023(4)	0.008(4)	-0.003(4)	-0.015(4)
C(35)	0.043(6)	0.027(5)	0.019(4)	-0.004(3)	0.004(4)	-0.012(4)
C(36)	0.025(5)	0.025(4)	0.022(4)	0.006(3)	0.004(3)	0.002(3)
C(41)	0.032(5)	0.017(4)	0.016(4)	-0.002(3)	0.009(3)	-0.000(3)
C(42)	0.035(5)	0.024(4)	0.019(4)	0.000(3)	0.012(3)	0.004(3)
C(43)	0.056(6)	0.030(5)	0.025(4)	0.007(3)	0.019(4)	0.015(4)
C(44)	0.084(8)	0.019(4)	0.031(5)	-0.000(4)	0.031(5)	0.003(5)
C(45)	0.060(7)	0.025(4)	0.033(5)	-0.007(3)	0.033(5)	-0.014(4)
C(46)	0.060(6)	0.020(4)	0.017(4)	-0.004(3)	0.018(4)	-0.007(4)
C(51)	0.018(4)	0.019(4)	0.016(4)	-0.002(3)	0.007(3)	-0.002(3)
C(52)	0.022(5)	0.031(4)	0.019(4)	0.001(3)	0.005(3)	-0.003(3)
C(53)	0.023(5)	0.037(5)	0.021(4)	-0.001(3)	0.009(3)	-0.005(4)
C(54)	0.029(5)	0.038(5)	0.019(4)	-0.008(3)	0.004(3)	-0.004(4)
C(55)	0.026(5)	0.023(4)	0.033(5)	-0.010(3)	0.010(4)	-0.007(3)
C(56)	0.019(4)	0.021(4)	0.026(4)	-0.007(3)	0.010(3)	-0.003(3)
C(61)	0.019(4)	0.010(3)	0.022(4)	-0.006(3)	0.006(3)	-0.003(3)
C(62)	0.029(5)	0.019(4)	0.022(4)	-0.002(3)	0.008(3)	-0.005(3)
C(63)	0.031(5)	0.029(4)	0.027(4)	-0.013(3)	0.013(4)	-0.009(4)
C(64)	0.021(5)	0.029(5)	0.045(5)	-0.018(4)	0.017(4)	-0.009(3)
C(65)	0.020(5)	0.027(4)	0.040(5)	-0.004(4)	0.009(4)	0.001(3)
C(66)	0.037(5)	0.017(4)	0.025(4)	-0.003(3)	0.009(4)	-0.003(3)
C(71)	0.015(4)	0.021(4)	0.011(3)	-0.003(3)	-0.001(3)	0.003(3)
C(72)	0.023(5)	0.020(4)	0.031(4)	-0.007(3)	0.009(4)	-0.002(3)
C(73)	0.015(5)	0.031(5)	0.046(5)	-0.003(4)	0.008(4)	0.005(3)
C(74)	0.021(5)	0.028(5)	0.035(5)	-0.013(4)	-0.000(4)	0.007(3)
C(75)	0.046(6)	0.026(4)	0.018(4)	-0.002(3)	-0.002(4)	0.011(4)
C(76)	0.033(5)	0.023(4)	0.019(4)	0.000(3)	0.005(3)	0.003(3)
C(81)	0.022(4)	0.021(4)	0.010(3)	0.002(3)	-0.005(3)	0.004(3)
C(82)	0.029(5)	0.025(4)	0.029(4)	-0.002(3)	0.009(4)	-0.006(4)
C(83)	0.036(6)	0.029(5)	0.035(5)	-0.010(4)	-0.003(4)	-0.011(4)
C(84)	0.059(7)	0.026(5)	0.026(5)	-0.007(4)	-0.002(4)	0.012(4)
C(85)	0.047(6)	0.039(5)	0.033(5)	-0.006(4)	0.016(4)	0.012(4)
C(86)	0.034(5)	0.027(4)	0.030(4)	-0.006(3)	0.013(4)	0.007(4)
C(91)	0.018(4)	0.014(4)	0.023(4)	-0.004(3)	0.008(3)	-0.003(3)
C(92)	0.029(5)	0.028(5)	0.029(4)	-0.001(3)	0.009(4)	-0.000(4)
C(93)	0.032(5)	0.041(5)	0.033(5)	-0.009(4)	0.017(4)	0.002(4)
C(94)	0.021(5)	0.042(5)	0.032(5)	-0.007(4)	0.004(4)	0.005(4)
C(95)	0.026(5)	0.032(5)	0.028(4)	-0.004(3)	0.006(4)	0.006(4)
C(96)	0.029(5)	0.023(4)	0.019(4)	0.002(3)	0.001(3)	0.003(3)
C(101)	0.025(4)	0.025(4)	0.014(4)	-0.005(3)	0.003(3)	0.009(3)
C(102)	0.044(6)	0.032(5)	0.029(5)	-0.001(4)	0.015(4)	0.009(4)
C(103)	0.049(6)	0.057(7)	0.021(5)	-0.009(4)	0.001(4)	0.015(5)
C(104)	0.026(5)	0.046(6)	0.041(6)	-0.029(4)	-0.004(4)	0.003(4)
C(105)	0.026(5)	0.035(5)	0.047(6)	-0.018(4)	0.007(4)	-0.001(4)
C(106)	0.012(4)	0.025(4)	0.032(4)	-0.009(3)	0.003(3)	0.001(3)

Table G.5 Bond lengths (Å) with estimated standard deviations in parentheses for $[(Ph_3Sb)_2(\mu\text{-}O)(\mu\text{-}O_2AsPh_2)_2].CHCl_3$ (3.6.$CHCl_3$)

Sb(1) - O(1)	1.967(5)	C(41) - C(42)	1.39(1)
Sb(1) - O(3)	2.148(5)	C(41) - C(46)	1.39(1)
Sb(1) - O(5)	2.152(5)	C(42) - C(43)	1.41(1)
Sb(1) - C(11)	2.135(7)	C(43) - C(44)	1.38(1)
Sb(1) - C(21)	2.156(7)	C(44) - C(45)	1.40(1)
Sb(1) - C(31)	2.158(7)	C(45) - C(46)	1.38(1)
Sb(2) - O(1)	1.947(4)	C(51) - C(52)	1.40(1)
Sb(2) - O(2)	2.169(4)	C(51) - C(56)	1.39(1)
Sb(2) - O(4)	2.141(5)	C(52) - C(53)	1.41(1)
Sb(2) - C(41)	2.167(7)	C(53) - C(54)	1.37(1)
Sb(2) - C(51)	2.166(7)	C(54) - C(55)	1.37(1)
Sb(2) - C(61)	2.148(7)	C(55) - C(56)	1.42(1)
As(1) - O(2)	1.699(5)	C(61) - C(62)	1.39(1)
As(1) - O(3)	1.680(4)	C(61) - C(66)	1.40(1)
As(1) - C(71)	1.926(7)	C(62) - C(63)	1.40(1)
As(1) - C(81)	1.921(7)	C(63) - C(64)	1.38(1)
As(2) - O(4)	1.686(5)	C(64) - C(65)	1.35(1)
As(2) - O(5)	1.677(5)	C(65) - C(66)	1.41(1)
As(2) - C(91)	1.919(7)	C(71) - C(72)	1.34(1)
As(2) - C(101)	1.923(7)	C(71) - C(76)	1.41(1)
Cl(1) - C(1)	1.72(1)	C(72) - C(73)	1.40(1)
Cl(2) - C(1)	1.741(9)	C(73) - C(74)	1.37(1)
Cl(3) - C(1)	1.77(1)	C(74) - C(75)	1.38(1)
C(11) - C(12)	1.42(1)	C(75) - C(76)	1.40(1)
C(11) - C(16)	1.39(1)	C(81) - C(82)	1.40(1)
C(12) - C(13)	1.38(1)	C(81) - C(86)	1.38(1)
C(13) - C(14)	1.38(1)	C(82) - C(83)	1.42(1)
C(14) - C(15)	1.40(1)	C(83) - C(84)	1.37(1)
C(15) - C(16)	1.38(1)	C(84) - C(85)	1.38(1)
C(21) - C(22)	1.39(1)	C(85) - C(86)	1.38(1)
C(21) - C(26)	1.40(1)	C(91) - C(92)	1.38(1)
C(22) - C(23)	1.39(1)	C(91) - C(96)	1.42(1)
C(23) - C(24)	1.40(1)	C(92) - C(93)	1.43(1)
C(24) - C(25)	1.38(1)	C(93) - C(94)	1.38(1)
C(25) - C(26)	1.40(1)	C(94) - C(95)	1.39(1)
C(31) - C(32)	1.39(1)	C(95) - C(96)	1.37(1)
C(31) - C(36)	1.42(1)	C(101)- C(102)	1.40(1)
C(32) - C(33)	1.39(1)	C(101)- C(106)	1.37(1)
C(33) - C(34)	1.38(1)	C(102)- C(103)	1.41(1)
C(34) - C(35)	1.38(1)	C(103)- C(104)	1.37(1)
C(35) - C(36)	1.39(1)	C(104)- C(105)	1.37(1)
		C(105)- C(106)	1.40(1)

Table G.6 Bond angles (°) with estimated standard deviations in parentheses for $[(Ph_3Sb)_2(\mu\text{-}O)(\mu\text{-}O_2AsPh_2)_2].CHCl_3$ ($3.6.CHCl_3$)

O(1) - Sb(1) - O(3)	86.6(2)	C(21) - C(26) - C(25)	118.4(8)
O(1) - Sb(1) - O(5)	86.4(2)	Sb(1) - C(31) - C(32)	120.2(5)
O(3) - Sb(1) - O(5)	80.2(2)	Sb(1) - C(31) - C(36)	121.3(5)
O(1) - Sb(1) - C(11)	168.4(2)	C(32) - C(31) - C(36)	118.0(7)
O(3) - Sb(1) - C(11)	86.3(2)	C(31) - C(32) - C(33)	121.4(8)
O(5) - Sb(1) - C(11)	83.4(2)	C(32) - C(33) - C(34)	120.2(8)
O(1) - Sb(1) - C(21)	90.9(2)	C(33) - C(34) - C(35)	119.6(7)
O(3) - Sb(1) - C(21)	89.5(2)	C(34) - C(35) - C(36)	120.7(7)
O(5) - Sb(1) - C(21)	169.4(2)	C(31) - C(36) - C(35)	120.1(8)
C(11) - Sb(1) - C(21)	98.1(3)	Sb(2) - C(41) - C(42)	122.3(6)
O(1) - Sb(1) - C(31)	87.7(2)	Sb(2) - C(41) - C(46)	117.9(6)
O(3) - Sb(1) - C(31)	168.7(2)	C(42) - C(41) - C(46)	119.8(7)
O(5) - Sb(1) - C(31)	89.7(2)	C(41) - C(42) - C(43)	120.0(8)
C(11) - Sb(1) - C(31)	97.7(3)	C(42) - C(43) - C(44)	119.9(8)
C(21) - Sb(1) - C(31)	100.4(3)	C(43) - C(44) - C(45)	119.9(8)
O(1) - Sb(2) - O(2)	86.3(2)	C(44) - C(45) - C(46)	120.1(8)
O(1) - Sb(2) - O(4)	85.9(2)	C(41) - C(46) - C(45)	120.4(9)
O(2) - Sb(2) - O(4)	82.8(2)	Sb(2) - C(51) - C(52)	118.9(5)
O(1) - Sb(2) - C(41)	166.2(3)	Sb(2) - C(51) - C(56)	120.8(5)
O(2) - Sb(2) - C(41)	83.3(2)	C(52) - C(51) - C(56)	120.2(7)
O(4) - Sb(2) - C(41)	83.9(2)	C(51) - C(52) - C(53)	119.2(7)
O(1) - Sb(2) - C(51)	91.9(2)	C(52) - C(53) - C(54)	120.3(7)
O(2) - Sb(2) - C(51)	173.1(2)	C(53) - C(54) - C(55)	120.8(7)
O(4) - Sb(2) - C(51)	90.4(2)	C(54) - C(55) - C(56)	120.2(7)
C(41) - Sb(2) - C(51)	97.4(3)	C(51) - C(56) - C(55)	119.2(7)
O(1) - Sb(2) - C(61)	92.6(2)	Sb(2) - C(61) - C(62)	120.7(5)
O(2) - Sb(2) - C(61)	86.7(2)	Sb(2) - C(61) - C(66)	121.1(5)
O(4) - Sb(2) - C(61)	169.4(2)	C(62) - C(61) - C(66)	118.0(7)
C(41) - Sb(2) - C(61)	95.7(3)	C(61) - C(62) - C(63)	120.7(7)
C(51) - Sb(2) - C(61)	100.1(3)	C(62) - C(63) - C(64)	119.3(7)
O(2) - As(1) - O(3)	118.8(2)	C(63) - C(64) - C(65)	122.1(7)
O(2) - As(1) - C(71)	109.2(3)	C(64) - C(65) - C(66)	118.7(8)
O(3) - As(1) - C(71)	103.8(3)	C(61) - C(66) - C(65)	121.0(7)
O(2) - As(1) - C(81)	106.0(3)	As(1) - C(71) - C(72)	120.0(6)
O(3) - As(1) - C(81)	109.5(3)	As(1) - C(71) - C(76)	117.8(6)
C(71) - As(1) - C(81)	109.3(3)	C(72) - C(71) - C(76)	122.1(7)
O(4) - As(2) - O(5)	118.6(2)	C(71) - C(72) - C(73)	120.3(8)
O(4) - As(2) - C(91)	104.8(3)	C(72) - C(73) - C(74)	119.0(8)
O(5) - As(2) - C(91)	109.2(3)	C(73) - C(74) - C(75)	120.9(8)
O(4) - As(2) - C(101)	109.5(3)	C(74) - C(75) - C(76)	120.6(8)
O(5) - As(2) - C(101)	107.5(3)	C(71) - C(76) - C(75)	117.1(8)
C(91) - As(2) - C(101)	106.8(3)	As(1) - C(81) - C(82)	118.3(6)
Sb(1) - O(1) - Sb(2)	151.7(3)	As(1) - C(81) - C(86)	120.8(6)
Sb(2) - O(2) - As(1)	125.9(2)	C(82) - C(81) - C(86)	120.9(7)
Sb(1) - O(3) - As(1)	129.1(3)	C(81) - C(82) - C(83)	117.8(8)
Sb(2) - O(4) - As(2)	128.6(2)	C(82) - C(83) - C(84)	120.1(9)
Sb(1) - O(5) - As(2)	127.4(2)	C(83) - C(84) - C(85)	121.1(8)
Cl(1) - C(1) - Cl(2)	111.9(6)	C(84) - C(85) - C(86)	119.8(9)
Cl(1) - C(1) - Cl(3)	110.1(5)	C(81) - C(86) - C(85)	120.3(8)
Cl(2) - C(1) - Cl(3)	110.5(5)	As(2) - C(91) - C(92)	120.9(6)
Sb(1) - C(11) - C(12)	124.2(5)	As(2) - C(91) - C(96)	117.0(6)
Sb(1) - C(11) - C(16)	119.1(6)	C(92) - C(91) - C(96)	121.9(7)
C(12) - C(11) - C(16)	116.7(7)	C(91) - C(92) - C(93)	118.9(8)

C(11) - C(12) - C(13)	120.8(7)	C(92) - C(93) - C(94)	117.7(8)
C(12) - C(13) - C(14)	121.6(9)	C(93) - C(94) - C(95)	123.2(8)
C(13) - C(14) - C(15)	118.4(8)	C(94) - C(95) - C(96)	119.1(8)
C(14) - C(15) - C(16)	119.8(7)	C(91) - C(96) - C(95)	119.1(8)
C(11) - C(16) - C(15)	122.7(8)	As(2) - C(101)- C(102)	118.0(6)
Sb(1) - C(21) - C(22)	119.3(5)	As(2) - C(101)- C(106)	120.0(5)
Sb(1) - C(21) - C(26)	121.4(5)	C(102)- C(101)- C(106)	121.8(7)
C(22) - C(21) - C(26)	119.4(7)	C(101)- C(102)- C(103)	117.6(8)
C(21) - C(22) - C(23)	121.8(7)	C(102)- C(103)- C(104)	120.3(8)
C(22) - C(23) - C(24)	118.9(8)	C(103)- C(104)- C(105)	121.1(8)
C(23) - C(24) - C(25)	119.3(7)	C(104)- C(105)- C(106)	119.6(9)
C(24) - C(25) - C(26)	122.1(8)	C(101)- C(106)- C(105)	119.5(8)

Experimental Details

Slightly more than one hemisphere of data were collected on a Delft Instruments FAST TV area detector, equipped with a rotating anode FR591 generator. The data were corrected for Lorentz and polarisation effects, merged and systematically absent reflections were rejected. The structure was solved direct methods (SIR-92)[5] and subsequent Fourier difference syntheses revealed the positions of all the other non-hydrogen atoms. Refinement was carried out against 'observed' F_o^2 data by full matrix procedures. Hydrogen atoms were placed in estimated positions (C–H = 1.00 Å) and assigned a common fixed thermal parameter (with the exception of the hydrogen of the chloroform molecule that was assigned a different thermal parameter) and refined 'riding' their respective carbon atoms. Data were corrected by a Chebyshev weighting scheme[6] (4 coefficient) and also for the effects of absorption[4], anomalous dispersion and isotropic extinction[7]. All crystallographic calculations were performed using the CRYSTALS suite of programs[8] and neutral atom scattering factors were taken from the usual sources[3].

APPENDIX H

Table H.1 Data collection and processing parameters for [((*p*-MeC_6H_4)$_3$Sb)$_2$(μ-O)(μ-O_2PMe_2)$_2$].0.5C_6H_{14} (3.7.0.5C_6H_{14})

Chemical formula	$C_{49}H_{61}O_5P_2Sb_2$
Formula weight	1035.47
Crystal size/mm	0.24 x 0.22 x 0.18
Crystal system	Monoclinic
Space group	$P2_1/n$
a / Å	12.038(12)
b / Å	17.127(13)
c / Å	23.35(2)
β / °	90.27(3)
Volume / Å^3	4814.63
Z	4
D_c/gcm^{-3}	1.429
Radiation (λ / Å)	Mo-K_α (0.71069)
μ / cm^{-1}	12.358
F(000)	2108
2θ limits / °	5-50
Index ranges (for unique data set)	-13<=h<=13, 0<=k<=19, 0<=l<=26
Temperature / K	150
Total data collected	23252
Unique data	7414 [(R(int) = 0.0937]
Observed data [$I > 2\sigma(I)$]	4900
Absorption correction	DIFABS (min, 0.849, max, 1.118)[4]
Structure solution	Direct (SIR-92)[5]
Refinement procedure	Full matrix-LS on F^2
Number of data / variables	4900 / 517
S	1.134
Max/min peaks in final diff. map / e Å^{-3}	+0.74, -0.49
R	0.0367
R_w	0.0912

Table H.2 Fractional atomic coordinates and equivalent isotropic displacement parameters ($Å^2$) with estimated standard deviations in parentheses for $[((p\text{-}MeC_6H_4)_3Sb)_2(\mu\text{-}O)(\mu\text{-}O_2PMc_2)_2].0.5C_6H_{14}$ ($3.7.0.5C_6H_{14}$)

Atom	x/a	y/b	z/c	U(eq)
Sb(1)	0.40770(4)	0.03565(3)	0.26423(2)	0.0224
Sb(2)	0.11880(4)	0.06862(3)	0.31587(2)	0.0214
P(1)	0.1990(2)	-0.0808(1)	0.22588(9)	0.0246
P(2)	0.3001(2)	-0.0460(1)	0.38457(8)	0.0260
O(1)	0.2665(4)	0.0870(3)	0.2842(2)	0.0230
O(2)	0.1357(4)	-0.0487(3)	0.2770(2)	0.0246
O(3)	0.3055(4)	-0.0364(3)	0.2108(2)	0.0246
O(4)	0.2169(4)	0.0208(3)	0.3882(2)	0.0245
O(5)	0.3638(4)	-0.0506(3)	0.3283(2)	0.0248
C(1)	0.1126(7)	-0.0790(5)	0.1637(3)	0.0366
C(2)	0.2319(8)	-0.1814(5)	0.2401(4)	0.0366
C(3)	0.2287(7)	-0.1365(5)	0.3943(4)	0.0336
C(4)	0.3972(7)	-0.0381(5)	0.4427(4)	0.0391
C(11)	0.5386(6)	-0.0459(4)	0.2445(3)	0.0244
C(12)	0.6271(7)	-0.0206(5)	0.2099(4)	0.0353
C(13)	0.7168(7)	-0.0685(6)	0.1985(4)	0.0370
C(14)	0.7209(7)	-0.1424(5)	0.2191(3)	0.0276
C(15)	0.6362(7)	-0.1690(5)	0.2543(3)	0.0312
C(16)	0.5448(6)	-0.1217(5)	0.2665(3)	0.0311
C(17)	0.8215(7)	-0.1943(5)	0.2063(4)	0.0413
C(21)	0.4317(6)	0.1124(5)	0.1918(3)	0.0276
C(22)	0.3798(7)	0.1030(5)	0.1399(4)	0.0386
C(23)	0.4022(8)	0.1524(6)	0.0942(4)	0.0437
C(24)	0.4777(7)	0.2128(5)	0.0991(4)	0.0351
C(25)	0.5277(8)	0.2239(5)	0.1520(4)	0.0339
C(26)	0.5047(7)	0.1750(5)	0.1972(4)	0.0356
C(27)	0.5065(8)	0.2647(5)	0.0483(4)	0.0392
C(31)	0.4986(6)	0.0996(4)	0.3289(3)	0.0230
C(32)	0.4540(7)	0.1665(5)	0.3534(3)	0.0292
C(33)	0.5105(7)	0.2068(5)	0.3958(4)	0.0358
C(34)	0.6138(8)	0.1830(5)	0.4148(4)	0.0331
C(35)	0.6602(8)	0.1176(6)	0.3896(5)	0.0423
C(36)	0.6025(7)	0.0759(5)	0.3483(4)	0.0301
C(37)	0.678(1)	0.2290(6)	0.4605(5)	0.0574
C(41)	-0.0149(6)	0.0117(4)	0.3596(3)	0.0208
C(42)	-0.0858(6)	-0.0434(5)	0.3331(3)	0.0292
C(43)	-0.1712(6)	-0.0781(5)	0.3632(4)	0.0288
C(44)	-0.1880(6)	-0.0617(5)	0.4210(3)	0.0278
C(45)	-0.1170(6)	-0.0066(5)	0.4481(3)	0.0289
C(46)	-0.0336(6)	0.0300(5)	0.4179(3)	0.0268
C(47)	-0.2778(8)	-0.1024(6)	0.4545(4)	0.0448
C(51)	0.1129(6)	0.1767(5)	0.3621(3)	0.0251
C(52)	0.1919(6)	0.1990(5)	0.4033(3)	0.0249
C(53)	0.1878(7)	0.2715(5)	0.4289(3)	0.0344
C(54)	0.1041(7)	0.3241(5)	0.4148(3)	0.0317
C(55)	0.0237(8)	0.3020(5)	0.3752(4)	0.0358
C(56)	0.0281(7)	0.2287(5)	0.3485(3)	0.0325
C(57)	0.0986(9)	0.4027(6)	0.4442(4)	0.0529
C(61)	0.0330(6)	0.1071(4)	0.2397(3)	0.0236

C(62)	-0.0807(7)	0.1000(5)	0.2315(3)	0.0315
C(63)	-0.1307(8)	0.1268(5)	0.1809(4)	0.0381
C(64)	-0.0710(8)	0.1594(5)	0.1376(4)	0.0350
C(65)	0.0418(8)	0.1662(5)	0.1446(4)	0.0429
C(66)	0.0955(8)	0.1404(5)	0.1949(3)	0.0360
C(67)	-0.128(1)	0.1874(7)	0.0829(5)	0.0580
C(100)	0.058(3)	0.007(2)	0.004(1)	0.078(8)
C(101)	0.111(2)	0.041(1)	-0.050(1)	0.065(6)
C(102)	0.240(2)	0.046(1)	-0.0407(8)	0.129(6)
C(103)	0.151(3)	0.015(2)	0.009(1)	0.11(1)
C(104)	0.048(4)	0.021(3)	-0.027(2)	0.15(2)

Table H.3 Calculated hydrogen coordinates and isotropic displacement parameters ($Å^2$) with estimated standard deviations in parentheses for $[((p\text{-}MeC_6H_4)_3Sb)_2(\mu\text{-}O)(\mu\text{-}O_2PMe_2)_2].0.5C_6H_{14}$ ($3.7.0.5C_6H_{14}$)

Atom	x/a	y/b	z/c	U(iso)
H(11)	0.0924(7)	-0.0238(5)	0.1546(3)	0.0600
H(12)	0.0435(7)	-0.1099(5)	0.1708(3)	0.0600
H(13)	0.1538(7)	-0.1022(5)	0.1307(3)	0.0600
H(21)	0.2802(8)	-0.1849(5)	0.2750(4)	0.0600
H(22)	0.1619(8)	-0.2115(5)	0.2466(4)	0.0600
H(23)	0.2723(8)	-0.2039(5)	0.2065(4)	0.0600
H(31)	0.1731(7)	-0.1436(5)	0.3627(4)	0.0600
H(32)	0.1896(7)	-0.1362(5)	0.4320(4)	0.0600
H(33)	0.2834(7)	-0.1805(5)	0.3935(4)	0.0600
H(41)	0.4393(7)	0.0120(5)	0.4391(4)	0.0600
H(42)	0.3565(7)	-0.0387(5)	0.4799(4)	0.0600
H(43)	0.4502(7)	-0.0830(5)	0.4414(4)	0.0600
H(121)	0.6247(7)	0.0334(5)	0.1937(4)	0.0462
H(131)	0.7791(7)	-0.0485(6)	0.1744(4)	0.0512
H(151)	0.6411(7)	-0.2226(5)	0.2712(3)	0.0423
H(161)	0.4829(6)	-0.1416(5)	0.2909(3)	0.0414
H(171)	0.8108(7)	-0.2465(5)	0.2247(4)	0.0617
H(172)	0.8901(7)	-0.1692(5)	0.2222(4)	0.0617
H(173)	0.8294(7)	-0.2011(5)	0.1640(4)	0.0617
H(221)	0.3240(7)	0.0602(5)	0.1352(4)	0.0537
H(231)	0.3627(8)	0.1446(6)	0.0569(4)	0.0609
H(251)	0.5801(8)	0.2687(5)	0.1573(4)	0.0467
H(261)	0.5428(7)	0.1838(5)	0.2348(4)	0.0496
H(271)	0.5630(8)	0.3043(5)	0.0603(4)	0.0556
H(272)	0.5372(8)	0.2321(5)	0.0166(4)	0.0556
H(273)	0.4378(8)	0.2919(5)	0.0347(4)	0.0556
H(321)	0.3803(7)	0.1857(5)	0.3395(3)	0.0389
H(331)	0.4757(7)	0.2539(5)	0.4136(4)	0.0466
H(351)	0.7363(8)	0.1006(6)	0.4015(5)	0.0638
H(361)	0.6365(7)	0.0278(5)	0.3316(4)	0.0456
H(371)	0.751(1)	0.2030(6)	0.4683(5)	0.0909
H(372)	0.634(1)	0.2307(6)	0.4965(5)	0.0909
H(373)	0.692(1)	0.2834(6)	0.4466(5)	0.0909
H(421)	-0.0731(6)	-0.0575(5)	0.2921(3)	0.0400

H(431)	-0.2218(6)	-0.1158(5)	0.3434(4)	0.0384
H(451)	-0.1274(6)	0.0052(5)	0.4897(3)	0.0424
H(461)	0.0142(6)	0.0700(5)	0.4372(3)	0.0374
H(471)	-0.2777(8)	-0.0830(6)	0.4949(4)	0.0665
H(472)	-0.2638(8)	-0.1600(6)	0.4542(4)	0.0665
H(473)	-0.3516(8)	-0.0913(6)	0.4364(4)	0.0665
H(521)	0.2513(6)	0.1611(5)	0.4147(3)	0.0334
H(531)	0.2458(7)	0.2869(5)	0.4575(3)	0.0447
H(551)	-0.0383(8)	0.3388(5)	0.3658(4)	0.0479
H(561)	-0.0294(7)	0.2133(5)	0.3196(3)	0.0447
H(571)	0.0336(9)	0.4326(6)	0.4290(4)	0.0688
H(572)	0.0900(9)	0.3950(6)	0.4864(4)	0.0688
H(573)	0.1685(9)	0.4325(6)	0.4366(4)	0.0688
H(621)	-0.1268(7)	0.0755(5)	0.2622(3)	0.0434
H(631)	-0.2130(8)	0.1222(5)	0.1760(4)	0.0507
H(651)	0.0867(8)	0.1898(5)	0.1131(4)	0.0589
H(661)	0.1779(8)	0.1453(5)	0.1993(3)	0.0446
H(671)	-0.072(1)	0.2096(7)	0.0560(5)	0.0922
H(672)	-0.185(1)	0.2284(7)	0.0925(5)	0.0922
H(673)	-0.167(1)	0.1420(7)	0.0643(5)	0.0922

Table H.4 Anisotropic thermal parameters ($Å^2$) with estimated standard deviations in parentheses for $[((p\text{-}MeC_6H_4)_3Sb)_2(\mu\text{-}O)(\mu\text{-}O_2PMe_2)_2].0.5C_6H_{14}$ (3.7.0.5C_6H_{14})

Atom	U(11)	U(22)	U(33)	U(23)	U(13)	U(12)
Sb(1)	0.0204(3)	0.0197(3)	0.0280(3)	-0.0012(2)	0.0019(2)	-0.0005(2)
Sb(2)	0.0204(3)	0.0238(3)	0.0204(3)	-0.0019(2)	-0.0012(2)	0.0016(2)
P(1)	0.025(1)	0.024(1)	0.028(1)	-0.0067(9)	0.0034(8)	-0.0044(8)
P(2)	0.025(1)	0.027(1)	0.027(1)	0.0020(9)	-0.0010(8)	0.0007(8)
O(1)	0.014(2)	0.025(3)	0.037(3)	-0.001(2)	0.000(2)	0.003(2)
O(2)	0.023(3)	0.024(3)	0.029(3)	-0.001(2)	0.002(2)	-0.005(2)
O(3)	0.030(3)	0.026(3)	0.028(3)	-0.011(2)	0.012(2)	-0.006(2)
O(4)	0.025(3)	0.031(3)	0.020(3)	-0.001(2)	-0.005(2)	0.003(2)
O(5)	0.024(3)	0.024(3)	0.029(3)	0.005(2)	0.004(2)	0.001(2)
C(1)	0.033(5)	0.045(6)	0.036(5)	-0.004(4)	0.001(4)	-0.010(4)
C(2)	0.049(6)	0.022(4)	0.050(6)	-0.008(4)	0.009(5)	-0.004(4)
C(3)	0.045(5)	0.033(5)	0.031(5)	0.010(4)	0.005(4)	-0.009(4)
C(4)	0.033(5)	0.038(5)	0.049(5)	-0.001(4)	-0.007(4)	0.005(4)
C(11)	0.023(4)	0.021(4)	0.036(4)	-0.006(4)	0.003(3)	0.006(3)
C(12)	0.033(5)	0.032(5)	0.046(5)	0.004(4)	0.012(4)	0.003(4)
C(13)	0.031(5)	0.042(6)	0.046(5)	-0.001(5)	0.015(4)	-0.004(4)
C(14)	0.035(5)	0.024(5)	0.030(5)	-0.009(4)	0.006(4)	0.004(4)
C(15)	0.040(5)	0.021(4)	0.038(5)	-0.004(4)	-0.000(4)	0.007(4)
C(16)	0.026(4)	0.034(5)	0.035(5)	-0.001(4)	0.004(4)	0.001(3)
C(17)	0.039(5)	0.040(6)	0.061(6)	-0.010(5)	0.011(5)	0.015(4)
C(21)	0.024(4)	0.027(5)	0.034(5)	0.003(4)	0.005(3)	0.003(3)
C(22)	0.046(5)	0.042(5)	0.037(5)	-0.003(4)	0.004(4)	-0.018(4)
C(23)	0.051(6)	0.057(7)	0.031(5)	-0.000(5)	-0.003(4)	-0.012(5)
C(24)	0.037(5)	0.034(5)	0.040(5)	0.001(4)	0.014(4)	0.003(4)
C(25)	0.059(6)	0.023(5)	0.038(5)	0.002(4)	-0.001(4)	-0.017(4)
C(26)	0.042(5)	0.032(5)	0.039(5)	-0.010(4)	0.004(4)	-0.010(4)
C(27)	0.061(6)	0.042(5)	0.030(5)	0.006(4)	0.017(4)	-0.004(5)

C(31)	0.025(4)	0.024(4)	0.021(4)	0.001(3)	-0.000(3)	-0.006(3)
C(32)	0.031(4)	0.034(5)	0.027(4)	0.009(4)	0.001(4)	-0.004(4)
C(33)	0.047(5)	0.030(5)	0.034(5)	-0.001(4)	0.001(4)	-0.007(4)
C(34)	0.059(6)	0.030(5)	0.037(5)	0.015(4)	-0.025(5)	-0.013(4)
C(35)	0.046(6)	0.036(6)	0.081(8)	0.023(5)	-0.033(5)	-0.002(5)
C(36)	0.036(5)	0.022(5)	0.046(5)	0.005(4)	-0.019(4)	0.001(4)
C(37)	0.094(9)	0.053(7)	0.067(8)	0.001(6)	-0.051(7)	-0.011(6)
C(41)	0.019(4)	0.024(4)	0.023(4)	0.005(3)	-0.000(3)	0.005(3)
C(42)	0.034(4)	0.027(5)	0.030(4)	-0.004(4)	0.004(4)	0.008(4)
C(43)	0.027(4)	0.020(4)	0.045(5)	0.001(4)	0.001(4)	-0.002(3)
C(44)	0.027(4)	0.031(5)	0.031(4)	0.006(4)	0.007(3)	0.009(4)
C(45)	0.031(4)	0.039(5)	0.024(4)	0.008(4)	0.003(4)	0.011(4)
C(46)	0.021(4)	0.034(5)	0.030(4)	0.002(4)	-0.005(3)	0.006(3)
C(47)	0.044(6)	0.042(6)	0.062(6)	0.002(5)	0.022(5)	-0.008(4)
C(51)	0.030(4)	0.025(4)	0.023(4)	-0.007(3)	0.000(3)	0.003(3)
C(52)	0.028(4)	0.034(5)	0.017(4)	-0.003(3)	0.003(3)	0.004(3)
C(53)	0.039(5)	0.044(5)	0.026(4)	-0.005(4)	0.003(4)	-0.009(4)
C(54)	0.048(5)	0.021(4)	0.033(5)	-0.006(4)	0.003(4)	0.000(4)
C(55)	0.052(6)	0.030(5)	0.035(5)	-0.000(4)	0.005(4)	0.015(4)
C(56)	0.037(5)	0.036(5)	0.029(4)	-0.006(4)	-0.001(4)	0.007(4)
C(57)	0.075(7)	0.043(6)	0.050(6)	-0.012(5)	0.008(5)	0.005(5)
C(61)	0.030(4)	0.021(4)	0.023(4)	-0.002(3)	-0.009(3)	0.005(3)
C(62)	0.033(5)	0.032(5)	0.033(5)	0.000(4)	-0.010(4)	0.001(4)
C(63)	0.046(6)	0.026(5)	0.057(6)	-0.007(5)	-0.019(5)	-0.002(4)
C(64)	0.058(6)	0.030(5)	0.031(5)	0.003(4)	-0.019(4)	-0.000(4)
C(65)	0.065(7)	0.036(6)	0.038(5)	0.012(4)	-0.005(5)	-0.001(5)
C(66)	0.050(5)	0.036(5)	0.027(5)	0.005(4)	-0.005(4)	-0.000(4)
C(67)	0.11(1)	0.055(7)	0.061(7)	0.018(6)	-0.046(7)	0.010(7)

Table H.5 Bond lengths (Å) with estimated standard deviations in parentheses for [((*p*-$McC_6H_4)_3Sb)_2(\mu$-O)(μ-$O_2PMe_2)_2$].0.5C_6H_{14} (3.7.0.5C_6H_{14})

Sb(1) - O(1)	1.972(5)	C(32) - C(33)	1.38(1)
Sb(1) - O(3)	2.139(5)	C(33) - C(34)	1.38(1)
Sb(1) - O(5)	2.170(5)	C(34) - C(35)	1.38(1)
Sb(1) - C(11)	2.158(7)	C(34) - C(37)	1.53(1)
Sb(1) - C(21)	2.163(8)	C(35) - C(36)	1.39(1)
Sb(1) - C(31)	2.159(7)	C(41) - C(42)	1.41(1)
Sb(2) - O(1)	1.954(5)	C(41) - C(46)	1.42(1)
Sb(2) - O(2)	2.215(5)	C(42) - C(43)	1.38(1)
Sb(2) - O(4)	2.213(5)	C(43) - C(44)	1.39(1)
Sb(2) - C(41)	2.144(7)	C(44) - C(45)	1.42(1)
Sb(2) - C(51)	2.144(7)	C(44) - C(47)	1.51(1)
Sb(2) - C(61)	2.156(7)	C(45) - C(46)	1.38(1)
P(1) - O(2)	1.521(5)	C(51) - C(52)	1.40(1)
P(1) - O(3)	1.533(5)	C(51) - C(56)	1.39(1)
P(1) - C(1)	1.783(8)	C(52) - C(53)	1.38(1)
P(1) - C(2)	1.800(8)	C(53) - C(54)	1.39(1)
P(2) - O(4)	1.524(5)	C(54) - C(55)	1.39(1)
P(2) - O(5)	1.526(5)	C(54) - C(57)	1.51(1)
P(2) - C(3)	1.788(8)	C(55) - C(56)	1.40(1)
P(2) - C(4)	1.792(8)	C(61) - C(62)	1.39(1)

C(11) - C(12)	1.41(1)	C(61) - C(66)	1.41(1)
C(11) - C(16)	1.40(1)	C(62) - C(63)	1.40(1)
C(12) - C(13)	1.38(1)	C(63) - C(64)	1.36(1)
C(13) - C(14)	1.36(1)	C(64) - C(65)	1.37(1)
C(14) - C(15)	1.39(1)	C(64) - C(67)	1.53(1)
C(14) - C(17)	1.53(1)	C(65) - C(66)	1.41(1)
C(15) - C(16)	1.40(1)	C(100)- C(100')	1.44(6)
C(21) - C(22)	1.37(1)	C(100)- C(101)	1.53(5)
C(21) - C(26)	1.39(1)	C(100)- C(103)	1.12(4)
C(22) - C(23)	1.39(1)	C(100)- C(104)	0.77(5)
C(23) - C(24)	1.38(1)	C(100')- C(104)	1.47(4)
C(24) - C(25)	1.39(1)	C(101)- C(102)	1.57(3)
C(24) - C(27)	1.52(1)	C(101)- C(103)	1.53(4)
C(25) - C(26)	1.38(1)	C(101)- C(104)	1.00(5)
C(31) - C(32)	1.39(1)	C(102)- C(103)	1.68(4)
C(31) - C(36)	1.39(1)	C(103)- C(104)	1.50(6)

Table H.6 Bond angles (°) with estimated standard deviations in parentheses for [((*p*-$MeC_6H_4)_3Sb)_2(\mu\text{-}O)(\mu\text{-}O_2PMe_2)_2].0.5C_6H_{14}$ ($3.7.0.5C_6H_{14}$)

O(1) - Sb(1) - O(3)	84.3(2)	Sb(1) - C(31) - C(36)	122.2(6)
O(1) - Sb(1) - O(5)	85.8(2)	C(32) - C(31) - C(36)	117.1(7)
O(3) - Sb(1) - O(5)	82.4(2)	C(31) - C(32) - C(33)	121.1(8)
O(1) - Sb(1) - C(11)	166.1(2)	C(32) - C(33) - C(34)	121.4(8)
O(3) - Sb(1) - C(11)	85.5(2)	C(33) - C(34) - C(35)	117.9(8)
O(5) - Sb(1) - C(11)	83.5(2)	C(33) - C(34) - C(37)	121.6(9)
O(1) - Sb(1) - C(21)	91.9(2)	C(35) - C(34) - C(37)	120.5(9)
O(3) - Sb(1) - C(21)	88.4(3)	C(34) - C(35) - C(36)	120.8(8)
O(5) - Sb(1) - C(21)	170.8(2)	C(31) - C(36) - C(35)	121.6(8)
C(11) - Sb(1) - C(21)	97.2(3)	Sb(2) - C(41) - C(42)	123.3(5)
O(1) - Sb(1) - C(31)	92.4(2)	Sb(2) - C(41) - C(46)	118.7(5)
O(3) - Sb(1) - C(31)	171.3(2)	C(42) - C(41) - C(46)	118.1(7)
O(5) - Sb(1) - C(31)	89.3(2)	C(41) - C(42) - C(43)	120.9(7)
C(11) - Sb(1) - C(31)	96.3(3)	C(42) - C(43) - C(44)	121.2(7)
C(21) - Sb(1) - C(31)	99.8(3)	C(43) - C(44) - C(45)	118.4(7)
O(1) - Sb(2) - O(2)	84.6(2)	C(43) - C(44) - C(47)	121.1(8)
O(1) - Sb(2) - O(4)	82.2(2)	C(45) - C(44) - C(47)	120.4(7)
O(2) - Sb(2) - O(4)	85.8(2)	C(44) - C(45) - C(46)	120.8(7)
O(1) - Sb(2) - C(41)	160.0(2)	C(41) - C(46) - C(45)	120.6(7)
O(2) - Sb(2) - C(41)	81.6(2)	Sb(2) - C(51) - C(52)	123.9(6)
O(4) - Sb(2) - C(41)	82.4(2)	Sb(2) - C(51) - C(56)	117.6(6)
O(1) - Sb(2) - C(51)	94.8(3)	C(52) - C(51) - C(56)	118.4(7)
O(2) - Sb(2) - C(51)	173.2(2)	C(51) - C(52) - C(53)	121.1(8)
O(4) - Sb(2) - C(51)	87.4(2)	C(52) - C(53) - C(54)	120.6(8)
C(41) - Sb(2) - C(51)	97.2(3)	C(53) - C(54) - C(55)	118.9(8)
O(1) - Sb(2) - C(61)	94.1(3)	C(53) - C(54) - C(57)	120.2(8)
O(2) - Sb(2) - C(61)	89.0(2)	C(55) - C(54) - C(57)	120.8(8)
O(4) - Sb(2) - C(61)	174.0(2)	C(54) - C(55) - C(56)	120.8(8)
C(41) - Sb(2) - C(61)	100.0(3)	C(51) - C(56) - C(55)	120.1(8)
C(51) - Sb(2) - C(61)	97.8(3)	Sb(2) - C(61) - C(62)	123.8(6)
O(2) - P(1) - O(3)	115.1(3)	Sb(2) - C(61) - C(66)	118.6(6)
O(2) - P(1) - C(1)	109.9(3)	C(62) - C(61) - C(66)	117.6(7)

O(3) - P(1) - C(1)	106.9(3)	C(61) - C(62) - C(63)	120.5(8)
O(2) - P(1) - C(2)	108.2(4)	C(62) - C(63) - C(64)	122.3(9)
O(3) - P(1) - C(2)	109.5(4)	C(63) - C(64) - C(65)	118.1(8)
C(1) - P(1) - C(2)	107.1(4)	C(63) - C(64) - C(67)	120.7(9)
O(4) - P(2) - O(5)	114.8(3)	C(65) - C(64) - C(67)	121.2(9)
O(4) - P(2) - C(3)	109.1(4)	C(64) - C(65) - C(66)	121.6(9)
O(5) - P(2) - C(3)	108.0(3)	C(61) - C(66) - C(65)	120.0(8)
O(4) - P(2) - C(4)	109.1(4)	C(100')- C(100)- C(101)	111.9(36)
O(5) - P(2) - C(4)	109.1(4)	C(100')- C(100)- C(103)	176.8(45)
C(3) - P(2) - C(4)	106.4(4)	C(101)- C(100)- C(103)	68.2(26)
Sb(1) - O(1) - Sb(2)	143.6(3)	C(100')- C(100)- C(104)	77.1(55)
Sb(2) - O(2) - P(1)	134.1(3)	C(101)- C(100)- C(104)	34.8(51)
Sb(1) - O(3) - P(1)	129.2(3)	C(103)- C(100)- C(104)	103.0(66)
Sb(2) - O(4) - P(2)	125.8(3)	C(100')- C(100)- C(104')	30.7(21)
Sb(1) - O(5) - P(2)	133.1(3)	C(101)- C(100)- C(104')	142.7(38)
Sb(1) - C(11) - C(12)	118.6(6)	C(103)- C(100)- C(104')	149.0(47)
Sb(1) - C(11) - C(16)	124.1(6)	C(104)- C(100)- C(104')	107.9(60)
C(12) - C(11) - C(16)	117.3(7)	C(100)- C(101)- C(102)	108.6(20)
C(11) - C(12) - C(13)	121.4(8)	C(100')- C(101)- C(103)	43.2(16)
C(12) - C(13) - C(14)	120.8(8)	C(102)- C(101)- C(103)	65.5(18)
C(13) - C(14) - C(15)	119.5(7)	C(100)- C(101)- C(104)	26.2(34)
C(13) - C(14) - C(17)	119.9(7)	C(102)- C(101)- C(104)	134.7(41)
C(15) - C(14) - C(17)	120.5(8)	C(103)- C(101)- C(104)	69.4(37)
C(14) - C(15) - C(16)	120.7(8)	C(101)- C(102)- C(103)	55.9(15)
C(11) - C(16) - C(15)	120.3(7)	C(100)- C(103)- C(101)	68.6(28)
Sb(1) - C(21) - C(22)	124.0(6)	C(100)- C(103)- C(102)	127.0(34)
Sb(1) - C(21) - C(26)	118.9(6)	C(101)- C(103)- C(102)	58.6(17)
C(22) - C(21) - C(26)	117.1(8)	C(100)- C(103)- C(104)	30.1(28)
C(21) - C(22) - C(23)	121.3(8)	C(101)- C(103)- C(104)	38.5(19)
C(22) - C(23) - C(24)	121.5(8)	C(102)- C(103)- C(104)	97.0(28)
C(23) - C(24) - C(25)	117.4(8)	C(100)- C(104)- C(100')	72.1(60)
C(23) - C(24) - C(27)	121.6(8)	C(100)- C(104)- C(101)	118.9(79)
C(25) - C(24) - C(27)	121.0(8)	C(100')- C(104)- C(101)	168.8(60)
C(24) - C(25) - C(26)	120.8(8)	C(100)- C(104)- C(103)	46.9(46)
C(21) - C(26) - C(25)	121.9(8)	C(100')- C(104)- C(103)	118.9(46)
Sb(1) - C(31) - C(32)	120.7(6)	C(101)- C(104)- C(103)	72.1(40)

Symmetry operation: (') = -x, -y, -z

Experimental Details

Slightly more than one hemisphere of data were collected on a Delft Instruments FAST TV area detector, equipped with a rotating anode FR591 generator. The data were corrected for Lorentz and polarisation effects, merged and systematically absent reflections were rejected. The structure was solved by direct methods (SIR-92)[5] and subsequent Fourier difference syntheses revealed the positions of all the other non-hydrogen atoms. Refinement was carried out against 'observed' F_o^2 data by full matrix procedures, using an anisotropic model for all non-hydrogen atoms except for the carbon atoms of the disordered solvent molecule which was modelled using one full occupancy carbon atom and four half occupancy atoms and refined isotropically. Hydrogen atoms were placed in estimated positions (C–H = 1.00 Å) with fixed isotropic parameters (1.3 x equivalent isotropic temperature factors of the carbon atom to which they were bonded) and refined 'riding' their respective carbon atoms. Data were corrected by a Chebyshev weighting scheme[6] (4 coefficient) and also for the effects of absorption[4], anomalous dispersion and isotropic extinction[7]. All crystallographic calculations were performed using the CRYSTALS suite of programs[8] and neutral atom scattering factors were taken from the usual sources[3].

APPENDIX I

Table I.1 Data collection and processing parameters for $Ph_2SbS_2PMe_2$ (3.11)

Chemical formula	$C_{14}H_{16}PS_2Sb$
Formula weight	401.13
Crystal size/mm	0.5 x 0.3 x 0.3
Crystal system	Triclinic
Space group	$P\bar{1}$
a / Å	9.389(3)
b / Å	10.032(3)
c / Å	10.177(3)
α / °	104.27(1)
β / °	116.67(2)
γ / °	94.93(2)
Volume / Å^3	808.49
Z	2
D_c/gcm^{-3}	1.648
Radiation (λ / Å)	Mo-K_α (0.71069)
μ / cm^{-1}	20.4
F(000)	396
2θ limits / °	5-50
Index ranges	-11<=h<=9, -11<=k<=11, 0<=l<=12
Temperature / K	298
Total unique data collected	4276
Observed data [$I > 3\sigma(I)$]	2717
Absorption correction	DIFABS (min, 0.749, max, 1.204)[4]
Structure solution	Patterson (CRYSTALS)[8]
Refinement procedure	Full matrix-LS on F
Number of data / variables	2717 / 163
Max/min peaks in final diff. map / e Å^{-3}	+1.2, -0.32
R	0.0387
R_w	0.0435

Table I.2 Fractional atomic coordinates and equivalent isotropic displacement parameters ($Å^2$) with estimated standard deviations in parentheses for $Ph_2SbS_2PMe_2$ (3.11)

Atom	x/a	y/b	z/c	U(eq)
Sb(1)	0.38865(2)	0.48677(2)	0.10004(2)	0.0430
P(1)	0.3531(1)	0.82679(9)	0.0886(1)	0.0483
S(1)	0.2378(1)	0.6734(1)	0.1350(1)	0.0493
S(2)	0.3827(2)	0.7639(1)	-0.0943(1)	0.0622
C(1)	0.1870(4)	0.3568(4)	-0.1213(4)	0.0470
C(2)	0.1097(5)	0.4109(5)	-0.2400(5)	0.0607
C(3)	-0.0123(7)	0.3254(7)	-0.3844(6)	0.0762
C(4)	-0.0571(7)	0.1839(7)	-0.4125(6)	0.0739
C(5)	0.0202(8)	0.1274(5)	-0.2967(7)	0.0784
C(6)	0.1415(6)	0.2140(5)	-0.1509(6)	0.0691
C(7)	0.3296(4)	0.3850(4)	0.2384(4)	0.0452
C(8)	0.4545(5)	0.3464(4)	0.3509(4)	0.0529
C(9)	0.4213(6)	0.2851(4)	0.4468(4)	0.0578
C(10)	0.2681(7)	0.2643(5)	0.4304(5)	0.0657
C(11)	0.1448(6)	0.3019(6)	0.3190(6)	0.0694
C(12)	0.1756(5)	0.3612(5)	0.2221(5)	0.0609
C(13)	0.2273(8)	0.9532(5)	0.0749(7)	0.0763
C(14)	0.5462(6)	0.9158(5)	0.2598(5)	0.0708

Table I.3 Calculated hydrogen coordinates and isotropic displacement parameters ($Å^2$) with estimated standard deviations in parentheses for $Ph_2SbS_2PMe_2$ (3.11)

Atom	x/a	y/b	z/c	U(iso)
H(21)	0.1425(5)	0.5141(5)	-0.2214(5)	0.1000
H(31)	-0.0680(7)	0.3675(7)	-0.4687(6)	0.1000
H(41)	-0.1455(7)	0.1222(7)	-0.5172(6)	0.1000
H(51)	-0.0113(8)	0.0237(5)	-0.3170(7)	0.1000
H(61)	0.1966(6)	0.1718(5)	-0.0666(6)	0.1000
H(81)	0.5672(5)	0.3624(4)	0.3635(4)	0.1000
H(91)	0.5102(6)	0.2557(4)	0.5271(4)	0.1000
H(101)	0.2457(7)	0.2220(5)	0.5004(5)	0.1000
H(111)	0.0324(6)	0.2863(6)	0.3070(6)	0.1000
H(121)	0.0850(5)	0.3875(5)	0.1400(5)	0.1000
H(131)	0.2141(8)	0.9848(5)	0.1790(7)	0.1000
H(132)	0.1238(8)	0.9097(5)	-0.0238(7)	0.1000
H(133)	0.2816(8)	1.0285(5)	0.0624(7)	0.1000
H(141)	0.6096(6)	0.8531(5)	0.2815(5)	0.1000
H(142)	0.5342(6)	0.9391(5)	0.3356(5)	0.1000
H(143)	0.5828(6)	0.9831(5)	0.2440(5)	0.1000

Table I.4 Anisotropic thermal parameters (Å^2) with estimated standard deviations in parentheses for $Ph_2SbS_2PMe_2$ (3.11)

Atom	U(11)	U(22)	U(33)	U(23)	U(13)	U(12)
Sb(1)	0.0444(2)	0.0403(2)	0.0416(2)	0.0103(1)	0.0203(1)	0.0047(1)
P(1)	0.0606(6)	0.0365(4)	0.0446(5)	0.0108(4)	0.0209(4)	0.0076(4)
S(1)	0.0550(5)	0.0445(5)	0.0514(5)	0.0151(4)	0.0278(4)	0.0126(4)
S(2)	0.0854(7)	0.0537(5)	0.0580(6)	0.0168(4)	0.0398(5)	0.0084(5)
C(1)	0.048(2)	0.044(2)	0.048(2)	0.005(1)	0.025(2)	0.005(1)
C(2)	0.067(2)	0.065(2)	0.044(2)	0.013(2)	0.021(2)	-0.001(2)
C(3)	0.075(3)	0.103(4)	0.046(2)	0.009(2)	0.021(2)	0.000(3)
C(4)	0.069(3)	0.090(4)	0.060(3)	-0.021(3)	0.028(2)	-0.018(3)
C(5)	0.092(4)	0.050(3)	0.093(4)	-0.010(3)	0.041(3)	-0.013(2)
C(6)	0.081(3)	0.046(2)	0.073(3)	0.005(2)	0.031(2)	-0.002(2)
C(7)	0.054(2)	0.043(2)	0.037(2)	0.013(1)	0.019(1)	0.006(1)
C(8)	0.059(2)	0.047(2)	0.045(2)	0.010(1)	0.019(2)	0.011(2)
C(9)	0.086(3)	0.052(2)	0.040(2)	0.018(2)	0.017(2)	0.017(2)
C(10)	0.088(3)	0.067(3)	0.053(2)	0.025(2)	0.033(2)	0.008(2)
C(11)	0.073(3)	0.086(3)	0.067(3)	0.032(2)	0.038(2)	0.006(2)
C(12)	0.059(2)	0.076(3)	0.059(2)	0.035(2)	0.026(2)	0.014(2)
C(13)	0.110(4)	0.051(2)	0.089(4)	0.024(2)	0.043(3)	0.035(3)
C(14)	0.076(3)	0.069(3)	0.054(2)	0.013(2)	0.017(2)	-0.009(2)

Table I.5 Bond lengths (Å) with estimated standard deviations in parentheses for $Ph_2SbS_2PMe_2$ (3.11)

Sb(1) - S(1)	2.4931(9)
Sb(1) - C(1)	2.158(3)
Sb(1) - C(7)	2.155(3)
P(1) - S(1)	2.072(1)
P(1) - S(2)	1.964(1)
P(1) - C(13)	1.794(5)
P(1) - C(14)	1.800(4)
C(1) - C(2)	1.373(6)
C(1) - C(6)	1.375(6)
C(2) - C(3)	1.381(6)
C(3) - C(4)	1.365(9)
C(4) - C(5)	1.367(9)
C(5) - C(6)	1.390(7)
C(7) - C(8)	1.389(5)
C(7) - C(12)	1.371(6)
C(8) - C(9)	1.401(6)
C(9) - C(10)	1.362(7)
C(10) - C(11)	1.369(7)
C(11) - C(12)	1.388(6)

Table I.6 Bond angles (°) with estimated standard deviations in parentheses for $Ph_2SbS_2PMe_2$ (3.11)

S(1) - Sb(1) - C(1)	94.2(1)
S(1) - Sb(1) - C(7)	92.5(1)
C(1) - Sb(1) - C(7)	96.1(1)
S(1) - P(1) - S(2)	116.67(6)
S(1) - P(1) - C(13)	102.4(2)
S(2) - P(1) - C(13)	112.9(2)
S(1) - P(1) - C(14)	108.3(2)
S(2) - P(1) - C(14)	110.7(2)
C(13) - P(1) - C(14)	105.0(3)
Sb(1) - S(1) - P(1)	98.96(5)
Sb(1) - C(1) - C(2)	121.5(3)
Sb(1) - C(1) - C(6)	120.2(3)
C(2) - C(1) - C(6)	118.1(4)
C(1) - C(2) - C(3)	121.3(5)
C(2) - C(3) - C(4)	120.2(6)
C(3) - C(4) - C(5)	119.5(4)
C(4) - C(5) - C(6)	120.2(5)
C(1) - C(6) - C(5)	120.8(5)
Sb(1) - C(7) - C(8)	118.1(3)
Sb(1) - C(7) - C(12)	122.5(3)
C(8) - C(7) - C(12)	119.4(3)
C(7) - C(8) - C(9)	119.4(4)
C(8) - C(9) - C(10)	120.3(4)
C(9) - C(10) - C(11)	120.3(4)
C(10) - C(11) - C(12)	120.0(5)
C(7) - C(12) - C(11)	120.6(4)

Experimental Details

A unique set of data were collected on a Hilger and Watts Y290 four-circle diffractometer and the data were corrected for Lorentz and polarisation effects. The Sb atom position was located from a Patterson synthesis and subsequent Fourier difference syntheses revealed the positions of all the other non-hydrogen atoms. Refinement was carried out against 'observed' F_o data by full matrix procedures. Phenyl hydrogen atoms were placed in estimated positions (C–H = 1.00 Å), whereas methyl hydrogen atoms were located by further Fourier difference syntheses, both types being assigned a common fixed thermal parameter and refined 'riding' their respective carbon atoms. Data were corrected by a Chebyshev weighting scheme[6] (5 coefficient) and also for the effects of absorption[4], anomalous dispersion and isotropic extinction[7]. All crystallographic calculations were performed using the CRYSTALS suite of programs[8] and neutral atom scattering factors were taken from the usual sources[3].

APPENDIX J

Table J.1 Data collection and processing parameters for $[Ph_3Sb(O_2CCF_3)]_2O$ (4.1)

Chemical formula	$C_{40}H_{30}F_6O_5Sb_2$
Formula weight	948.14
Crystal size/mm	0.32 x 0.12 x 0.10
Crystal system	Monoclinic
Space group	$P2_1/c$
a / Å	20.436(2)
b / Å	10.1755(9)
c / Å	19.518(5)
β / °	112.494(13)
Volume / Å^3	3749.8(11)
Z	4
D_c/gcm^{-3}	1.679
Radiation (λ / Å)	Mo-K_α (0.71069)
μ / cm^{-1}	15.14
F(000)	1864
2θ limits / °	4.20 to 49.92
Index ranges	-23<=h<=23, -11<=k<=11, -22<=l<=17
Temperature / K	150
Total data collected	15116
Unique data	5579 [R(int) = 0.0884]
Absorption correction	None
Structure solution	Direct (SHELXS-86)[1]
Refinement procedure	Full matrix-LS on F^2
Number of data / variables	5572 / 478
Goodness-of-fit on F^2	0.935
Max/min peaks in final diff. map / e Å^{-3}	+2.139, -1.149
R observed data [$I > 2\sigma(I)$], (all data)	0.0466, (0.0608)
R_w observed data, (all data)	0.1131, (0.1252)

Table J.2 Atomic coordinates (x 10^4) and equivalent isotropic displacement parameters ($Å^2$ x 10^3) with estimated standard deviations in parentheses for $[Ph_3Sb(O_2CCF_3)]_2O$ (4.1)

Atom	x	y	z	U(eq)
Sb(1)	1775(1)	1813(1)	3801(1)	24(1)
Sb(2)	2901(1)	4450(1)	3555(1)	28(1)
O(1)	2073(2)	3605(3)	3645(2)	27(1)
C(1)	826(2)	-571(4)	3541(3)	31(1)
C(2)	667(3)	-1987(5)	3645(3)	39(2)
F(1)	941(2)	-2407(3)	4345(2)	52(1)
F(2)	940(3)	-2790(4)	3282(2)	73(1)
F(3)	-20(2)	-2227(4)	3402(3)	77(1)
O(2)	1426(2)	-211(4)	3990(2)	31(1)
O(3)	385(2)	64(4)	3035(2)	39(1)
C(3)	3854(2)	6558(4)	3260(2)	53(2)
C(4)	4497(3)	6858(5)	3081(3)	53(2)
F(4)	4509(2)	8050(3)	2811(2)	67(1)
F(5)	4529(3)	6042(5)	2555(3)	116(2)
F(6)	5087(2)	6710(6)	3668(3)	132(3)
O(4)	3830(2)	5391(4)	3429(3)	49(1)
O(5)	3435(3)	7464(4)	3218(3)	67(2)
C(11)	907(3)	2593(5)	3999(3)	24(1)
C(12)	506(3)	3604(6)	3580(4)	34(1)
C(13)	-43(3)	4137(6)	3757(4)	37(2)
C(14)	-154(3)	3705(7)	4357(4)	38(2)
C(15)	261(3)	2701(6)	4804(4)	37(2)
C(16)	784(3)	2138(6)	4612(3)	32(1)
C(21)	2646(3)	1455(6)	4798(3)	25(1)
C(22)	2815(3)	2456(6)	5328(3)	34(1)
C(23)	3375(4)	2297(7)	6002(4)	47(2)
C(24)	3774(3)	1141(8)	6132(4)	51(2)
C(25)	3613(3)	178(7)	5617(4)	48(2)
C(26)	3036(3)	313(6)	4940(4)	40(2)
C(31)	1797(3)	1065(6)	2802(3)	28(1)
C(32)	2041(3)	-214(6)	2762(4)	35(2)
C(33)	2117(3)	-601(6)	2121(4)	41(2)
C(34)	1934(4)	251(7)	1514(4)	42(2)
C(35)	1680(3)	1496(7)	1552(4)	42(2)
C(36)	1613(3)	1899(6)	2199(3)	30(1)
C(41)	2275(3)	5143(5)	2484(3)	30(1)
C(42)	1577(3)	5496(6)	2331(4)	34(2)
C(43)	1139(3)	5871(6)	1628(3)	36(2)
C(44)	1395(4)	5854(6)	1067(4)	41(2)
C(45)	2082(4)	5493(6)	1212(4)	39(2)
C(46)	2530(3)	5142(6)	1915(4)	33(2)
C(51)	3555(3)	2806(6)	3664(3)	29(1)
C(52)	4090(4)	2512(6)	4346(4)	40(2)
C(53)	4540(4)	1485(8)	4412(4)	50(2)
C(54)	4456(4)	673(6)	3803(4)	46(2)
C(55)	3925(3)	964(7)	3123(4)	48(2)
C(56)	3486(3)	2019(6)	3049(4)	41(2)
C(61)	3120(3)	5550(5)	4534(3)	34(2)
C(62)	2546(4)	5974(6)	4702(4)	39(2)
C(63)	2666(5)	6635(6)	5354(4)	50(2)
C(64)	3365(6)	6804(7)	5866(5)	66(3)
C(65)	3921(5)	6400(8)	5691(5)	73(3)
C(66)	3817(4)	5789(7)	5032(4)	52(2)

Table J.3 Calculated hydrogen coordinates (x 10^4) and isotropic displacement parameters ($Å^2$ x 10^3) with estimated standard deviations in parentheses for $[Ph_3Sb(O_2CCF_3)]_2O$ (4.1)

Atom	x	y	z	U(iso)
H(12A)	597(3)	3934(6)	3182(4)	40
H(13A)	-331(3)	4791(6)	3459(4)	45
H(14A)	-512(3)	4081(7)	4475(4)	45
H(15A)	187(3)	2418(6)	5222(4)	45
H(16A)	1054(3)	1451(6)	4894(3)	38
H(22A)	2551(3)	3228(6)	5228(3)	40
H(23A)	3484(4)	2949(7)	6362(4)	57
H(24A)	4156(3)	1033(8)	6581(4)	61
H(25A)	3888(3)	-580(7)	5712(4)	58
H(26A)	2917(3)	-359(6)	4591(4)	48
H(32A)	2148(3)	-788(6)	3161(4)	42
H(33A)	2292(3)	-1434(6)	2091(4)	49
H(34A)	1984(4)	-22(7)	1081(4)	51
H(35A)	1556(3)	2058(7)	1146(4)	50
H(36A)	1442(3)	2736(6)	2228(3)	36
H(42A)	1404(3)	5478(6)	2707(4)	41
H(43A)	676(3)	6132(6)	1531(3)	43
H(44A)	1099(4)	6089(6)	588(4)	49
H(45A)	2247(4)	5487(6)	829(4)	47
H(46A)	2996(3)	4906(6)	2011(4)	40
H(52A)	4141(4)	3019(6)	4760(4)	48
H(53A)	4906(4)	1321(8)	4866(4)	60
H(54A)	4751(4)	-47(6)	3854(4)	55
H(55A)	3866(3)	438(7)	2714(4)	58
H(56A)	3139(3)	2215(6)	2587(4)	49
H(62A)	2085(4)	5809(6)	4373(4)	47
H(63A)	2289(5)	6966(6)	5455(4)	61
H(64A)	3450(6)	7191(7)	6324(5)	79
H(65A)	4381(5)	6543(8)	6029(5)	88
H(66A)	4201(4)	5539(7)	4917(4)	63

Table J.4 Anisotropic thermal parameters ($Å^2$ x 10^3) with estimated standard deviations in parentheses for $[Ph_3Sb(O_2CCF_3)]_2O$ (4.1)

Atom	U11	U22	U33	U23	U13	U12
Sb(1)	24(1)	25(1)	23(1)	2(1)	9(1)	4(1)
Sb(2)	27(1)	28(1)	32(1)	7(1)	13(1)	7(1)
O(1)	31(2)	20(2)	34(3)	4(2)	17(2)	3(2)
C(1)	32(4)	31(3)	35(4)	-13(3)	20(3)	-3(3)
C(2)	38(4)	44(4)	37(5)	-2(3)	18(3)	-2(3)
F(1)	59(3)	45(2)	50(3)	4(2)	19(2)	-11(2)
F(2)	125(4)	39(2)	82(4)	-15(2)	70(3)	-5(3)
F(3)	40(3)	70(3)	102(4)	18(3)	8(2)	-19(2)
O(2)	32(2)	30(2)	28(3)	0(2)	10(2)	2(2)
O(3)	33(3)	37(2)	38(3)	-2(2)	3(2)	4(2)
C(3)	68(5)	31(4)	94(6)	-40(4)	68(5)	-41(4)
C(4)	44(4)	44(4)	60(5)	2(4)	10(4)	-17(4)
F(4)	70(3)	50(3)	76(3)	14(2)	21(2)	-19(2)

F(5)	154(6)	74(4)	185(7)	-30(4)	137(6)	-32(4)
F(6)	45(3)	151(6)	154(6)	90(5)	-12(3)	-36(3)
O(4)	42(3)	58(3)	51(3)	22(2)	21(2)	19(2)
O(5)	55(4)	46(3)	100(5)	6(3)	31(3)	4(3)
C(11)	21(3)	31(3)	19(4)	-5(2)	6(2)	2(2)
C(12)	26(3)	31(3)	43(4)	-2(3)	13(3)	2(3)
C(13)	26(3)	33(3)	48(5)	0(3)	9(3)	2(3)
C(14)	30(4)	50(4)	33(4)	-21(3)	11(3)	2(3)
C(15)	28(3)	53(4)	31(4)	-12(3)	11(3)	-5(3)
C(16)	29(3)	43(4)	21(4)	-7(3)	7(3)	-3(3)
C(21)	15(3)	38(3)	16(3)	8(2)	0(2)	1(2)
C(22)	27(3)	42(4)	28(4)	10(3)	7(3)	0(3)
C(23)	41(4)	57(5)	41(5)	5(3)	12(3)	-16(4)
C(24)	29(4)	67(5)	40(5)	24(4)	-5(3)	-15(4)
C(25)	27(4)	45(4)	66(6)	29(4)	11(3)	6(3)
C(26)	28(4)	32(3)	53(5)	6(3)	9(3)	-1(3)
C(31)	23(3)	37(3)	25(4)	-8(3)	11(2)	-5(3)
C(32)	33(4)	33(3)	40(4)	-3(3)	16(3)	3(3)
C(33)	39(4)	42(4)	43(5)	-17(3)	18(3)	2(3)
C(34)	41(4)	62(5)	24(4)	-15(3)	13(3)	-2(3)
C(35)	28(4)	59(4)	31(4)	1(3)	4(3)	0(3)
C(36)	23(3)	41(4)	21(4)	-1(3)	4(2)	2(3)
C(41)	33(4)	25(3)	33(4)	10(2)	14(3)	7(3)
C(42)	36(4)	33(3)	40(4)	9(3)	22(3)	8(3)
C(43)	40(4)	28(3)	39(5)	9(3)	15(3)	7(3)
C(44)	53(5)	31(3)	35(4)	9(3)	14(3)	6(3)
C(45)	55(5)	28(3)	38(5)	0(3)	23(3)	-3(3)
C(46)	36(4)	26(3)	43(5)	4(3)	21(3)	2(3)
C(51)	23(3)	32(3)	37(4)	10(3)	16(3)	9(3)
C(52)	47(4)	46(4)	26(4)	9(3)	12(3)	18(3)
C(53)	46(4)	67(5)	31(5)	15(3)	8(3)	24(4)
C(54)	40(4)	38(4)	59(5)	15(3)	20(4)	23(3)
C(55)	35(4)	59(5)	47(5)	-4(3)	11(3)	16(4)
C(56)	34(4)	43(4)	39(5)	2(3)	6(3)	12(3)
C(61)	39(4)	22(3)	32(4)	4(2)	3(3)	-6(3)
C(62)	47(4)	32(3)	41(4)	0(3)	18(3)	-4(3)
C(63)	80(6)	30(4)	51(5)	-7(3)	35(4)	-10(4)
C(64)	109(8)	41(5)	39(5)	-10(3)	19(5)	-27(5)
C(65)	70(6)	48(5)	68(7)	-2(4)	-11(5)	-28(5)
C(66)	47(4)	42(4)	53(5)	-3(3)	3(4)	-15(4)

Table J.5 Bond lengths (Å) with estimated standard deviations in parentheses for $[Ph_3Sb(O_2CCF_3)]_2O$ (4.1)

Sb(1)-O(1)	1.983(4)	C(21)-C(22)	1.397(9)
Sb(1)-C(31)	2.109(5)	C(22)-C(23)	1.383(9)
Sb(1)-C(21)	2.107(5)	C(23)-C(24)	1.398(10)
Sb(1)-C(11)	2.109(5)	C(24)-C(25)	1.352(11)
Sb(1)-O(2)	2.255(4)	C(25)-C(26)	1.402(9)
Sb(2)-O(1)	1.966(4)	C(31)-C(36)	1.381(8)
Sb(2)-C(51)	2.100(6)	C(31)-C(32)	1.407(8)
Sb(2)-C(41)	2.112(6)	C(32)-C(33)	1.377(9)
Sb(2)-C(61)	2.108(6)	C(33)-C(34)	1.399(9)

Sb(2)-O(4)	2.222(4)	C(34)-C(35)	1.381(10)
C(1)-O(3)	1.235(5)	C(35)-C(36)	1.384(9)
C(1)-O(2)	1.258(5)	C(41)-C(42)	1.388(8)
C(1)-C(2)	1.509(6)	C(41)-C(46)	1.394(8)
C(2)-F(2)	1.336(6)	C(42)-C(43)	1.374(9)
C(2)-F(3)	1.322(6)	C(43)-C(44)	1.382(9)
C(2)-F(1)	1.333(5)	C(44)-C(45)	1.372(9)
C(3)-O(5)	1.240(5)	C(45)-C(46)	1.375(9)
C(3)-O(4)	1.239(5)	C(51)-C(52)	1.393(9)
C(3)-C(4)	1.513(7)	C(51)-C(56)	1.406(9)
C(4)-F(6)	1.316(6)	C(52)-C(53)	1.365(9)
C(4)-F(5)	1.341(6)	C(53)-C(54)	1.403(10)
C(4)-F(4)	1.326(5)	C(54)-C(55)	1.386(10)
C(11)-C(12)	1.373(8)	C(55)-C(56)	1.370(9)
C(11)-C(16)	1.393(8)	C(61)-C(66)	1.405(9)
C(12)-C(13)	1.402(8)	C(61)-C(62)	1.403(9)
C(13)-C(14)	1.349(9)	C(62)-C(63)	1.375(9)
C(14)-C(15)	1.400(9)	C(63)-C(64)	1.406(12)
C(15)-C(16)	1.385(8)	C(64)-C(65)	1.368(12)
C(21)-C(26)	1.376(8)	C(65)-C(66)	1.371(12)

Table J.6 Bond angles (°) with estimated standard deviations in parentheses for $[Ph_3Sb(O_2CCF_3)]_2O$ (4.1)

O(1)-Sb(1)-C(31)	94.2(2)	C(11)-C(12)-C(13)	119.7(6)
O(1)-Sb(1)-C(21)	95.7(2)	C(14)-C(13)-C(12)	120.2(6)
C(31)-Sb(1)-C(21)	118.9(2)	C(13)-C(14)-C(15)	121.1(6)
O(1)-Sb(1)-C(11)	90.6(2)	C(16)-C(15)-C(14)	118.6(6)
C(31)-Sb(1)-C(11)	128.5(2)	C(15)-C(16)-C(11)	120.5(6)
C(21)-Sb(1)-C(11)	111.6(2)	C(26)-C(21)-C(22)	120.5(5)
O(1)-Sb(1)-O(2)	179.03(14)	C(26)-C(21)-Sb(1)	123.4(5)
C(31)-Sb(1)-O(2)	86.7(2)	C(22)-C(21)-Sb(1)	116.1(4)
C(21)-Sb(1)-O(2)	84.2(2)	C(23)-C(22)-C(21)	119.9(6)
C(11)-Sb(1)-O(2)	88.5(2)	C(22)-C(23)-C(24)	119.0(7)
O(1)-Sb(2)-C(51)	100.3(2)	C(25)-C(24)-C(23)	121.0(6)
O(1)-Sb(2)-C(41)	91.0(2)	C(24)-C(25)-C(26)	120.5(7)
C(51)-Sb(2)-C(41)	119.2(2)	C(21)-C(26)-C(25)	119.1(6)
O(1)-Sb(2)-C(61)	92.5(2)	C(36)-C(31)-C(32)	120.5(5)
C(51)-Sb(2)-C(61)	115.1(2)	C(36)-C(31)-Sb(1)	118.1(4)
C(41)-Sb(2)-C(61)	123.9(2)	C(32)-C(31)-Sb(1)	121.2(4)
O(1)-Sb(2)-O(4)	178.8(2)	C(33)-C(32)-C(31)	118.7(6)
C(51)-Sb(2)-O(4)	79.5(2)	C(32)-C(33)-C(34)	120.4(6)
C(41)-Sb(2)-O(4)	88.1(2)	C(35)-C(34)-C(33)	120.5(6)
C(61)-Sb(2)-O(4)	88.7(2)	C(36)-C(35)-C(34)	119.5(6)
Sb(2)-O(1)-Sb(1)	137.9(2)	C(35)-C(36)-C(31)	120.4(6)
O(3)-C(1)-O(2)	128.6(4)	C(42)-C(41)-C(46)	119.6(6)
O(3)-C(1)-C(2)	118.6(4)	C(42)-C(41)-Sb(2)	118.9(4)
O(2)-C(1)-C(2)	112.8(4)	C(46)-C(41)-Sb(2)	121.2(4)
F(2)-C(2)-F(3)	107.3(5)	C(43)-C(42)-C(41)	120.7(6)
F(2)-C(2)-F(1)	104.6(4)	C(42)-C(43)-C(44)	119.1(6)
F(3)-C(2)-F(1)	106.3(4)	C(45)-C(44)-C(43)	120.6(6)
F(2)-C(2)-C(1)	110.9(4)	C(46)-C(45)-C(44)	120.8(6)

F(3)-C(2)-C(1)	112.5(4)	C(45)-C(46)-C(41)	119.1(6)
F(1)-C(2)-C(1)	114.6(4)	C(52)-C(51)-C(56)	118.6(6)
C(1)-O(2)-Sb(1)	115.8(3)	C(52)-C(51)-Sb(2)	120.3(5)
O(5)-C(3)-O(4)	129.2(5)	C(56)-C(51)-Sb(2)	121.0(4)
O(5)-C(3)-C(4)	118.3(4)	C(53)-C(52)-C(51)	120.6(6)
O(4)-C(3)-C(4)	112.5(4)	C(52)-C(53)-C(54)	120.7(6)
F(6)-C(4)-F(5)	107.4(5)	C(55)-C(54)-C(53)	118.8(6)
F(6)-C(4)-F(4)	107.4(4)	C(54)-C(55)-C(56)	120.6(7)
F(5)-C(4)-F(4)	104.4(4)	C(55)-C(56)-C(51)	120.5(6)
F(6)-C(4)-C(3)	111.3(4)	C(66)-C(61)-C(62)	120.2(7)
F(5)-C(4)-C(3)	110.7(4)	C(66)-C(61)-Sb(2)	121.8(5)
F(4)-C(4)-C(3)	115.2(4)	C(62)-C(61)-Sb(2)	117.9(4)
C(3)-O(4)-Sb(2)	124.5(3)	C(63)-C(62)-C(61)	119.8(7)
C(12)-C(11)-C(16)	119.8(5)	C(62)-C(63)-C(64)	119.5(7)
C(12)-C(11)-Sb(1)	121.7(4)	C(65)-C(64)-C(63)	120.0(8)
C(16)-C(11)-Sb(1)	118.3(4)	C(64)-C(65)-C(66)	121.8(8)
		C(65)-C(66)-C(61)	118.6(8)

Experimental Details

Slightly more than one hemisphere of data were collected on a Delft Instruments FAST TV area detector, equipped with a rotating anode FR591 generator. The data were corrected for Lorentz and polarisation effects, merged and systematically absent reflections were rejected. The structure was solved by direct methods (SHELXS-86)[1] and subsequent Fourier difference syntheses revealed the positions of all the other non-hydrogen atoms. Refinement was carried out against all F_o^2 data by full matrix procedures (SHELXL-93)[2] with the disordered C(3) trifluoroacetate group restrained to have similar parameters to the C(1) group. The fluorine atoms of the C(3) trifluoroacetate group gave relatively large equivalent isotropic displacement parameters, but attempts to define a fractionally disordered model were unsuccessful and it was treated fully ordered. Hydrogen atoms were placed in estimated positions [C–H = 0.95 Å], with fixed isotropic parameters (1.2 x equivalent isotropic temperature factors of the carbon atom to which they were bonded) and refined 'riding' their respective carbon atoms. A standard weighting scheme was applied but no extinction correction was found to be necessary. All crystallographic calculations were performed using the SHELXS-86[1] and SHELXL-93[2] programs and neutral atom scattering factors were taken from the usual sources[3].

APPENDIX K

Table K.1 Data collection and processing parameters for $[Me_3Sb(O_2CMe)]_2O$ (4.7)

Chemical formula	$C_{10}H_{24}O_5Sb_2$
Formula weight	467.79
Crystal size/mm	0.28 x 0.21 x 0.07
Crystal system	Monoclinic
Space group	*C2/c*
a / Å	14.249(3)
b / Å	8.684(3)
c / Å	14.177(3)
β / °	114.58(2)
Volume / Å^3	1595.3(7)
Z	4
D_c/gcm^{-3}	1.948
Radiation (λ / Å)	Mo-K_α (0.71069)
μ / cm^{-1}	33.93
F(000)	904
2θ limits / °	5.64 to 49.84
Index ranges	-15<=h<=12, -9<=k<=10, -12<=l<=16
Temperature / K	150
Total data collected	3168
Unique data	1236 [R(int) = 0.1220]
Absorption correction	None
Structure solution	Direct (SHELXS-86)[1]
Refinement procedure	Full matrix-LS on F^2
Number of data / variables	1204 / 83
Goodness-of-fit on F^2	1.100
Max/min peaks in final diff. map / e Å^{-3}	+4.292, -2.036
R observed data [$I > 2\sigma(I)$], (all data)	0.0609, (0.0674)
R_w observed data, (all data)	0.1337, (0.1464)

Table K.2 Atomic coordinates (x 10^4) and equivalent isotropic displacement parameters ($Å^2$ x 10^3) with estimated standard deviations in parentheses for $[Me_3Sb(O_2CMe)]_2O$ (4.7)

Atom	x	y	z	U(eq)
Sb(1)	3567(1)	9173(1)	1967(1)	17(1)
O(1)	5000	9949(8)	2500	27(2)
C(1)	3798(5)	7128(7)	1295(5)	25(2)
C(2)	3556(6)	9257(7)	3441(6)	26(2)
C(3)	3052(6)	11014(8)	913(6)	30(2)
O(2)	1978(3)	8300(5)	1375(4)	24(1)
O(3)	1381(4)	10478(6)	1751(4)	31(1)
C(4)	1247(6)	9170(7)	1410(7)	25(2)
C(5)	206(5)	8406(8)	1045(6)	33(2)

Table K.3 Calculated hydrogen coordinates (x 10^4) and isotropic displacement parameters ($Å^2$ x 10^3) with estimated standard deviations in parentheses for $[Me_3Sb(O_2CMe)]_2O$ (4.7)

Atom	x	y	z	U(iso)
H(1A)	3441(29)	7201(22)	538(5)	38
H(1B)	3523(32)	6254(10)	1538(27)	38
H(1C)	4538(6)	6978(28)	1496(29)	38
H(2A)	3024(25)	8559(40)	3460(12)	40
H(2B)	3406(35)	10310(13)	3585(16)	40
H(2C)	4232(13)	8941(51)	3965(7)	40
H(3A)	2317(12)	11197(42)	726(34)	45
H(3B)	3152(40)	10761(27)	287(19)	45
H(3C)	3446(29)	11943(17)	1233(16)	45
H(5A)	261(10)	7485(36)	1465(28)	49
H(5B)	-29(19)	8111(56)	315(13)	49
H(5C)	-289(11)	9125(23)	1119(40)	49

Table K.4 Anisotropic thermal parameters ($Å^2$ x 10^3) with estimated standard deviations in parentheses for $[Me_3Sb(O_2CMe)]_2O$ (4.7)

Atom	U11	U22	U33	U23	U13	U12
Sb(1)	15(1)	11(1)	23(1)	0(1)	7(1)	1(1)
O(1)	14(3)	21(4)	41(4)	0	8(3)	0
C(1)	31(4)	16(4)	28(3)	-7(3)	13(3)	0(3)
C(2)	39(5)	20(4)	20(4)	-1(2)	11(3)	-3(3)
C(3)	27(4)	27(4)	35(4)	8(3)	13(3)	1(3)
O(2)	18(2)	17(2)	37(2)	-4(2)	12(2)	-1(2)
O(3)	25(3)	16(2)	55(3)	-9(2)	20(2)	-3(2)
C(4)	28(4)	16(4)	38(5)	4(3)	20(4)	-1(3)
C(5)	18(4)	27(4)	52(5)	2(3)	13(3)	0(3)

Table K.5 Bond lengths (Å) with estimated standard deviations in parentheses for $[Me_3Sb(O_2CMe)]_2O$ (4.7)

Sb(1)-O(1)	1.978(2)
Sb(1)-C(2)	2.098(8)
Sb(1)-C(3)	2.102(7)
Sb(1)-C(1)	2.104(6)
Sb(1)-O(2)	2.197(4)
O(1)-Sb(1a)	1.978(2)
O(2)-C(4)	1.304(9)
O(3)-C(4)	1.218(8)
C(4)-C(5)	1.506(11)

Table K.6 Bond angles (°) with estimated standard deviations in parentheses for $[Me_3Sb(O_2CMe)]_2O$ (4.7)

O(1)-Sb(1)-C(2)	92.4(2)
O(1)-Sb(1)-C(3)	90.7(3)
C(2)-Sb(1)-C(3)	122.5(3)
O(1)-Sb(1)-C(1)	97.4(2)
C(2)-Sb(1)-C(1)	123.2(3)
C(3)-Sb(1)-C(1)	113.2(3)
O(1)-Sb(1)-O(2)	179.8(2)
C(2)-Sb(1)-O(2)	87.6(2)
C(3)-Sb(1)-O(2)	89.5(3)
C(1)-Sb(1)-O(2)	82.4(2)
Sb(1)-O(1)-Sb(1a)	140.1(4)
C(4)-O(2)-Sb(1)	119.9(4)
O(3)-C(4)-O(2)	124.0(7)
O(3)-C(4)-C(5)	121.1(7)
O(2)-C(4)-C(5)	114.8(6)

Symmetry transformations used to generate equivalent atoms:

a = -x+1,y,-z+1/2

Experimental Details

Slightly more than one hemisphere of data were collected on a Delft Instruments FAST TV area detector, equipped with a rotating anode FR591 generator. The data were corrected for Lorentz and polarisation effects, merged and systematically absent reflections were rejected. The structure was solved by direct methods (SHELXS-86)[1] and subsequent Fourier difference syntheses revealed the positions of all the other non-hydrogen atoms. Refinement was carried out against all F_o^2 data by full matrix procedures (SHELXL-93)[2] and hydrogen atoms were placed in estimated positions [C–H = 0.98 Å], with fixed isotropic parameters (1.5 x equivalent isotropic temperature factors of the carbon atom to which they were bonded) and refined 'riding' their respective carbon atoms. A standard weighting scheme was applied but no extinction correction was found to be necessary. Substantial electron density (+4.292 e $Å^{-3}$) was noted in a final difference map at the antimony atom, likely to be an artefact of uncorrected absorption. All crystallographic calculations were performed using the SHELXS-86[1] and SHELXL-93[2] programs and neutral atom scattering factors were taken from the usual sources[3].

APPENDIX L

Table L.1 Data collection and processing parameters for $[Ph_8Sb_4(\mu\text{-}O)_4(\mu\text{-}OH)(\mu\text{-}OEt)(\mu\text{-}O_2CMe)_2].CH_2Cl_2$ (4.10.CH_2Cl_2)

Chemical formula	$C_{55}H_{54}Cl_2O_{10}Sb_4$
Formula weight	1432.88
Crystal size/mm	0.25 x 0.15 x 0.10
Crystal system	Monoclinic
Space group	$P2_1/c$
a / Å	12.634(6)
b / Å	21.946(6)
c / Å	20.627(5)
β / °	106.61(2)
Volume / Å^3	5481(3)
Z	4
D_c/gcm^{-3}	1.737
Radiation (λ / Å)	Mo-K_α (0.71069)
μ / cm^{-1}	21.04
F(000)	2808
2θ limits / °	3.88 to 49.86
Index ranges	-13<=h<=10, -25<=k<=22, -22<=l<= 24
Temperature / K	150
Total data collected	15512
Unique data	7521 [(R(int) = 0.0367]
Absorption correction	DIFABS (min, 0.927, max, 1.001)[9]
Structure solution	Direct (SHELXS-86)[1]
Refinement procedure	Full matrix-LS on F^2
Number of data / variables	7521 / 576
Goodness-of-fit on F^2	1.033
Max/min peaks in final diff. map / e Å^3	+2.751, -0.846
R observed data [$I > 2\sigma(I)$], (all data)	0.0368, (0.0425)
R_w observed data, (all data)	0.0899, (0.0913)

Table L.2 Atomic coordinates (x 10^4) and equivalent isotropic displacement parameters ($Å^2$ x 10^3) with estimated standard deviations in parentheses for $[Ph_8Sb_4(\mu\text{-}O)_4(\mu\text{-}OH)(\mu\text{-}OEt)(\mu\text{-}O_2CMe)_2].CH_2Cl_2$ ($4.10.CH_2Cl_2$)

	x	y	z	U(eq)
Sb(1)	1862.7(2)	2214.7(1)	2450.7(2)	15.0(1)
Sb(2)	2042.3(2)	3838.9(1)	2902.2(2)	13.9(1)
Sb(3)	4736.6(2)	3739.2(1)	3318.6(2)	14.8(1)
Sb(4)	4506.9(2)	2106.2(1)	2925.3(2)	15.2(1)
O(1)	1692(3)	2980(1)	2898(2)	18(1)
O(2)	4876(3)	2863(1)	3435(2)	18(1)
O(3)	3343(2)	3710(1)	2570(2)	16(1)
O(4)	3153(2)	1952(2)	3184(2)	16(1)
O(5)	3238(3)	2536(2)	2134(2)	17(1)
O(6)	2609(3)	4797(1)	3040(2)	19(1)
O(7)	4456(3)	4716(1)	3296(2)	19(1)
O(8)	2149(3)	1383(2)	1939(2)	21(1)
O(9)	3998(3)	1283(1)	2303(2)	20(1)
O(10)	3426(3)	3763(1)	3797(2)	18(1)
C(1)	3565(4)	5023(2)	3148(2)	17(1)
C(2)	3681(4)	5697(2)	3129(3)	29(1)
C(3)	3033(4)	1086(2)	2008(3)	23(1)
C(4)	2945(5)	473(3)	1692(4)	42(2)
C(5)	3428(4)	3361(2)	4359(2)	24(1)
C(6)	3351(5)	3712(3)	4971(3)	38(2)
C(111)	812(2)	2473(1)	1483(1)	21(1)
C(112)	-149(3)	2785(2)	1473(1)	22(1)
C(113)	-865(2)	2975(2)	861(2)	29(1)
C(114)	-619(3)	2852(2)	259(1)	35(2)
C(115)	342(3)	2539(2)	269(1)	33(1)
C(116)	1058(2)	2350(2)	881(2)	27(1)
C(121)	727(2)	1711(1)	2834(1)	17(1)
C(122)	47(3)	1278(1)	2427(1)	22(1)
C(123)	-670(2)	935(1)	2680(2)	27(1)
C(124)	-708(3)	1024(2)	3341(2)	33(1)
C(125)	-28(3)	1457(2)	3748(1)	32(1)
C(126)	689(3)	1800(1)	3495(1)	25(1)
C(211)	956(2)	4050(1)	3514(2)	16(1)
C(212)	335(3)	3582(1)	3676(2)	25(1)
C(213)	-419(3)	3709(1)	4035(2)	32(1)
C(214)	-551(3)	4303(2)	4231(2)	30(1)
C(215)	70(3)	4771(1)	4069(2)	31(1)
C(216)	824(3)	4644(1)	3710(2)	26(1)
C(221)	1066(2)	4139(2)	1927(1)	19(1)
C(222)	62(2)	4427(2)	1865(1)	22(1)
C(223)	-573(2)	4630(2)	1235(2)	28(1)
C(224)	-204(2)	4545(2)	668(1)	30(1)
C(225)	800(3)	4257(2)	730(1)	29(1)
C(226)	1435(2)	4054(2)	1360(2)	26(1)
C(311)	5941(2)	3886(1)	4282(1)	16(1)
C(312)	5999(2)	4427(1)	4641(2)	24(1)
C(313)	6834(3)	4512(1)	5241(2)	28(1)

C(314)	7611(2)	4056(1)	5482(1)	28(1)
C(315)	7552(2)	3515(1)	5123(2)	23(1)
C(316)	6717(2)	3430(1)	4523(1)	21(1)
C(321)	5675(2)	3911(2)	2627(2)	22(1)
C(322)	6805(3)	3798(2)	2824(2)	31(1)
C(323)	7427(2)	3919(2)	2381(2)	38(2)
C(324)	6919(3)	4152(2)	1741(2)	43(2)
C(325)	5789(3)	4265(2)	1545(2)	56(2)
C(326)	5167(2)	4145(2)	1988(2)	41(2)
C(411)	5616(2)	2211(2)	2330(2)	21(1)
C(412)	5255(2)	2261(2)	1629(2)	27(1)
C(413)	6018(3)	2298(2)	1262(1)	36(1)
C(414)	7143(2)	2286(2)	1594(2)	31(1)
C(415)	7503(2)	2237(2)	2295(2)	30(1)
C(416)	6740(2)	2199(2)	2663(1)	24(1)
C(421)	5487(3)	1562(1)	3741(1)	20(1)
C(422)	5733(3)	1796(1)	4393(2)	32(1)
C(423)	6374(3)	1460(2)	4935(1)	36(1)
C(424)	6769(3)	889(2)	4824(2)	39(2)
C(425)	6523(3)	656(1)	4172(2)	54(2)
C(426)	5882(3)	992(2)	3630(1)	40(2)
C(7)	3292(8)	3642(2)	-376(4)	99(4)
Cl(11)	2925(12)	3213(5)	209(5)	68(3)
Cl(21)	3450(12)	4406(2)	-276(6)	101(5)
Cl(12)	3067(34)	3140(13)	195(15)	89(13)
Cl(13)	3369(35)	3420(15)	423(7)	164(15)
Cl(14)	3522(13)	3218(6)	338(5)	33(3)
Cl(22)	2796(9)	4361(3)	-413(7)	56(3)
Cl(23)	3515(49)	4395(6)	-461(27)	188(29)
Cl(24)	3525(34)	4386(6)	-166(24)	92(13)

Table L.3 Calculated hydrogen coordinates (x 10^4) and isotropic displacement parameters ($Å^2$ x 10^3) with estimated standard deviations in parentheses for $[Ph_8Sb_4(\mu\text{-}O)_4(\mu\text{-}OH)(\mu\text{-}OEt)(\mu\text{-}O_2CMe)_2].CH_2Cl_2$ (4.10.CH_2Cl_2)

	x	y	z	Uiso
H(5)	3253(41)	2924(24)	2193(26)	21(15)
H(2A)	4437(7)	5799(2)	3173(18)	44
H(2B)	3462(27)	5876(3)	3496(10)	44
H(2C)	3219(21)	5850(3)	2707(7)	44
H(4A)	2881(31)	171(3)	2015(7)	63
H(4B)	3593(15)	394(8)	1552(18)	63
H(4C)	2304(18)	458(6)	1307(11)	63
H(5A)	4101(4)	3121(2)	4477(2)	28
H(5B)	2808(4)	3082(2)	4221(2)	28
H(6A)	3388(31)	3434(3)	5337(6)	56
H(6B)	2664(15)	3929(14)	4865(6)	56
H(6C)	3953(18)	3995(12)	5103(12)	56
H(112)	-313(4)	2868(2)	1876(2)	26
H(113)	-1508(3)	3184(2)	855(2)	35
H(114)	-1098(3)	2979(2)	-150(2)	42
H(115)	506(4)	2457(2)	-134(2)	40
H(116)	1701(3)	2140(2)	888(2)	32
H(122)	73(4)	1218(2)	1986(1)	26
H(123)	-1125(3)	645(2)	2408(2)	32
H(124)	-1188(4)	795(2)	3510(2)	40
H(125)	-53(4)	1517(2)	4189(2)	39
H(126)	1144(4)	2090(2)	3767(2)	31
H(212)	423(4)	3184(1)	3545(3)	30
H(213)	-834(4)	3396(2)	4143(3)	39
H(214)	-1055(4)	4388(2)	4471(2)	36
H(215)	-18(4)	5169(1)	4200(3)	38
H(216)	1239(4)	4957(1)	3602(3)	31
H(222)	-185(3)	4483(2)	2244(2)	26
H(223)	-1245(2)	4823(2)	1194(2)	34
H(224)	-629(3)	4681(2)	247(1)	36
H(225)	1047(4)	4201(2)	351(2)	35
H(226)	2107(3)	3862(2)	1401(2)	31
H(312)	5480(3)	4732(2)	4480(2)	29
H(313)	6873(4)	4874(1)	5481(2)	34
H(314)	8169(3)	4113(2)	5883(2)	33
H(315)	8071(3)	3210(2)	5284(2)	27
H(316)	6678(4)	3068(1)	4283(2)	25
H(322)	7145(3)	3641(3)	3252(2)	37
H(323)	8182(2)	3843(3)	2513(3)	45
H(324)	7334(4)	4233(3)	1445(2)	52
H(325)	5449(4)	4422(3)	1117(2)	67
H(326)	4411(2)	4220(3)	1856(2)	49
H(412)	4503(2)	2268(2)	1407(2)	32
H(413)	5777(4)	2332(2)	793(1)	43
H(414)	7654(3)	2312(2)	1348(2)	38
H(415)	8256(2)	2229(2)	2518(2)	36
H(416)	6981(3)	2166(2)	3132(1)	28
H(422)	5469(4)	2178(1)	4468(2)	38
H(423)	6538(4)	1616(2)	5372(1)	43
H(424)	7197(4)	664(2)	5187(2)	47
H(425)	6787(5)	274(2)	4098(3)	65
H(426)	5717(5)	836(2)	3194(2)	48

Table L.4 Anisotropic thermal parameters ($Å^2 \times 10^3$) with estimated standard deviations in parentheses for $[Ph_8Sb_4(\mu\text{-}O)_4(\mu\text{-}OH)(\mu\text{-}OEt)(\mu\text{-}O_2CMe)_2].CH_2Cl_2$ ($4.10.CH_2Cl_2$)

	U11	U22	U33	U23	U13	U12
Sb(1)	13(1)	14(1)	18(1)	-1(1)	5(1)	-1(1)
Sb(2)	13(1)	13(1)	16(1)	0(1)	4(1)	0(1)
Sb(3)	12(1)	13(1)	19(1)	0(1)	4(1)	-1(1)
Sb(4)	14(1)	13(1)	19(1)	-1(1)	5(1)	1(1)
O(1)	19(2)	12(2)	24(2)	-1(1)	10(1)	-2(1)
O(2)	17(2)	12(2)	21(2)	-2(1)	2(1)	0(1)
O(3)	8(2)	18(2)	21(2)	-1(1)	4(1)	-2(1)
O(4)	10(2)	21(2)	17(2)	1(1)	3(1)	1(1)
O(5)	16(2)	12(2)	24(2)	-1(1)	8(1)	2(2)
O(6)	17(2)	12(2)	28(2)	-3(1)	8(2)	-2(2)
O(7)	18(2)	11(2)	28(2)	1(1)	5(1)	-3(2)
O(8)	17(2)	18(2)	29(2)	-5(2)	7(2)	-2(2)
O(9)	16(2)	16(2)	30(2)	-4(1)	9(2)	-1(2)
O(10)	14(2)	20(2)	19(2)	2(1)	6(1)	1(1)
C(1)	20(3)	17(3)	17(3)	-3(2)	9(2)	2(2)
C(2)	25(3)	16(3)	49(4)	3(2)	15(3)	-2(2)
C(3)	22(3)	20(3)	29(3)	-3(2)	12(2)	-2(2)
C(4)	28(3)	19(3)	78(5)	-18(3)	13(3)	-6(3)
C(5)	21(3)	28(3)	21(3)	5(2)	5(2)	0(2)
C(6)	51(4)	39(4)	25(3)	4(2)	14(3)	4(3)
C(111)	23(3)	15(3)	20(3)	1(2)	-4(2)	-8(2)
C(112)	19(3)	18(3)	28(3)	2(2)	6(2)	-6(2)
C(113)	23(3)	29(3)	33(4)	8(2)	2(2)	-6(2)
C(114)	27(3)	36(4)	32(4)	9(2)	-7(3)	-16(3)
C(115)	41(4)	40(4)	20(3)	0(2)	9(3)	-7(3)
C(116)	29(3)	24(3)	30(3)	-6(2)	13(2)	1(2)
C(121)	12(3)	16(3)	26(3)	4(2)	9(2)	1(2)
C(122)	19(3)	19(3)	27(3)	-2(2)	6(2)	1(2)
C(123)	23(3)	13(3)	43(4)	-3(2)	6(2)	-4(2)
C(124)	24(3)	28(3)	54(4)	12(3)	22(3)	-1(3)
C(125)	45(4)	28(3)	33(3)	3(2)	24(3)	0(3)
C(126)	31(3)	21(3)	25(3)	-4(2)	8(2)	-6(2)
C(211)	15(3)	17(3)	16(3)	0(2)	4(2)	1(2)
C(212)	28(3)	19(3)	33(3)	4(2)	17(2)	2(2)
C(213)	17(3)	39(4)	44(4)	10(3)	13(3)	0(2)
C(214)	23(3)	39(4)	34(4)	0(2)	19(3)	6(3)
C(215)	29(3)	31(3)	39(4)	-13(3)	16(3)	1(3)
C(216)	26(3)	24(3)	30(3)	-2(2)	13(2)	-4(2)
C(221)	20(3)	11(3)	24(3)	3(2)	5(2)	-5(2)
C(222)	17(3)	20(3)	27(3)	3(2)	4(2)	-4(2)
C(223)	18(3)	31(3)	30(3)	7(2)	-1(2)	-1(2)
C(224)	24(3)	36(4)	24(3)	14(2)	-2(2)	-7(3)
C(225)	24(3)	39(4)	22(3)	6(2)	4(2)	-7(3)
C(226)	22(3)	24(3)	33(3)	1(2)	11(2)	-2(2)
C(311)	15(3)	18(3)	16(3)	-3(2)	3(2)	-4(2)
C(312)	25(3)	20(3)	25(3)	-1(2)	3(2)	4(2)

C(313)	29(3)	25(3)	28(3)	-8(2)	3(2)	-1(2)
C(314)	25(3)	32(3)	20(3)	0(2)	-4(2)	-6(3)
C(315)	19(3)	18(3)	29(3)	1(2)	5(2)	4(2)
C(316)	22(3)	14(3)	26(3)	-2(2)	6(2)	-2(2)
C(321)	26(3)	13(3)	30(3)	-3(2)	14(2)	-5(2)
C(322)	28(3)	31(3)	36(4)	10(2)	13(3)	5(2)
C(323)	17(3)	43(4)	58(5)	5(3)	19(3)	-2(3)
C(324)	45(4)	55(4)	43(4)	-5(3)	34(3)	-18(3)
C(325)	43(4)	95(6)	32(4)	11(4)	14(3)	-19(4)
C(326)	28(3)	62(5)	33(4)	9(3)	8(3)	-4(3)
C(411)	24(3)	13(3)	27(3)	-4(2)	9(2)	0(2)
C(412)	31(3)	20(3)	32(3)	1(2)	12(3)	1(2)
C(413)	45(4)	36(4)	31(4)	0(3)	19(3)	-3(3)
C(414)	23(3)	24(3)	56(4)	-2(3)	27(3)	-2(2)
C(415)	21(3)	20(3)	59(4)	-3(2)	25(3)	-2(2)
C(416)	21(3)	20(3)	29(3)	-2(2)	8(2)	1(2)
C(421)	13(3)	18(3)	27(3)	6(2)	4(2)	2(2)
C(422)	36(3)	23(3)	29(3)	-1(2)	-3(2)	-3(3)
C(423)	32(3)	34(4)	35(4)	2(3)	-2(3)	1(3)
C(424)	33(4)	38(4)	37(4)	15(3)	-3(3)	9(3)
C(425)	77(5)	41(4)	43(4)	14(3)	15(4)	36(4)
C(426)	59(4)	32(4)	27(4)	5(3)	8(3)	20(3)
C(7)	143(9)	91(7)	90(8)	-47(6)	76(7)	-49(7)
Cl(11)	96(7)	63(4)	37(3)	-8(2)	4(3)	24(4)
Cl(21)	151(10)	43(3)	69(7)	-4(2)	-31(5)	36(3)

Table L.5 Bond lengths (Å) and angles (°) with estimated standard deviations in parentheses for $[Ph_8Sb_4(\mu\text{-}O)_4(\mu\text{-}OH)(\mu\text{-}OEt)(\mu\text{-}O_2CMe)_2].CH_2Cl_2$ ($4.10.CH_2Cl_2$)

Sb(1)...Sb(4)	3.210(2)	Sb(2)...Sb(3)	3.271(2)
Sb(1)-O(1)	1.957(3)	Sb(1)-O(4)	1.966(3)
Sb(1)-O(5)	2.143(3)	Sb(1)-O(8)	2.190(3)
Sb(1)-C(111)	2.133(2)	Sb(1)-C(121)	2.135(2)
Sb(2)-O(1)	1.937(3)	Sb(2)-O(3)	1.973(3)
Sb(2)-O(6)	2.213(3)	Sb(2)-O(10)	2.155(3)
Sb(2)-C(211)	2.164(2)	Sb(2)-C(221)	2.141(2)
Sb(3)-O(2)	1.939(3)	Sb(3)-O(3)	1.984(3)
Sb(3)-O(7)	2.170(3)	Sb(3)-O(10)	2.157(3)
Sb(3)-C(311)	2.154(2)	Sb(3)-C(321)	2.133(2)
Sb(4)-O(2)	1.950(3)	Sb(4)-O(4)	1.961(3)
Sb(4)-O(5)	2.151(3)	Sb(4)-O(9)	2.203(3)
Sb(4)-C(411)	2.122(2)	Sb(4)-C(421)	2.144(2)
O(5)-H(5)	0.86(5)	O(6)-C(1)	1.265(5)
O(7)-C(1)	1.272(5)	O(8)-C(3)	1.266(6)
O(9)-C(3)	1.273(6)	O(10)-C(5)	1.457(6)
C(1)-C(2)	1.488(7)	C(3)-C(4)	1.485(7)
C(5)-C(6)	1.505(7)		
O(1)-Sb(1)-O(4)	93.86(13)	O(1)-Sb(1)-C(111)	95.21(13)
O(4)-Sb(1)-C(111)	162.64(12)	O(1)-Sb(1)-C(121)	95.36(12)
O(4)-Sb(1)-C(121)	93.46(13)	C(111)-Sb(1)-C(121)	100.38(13)
O(1)-Sb(1)-O(5)	93.99(13)	O(4)-Sb(1)-O(5)	76.38(13)
C(111)-Sb(1)-O(5)	88.24(13)	C(121)-Sb(1)-O(5)	166.63(13)
O(1)-Sb(1)-O(8)	176.37(12)	O(4)-Sb(1)-O(8)	84.92(13)
C(111)-Sb(1)-O(8)	85.11(12)	C(121)-Sb(1)-O(8)	88.13(12)
O(5)-Sb(1)-O(8)	82.40(13)	O(1)-Sb(2)-O(3)	94.04(13)
O(1)-Sb(2)-C(221)	103.05(13)	O(3)-Sb(2)-C(221)	91.76(12)
O(1)-Sb(2)-O(10)	93.26(13)	O(3)-Sb(2)-O(10)	74.61(13)
C(221)-Sb(2)-O(10)	159.52(12)	O(1)-Sb(2)-C(211)	91.64(12)
O(3)-Sb(2)-C(211)	164.47(13)	C(221)-Sb(2)-C(211)	101.03(12)
O(10)-Sb(2)-C(211)	90.66(13)	O(1)-Sb(2)-O(6)	172.27(13)
O(3)-Sb(2)-O(6)	84.83(12)	C(221)-Sb(2)-O(6)	84.64(13)
O(10)-Sb(2)-O(6)	79.06(12)	C(211)-Sb(2)-O(6)	87.60(11)
O(2)-Sb(3)-O(3)	95.33(13)	O(2)-Sb(3)-C(321)	102.09(13)
O(3)-Sb(3)-C(321)	91.41(13)	O(2)-Sb(3)-C(311)	91.10(12)
O(3)-Sb(3)-C(311)	163.49(12)	C(321)-Sb(3)-C(311)	102.10(13)
O(2)-Sb(3)-O(10)	91.27(12)	O(3)-Sb(3)-O(10)	74.34(13)
C(321)-Sb(3)-O(10)	161.40(12)	C(311)-Sb(3)-O(10)	90.37(13)
O(2)-Sb(3)-O(7)	171.89(13)	O(3)-Sb(3)-O(7)	84.97(12)
C(321)-Sb(3)-O(7)	85.99(13)	C(311)-Sb(3)-O(7)	86.55(12)
O(10)-Sb(3)-O(7)	80.99(12)	O(2)-Sb(4)-O(4)	95.34(13)
O(2)-Sb(4)-C(411)	97.10(13)	O(4)-Sb(4)-C(411)	161.27(12)
O(2)-Sb(4)-C(421)	93.22(13)	O(4)-Sb(4)-C(421)	92.52(13)
C(411)-Sb(4)-C(421)	100.68(13)	O(2)-Sb(4)-O(5)	92.67(13)
O(4)-Sb(4)-O(5)	76.29(12)	C(411)-Sb(4)-O(5)	89.18(12)
C(421)-Sb(4)-O(5)	167.80(12)	O(2)-Sb(4)-O(9)	176.18(13)
O(4)-Sb(4)-O(9)	83.44(12)	C(411)-Sb(4)-O(9)	83.23(12)
C(421)-Sb(4)-O(9)	90.45(13)	O(5)-Sb(4)-O(9)	83.53(13)

Sb(2)-O(1)-Sb(1)	141.4(2)	Sb(3)-O(2)-Sb(4)	141.2(2)
Sb(2)-O(3)-Sb(3)	111.5(2)	Sb(4)-O(4)-Sb(1)	109.7(2)
Sb(1)-O(5)-Sb(4)	96.76(13)	Sb(1)-O(5)-H(5)	106(3)
Sb(4)-O(5)-H(5)	110(4)	C(1)-O(6)-Sb(2)	130.7(3)
C(1)-O(7)-Sb(3)	131.0(3)	C(3)-O(8)-Sb(1)	129.6(3)
C(3)-O(9)-Sb(4)	129.6(3)	C(5)-O(10)-Sb(2)	123.0(3)
C(5)-O(10)-Sb(3)	121.5(3)	Sb(2)-O(10)-Sb(3)	98.70(13)
O(6)-C(1)-O(7)	124.7(4)	O(6)-C(1)-C(2)	118.7(4)
O(7)-C(1)-C(2)	116.5(4)	O(8)-C(3)-O(9)	125.0(5)
O(8)-C(3)-C(4)	117.6(5)	O(9)-C(3)-C(4)	117.3(4)
O(10)-C(5)-C(6)	111.8(4)	C(112)-C(111)-C(116)	120.0
C(112)-C(111)-Sb(1)	116.9(2)	C(116)-C(111)-Sb(1)	123.1(2)
C(122)-C(121)-Sb(1)	119.7(2)	C(126)-C(121)-Sb(1)	120.3(2)
C(212)-C(211)-Sb(2)	118.6(2)	C(216)-C(211)-Sb(2)	121.3(2)
C(222)-C(221)-Sb(2)	119.5(2)	C(226)-C(221)-Sb(2)	120.5(2)
C(312)-C(311)-Sb(3)	122.4(2)	C(316)-C(311)-Sb(3)	117.5(2)
C(322)-C(321)-Sb(3)	119.6(2)	C(326)-C(321)-Sb(3)	120.4(2)
C(412)-C(411)-Sb(4)	122.4(2)	C(416)-C(411)-Sb(4)	117.6(2)
C(422)-C(421)-Sb(4)	118.3(2)	C(426)-C(421)-Sb(4)	121.7(2)

Experimental Details

Slightly more than one hemisphere of data were collected on a Delft Instruments FAST TV area detector, equipped with a rotating anode FR591 generator. The data were corrected for absorption (DIFABS)[9], Lorentz and polarisation effects, merged and systematically absent reflections were rejected. The structure was solved by direct methods (SHELXS-86)[1] and subsequent Fourier difference syntheses revealed the positions of all the other non-hydrogen atoms. Refinement was carried out against all F_o^2 data by full matrix procedures (SHELXL-93)[2]. The dichloromethane solvate was found to be disordered and modelled on several partially occupied chlorine positions. The carbon and two half-occupied chlorine atoms of the solvate were refined anisotropically, whilst the other chlorine atoms were refined isotropically. All other non-hydrogen atoms were refined anisotropically, with the phenyl groups restrained as idealised hexagons. The hydroxyl hydrogen atom was experimentally located and isotropically refined without any constraint; other hydrogens were placed in estimated positions, with fixed isotropic parameters (U_{iso} tied to the U_{eq} of the parent atom) and refined 'riding' their respective carbon atoms. A standard weighting scheme was applied and the data was corrected for isotropic extinction. All crystallographic calculations were performed using the SHELXS-86[1] and SHELXL-93[2] programs and neutral atom scattering factors were taken from the usual sources[3].

APPENDIX M

Table M.1 Data collection and processing parameters for $PhSb(2,2'-C_{12}H_8)Br_2$ (5.2)

Chemical formula	$C_{18}H_{13}Br_2Sb$
Formula weight	510.86
Crystal size/mm	0.50 x 0.40 x 0.20
Crystal system	Monoclinic
Space group	$P2_1/c$
a / Å	11.924(2)
b / Å	13.164(4)
c / Å	11.067(2)
β / °	109.83(2)
Volume / Å^3	1634.15
Z	4
D_c/gcm^{-3}	2.077
Radiation (λ / Å)	Mo-K_α (0.71069)
μ / cm^{-1}	65.34
F(000)	968
2θ limits / °	5-50
Index ranges	-14<=h<=13, 0<=k<=15, 0<=l<=13
Temperature / K	298
Total unique data collected	3022
Observed data [$I > 3\sigma(I)$]	2194
Absorption correction	DIFABS (min, 0.843, max, 1.241)[4]
Structure solution	Patterson (CRYSTALS)[8]
Refinement procedure	Full matrix-LS on F
Number of data / variables	2194 / 191
S	1.120
Max/min peaks in final diff. map / e Å^{-3}	+1.36, -0.595
R	0.0390
R_w	0.0422

Table M.2 Fractional atomic coordinates and equivalent isotropic displacement parameters ($Å^2$) with estimated standard deviations in parentheses for $PhSb(2,2'\text{-}C_{12}H_8)Br_2$ (5.2)

Atom	x/a	y/b	z/c	U(eq)
Sb(1)	0.36228(4)	0.00163(3)	0.10418(4)	0.0412
Br(2)	0.28611(7)	-0.15801(6)	0.18970(7)	0.0594
Br(1)	0.45999(6)	0.14680(5)	-0.00241(6)	0.0506
C(1)	0.5184(6)	0.0017(5)	0.2699(6)	0.0459
C(2)	0.5754(6)	-0.0858(6)	0.3232(7)	0.0536
C(3)	0.6683(7)	-0.0806(7)	0.4389(7)	0.0612
C(4)	0.6970(7)	0.0087(7)	0.5029(7)	0.0622
C(5)	0.6408(8)	0.0964(6)	0.4499(7)	0.0614
C(6)	0.5499(6)	0.0949(6)	0.3299(6)	0.0506
C(7)	0.2363(6)	0.1060(5)	0.1253(6)	0.0455
C(8)	0.2467(7)	0.1701(5)	0.2287(7)	0.0527
C(9)	0.1562(8)	0.2361(7)	0.2210(8)	0.0683
C(10)	0.0556(8)	0.2356(7)	0.1130(9)	0.0717
C(11)	0.0453(8)	0.1718(6)	0.0110(8)	0.0644
C(12)	0.1365(6)	0.1060(5)	0.0172(6)	0.0440
C(13)	0.1324(5)	0.0350(5)	-0.0904(6)	0.0438
C(14)	0.2331(5)	-0.0252(5)	-0.0791(6)	0.0405
C(15)	0.2362(6)	-0.0909(5)	-0.1742(7)	0.0542
C(16)	0.1372(7)	-0.0967(6)	-0.2858(7)	0.0586
C(17)	0.0381(7)	-0.0399(6)	-0.2989(7)	0.0603
C(18)	0.0351(6)	0.0263(6)	-0.2020(7)	0.0526

Table M.3 Calculated hydrogen coordinates and isotropic displacement parameters ($Å^2$) with estimated standard deviations in parentheses for $PhSb(2,2'\text{-}C_{12}H_8)Br_2$ (5.2)

Atom	x/a	y/b	z/c	U(iso)
H(21)	0.5499(6)	-0.1521(6)	0.2781(7)	0.1000
H(31)	0.7148(7)	-0.1432(7)	0.4760(7)	0.1000
H(41)	0.7596(7)	0.0104(7)	0.5901(7)	0.1000
H(51)	0.6652(8)	0.1623(6)	0.4965(7)	0.1000
H(61)	0.5080(6)	0.1584(6)	0.2888(6)	0.1000
H(81)	0.3199(7)	0.1683(5)	0.3069(7)	0.1000
H(91)	0.1622(8)	0.2842(7)	0.2928(8)	0.1000
H(101)	-0.0112(8)	0.2832(7)	0.1078(9)	0.1000
H(111)	-0.0288(8)	0.1721(6)	-0.0663(8)	0.1000
H(151)	0.3082(6)	-0.1339(5)	-0.1625(7)	0.1000
H(161)	0.1389(7)	-0.1426(6)	-0.3572(7)	0.1000
H(171)	-0.0333(7)	-0.0462(6)	-0.3787(7)	0.1000
H(181)	-0.0377(6)	0.0680(6)	-0.2127(7)	0.1000

Table M.4 Anisotropic thermal parameters ($Å^2$) with estimated standard deviations in parentheses for $PhSb(2,2'-C_{12}H_8)Br_2$ (5.2)

Atom	U(11)	U(22)	U(33)	U(23)	U(13)	U(12)
Sb(1)	0.0399(2)	0.0430(2)	0.0398(2)	-0.0003(2)	0.0124(2)	0.0004(2)
Br(2)	0.0615(5)	0.0531(4)	0.0688(5)	0.0098(4)	0.0220(4)	-0.0077(3)
Br(1)	0.0523(4)	0.0512(4)	0.0510(4)	0.0042(3)	0.0199(3)	-0.0017(3)
C(1)	0.047(3)	0.055(4)	0.039(3)	0.004(3)	0.016(3)	-0.001(3)
C(2)	0.048(4)	0.056(4)	0.055(4)	-0.003(3)	0.015(3)	0.002(3)
C(3)	0.057(5)	0.074(5)	0.055(4)	0.012(4)	0.015(4)	0.013(4)
C(4)	0.058(4)	0.082(6)	0.047(4)	-0.004(4)	0.011(3)	0.001(4)
C(5)	0.074(5)	0.071(5)	0.043(4)	-0.010(4)	0.014(4)	-0.005(4)
C(6)	0.050(4)	0.058(4)	0.042(4)	0.000(3)	0.011(3)	-0.006(3)
C(7)	0.046(4)	0.047(4)	0.046(3)	0.003(3)	0.017(3)	0.001(3)
C(8)	0.056(4)	0.059(4)	0.048(4)	-0.005(3)	0.018(3)	0.009(3)
C(9)	0.087(6)	0.075(6)	0.067(5)	-0.012(4)	0.038(5)	0.015(5)
C(10)	0.077(6)	0.072(5)	0.082(6)	-0.003(5)	0.029(5)	0.027(5)
C(11)	0.064(5)	0.066(5)	0.069(5)	-0.004(4)	0.019(4)	0.020(4)
C(12)	0.042(3)	0.050(4)	0.048(4)	0.003(3)	0.022(3)	0.004(3)
C(13)	0.039(4)	0.044(3)	0.049(4)	0.001(3)	0.016(3)	0.001(3)
C(14)	0.039(3)	0.045(3)	0.039(3)	-0.001(3)	0.015(3)	-0.001(3)
C(15)	0.046(4)	0.054(4)	0.066(5)	-0.006(3)	0.020(3)	-0.003(3)
C(16)	0.064(5)	0.059(5)	0.056(4)	-0.016(4)	0.017(4)	-0.004(4)
C(17)	0.056(4)	0.068(5)	0.053(4)	-0.005(4)	0.008(3)	0.005(4)
C(18)	0.044(4)	0.061(4)	0.051(4)	-0.002(3)	0.010(3)	0.004(3)

Table M.5 Bond lengths (Å) with estimated standard deviations in parentheses for $PhSb(2,2'-C_{12}H_8)Br_2$ (5.2)

Sb(1) - Br(2)	2.5924(8)
Sb(1) - Br(1)	2.7080(8)
Sb(1) - C(1)	2.124(6)
Sb(1) - C(7)	2.106(6)
Sb(1) - C(14)	2.119(6)
C(1) - C(2)	1.37(1)
C(1) - C(6)	1.39(1)
C(2) - C(3)	1.38(1)
C(3) - C(4)	1.36(1)
C(4) - C(5)	1.36(1)
C(5) - C(6)	1.40(1)
C(7) - C(8)	1.393(9)
C(7) - C(12)	1.372(9)
C(8) - C(9)	1.36(1)
C(9) - C(10)	1.38(1)
C(10) - C(11)	1.38(1)
C(11) - C(12)	1.37(1)
C(12) - C(13)	1.503(9)
C(13) - C(14)	1.408(9)
C(13) - C(18)	1.382(9)
C(14) - C(15)	1.372(9)
C(15) - C(16)	1.39(1)
C(16) - C(17)	1.36(1)
C(17) - C(18)	1.39(1)

Table M.6 Bond angles (°) with estimated standard deviations in parentheses for PhSb(2,2'-$C_{12}H_8$)Br_2 (5.2)

Br(2) - Sb(1) - Br(1)	170.72(3)
Br(2) - Sb(1) - C(1)	89.9(2)
Br(1) - Sb(1) - C(1)	89.7(2)
Br(2) - Sb(1) - C(7)	97.9(2)
Br(1) - Sb(1) - C(7)	90.9(2)
C(1) - Sb(1) - C(7)	110.7(3)
Br(2) - Sb(1) - C(14)	89.0(2)
Br(1) - Sb(1) - C(14)	88.9(2)
C(1) - Sb(1) - C(14)	165.0(2)
C(7) - Sb(1) - C(14)	84.3(2)
Sb(1) - C(1) - C(2)	122.3(5)
Sb(1) - C(1) - C(6)	115.5(5)
C(2) - C(1) - C(6)	121.7(6)
C(1) - C(2) - C(3)	118.9(7)
C(2) - C(3) - C(4)	120.5(7)
C(3) - C(4) - C(5)	120.7(7)
C(4) - C(5) - C(6)	120.3(7)
C(1) - C(6) - C(5)	117.6(7)
Sb(1) - C(7) - C(8)	128.2(5)
Sb(1) - C(7) - C(12)	110.1(5)
C(8) - C(7) - C(12)	121.6(6)
C(7) - C(8) - C(9)	119.1(7)
C(8) - C(9) - C(10)	119.2(7)
C(9) - C(10) - C(11)	121.6(8)
C(10) - C(11) - C(12)	119.6(8)
C(7) - C(12) - C(11)	118.8(6)
C(7) - C(12) - C(13)	118.4(6)
C(11) - C(12) - C(13)	122.7(6)
C(12) - C(13) - C(14)	118.8(6)
C(12) - C(13) - C(18)	123.4(6)
C(14) - C(13) - C(18)	117.7(6)
Sb(1) - C(14) - C(13)	108.2(4)
Sb(1) - C(14) - C(15)	129.7(5)
C(13) - C(14) - C(15)	122.0(6)
C(14) - C(15) - C(16)	118.7(7)
C(15) - C(16) - C(17)	120.5(7)
C(16) - C(17) - C(18)	120.6(7)
C(13) - C(18) - C(17)	120.5(7)

Experimental Details

A unique set of data were collected on a Hilger and Watts Y290 four-circle diffractometer and the data were corrected for Lorentz and polarisation effects. The Sb atom position was located from a Patterson synthesis and subsequent Fourier difference syntheses revealed the positions of all the other non-hydrogen atoms. Refinement was carried out against 'observed' F_o data by full matrix procedures. Phenyl hydrogen atoms were placed in estimated positions (C–H = 1.00 Å) and assigned a common fixed thermal parameter and refined 'riding' their respective carbon atoms. Data were corrected by a Chebyshev weighting scheme[6] (4 coefficient) and also for the effects of absorption[4], anomalous dispersion and isotropic extinction[7]. All crystallographic calculations were performed using the CRYSTALS suite of programs[8] and neutral atom scattering factors were taken from the usual sources[3].

APPENDIX N

Table N.1 Data collection and processing parameters for $PhSb(2,2'\text{-}C_{12}H_8)Cl_2$ (5.3)

Chemical formula	$C_{18}H_{13}Cl_2Sb$
Formula weight	421.96
Crystal size/mm	0.30 x 0.20 x 0.15
Crystal system	Monoclinic
Space group	$P2_1/c$
a / Å	11.692(3)
b / Å	12.935(4)
c / Å	10.946(4)
β / °	109.32(2)
Volume / Å^3	1562.20
Z	4
D_c/gcm^{-3}	1.794
Radiation (λ / Å)	Mo-K_α (0.71069)
μ / cm^{-1}	21.115
F(000)	824
2θ limits / °	4-50
Index ranges	-13<=h<=12, 0<=k<=15, 0<=l<=12
Temperature / K	298
Total unique data collected	2694
Observed data [$I > 3\sigma(I)$]	1495
Absorption correction	DIFABS (min, 0.721, max, 1.136)[4]
Structure solution	Patterson (CRYSTALS)[8]
Refinement procedure	Full matrix-LS on F
Number of data / variables	1495 / 190
S	1.022
Max/min peaks in final diff. map / e Å^{-3}	+1.64, -0.862
R	0.0793
R_w	0.0935

Table N.2 Fractional atomic coordinates and equivalent isotropic displacement parameters ($Å^2$) with estimated standard deviations in parentheses for $PhSb(2,2'-C_{12}H_8)Cl_2$ (5.3)

Atom	x/a	y/b	z/c	U(eq)
Sb(1)	0.36410(7)	0.0007(1)	0.10186(8)	0.0415
Cl(1)	0.4589(3)	0.1374(3)	-0.0017(3)	0.0492
Cl(2)	0.2920(4)	-0.1518(4)	0.1863(4)	0.0572
C(1)	0.521(1)	0.003(1)	0.270(1)	0.0412
C(2)	0.578(1)	-0.087(2)	0.323(2)	0.0561
C(3)	0.672(1)	-0.081(1)	0.441(2)	0.0552
C(4)	0.698(2)	0.013(2)	0.505(2)	0.0611
C(5)	0.638(2)	0.095(2)	0.452(2)	0.0648
C(6)	0.549(1)	0.093(1)	0.331(1)	0.0490
C(7)	0.237(1)	0.110(1)	0.123(1)	0.0315
C(8)	0.244(1)	0.171(1)	0.224(1)	0.0462
C(9)	0.152(1)	0.243(1)	0.213(2)	0.0561
C(10)	0.049(2)	0.239(2)	0.106(2)	0.0751
C(11)	0.039(2)	0.171(1)	0.004(2)	0.0590
C(12)	0.134(1)	0.104(1)	0.011(1)	0.0381
C(13)	0.133(1)	0.032(1)	-0.094(1)	0.0484
C(14)	0.235(1)	-0.029(1)	-0.080(1)	0.0328
C(15)	0.241(1)	-0.102(1)	-0.172(1)	0.0500
C(16)	0.139(1)	-0.108(1)	-0.288(2)	0.0556
C(17)	0.040(1)	-0.050(2)	-0.301(2)	0.0572
C(18)	0.036(1)	0.0190(8)	-0.206(2)	0.0236

Table N.3 Calculated hydrogen coordinates and isotropic displacement parameters ($Å^2$) with estimated standard deviations in parentheses for $PhSb(2,2'-C_{12}H_8)Cl_2$ (5.3)

Atom	x/a	y/b	z/c	U(iso)
H(21)	0.549(1)	-0.155(2)	0.281(2)	0.1000
H(31)	0.722(1)	-0.143(1)	0.479(2)	0.1000
H(41)	0.762(2)	0.018(2)	0.593(2)	0.1000
H(51)	0.659(2)	0.163(2)	0.498(2)	0.1000
H(61)	0.501(1)	0.156(1)	0.289(1)	0.1000
H(81)	0.317(1)	0.170(1)	0.304(1)	0.1000
H(91)	0.158(1)	0.292(1)	0.285(2)	0.1000
H(101)	-0.019(2)	0.288(2)	0.101(2)	0.1000
H(111)	-0.037(2)	0.169(1)	-0.073(2)	0.1000
H(151)	0.315(1)	-0.147(1)	-0.157(1)	0.1000
H(161)	0.139(1)	-0.158(1)	-0.358(2)	0.1000
H(171)	-0.029(1)	-0.051(2)	-0.384(2)	0.1000
H(181)	-0.041(1)	0.0576(8)	-0.215(2)	0.1000

Table N.4 Anisotropic thermal parameters ($Å^2$) with estimated standard deviations in parentheses for $PhSb(2,2'-C_{12}H_8)Cl_2$ (5.3)

Atom	U(11)	U(22)	U(33)	U(23)	U(13)	U(12)
Sb(1)	0.0354(5)	0.0441(6)	0.0445(6)	0.0013(5)	0.0114(4)	0.0004(5)
Cl(1)	0.043(2)	0.054(3)	0.053(2)	-0.001(2)	0.017(2)	-0.006(2)
Cl(2)	0.059(2)	0.053(3)	0.065(2)	0.017(2)	0.016(2)	-0.007(2)
C(1)	0.040(7)	0.054(9)	0.052(8)	-0.028(9)	0.018(6)	0.002(9)
C(2)	0.041(9)	0.07(1)	0.06(1)	-0.002(9)	0.012(7)	0.002(9)
C(3)	0.048(9)	0.06(1)	0.06(1)	0.004(9)	0.005(8)	0.011(8)
C(4)	0.06(1)	0.06(2)	0.06(1)	-0.009(9)	0.004(8)	0.01(1)
C(5)	0.07(1)	0.10(2)	0.06(1)	-0.02(1)	0.020(9)	0.03(1)
C(6)	0.053(9)	0.05(1)	0.052(9)	0.006(8)	0.024(8)	0.013(7)
C(7)	0.044(7)	0.019(7)	0.049(8)	-0.004(6)	0.021(6)	0.006(5)
C(8)	0.059(9)	0.04(1)	0.053(8)	-0.014(7)	0.022(7)	0.001(7)
C(9)	0.06(1)	0.06(1)	0.058(9)	-0.012(8)	0.029(8)	0.008(9)
C(10)	0.06(1)	0.12(2)	0.07(1)	0.02(1)	0.028(9)	0.04(1)
C(11)	0.07(1)	0.06(1)	0.06(1)	0.020(9)	0.032(9)	0.017(9)
C(12)	0.035(7)	0.036(9)	0.060(9)	0.012(6)	0.019(6)	0.016(6)
C(13)	0.038(8)	0.05(1)	0.06(1)	-0.002(7)	0.015(7)	-0.007(6)
C(14)	0.048(8)	0.022(9)	0.043(7)	0.012(5)	0.020(6)	0.004(5)
C(15)	0.044(8)	0.05(1)	0.055(9)	0.000(7)	0.014(7)	-0.009(7)
C(16)	0.06(1)	0.07(1)	0.050(9)	-0.026(8)	0.011(7)	-0.005(8)
C(17)	0.048(9)	0.07(1)	0.052(9)	-0.013(9)	0.003(7)	0.003(9)
C(18)	0.045(8)	0.00(1)	0.08(1)	0.007(6)	0.011(7)	0.000(5)

Table N.5 Bond lengths (Å) with estimated standard deviations in parentheses for $PhSb(2,2'-C_{12}H_8)Cl_2$ (5.3)

Sb(1) - Cl(1)	2.544(4)
Sb(1) - Cl(2)	2.444(4)
Sb(1) - C(1)	2.13(1)
Sb(1) - C(7)	2.12(1)
Sb(1) - C(14)	2.10(1)
C(1) - C(2)	1.37(2)
C(1) - C(6)	1.33(2)
C(2) - C(3)	1.39(2)
C(3) - C(4)	1.39(2)
C(4) - C(5)	1.30(3)
C(5) - C(6)	1.39(2)
C(7) - C(8)	1.34(2)
C(7) - C(12)	1.40(2)
C(8) - C(9)	1.40(2)
C(9) - C(10)	1.38(2)
C(10) - C(11)	1.39(3)
C(11) - C(12)	1.39(2)
C(12) - C(13)	1.48(2)
C(13) - C(14)	1.40(2)
C(13) - C(18)	1.37(2)
C(14) - C(15)	1.41(2)
C(15) - C(16)	1.42(2)
C(16) - C(17)	1.35(2)
C(17) - C(18)	1.38(2)

Table N.6 Bond angles (°) with estimated standard deviations in parentheses for PhSb(2,2'-$C_{12}H_8$)Cl_2 (5.3)

Cl(1) - Sb(1) - Cl(2)	170.2(1)
Cl(1) - Sb(1) - C(1)	90.0(5)
Cl(2) - Sb(1) - C(1)	89.3(5)
Cl(1) - Sb(1) - C(7)	90.6(4)
Cl(2) - Sb(1) - C(7)	98.9(4)
C(1) - Sb(1) - C(7)	109.6(5)
Cl(1) - Sb(1) - C(14)	89.2(4)
Cl(2) - Sb(1) - C(14)	89.0(4)
C(1) - Sb(1) - C(14)	165.4(5)
C(7) - Sb(1) - C(14)	85.0(5)
Sb(1) - C(1) - C(2)	121.0(12)
Sb(1) - C(1) - C(6)	116.0(12)
C(2) - C(1) - C(6)	122.2(14)
C(1) - C(2) - C(3)	118.0(16)
C(2) - C(3) - C(4)	119.4(15)
C(3) - C(4) - C(5)	119.6(16)
C(4) - C(5) - C(6)	122.6(19)
C(1) - C(6) - C(5)	118.1(16)
Sb(1) - C(7) - C(8)	128.7(11)
Sb(1) - C(7) - C(12)	107.4(9)
C(8) - C(7) - C(12)	123.8(12)
C(7) - C(8) - C(9)	118.8(14)
C(8) - C(9) - C(10)	118.9(16)
C(9) - C(10) - C(11)	121.5(17)
C(10) - C(11) - C(12)	119.8(16)
C(7) - C(12) - C(11)	116.7(14)
C(7) - C(12) - C(13)	119.9(11)
C(11) - C(12) - C(13)	123.3(14)
C(12) - C(13) - C(14)	118.7(13)
C(12) - C(13) - C(18)	124.2(13)
C(14) - C(13) - C(18)	117.1(15)
Sb(1) - C(14) - C(13)	108.9(10)
Sb(1) - C(14) - C(15)	127.7(11)
C(13) - C(14) - C(15)	123.2(14)
C(14) - C(15) - C(16)	116.5(15)
C(15) - C(16) - C(17)	119.9(15)
C(16) - C(17) - C(18)	121.8(14)
C(13) - C(18) - C(17)	121.3(14)

Experimental Details

A unique set of data were collected on a Hilger and Watts Y290 four-circle diffractometer and the data were corrected for Lorentz and polarisation effects with systematically absent reflections rejected. The Sb atom position was located by a Patterson map and subsequent Fourier difference syntheses revealed the positions of all the other non-hydrogen atoms. Hydrogen atoms were placed in estimated positions (C–H = 1.00 Å), assigned a common fixed thermal parameter and refined 'riding' their respective carbon atoms. Data were corrected by a Chebyshev weighting scheme[6] (5 coefficient) and also for the effects of absorption[4], anomalous dispersion and isotropic extinction[7]. All crystallographic calculations were performed using the CRYSTALS suite of programs[8] and neutral atom scattering factors were taken from the usual sources.

APPENDIX O

Table O.1 Data collection and processing parameters for PhSb(2,2'-$C_{12}H_8$)$(NCS)_2$ (5.5)

Chemical formula	$C_{20}H_{13}N_2S_2Sb$
Formula weight	467.21
Crystal size/mm	0.20 x 0.12 x 0.08
Crystal system	Triclinic
Space group	$P\bar{1}$
a / Å	8.832(3)
b / Å	10.706(5)
c / Å	10.908(3)
α / °	75.65(3)
β / °	70.63(2)
γ / °	80.54(3)
Volume / Å^3	938.85
Z	2
D_c/gcm^{-3}	1.653
Radiation (λ / Å)	Mo-K_α (0.71069)
μ / cm^{-1}	16.955
F(000)	460
2θ limits / °	5-50
Index ranges (for unique data set)	-8<=h<=10, -11<=k<=11, 0<=l<=12
Temperature / K	150
Total data collected	4089
Unique data	2615 [(R(int) = 0.0381]
Observed data [$I > 3\sigma(I)$]	2271
Absorption correction	DIFABS (min, 0.918, max, 1.189)[4]
Structure solution	Direct (SIR-92)[5]
Refinement procedure	Full matrix-LS on F^2
Number of data / variables	2271 / 227
S	1.129
Max/min peaks in final diff. map / e Å^{-3}	+0.952, -0.771
R, R_w	0.0328, 0.0668

Table O.2 Fractional atomic coordinates and equivalent isotropic displacement parameters ($Å^2$) with estimated standard deviations in parentheses $PhSb(2,2'-C_{12}H_8)(NCS)_2$ (5.5)

Atom	x/a	y/b	z/c	U(eq)
Sb(1)	0.59339(4)	0.25979(3)	0.68649(3)	0.0235
S(100)	0.2424(1)	0.4777(1)	0.4017(1)	0.0282
S(200)	1.0576(2)	0.2556(2)	0.7976(2)	0.0552
N(100)	0.4422(5)	0.3459(4)	0.5547(4)	0.0267
N(200)	0.7598(5)	0.2027(4)	0.8000(4)	0.0268
C(1)	0.4367(5)	0.3664(4)	0.8290(5)	0.0236
C(2)	0.3293(6)	0.4704(5)	0.7969(5)	0.0307
C(3)	0.2273(6)	0.5322(5)	0.8980(5)	0.0326
C(4)	0.2335(6)	0.4897(5)	1.0270(5)	0.0366
C(5)	0.3424(6)	0.3884(5)	1.0574(5)	0.0372
C(6)	0.4432(6)	0.3247(5)	0.9590(5)	0.0330
C(7)	0.5188(5)	0.0751(4)	0.7226(5)	0.0255
C(8)	0.3899(6)	0.0169(5)	0.8251(5)	0.0291
C(9)	0.3559(6)	-0.1052(5)	0.8276(5)	0.0331
C(10)	0.4503(6)	-0.1690(5)	0.7280(5)	0.0363
C(11)	0.5808(6)	-0.1143(5)	0.6255(5)	0.0335
C(12)	0.6142(5)	0.0099(4)	0.6226(5)	0.0243
C(13)	0.7499(5)	0.0778(4)	0.5144(4)	0.0237
C(14)	0.7723(5)	0.2054(4)	0.5167(5)	0.0232
C(15)	0.8956(6)	0.2732(5)	0.4218(5)	0.0338
C(16)	1.0008(6)	0.2145(5)	0.3200(5)	0.0373
C(17)	0.9794(6)	0.0897(5)	0.3143(5)	0.0332
C(18)	0.8561(6)	0.0221(5)	0.4108(5)	0.0306
C(100)	0.3596(5)	0.4013(4)	0.4911(4)	0.0194
C(200)	0.8860(6)	0.2262(5)	0.7968(5)	0.0293

Table O.3 Calculated hydrogen coordinates and isotropic displacement parameters ($Å^2$) with estimated standard deviations in parentheses for $PhSb(2,2'-C_{12}H_8)(NCS)_2$ (5.5)

Atom	x/a	y/b	z/c	U(iso)
H(21)	0.3260(6)	0.5006(5)	0.7033(5)	0.0401
H(31)	0.1492(6)	0.6068(5)	0.8769(5)	0.0444
H(41)	0.1589(6)	0.5331(5)	1.0989(5)	0.0473
H(51)	0.3484(6)	0.3605(5)	1.1503(5)	0.0494
H(61)	0.5202(6)	0.2496(5)	0.9812(5)	0.0424
H(81)	0.3231(6)	0.0639(5)	0.8964(5)	0.0418
H(91)	0.2647(6)	-0.1474(5)	0.9003(5)	0.0474
H(101)	0.4238(6)	-0.2568(5)	0.7295(5)	0.0498
H(111)	0.6486(6)	-0.1625(5)	0.5555(5)	0.0489
H(151)	0.9088(6)	0.3627(5)	0.4265(5)	0.0433
H(161)	1.0912(6)	0.2616(5)	0.2515(5)	0.0464
H(171)	1.0530(6)	0.0489(5)	0.2402(5)	0.0448
H(181)	0.8425(6)	-0.0674(5)	0.4063(5)	0.0414

Table O.4 Anisotropic thermal parameters ($Å^2$) with estimated standard deviations in parentheses for $PhSb(2,2'-C_{12}H_8)(NCS)_2$ (5.5)

Atom	U(11)	U(22)	U(33)	U(23)	U(13)	U(12)
Sb(1)	0.0248(2)	0.0218(2)	0.0237(2)	-0.0055(1)	-0.0071(1)	-0.0002(1)
S(100)	0.0286(6)	0.0261(6)	0.0335(8)	-0.0025(5)	-0.0145(5)	-0.0029(5)
S(200)	0.0298(8)	0.071(1)	0.116(2)	-0.049(1)	-0.0239(9)	0.0048(7)
N(100)	0.026(2)	0.023(2)	0.034(2)	-0.005(2)	-0.011(2)	-0.002(2)
N(200)	0.022(2)	0.034(2)	0.029(2)	-0.007(2)	-0.012(2)	0.005(2)
C(1)	0.023(2)	0.027(2)	0.023(3)	-0.011(2)	-0.002(2)	0.000(2)
C(2)	0.035(3)	0.027(3)	0.033(3)	-0.008(2)	-0.012(2)	0.001(2)
C(3)	0.027(3)	0.032(3)	0.041(3)	-0.014(2)	-0.003(2)	-0.000(2)
C(4)	0.035(3)	0.042(3)	0.033(3)	-0.014(2)	0.002(2)	-0.006(2)
C(5)	0.038(3)	0.053(3)	0.024(3)	-0.010(2)	-0.000(2)	-0.003(3)
C(6)	0.030(3)	0.036(3)	0.029(3)	-0.004(2)	-0.004(2)	-0.002(2)
C(7)	0.025(2)	0.024(2)	0.029(3)	-0.001(2)	-0.012(2)	-0.002(2)
C(8)	0.034(3)	0.029(3)	0.028(3)	0.004(2)	-0.015(2)	-0.008(2)
C(9)	0.037(3)	0.032(3)	0.036(3)	0.010(2)	-0.015(2)	-0.011(2)
C(10)	0.045(3)	0.028(3)	0.044(3)	0.001(2)	-0.022(3)	-0.006(2)
C(11)	0.043(3)	0.030(3)	0.035(3)	-0.009(2)	-0.018(2)	0.000(2)
C(12)	0.030(2)	0.023(2)	0.024(3)	-0.003(2)	-0.015(2)	0.001(2)
C(13)	0.026(2)	0.028(2)	0.022(3)	-0.005(2)	-0.012(2)	0.001(2)
C(14)	0.022(2)	0.026(2)	0.023(3)	-0.006(2)	-0.008(2)	0.005(2)
C(15)	0.035(3)	0.032(3)	0.033(3)	-0.006(2)	-0.010(2)	-0.001(2)
C(16)	0.030(3)	0.044(3)	0.033(3)	-0.000(2)	-0.001(2)	0.000(2)
C(17)	0.038(3)	0.042(3)	0.025(3)	-0.011(2)	-0.007(2)	0.012(2)
C(18)	0.037(3)	0.033(3)	0.027(3)	-0.007(2)	-0.015(2)	0.007(2)
C(100)	0.020(2)	0.016(2)	0.024(3)	-0.007(2)	0.005(2)	-0.004(2)
C(200)	0.038(3)	0.029(3)	0.025(3)	-0.011(2)	-0.004(2)	0.010(2)

Table O.5 Bond lengths (Å) with estimated standard deviations in parentheses for $PhSb(2,2'-C_{12}H_8)(NCS)_2$ (5.5)

Sb(1) - N(100)	2.216(4)
Sb(1) - N(200)	2.146(4)
Sb(1) - C(1)	2.137(4)
Sb(1) - C(7)	2.090(4)
Sb(1) - C(14)	2.135(4)
S(100)- C(100)	1.639(5)
S(200)- C(200)	1.601(6)
N(100)- C(100)	1.165(6)
N(200)- C(200)	1.169(6)
C(1) - C(2)	1.393(7)
C(1) - C(6)	1.395(7)
C(2) - C(3)	1.404(7)
C(3) - C(4)	1.384(8)
C(4) - C(5)	1.379(7)
C(5) - C(6)	1.392(7)
C(7) - C(8)	1.406(7)
C(7) - C(12)	1.400(7)
C(8) - C(9)	1.380(7)
C(9) - C(10)	1.386(8)
C(10) - C(11)	1.402(7)
C(11) - C(12)	1.399(7)

C(12) - C(13)	1.510(6)
C(13) - C(14)	1.420(7)
C(13) - C(18)	1.400(7)
C(14) - C(15)	1.387(7)
C(15) - C(16)	1.400(7)
C(16) - C(17)	1.399(8)
C(17) - C(18)	1.392(7)

Table O.6 Bond angles (°) with estimated standard deviations in parentheses for PhSb(2,2'-$C_{12}H_8$)$(NCS)_2$ (5.5)

N(100)- Sb(1) - N(200)	171.1(1)
N(100)- Sb(1) - C(1)	88.5(2)
N(200)- Sb(1) - C(1)	91.1(2)
N(100)- Sb(1) - C(7)	93.0(2)
N(200)- Sb(1) - C(7)	95.5(2)
C(1) - Sb(1) - C(7)	110.7(2)
N(100)- Sb(1) - C(14)	87.2(2)
N(200)- Sb(1) - C(14)	90.8(2)
C(1) - Sb(1) - C(14)	164.0(2)
C(7) - Sb(1) - C(14)	84.9(2)
Sb(1) - N(100)- C(100)	173.5(4)
Sb(1) - N(200)- C(200)	139.6(4)
Sb(1) - C(1) - C(2)	122.7(3)
Sb(1) - C(1) - C(6)	116.6(3)
C(2) - C(1) - C(6)	120.7(4)
C(1) - C(2) - C(3)	118.7(5)
C(2) - C(3) - C(4)	120.3(5)
C(3) - C(4) - C(5)	120.5(5)
C(4) - C(5) - C(6)	120.1(5)
C(1) - C(6) - C(5)	119.6(5)
Sb(1) - C(7) - C(8)	129.2(4)
Sb(1) - C(7) - C(12)	110.2(3)
C(8) - C(7) - C(12)	120.5(4)
C(7) - C(8) - C(9)	120.2(5)
C(8) - C(9) - C(10)	119.1(5)
C(9) - C(10) - C(11)	122.1(5)
C(10) - C(11) - C(12)	118.7(5)
C(7) - C(12) - C(11)	119.5(4)
C(7) - C(12) - C(13)	118.2(4)
C(11) - C(12) - C(13)	122.4(4)
C(12) - C(13) - C(14)	118.7(4)
C(12) - C(13) - C(18)	123.7(4)
C(14) - C(13) - C(18)	117.5(4)
Sb(1) - C(14) - C(13)	107.9(3)
Sb(1) - C(14) - C(15)	130.0(4)
C(13) - C(14) - C(15)	122.0(4)
C(14) - C(15) - C(16)	119.1(5)
C(15) - C(16) - C(17)	119.9(5)
C(16) - C(17) - C(18)	120.5(5)
C(13) - C(18) - C(17)	120.9(5)
S(100)- C(100)- N(100)	179.3(4)
S(200)- C(200)- N(200)	178.0(5)

Experimental Details

Slightly more than one hemisphere of data were collected on a Delft Instruments FAST TV area detector, equipped with a rotating anode FR591 generator. The data were corrected for Lorentz and polarisation effects, merged and systematically absent reflections were rejected. The structure was solved by direct methods (SIR-92)[5]. Refinement was carried out against 'observed' F_o^2 data by full matrix procedures. Hydrogen atoms were placed in estimated positions (C–H = 1.00 Å) with fixed isotropic parameters (1.3 x equivalent isotropic temperature factors of the carbon atom to which they are bonded) and refined 'riding' their respective carbon atoms. Data were corrected by a Chebyshev weighting scheme[6] (4 coefficient) and also for the effects of absorption[4], anomalous dispersion and isotropic extinction[7]. All crystallographic calculations were performed using the CRYSTALS suite of programs[8] and neutral atom scattering factors were taken from the usual sources[3].

APPENDIX P

Table P.1 Data collection and processing parameters for PhSb(*o*-$O_2C_6Cl_4$)Cl_2.OEt_2 (5.6)

Chemical formula	$C_{16}H_{15}Cl_6O_3Sb$
Formula weight	589.73
Crystal size/mm	0.80 x 0.39 x 0.21
Crystal system	Monoclinic
Space group	$P2_1/n$
a / Å	7.498(6)
b / Å	22.32(2)
c / Å	12.898(4)
β / °	103.83(3)
Volume / Å^3	2096(3)
Z	4
D_c/gcm^{-3}	1.869
Radiation (λ / Å)	Mo-K_α (0.71069)
μ / cm^{-1}	20.95
F(000)	1152
2θ limits / °	5.76 to 49.96
Index ranges	-8<=h<=8, -2<=k<=26, -1<=l<=15
Temperature / K	298
Total data collected	4125
Unique data	3671 [R(int) = 0.0280]
Absorption correction	Psi scans (min = 0.313, max = 0.532)
Structure solution	Direct (SHELXS-86)[1]
Refinement procedure	Full matrix-LS on F^2
Number of data / variables	3647 / 235
Goodness-of-fit on F^2	1.146
Max/min peaks in final diff. map / e Å^{-3}	+0.635, -1.280
R observed data [$I > 2\sigma(I)$], (all data)	0.0346, (0.0429)
R_w observed data, (all data)	0.0880, (0.1127)

Table P.2 Atomic coordinates (x 10^4) and equivalent isotropic displacement parameters ($Å^2$ x 10^3) with estimated standard deviations in parentheses for $PhSb(o\text{-}O_2C_6Cl_4)Cl_2.OEt_2$ (5.6)

Atom	x	y	z	U(eq)
Sb	-1735(1)	-1751(1)	-3994(1)	32(1)
Cl(1)	-4805(2)	-2046(1)	-4607(1)	62(1)
Cl(2)	-644(2)	-2719(1)	-3497(1)	55(1)
O(21)	-2413(4)	-871(1)	-4017(2)	38(1)
O(22)	-1955(5)	-1684(1)	-2490(2)	40(1)
C(21)	-2515(5)	-681(2)	-3045(3)	32(1)
C(22)	-2242(6)	-1110(2)	-2231(3)	33(1)
C(23)	-2245(6)	-946(2)	-1194(3)	37(1)
C(24)	-2547(6)	-348(2)	-962(3)	38(1)
C(25)	-2841(6)	75(2)	-1769(4)	39(1)
C(26)	-2821(6)	-89(2)	-2812(3)	35(1)
Cl(23)	-1913(2)	-1492(1)	-230(1)	60(1)
Cl(24)	-2453(2)	-145(1)	336(1)	63(1)
Cl(25)	-3244(2)	811(1)	-1494(1)	63(1)
Cl(26)	-3199(2)	426(1)	-3833(1)	56(1)
C(11)	-1041(6)	-1717(2)	-5490(3)	32(1)
C(12)	460(6)	-2038(2)	-5627(3)	43(1)
C(13)	903(7)	-2025(3)	-6613(4)	53(1)
C(14)	-160(7)	-1693(2)	-7429(4)	54(1)
C(15)	-1655(7)	-1374(3)	-7284(4)	54(1)
C(16)	-2135(7)	-1386(2)	-6306(4)	44(1)
C(1)	2824(20)	-1379(7)	-1363(8)	73(4)
C(1')	2310(18)	-1628(6)	-1325(7)	58(3)
C(2)	2557(9)	-1683(3)	-2427(4)	66(2)
O(1)	1157(4)	-1385(2)	-3247(2)	44(1)
C(3)	1888(8)	-901(2)	-3781(4)	56(1)
C(4)	2194(10)	-331(3)	-3170(6)	85(2)

Table P.3 Calculated hydrogen coordinates (x 10^4) and isotropic displacement parameters ($Å^2$ x 10^3) with estimated standard deviations in parentheses for $PhSb(o\text{-}O_2C_6Cl_4)Cl_2.OEt_2$ (5.6)

Atom	x	y	z	U(iso)
H(12A)	1166(6)	-2259(2)	-5066(3)	52
H(13A)	1907(7)	-2240(3)	-6720(4)	63
H(14A)	135(7)	-1683(2)	-8089(4)	64
H(15A)	-2348(7)	-1149(3)	-7844(4)	65
H(16A)	-3156(7)	-1178(2)	-6205(4)	52
H(1A)	3752(20)	-1587(7)	-847(8)	110
H(1B)	1690(20)	-1385(7)	-1141(8)	110
H(1C)	3202(20)	-972(7)	-1421(8)	110
H(1A')	3286(18)	-1836(6)	-842(7)	87
H(1B')	1153(18)	-1801(6)	-1291(7)	87
H(1C')	2332(18)	-1213(6)	-1130(7)	87
H(2A)	3711(9)	-1683(3)	-2642(4)	79
H(2B)	2199(9)	-2096(3)	-2362(4)	79
H(3A)	1044(8)	-826(2)	-4466(4)	67
H(3B)	3045(8)	-1030(2)	-3919(4)	67
H(4A)	2674(10)	-35(3)	-3571(6)	127
H(4B)	3055(10)	-397(3)	-2499(6)	127
H(4C)	1051(10)	-193(3)	-3046(6)	127

Table P.4 Anisotropic thermal parameters ($Å^2 \times 10^3$) with estimated standard deviations in parentheses for $PhSb(o\text{-}O_2C_6Cl_4)Cl_2.OEt_2$ (5.6)

Atom	U11	U22	U33	U23	U13	U12
Sb	39(1)	29(1)	30(1)	-1(1)	12(1)	0(1)
Cl(1)	44(1)	76(1)	68(1)	-16(1)	19(1)	-17(1)
Cl(2)	82(1)	30(1)	58(1)	4(1)	25(1)	8(1)
O(21)	55(2)	32(2)	28(1)	3(1)	16(1)	8(1)
O(22)	66(2)	29(2)	31(2)	2(1)	21(1)	4(1)
C(21)	34(2)	32(2)	32(2)	-3(2)	9(2)	2(2)
C(22)	36(2)	34(2)	30(2)	-1(2)	12(2)	0(2)
C(23)	44(2)	43(2)	26(2)	1(2)	11(2)	-3(2)
C(24)	44(2)	42(2)	32(2)	-9(2)	16(2)	-2(2)
C(25)	41(2)	32(2)	47(3)	-5(2)	15(2)	0(2)
C(26)	35(2)	34(2)	37(2)	1(2)	9(2)	3(2)
Cl(23)	96(1)	52(1)	33(1)	9(1)	17(1)	3(1)
Cl(24)	92(1)	65(1)	37(1)	-15(1)	22(1)	1(1)
Cl(25)	90(1)	37(1)	68(1)	-11(1)	33(1)	7(1)
Cl(26)	83(1)	39(1)	50(1)	12(1)	22(1)	14(1)
C(11)	37(2)	34(2)	25(2)	-4(2)	7(2)	-3(2)
C(12)	44(3)	53(3)	32(2)	0(2)	10(2)	8(2)
C(13)	46(3)	68(3)	49(3)	-7(3)	22(2)	5(2)
C(14)	58(3)	76(4)	31(2)	-7(2)	19(2)	-11(3)
C(15)	60(3)	65(3)	34(2)	7(2)	7(2)	2(3)
C(16)	49(3)	46(3)	36(2)	3(2)	11(2)	8(2)
C(2)	60(3)	66(4)	61(3)	0(3)	-4(3)	9(3)
O(1)	41(2)	50(2)	37(2)	1(1)	4(1)	-3(1)
C(3)	57(3)	54(3)	58(3)	-4(3)	17(3)	-17(2)
C(4)	85(5)	64(4)	115(6)	-17(4)	43(4)	-22(4)

Table P.5 Bond lengths (Å) with estimated standard deviations in parentheses for $PhSb(o\text{-}O_2C_6Cl_4)Cl_2.OEt_2$ (5.6)

Sb-O(22)	1.991(3)	C(24)-Cl(24)	1.720(4)
Sb-O(21)	2.026(3)	C(25)-C(26)	1.398(6)
Sb-C(11)	2.117(4)	C(25)-Cl(25)	1.722(5)
Sb-O(1)	2.302(3)	C(26)-Cl(26)	1.719(4)
Sb-Cl(1)	2.342(2)	C(11)-C(12)	1.380(6)
Sb-Cl(2)	2.346(2)	C(11)-C(16)	1.384(6)
O(21)-C(21)	1.343(5)	C(12)-C(13)	1.390(6)
O(22)-C(22)	1.354(5)	C(13)-C(14)	1.375(7)
C(21)-C(26)	1.387(6)	C(14)-C(15)	1.377(7)
C(21)-C(22)	1.399(6)	C(15)-C(16)	1.393(6)
C(22)-C(23)	1.387(6)	C(1)-C(2)	1.499(8)
C(23)-C(24)	1.398(6)	C(1')-C(2)	1.481(8)
C(23)-Cl(23)	1.716(4)	C(2)-O(1)	1.460(6)
C(24)-C(25)	1.384(6)	O(1)-C(3)	1.457(6)
		C(3)-C(4)	1.485(8)

Table P.6 Bond angles (°) with estimated standard deviations in parentheses for PhSb(*o*-$O_2C_6Cl_4$)Cl_2.OEt_2 (5.6)

O(22)-Sb-O(21)	82.15(11)	C(22)-C(23)-Cl(23)	118.6(3)
O(22)-Sb-C(11)	168.86(14)	C(24)-C(23)-Cl(23)	121.7(3)
O(21)-Sb-C(11)	93.88(13)	C(25)-C(24)-C(23)	119.8(4)
O(22)-Sb-O(1)	81.67(13)	C(25)-C(24)-Cl(24)	120.9(3)
O(21)-Sb-O(1)	82.56(13)	C(23)-C(24)-Cl(24)	119.3(3)
C(11)-Sb-O(1)	87.50(14)	C(24)-C(25)-C(26)	120.5(4)
O(22)-Sb-Cl(1)	92.68(11)	C(24)-C(25)-Cl(25)	120.1(3)
O(21)-Sb-Cl(1)	92.58(10)	C(26)-C(25)-Cl(25)	119.4(3)
C(11)-Sb-Cl(1)	97.91(12)	C(21)-C(26)-C(25)	119.9(4)
O(1)-Sb-Cl(1)	172.98(9)	C(21)-C(26)-Cl(26)	118.5(3)
O(22)-Sb-Cl(2)	84.69(9)	C(25)-C(26)-Cl(26)	121.6(3)
O(21)-Sb-Cl(2)	165.20(9)	C(12)-C(11)-C(16)	122.2(4)
C(11)-Sb-Cl(2)	97.81(11)	C(12)-C(11)-Sb	119.0(3)
O(1)-Sb-Cl(2)	88.89(10)	C(16)-C(11)-Sb	118.8(3)
Cl(1)-Sb-Cl(2)	94.76(7)	C(11)-C(12)-C(13)	119.2(4)
C(21)-O(21)-Sb	111.2(2)	C(14)-C(13)-C(12)	119.3(4)
C(22)-O(22)-Sb	111.4(2)	C(13)-C(14)-C(15)	121.1(4)
O(21)-C(21)-C(26)	123.5(4)	C(14)-C(15)-C(16)	120.5(5)
O(21)-C(21)-C(22)	116.9(4)	C(11)-C(16)-C(15)	117.7(4)
C(26)-C(21)-C(22)	119.5(4)	O(1)-C(2)-C(1')	115.1(6)
O(22)-C(22)-C(23)	121.6(4)	O(1)-C(2)-C(1)	111.9(7)
O(22)-C(22)-C(21)	117.8(3)	C(3)-O(1)-C(2)	113.2(4)
C(23)-C(22)-C(21)	120.6(4)	C(3)-O(1)-Sb	119.3(3)
C(22)-C(23)-C(24)	119.7(4)	C(2)-O(1)-Sb	125.7(3)
		O(1)-C(3)-C(4)	114.4(5)

Experimental Details

Slightly more than a unique set of data were collected on a Stoe Stadi-4 four-circle diffractometer and the data were corrected for absorption, Lorentz and polarisation effects. Systematically absent data were then removed and the data merged to give a unique set. The structure was solved by direct methods (SHELXS-86)[1] and subsequent Fourier difference syntheses revealed the positions of all the other non-hydrogen atoms. Refinement was carried out against all F_o^2 data by full matrix procedures (SHELXL-93)[2]. One of the methyl groups in the diethyl ether ligand is disordered equally over two sites and the half occupancy atoms C(1) and C(1') were refined with isotropic thermal parameters and their distances from the neighbouring methylene carbon atoms restrained to 1.52 Å. The phenyl group was restrained to have local C_{2v} symmetry. Hydrogen atoms were placed in estimated [C–H = 0.93 (phenyl hydrogens), 0.96 (methyl hydrogens) and 0.97 (methylene hydrogens) Å], with fixed isotropic parameters (1.2 x equivalent isotropic temperature factors of the carbon atom to which they were bonded for phenyl and methylene protons and 1.5 x for methyl protons) and refined 'riding' their respective carbon atoms. A standard weighting scheme was applied and the data were corrected for the effects of extinction. All crystallographic calculations were performed using the SHELXS-86[1] and SHELXL-93[2] programs and neutral atom scattering factors were taken from the usual sources[3].

APPENDIX Q

Table Q.1 Data collection and processing parameters for [{μ-Ph_2Sb}$_2${$Mo(CO)_2(\eta$-$C_5H_5)$}$_2$].$CHCl_3$ (6.1.$CHCl_3$)

Chemical formula	$C_{39}H_{31}Cl_3Mo_2O_4Sb_2$
Formula weight	1105.41
Crystal size/mm	0.45 x 0.25 x 0.20
Crystal system	Monoclinic
Space group	$P2_1/c$
a / Å	14.662(3)
b / Å	14.896(3)
c / Å	18.759(4)
β / °	107.54(1)
Volume / Å^3	3906.47
Z	4
D_c/gcm^{-3}	1.880
Radiation (λ / Å)	Mo-K_α (0.71069)
μ / cm^{-1}	22.361
F(000)	2136
2θ limits / °	4-50
Index ranges	-15<=h<=14, 0<=k<=15, 0<=l<=19
Temperature / K	298
Total unique data collected	5059
Observed data [$I > 3\sigma(I)$]	4028
Absorption correction	DIFABS (min, 0.885, max, 1.116)[4]
Structure solution	Patterson (SHELXS-86)[1]
Refinement procedure	Full matrix-LS on F
Number of data / variables	4028 / 432
S	1.038
Max/min peaks in final diff. map / e Å^{-3}	+2.08, -1.50
R	0.0488
R_w	0.0542

Table Q.2 Fractional atomic coordinates and equivalent isotropic displacement parameters ($Å^2$) with estimated standard deviations in parentheses for [{μ-Ph_2Sb}$_2${$Mo(CO)_2$(η-C_5H_5)}$_2$].$CHCl_3$ (6.1.$CHCl_3$)

Atom	x/a	y/b	z/c	U(eq)
Sb(1)	0.12692(4)	0.19549(4)	0.17612(3)	0.0423
Sb(2)	0.28483(4)	0.08165(4)	0.28598(3)	0.0396
Mo(1)	0.20685(6)	0.04049(5)	0.13563(4)	0.0409
Mo(2)	0.14214(6)	0.17003(6)	0.32590(5)	0.0470
O(1)	0.1764(6)	-0.1379(5)	0.2113(5)	0.0725
O(2)	-0.0095(6)	-0.0025(6)	0.0870(5)	0.0778
O(3)	0.1174(8)	0.3777(6)	0.3163(6)	0.0969
O(4)	0.3195(7)	0.2283(7)	0.4560(5)	0.0879
C(1)	0.1905(7)	-0.0699(7)	0.1851(6)	0.0537
C(2)	0.0701(8)	0.0176(7)	0.1042(6)	0.0544
C(3)	0.1274(9)	0.3009(8)	0.3179(7)	0.0657
C(4)	0.2538(9)	0.2064(8)	0.4063(7)	0.0633
C(11)	-0.0153(7)	0.2248(7)	0.1073(6)	0.0498
C(12)	-0.0805(7)	0.2672(7)	0.1376(7)	0.0608
C(13)	-0.1683(8)	0.2971(8)	0.0909(7)	0.0650
C(14)	-0.1915(8)	0.2834(8)	0.0155(8)	0.0649
C(15)	-0.1283(8)	0.2425(8)	-0.0151(7)	0.0680
C(16)	-0.0415(8)	0.2116(7)	0.0306(6)	0.0554
C(21)	0.1820(7)	0.3194(6)	0.1456(5)	0.0484
C(22)	0.2783(8)	0.3263(7)	0.1457(6)	0.0602
C(23)	0.3103(9)	0.4055(8)	0.1214(7)	0.0680
C(24)	0.249(1)	0.4770(8)	0.0979(7)	0.0657
C(25)	0.1579(9)	0.4713(8)	0.1004(6)	0.0685
C(26)	0.1251(8)	0.3914(7)	0.1233(6)	0.0580
C(31)	0.3504(6)	-0.0269(6)	0.3593(5)	0.0448
C(32)	0.3641(7)	-0.0204(8)	0.4348(6)	0.0554
C(33)	0.4120(8)	-0.085(1)	0.4833(7)	0.0655
C(34)	0.4467(9)	-0.159(1)	0.4557(9)	0.0744
C(35)	0.4350(9)	-0.1670(9)	0.381(1)	0.0775
C(36)	0.3866(8)	-0.1012(7)	0.3323(6)	0.0598
C(41)	0.4164(7)	0.1546(7)	0.3033(5)	0.0491
C(42)	0.4221(8)	0.2454(7)	0.3179(7)	0.0673
C(43)	0.506(1)	0.2905(9)	0.326(1)	0.0875
C(44)	0.586(1)	0.245(1)	0.3219(8)	0.0805
C(45)	0.5816(8)	0.1557(9)	0.3071(7)	0.0695
C(46)	0.4969(7)	0.1112(8)	0.2982(6)	0.0590
C(51)	0.278(2)	0.117(1)	0.057(1)	0.0811
C(52)	0.215(1)	0.066(1)	0.0173(7)	0.0751
C(53)	0.235(2)	-0.016(1)	0.032(1)	0.0755
C(54)	0.322(2)	-0.018(2)	0.091(2)	0.0749
C(55)	0.344(1)	0.070(2)	0.1045(9)	0.0888
C(61)	0.052(1)	0.133(1)	0.4019(8)	0.0779
C(62)	-0.0130(8)	0.1516(9)	0.3296(9)	0.0751
C(63)	0.0004(9)	0.0848(9)	0.2812(7)	0.0730
C(64)	0.0705(9)	0.0275(8)	0.3203(7)	0.0677
C(65)	0.1032(8)	0.0562(9)	0.3959(7)	0.0673
C(200)	0.680(2)	0.011(2)	0.119(2)	0.16(1)
Cl(201)	0.6762(7)	-0.0257(6)	0.2046(5)	0.214(3)
Cl(202)	0.739(1)	0.118(1)	0.1482(8)	0.328(7)
Cl(203)	0.581(1)	0.074(1)	0.0708(8)	0.322(7)

Table Q.3 Calculated hydrogen coordinates and isotropic displacement parameters ($Å^2$) with estimated standard deviations in parentheses for $[\{\mu\text{-}Ph_2Sb\}_2\{Mo(CO)_2(\eta\text{-}C_5H_5)\}_2].CHCl_3$ ($6.1.CHCl_3$)

Atom	x/a	y/b	z/c	U(iso)
H(121)	-0.0635(7)	0.2757(7)	0.1929(7)	0.0850
H(131)	-0.2143(8)	0.3282(8)	0.1125(7)	0.0850
H(141)	-0.2555(8)	0.3030(8)	-0.0176(8)	0.0850
H(151)	-0.1450(8)	0.2348(8)	-0.0705(7)	0.0850
H(161)	0.0043(8)	0.1803(7)	0.0088(6)	0.0850
H(221)	0.3230(8)	0.2746(7)	0.1632(6)	0.0850
H(231)	0.3781(9)	0.4096(8)	0.1207(7)	0.0850
H(241)	0.273(1)	0.5330(8)	0.0800(7)	0.0850
H(251)	0.1136(9)	0.5236(8)	0.0847(6)	0.0850
H(261)	0.0573(8)	0.3874(7)	0.1242(6)	0.0850
H(321)	0.3379(7)	0.0329(8)	0.4546(6)	0.0850
H(331)	0.4221(8)	-0.080(1)	0.5383(7)	0.0850
H(341)	0.4809(9)	-0.207(1)	0.4907(9)	0.0850
H(351)	0.4607(9)	-0.2203(9)	0.361(1)	0.0850
H(361)	0.3773(8)	-0.1064(7)	0.2775(6)	0.0850
H(421)	0.3641(8)	0.2775(7)	0.3222(7)	0.0850
H(431)	0.510(1)	0.3563(9)	0.337(1)	0.0850
H(441)	0.647(1)	0.279(1)	0.3285(8)	0.0850
H(451)	0.6394(8)	0.1230(9)	0.3030(7)	0.0850
H(461)	0.4930(7)	0.0454(8)	0.2874(6)	0.0850
H(511)	0.278(2)	0.185(1)	0.056(1)	0.0850
H(521)	0.157(1)	0.087(1)	-0.0227(7)	0.0850
H(531)	0.197(2)	-0.069(1)	0.008(1)	0.0850
H(541)	0.359(2)	-0.071(2)	0.116(2)	0.0850
H(551)	0.402(1)	0.094(2)	0.1433(9)	0.0850
H(611)	0.059(1)	0.169(1)	0.4481(8)	0.0850
H(621)	-0.0594(8)	0.2027(9)	0.3161(9)	0.0850
H(631)	-0.0354(9)	0.0797(9)	0.2268(7)	0.0850
H(641)	0.0948(9)	-0.0262(8)	0.2996(7)	0.0850
H(651)	0.1535(8)	0.0268(9)	0.4375(7)	0.0850

Table Q.4 Anisotropic thermal parameters ($Å^2$) with estimated standard deviations in parentheses for $[\{\mu\text{-}Ph_2Sb\}_2\{Mo(CO)_2(\eta\text{-}C_5H_5)\}_2].CHCl_3$ (6.1.$CHCl_3$)

Atom	U(11)	U(22)	U(33)	U(23)	U(13)	U(12)
Sb(1)	0.0412(4)	0.0423(4)	0.0436(4)	0.0027(3)	0.0124(3)	0.0032(3)
Sb(2)	0.0395(4)	0.0380(4)	0.0400(4)	-0.0008(3)	0.0098(3)	-0.0005(3)
Mo(1)	0.0430(5)	0.0414(5)	0.0394(5)	-0.0017(3)	0.0135(4)	-0.0025(3)
Mo(2)	0.0492(5)	0.0519(5)	0.0441(5)	-0.0015(4)	0.0179(4)	0.0054(4)
O(1)	0.100(6)	0.050(5)	0.080(6)	0.008(4)	0.017(5)	-0.018(4)
O(2)	0.055(5)	0.100(7)	0.090(6)	-0.002(5)	0.009(4)	-0.026(5)
O(3)	0.15(1)	0.062(6)	0.116(8)	-0.010(5)	0.049(7)	0.024(6)
O(4)	0.090(6)	0.128(8)	0.067(6)	-0.040(6)	0.007(5)	0.006(6)
C(1)	0.061(7)	0.045(6)	0.057(6)	-0.006(5)	0.017(5)	-0.006(5)
C(2)	0.056(7)	0.055(6)	0.054(6)	-0.008(5)	0.017(5)	-0.005(5)
C(3)	0.089(9)	0.050(7)	0.081(8)	0.003(6)	0.040(7)	0.019(6)
C(4)	0.077(8)	0.064(7)	0.061(7)	-0.019(6)	0.021(7)	0.009(6)
C(11)	0.045(6)	0.051(6)	0.053(6)	0.009(5)	0.011(5)	0.004(5)
C(12)	0.048(6)	0.063(7)	0.076(8)	0.009(6)	0.018(6)	0.008(5)
C(13)	0.051(6)	0.065(7)	0.087(9)	0.010(6)	0.017(6)	0.016(6)
C(14)	0.049(7)	0.060(7)	0.09(1)	0.017(6)	-0.002(6)	0.012(6)
C(15)	0.067(8)	0.066(7)	0.066(7)	0.008(6)	0.001(6)	-0.000(6)
C(16)	0.063(7)	0.054(6)	0.050(6)	0.008(5)	0.012(5)	0.005(5)
C(21)	0.059(6)	0.041(5)	0.048(6)	0.004(4)	0.016(5)	0.006(5)
C(22)	0.055(6)	0.059(7)	0.068(7)	-0.001(5)	0.019(5)	-0.004(5)
C(23)	0.061(7)	0.069(8)	0.086(9)	-0.005(7)	0.028(6)	-0.019(6)
C(24)	0.10(1)	0.053(7)	0.064(7)	-0.000(6)	0.034(7)	-0.018(7)
C(25)	0.081(9)	0.066(8)	0.063(7)	0.010(6)	0.023(6)	0.008(6)
C(26)	0.056(6)	0.048(6)	0.076(7)	0.006(5)	0.023(6)	0.002(5)
C(31)	0.040(5)	0.041(5)	0.055(6)	0.005(4)	0.006(4)	-0.010(4)
C(32)	0.048(6)	0.066(7)	0.051(7)	0.009(5)	-0.003(5)	-0.011(5)
C(33)	0.054(7)	0.10(1)	0.060(7)	0.029(7)	-0.004(6)	-0.014(7)
C(34)	0.055(7)	0.075(9)	0.11(1)	0.039(9)	0.008(7)	0.002(7)
C(35)	0.070(8)	0.068(8)	0.13(1)	0.036(8)	0.035(8)	0.018(7)
C(36)	0.067(7)	0.057(7)	0.059(7)	0.007(5)	0.021(5)	0.006(6)
C(41)	0.044(6)	0.057(7)	0.047(6)	0.010(5)	0.007(4)	-0.006(5)
C(42)	0.058(7)	0.046(7)	0.11(1)	-0.006(6)	0.014(6)	-0.008(5)
C(43)	0.08(1)	0.055(8)	0.17(2)	-0.010(9)	0.02(1)	-0.026(8)
C(44)	0.063(9)	0.09(1)	0.11(1)	0.024(8)	0.006(7)	-0.029(8)
C(45)	0.049(7)	0.088(9)	0.081(8)	0.018(7)	0.017(6)	-0.001(6)
C(46)	0.054(7)	0.064(7)	0.063(7)	0.011(5)	0.018(5)	-0.004(6)
C(51)	0.16(2)	0.08(1)	0.09(1)	-0.008(9)	0.09(1)	-0.04(1)
C(52)	0.077(9)	0.14(1)	0.046(7)	-0.007(8)	0.026(6)	-0.01(1)
C(53)	0.17(2)	0.058(9)	0.13(1)	-0.042(9)	0.11(1)	-0.03(1)
C(54)	0.20(3)	0.18(2)	0.21(3)	0.15(2)	0.17(2)	0.17(2)
C(55)	0.060(9)	0.32(3)	0.045(8)	-0.01(1)	0.018(7)	-0.05(2)
C(61)	0.084(9)	0.10(1)	0.081(9)	0.002(8)	0.050(8)	0.004(8)
C(62)	0.054(7)	0.090(9)	0.12(1)	0.027(9)	0.045(7)	0.012(6)
C(63)	0.068(8)	0.093(9)	0.069(8)	0.006(7)	0.025(7)	-0.015(7)
C(64)	0.072(8)	0.065(7)	0.082(9)	-0.001(6)	0.035(7)	-0.016(6)
C(65)	0.064(7)	0.089(9)	0.065(8)	0.028(6)	0.025(6)	0.006(7)

Table Q.5 Bond lengths (Å) with estimated standard deviations in parentheses for [{μ-Ph_2Sb}$_2${$Mo(CO)_2(\eta$-$C_5H_5)$}$_2$].$CHCl_3$ (6.1.$CHCl_3$)

Sb(1) - Sb(2)	3.0996(8)	C(15) - C(16)	1.38(2)
Sb(1) - Mo(1)	2.796(1)	C(21) - C(22)	1.41(1)
Sb(1) - Mo(2)	2.777(1)	C(21) - C(26)	1.35(1)
Sb(1) - C(11)	2.140(9)	C(22) - C(23)	1.40(2)
Sb(1) - C(21)	2.16(1)	C(23) - C(24)	1.37(2)
Sb(2) - Mo(1)	2.774(1)	C(24) - C(25)	1.36(2)
Sb(2) - Mo(2)	2.760(1)	C(25) - C(26)	1.40(2)
Sb(2) - C(31)	2.152(9)	C(31) - C(32)	1.37(1)
Sb(2) - C(41)	2.152(9)	C(31) - C(36)	1.39(1)
Mo(1) - C(1)	1.94(1)	C(32) - C(33)	1.37(2)
Mo(1) - C(2)	1.94(1)	C(33) - C(34)	1.37(2)
Mo(1) - C(51)	2.34(1)	C(34) - C(35)	1.36(2)
Mo(1) - C(52)	2.29(1)	C(35) - C(36)	1.38(2)
Mo(1) - C(53)	2.26(1)	C(41) - C(42)	1.38(2)
Mo(1) - C(54)	2.27(1)	C(41) - C(46)	1.37(1)
Mo(1) - C(55)	2.30(1)	C(42) - C(43)	1.37(2)
Mo(2) - C(3)	1.96(1)	C(43) - C(44)	1.37(2)
Mo(2) - C(4)	1.94(1)	C(44) - C(45)	1.36(2)
Mo(2) - C(61)	2.29(1)	C(45) - C(46)	1.37(2)
Mo(2) - C(62)	2.31(1)	C(51) - C(52)	1.26(2)
Mo(2) - C(63)	2.36(1)	C(51) - C(55)	1.31(3)
Mo(2) - C(64)	2.36(1)	C(52) - C(53)	1.27(2)
Mo(2) - C(65)	2.32(1)	C(53) - C(54)	1.42(3)
O(1) - C(1)	1.17(1)	C(54) - C(55)	1.35(3)
O(2) - C(2)	1.15(1)	C(61) - C(62)	1.43(2)
O(3) - C(3)	1.15(1)	C(61) - C(65)	1.39(2)
O(4) - C(4)	1.17(1)	C(62) - C(63)	1.40(2)
C(11) - C(12)	1.40(1)	C(63) - C(64)	1.37(2)
C(11) - C(16)	1.39(1)	C(64) - C(65)	1.42(2)
C(12) - C(13)	1.39(2)	C(200)- Cl(201)	1.71(3)
C(13) - C(14)	1.37(2)	C(200)- Cl(202)	1.82(3)
C(14) - C(15)	1.37(2)	C(200)- Cl(203)	1.73(3)

Table Q.6 Bond angles (°) with estimated standard deviations in parentheses for [{μ-Ph_2Sb}$_2${$Mo(CO)_2(\eta$-$C_5H_5)$}$_2$].$CHCl_3$ (6.1.$CHCl_3$)

Sb(2) - Sb(1) - Mo(1)	55.85(2)	C(4) - Mo(2) - C(64)	123.2(5)
Sb(2) - Sb(1) - Mo(2)	55.69(2)	C(61) - Mo(2) - C(64)	58.4(5)
Mo(1) - Sb(1) - Mo(2)	104.45(3)	C(62) - Mo(2) - C(64)	57.7(5)
Sb(2) - Sb(1) - C(11)	155.4(3)	Sb(1) - Mo(2) - C(65)	135.6(3)
Mo(1) - Sb(1) - C(11)	114.6(3)	Sb(2) - Mo(2) - C(65)	98.1(3)
Mo(2) - Sb(1) - C(11)	113.9(3)	C(3) - Mo(2) - C(65)	136.9(5)
Sb(2) - Sb(1) - C(21)	112.3(3)	C(4) - Mo(2) - C(65)	93.4(5)
Mo(1) - Sb(1) - C(21)	114.4(3)	C(61) - Mo(2) - C(65)	35.2(4)
Mo(2) - Sb(1) - C(21)	117.6(3)	C(62) - Mo(2) - C(65)	58.9(4)
C(11) - Sb(1) - C(21)	92.3(4)	C(63) - Mo(2) - C(64)	33.7(4)
Sb(1) - Sb(2) - Mo(1)	56.53(2)	C(63) - Mo(2) - C(65)	57.8(4)
Sb(1) - Sb(2) - Mo(2)	56.22(2)	C(64) - Mo(2) - C(65)	35.3(4)

Mo(1) - Sb(2) - Mo(2)	105.51(3)	Mo(1) - C(1) - O(1)	176.1(9)
Sb(1) - Sb(2) - C(31)	159.4(2)	Mo(1) - C(2) - O(2)	175.0(10)
Mo(1) - Sb(2) - C(31)	116.8(3)	Mo(2) - C(3) - O(3)	176.6(11)
Mo(2) - Sb(2) - C(31)	114.5(3)	Mo(2) - C(4) - O(4)	178.2(11)
Sb(1) - Sb(2) - C(41)	106.3(3)	Sb(1) - C(11) - C(12)	120.5(8)
Mo(1) - Sb(2) - C(41)	109.9(3)	Sb(1) - C(11) - C(16)	120.8(7)
Mo(2) - Sb(2) - C(41)	115.9(3)	C(12) - C(11) - C(16)	118.4(9)
C(31) - Sb(2) - C(41)	94.3(3)	C(11) - C(12) - C(13)	120.2(11)
Sb(1) - Mo(1) - Sb(2)	67.63(2)	C(12) - C(13) - C(14)	119.9(11)
Sb(1) - Mo(1) - C(1)	116.6(3)	C(13) - C(14) - C(15)	120.7(10)
Sb(2) - Mo(1) - C(1)	76.9(3)	C(14) - C(15) - C(16)	120.0(12)
Sb(1) - Mo(1) - C(2)	75.4(3)	C(11) - C(16) - C(15)	120.8(11)
Sb(2) - Mo(1) - C(2)	114.8(3)	Sb(1) - C(21) - C(22)	121.0(7)
C(1) - Mo(1) - C(2)	74.4(5)	Sb(1) - C(21) - C(26)	121.1(8)
Sb(1) - Mo(1) - C(51)	93.9(4)	C(22) - C(21) - C(26)	117.9(9)
Sb(2) - Mo(1) - C(51)	113.9(5)	C(21) - C(22) - C(23)	119.6(10)
C(1) - Mo(1) - C(51)	149.2(5)	C(22) - C(23) - C(24)	120.6(11)
C(2) - Mo(1) - C(51)	120.6(7)	C(23) - C(24) - C(25)	119.6(11)
Sb(1) - Mo(1) - C(52)	105.9(5)	C(24) - C(25) - C(26)	119.9(11)
Sb(2) - Mo(1) - C(52)	145.4(4)	C(21) - C(26) - C(25)	122.3(10)
C(1) - Mo(1) - C(52)	131.0(6)	Sb(2) - C(31) - C(32)	120.3(8)
C(2) - Mo(1) - C(52)	94.8(5)	Sb(2) - C(31) - C(36)	120.9(7)
C(51) - Mo(1) - C(52)	31.5(5)	C(32) - C(31) - C(36)	118.6(9)
Sb(1) - Mo(1) - C(53)	137.6(6)	C(31) - C(32) - C(33)	121.5(12)
Sb(2) - Mo(1) - C(53)	145.9(6)	C(32) - C(33) - C(34)	119.2(13)
C(1) - Mo(1) - C(53)	100.2(5)	C(33) - C(34) - C(35)	121.0(12)
C(2) - Mo(1) - C(53)	96.5(6)	C(34) - C(35) - C(36)	119.9(13)
C(51) - Mo(1) - C(53)	54.1(5)	C(31) - C(36) - C(35)	119.9(12)
C(52) - Mo(1) - C(53)	32.3(6)	Sb(2) - C(41) - C(42)	121.6(8)
Sb(1) - Mo(1) - C(54)	146.6(8)	Sb(2) - C(41) - C(46)	120.1(8)
Sb(2) - Mo(1) - C(54)	109.5(9)	C(42) - C(41) - C(46)	118.3(10)
C(1) - Mo(1) - C(54)	93.7(6)	C(41) - C(42) - C(43)	120.1(12)
C(2) - Mo(1) - C(54)	129.5(11)	C(42) - C(43) - C(44)	120.4(13)
C(51) - Mo(1) - C(54)	55.6(6)	C(43) - C(44) - C(45)	120.2(12)
C(52) - Mo(1) - C(54)	56.4(6)	C(44) - C(45) - C(46)	119.0(12)
Sb(1) - Mo(1) - C(55)	112.4(8)	C(41) - C(46) - C(45)	121.9(11)
Sb(2) - Mo(1) - C(55)	95.3(4)	Mo(1) - C(51) - C(52)	72.0(8)
C(1) - Mo(1) - C(55)	121.8(9)	Mo(1) - C(51) - C(55)	72.1(9)
C(2) - Mo(1) - C(55)	149.2(5)	C(52) - C(51) - C(55)	109.8(18)
C(51) - Mo(1) - C(55)	32.7(7)	Mo(1) - C(52) - C(51)	76.4(8)
C(52) - Mo(1) - C(55)	54.4(5)	Mo(1) - C(52) - C(53)	72.7(8)
C(53) - Mo(1) - C(54)	36.4(9)	C(51) - C(52) - C(53)	111.8(17)
C(53) - Mo(1) - C(55)	56.9(7)	Mo(1) - C(53) - C(52)	75.0(7)
C(54) - Mo(1) - C(55)	34.4(8)	Mo(1) - C(53) - C(54)	72.3(9)
Sb(1) - Mo(2) - Sb(2)	68.09(3)	C(52) - C(53) - C(54)	106.8(16)
Sb(1) - Mo(2) - C(3)	79.2(4)	Mo(1) - C(54) - C(53)	71.4(8)
Sb(2) - Mo(2) - C(3)	121.9(3)	Mo(1) - C(54) - C(55)	74.0(10)
Sb(1) - Mo(2) - C(4)	122.7(4)	C(53) - C(54) - C(55)	103.5(13)
Sb(2) - Mo(2) - C(4)	79.2(3)	Mo(1) - C(55) - C(51)	75.2(9)
C(3) - Mo(2) - C(4)	80.2(5)	Mo(1) - C(55) - C(54)	71.6(9)
Sb(1) - Mo(2) - C(61)	141.1(4)	C(51) - C(55) - C(54)	108.0(18)
Sb(2) - Mo(2) - C(61)	133.1(4)	Mo(2) - C(61) - C(62)	72.9(6)
C(3) - Mo(2) - C(61)	102.5(5)	Mo(2) - C(61) - C(65)	73.6(6)
C(4) - Mo(2) - C(61)	95.4(5)	C(62) - C(61) - C(65)	107.7(12)
Sb(1) - Mo(2) - C(62)	105.5(4)	Mo(2) - C(62) - C(61)	71.0(6)
Sb(2) - Mo(2) - C(62)	141.7(4)	Mo(2) - C(62) - C(63)	74.5(7)
C(3) - Mo(2) - C(62)	91.9(5)	C(61) - C(62) - C(63)	107.1(12)
C(4) - Mo(2) - C(62)	128.1(5)	Mo(2) - C(63) - C(62)	70.7(7)

C(61) - Mo(2) - C(62)	36.2(5)	Mo(2) - C(63) - C(64)	72.9(7)
Sb(1) - Mo(2) - C(63)	85.4(3)	C(62) - C(63) - C(64)	109.0(12)
Sb(2) - Mo(2) - C(63)	107.8(3)	Mo(2) - C(64) - C(63)	73.4(7)
C(3) - Mo(2) - C(63)	116.2(5)	Mo(2) - C(64) - C(65)	70.9(7)
C(4) - Mo(2) - C(63)	150.7(5)	C(63) - C(64) - C(65)	108.7(12)
C(61) - Mo(2) - C(63)	58.6(5)	Mo(2) - C(65) - C(61)	71.3(7)
C(62) - Mo(2) - C(63)	34.8(5)	Mo(2) - C(65) - C(64)	73.8(6)
Sb(1) - Mo(2) - C(64)	100.3(3)	C(61) - C(65) - C(64)	107.5(11)
Sb(2) - Mo(2) - C(64)	85.5(3)	Cl(201- C(200)- Cl(202)	98.3(16)
C(3) - Mo(2) - C(64)	148.7(5)	Cl(201- C(200)- Cl(203)	114.2(18)
		Cl(202- C(200)- Cl(203)	85.6(16)

Experimental Details

A unique set of data were collected on a Hilger and Watts Y290 four-circle diffractometer and the data were corrected for Lorentz and polarisation effects. The Sb and Mo atoms were located from a Patterson synthesis[1] and subsequent Fourier difference syntheses revealed the positions of all the other non-hydrogen atoms. Refinement was carried out against 'observed' F_o data by full matrix procedures using an anisotropic model for all non-hydrogen atoms, except for those associated with the disordered chloroform solvate molecule that were refined isotropically. Hydrogen atoms were placed in estimated positions (C–H = 1.00 Å), with the exception of the hydrogen associated with the disordered chloroform solvate that was ignored. The hydrogen atoms were assigned a common fixed thermal parameter and refined 'riding' their respective carbon atoms. Data were corrected by a Chebyshev weighting scheme[6] (4 coefficient) and also for the effects of absorption[4], anomalous dispersion and isotropic extinction[7]. All crystallographic calculations were performed using the CRYSTALS suite of programs[8] and neutral atom scattering factors were taken from the usual sources[3].

APPENDIX R

Table R.1 Data collection and processing parameters for [PhSb{Fe(CO)$_2$(η-C$_5$H$_5$)}$_2$] (6.4)

Chemical formula	$C_{20}H_{15}Fe_2O_4Sb$
Formula weight	552.77
Crystal size/mm	0.50 x 0.40 x 0.20
Crystal system	Orthorhombic
Space group	$Pca2_1$
a / Å	18.003(4)
b / Å	7.634(2)
c / Å	14.521(3)
Volume / Å^3	1995.7(7)
Z	4
D_c/gcm^{-3}	1.840
Radiation (λ / Å)	Mo-K$_\alpha$ (0.71069)
μ / cm^{-1}	28.00
F(000)	1080
2θ limits / °	4.52 to 59.86
Index ranges	-1<=h<=25, 0<=k<=10, 0<=l<=20
Temperature / K	298
Total data collected	3215
Unique data	3001 [R(int) = 0.0593]
Absorption correction	Psi scans (min = 0.4063, max = 0.9558)
Structure solution	Direct (SHELXS-86)[1]
Refinement procedure	Full matrix-LS on F^2
Number of data / variables	2945 / 245
Goodness-of-fit on F^2	0.848
Max/min peaks in final diff. map / e Å^{-3}	+0.801, -1.657
Absolute structure parameter	0.00(5)
R observed data [$I > 2\sigma(I)$], (all data)	0.0340, (0.2034)
R_w observed data, (all data)	0.0686, (0.2580)

Table R.2 Atomic coordinates (x 10^4) and equivalent isotropic displacement parameters ($Å^2$ x 10^3) with estimated standard deviations in parentheses for [PhSb{Fe(CO)$_2$(η-C_5H_5)}$_2$] (6.4)

Atom	x	y	z	U(eq)
Sb(1)	5305(1)	3450(1)	-15(1)	42(1)
Fe(1)	6253(1)	3827(2)	-1387(1)	41(1)
Fe(2)	4191(1)	1377(2)	-456(1)	41(1)
O(1)	7316(4)	4869(12)	-4(9)	96(2)
O(2)	6677(4)	201(8)	-1303(5)	61(2)
O(3)	3634(4)	4201(11)	-1608(7)	90(3)
O(4)	5014(5)	-281(10)	-1924(6)	70(2)
C(1)	5975(5)	1773(12)	869(6)	46(2)
C(2)	6057(6)	-34(14)	770(6)	55(2)
C(3)	6491(6)	-986(15)	1363(8)	61(3)
C(4)	6856(7)	-153(25)	2084(10)	88(4)
C(5)	6781(6)	1624(21)	2189(8)	72(4)
C(6)	6339(6)	2554(16)	1623(7)	54(3)
C(7)	6693(9)	5348(20)	-2458(10)	85(4)
C(8)	6133(10)	6287(13)	-1975(11)	89(4)
C(9)	5456(7)	5391(15)	-2080(8)	71(3)
C(10)	5604(7)	3899(15)	-2600(7)	63(3)
C(11)	6334(8)	3872(16)	-2821(8)	72(3)
C(12)	6872(6)	4481(15)	-538(7)	56(3)
C(13)	6476(5)	1617(11)	-1316(7)	44(2)
C(14)	4129(8)	807(23)	969(8)	84(4)
C(15)	4145(8)	-773(18)	446(11)	88(4)
C(16)	3512(7)	-760(18)	-131(11)	83(4)
C(17)	3124(5)	757(17)	22(11)	71(3)
C(18)	3502(6)	1720(20)	680(8)	74(3)
C(19)	3873(5)	3102(14)	-1143(7)	54(3)
C(20)	4708(5)	387(11)	-1337(6)	44(2)

Table R.3 Anisotropic thermal parameters ($Å^2$ x 10^3) with estimated standard deviations in parentheses for [PhSb{Fe(CO)$_2$(η-C_5H_5)}$_2$] (6.4)

Atom	U11	U22	U33	U23	U13	U12
Sb(1)	42(1)	44(1)	40(1)	-11(1)	-6(1)	4(1)
Fe(1)	45(1)	36(1)	43(1)	4(1)	-4(1)	-6(1)
Fe(2)	34(1)	57(1)	32(1)	-2(1)	0(1)	-1(1)
O(1)	85(5)	135(7)	67(4)	-5(7)	-9(7)	-54(5)
O(2)	65(5)	42(4)	78(5)	8(4)	1(4)	13(3)
O(3)	76(6)	100(5)	94(6)	36(5)	-16(5)	32(5)
O(4)	63(4)	81(5)	66(4)	-34(5)	16(4)	1(4)
C(1)	43(5)	63(6)	32(4)	16(4)	-2(4)	8(5)
C(2)	59(6)	74(6)	32(5)	1(5)	-2(5)	-4(5)
C(3)	47(6)	70(7)	65(7)	12(6)	13(6)	15(6)
C(4)	38(6)	154(14)	71(8)	45(9)	-5(6)	-6(8)
C(5)	46(6)	127(12)	43(5)	27(8)	-11(5)	-16(8)
C(6)	52(6)	70(7)	40(5)	3(5)	-6(5)	-10(6)
C(7)	72(9)	107(11)	76(8)	58(8)	-19(7)	-13(9)
C(8)	138(13)	37(5)	91(10)	19(6)	-28(10)	-18(8)
C(9)	85(9)	65(7)	64(7)	23(6)	-4(7)	17(7)
C(10)	73(8)	70(7)	45(6)	19(5)	-11(5)	-8(6)

C(11)	96(10)	78(7)	42(6)	5(6)	-4(6)	1(8)
C(12)	47(6)	76(7)	46(6)	-4(5)	-1(5)	-11(5)
C(13)	46(5)	41(5)	44(5)	11(5)	7(5)	-4(4)
C(14)	69(9)	149(13)	33(6)	15(8)	8(6)	-30(9)
C(15)	85(9)	85(8)	93(10)	35(8)	36(9)	-5(8)
C(16)	77(8)	109(9)	62(9)	2(8)	-1(7)	-53(8)
C(17)	38(5)	116(8)	58(6)	-4(10)	22(8)	-17(6)
C(18)	51(6)	126(10)	47(6)	-15(7)	11(5)	-4(8)
C(19)	37(5)	71(6)	53(6)	-1(5)	0(5)	3(5)
C(20)	36(5)	51(5)	44(5)	-5(4)	-5(5)	-4(4)

Table R.4 Bond lengths (Å) with estimated standard deviations in parentheses for [PhSb{Fe(CO)$_2$(η-C$_5$H$_5$)}$_2$] (6.4)

Sb(1)-C(1)	2.177(9)	O(2)-C(13)	1.140(9)
Sb(1)-Fe(2)	2.6338(14)	O(3)-C(19)	1.160(11)
Sb(1)-Fe(1)	2.639(2)	O(4)-C(20)	1.137(11)
Fe(1)-C(12)	1.736(11)	C(1)-C(2)	1.395(14)
Fe(1)-C(13)	1.737(8)	C(1)-C(6)	1.408(13)
Fe(1)-C(8)	2.074(10)	C(2)-C(3)	1.37(2)
Fe(1)-C(11)	2.087(11)	C(3)-C(4)	1.39(2)
Fe(1)-C(7)	2.096(12)	C(4)-C(5)	1.37(2)
Fe(1)-C(10)	2.114(11)	C(5)-C(6)	1.35(2)
Fe(1)-C(9)	2.120(11)	C(7)-C(11)	1.40(2)
Fe(2)-C(19)	1.749(11)	C(7)-C(8)	1.42(2)
Fe(2)-C(20)	1.753(10)	C(8)-C(9)	1.41(2)
Fe(2)-C(18)	2.081(11)	C(9)-C(10)	1.39(2)
Fe(2)-C(16)	2.093(11)	C(10)-C(11)	1.35(2)
Fe(2)-C(17)	2.097(9)	C(14)-C(18)	1.39(2)
Fe(2)-C(15)	2.101(12)	C(14)-C(15)	1.43(2)
Fe(2)-C(14)	2.117(12)	C(15)-C(16)	1.42(2)
O(1)-C(12)	1.151(13)	C(16)-C(17)	1.37(2)
		C(17)-C(18)	1.38(2)

Table R.5 Bond angles (°) with estimated standard deviations in parentheses for [PhSb{Fe(CO)$_2$(η-C$_5$H$_5$)}$_2$] (6.4)

C(1)-Sb(1)-Fe(2)	102.2(3)	C(2)-C(1)-Sb(1)	125.4(8)
C(1)-Sb(1)-Fe(1)	98.7(2)	C(6)-C(1)-Sb(1)	117.9(7)
Fe(2)-Sb(1)-Fe(1)	111.96(5)	C(3)-C(2)-C(1)	121.3(11)
C(12)-Fe(1)-C(13)	95.1(5)	C(2)-C(3)-C(4)	120.0(12)
C(12)-Fe(1)-C(8)	95.7(5)	C(5)-C(4)-C(3)	119.3(12)
C(13)-Fe(1)-C(8)	158.1(6)	C(6)-C(5)-C(4)	120.8(13)
C(12)-Fe(1)-C(11)	131.2(5)	C(5)-C(6)-C(1)	121.8(11)
C(13)-Fe(1)-C(11)	93.4(5)	C(11)-C(7)-C(8)	105.3(12)
C(12)-Fe(1)-C(7)	97.2(5)	C(11)-C(7)-Fe(1)	70.1(7)
C(13)-Fe(1)-C(7)	119.6(6)	C(8)-C(7)-Fe(1)	69.2(7)
C(12)-Fe(1)-C(10)	159.9(5)	C(9)-C(8)-C(7)	108.4(11)
C(13)-Fe(1)-C(10)	101.7(5)	C(9)-C(8)-Fe(1)	72.2(6)
C(12)-Fe(1)-C(9)	127.6(5)	C(7)-C(8)-Fe(1)	70.9(6)
C(13)-Fe(1)-C(9)	137.0(5)	C(10)-C(9)-C(8)	106.9(12)

C(12)-Fe(1)-Sb(1)	84.8(3)	C(10)-C(9)-Fe(1)	70.6(6)
C(13)-Fe(1)-Sb(1)	89.9(3)	C(8)-C(9)-Fe(1)	68.7(7)
C(8)-Fe(1)-Sb(1)	110.0(5)	C(11)-C(10)-C(9)	109.1(11)
C(11)-Fe(1)-Sb(1)	143.2(4)	C(11)-C(10)-Fe(1)	70.1(7)
C(7)-Fe(1)-Sb(1)	149.9(5)	C(9)-C(10)-Fe(1)	71.0(6)
C(10)-Fe(1)-Sb(1)	105.9(4)	C(10)-C(11)-C(7)	110.3(12)
C(9)-Fe(1)-Sb(1)	89.0(3)	C(10)-C(11)-Fe(1)	72.3(7)
C(19)-Fe(2)-C(20)	94.7(4)	C(7)-C(11)-Fe(1)	70.8(7)
C(19)-Fe(2)-C(18)	99.3(5)	O(1)-C(12)-Fe(1)	176.0(11)
C(20)-Fe(2)-C(18)	161.7(5)	O(2)-C(13)-Fe(1)	174.3(8)
C(19)-Fe(2)-C(16)	121.6(6)	C(18)-C(14)-C(15)	106.2(13)
C(20)-Fe(2)-C(16)	97.9(5)	C(18)-C(14)-Fe(2)	69.2(7)
C(19)-Fe(2)-C(17)	93.3(5)	C(15)-C(14)-Fe(2)	69.6(7)
C(20)-Fe(2)-C(17)	129.0(5)	C(16)-C(15)-C(14)	107.1(13)
C(19)-Fe(2)-C(15)	158.5(5)	C(16)-C(15)-Fe(2)	70.0(7)
C(20)-Fe(2)-C(15)	98.0(5)	C(14)-C(15)-Fe(2)	70.9(7)
C(19)-Fe(2)-C(14)	134.0(6)	C(17)-C(16)-C(15)	108.7(13)
C(20)-Fe(2)-C(14)	130.7(6)	C(17)-C(16)-Fe(2)	71.0(6)
C(19)-Fe(2)-Sb(1)	86.3(3)	C(15)-C(16)-Fe(2)	70.6(6)
C(20)-Fe(2)-Sb(1)	91.9(3)	C(16)-C(17)-C(18)	108.1(13)
C(18)-Fe(2)-Sb(1)	100.7(3)	C(16)-C(17)-Fe(2)	70.8(6)
C(16)-Fe(2)-Sb(1)	149.2(5)	C(18)-C(17)-Fe(2)	70.0(5)
C(17)-Fe(2)-Sb(1)	138.8(4)	C(17)-C(18)-C(14)	109.9(13)
C(15)-Fe(2)-Sb(1)	110.4(5)	C(17)-C(18)-Fe(2)	71.3(6)
C(14)-Fe(2)-Sb(1)	85.8(4)	C(14)-C(18)-Fe(2)	72.1(7)
C(2)-C(1)-C(6)	116.7(9)	O(3)-C(19)-Fe(2)	177.0(9)
		O(4)-C(20)-Fe(2)	177.0(8)

Experimental Details

Slightly more than a unique set of data were collected on a Enraf-Nonius CAD-4 four-circle diffractometer. The data were corrected for Lorentz, polarisation and absorption (semi-emperical from ψ-scans) effects, merged and systematically absent reflections were rejected. The structure was solved direct methods (SHELXS-86)[1] and subsequent Fourier difference syntheses revealed the positions of all the other non-hydrogen atoms. Refinement was carried out against all F_o^2 data by full matrix procedures (SHELXL-93)[2]. Hydrogen atoms were placed in estimated positions [C–H = 0.95 Å], with fixed isotropic parameters (1.2 x equivalent isotropic temperature factors of the carbon atom to which they were bonded) and refined 'riding' their respective carbon atoms. A standard weighting scheme was applied and the data was corrected for isotropic extinction. All crystallographic calculations were performed using the SHELXS-86[1] and SHELXL-93[2] programs and neutral atom scattering factors were taken from the usual sources[3].

REFERENCES

1. G.M.Sheldrick, *Acta Crystallogr.*, 1990, **A46**, 467.

2. G.M.Sheldrick, *SHELXL-93*, Institut. Für Anorganische Chemie der Universität Göttingen, Germany, 1993.

3. *International Tables for Crystallography*, Kynoch Press, Birmingham, 1974, Vol. 4.

4. N.Walker, D.Stuart, *Acta Crystallogr.*, 1983, **A39**, 158.

5. A.Altomare, G.Cascarano, C.Giacovazzo, A.Guagliardi, *J. Appl. Cryst.*, 1993, **26**, 343.

6. J.S.Rollet, *Computing Methods in Crystallography*, Pergamon Press, Oxford, 1965.

7. A.C.Larson, *Acta Crystallogr.*, 1967, **A23**, 664.

8. D.J.Watkin, J.R.Carruthers, P.W.Betteridge, *CRYSTALS User Guide*, Chemical Crystallography Laboratory, University of Oxford, 1985.

9. N.Walker, D.Stuart, *Acta Crystallogr.*, 1983, **A39**, 158; adapted for FAST geometry by A.I.Karaulov, University of Wales, 1991.